



UNITED STATES  
NUCLEAR REGULATORY COMMISSION  
WASHINGTON, D.C. 20555-0001

GT9990406  
RC

September 8, 2004

RECEIVED  
ACRS/ACNW  
US NRC

SEP 10 2004

MEMORANDUM TO: John T. Larkins, Executive Director  
Advisory Committee on Reactor Safeguards

FROM: Suzanne C. Black, Director  
Division of Systems Safety and Analysis  
Office of Nuclear Reactor Regulation

*John T. Larkins, for*

SUBJECT: REQUEST FOR ACRS REVIEW OF THE DRAFT SAFETY  
EVALUATION BY THE OFFICE OF NUCLEAR REACTOR  
REGULATION RELATED TO NRC GENERIC LETTER 2004-xx,  
NUCLEAR ENERGY INSTITUTE GUIDANCE REPORT (PROPOSED  
DOCUMENT NUMBER NEI 04-07), "PRESSURIZED WATER REACTOR  
SUMP PERFORMANCE EVALUATION METHODOLOGY"

The Office of Nuclear Reactor Regulation (NRR) requests that the Advisory Committee on Reactor Safeguards (ACRS) review and give final endorsement to the subject Safety Evaluation Report (SER). The draft version of the SER is currently scheduled to be issued for public release September 20, 2004.

The attached SER is part of the staff's resolution of Generic Safety Issue (GSI) 191, "Assessment of Debris Accumulation on PWR Sump Performance." The objective of GSI-191 is to ensure that post-accident debris blockage will not impede or prevent the operation of the emergency core cooling system (ECCS) or containment spray system (CSS) in the recirculation mode at pressurized water reactor during loss of coolant accidents or other high energy line breaks accidents for which sump recirculation is required. Because of the issues identified during the resolution of GSI-191, the staff has concluded that the subject SER should be issued to licensee's to provide staff acceptable guidance for evaluation of the ECCS or CSS recirculation functions and, if appropriate, take additional actions to ensure their compliance with 10 CFR 50.465(b)(5).

Attachment: As stated

CONTACT: T. Hafera, NRR/DSSA/SPLB  
415-4097

**ACRS OFFICE COPY**  
**DO NOT REMOVE FROM ACRS OFFICE**

GT 999

**SAFETY EVALUATION BY  
THE OFFICE OF NUCLEAR REACTOR REGULATION  
RELATED TO NRC GENERIC LETTER 2004-XX,  
NUCLEAR ENERGY INSTITUTE  
GUIDANCE REPORT  
(PROPOSED DOCUMENT NUMBER NEI 04-07),  
“PRESSURIZED WATER REACTOR  
SUMP PERFORMANCE EVALUATION METHODOLOGY”**

This page is intentionally blank.

## FOREWORD

The objective of a safety evaluation report (SER) issued by the U.S. Nuclear Regulatory Commission (NRC, the staff) is typically to determine and describe the acceptability of a submittal from a domestic licensee, vendor, or nuclear industry organization related to a nuclear power plant(s). However, the objective of this SER on (proposed document number NEI 04-07) "Pressurized Water Reactor Sump Performance Evaluation Methodology" (NEI, 2004a), submitted by the Nuclear Energy Institute (NEI) to the NRC, is to provide an acceptable methodology guidance for licensees of pressurized water reactors (PWRs) through the use of the combination of the submittal and this SER in their responses to recently-issued NRC Generic Letter 2004-XX, "Potential Impact of Debris Blockage on Emergency Recirculation During Design Basis Accidents at Pressurized-Water Reactors" (GL-04-xx), as the cited NRC approved methodology for their evaluation of plant-specific sump performance.

In the staff's review of the NEI submittal, it found that portions of the proposed guidance were acceptable as is; and other portions were found to need additional justification and/or modification. Therefore, in an effort to expedite the resolution of Generic Safety Issue (GSI)-191, "Assessment of Debris Accumulation on PWR Sump Performance," the staff has provided identified conditions, limitations, and required modifications, including alternative guidance to supplement those portions determined by the staff to need additional justification and/or modification in the NEI submittal. The resultant combination of the NEI submittal and staff safety evaluation, provide an acceptable overall guidance methodology for the plant-specific evaluation of emergency core cooling system (ECCS) or core spray system (CSS) sump performance following all postulated accidents for which ECCS or CSS recirculation is required, with specific attention given to the potential for debris accumulation that could impede or prevent ECCS or CSS from performing its intended safety functions.

## EXECUTIVE SUMMARY

The Nuclear Energy Institute (NEI) submitted (proposed document number NEI 04-07) "Pressurized Water Reactor Sump Performance Evaluation Methodology" (NEI, 2004a, referred to herein as the Guidance Report or GR), for review by the U.S. Nuclear Regulatory Commission (NRC, the staff). NRC approval of this methodology guidance would allow licensees of pressurized water reactors (PWRs) to use the document in their responses to recently-issued NRC Generic Letter 2004-XX, "Potential Impact of Debris Blockage on Emergency Recirculation During Design Basis Accidents at Pressurized-Water Reactors" (GL-04-xx), as the cited NRC approved methodology for their evaluation of plant-specific sump performance. The Generic Letter identifies inadequacies in previous approaches for modeling sump screen debris blockage and related effects, such that the staff no longer considers many licensing-basis analyses acceptable for confirming compliance with NRC regulations. The NEI submittal offers guidance to all PWR licensees in response to those inadequacies identified during resolution of Generic Safety Issue (GSI)-191, "Assessment of Debris Accumulation on PWR Sump Performance," documented in the Generic Letter.

The resultant combination of the NEI submittal and staff safety evaluation, provide an acceptable overall guidance methodology for the plant-specific evaluation of ECCS (or CSS) sump performance following all postulated accidents for which ECCS or CSS recirculation is required, with specific attention given to the potential for debris accumulation that could impede or prevent ECCS or CSS from performing its intended safety functions.

The GR is divided into two primary sections, the baseline evaluation and the refinements sections. The baseline is intended by NEI to provide a conservative approach for utilities to perform a "baseline evaluation" of their PWR containment sump using a sample calculation for a consistent and simplified first-step in determining susceptibility to head loss. The refinements sections are intended to address, for those plants that do not "pass" the baseline evaluation, options for refinements to the baseline calculation that result in acceptable results, or hardware "fixes" to provide acceptable results. This NEI submittal addresses the following major areas:

- Pipe Break Characterization
- Debris Generation/Zone-of-Influence
- Latent Debris Accumulation within Containment
- Debris Transport to the Sump Screen(s)
- Head Loss as a Result of Debris Accumulation
- Analytical Refinements to Remove Conservatism(s) from the Evaluation
- Physical Refinements to Plant
- Risk-Informed Evaluation
- Sump Structural Analysis
- Upstream Effects of Debris Accumulation
- Downstream Effects of Debris Accumulation
- Chemical Precipitation Effects of Debris Accumulation

The following is a brief summary of each major area of the staff's evaluation.

### ES.1 PIPE BREAK CHARACTERIZATION

Analysis of the most challenging postulated accident with regard to sump performance during long-term core cooling, involves selection of the most limiting pipe break size, location, and debris combination within containment. For a PWR, RG 1.82, Rev. 3, "Water Sources for Long-Term Recirculation Cooling Following a Loss-of-Coolant Accident," (RG 1.82-3), Section C, Regulatory Position 1.3.2.3, specifies that a sufficient number of breaks in each high-pressure system that relies on recirculation should be considered to reasonably bound variations in debris generation by size, quantity and type of debris. Regulatory Guide 1.82 stipulates the following set of break locations to be considered as a minimum:

- Breaks in the reactor coolant system (RCS) and, depending on the plant licensing basis, main steam and main feedwater lines with the largest amount of potential debris within the postulated zone-of-influence (ZOI),
- Large breaks with the most variety of debris, within the expected ZOI,
- Breaks in areas with the most direct path to the sump,
- Medium and large breaks with the largest potential particulate debris to insulation ratio by weight, and
- Breaks that generate an amount of fibrous debris that, after its transport to the sump screen, could form a uniform thin bed that could subsequently filter sufficient particulate debris to create a relatively high head loss referred to as the "thin-bed effect." The minimum thickness of fibrous debris needed to form a thin bed has typically been estimated at 1/8 inch thick.

The GR states the objective of the break selection process is to identify the break size and location which results in debris generation that produces the maximum head loss across the sump screen. All phases of the accident scenario must be considered for each postulated break location, including debris generation, debris transport, and sump screen head loss calculations. The break selection process outlined in the GR identifies limiting break locations as those that result in:

- The maximum amount of debris that is transported to the sump screen.
- The worst combination of debris mixes that are transported to the sump screen.

The GR also provides the following guidance:

- Break exclusion zones are disregarded for this evaluation (pipe breaks must be postulated in pre-existing break exclusion zones).
- Exclude consideration of NRC Branch Technical Position MEB 3-1, as a basis, since limiting conditions for ECCS sump concerns are not related to the pipe vulnerability issues addressed in MEB 3-1.
- For plants needing to consider main steam and feedwater line breaks, break locations should be consistent with the plant's current licensing basis.
- Consider locations that result in a unique debris source term (i.e., not multiple identical locations).
- Consider locations with high concentrations of problematic insulation.

- Consider breaks that generate an amount of fibrous debris that could create a thin-bed effect.
- Small breaks less than 2 inches in diameter (for piping attached to the RCS) need not be considered.
- If a significant amount of fibrous debris is not generated, consider breaks that produce the greatest contribution of latent debris sources which may produce the limiting debris loading condition for sump screen blockage concerns.

The staff finds that the GR is consistent with staff positions, with the following exceptions:

1. The GR does not provide guidance for those plants that can substantiate no thin bed effect, which may impact head loss results and limiting break location.
2. For plants needing to evaluate secondary-side piping such as main steam and feedwater pipe breaks, break locations should be postulated in a manner consistent with the guidance in Section 3.3 of this SER.

To address these exceptions, the staff has provided enhanced guidance in Sections 3.3 and 3.4 of this SER, and in combination with the enhanced guidance offered in the SER, the staff finds this section to be acceptable.

## **ES.2 DEBRIS GENERATION/ZONE-OF-INFLUENCE**

With the rupture of piping come shock waves and jets of coolant that project from within the piping via the closed system pressure, until that pressure dissipates. Debris is generated as the shock waves and jets impact surrounding insulation, coatings, surfaces, and other materials within the zone. The volume of space affected by this impact, or zone-of-influence (ZOI), is modeled in order to define and characterize the debris generated.

The ZOI recommended in GR Section 3.4, is a spherical boundary with the center of the sphere located at the break site. The use of a spherical ZOI is intended to encompass the effects of jet expansion resulting from impingement on structures and components, truncating the sphere wherever it intersects any structural boundary or large robust equipment. The GR recommends that ZOI sizing be determined through the use of ANSI/ANS 58.2-1988 standard for a freely expanding jet, and for the baseline is to be based on the insulation type that generates the largest ZOI of all potentially affected insulation types located inside containment—i.e., the insulation type with the lowest destruction pressure. The resulting ZOI will then be applied to all insulation types.

Coating debris generation, however, is treated separately. Coating debris in the GR, are generated from postulated failure (destruction) of both DBA-qualified and unqualified coatings within the ZOI and from postulated failure of all unqualified coatings outside the ZOI. For coatings, the GR recommends a ZOI destruction pressure of 1000 psi, with a corresponding ZOI radius of one pipe diameter. The GR assumes that all coating debris will fail to a particulate size equivalent to the basic material constituent.

Debris characteristics are described in the GR in terms of size distribution, size and shape, and density. The GR identifies two size distributions for material within the ZOI, i.e., small fines and large pieces. Small fines are defined as debris able to pass through the largest openings of the gratings, trash racks, and radiological fences, which are less than a nominal four inches. Debris that cannot pass through these barriers is classified as large pieces.

For debris sizing assumed within the ZOI, most fibrous debris is assumed to degrade to 60% small fines and 40% large pieces. Some fibrous debris is considered to degrade to 100% small fines and no large pieces. Reflective metallic insulation (RMI) is assumed to degrade to 75% small fines and 25% large pieces. And most other debris types are considered to degrade to 100% small fines and no large pieces. Erosion is neglected based on the assumption that the small fines are already reduced to their basic constituents of individual particles and fibers. Jacketed large debris is also assumed not to erode.

Debris material densities and size distributions were tabulated in the GR for select debris types. Properties of materials for which limited data is available are listed as "best available." For those materials for which no data is available, maximum destruction is assumed.

The GR assumes that coatings will fail as particulate. The amount of particulate is a function of coating properties including the thickness and area. The GR indicates that where plant-specific data does not exist regarding the thickness of unqualified coatings, an equivalent thickness of 3 mils of inorganic zinc (IOZ) be used.

The staff has reviewed the use of a spherical model sized in accordance with the ANSI/ANS standard, and finds this approach acceptable. The spherical geometry proposed encompasses a zone which considers multiple jet reflections at targets, offset between broken ends of a guillotine break, and pipe whip. The confirmatory analysis performed by the staff (Appendix I) verifies the applicability of the ANSI/ANS standard for determining the size of this zone. Use of a ZOI model is identified as an acceptable approach for analyzing debris generation per RG 1.82, Rev. 3. (This approach was also used and approved by the staff in the BWR sump performance SER.) The GR recommendation to truncate the spherical ZOI when a robust barrier or large piece of equipment is encountered is acceptable to the staff. The refinement offered in the GR to apply spherical ZOIs that correspond to material-specific destruction pressures for each material that may be affected in the vicinity of a break, is also acceptable.

A LWR LOCA jet is a two-phase steam/water jet. The destruction pressures cited in the GR are referenced from the BWROG URG which were determined using an air jet. Based on staff study of this difference and due to limited experimental evidence from two-phase jets, the BWROG destruction pressures could be too high and thus could underestimate debris quantities. The staff position in this Safety Evaluation is to lower the debris destruction pressure by 40% in order to account for two-phase jet effects (see Section 3.4.2.2).

With regard to coatings, the staff agrees with the approach taken; however the staff considers there to be insufficient technical justification to support a value of 1000 psi as a destruction pressure, with corresponding ZOI of one pipe diameter. The staff position is that the licensees should use a coatings ZOI equivalent to 10D or a ZOI determined

by plant specific analysis, based on experimental data that correlate to plant materials over the range of temperatures and pressures of concern. Note that an equivalent to ten pipe diameters was used for coatings characterization and was approved by the staff in the BWR sump performance SER.

The staff concurs with the characterization of debris in GR Section 3.4.3. Confirmatory analyses provided in Appendix II, verifies the acceptability of the size distributions recommended in the GR. However, the staff position is that licensees apply insulation-specific debris size information where available.

For the characterization of coatings in Section 3.4.3.4, the staff finds that the alternative offered to use of plant-specific data for the determination of coatings thicknesses will require plant-specific justification. The equivalent inorganic zinc (IOZ) thickness of 3 mils recommended may be nonconservative and unsubstantiated because, although the assumption that all unqualified coatings outside the ZOI fail, is consistent with the position provided in NUREG-0800, Section 6.1.2, "Protective Coatings Systems;" the staff is aware of numerous cases in which containment coatings, qualified and unqualified, are much thicker than the recommended 3 mil IOZ equivalent thickness.

Also, for those plants that substantiate no formation of a fibrous thin bed, the assumptions and guidance provided in the GR may be nonconservative in that the particulate-sized debris assumed would simply pass through the screens, thereby not causing a head loss concern. Therefore, for any such plant, the staff position is that assumptions as to debris characterization, particularly for coatings characterization, be realistically-conservative based upon the plant-specific environment and susceptibilities identified by the licensee.

### **ES.3 LATENT DEBRIS**

Section 3.5 of the GR provides guidance for estimating the amount latent debris as a source for contribution to head loss across the ECCS sump screen. Generally, miscellaneous fiber, dust, and dirt are primary sources of this debris type. It is noted that for all-RMI plants, the primary contribution of fibrous debris toward formation of a thin fibrous bed may come from latent debris sources.

The staff has reviewed the guidance provided for estimating the impact of latent debris and agrees that it is necessary to determine the types, quantities and locations of latent debris sources. The staff also agrees that it is not appropriate for licensees to assume that their existing foreign material exclusion (FME) programs have entirely eliminated miscellaneous debris. Results from plant specific walkdowns must be used to determine a realistic amount of latent debris in containment and to monitor cleanliness programs for compliance to committed estimates.

The guidance provided in the GR for consideration of effects of latent debris is considered acceptable for: general considerations for latent debris; estimates of some surface areas for evaluation of latent debris; and some attributes associated with evaluation of debris buildup, quantity of miscellaneous debris, and defining debris characteristics Alternate guidance is provided in Section 3.5 of the SER for statistical sampling and sample analysis to allow licensees to more accurately determine the impact of latent debris on sump screen performance. This revised approach is based on

generic characterization of actual PWR debris samples. If desired, a licensee could pursue plant-specific characterization as a refinement.

#### **ES.4 DEBRIS TRANSPORT**

Debris transport is described in Section 3.6, and is separately specified for each of three containment types—highly-compartmentalized, mostly un-compartmentalized, and ice condenser containments. Transport of the two size distributions identified in ES.2, above, and discussed in Section 3.4.3 (i.e., small fines and large pieces) are considered in the staff's review of debris transport.

The staff finds that the transport guidance for small fines of debris is acceptable. However, the guidance for the large pieces of debris is because of the unrealistic assumption that large pieces of debris will not transport. Specifically, plants with configurations conducive to fast pool velocities will realistically transport some large pieces, therefore the staff position is that consideration for transport of large pieces of debris is necessary.

The staff also finds that the method recommended for determining the quantity of fine debris trapped in inactive pools based on the volume ratio of inactive pools to the total pools is unrealistic for plants with large inactive pools. Therefore the staff position is that licensees should limit the maximum fraction of fine debris being trapped in inactive pools to 15% to avoid nonconservative results.

#### **ES.5 HEAD LOSS**

Computation of head loss in the GR involves input of design characteristics and reflection of thermal-hydraulic conditions into a head loss correlation (NUREG/CR-6224). The approach is acceptable to the staff, with specific areas of additional guidance offered in Section 3.7.2.2 and 3.7.2.3 of this SER.

The following additional guidance is necessary in the consideration of fibrous thin bed formation:

- Use of the appropriate density in the determination of the quantity of debris needed to form a thin bed—i.e., the as-manufactured density.
- Careful evaluation of the limiting porosity for the particular particulate or mixture of particulates in the debris bed.
- Consideration of uncertainties in specifying a one-eighth-inch bed thickness criteria—e.g., the strong indication that calcium silicate can form a debris bed without supporting fibers.
- Consideration of other uncertainties—e.g., uncertainties associated with mixing of constituents, or uncertainties associated with latent debris data collection.

#### **ES.6 ANALYTICAL REFINEMENTS**

Three analytical topics are identified in this section—i.e., debris generation, debris transport, and head loss. A fourth, break selection, is addressed in Section 6.0.

For debris generation, the GR recommends two refinements for insulation materials. First, the GR proposes use of debris-specific ZOI's versus use of the most conservative debris type applied to all. Second, the GR proposes use of two freely-expanding jets emanating from each broken pipe section versus use of spherical ZOI. The staff finds both debris generation refinements to be acceptable.

For debris transport, two methods for computing flow velocities in a sump pool—i.e., the network method and the computational fluid dynamics method—are provided in the Analytical Refinements section of the GR. However, the staff finds the guidance offered in either option to be insufficient to provide an acceptable alternative to the baseline approach.

For head loss, only refinements offered in GR Section 3.7.2.3.2.3, "Thin Fibrous Beds," are offered. This section addresses the need for consideration of fibrous thin bed formation, and the alternative consideration of latent debris as the primary contributor to this thin bed for all-RMI plants. The staff finds no specific refinement offered for the head loss analysis.

## **ES.7 PHYSICAL REFINEMENTS TO PLANT**

GR Section 5.0 provides guidance for refinements in the areas of debris source term, debris transport obstructions, and screen modifications.

The five following areas for refinement are offered for debris source term:

- Housekeeping and foreign material exclusion (FME) programs
- Change-out of insulation
- Modify existing insulation
- Modify other equipment or systems
- Modify or improve coatings program

The staff has reviewed these refinements and finds them to be acceptable. However, with regard to insulation change-out or modification, the staff emphasizes that minimum loadings required to form a thin-bed be considered. Also, on the coatings area, the statement that DBA-qualified coatings have very high destruction pressures, has not been proven (see Sections 3.4.2, 3.4.2, and 4.2.2.2.3).

This section of the GR also discusses the potential use of floor obstructions to provide a barrier to prevent debris transport to the sump. It mentions that barriers can be used either near the sump or closer to the debris source. Key considerations regarding the use of floor obstructions and barriers are that the barrier be located where flow velocities and turbulence are insufficient to lift debris over the barriers, and the barrier should cover the entire cross-section of flow.

This section provides little specific information regarding the methods for determining proper debris transport obstruction design. The lack of detail and simplified concepts presented would require each plant to perform a plant specific evaluation of their proposed debris obstruction to determine their effectiveness and structural capability

under post-accident conditions. To credit debris transport obstructions for trapping debris, plant specific documentation should be available on site to demonstrate an appropriate correlation to the test results in terms of debris type and velocity limits.

With regard to screen modifications, those discussed in the GR are found to be acceptable; however, licensees are not limited to those identified.

## **ES.8 ALTERNATE EVALUATION**

NEI has proposed an alternative evaluation approach which incorporates realistic and risk-informed elements to the PWR sump analysis. The following steps are proposed for this alternative approach, or "Option B":

- Define a "debris generation" LOCA break size to distinguish between customary and more realistic design basis PWR sump analyses
- Perform customary design basis analyses for break sizes up through the debris generation break size identified above (Region I analyses)
- Perform analyses demonstrating long-term cooling and mitigative capability for break sizes larger than the debris generation break size up through the double-ended rupture of the largest RCS piping (Region II analyses)

The GR proposes realistic treatment of Region II break sizes based on the low probability of these larger breaks. Models, assumptions, and equipment availability for mitigation used for this analysis are proposed to be realistic and demonstrated as functionally reliable, and may not necessarily be safety-related or single failure-proof. Risk evaluations would be performed as a basis for plant modifications and credit taken for operator actions. Such analyses may require plant-specific exemption and/or license amendment requests.

- The staff concludes that GR Section 6.0 provides an acceptable approach for evaluating PWR sump performance. Application of more realistic and risk-informed elements is technically justified based on the low likelihood of such breaks occurring.

## **ES.9 SUMP STRUCTURAL ANALYSIS**

formation to show that structural loads on a sump screen should be computed using the total pressure drop across the screen. The limiting conditions correspond to the break location and debris source term that induce the maximum total head loss at the sump screen after full consideration of transport and degradation mechanisms. This represents the minimum required performance criterion for judging recirculation-sump operability. In other words, the recirculation sump must be able to accommodate both the clean-screen head loss and the debris-induced head loss associated with the limiting break while providing adequate flow through both the ECCS injection pumps and the CS pumps if needed. For some licensees, the minimum structural design criterion for the sump screen can depend on the plant NPSH margin. Revised plant-specific licensing bases may dictate the structural capacity of the sump screen for supporting water flow through a debris bed under recirculation velocities depending on screen geometry (fully-submerged versus partially-submerged designs).

## **ES.10 UPSTREAM EFFECTS**

The GR states that certain hold-up or choke points exist which could reduce flow to and possibly cause blockage upstream of the sump. Such areas within containment are: (1) narrowing of hallways or passages; (2) gates or screens that restrict access to areas of containment such as behind the bioshield or crane wall; and (3) refueling canal drain.

The staff finds the guidance with respect to upstream blockage to be acceptable.

## **ES.11 DOWNSTREAM EFFECTS**

This section provides guidance on the evaluation of entrained debris downstream of the sump causing downstream blockage. The three areas of concern identified are: (1) blockage of flow paths in equipment such as containment spray nozzles and tight-clearance valves, (2) wear and abrasion of surfaces such as pump running surfaces, and heat exchanger tubes and orifices, and (3) blockage of flow clearances through fuel assemblies.

The staff finds this section to need clarification and additional considerations and provides the following alternative guidance with regard to downstream blockage:

- Licensees should consider particles larger than the flow openings in a sump screen will deform and flow through or orient axially and flow through, and determine what percentage of debris would likely pass through their sump screen and be available for blockage of piping, core spray nozzles, and instrument tubing at downstream locations.
- Licensees should consider term of operating line-up (short or long), conditions of operation, and mission times.
- Licensees should consider wear and abrasion of pumps and rotating equipment, piping, spray nozzles, instrumentation tubing, and HPSI throttle valves. The potential for wear to alter system flow distribution and/or form plating of slurry materials (in heat exchangers) should be included.
- Licensees should consider leakage past seals and rings due to wear from debris fines to areas outside containment, with respect to license basis dose consequences.
- An overall ECCS or CS system evaluation should be performed considering the potential for reduced pump/system capacity due to internal bypass leakage or through external leakage.
- Licensees should consider flow blockage associated with core grid supports, mixing vanes, and debris filter, and their effects on fuel rod temperature.

## **ES.12 CHEMICAL EFFECTS**

GR Section 7.4 addresses how reaction products formed in a post-LOCA environment can contribute to blockage of the sump screens and increase the associated head loss across the screens. The GR also defers guidance for dealing with these effects until current testing is completed and the data has been appropriately evaluated.

The staff has considered NEI's response and finds that chemical effects must be addressed on a plant-specific basis. Initially, licensees must evaluate whether the current chemical test parameters are sufficiently bounding for their plant specific conditions. If they are not, then licensees must provide technical justification in order to use any of the results from the tests in their plant-specific evaluation. If chemical effects are observed during these tests, then licensees must evaluate the sump screen head loss consequences of this effect. A licensee who chooses to modify their sump screen before tests are complete should consider potential chemical effects in order to avoid additional screen modification should deleterious chemical effects be observed during testing.

## GUIDANCE DEVELOPMENT BACKGROUND

The staff began working with NEI on the resolution of GSI-191 in 1997, with the establishment of the PWR Industry Sump Performance Task Force. The staff also conducted a study on the susceptibility of PWRs to ECCS sump blockage following a LOCA. This study was entitled, "GSI-191: Parametric Evaluations for Pressurized Water Reactor Recirculation Sump Performance" (Rao, 2001), and was performed by Los Alamos National Laboratory (LANL) in support of the NRC's GSI-191 technical assessment to determine if sump failure is a plausible concern for PWRs.

On July 26 and 27, 2001, the NRC held a public meeting with the industry and other stakeholders including NEI, the Westinghouse Owners Group, the Babcock and Wilcox Owners Group, and the Combustion Engineering Owners Group, on the preliminary findings of that study. This meeting was documented in a meeting summary dated August 14, 2001 (Mtg, 2001). The preliminary results of the study indicated that significant quantities of fibrous and particulate debris will be generated during various size LOCAs, and that a sufficient fraction of this debris may be transported to the sump screen and cause sump screen blockage. However, before determining what regulatory action was needed, the staff presented the results to the industry and interested stakeholders, to discuss the assumptions and calculations in the report. Since that time, the parametric report was approved and issued (NUREG/CR-6762), and the staff concluded that GSI-191 is a credible concern for the population of domestic PWRs and that detailed plant-specific evaluations are needed to determine the susceptibility of each U.S.-licensed PWR to ECCS sump blockage.

The staff has worked closely with NEI, providing feedback into the development of an acceptable approach to resolution of GSI-191, through a series of public meetings held between July 2001 and October 2003, until the submittal of NEI's October 31, 2003, "PWR Containment Sump Evaluation Methodology" (NEI, 2003b). Following the public meeting on July 26 and 27, 2001, described above, which involved discussions of risk considerations as well as the parametric evaluation results, a public meeting was held on March 28, 2002, described in a meeting summary dated April 16, 2002 (Mtg, 2002a). The staff presented their approach toward resolution of GSI-191, as did the industry, making references to the revision of Regulatory Guide (RG) 1.82, "Water Sources for Long-Term Recirculation Cooling Following a Loss-of-Coolant Accident (DG-1107)," issuance of a generic letter, Standard Review Plan update, chemical testing, data collection guidance, and evaluation guidance. Industry also committed to take the lead for issue resolution.

By the next meeting on May 30, 2002, NEI had issued NEI 02-01, "Condition Assessment Guidelines: Debris Sources Inside PWR Containments," dated April 19, 2002 (NEI, 2002a). The staff's comments in response to NEI 02-01 identified minor concerns with a lack of firm direction in some areas of data collection although providing reasonable overall guidance; . The staff's conclusions; are included in Attachment 3 to the meeting summary dated June 6, 2002, ,, as are status presentations from the staff NEI, and the industry (Mtg, 2002b).

In the next two public meetings on July 2, 2002, and August 29, 2002, the staff raised discussions on the schedule for the draft generic letter, the development of temporary instructions for NRC inspectors regarding GSI-191, concerns surrounding downstream effects such as high pressure safety injection (HPSI) throttle valve blockage, and

presented fault tree modeling for ECCS injection. NEI's discussion focused on Interim Plant Assessment templates and guidance on related compensatory measures, as well as their response to the staff's comments on NEI 02-01. The discussions in both meetings are documented in meeting summaries dated July 31, 2002 (Mtg, 2002c), and September 5, 2002 (Mtg, 2002d), respectively.

The following two public meetings on October 24, 2002, and December 12, 2002, revolved around NEI's proposed ground rules for the sump evaluation guidance, discussion of head loss behavior and leak-before-break (LBB) considerations for break selection, as well as the HPSI issue. The staff objected to the use of LBB as applied to break selection assumptions. "NEI Draft Evaluation Methodology Ground Rules" was issued on December 12, 2002 (NEI, 2002b). The material presented during both meetings is included in the meeting summaries dated October 31, 2002 (Mtg, 2002e), and December 31, 2002 (Mtg, 2002f), respectively.

The staff, NEI, LANL, and interested stakeholders participated in discussions of standing GSI-191 issues and toured the University of New Mexico (UNM) experimental facilities on March 5, 2003. NRC presented the schedule for generic letter issuance, chemical testing status and expectations, response to NEI's ground rules for sump evaluation guidance, and supporting data and research by LANL including debris accumulation, ECCS vulnerability, and pool flow analysis. NEI presented material on the use of LBB for break selection, the use of a Nodal Network Method as an alternative to Computational Fluid Dynamics computer modeling for debris transport analysis, and the use of fracture mechanics for debris generation. A meeting summary was generated, and several individual presentations were documented (Mtg, 2003a).

NEI requested a meeting on April 29, 2003, summarized in a meeting summary dated May 15, 2003 (Mtg, 2003b), where the technical basis for using LBB arguments for break selection was discussed at length. The staff recommended that NEI provide for staff consideration an official submittal on their proposed approach to break selection. The staff presented the proposed Bulletin in the meeting, which was titled "Potential Impact of Debris Blockage on Emergency Sump Recirculation at Pressurized-Water Reactors."

On June 30, 2003, the staff held a public meeting with NEI and interested stakeholders on the issuance of NRC Bulletin 2003-01, "Potential Impact of Debris Blockage on Emergency Recirculation during Design-Basis Accidents at Pressurized-Water Reactors," dated June 9, 2003 (NRCB, 2003). NEI had forwarded 73 industry questions and comments on the bulletin, to which the staff responded in a handout distributed at this meeting. The effect of the bulletin on the overall GSI-191 resolution schedule was also raised by the public. All meeting material was attached to the meeting summary dated August 12, 2003 (Mtg, 2003c).

On July 1, 2003, a separate public meeting was held between the staff, and NEI and the industry, where sections of the draft methodology guidance were presented to the staff. The staff discussed progress in four major regulatory areas: RG 1.82, Revision 3 (issuance), head loss task report, debris characterization project, and chemical effects testing. The public raised the question of ranking the plants' susceptibility to sump blockage; to which the staff replied that no ranking was intended beyond the parametric study results for 69 "cases" already issued. The associated meeting summary is dated August 11, 2003 (Mtg, 2003d).

The NRC participated in a public workshop on Debris Impact on ECCS Recirculation held in Baltimore, MD, on July 30 and 31, 2003, where NRC and LANL presented material on sump evaluation methodology and the use of computer codes and volunteer plant studies in sump evaluation analyses. The NRC presentations were documented (Wkshp, 2003).

A public meeting between the staff and NEI and the industry was held on September 10, 2003, the results of which were documented in a meeting summary dated October 16, 2003 (Mtg, 2003e). The NRC staff expressed concern over chemical effects on sump screen blockage based on testing. NEI and the industry also presented material on chemical effects. Considerable discussion centered around the formation of gelatinous material due to chemical effects.

On October 31, 2003, NEI submitted to the staff the "PWR Containment Sump Evaluation Methodology" (NEI, 2003b). The staff provided to NEI a preliminary review of the October 31, 2003, submittal, by letter dated February 9, 2004 (NRC, 2004a). The staff transmitted two requests for additional information (RAIs) by electronic mail to NEI on March 10, 2004, and June 28, 2004, respectively. The staff met with NEI and stakeholders in a public meeting on March 23 and 24, 2004, to discuss the draft submittal and the March 10, 2004, RAIs. The results of this meeting are described in a meeting summary dated April 22, 2004 (Mtg, 2004a). NEI responded to the staff's RAIs by letters dated June 10, 2004 (NEI, 2004c), and July 8, 2004 (NEI, 2004d), respectively.

On April 19, 2004, NEI submitted to the staff a preliminary version of a Baseline Evaluation Method (NEI, 2004b), or Section 3.0 of the proposed GR. On May 28, 2004, NEI submitted the final version of the "PWR Containment Sump Evaluation Methodology" (NEI, 2004a), including a revised Section 3.0, and including a draft version of Section 6.0. On July 7, 2004, NEI provided the staff with a "Table of Refinements," via electronic mail, clarifying what refinements were being offered in the GR. On July 13, 2004, NEI submitted a final version of the Risk-Informed Section, or Section 6.0 (NEI, 2004e) of the GR.

NEI submitted a total of three draft versions of the GR, which were reviewed by the staff. They are: a draft of key sections of the evaluation guidance submitted July 1, 2003 (NEI, 2003a); a first draft of the "PWR Containment Sump Evaluation Methodology," submitted October 31, 2003 (NEI, 2003b); and a preliminary version of the current Baseline Evaluation Method, or Section 3.0 of the proposed GR, submitted April 19, 2004 (NEI, 2004b). The final GR was submitted to the NRC staff for review on May 28, 2004 (except Section 6.0, which was submitted to the staff on July 13, 2004), and is the subject of this safety evaluation. The final GR provides "baseline" guidance to utilities for evaluating plant-specific issues of pipe break selection, debris generation, latent debris, debris transport, sump screen head loss, and ECCS pump NPSH. In addition the GR provides "supplemental" guidance that can be used by licensees to refine their analysis and evaluations. The GR baseline guidance does not provide detailed guidance for several important related issues, including long-term chemical effects and head-loss correlations for particular insulation materials (e.g., calcium silicate), nor does it provide guidance for evaluating the impacts of debris passing through the screens and being ingested into the ECCS (downstream effects). The GR does note that licensees

must consider these additional elements in the overall performance evaluation in their plant-specific analysis.

The process used between the industry and the staff involved (1) direct discussions between the industry and the staff on key issues, (2) the NRC staff's independent research in support of the GSI-191 resolution effort, and (3) the submittal by NEI of three separate versions of the GR, which significantly contributed to the development of the technical basis for an acceptable methodology which is described in this SER.

## Table of Contents

FOREWORD .....	iii
EXECUTIVE SUMMARY .....	iv
GUIDANCE DEVELOPMENT BACKGROUND .....	xiv
List of Figures.....	xxii
List of Tables.....	xxiii
Acronym List.....	xxiv
1.0 INTRODUCTION .....	1
1.1 BACKGROUND .....	2
1.2 OVERVIEW.....	4
2.0 REGULATORY EVALUATION.....	8
3.0 BASELINE EVALUATION.....	10
3.1 INTRODUCTION.....	10
3.2 METHOD OVERVIEW .....	11
3.3 BREAK SELECTION.....	11
3.3.1 Introduction .....	11
3.3.2 Discussion.....	11
3.3.3 Postulated Break Size .....	12
3.3.4 Identifying Break Locations.....	12
3.3.5 Evaluation of Break Consequences.....	15
3.4 DEBRIS GENERATION .....	17
3.4.1 Introduction .....	17
3.4.2 Zone of Influence (ZOI) .....	17
3.4.3 Quantification of Debris Characteristics .....	31
3.5 LATENT DEBRIS.....	40
3.5.1 Discussion.....	40
3.5.2 Baseline Approach .....	41
3.5.3 Sample Calculation .....	51
3.6 DEBRIS TRANSPORT.....	51
3.6.1 Definition .....	51
3.6.2 Discussion.....	52
3.6.3 Debris Transport.....	52
3.6.4 Calculate Transport Factors .....	56
3.7 HEAD LOSS .....	57

3.7.1	Introduction and Scope.....	57
3.7.2	Inputs for Head Loss Evaluation.....	57
3.8	ACCEPTANCE OF NEI BASELINE GUIDANCE.....	70
4.0	ANALYTICAL REFINEMENTS.....	81
4.1	INTRODUCTION.....	86
4.2	METHOD DESCRIPTION.....	86
4.2.1	Break Selection.....	86
4.2.2	Debris Generation.....	88
4.2.3	Latent Debris.....	94
4.2.4	Debris Transport.....	94
4.2.5	Head Loss.....	98
5.0	DESIGN AND ADMINISTRATIVE CONTROL REFINEMENTS.....	99
5.1	DEBRIS SOURCE TERM.....	100
5.2	DEBRIS TRANSPORT OBSTRUCTIONS.....	101
5.2.1	Floor Obstruction Design Considerations.....	101
5.2.2	Debris Obstruction Rack Design Considerations.....	101
5.3	SCREEN MODIFICATION.....	102
5.3.1	Considerations for Passive Strainer Designs.....	103
5.3.2	Considerations for a Backwash Strainer Design.....	103
5.3.3	Considerations for an Active Strainer Design.....	104
5.3.4	Summary.....	105
6.0	ALTERNATE EVALUATION.....	106
6.1	BACKGROUND AND OVERVIEW.....	106
6.2	ALTERNATE BREAK SIZE.....	108
6.3	REGION I ANALYSIS.....	111
6.4	REGION II ANALYSIS.....	114
6.5	RISK INSIGHTS.....	120
7.0	ADDITIONAL DESIGN CONSIDERATIONS.....	124
7.1	SUMP STRUCTURAL ANALYSIS.....	124
7.2	UPSTREAM EFFECTS.....	125
7.3	DOWNSTREAM EFFECTS.....	126
7.4	CHEMICAL EFFECTS.....	129
8.0	CONDITIONS AND LIMITATIONS.....	132
9.0	CONCLUSION.....	136

10.0 REFERENCES .....143

## **Review of NEI Guidance Appendices**

Review of Appendix A, “Defining Coating Destruction Pressures and Coating Debris Sizes for DBA-Qualified and Acceptable Coatings in Pressurized Water Reactor (PWR) Containments”

Review of Appendix B, “Example of a Latent Debris Survey”

Review of Appendix C, “Comparison of Nodal Network and CFD Analysis”

Review of Appendix D, “Isobar Maps for Zone of Influence Determination”

Review of Appendix E, “Additional Information Regarding Debris Head Loss”

## **Confirmatory Analysis and Alternative Guidance Appendices**

Appendix I: ANSI/ANS Jet Model

Appendix II: Confirmatory Debris Generation Analyses

Appendix III: Volunteer Plant Containment Pool CFD Analysis

Appendix IV: Debris Transport Comparison

Appendix V: Confirmatory Head Loss Analyses

Appendix VI: Detailed Blowdown/Washdown Transport Analysis for  
Pressurized-Water-Reactor Volunteer Plant

Appendix VII: Characterization of PWR Latent Debris

## List of Figures

Figure 3-1. Comparison of GR Isobar Map with Isobars from Independently Evaluated ANSI Jet Model .....	24
---	----

## List of Tables

Table 3-1. Comparison of Computed Spherical ZOI Radii from Independent Evaluations of the ANSI Jet Model .....	25
Table 3-2. Revised Damage Pressures and Corresponding Volume-Equivalent Spherical ZOI Radii .....	28
Table 3-3. NEI Recommended Debris Size Distributions .....	35
Table 3-4. Summary of Debris Transport Assumptions for Small Fines Debris from ZOI .....	53
Table 3-5. Recommended Conservative Calcium Silicate NUREG/CR-6224 Correlation Parameters .....	63
Table 3-6. Conservative Assumptions in the Baseline Evaluation Methodology.....	71
Table 3-7. Non-Conservative Assumptions in the Baseline Evaluation Methodology .....	74
Table 3-8. Baseline Guidance Application to Divergent Hypothetical Plants A and B .....	78
Table 4-1. Pressurized Water Reactor Sump Performance Evaluation Methodology Refinements Table.....	82

## Acronym List

ACRS	Advisory Committee on Reactor Safeguards
AJIT	air jet impact test
ANSI	American National Standards Institute
ASME	American Society of Mechanical Engineers
BWR	boiling water reactor
BWROG	Boiling Water Reactor Owners' Group
B&W	Babcock and Wilcox
CalSil	calcium silicate
CDF	core damage frequency
CFD	computational fluid dynamics
CP	corrosion products
CS	containment spray
CSS	containment spray system
DBA	design basis accident
DGBS	"debris generation" break size
DDTS	Drywell Debris Transport Study
DEGB	double-ended guillotine break
DPSC	Diamond Power Specialty Co.
ECC	emergency core cooling
ECCS	emergency core cooling system
GDC	General Design Criteria
GR	NEI PWR Sump Performance Evaluation Methodology guidance report
GSI	Generic Safety Issue
HELB	high-energy line break
HPSI	high-pressure safety injection
IEF	initiating event frequency
IOZ	inorganic zinc
LANL	Los Alamos National Laboratory
LBB	leak before break
LBLOCA	large break loss of coolant accident
LDFG	low density fiberglass
LOCA	loss-of-coolant accident

NEI	Nuclear Energy Institute
NIST	National Institute for Standards and Technology
NPSH	net positive suction head
NRC	Nuclear Regulatory Commission
PE	Parametric Evaluation
PWR	pressurized water reactor
RAI	Request for Additional Information
RCS	Reactor Coolant System
RG	Regulatory Guide
RMI	reflective metal insulation
SEM	scanning electron microscope
SER	Safety Evaluation Report
SMC:FP	sump mitigation capability failure probability
SS	stainless steel
TMI	Three Mile Island
TPI	Transco Products, Inc.
TR	target reliability
UNM	University of New Mexico
ZOI	zone of influence

This page is intentionally blank.



SAFETY EVALUATION BY THE OFFICE OF NUCLEAR REACTOR REGULATION

RELATED TO NRC GENERIC LETTER 2004-XX,

NUCLEAR ENERGY INSTITUTE

GUIDANCE REPORT (PROPOSED DOCUMENT NUMBER NEI 04-07)

"PRESSURIZED WATER REACTOR SUMP PERFORMANCE

EVALUATION METHODOLOGY"

1.0 INTRODUCTION

By letter dated May 28, 2004, the Nuclear Energy Institute (NEI) submitted for review by the U.S. Nuclear Regulatory Commission (NRC, the staff) a document entitled (proposed document number NEI 04-07,) "Pressurized Water Reactor Sump Performance Evaluation Methodology" (NEI, 2004a), herein referred to as the guidance report (GR). NRC approval of the GR would allow licensees of pressurized water reactors (PWRs) to use the GR in their response to NRC Generic Letter 2004-XX, "Potential Impact of Debris Blockage on Emergency Recirculation During Design Basis Accidents at Pressurized-Water Reactors" (GL-04-xx), as the cited "NRC approved methodology" for their evaluation of plant-specific sump performance. The Generic Letter identifies inadequacies in many of the current PWR licensing-basis analyses for modeling sump screen debris blockage and related effects, such that the staff no longer considers those analyses acceptable for confirming compliance with NRC regulations. The NEI GR offers guidance to all PWR licensees in response to those inadequacies raised during resolution of Generic Safety Issue (GSI) 191, "Assessment of Debris Accumulation on PWR Sump Performance," which are documented in the Generic Letter.

The staff has completed its review of the GR and associated documentation, and the conclusions are documented in this safety evaluation report (SER). In general, the staff found that portions of the GR are acceptable for use in conducting plant-specific analyses of emergency core cooling system (ECCS) sump screen blockage and resultant ECCS and/or core spray system (CSS) loss of net positive suction head (NPSH) for pumps required following a loss-of-coolant-accident (LOCA). However, the staff found that several portions of the GR are not acceptable because the methods lack sufficient guidance, supporting data, or analysis to justify their technical basis. For each of these areas, the staff has provided a recommendation and/or alternative guidance to that offered in the GR. This SER discusses each section of the GR, along with the basis for the staff's conclusions.

This SER addresses each part of a plant-specific analysis of sump performance, and is organized so that its discussions parallel the guidance discussions presented in the GR. The SER includes sections on each of the following topics:

- Pipe Break Characterization (Section 3.3)
- Debris Generation/Zone of Influence (Section 3.4)

- Latent Debris (Section 3.5)
- Debris Transport (Section 3.6)
- Head Loss (Section 3.7)
- Analytical Refinements (Section 4.0)
- Design and Administrative Refinements (Section 5.0)
- Debris Source Term Refinements (Section 5.1)
- Refinements by use of Debris Transport Obstructions (Section 5.2)
- Refinements via Sump Screen Modifications (Section 5.3)
- Risk-Informed Evaluation (Section 6.0)
- Sump Structural Analysis (Section 7.1)
- Upstream Effects (Section 7.2)
- Downstream Effects (Section 7.3)
- Chemical Effects (Section 7.4)

## 1.1 BACKGROUND

In 1979, Unresolved Safety Issue (USI) A-43, "Containment Emergency Sump Performance," was established as a result of evolving staff concerns related to the adequacy of PWR recirculation sump designs. After extensive research, the staff found that the design assumption of 50 percent sump blockage used by licensees was nonconservative under certain conditions, and published the technical findings in NUREG-0897, "Containment Emergency Sump Performance," dated October 1985. Although the staff's regulatory analysis concerning USI A-43 did not support imposing new sump performance requirements, the staff issued GL 85-22, "Potential for Loss of Post-LOCA Recirculation Capability Due to Insulation Debris Blockage," dated December 3, 1985, to document the resolution of USI A-43, recommending that all reactor licensees replace the 50 percent blockage assumption with a comprehensive mechanistic assessment of plant-specific debris blockage potential for future modifications related to sump performance, such as thermal insulation changeouts. The staff also updated the NRC's regulatory guidance, including Section 6.2.2 of the Standard Review Plan (NUREG-0800) and Regulatory Guide (RG) 1.82, "Water Sources for Long-Term Recirculation Cooling Following a Loss-of-Coolant Accident" (RG 1.82), to reflect the USI A-43 technical findings documented in NUREG-0897.

Following the resolution of USI A-43 in 1985, several events challenged the staff's conclusion that no new requirements were necessary to prevent the clogging of ECCS strainers at operating BWRs:

- On July 28, 1992, at Barseback Unit 2, a Swedish BWR, the spurious opening of a pilot-operated relief valve led to the plugging of two containment vessel spray system suction strainers with mineral wool and required operators to shut down the spray pumps and backflush the strainers.

- In 1993, at Perry Unit 1, ECCS strainers twice became plugged with debris. On January 16, ECCS strainers were plugged with suppression pool particulate matter, and on April 14, an ECCS strainer was plugged with glass fiber from ventilation filters that had fallen into the suppression pool. On both occasions, the affected ECCS strainers were deformed by excessive differential pressure created by the debris plugging.
- On September 11, 1995, at Limerick Unit 1, following a manual scram due to a stuck-open safety/relief valve, operators observed fluctuating flow and pump motor current on the 'A' loop of suppression pool cooling. The licensee later attributed these indications to a thin mat of fiber and sludge which had accumulated on the suction strainer.

In response to these ECCS suction strainer plugging events, the NRC issued several generic communications, including Bulletin 93-02, Supplement 1, "Debris Plugging of Emergency Core Cooling Suction Strainers," dated February 18, 1994; Bulletin 95-02, "Unexpected Clogging of a Residual Heat Removal (RHR) Pump Strainer While Operating in Suppression Pool Cooling Mode," dated October 17, 1995; and Bulletin 96-03, "Potential Plugging of Emergency Core Cooling Suction Strainers by Debris in Boiling-Water Reactors," dated May 6, 1996. Through these bulletins the staff requested that BWR licensees implement appropriate procedural measures, maintenance practices, and plant modifications to minimize the potential for the clogging of ECCS suction strainers by debris accumulation following a loss-of-coolant accident (LOCA). Bulletin 96-03, in particular, noted the experience-based finding that clogging by fibrous debris is not limited to fibrous insulation as a debris source. These bulletins were adequately addressed by all BWR licensees.

However, findings from research to resolve the BWR strainer clogging issue in the 1990s raised questions concerning the adequacy of PWR sump designs by confirming what the aforementioned BWR strainer clogging events had earlier indicated: (1) that the amount of debris generated by a HELB could be greater than estimated by the USI A-43 research program, (2) that the debris could be finer (and, thus, more easily transportable), and (3) that certain combinations of debris (e.g., fibrous material plus particulate material) could result in a substantially greater head loss than an equivalent amount of either type of debris alone. Therefore, in 1996 the staff identified GSI-191, to ensure that post-accident debris blockage would not impede or prevent the operation of the ECCS and CSS in the recirculation mode at PWRs in the event of a LOCA or other HELB accidents for which sump recirculation is required. The staff began evaluating the potential vulnerability of PWRs and contracted LANL to evaluate the potential for debris to cause degraded PWR recirculating sump performance. In July 2001, preliminary parametric calculations were completed on PWR sump performance, which confirmed the potential for debris accumulation in a representative number of operating PWRs.

On June 9, 2003, having completed its technical assessment of GSI-191 (summarized below in the Overview section), the NRC issued Bulletin 2003-01, "Potential Impact of Debris Blockage on Emergency Recirculation During Design-Basis Accidents at Pressurized-Water Reactors," requesting an expedited response from PWR licensees as to the status of their compliance, on a mechanistic basis, with regulatory requirements concerning the ECCS and CSS recirculation functions. PWR licensees unable to assure regulatory compliance pending further analysis were asked to describe any interim compensatory measures that have been implemented or will be implemented to reduce

risk until the analysis could be completed. All PWR licensees have since responded to Bulletin 2003-01.

In developing Bulletin 2003-01, the NRC staff recognized that it may be necessary for PWR licensees to undertake complex evaluations to determine whether regulatory compliance exists in light of the concerns identified in the bulletin and that the methodology to perform such evaluations was not currently available. As a result, that information was not requested in the bulletin but PWR licensees were informed that the staff was preparing a generic letter that would request this information. On August xx, 2004, that generic letter was issued as GL 2004-xx, "Potential Impact of Debris Blockage on Emergency Recirculation During Design Basis Accidents at Pressurized-Water Reactors."

## **1.2 OVERVIEW**

In the event of a HELB inside the containment of a PWR, energetic pressure waves and fluid jets would impinge upon materials in the vicinity of the break, such as thermal insulation, coatings, and concrete, causing them to become damaged and dislodged. Debris could also be generated through secondary mechanisms, such as severe post-accident temperature and humidity conditions, flooding of the lower containment, and the impact of containment spray droplets. In addition to debris generated by jet forces from the pipe rupture, debris can be created by the chemical reaction between the chemically reactive spray solutions used following a LOCA and the materials in containment. These reactions may result in additional debris such as disbonded coatings and chemical precipitants being generated. Through transport methods such as entrainment in the steam/water flows issuing from the break and containment spray washdown, a fraction of the generated debris and foreign material in the containment would be transported to the pool of water formed on the containment floor. Subsequently, if the ECCS or CSS pumps were to take suction from the recirculation sump, the debris suspended in the containment pool would begin to accumulate on the sump screen or be transported through the associated system. The accumulation of this suspended debris on the sump screen could create a roughly uniform covering on the screen, referred to as a debris bed, which would tend to increase the head loss across the screen through a filtering action. If a sufficient amount of debris were to accumulate, the debris bed would reach a critical thickness at which the head loss across the debris bed would exceed the net positive suction head (NPSH) margin required to ensure the successful operation of the ECCS and CSS pumps in recirculation mode. A loss of NPSH margin for the ECCS or CSS pumps as a result of the accumulation of debris on the recirculation sump screen, referred to as sump clogging, could result in degraded pump performance and eventual pump failure. Debris could also plug or wear close tolerance components within the ECCS or CSS systems. The effect of this plugging or wear may cause a component to degrade to the point where it may be unable to perform its designated function (e.g. pump fluid, maintain system pressure, or pass and control system flow).

Assessing the likelihood of the ECCS and CSS pumps at domestic PWRs experiencing a debris-induced loss of NPSH margin during sump recirculation was the primary objective of the NRC's technical assessment of GSI-191. The NRC's technical assessment culminated in a parametric study that mechanistically treated phenomena associated with debris blockage using analytical models of domestic PWRs generated with a combination of generic and plant-specific data. As documented in Volume 1 of NUREG/CR-6762, "GSI-191 Technical Assessment: Parametric Evaluations for

Pressurized Water Reactor Recirculation Sump Performance,” dated August 2002 (NUREG/CR-6762-1), the GSI-191 parametric study concludes that recirculation sump clogging is a credible concern for domestic PWRs. As a result of limitations with respect to plant-specific data and other modeling uncertainties, however, the parametric study does not definitively identify whether or not particular PWR plants are vulnerable to sump clogging when phenomena associated with debris blockage are modeled mechanistically.

The methodology employed by the GSI-191 parametric study is based upon the substantial body of test data and analyses that are documented in technical reports generated during the NRC’s GSI-191 research program and earlier technical reports generated by the NRC and the industry during the resolution of the BWR strainer clogging issue and USI A-43. These pertinent technical reports, which cover debris generation, transport, accumulation, and head loss, are incorporated by reference into the GSI-191 parametric study:

- NUREG/CR-6770, “GSI-191: Thermal-Hydraulic Response of PWR Reactor Coolant System and Containments to Selected Accident Sequences,” dated August 2002.
- NUREG/CR-6762, Vol. 3, “GSI-191 Technical Assessment: Development of Debris Generation Quantities in Support of the Parametric Evaluation,” dated August 2002.
- NUREG/CR-6762, Vol. 4, “GSI-191 Technical Assessment: Development of Debris Transport Fractions in Support of the Parametric Evaluation,” dated August 2002.
- NUREG/CR-6224, “Parametric Study of the Potential for BWR ECCS Strainer Blockage Due to LOCA Generated Debris,” dated October 1995.

In light of the new information identified during the efforts to resolve GSI-191, the NRC staff has determined that the previous guidance used to develop current licensing-basis analyses does not adequately and completely model sump screen debris blockage and related effects. As a result, due to the deficiencies in the previous guidance, an analytical error could be introduced which results in ECCS and CSS performance that does not conform with the existing applicable regulatory requirements outlined in this generic letter. Therefore, the staff has revised its guidance for determining the susceptibility of PWR recirculation sump screens to the adverse effects of debris blockage during design basis accidents requiring recirculation operation of the ECCS or CSS (RG 1.82-3). Therefore, the NRC staff determined that it is appropriate to request that addressees perform new, more realistic analyses and submit information to confirm their plant-specific compliance with NRC regulations and other existing regulatory requirements listed in this generic letter pertaining to post-accident debris blockage.

In addition to demonstrating the potential for debris to clog containment recirculation sumps, operational experience and the NRC’s technical assessment of GSI 191 have also identified three integrally related modes by which post-accident debris blockage could adversely affect the sump screen’s design function of intercepting debris that could impede or prevent the operation of the ECCS and CSS in recirculation mode.

First, as a result of the 50-percent blockage assumption, most PWR sump screens were designed assuming that relatively small structural loadings would result from the differential pressure associated with debris blockage. Consequently, PWR sump screens may not be capable of accommodating the increased structural loadings that would occur due to mechanistically determined debris beds that cover essentially the entire screen surface. Inadequate structural reinforcement of a sump screen may result in its deformation, damage, or failure, which could allow large quantities of debris to be ingested into the ECCS and CSS piping, pumps, and other components, potentially leading to their clogging or failure. The ECCS strainer plugging and deformation events that occurred at Perry Unit 1 (further described in Information Notice (IN) 93-34, "Potential for Loss of Emergency Cooling Function Due to a Combination of Operational and Post LOCA Debris in Containment," dated April 26, 1993, and LER 50 440/93-011, "Excessive Strainer Differential Pressure Across the RHR Suction Strainer Could Have Compromised Long Term Cooling During Post LOCA Operation," submitted May 19, 1993), demonstrate the credibility of this concern for screens and strainers that have not been designed with adequate reinforcement.

Second, in some PWR containments, the flowpaths by which containment spray or break flows return to the recirculation sump may include "choke-points," where the flowpath becomes so constricted that it could become blocked with debris following a HELB. Examples of potential choke-points are drains for pools, cavities, isolated containment compartments, and constricted drainage paths between physically separated containment elevations. Debris blockage at certain choke-points could hold up substantial amounts of water required for adequate recirculation or cause the water to be diverted into containment volumes that do not drain to the recirculation sump. The holdup or diversion of water assumed to be available to support sump recirculation could result in an available NPSH for ECCS and CSS pumps that is lower than the analyzed value, thereby reducing assurance that recirculation would successfully function. A reduced available NPSH directly concerns sump screen design because the NPSH margin of the ECCS and CSS pumps must be conservatively calculated to determine correctly the required surface area of passive sump screens when mechanistically determined debris loadings are considered. Although the parametric study (NUREG/CR-6762, Volume 1) did not analyze in detail the potential for the holdup or diversion of recirculation sump inventory, the NRC's GSI 191 research identified this phenomenon as an important and potentially credible concern. A number of LERs associated with this concern have also been generated, which further confirms its credibility and potential significance:

- LER 50-369/90-012, "Loose Material Was Located in Upper Containment During Unit Operation Because of an Inappropriate Action," McGuire Unit 1, submitted August 30, 1990.
- LER 50-266/97-006, "Potential Refueling Cavity Drain Failure Could Affect Accident Mitigation," Point Beach Unit 1, submitted February 19, 1997.
- LER 50-455/97-001, "Unit 2 Containment Drain System Clogged Due to Debris," Byron Unit 2, submitted April 17, 1997.
- LER 50-269/97-010, "Inadequate Analysis of ECCS Sump Inventory Due to Inadequate Design Analysis," Oconee Unit 1, submitted January 8, 1998.
- LER 50-315/98-017, "Debris Recovered from Ice Condenser Represents Unanalyzed Condition," D.C. Cook Unit 1, submitted July 1, 1998.

Third, debris blockage at flow restrictions within the ECCS recirculation flowpath downstream of the sump screen is a potential concern for PWRs. Debris that is capable of passing through the recirculation sump screen may have the potential to become lodged at a downstream flow restriction, such as a high-pressure safety injection (HPSI) throttle valve or fuel assembly inlet debris screen. Debris blockage at such flow restrictions in the ECCS flowpath could impede or prevent the recirculation of coolant to the reactor core, thereby leading to inadequate core cooling. Similarly, debris blockage at flow restrictions in the CSS flowpath, such as a containment spray nozzle, could impede or prevent CSS recirculation, thereby leading to inadequate containment heat removal. Debris may also accumulate in close tolerance sub-components of pumps and valves. The effect may either be to plug the sub-component thereby rendering the component unable to perform its function or to wear critical close tolerance sub-components to the point at which component or system operation is degraded and unable to fully perform its function. Considering the recirculation sump screen's design function of intercepting potentially harmful debris, it is essential that the screen openings are adequately sized and that the sump screen's current configuration is free of gaps or breaches which could compromise the ECCS and CSS recirculation functions. It is also essential that system components are designed and evaluated to be able to operate with debris laden fluid as necessary post-LOCA.

To assist in determining, on a plant-specific basis, whether compliance exists with 10 CFR 50.46(b)(5), licensees may use the guidance contained in RG 1.82, Revision 3, "Water Sources for Long-Term Recirculation Cooling Following a Loss-of-Coolant Accident," dated November 2003. Revision 3 enhanced the debris blockage evaluation guidance for PWRs provided in Revision 1 of the RG to better model sump screen debris blockage and related effects. The NRC staff determined after the issuance of Revision 2, that research for PWRs indicated that the guidance in that revision was not comprehensive enough to ensure adequate evaluation of a PWR plant's susceptibility to the detrimental effects caused by debris accumulation on debris interceptors (e.g., trash racks and sump screens). Revision 2 altered the debris blockage evaluation guidance found in Revision 1 following the evaluation of blockage events, such as the Barsebäck Unit 2 event mentioned above, but for BWRs only. Revision 1 replaced the 50-percent blockage assumption in Revision 0 with a comprehensive, mechanistic assessment of plant-specific debris blockage potential for future modifications related to sump performance, such as thermal insulation changeouts. This was in response to the findings of USI A-43.

The NEI GR expands on RG 1.82, Rev. 3 (requirements for long-term cooling), using portions of NUREG/CR-6808 (knowledge-base report) and other NRC and industry related documents. The NEI research contributions are (1) in the area of alternate break size, including options for risk-informing the analysis as it relates to the initial postulated break size, and (2) on the behavior of protective coatings (a potential debris type) under high-pressure, two-phase jet impact.

In support of the GSI-191 resolution effort, the staff also contracted research which was not completed, for a plant-specific sump performance analysis based on sample plant data. Although the work was not published, some of the work was completed and simply not documented. Therefore, the staff has provided results from specific areas of this research, to supplement areas in the GR that lack supporting data and experimentation, as a basis for alternative guidance and has provided details in such cases, in Appendices III and VI to this SER.

## 2.0 REGULATORY EVALUATION

This section details the regulatory requirements, associated guidance, and precedent upon which the staff based its review of the GR submitted by NEI to be used for the evaluation of PWR sump recirculation performance.

In accordance with Title 10 of the Code of Federal Regulations (10 CFR) Part 50.46, Sub-sections (b) (5), licensees of domestic nuclear power plants are required to provide long-term cooling of the reactor core “after any calculated successful initial operation of the ECCS.” Furthermore, the “calculated core temperature shall be maintained at an acceptably low value and decay heat shall be removed for the extended period of time required by the long-lived radioactivity remaining in the core.” For this evaluation of PWR recirculation performance, the staff has considered this extended time to be thirty days, and requires cooling by recirculation of coolant via the ECCS sump, where coolant is accumulated for this purpose. However, if debris collects and clogs the sump screen or other components or pathways that prevent adequate suction for ECCS or CSS pumps, then compliance with this regulation may be in question.

Guidance for determining compliance with 10 CFR 50.46(b) (5), is contained in RG 1.82, Revision 3. The staff review guidance for evaluating licensee compliance with 10 CFR 50.46(b) (5), is contained in Standard Review Plan (SRP) 6.2.2, “Containment Heat Removal Systems.” Additionally, SRP 6.1.1, “Engineered Safety Features Materials,” provides the review process for thermal insulation and coating systems, which impact long-term cooling evaluation; and SRP 9.2.5, “Ultimate Heat Sink,” provides review guidance from which the extended time for recirculation performance is derived.

For PWRs licensed to General Design Criteria (GDC) in Appendix A to 10 CFR Part 50, GDC 35 specifies additional ECCS requirements, GDC 38 specifies heat removal systems requirements, and GDC 41 provides requirements for containment atmosphere cleanup. Many PWR licensees credit a CSS, at least in part, with performing the safety functions to satisfy these requirements, and PWRs that are not licensed to the GDC may credit a CSS to satisfy similar plant-specific licensing basis requirements. In addition, PWR licensees may credit a CSS with reducing the accident source term to meet the limits of 10 CFR Part 100 or 10 CFR 50.67.

Technical specifications pertain to the ECCS and CSS insofar as they require the operability of these systems for the mitigation of certain design basis accidents. Other plant-specific licensing commitments concerning the ECCS and CSS are also documented in the Final Safety Analysis Report.

The staff considered the NRC’s August 28, 1998, SER on the Utility Resolution Guidance (URG) for ECCS Suction Strainer Blockage (NEDO-32686-A), (URG SER) used for resolution of the related strainer blockage issue for BWRs in its evaluation of the GR. This approach helped to assure consistency and efficiency. In some areas, departures from the GR and the URG SER were warranted due to differences in the design features of BWRs and PWRs, as well as later information obtained through regulatory research.

The Commission’s staff requirements memorandum from A. L. Vietti-Cook to L. A. Reyes, SECY-04-0037, “Issues Related to Proposed Rulemaking to Risk-Inform Requirements Related to Large Break Loss-of-Coolant-Accident (LOCA) Break Size and

Plans for Rulemaking on LOCA with Coincident Loss-of-Offsite-Power,” dated July 1, 2004 (SECY-04-0037) was considered in the review of industry-proposed alternatives, and in the realistic and risk-informed options with regard to break size selection and mitigative equipment requirements.

### 3.0 BASELINE EVALUATION

Section 3 of the GR provide an evaluation methodology referred to as a baseline set of methods that help identify the dominant design factors for a given plant. The baseline evaluation methodology is intended to serve as an approach with sufficient conservatism such that simpler analytical methods can be used.

#### 3.1 INTRODUCTION

Section 3.1 of the GR describes the purpose of the baseline, and it presents background information regarding general accident scenarios of concern and accident phenomena. This section also notes the limitations of the evaluation method. It makes reference to supplemental guidance for refinements, and data collection to support base evaluations.

Key introductory points include the following:

1. This section states: “If a plant uses this method and guidance to determine that sufficient head loss margin exists for proper long-term Emergency Core Cooling (ECC) and Containment Spray (CS) function, no additional evaluation for head loss is required.”
2. The baseline evaluation method only addresses the phenomena and issues up to and including head loss across the sump screen. Insufficient information presently exists to evaluate the effects of chemical reaction products on head loss across a sump screen and the associated debris bed. Also, the Baseline Methodology does not include the evaluation of holdup of flow by debris upstream of the sump screen, the structural integrity of the sump screen, or the effects resulting from debris passing through the sump screen and being ingested into the ECC or CS systems.
3. The baseline evaluation guidance provides a conservative approach for evaluating the generation and transport of debris, and the resulting head loss across the sump screen. If a plant determines that the results of the baseline approach are not acceptable, or additional design margin is desirable, the refinement guidance provided in subsequent sections may be used to further evaluate the post-accident performance of the ECC sump.

**Staff Evaluation for Section 3.1:** The baseline guidance acknowledges that the chemical reaction product effects on the head loss, the downstream effects, and the upstream effects were not fully considered in the baseline evaluation methodology. However, the guidance does not make it explicitly clear that the plant must still address these issues even if the plant successfully applied the baseline method to their plant. Therefore, the staff position is that licensees address these effects in accordance with the staff positions specified in Section 7.0 of this SER.

The staff questions the GR statement that the baseline provides a conservative approach. Aspects of the baseline guidance have been identified that are clearly not conservative while other aspects are conservative. The subject aspects are identified at the appropriate locations in the guidance review. Acceptance of the baseline evaluation requires that the baseline approach results in an evaluation that, overall, is realistically

conservative. The staff has sponsored research to confirm whether or not specific aspects of the guidance are truly conservative as stated by the guidance. Results of this research are included in Appendices III and VI, to this SER, and are referenced appropriately in the pertinent section of this document. Section 3.8 documents the staff evaluation of assumptions for which conservatism is in question, and provides alternative guidance toward ensuring an overall realistic conservatism for the baseline.

### **3.2 METHOD OVERVIEW**

Section 3.2 presents the five major areas of the baseline guidance as break selection, debris generation, latent debris, debris transport, and head loss.

### **3.3 BREAK SELECTION**

This section of the GR presents considerations and guidance for selecting an appropriate postulated break size and location for use in the baseline analysis. The stated objective of the selection process is to identify the break conditions that present the greatest challenge to post-accident sump performance.

#### **3.3.1 Introduction**

Break selection is described in the GR as a two-step process involving selection of (1) the size of the break and (2) the location of the break.

**Staff Evaluation of Section 3.3.1:** The staff notes that DEGB breaks need to be assumed for the baseline analysis of primary system piping (GR section 3.3.3), so the size of the break is then determined by the diameter of the pipe. Other break-size criteria may be adopted for postulated breaks in secondary piping depending on assumptions in the plant licensing basis.

The GR states that the objective of the break selection process is to identify the break size and location that results in debris generation that is determined to produce the maximum head loss across the sump screen. The staff finds this objective to be acceptable. Because the assessment will address several complex phenomena for each break location, the location of the most challenging break cannot be identified with confidence until a number of postulated-break locations have been evaluated.

#### **3.3.2 Discussion**

As stated in the GR, the criterion used to define the most challenging break conditions is the estimated head loss across the sump screen. The break location that maximizes estimated head loss is referred to in the GR as the "limiting break location." All phases of the accident scenario must be considered for each postulated break location including debris generation, debris transport, and sump-screen head loss calculations. The outcome of head loss predictions from each candidate break location should be performed systematically, and should be self-contained.

Two attributes of break selection which are emphasized in the GR that can contribute to head loss are (1) the maximum amount of debris transported to the screen and (2) the worst combination of debris mixes that are transported to the screen. The proper metric for comparison, head-loss effect upon arrival at the screen, has been emphasized. The

GR requires that break locations be surveyed to provide for both items 1 and 2 because under given circumstances, either could represent the limiting break. For example, relatively small quantities of fiber in combination with LOCA-generated or latent-debris particulate can induce head losses that exceed the effects of much larger debris beds. Regulatory Guide 1.82, Rev. 3 [RG 1.82-3] itemizes additional features of a break that may dominate effects on the screen, but these two criteria stated in the GR encompass quantity, type, transport and mixed composition as key issues.

### **3.3.3 Postulated Break Size**

**Staff Evaluation of Section 3.3.3:** The NRC agrees that double-ended guillotine breaks (DEGB) with full piping separation and offset should be used for baseline evaluation of LOCA debris generation for breaks assumed to occur in primary system piping (RCS main loop piping and attached auxiliary piping). For plants that require recirculation to maintain long-term cooling after secondary-system pipe ruptures, either DEGB conditions may be assumed or conditions consistent with the plant's licensing basis for those breaks may be used for size characterization (typically, a spectrum of break sizes is evaluated, up through a double ended rupture). The staff finds the GR guidance with respect to break size is acceptable because this approach provides for large volumes of debris and worst combinations of debris.

### **3.3.4 Identifying Break Locations**

**Staff Evaluation of Section 3.3.4:** The NRC agrees that all reactor coolant system (RCS) piping, and connected piping, must be considered in the evaluation of locations to identify the limiting break. As stated in the GR, some plant designs require eventual coolant recirculation from the sump for pipe ruptures other than a LOCA. If recirculation is required under the plant licensing basis to mitigate these events, then breaks must be examined in this piping as well. Any actuation of the recirculation pumps implies an initiating event that should be examined for potential debris generation regardless of whether the recirculation supplies containment spray or safety injection systems.

#### **3.3.4.1 General Guidance**

The staff position is provided here for each of the seven principles of break selection guidance offered in the GR.

1. The GR states that break exclusion zones must be disregarded for this evaluation. The staff finds this to be acceptable because all piping locations must be considered. The GR also states that for main steam and feedwater line breaks, licensees should evaluate the licensing basis and include potential break locations in the evaluation, if necessary. The staff finds this to be acceptable. However, the staff position is that if secondary breaches such as main steam line and feedwater line breaks rely on sump recirculation, as described in the plant licensing basis, breaks should be postulated in these systems at locations chosen in a manner consistent with the remaining guidance in this section.
2. The GR states that application of NRC Branch Technical Position MEB 3-1 is not appropriate for determining potential LOCA break locations. The staff finds

this to be acceptable (see section 4.2.1 of this SER for a more detailed discussion of the staff position).

3. The GR states that for plants for which secondary-system breaks such as main steam line and feedwater line breaks rely on sump recirculation as described in the licensing basis, , postulated break locations should be consistent with the plant's current licensing basis. The staff finds this position to be unacceptable. The staff position is that secondary side break locations should be postulated in a manner consistent with the remaining guidance in this section.
4. The GR recommends that pipe breaks be postulated at locations that result in unique debris source terms to avoid multiple locations with identical composition and quantity of debris. However, in order to assess the potential head loss on the sump screen, the uniqueness of a break location must also be judged based on the degree of transport that is expected. position is Licensees may find it to be beneficial to analyze the first few break locations be analyzed in full detail, quantifying all phases of the accident sequence. Additional breaks may then be addressed by comparison to these examples of their debris composition, debris quantity and debris transport potential without full quantification. This approach will avoid some duplication of effort while also permitting a systematic survey of break locations.
5. The GR states that pipe breaks shall be postulated that affect locations containing high concentrations of problematic insulation (microporous insulation, calcium-silicate, fire barrier material, etc.). The staff finds this position to be acceptable. Additionally, in keeping with the objective of identifying limiting break conditions, zones of problematic insulation might be affected by smaller breaks in their vicinity or by larger breaks that encompass them. Both possibilities should be considered because the overall composition of the debris arriving at the screen may be different.
6. As discussed above, the initial quantity and composition of the debris source are important attributes of break selection, but potential transport must needs to be considered also. The GR states that "Pipe breaks shall be postulated with the goal of creating the largest quantity of debris and/or the worst-cast combination of debris types at the sump screen." The staff agrees that these conditions need to be evaluated, however, the GR correctly notes that the largest quantity at the screen may not produce the highest head loss. Additional discussion of screen head loss analysis found in Section 3.7 of the SER may help guide the selection of break locations that may create adverse conditions at the sump screen.
7. The GR proposes that piping less than 2 inches in diameter need not be considered in order to identify the limiting break conditions. The staff finds this to be acceptable. While it may be possible for a 2-inch break to challenge net-positive-suction-head (NPSH) margins for some existing screens, larger breaks postulated with minimal transport would pose an identical challenge. Larger breaks with higher transport potential will certainly bound the maximum on-screen debris permitted by a 2-inch break. Eliminating 2-inch diameter breaks from the baseline greatly simplifies the systematic survey.

#### 3.3.4.2 Piping Runs to Consider

The staff agrees that breaks, ruptures and leaks other than a LOCA must be considered in this analysis if these scenarios eventually require recirculation for any purpose and if they are part of the plant licensing basis.

The staff's position is that all broken lines, regardless of piping system, that meet the following criteria must be considered: (1) incorporated in the licensing basis; (2) capable of generating debris; and (3) lead to a recirculation demand on the sumps. This position is not meant to imply that breaks must be fully analyzed in every length of every system. Many postulated locations will be eliminated by comparison with other collocated break possibilities of their respective debris volume, composition, and transport potential. Note that all piping in containment must be considered regardless of its location within containment because breaks in secondary systems may also be of interest if the above criteria for consideration are satisfied (e.g., main steam and feedwater piping). The level of detail pursued in the application of breaks in alternative piping systems depends largely on assumptions made in other steps of the accident analysis. For example, if assumptions made in the transport and head loss analyses both require the assessment of thin-bed formation, then break selection can focus on (1) particulate sources that may contribute to the thin-bed, and (2) maximum debris quantities that may dominate the thin bed. A hypothetical example of a case where detailed examination of an alternative system might be required is a line with debris-generation potential but lower than system operating pressure that is either insulated with or that might affect problematic or diverse insulation types in locations outside the range of larger pipe breaks. Locations of this type might be found in upper containment near in component cooling lines near the pressurizer, for example. Scenarios of this type could be conservatively analyzed using bounding jet parameters relevant to the primary system piping or a new jet calculation could be performed specific to the conditions of the line in question. The actuation of spray for breaks postulated in alternative systems is also a key consideration in their assessment as potentially limiting conditions, because containment spray will enhance transport to the recirculation pool and to the sump screen.

Note that the explicit assumption of thin-bed formation regardless of break size or location offers a significant simplification for break selection, because more focus can be placed on the larger piping systems that envelope more spatial volume. Breaks outside of the crane wall may require more detailed examination for pipe size, pipe pressure, nearby insulation types, and transport potential.

#### 3.3.4.3 Other Considerations for Selecting Break Locations

Three additional considerations for selecting break locations are presented in the GR. The staff position regarding each respective consideration is discussed here.

1. The staff finds that the GR correctly emphasizes proper consideration of relative locations between the postulated break location and the affected containment material targets. Additionally, the staff notes that a good understanding of spatial volume obtained from the ZOI discussion in Section 3.4.2 of this SER and related calculations will assist in determining the level of detail needed for the break location survey.
2. The second consideration focuses on the potential for the formation of a thin fiber layer on the screen that filters particulates very efficiently, the so-called

“thin-bed” effect. In general, state-of-the art debris transport methods are not sufficiently advanced to preclude the formation of a thin bed when fibrous insulation are damaged within any ZOI. The degree of vulnerability to this effect is specific to the sump screen in question. This GR consideration for break selection sets a de minimus value for debris generation that might already be bounded by larger breaks with minimal transport. The staff agrees that the “thin-bed” effect needs to be evaluated. Additionally, the staff’s position is that smaller breaks affecting unique combinations of insulation not encompassed by larger break should still be examined for potential thin-bed formation. When computing the volume of fibrous debris needed to form a 1/8-inch thick uniform layer on a given sump screen, the dry-bed or “as-manufactured” density should be used, and only the wetted screen area relevant to the break in question should be credited.

3. The GR offers an additional consideration that recognizes the importance of latent debris inventory as a potentially limiting debris source for plants with little or no fibrous insulation. The staff agrees with this consideration, and refers to Section 3.5 of this SER for a more complete discussion of latent debris characterization. The staff notes that the use of an appropriate dry-bed density for latent fiber and a wetted screen area can be used by plants with non-fiber insulation to establish a plant cleanliness criterion for their FME programs.

#### 3.3.4.4 Selecting the Initial Break Locations

The staff finds that the guidance offered in the GR for initial break location selection is acceptable and notes that spatial perspectives gained from implementation of the ZOI models will be helpful at directing the break-location survey further. In general, the survey should first consider larger breaks with more complex debris composition and proceed down to smaller breaks with more unique debris compositions that have not yet been captured in the survey. The degree of transport, which can be affected by the use of containment spray should be considered during the comparison of potential break locations. Starting with this initial break location and moving to other large breaks that envelope any previously identified debris-source concerns will quickly build a set of comparative source-term and transport factors that can be used to judge other locations and classes of postulated breaks without as much detailed quantification. Comparative rationale that disqualify a candidate location from designation as a limiting break condition should be documented to illustrate the systematic and comprehensive scope of the break-selection survey.

#### 3.3.5 Evaluation of Break Consequences

Staff Evaluation of Section 3.3.5:

The staff finds that the proper metric of comparison between break locations has been emphasized in the GR, i.e., head loss across the sump screen as a result of generation, transport, and accumulation of debris on the sump screen. Break locations cannot be eliminated from consideration based on any single attribute alone. The staff agrees that all breaks should be evaluated in the context of the complete accident sequence and the potential effect on sump-screen head loss. Nevertheless, many comparisons will be found that are useful. For example, all large break locations within a compartment may

be found to have similar transport characteristics and spatial volume, so only one or two locations within the compartment are needed to bound the variation in debris composition.

#### 3.3.5.1 Purpose of Break Consequence Evaluation

Once the limiting break condition(s) have been identified, the corresponding head loss will be compared to the required NPSH either as a measure of vulnerability to sump blockage or as a design criterion for sump-screen modifications. The staff finds that the GR provides an acceptable and concise summary in this section of the steps involved with evaluating each candidate break location against the criterion of maximum sump-screen head loss.

#### 3.3.5.2 Selection of Intervals for Additional Break Locations

This section of the GR describes a systematic approach to break selection along individual piping runs that starts at an initial location along a pipe, generally a terminal end, and steps along in equal increments (3 foot increments) placing breaks at each sequential location. The staff position is that break intervals can be relaxed to 5-ft increments along the pipe in question and notes that the concept of equal increments is only a reminder to be systematic and thorough. Earlier work reported by NRC contractors using automated analysis tools to evaluate higher spatial resolution (1 to 3 ft increments) was motivated by a risk assessment approach that required an accurate sampling of piping lengths and break sizes to represent their proportional contribution to the overall frequency of sump screen failure. For the purpose of identifying limiting break conditions, a more discrete approach driven by the comparison of debris source term and transport potential can be effective at placing postulated breaks. The key difference between many breaks (especially large breaks) will not be the exact location along the pipe, but rather the envelope of containment material targets that is affected.

The staff agrees that as the plant-specific analysis develops, many breaks locations along a pipe will be determined by inspection of potential debris inventory, similarity of transport paths, and piping physical characteristics compared to a smaller number of fully quantified break scenarios

As discussed previously, the staff does not accept the GR position regarding the treatment of secondary break locations. The staff position is that if secondary break scenarios involve a recirculation-sump demand and if these scenarios are part of the plant licensing basis, the same considerations for break location must be applied as discussed in this section for LOCA events in primary piping. The reasons supporting this position is that inclusion of secondary-break scenarios in the licensing basis acknowledges the possible need for recirculation, but the break locations evaluated in the licensing basis may not have been defined specific to sump performance and could not have anticipated the range of concerns identified in the course of resolving GSI-191.

The staff accepts the GR-stated position regarding breaks in attached piping beyond isolation points so long as there is no possible need for recirculation should a break occur in these sections. The decision whether to include piping segments beyond the isolation points should consider possible failure of the isolation valves in a manner consistent with the licensing basis.

## 3.4 DEBRIS GENERATION

### 3.4.1 Introduction

This section of the GR discusses the process of determining, for each postulated pipe break location, the zone within which the break jet forces will be sufficient to damage materials and create debris, the amount of debris generated by the break jet forces and the need to determine the characteristics of the debris.

**Staff Evaluation for Section 3.4.1:** Section 3.4.1 is an acceptable introduction to the debris generation section.

### 3.4.2 Zone of Influence (ZOI)

The GR in Section 3.4.2 recommends a spherical boundary for the ZOI with the center of the sphere located at the break site. The ZOI is defined as the volume about the break in which the fluid escaping from the break has sufficient energy to generate debris from insulation, coatings, and other materials within the zone. The use of a spherical ZOI is intended to encompass the effects of jet expansion resulting from impingement on structures and components.

**Staff Evaluation for Section 3.4.2:** The recommended spherical ZOI is a key feature to the baseline evaluation and any alternatives other than spherical or alternatives specifically reviewed and approved by the staff for use within the baseline as described in Section 6 of this safety evaluation report will not be considered valid for the baseline. The staff evaluation of refinements to the spherical ZOI are addressed in Section 4.2.2 of this SE.

The spherical zone is a practical convenience that accounts for multiple jet reflections and mutual interference of jets from opposing sides of a guillotine break as well as pipe whip. It is important to note that when the spherical volume is computed using an acceptable approximation for unimpeded free-jet expansion, the actual energy loss involved in multiple reflections is conservatively neglected to maximize the size of the ZOI. The staff concurs with the use of spherical ZOI as a practical approximation for jet-impingement damage zones.

#### 3.4.2.1 Recommended Size of Zone of Influence

The GR recommends using the ANSI/ANS 58.2-1988 standards [ANSI/ANS 58.2-1988] to determine the radius of the spherical ZOI that represents the effects of the jet originating from a postulated pipe break. Appendices B, C, and D of the ANSI/ANS standard provide guidance necessary to determine the geometry of a freely expanding jet for jets originating from a variety of reservoir conditions, including subcooled conditions. This section of the GR reviews the key steps used in the ANSI/ANS 58.2-1988 procedure that determine the size of the ZOI.

Section 3.4.2.1 of the GR also specifically addresses the break jet pressures that will result in coating debris generation within the ZOI.

Table 3-1 presented in this section of the GR contains the recommended destruction pressures for typical protective coatings and for several types of insulation.

**Staff Evaluation for Section 3.4.2.1:** The staff agrees that ANSI/ANS 58.2-1988 Standard (cited as reference 3 in the GR) provides a suitable basis for computing spatial volumes inside a damage zone defined by a jet impingement pressure isobar. Appendices in the standard do provide a set of equations that can be evaluated for this purpose, but the presentation is somewhat confusing, and the physical limitations of the model are not discussed thoroughly. For these reasons, Appendix I has been provided in this document to add guidance on the proper evaluation and interpretation of results from the ANSI model.

Six steps are outlined in the GR for performing ZOI calculations using the ANSI jet model:

1. The mass flux from the postulated break was determined using the Henry-Fauske model, as recommended in Appendix B of the Standard, for subcooled water blowdown through nozzles, based on a homogeneous non-equilibrium flow process. No irreversible losses were considered.
2. The initial and steady-state thrust forces were calculated based on the guidance in Appendix B of the Standard, with reservoir conditions postulated.
3. The jet outer boundary and regions were mapped using the guidance in Appendix C, Section 1.1 of the Standard for a circumferential break with full separation.
4. A spectrum of isobars was mapped using the guidance in Appendix D of the Standard.
5. The volume encompassed by the various isobars was calculated using a trapezoidal approximation to the integral with results doubled to represent a DEGB.
6. The radius of an equivalent sphere was calculated to encompass the same volume as twice the volume of a freely expanding jet.

These steps are acceptable for generic implementation of the model and conversion of isobar volumes to a volume-equivalent spherical radius. However, the following observations are provided in this SE which concern details of implementation of this method that need to be considered when using the model. These details are further explained in Appendix I:

1. Plots of metrics related to the Henry-Fauske mass flux presented in the standard do not extend to the desired state point, so it is not clear exactly how the mass flux was evaluated in the GR. Licensees using this technique should refer to confirmatory Appendix I for guidance.
2. It should be noted that neglect of irreversible losses refers to internal pipe and pipe-component friction losses between the upstream reservoir and the location of the break.

3. Only the steady-state thrust coefficient should be used in this calculation as a conservative bound.
4. Insulation damage pressures such as the 10 psi cited for Nukon fiberglass can only be interpreted with a full understanding of the test conditions under which they were experimentally measured. The computed jet conditions will not match the experimental test conditions, therefore care should be taken to assure that equivalent damage effects are considered. Finally, it should be noted that the GR exercised the model for a spectrum of pressure isobar values because different materials have different resistances to damage from jet impingement.

Regarding the three conditions offered for jet expansion calculations, the staff agrees that DEGB break configurations with circular geometries, and full separation and offset between the broken ends provides the maximum debris generation volume. However, as further discussed in Appendix I, the choice of fluid reservoir conditions is not justified as bounding for the baseline evaluation and the reported thermodynamic properties do not match the stated conditions. Using automated NIST/ASME steam tables [NIS96], the stagnation enthalpy and degree of subcooling for the stated conditions of 2250 psia and 540 °F are 534.9 Btu/lbm and 112.7 °F, respectively. However, Appendix I confirms that these conditions bound nominal conditions for a hot-leg break, and some guidance is offered there for licensees to estimate the effects of minor system-pressure increases without the need for reevaluating the model.

The staff agrees with the GR choice of ambient containment pressure, versus crediting containment backpressure. The staff considers this choice necessary since zone-of-influence volumes are strongly driven by the system stagnation pressure, which is highest when the containment is at ambient conditions. The maximum debris generation would occur instantaneously within this ZOI. Furthermore, the use of atmospheric pressure may not be non-conservative for subatmospheric containment designs that would permit the discharge of a slightly higher mass flux across a break. However, the effect is judged to be small and is compensated by jet pressure equations in the standard that do neglect ambient pressure in containment. See Appendix I for a discussion of mass flux calculations and the dependence of ANSI correlations for thrust coefficient on the choice of psia.

The staff finds that the citation of 10-diameter limits for jet damage recommended in NUREG/CR-2913 [WEI83] for structural loadings on equipment and components is not applicable to the present concern regarding insulation and coatings damage. The criteria for onset of damage and the implications of structural damage vs debris generation are not directly related. Furthermore, any comparison of conservatism between methods should consider the range of damage pressures for various insulation types.

### **Protective Coatings Destruction**

The potential debris term generated by failed coatings can be a significant contributor to the total containment sump debris term for some plants. Consistent with convention, the GR assumes the following LOCA effects on coatings:

- that all coatings in the ZOI will fail;
- that all qualified (DBA-qualified or Acceptable) coatings outside the ZOI remain intact; and
- that all Unqualified coatings will fail.

The GR also assumes that coating failure will generate debris in the form of fine particulate which is equivalent in size to the basic material constituents. This is descriptive of the size of the average zinc particle in inorganic zinc (IOZ) coatings or the pigment used in epoxy coatings, which is approximately a 10µm (in diameter) spherical particle in both cases. The GR states that because there is a lack of experimental data regarding coating debris size values, a debris size distribution of 100% small fines (10µm IOZ equivalent) is adopted for all coatings inside the ZOI. For coatings outside the ZOI, the GR states that all indeterminate and DBA-unqualified and unacceptable coatings should be treated as a single category of coating which produces debris of the same characteristic independent of the type of coating. As such, the coating debris size within the ZOI is applicable to all unqualified, indeterminate and unacceptable coatings that fail outside the ZOI as well.

Outside the ZOI, the GR assumes that all qualified coatings remain intact and do not contribute to the debris term. Although the GR assumes that all unqualified coatings will fail and break down into 10µm particles, it also indicates that plant specific data should be used to estimate the area and thickness of the unqualified coating in order to determine the amount of debris generated.

The GR indicates that “the ZOI for DBA-qualified coatings or coatings determined to be ‘Acceptable,’ applied to PWR containment surfaces, which results from fluid impingement from the break jet, has not been clearly defined.” However, two key pieces of evidence are offered in the GR to support the argument that DBA qualified and acceptable coatings are resistant to direct jet impingement: (1) DBA qualification tests subject samples to elevated temperatures with no apparent loss of structural integrity or performance degradation; and (2) water-jet pressures in excess 2250 psia are commonly required to efficiently remove coatings in industrial applications.

This GR-assumed destruction pressure is tied to experience for removing coatings by the commercial water blast industry and industry waterjet testing detailed in Appendix A of the GR. This testing was performed using a 3500 psig positive displacement pump, hose and nozzle attachment (high pressure washer) at two temperatures, i.e., approximately 80°F and 150°F, to investigate coating degradation under jet impingement conditions. The test apparatus was used at various distances from substrates coated with qualified coatings. The testing indicated that coating debris generated in the ZOI would fail as the result of erosion and would generate debris sized roughly equivalent to the coating pigment size. Both IOZ and epoxy were tested. The testing also indicated that coating degradation was influenced by temperature.

**Staff Evaluation for Protective Coatings Destruction:** The staff finds that the following bases should be applied with regard to coating debris destruction subjected to a LOCA jet:

- Qualified coatings outside the ZOI are assumed to remain intact and will not contribute to the sump debris load during a postulated event.

- All unqualified coatings outside the ZOI are assumed to fail and act as a potential contributor to the debris load during a postulated event.
- All coatings, regardless of qualification are assumed to fail within the LOCA jet ZOI. The baseline guidance does not provide sufficient technical justification to support use of a 1000 psig coating destruction pressure and corresponding ZOI equivalent to 1 pipe diameter. The staff position is that licensees should use a coatings ZOI equivalent to 10D or a ZOI determined by plant specific analysis. The specified ZOI of 10D is based upon the previous staff position used for BWR sump analysis. Any plant specific analysis should incorporate at a minimum the temperature and pressure effects of the jet on plant coating systems in the ZOI. Such an analysis should be based on experimental data over the range of pressures and temperatures of concern using coating samples correlatable to plant materials. The analysis should also seek to accurately estimate the amount of coating on a plant specific basis within the ZOI. If a realistically conservative approach is taken, the basis and justification why the method is realistically conservative must be provided.

The staff agrees that it is conservative to treat coating debris as highly transportable particulates in the range of 10 to 50 microns in diameter, based on plant susceptibility to thin bed formation at the sump screen. However, for those plants that can substantiate no formation of a thin bed at the sump, this assumption may be non-conservative with regard to sump blockage since fine particulates would pass through the sump screen and generate no blockage concerns. Therefore, for those plants that are susceptible to thin bed formation at the sump screen, use of the basic material constituent (10  $\mu\text{m}$  sphere) to size coating debris is acceptable. However, for those plants that can substantiate no formation of a thin bed at which particulate debris can collect, the staff finds that coating debris should be sized based on plant specific analyses for debris generated from within ZOI and from outside the ZOI. Such an analysis should conservatively assess the coating debris generated with appropriate justification for the assumed particulate size or debris size distribution. Degraded qualified coatings that have not been remediated should be treated as unqualified coatings. Finally, testing regarding jet interaction and coating debris formation could provide insight into coating debris formation and help remove some of the potential conservatism associated with treating coatings debris as highly transportable particulate. If coatings, when tested at corresponding LOCA jet pressures and temperatures, are found to fail by means other than erosion or the erosion is limited, the majority of debris may be larger, less transportable or pose less of a concern for head loss.

The staff agrees with the assumption that qualified coatings outside the ZOI remain intact during a postulated event and will not contribute to the ECCS sump debris load, because it is based on qualified coatings meeting established quality criteria and acceptance testing and is consistent with the position outlined in NUREG 0800, Section 6.1.2 Protective Coating Systems. The assumption is also based on the coatings being in good condition at the initiation of the postulated LOCA. However, operating experience indicates qualified coatings require periodic maintenance throughout the coating service life and operating experience has identified cases where qualified coatings have exhibited significant degradation during the coatings normal service life. Therefore, the staff recommends that a periodic coating condition assessment be identified, described and implemented during routing outages, to assure that qualified

coatings remain capable of performing in a manner consistent with assumptions used to evaluate sump debris loads . Further the staff has concluded that qualified coatings which have degraded, but which have not yet been remediated must be considered to fail during a postulated accident and will potentially contribute to the debris load. The staff finds that the estimated quantity of debris from degraded qualified coatings (if any) should be based on plant specific data and should follow the guidance for debris resulting from unqualified coatings.

The staff agrees with the assumption that all unqualified coatings outside the ZOI fail, based on the position outlined in NUREG 0800, Section 6.1.2 Protective Coating Systems.

The staff agrees with the assumption that all coatings, regardless of type and qualification will fail within the ZOI because it conservatively addresses the LOCA jet interaction with all coatings (unqualified coatings are assumed to fail regardless of location) in this zone; however, the staff believes there is insufficient technical justification for the assumption of a 1000 psig destruction pressure and corresponding spherical ZOI with a radius equivalent to one pipe diameter.

Although Appendix A of the GR provides useful test data illustrating the erosion effects of high pressure water jets on coating systems, no test data are offered that combine both the effects of mechanical insult and elevated temperature in the same test, and no data appear to be available on the effects of very rapid thermal transients on coating performance. Specifically, the initial conditions of the LOCA jet established in the baseline methodology are 540°F and 2250 psig, while industry testing referenced in Appendix A of the GR was performed at approximately 3500 psig and 150°F. Although the initial LOCA jet pressure is expected to be lower than the industry test pressure used (~3500 psig) and waterjet pressure data, the initial LOCA jet temperature expected is significantly higher than the industry test temperatures used (150°F). No correlation or extrapolation was provided in the NEI baseline methodology illustrating how the elevated test pressure accounts for the reduced test temperature to produce a similar damage mechanism and degree of damage as the combined temperature and pressure from a LOCA jet and thus can be used to adequately establish the coating ZOI. Therefore, the staff finds the results of the waterjet testing to be inconclusive in this regard.

Additional information offered in Appendix I of this report presents spatial contours of estimated jet impingement temperature for a reference cold-leg break condition. Temperature zones exceeding 300 °F are observed to extend out to 10 pipe diameters from the break, and exceed 220 °F for most of the jet envelope. Given the small thickness of the paint and the differences in heat conduction between the layer and the substrate, it is presumed that the coating would reach the impingement temperature almost instantly when directly hit by the break jet. Thermal shock may affect bonding with the substrate, induce expansion cracking in the coating layer, and change its tensile properties. All of these potential effects increase the vulnerability of paint to jet impingement. The occurrence of very rapid thermal transients in combination with the mechanical insult of water-laden jet impact is a unique environment that deserves experimental study.

The NRC staff acknowledges that the five reasons given to defend the selection of 1000 psi as a destruction pressure for DBA-qualified or "Acceptable" coatings are factual, while the GR arguments do not address important phenomenology of the accident

environment. It is premature to accept the proposed value of 1000 psi as either appropriate or conservative. Individual licensees should provide data to support the robustness of their DBA-qualified and "Acceptable" coatings system for use in the baseline analysis. Spatial contours of jet-impingement temperature such as that offered in Appendix I may be useful in judging the cost-benefit of alternative test conditions.

Because (1) the temperature effect may be influenced by the coating system, i.e., IOZ alone, IOZ topcoated with epoxy or multiple coats of epoxy, (2) epoxy and IOZ each would be expected to have a different temperature response, and (3) no testing replicating the effects of LOCA jet pressures and temperatures on coatings (epoxy, IOZ, qualified or unqualified coatings) have been performed or referenced; the staff position is that the coating ZOI should be determined by plant specific analysis. This analysis should incorporate, at a minimum, the combined temperature and pressure effects of the jet on potential coating systems in the ZOI. Such an analysis should be based on experimental data over the range of pressures and temperatures of concern using coating samples correlatable to plant materials. The analysis should also seek to accurately estimate the amount of coating on a plant specific basis within the ZOI. If a bounding approach is taken, the basis and justification why the method is conservatively bounding must be provided. The staff believes that a comprehensive test program investigating the effects of direct impingement of a LOCA jet (accounting for jet pressure and temperature) on coating degradation needs to be performed in order to have a sound basis for the destruction pressure and size of the coating ZOI.

#### 3.4.2.2 Selecting a Zone of Influence

Section 3.4.2.2 recommends that for the baseline calculation, the ZOI for a break is selected based on the potentially affected insulation inside containment with the minimum destruction pressure. This ZOI is then applied to all insulation types.

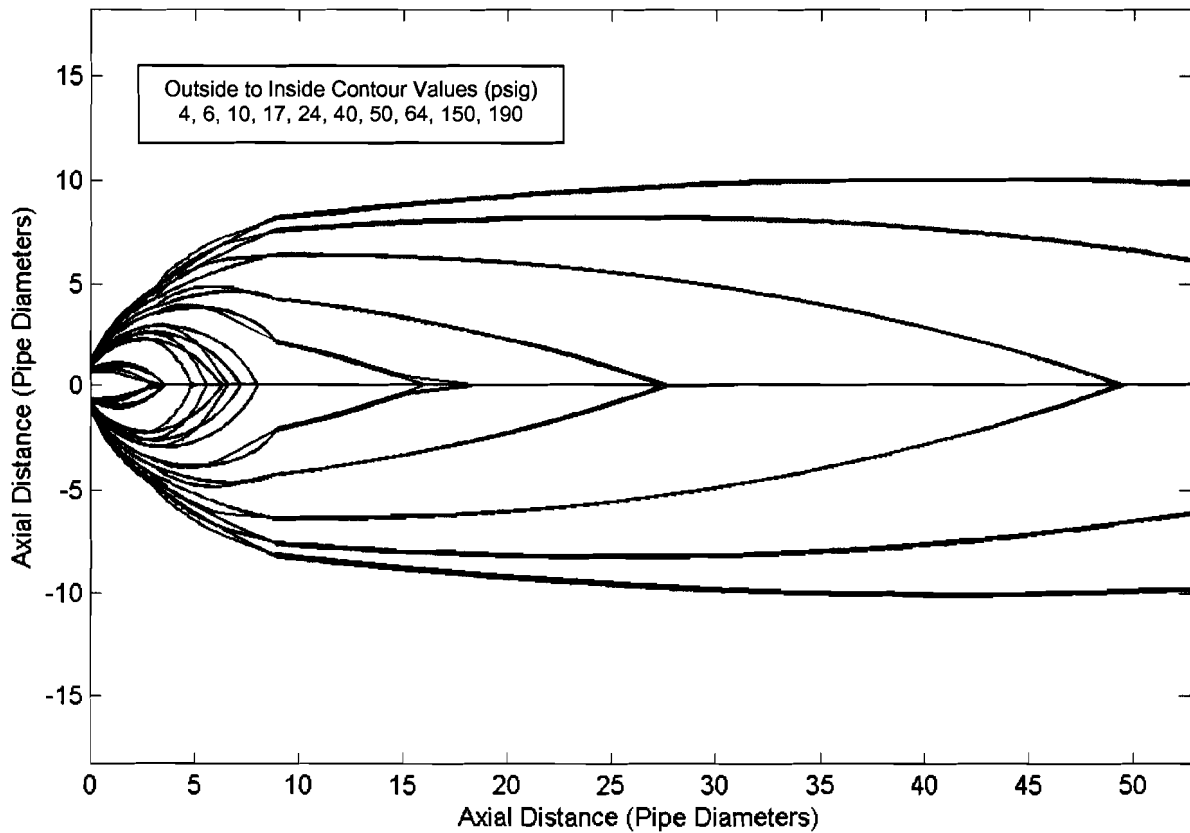
**Staff Evaluation for Section 3.4.2.2:** The baseline approach of selecting ZOI size based on the potentially affected insulation type in containment with the lowest destruction pressure is acceptable to the staff provided that 1) there are no other materials in containment more fragile than insulation that might pose a debris generation potential, and that 2) defensible damage pressures are available or can be ascertained conservatively with engineering judgment, for all insulation types, coatings and other materials of concern. The implication of this assumption that the presence of a single vulnerable material means that all candidate debris materials should be presumed damaged to the same level. Credit for the individual response of well-characterized insulation types can be given under the refinement offered in Chapter 4 of the GR.

Table 3-1 is offered in the GR as a mechanism for matching experimentally determined damage pressures with "calculated" values of volume-equivalent spherical ZOI radii. Presumably, the calculations were performed in the manner described in Appendix D of the GR, but no cross reference or explanation is offered. Appendix D cites an evaluation of the ANSI/ANS 58.2-1988 that was used to generate spatial jet pressure contours, but no insights are offered in the GR for how to interpret the resulting pressures with respect to material damage.

In order to confirm that the ANSI jet model was implemented properly the model was independently programmed and the results compared with the isobar map tabulated in Table D-1 of the GR. This comparison is shown in Fig. 3-1 where the blue contour lines

represent the GR evaluation of a break at 2250 psia and 540 °F and the black contour lines represent a reference cold-leg break at 2250 psia and 530 °F. See Appendix I of this SER for an explanation of the independent calculation and additional guidance on interpreting results of the ANSI jet model.

Good agreement is seen between the calculations for downrange behavior (Zone 3), but discrepancies exist in Zones 1 and 2. It appears that contour termination points on the centerline are not accurate and that the quadratic behavior of the Zone 2 isobar equations is not implemented correctly. These differences will have a negligible effect on volume integrals for jet pressures less than 20 psig, but may become more of a concern for higher pressures near the break. To quantify the magnitude of the difference, Table 3-1 below presents a comparison of ZOI radii computed from both methods. In particular, the GR approach may not have preserved the system stagnation pressure throughout the volume of the liquid core region as specified by the standard. However, the GR recommended values essentially bound both sets of calculated values.



**Figure 3-1. Comparison of GR Isobar Map with Isobars from Independently Evaluated ANSI Jet Model**

**Table 3-1. Comparison of Computed Spherical ZOI Radii from Independent Evaluations of the ANSI Jet Model**

Impingement Pressure (psig)	ZOI Radius/Break Diameter		
	Guidance Report Recommendation	Calculated Value	SER Appendix I
1000	1.0	0.24	0.89 <sup>a</sup>
333	1.0	0.55	0.90
190	1.3	1.11	1.05
150	1.6	1.51	1.46
40	3.8	3.73	4.00
24	5.5	5.45	5.40
17	7.8	7.72	7.49
10	12.1	12.07	11.92
6	17	16.97	16.95
4	21.6	21.53	21.60

<sup>a</sup> The core volume at stagnation pressure P0 gives a minimum possible ZOI radius of 0.88 diameters.

The larger question of what damage pressure to recommend for each material type requires an understanding of both the limits of the jet model and the knowledge base of existing experimental data.

First, as discussed in Appendix I, the jet model predicts impingement pressures in the longitudinal (downstream) direction only and may underestimate the radial extent of isobars in Zones 1 and 2 when considering the impingement pressure that would develop on the face of a target perpendicular to the local flow velocity.

Second, the ANSI model appears to be unbounded in the downstream direction. This means that for very small impingement pressures the isobar volume will grow unrealistically large. These two limitations compensate to some extent when volume-equivalent spherical radii are computed, and because the jet envelope provides a rigid constraint to radial growth of the contours, unbounded downstream growth will eventually dominate.

Unreasonable growth of low-pressure isobars can be illustrated by comparing the spherical radius plot in Figure I-13 (Appendix I) to Figure 3-3 in the parametric evaluation (PE) supplement [NUREG/CR-6762-3]. The PE study plots a function of spherical ZOI radii that was determined by the BWROG using the NPARC computational fluid dynamics (CFD) model for BWR blowdown conditions. Despite the differences in thermodynamic state point, the differences in qualitative behavior for target pressures less than 20 psig is evident; the ANSI trend appears to be diverging while the BWROG correlation appears to approach a finite maximum at zero pressure. The NRC reviewed the BWROG calculations and found the NPARC code to be a more capable method of modeling steam jets than the ANSI model.

The staff notes that a comparison using a CFD model for PWR break conditions was not performed for either the GR nor this safety evaluation. Caution should be used in the comparison of calculated and experimentally determined pressures to ensure that the computed parameter of the field matches the measured parameter as closely as possible. For example, while it is trivial to fractionate a computed pressure into static

and dynamic components over any incident angle, it may be difficult to obtain high-fidelity measurements under equivalent conditions and diagnostic orientations.

Third, the correlation between any prediction of jet pressure and an experimental observation of "damage pressure" depends on how the measurements were taken, how the debris was characterized, and what the thermodynamic conditions of the test actually were. Data from the references cited in Table 3-1 of the GR are dominated by tests conducted for resolving the strainer blockage issue for BWRs using high-pressure air as a working fluid. Therefore, much of the test data is not directly applicable to PWR or BWR blowdown conditions where jets consist of steam and water mixtures. Without directly applicable data and/or high-fidelity predictive models, this surrogate information can only be applied with appropriate caution. The NRC was concerned enough about potential differences in debris generation between air surrogates and two-phase jets to initiate a joint test program with Ontario Power Generation (OPG). Testing of low-density fiberglass ended prematurely after only one test and the concerns were not fully resolved, but the available results are documented in Vol. 3 of the PE report [NUREG/CR-6762-3] and in Reference 7 of the GR. These data were cited but not discussed in GR Table 3-1 in reference to damage pressures for calcium silicate. Therefore, there is a very limited set of data to evaluate the effects of two-phase jets on low-density fiberglass.

One recurring problem with definitions of damage pressure is inconsistency in the degree of damage that is correlated to the pressure value. Two obvious choices exist. The first option is to define the minimum pressure (threshold) at which jacketing is breached in any way. Issues regarding contribution to potential screen blockage are then handled with a complete description of the debris size distribution from fines to partially intact cassettes and blankets. The second option is to presume a debris size that is suspected to contribute to the blockage potential and to report the damage pressure as the point where significant quantities of this debris size are generated. The second option will have higher values of damage pressure than the first, and the debris size distribution will be skewed towards smaller, and therefore more transportable, pieces if the two options are to give equivalent results in a vulnerability assessment. The second method also requires more a priori subjective judgment. Damage-pressure values reported in Table 3-1 of the GR are based on the second approach. The single fiberglass test performed by OPG resulted in conversion of approximately 50% of the insulation volume into debris of sufficiently small size to be a concern. It is assumed that this test meets by a significant margin the criteria for significant quantity implicit in the second damage-pressure definition.

The OPG test for fiberglass was conducted at a distance of 10D on the centerline downstream of a heated vessel of water at 1450 psia. ANSI jet modeling of this condition suggested an impingement pressure of 6.4 psig at that target location. This result is substantially lower than the BWROG-recommended and NRC accepted pressure of 10 psig cited in Table 3-1 of the GR. Further comparisons with more extensive OPG data for calcium-silicate suggested [NUREG/CR-6762-3] that the lower threshold for fiberglass damage in two-phase jets might be as low as 4 psig. The actual range can only be determined by bracketing with two tests at differing distance the transition from significant damage to negligible damage. While it is true that the insulation products tested by OPG were not identical to those tested in the BWROG air-jet tests, substantially different debris characteristics were observed.

In the absence of more complete test data, it is prudent to attribute the observed effects to the differences in the jet medium, i.e. the difference between air used in the BWROG tests and the two-phase steam/water mixture used by OPG. Several plausible physical mechanisms may contribute to enhanced debris generation in two-phase jets including penetration and erosion from impingement of entrained droplets, increased shear forces within the jet caused by radial velocity components of the expanding fluid, and higher local velocities because of the lower density of water vapor compared to air. To judge the potential contributions of these effects without more extensive data would be speculative, as would be any counter arguments offered to refute their importance. The potential for material degradation by erosion has already been acknowledged in the GR in relation to coatings damage. Although offered there as an ostensible conservatism, the same phenomenon should be considered for all material types.

Based on the OPG test results, an argument could be made for reducing damage pressures determined through air-jet testing by a factor of 2 or more. That approach was recommended, in fact, in the PE study by reducing the damage pressure for fiberglass from 10 psig to 4 psig. A corresponding spherical ZOI radius was then recommended based, not on the ANSI model for PWR break conditions, but rather, on the BWROG correlation for BWR break conditions that were similar to the OPG test. The corresponding radius was reported to be 12-D for an incident pressure of 4 psig while the ANSI model predicts a 21.6-D radius for nominal PWR break conditions at the same impingement pressure. Hence, there appears to be an inconsistency in the PE report because no compensation was made for increased ZOI volume induced by the higher initial pressure of a PWR break.

Given the uncertainties discussed above regarding: (1) interpretations and applicability of the ANSI jet model and its performance compared to CFD correlations for very low impingement pressures; (2) the dissimilarity of insulation types, jacketing and target orientation used in the OPG test compared to U.S. PWRs; and (3) the practical definition of damage pressure and its empirical correlation to the degree of insult, it would be an extreme penalty to assess the full damage-pressure reduction derived in the PE report. Therefore, based on the 50% destruction of fiberglass observed in the only publicly accessible two-phase debris generation test for this insulation type, and on the similarity of this degree of damage to the definitions used in Table 3-1 of the GR, the NRC staff position is that damage pressures for all material types characterized with air jet testing need to be reduced by 40% to account for potentially enhanced debris generation in a two-phase PWR jet.

This reduction corresponds to the differences observed between fiberglass tested in air (10 psig) and fiberglass tested in a water-laden steam jet (~6 psig). Of course, specific materials may respond differently (if at all) to the effects of a two-phase jet, but this reduction in damage pressure provides adequate recognition of the issue and could focus some attention on the remediation or mitigation of high-debris volume accident scenarios. When available, the reduced damage pressure thresholds should be replaced with material-specific test data, so the GR recommendation of 24 psig for the damage pressure of calcium silicate is appropriate based on the findings of the OPG study. Table 3-2 lists the revised destruction pressures and the corresponding ZOI diameters computed as described in Appendix I for the reference cold-leg break.

**Table 3-2. Revised Damage Pressures and Corresponding Volume-Equivalent Spherical ZOI Radii**

Insulation Types	Destruction Pressure (psig)	ZOI Radius/ Break Diameter
Protective Coatings (epoxy and epoxy-phenolic paints)	TBD <sup>1</sup>	NA <sup>2</sup>
Protective Coatings (untopcoated inorganic zinc)	TBD <sup>1</sup>	NA <sup>2</sup>
Transco RMI Darchem DARMET	114	2.0
Jacketed Nukon with Sure-Hold® bands	90	2.4
Mirror® with Sure-Hold® bands		
K-wool	24	5.4
Cal-Sil (Al. cladding, SS bands)	14.4	8.8
Temp-Mat with stainless steel wire retainer	10.2	11.7
Unjacketed Nukon, Jacketed Nukon with standard bands	6	17.0
Knaupf		
Koolphen-K	3.6	22.9
Min-K Mirror® with standard bands	2.4	28.6

<sup>1</sup> To be determined by experiment.

<sup>2</sup> Not available for evaluation at this time.

### 3.4.2.3 The ZOI and Robust Barriers

Section 3.4.2.3 recommends truncating the spherical ZOI whenever the ZOI intersects a robust barrier such as walls and components such as supports, pressurizer, steam generator, reactor coolant pump or jet shields. Such barriers will terminate further expansion of the ZOI. The area in the shadow of the component or structure will be free from damage. The baseline assumes there is sufficient conservatism in drawing the sphere that it is not reasonable that a jet reflected off of a wall or structure would extend further than the unrestrained sphere.

**Staff Evaluation for Section 3.4.2.3:** Conceptually, the volume integral under a computed jet expansion isobar represents the potential for material degradation at pressures equal to the isobar value and higher. Multiple reflections and deflections of a LOCA jet within a confined space would dissipate energy, so conservation of the jet volume under an impingement pressure isobar provides an upper bound on the integral volume of the spatial damage zone, regardless of the shape it is mapped into either by the local geometry of obstacles or by convention for the purpose of analysis. Spherical zones were originally conceived as an adequate approximation for opposing jets from

each side of a guillotine break in the congested piping environment of a BWR containment structure. Spherical zones also provide significant convenience for mapping onto piping layouts.

The only conservatism inherent to the ZOI mapping within containment is the conservation of damage potential computed as the volume under a relevant damage-pressure isobar. The degree of conservatism depends on the piping and equipment congestion in the vicinity of the break. More deflections and redirections lead to greater local deposition of energy, and hence, to greater conservatism in the preservation of damage volume, which maximizes the size of the ZOI by assuming no interference with jet development. It is difficult to quantify the degree of conservatism introduced by ignoring jet reflections, but for BWR break conditions, CFD calculations were performed in a spatial domain with contrived obstacles and flow paths to demonstrate rapid dissipation of the potential damage volume. Similar examples have not been offered in the GR to support the judgment of sufficient conservatism that is needed to rationalize the truncation of spherical ZOI. Relevant attributes of this calculation would include representative spatial complexity and scale relative to the damage volume for PWR break conditions.

PWR containment structures often have structural paths that are designed to direct the principle expansion flow. These features include the ice columns in ice-condenser plants and steam generator compartments in large-dry plants that are vented to upper containment domes with spray deluge systems. Given the potentially large damage volumes that may be predicted from the previous section, it seems reasonable it seems reasonable that these spherical ZOI will be redirected along the designed flow paths for many break scenarios.

The potential benefits of shadowing by equipment and components are also difficult to quantify, and there is not adequate guidance offered to make this a viable credit for the baseline analysis. Undoubtedly, shadowing is a relevant effect for impingement on a large steam generator from one side in a relatively unconfined location, but within a doghouse enclosure, flows may accelerate completely around the generator causing damage on all sides. Shadowing effects cannot be approximated by strict geometric obstruction angles. Insufficient guidance is provided here on the practical implementation of proposed method.

For the baseline analysis, the NRC staff position is that licensees should center the spherical ZOI at the location of the break. Where the sphere extends beyond robust barriers such as walls or encompasses large components such as tanks and steam generators, both the extended and encompassed volumes should be added back to the contiguous ZOI in the direction of the principle expansion flow relevant to the assumed break location. If the direction of the flow is not obvious, the extra volume should be added to a region of the contiguous ZOI that affects the largest volume of potential debris targets. Volume mapping is recognized to be an approximate exercise that requires engineering judgment. A goal of  $\pm 25\%$  accuracy is desirable, and only "large" obstructions need to be considered.

#### 3.4.2.4 Simplifying the Determination of the ZOI

Section 3.4.2.4 offers a conservative simplification for the determination of the ZOI. Given the complexity of the analysis as a whole, it may be desired to make conservative assumptions with the goal of simplifying the analysis. For example, for some breaks it may be only slightly more conservative and much simpler to assume that an entire subcompartment (but not outside the subcompartment) becomes the ZOI.

**Staff Evaluation for Section 3.4.2.4:** The staff concurs that simplifications may be desirable. As a point of practical guidance, it may be useful to precalculate the free volume of subcompartments and rooms that may host a break location or be affected by an adjacent break location. This will facilitate cumulative volume estimates for the total affected zone.

The staff finds the example simplification acceptable, provided the simplification procedure properly justifies that significant jet destruction cannot occur beyond the assumed boundaries of the affected compartments.

#### 3.4.2.5 Evaluating Debris Generation within the ZOI

Section 3.4.2.5 provides a general statement regarding the assessments of debris within the ZOI and refers to the following section (Section 3.4.3). It notes that plant-specific information on the type, location, and amount of debris sources within containment is needed. This information is obtained from plant drawings and the results of condition assessment walkdowns.

**Staff Evaluation for Section 3.4.2.5:** The general statement in GR Section 3.4.2.5 is acceptable. As a point of clarification the staff suggests that once the spatial region of the ZOI has been determined, the next step is to calculate the volume of insulation, the surface area of coatings both qualified and unqualified, and the amounts of any other potentially frangible debris sources within that ZOI. Guidance provided in other sections determines how this insulation is distributed by size and character into debris.

#### 3.4.2.6 Sample Calculation

A sample calculation is provided in Section 3.4.2.6 of the GR. The sample postulates the break of a 10-inch diameter pipe attached to the RCS. The break occurs at the base of a steam generator. Two types of insulation materials are specified (Nukon and RMI), and the quantities of each in the affected zone are given. A ZOI radius is determined based on the pertinent ZOI/break diameter values given in Table 3-1 of the GR. All of the insulation material within the affected zone is assumed to be damaged and becomes debris. The sample also calculates the surface area of coatings estimated to be destructed by the break jet forces.

**Staff Evaluation for Section 3.4.2.6:** Separation of the containment into inventory zones appears to be a very effective aide in moving through the break selection and ZOI mapping processes in a systematic way. Alternative segmentation schemes (or useful subdivisions) other than the uniform grid shown in Fig. 3-1 of the GR might be based on structural barriers or groupings of diverse but collocated insulation types. In Step 4, the volume of the evaluation zone and the estimated surface area of coatings (both qualified

and unqualified) are not provided even though this step should represent all available information about the potential impacts of a break in the postulated location.

The sample calculation is inconsistent with the baseline methodology discussed above because it implies that the potentially affected insulation type with the minimum destruction pressure can be selected from within an accounting region in the vicinity of the break rather than from the entire containment inventory as specified in Section 3.4.2.2. For example, if Min-K were present in an adjacent evaluation zone (or anywhere else in containment), the ZOI radius would have to be larger to account for the lower damage pressure of that insulation type. ZOI may easily overlap several evaluation zones for large breaks.

If Nukon is the most fragile insulation in containment, then the example is consistent through step 5 except that, using the revised damage pressures presented in Table 2 above for two-phase jet impingement, the ZOI radius would be 17 pipe diameters, the ZOI radius would be 14.1 ft, and the ZOI spherical volume would be 11,742 ft<sup>3</sup>. All potential debris generation materials within this zone should be included in the debris inventory.

Step 6 appears to invoke the simplification of assuming 100% inventory within the zone. The decision to make this simplification might be assisted by comparing the ratio of the ZOI volume to the volume of the evaluation zone. It is further reinforced by considering the relative volume of the ZOI obstructed by the steam generator and major piping. When this additional volume is added back to account for flow divergence, the ZOI occupies an even larger proportion of the evaluation zone.

For strict compliance with the baseline methodology, step 6 should also include all of the coatings within the evaluation zone as debris, both qualified and unqualified. Instead, step 7 illustrates an example of a proposed refinement presented in Chapter 4 of the GR where a ZOI specific to a material type is computed to account for the possible higher resistance of coatings to jet impact. Under this refinement, a separate ZOI radius can be computed for each potentially affected debris source. It is likely that many licensees will choose this refinement rather than accept the conservatism of applying at all break locations damage zones defined by the most vulnerable material in containment.

Concurrence with step 7 cannot be extended because acceptable damage pressures for coatings have not been developed. However, once a ZOI has been established, the total area (or equivalent mass) of qualified paint within the zone should be added to the initial debris inventory. There is no basis for the assumption of a coating area equal to the surface area of the ZOI except to satisfy the intent of conservatism for very small damage zones. This assumption of a minimum coating contribution is not required if there is no paint present within the potential ZOI that is eventually defined by a coatings damage pressure.

### **3.4.3 Quantification of Debris Characteristics**

#### **3.4.3.1 Definition**

Section 3.4.3.1 defines debris characteristics as post-accident size distribution of material, material size and shape, and material densities. The input information needed to determine debris characteristics is also noted.

### 3.4.3.2 Discussion

Section 3.4.3.2 provides a discussion of the debris size distributions that have been used in various studies and specifies the distribution recommended for the baseline evaluation. The GR adopts a two-size distribution for material inside the ZOI of a postulated break. These two size groups are small fines and large pieces. Small fines were defined as any material that could transport through gratings, trash racks, or radiological protection fences by blowdown, containment sprays, or post-accident pool flows. Furthermore, the small fines are assumed to be the basic constituent of the material for fibrous blankets and coatings (i.e. individual fibers and pigments, respectively). The GR assumes the largest openings of the gratings, trash racks, or radiological protection fences to be less than a nominal 4 inches (less than 20 square inches total open area). The remaining material that cannot pass through gratings, trash racks, and radiological fences is classified as large pieces.

The erosion and potential disintegration of some debris materials by post-DBA environment water flows are also discussed in Section 3.4.3.2. Because the small fines were already classified as reduced down to the basic constituent, further erosion of the small fines does not apply (e.g., fibrous and coating debris). For fibrous insulation material, the large pieces are assumed to be jacketed or canvassed. According to NUREG/CR-6369, jacketed pieces are not subjected to further erosion. Also, for material outside the ZOI, all insulation material that is jacketed is assumed not to undergo erosion or disintegration by containment spray or break flow.

The discussion noted that NUKON™ debris size distribution on the test of the insulation that had the most data points and that produced the smallest fines and adapted this point as the bounding value of fines production for unjacketed fibrous blankets. The GR references the OPG testing (OPG, 2001) for a low-density fiberglass, which indicated that 52% of the debris was in the category defined as small fines.

The GR assumes that if a material has a higher destruction pressure than NUKON™ then it signifies that the material has a higher resistance to damage, hence the size distribution would be larger than a more fragile material indicated by a lower destruction pressure. Therefore, it is conservative to adopt the NUKON™ blanket size distribution for material with a higher destruction pressure.

**Staff Evaluation for Section 3.4.3.2:** The categories in any size distribution must correlate to the transport model assumptions. The recommended two category size distribution (i.e., small fines and larger pieces) adapted by the NEI baseline for material inside the ZOI of a postulated break is suitable to the baseline transport assumptions, which are based on the transport of either the basic constituent (e.g. individual fibers) or large pieces. The division between the two categories of a nominal 4-in size is adequate in that it agrees well with debris generation testing data. The two-category size distribution, however, is likely to become highly problematic for debris transport refinements that more realistically treat the transport processes. For example, a transport model designed to treat small fibrous debris that transport along the pool floor rather than as suspended fibers will require the small fines in the NEI baseline to be further subdivided into suspended fines and small pieces. The staff finds the two-category size distribution suitable to the baseline but the use of this size distribution

must be reevaluated when debris transport refinements are proposed, such as the refinements proposed in Section 4 of the GR.

The baseline approach contains the assumption that all large pieces of fibrous insulation material would be jacketed or canvassed and therefore would not be subject to further erosion due to water flows. Although this assumption is inconsistent with debris generation data acquired through NRC-sponsored tests, the staff position is that the overall impact of this nonconservatism on the results of this analysis, is relatively minor in regards to the acceptance of the baseline guidance, and therefore acceptable. Further, it is agreed that for material outside the ZOI, all insulation material that is jacketed will not undergo significant erosion or disintegration by containment spray or break flow.

The NEI baseline guidance for determining a conservative fraction for the small fines based on one insulation type, i.e. NUKON™, is not realistic even though the 60% determination is adequate. The GR indicates that the debris generation test with the most destruction for their determination is the low-density fiberglass test conducted by OPG and documented in NUREG/CR-6808, which indicated 52% of the debris was in the category defined as small fines, which is in close agreement with the GR assumption of 60%. During the debris generation for the drywell debris transport tests (DDTS) documented in NUREG/CR-6369, Transco™ fiberglass blankets (similar to NUKON™ blankets) were located at a distance in front of the air jet nozzle so that the blankets were routinely completely or nearly completely destroyed (so noted on Page 3-20 in NUREG/CR-6369). Therefore, it must be concluded that fiberglass blankets will be essentially totally destructed into small fines given sufficient jet pressures (approximately 17 psi for Transco™). However, because this testing was based on a small distance between the nozzle and the insulation target, a realistic determination of the fraction of the insulation in a spherical ZOI that would be destructed to small fines requires integration over the sphere based on damage versus pressure and a mapping of the test jets into the spherical ZOI. Analyses documented in Appendix II confirmed the adequacy of the recommendation of 60% for the fraction of small fines debris generation for NUKON™ fiberglass insulation. Further, this analysis confirmed the 60% number for Transco and Knauf insulations, which are similar to NUKON™ (all low density fiberglass insulations). The Appendix II analyses also illustrate the correct process to determine the debris size recommendation.

The baseline guidance assumes it is conservative to adopt the NUKON™ blanket size distribution for other materials with a higher destruction pressure than NUKON™. This assumption has been supported, but not conclusively assured, by debris generation confirmatory analyses documented in Appendix II. This assumption should only be applied if insulation-specific debris size information is not available.

In addition, although the GR provides damage pressures for a number of insulation products, this list reflects only those products that have received some type of prior testing. The list is not comprehensive either in trade name or by mechanical insulation type. Acceptable default assumptions regarding material damage have been discussed, but product-specific test data can be performed in order to avoid unnecessary conservatism. Test data will be required to quantify the performance of mitigation strategies such as double cladding, double banding, or other redesigned insulation-application methods.

### 3.4.3.3 Size Distribution

Section 3.4.3.3 provides the recommended size distributions (i.e., percentages that are small fines versus large pieces) for fibrous materials in a ZOI, reflective metallic insulation (RMI) in a ZOI, other material in ZOI, and material outside the ZOI. These recommendations are summarized in Table 3-3.

**Table 3-3. NEI Recommended Debris Size Distributions**

<b>Material</b>	<b>Percentage Small Fines</b>	<b>Percentage Large Pieces</b>
<b><i>Fibrous Materials in a ZOI</i></b>		
NUKON Fiber Blankets	60	40
Transco Fiber Blankets	60	40
Knaupf	60	40
Temp-Mat	60	40
K-Wool	60	40
Min-K	100	0
Generic Low-Density Fiberglass	100	0
Generic High-Density Fiberglass	100	0
Generic Mineral Wool	100	0
<b><i>Reflective Metallic Insulation in a ZOI</i></b>		
All Types	75	25
<b><i>Other Material in ZOI</i></b>		
Calcium Silicate	100	0
Microtherm	100	0
Koolphen	100	0
Fire Barrier	100	0
Lead Wool	100	0
Coatings	100	0
<b><i>Material Outside the ZOI</i></b>		
Covered Undamaged Insulation	0	0
Fire Barrier (Covered)	0	0
Fire Barrier (Uncovered)	100	0
Lead Wool (Covered)	0	0
Unjacketed Insulation	100	0
Qualified Coatings	0	0
Unqualified Coatings	100	0

**Staff Evaluation for Section 3.4.3.3:** The baseline recommendations can be grouped as follows:

- Materials for which adequate debris generation data exists to evaluate the debris size distribution, i.e., NUKON™ fiberglass and DPSC Mirror™ RMI insulations.
- Materials deemed to have a size distribution no finer than the materials for which debris generation data is available.
- Materials for which the debris generation is not known well enough to conservatively estimate debris size distributions, therefore maximum destruction is assumed.
- Materials outside the ZOI that are not expected to form debris due to protective coverings.

The size distribution for materials located within the ZOI should be specified in conjunction with the specification of the spherical ZOI radius. Insulation damage progresses from total destruction at the location of the break to substantially less damage near the outer boundary of the ZOI. The specification of the outer boundary is based on a judgment of the conditions under which the damage becomes relatively insignificant. For example, with NUKON™ insulation where the destruction pressure of 10 psi has been accepted even though significant damage was seen at 6 psi in a debris generation test [BWROG AJIT Test 6-2 documented in the BWROG URG], the general test results indicate that a larger portion of the 10 psi ZOI would be in small fines than if the ZOI was based on 6 psi. Therefore, within the ZOI, the size distribution used should be based on the radius of the spherical ZOI determined.

For section 3.4.3.3 of the GR, the staff finds the following:

1. Analyses documented in Appendix II confirmed the adequacy of the recommendation of 60% for the fraction of small fines debris generation for NUKON™ fiberglass insulation. Further, this analysis confirmed the 60% number for Transco and Knauf insulations, which are similar to NUKON™. The small fine generation fraction of 60% is a realistic value that is only slightly conservative.
2. The GR assumes it is conservative to adopt the NUKON™ blanket size distribution for other materials with a higher destruction pressure than NUKON™. This NEI assumption has been supported but not conclusively assured by debris generation confirmatory analyses documented in Appendix II. This assumption should only be applied if insulation-specific debris size information is not available.
3. The staff agrees with the assumption of 100% of the materials becoming small fines for materials for which the debris generation is not known well enough to conservatively estimate debris size distributions.

However, for those plants that can substantiate no formation of a thin bed at the sump, this assumption would be nonconservative with regard to sump blockage since fine particulates would pass through the sump screen and generate no blockage concerns. Therefore, for those plants that can substantiate no formation of a thin bed at the sump at which particulate debris can collect, the staff finds that debris generated should be assumed to be sized with realistic conservatism based on the plant-specific environment and susceptibilities identified for that facility, with appropriate justification for the sizing used.

4. The staff agrees that covered insulations and fire barrier material outside the ZOI will not form significant debris provided the covering is substantial enough to remain intact and to stop significant water from passing through the insulating materials. For example, an exception would be a vinyl covering of fibrous or particulate material that might melt at post-LOCA containment temperatures, and thus would not protect the materials inside from the effects of water erosion.

#### 3.4.3.4 Calculate Quantities of Each Size Distribution

Section 3.4.3.4 provides guidance for estimating the quantities of debris for each material and each size distribution category. For materials located within the ZOI, other than coatings, the volumes of materials are simply multiplied by the respective size distribution fractions for either small fines debris or large piece debris to obtain the debris volumes of small fines and large pieces, respectively.

**Staff Evaluation for Section 3.4.3.4:** The staff agrees that for materials other than coatings, it is appropriate to multiply the volumes of the ZOI by the appropriate debris size distribution fractions to determine the volumes of debris.

#### **Protective Coatings Quantification**

The ZOI for protective coatings is based on the coating destruction pressure assumed in the GR. The same approach used to map the ZOI for other debris types (described in Section 3.4.2) is also used to map the ZOI for coatings, that is, modeling the ZOI as a spherical volume resulting from the freely expanding LOCA jet that will be exposed to pressures greater than or equal to the assumed destruction pressure. Depending on the break location, coated components may or may not exist within this sphere. Where plant specific data does not exist regarding the amount of coating within the ZOI, the GR assumes that coated components equivalent to the surface area of the sphere will exist within this volume and will fail, generating fine particulate debris. The amount of coating debris is a function of the coating thickness as well as the surface area. If plant specific coating thicknesses are not available, then the GR provides guidance on assuming a coating thickness in the ZOI that consists of 3 mils of IOZ primer plus 6 mils of epoxy topcoat.

**Staff Evaluation for Protective Coatings Quantification:** The staff finds that the quantity of coating debris that will be generated as a result of a LOCA jet should be based on the following:

- For plants that substantiate a thin bed, use of the basic material constituent (10  $\mu\text{m}$  sphere) to size coating debris is acceptable.
- For those plants that can substantiate no formation of a thin bed at which particulate debris can collect, the staff finds that coating debris should be sized based on plant specific analyses for debris generated from within ZOI and from outside the ZOI. Such an analysis should conservatively assess the coating debris generated with appropriate justification for the assumed particulate size or debris size distribution. Degraded qualified coatings that have not been remediated should be treated as unqualified coatings. Finally, testing regarding jet interaction and coating debris formation could provide insight into coating debris formation and help remove some of the potential conservatism associated with treating coatings debris as highly transportable particulate. If coatings, when tested at corresponding LOCA jet pressures and temperatures, are found fail by means other than erosion or the erosion is limited, the majority of debris may be larger, less transportable or pose less of a concern for head loss.

-

The GR stipulates that all unqualified coatings outside the ZOI are assumed to fail. This assumption is consistent with the position provided in NUREG 0800, Section 6.1.2. "Protective Coating Systems." The amount of debris will be a function of the area of unqualified coating and the coating thickness as described in the GR, but the staff recommends that plant-specific values regarding the unqualified coating properties and thickness should be used. The GR recommendation to use 3 mils of IOZ as a default thickness for unqualified coatings outside of the ZOI was based on the fact that 3 mils of IOZ, being 4.5 to 5 times more dense than epoxy, epoxy phenolic or alkyd coatings, would yield approximately the same mass as 13.5 to 15 mils of epoxy coating film. .

Further, the staff is aware of numerous instances where containment coatings, qualified and unqualified, are much thicker than the assumed equivalent thickness of 13.5 to 15 mils, so the assumed equivalent thickness may not be conservative. The staff concludes that the GR alternative is not acceptable without plant specific justification and recommends that plant-specific evaluation of the plant's unqualified coatings be performed to determine conservative coating properties and thicknesses. The staff recognizes that the amount of unqualified coating in a plant may change due to changes in plant equipment and modifications which could affect the sump debris load. Therefore, the staff recommends that licensees to periodically assess the amount of unqualified coating identified and used in the sump analysis to ensure the quantity remains bounding and if non-conservative changes in the amount of unqualified coating occur, that the impact of this change be evaluated.

**Staff Conclusions Regarding Section 3.4.3.4:** The staff concludes that the baseline alternatives to plant specific data for the determination of the coatings thickness may not be conservative and are not acceptable without plant specific justification. Rather, the staff concludes that each plant should perform a plant specific evaluation of their respective coatings to determine conservative coating thicknesses. This conclusion was drawn despite the perceived conservatism of the recommendations of assuming all the unqualified coatings in containment fail and all coating debris forms a fine 10 micron particulate. It is considered reasonable for each plant to assess their respective coating thicknesses as well as the soundness of their coatings rather than assume an indefensible default recommendation.

#### 3.4.3.5 Sample Calculation

Section 3.4.3.5 provides a sample calculation for estimating the quantities of debris from the ZOI by size category and for the DBA-unqualified coatings outside the ZOI.

**Staff Evaluation for Section 3.4.3.5:** The staff found the sample calculation presented in this section of the GR to be adequate in concept and practice, but numerically inconsistent with revised guidance explained in this SER, particularly in its treatment of coatings debris. First, the size distribution of fine and large pieces for both fiberglass and RMI insulation should be reviewed for consistency with SER recommendations in Section 3.4.3. Second, the estimate of coating debris from within the ZOI should be based on plant-specific characterization of coating thickness and a defensible ZOI radius. Finally, the estimate of coating debris from outside the ZOI should also be based on a plant-specific characterization of unqualified coating thickness and total inventory, not the suggested default thickness.

#### 3.4.3.6 Debris Characteristics for Use in Debris Transport and Head Loss

Section 3.4.3.6 provides Tables 3-2 and 3-3 that compile selected debris characteristics for a variety of materials, specifically material densities and characteristic sizes. The baseline guidance declared the characteristic sizes to be the most conservative values that can be associated with debris transport and head loss. The tables include data for fibrous, cellular, RMI, and particulate (granular) insulation materials. It is noted that the manufacturer should be contacted to obtain information for materials not listed.

**Staff Evaluation for Section 3.4.3.6:** The staff notes the following concerns regarding the use of the data Tables 3-2 and 3-3:

1. The range of variation for several data entries is substantial, e.g., the as-fabricated density for Kaowool ranges from 3 to 12 lb/ft<sup>3</sup>. The reason for such wide variation was not provided but is likely due to the variability in the manufacture of that insulation. Further, the specification of such a wide range is not specific enough for head loss predictions because using 3 versus 12 lb/ft<sup>3</sup> for an as-manufactured density could easily make a drastic difference in the prediction. For example, it would take four times the volume of insulation to form a uniform 1/8-in thick layer if the density was 12 rather than 3. It is important that each plant locate data specific to their installed insulation.
2. An inconsistency exists in the guidance regarding the particulate size for coatings debris outside the ZOI. The characteristic size for epoxy and epoxy phenolic coating chips (outside the ZOI) in Table 3-3 is listed as 25 microns. But the discussion on Page 3-25 appears to recommend a 10 micron particulate size for all unqualified coatings. It is the staff's understanding that the intent of the baseline guidance was to recommend the 10 micron size for the coating particulate; therefore acceptance of the baseline is based on the 10 micron recommendation.
3. The data in Tables 3-2 and 3-3 are not complete with respect to the materials typical of PWR containments. For example, the insulation known as Min-K is missing. For insulation types without a destruction pressure, the GR recommends using the lowest destruction pressure available.
4. The data tables provide a characteristic size to represent the material in head loss calculations rather than the specific surface area required when using a correlation such as the NUREG/CR-6224 head loss correlation. In head loss discussions in Section 3.7 of the GR, the characteristic size is used to estimate the specific surface area from simple geometric formulas. The staff is concerned with the method of converting characteristic dimensions into specific surface area because it has been demonstrated that the method shown in Section 3.7 is not reliable. This concern is particularly important when estimating a specific surface area for a particulate with a distribution of particle sizes where the tendency of using the mean of the size distribution is incorrect and leads to an underestimate of the specific surface area that, in turn, can lead to a serious underestimate of the head loss. Further discussion of this issue is deferred to the staff evaluation of Section 3.7. Confirmatory research presented in Appendix V was performed that illustrates the application of simple geometric equations (e.g.,  $4/d$  for fibers and  $6/d$  for particles).

**Staff Conclusions Regarding Section 3.4.3.6:** The staff concludes that acceptance of this section depends upon each plant-specific evaluation properly determining that the parameters selected for the analysis adequately reflect the insulation types actually used in that containment, and that the specific surface area used in the head loss calculation is properly determined.

The staff did not independently verify all the data located in GR Tables 3-2 and 3-3, however, the values presented agree with analyst perceptions for these materials.

## **Failed Coatings**

The GR assumes that all failed coatings generate debris sizes equivalent to the coatings basic constituent or pigment sizes which the methodology identifies as 10 $\mu$ m. The GR chose this value because experimental evidence was lacking regarding coating debris size generation during a postulated event. The industry pressure wash testing detailed in Appendix A of the GR provided some insight that coatings within the ZOI will likely fail by erosion resulting in debris sized in the range of 10 $\mu$ m - 50 $\mu$ m spheres. The testing also provided insight that the qualified epoxy and qualified IOZ coating that were tested would not fail as chips or sheets during simulated jet impingement testing. Coatings outside the ZOI that fail are also assumed to generate debris in sizes equivalent to their basic constituents or pigment sizes. This debris on the order of 10 $\mu$ m spheres.

**Staff Conclusions Regarding Failed Coatings:** For plants that substantiate a thin bed, use of the basic material constituent (10  $\mu$ m sphere) to size coating debris is acceptable.

For those plants that can substantiate no formation of a thin bed at which particulate debris can collect, the staff finds that coating debris should be sized based on plant specific analyses for debris generated from within ZOI and from outside the ZOI. Such an analysis should conservatively assess the coating debris generated with appropriate justification for the assumed particulate size or debris size distribution. Degraded qualified coatings that have not been remediated should be treated as unqualified coatings.

Finally, testing regarding jet interaction and coating debris formation could provide insight into coating debris formation and help remove some of the potential conservatism associated with treating coatings debris as highly transportable particulate. If coatings, when tested at corresponding LOCA jet pressures and temperatures, are found to fail by means other than erosion or the erosion is limited, the majority of debris may be larger, less transportable or pose less of a concern for head loss.

## **3.5 LATENT DEBRIS**

### **3.5.1 Discussion**

Section 3.5.1 of the GR provides a discussion of general considerations for latent debris regarding its potential impact on sump screen blockage and some variables that must be addressed on a plant specific basis. The four bulleted generic activities outlined in the GR (calculation of horizontal and vertical surface areas inside containment, evaluate resident debris buildup, define the debris characteristics, and calculate the total quantity and composition of debris) needed to quantify and characterize latent debris inside containment provide a working outline of the process.

**Staff Evaluation for Section 3.5.1:** The staff finds the GR guidance with respect to general considerations for latent debris to be acceptable. The staff agrees with the position in the GR that latent debris present in containment during operation may contribute to head loss across the emergency core-cooling sump-screens, and that it is necessary to determine the types, quantities and locations of latent debris. The staff also agrees that it is not appropriate for licensees to claim that their existing Foreign Materials Exclusion (FME) programs have entirely eliminated miscellaneous latent debris. Results from plant-specific walkdowns should be used to determine a realistic amount of dust and dirt in containment and to monitor cleanliness metrics that may be deemed necessary following the overall sump screen blockage vulnerability assessment.

For more detailed analysis, the staff believes that when characterizing the resident debris buildup it would be useful to partition the inventory not only by vertical and horizontal location but also by relationship to spray impingement and washing by containment-spray drainage.

### **3.5.2 Baseline Approach**

The introduction provided in this section of the GR provides practical insights into the level of importance that latent debris may take in the overall vulnerability assessment and helps licensees to judge the level of effort needed to characterize their plants. In this section, NEI acknowledges that latent debris should be considered as an input to sump screen head loss, and recommends the use of conservative strategies rather than evaluating the effects of latent debris to a high level of detail.

**Staff Evaluation for Section 3.5.1:** The staff finds the GR guidance with respect to the introduction of the baseline approach for consideration of latent debris to be acceptable. For plants that expect to have fibrous insulation debris generated in the ZOI, the additional contribution to head loss from the latent fiber component may be small by comparison and reasonable approximations of inventory will suffice. However, for predominantly RMI plants, the latent fiber component represents the dominant potential for thin-bed formation across the screen. In any case, accurate fiber inventories can provide valuable insight for critical decisions regarding sump-screen vulnerability.

#### **3.5.2.1 Estimate Horizontal and Vertical Surface Area Inside Containment**

This section of the GR provides a general outline of steps required to estimate the horizontal and vertical surface areas in containment. The bulleted list of items that should be included in the surface area calculation (floor area, walls, cable trays, major ductwork, control rod drive mechanism coolers, tops of reactor coolant pumps, and equipment such as valve operators, air handlers, etc.) provides a starting point for licensees to consider for major inputs. The five steps provided for surface-area calculations (flat surface considerations, round surface area considerations, vertical surface area considerations, thorough calculation of surface areas in containment, and use of estimated dimensions when exact dimensions are unavailable) are informative.

**Staff Evaluation for Section 3.5.2.1:** The staff finds the GR guidance for estimating surface areas within containment to be acceptable with provisions outlined below for specific sections/attributes.

The staff agrees that the quantity of ambient dust and dirt collected on vertical surfaces by settling from the air is small compared to that collected on horizontal surfaces in the absence of factors that promote adhesion to those vertical surfaces. Any special factors that might promote adhesion to vertical surface should be noted and examined more carefully for dust accumulation. A list of potential adhesive factors includes oil leaks, moisture or condensate laden surfaces, residue from previously sprayed oils or solutions, and detergent films. Dust that accumulates on vertical surfaces is very small and should be assumed 100% transportable if affected by water during a LOCA.

Other surfaces that should be considered for inclusion in plant-specific inventory estimates include steam generators, pressurizers and pressurizer relief tanks, cooling fans, other large equipment, structural supports like I-beams and seismic restraint collars, access gratings and steps, and piping. In general, the area inventory refers to external surfaces that can be affected by spray wash down. Internal compartments and cabinets with known loadings of dust and debris that are not typical of most surface conditions after containment close out should be examined carefully for water infiltration and potential flushing. Areas of this type include inlet-air filter housings and confined crawl spaces that are accessed infrequently.

The guidance provided for surface-area calculations treats the contribution of vertical surfaces in an inconsistent manner. In general, the staff agrees that practical simplifications can be made to simplify estimates of surface area, and the 10% factor proposed for general vertical surfaces is an acceptable estimation based on engineering judgment. However, vertical surfaces that are subject to enhanced dust and debris accumulation should be added to the latent debris load estimation separately as part of the resident debris buildup evaluation in Section 3.5.2.2. Additional guidance for considerations to be included in containment surveys for latent debris loading is provided under that section.

The staff agrees that the containment dome does not need to be considered from the point of view of dust accumulation. However, the dome may be a contributor of degraded coatings that are dislodged during vapor expansion and should be addressed as such in the determination of the coatings debris source term.

In its present form, the baseline guidance requires detailed calculations of both horizontal and vertical surface areas and physical surveys of dust accumulation on horizontal surfaces (Section 3.5.2.2.1). To improve consistency in the treatment of vertical surfaces, the staff provides the following two acceptable alternative options for baseline analysis based on the best available information documented by the industry:

Option 1: Adopt a default vertical-surface inventory of 30 lbs to be characterized by the smallest size fraction found in the horizontal-surface inventory and document a simplified but realistic calculation of vertical surface area. Consideration should still be given to the unique deposition areas discussed above and the results should be added to the default vertical inventory. This value is approximately 5 times higher than the vertical inventory reported in Appendix B for concrete walls and the containment liner and should be sufficiently high to bound variations in surface area, plant cleanliness and the additional vertical areas represented by piping and equipment.

Option 2: Conduct swipes for three categories (a, b, c) of vertical surfaces in the manner illustrated in Appendix B of the GR. It should be noted that repeated wiping with a lint-

free cloth (Maslin) under manual pressure or HEPA-filtered vacuuming with mild brush agitation of the surface are both effective methods for collecting the full spectrum of particle sizes found on surfaces, and both methods provide collection media that can be weighed before and after collection to determine the mass of debris in the sample (see Appendix VII). Concrete walls (a), the liner (b), and vertical piping/equipment (c) should each be sampled at a minimum of three locations selected and documented by simple rationale to represent typical variations in expected dust loadings within containment. For example, walls near the equipment hatch might represent maxima and the upper containment liner might represent minima. Document a simplified but realistic calculation of vertical surface area for each category of surface that is sampled and use the average of the three (or more) measurements to determine the mass present on vertical surfaces of each surface category. Add the three subtotals to the inventory estimate obtained from any unique deposition areas. If recently cleaned surfaces are used to establish the minima for a surface category, a documented cleanliness plan should be referenced that describes the frequency of this cleaning treatment. This option represents a minimal increase in effort over that required in the GR, namely the collection of vertical-surface swipes, and yet allows maximum credit for individual variations in plant cleanliness.

The staff agrees with Step 2 in the GR regarding the treatment of round surfaces, but notes that piping surfaces should be considered. Steps 4 and 5 also provide some practical recommendations that are acceptable.

#### 3.5.2.2 Evaluate Resident Debris Buildup

Section 3.5.2.2 of the GR provides a high level discussion of general practices needed to evaluate latent debris buildup in containment. The GR cites recent sampling of surfaces inside of containment at a number of plants, and recommends surveys of the containment be performed with the objective of determining the quantity of latent debris. This information is not referenced in the public domain to allow confirmation of consistency in the sampling methods and reporting practices, so any statement of expected maximum dust inventory should be considered speculative. The GR references NEI 02-01 to provide guidance for conduct of these containment surveys and evaluation of the presence of foreign material found. The GR also suggests that the degree of rigor for containment survey and surface swiping be applied in inverse proportion to the attention given to foreign material exclusion under normal operations.

**Staff Evaluation for Section 3.5.2.2:** The staff finds the GR guidance with respect to the practices for overall evaluation of latent debris to be acceptable provided the provisions outlined below are incorporated into the site-specific surveys for latent debris in containment. These surveys will produce opportunities to maximize credit for plant cleanliness, and identify areas of higher than expected debris loadings.

To ensure a comprehensive evaluation of containment debris, the following items should be considered as part of the containment survey: Phenomena that can enhance dust collection on both vertical and horizontal surfaces include temperature gradients (thermophoresis) and static electrical charge (electrophoresis). The vertical surfaces of cooling fins, heat exchangers and warm electrical panels may attract higher concentrations of dust than painted concrete structures. Hanging lamp shades inside containment are a common location for enhanced dust collection caused by the thermal gradient. Static charge may be accumulated on any surface exposed regularly to air

flow. Dielectric materials such as plastics and exposed cable jackets may be principle candidates for inspection. For some plants, these effects and locations may be minor contributors to the total dust inventory, and can be dismissed with proper examination. However, these issues should be considered and their disposition documented.

For the purposes of latent debris characterization, surveys taken after every second outage should be sufficient. Exceptions to this schedule warrant surveys after any invasive or extended maintenance like steam-generator replacement.

#### 3.5.2.2.1 Evaluate the Resident Debris Buildup on Surfaces

This section of the GR focuses on the measurement of dust and dirt found on horizontal surfaces of containment. The four steps presented in the GR (1. Divide the containment into areas based on robust barriers, 2. Determine representative surfaces for each section of containment, 3. Survey the representative surfaces in each section to measure debris quantity, and 4. Calculate the thickness of the debris layer) describe the process. Of these, steps 1 and 2 offer practical and thorough guidance for performing a systematic survey. The primary method for determining latent debris inventory suggested in items 3 and 4 of the GR is direct measurement of debris thickness.

**Staff Evaluation for Section 3.5.2.2.1:** The staff finds the GR guidance with respect to division of containment areas (step 1) and determination of representative surfaces (Step 2) to be acceptable, however, the methods identified for measuring and evaluating the buildup of debris on surfaces to be unacceptable. The recommendation in the GR for direct measurement of dust thickness is considered impractical, subjective, and inaccurate. A revised approach for the assessment is offered here that is based on generic characterization of actual PWR debris samples. The revised approach also addresses the question of particulate to fiber ratio as it relates to thin bed effect. If desired, a limited plant-specific characterization can also be pursued as a refinement using this guidance.

Attempting to directly measure is not recommended for the following reasons: (1) masses can be measured much more accurately than thickness, (2) comparison of dirt layers to reference thickness standards is subjective and prone to error because of heterogeneous small objects that may reside on the surface and because of nonuniform dust thickness across a surface like piping, (3) in situ estimates of thickness do not satisfy the requirements to characterize size distributions, particulate-to-fiber mass ratios or densities that are needed to define hydraulic head-loss properties. These problems can be avoided by measuring total masses within a known surface area and then partitioning the fiber and particulate mass fractions either by physical measurement or by generic assumptions described in the next section. Head-loss correlations require the mass and packed-bed density for particulates and the mass and dry (or as-manufactured) density of fiber. The process of debris partitioning will be discussed in Section 3.5.2.3 and generic property values will be recommended.

Statistical sample mass collection is an acceptable method for quantifying latent debris inventories. This approach will not pose an undue burden if planned for in advance and incorporated with other survey activities. A list of unique debris sample locations should be developed starting with the previous discussion in Section 3.5.2.1 that can be

checked for each evaluation zone that is defined in containment. For convenient cross reference these evaluation zones should be defined to coincide with the break zones discussed in Section 3.4. For later input in debris transport assessment, the potential for exposure to water from either direct containment spray, containment-spray drainage, or recirculation-pool immersion, should be noted for the surfaces in each evaluation zone. Other areas that should be included in the survey include annular compartments outside of the bioshield and the reactor cavity if the area participates in circulatory flow with the sump pool during recirculation. Using the practical guidance offered in GR Section 3.4.2.2.1 item 2 for selecting typically loaded surfaces within each inventory evaluation zone, several classes of horizontal surfaces should be defined to represent places where latent debris are found. For example, high and low traffic floor areas, tops of equipment, floor near curbing, cable trays, etc. At least three samples should be taken from each category as they appear throughout containment and the results should be treated in the same manner described for vertical surfaces.

The goal of defining debris characteristics is satisfied by collecting swipe or vacuum-filter samples that can be weighed before and after collection to determine the total mass of debris within a measured area. It is important that the collection method adequately capture the full range of particulate sizes from very small ( $< 10 \mu\text{m}$ ) up to the large miscellaneous chips and pieces, and all fibers in the sample region. Both HEPA-filtered vacuuming with light brush agitation of the surface and repeated swiping under manual pressure with a Maslin cloth were found to be effective collection methods for fine particulates and fiber. Vacuuming is considered more efficient for collecting larger grains and miscellaneous objects. Scraping with a metal blade or sweeping with a bristle-type brush will not adequately collect the full range of debris [DIN04].

#### 3.5.2.2.2 Evaluate the Quantity of Other Miscellaneous Debris

Section 3.5.2.2.2 of the GR provides general guidance for considerations to be used for identifying and evaluating potential sources of miscellaneous debris in containment. The GR refers to and endorses the use of NEI 02-01 to provide guidance for performance of containment surveys. A list of three bulletized items; Equipment tags, Tape, and Stickers or placards affixed by adhesives; is provided to provide guidance for sources to be considered in this section.

**Staff Evaluation for Section 3.5.2.2.2:** The staff finds the GR guidance with respect to the methods to identify and evaluate miscellaneous debris acceptable provided the guidance is supplemental with the additional direction identified below. The staff agrees that surveys of containment for the presence of miscellaneous debris need to be performed and that miscellaneous debris types need to be assessed for potential contributions to sump-screen head loss. In addition to the three categories of miscellaneous debris discussed in the GR, the quantity, characteristics and location of any failed qualified coatings should also be noted in the survey. This issue may be addressed elsewhere in the GR, but it warrants emphasis in this section as well. The following additional guidance is offered on the evaluation of the categories of latent debris.

- General observation: Without specific data to cite regarding the behavior of miscellaneous debris types, the phrases “available for transport” and “transportable debris” should be interpreted as “complete transport to the

screen,” under the conditions of interaction with water. Larger miscellaneous debris types must be evaluated on a case by case basis for susceptibility to transport as outlined in section 3.6. If applicable data on disintegration and transport become available, they should be documented and used as an acceptable refinement to quantify an assumption of partial degradation or partial transport. If applicable, refinements should include a plausible timeline or necessary operating condition for failure. For example, if adhesives are shown to fail after hours in containment, large or heavy stickers and signs may become detached, but still may not transport in low-velocity recirculation conditions. Or, delayed failure of adhesives on upper levels of containment may not lead to transport if containment sprays are no longer operating. Proper consideration should be given to the location of these items and the logic of the rationale that is used. For example, slow softening of adhesive in a high-humidity environment is much different than erosion by spray-water cascade or break-jet impingement

- **Equipment tags:** The guidance provided on the post-LOCA status of paper tags is ambiguous. There is an implied assumption that complete tags arriving at the screen will induce more head loss than shredded or dissolved paper fiber contributing to a mixed debris bed. Regardless of their physical condition, tags can only contribute to head loss if they are transportable. Robust lanyards and attachment methods should prevent most equipment tags that exist outside the ZOI from becoming detached (equipment tags within the ZOI shall be assumed to become detached). The size and weight of detached equipment tags and broken lanyards should be evaluated against criteria in Section 3.6 to determine if they should be considered transportable debris. For all equipment tags that are found to be potentially transportable, it is necessary to determine the number and location of tags by type for contribution to screen head loss. If transportability or the capability of tags to remain intact cannot be determined, to preserve conservatism it should be assumed that they remain intact and are transported to the sump screen. In this case, the wetted sump-screen flow area should be reduced by an area equivalent to the original single-sided surface area of the tags. If there is information that indicates the tags will not remain intact, the staff recommends that the equivalent mass of the tags be treated as latent fiber.
- **Tape:** The GR mentions some specific applications of tape and recommends that all tape be assumed to fail as transportable debris. Because no distinction is made between types or applications of tape, this implies that all tape fails and arrives on the sump screen. The staff position is that the size, weight, and composition of tape that would interact with water should be evaluated for transportability per Section 3.6 to determine the realistic amount that would arrive on the sump screen. As stated in the GR, for equipment tags, the staff requires that, without documentation or evidence, all failed tape that is determined to be transportable should be assumed to arrive on the screen intact and obstruct an area equivalent to its original single-sided surface area. If there is evidence that the tapes will not remain intact, for example prior in-service disintegration, then the equivalent mass of the tape should be assumed to be transported to the screen in the form of latent fiber.
- **Stickers or placards affixed by adhesives:** The staff agrees that adhesives may fail in post-accident conditions. Under the present guidance offered in the GR, all items attached by adhesives should be assumed to fail and be evaluated for transport to the sump screen as outlined in Section 3.6. Where evidence is

available that these items will degrade, the staff recommends that the equivalent mass of the items be assumed to be transported to the sump screen in the form of latent fiber. Otherwise, the wetted flow area of the sump screen should be reduced by the original single-sided area of the items in question.

### 3.5.2.3 Define Debris Characteristics

This section of the GR notes that two generic methods can be applied for defining debris characteristics – Method 1 - analysis of samples, or Method 2 - assume composition and properties based on conservative values. NEI indicates that the second option (assume conservative values for debris composition properties) is preferable, and provides parameter values for fiber density, particle density, and particle diameter. The GR notes that for this option to be used, an appropriate fiber/particulate mix for the plant being evaluated should be used. The GR goes on to describe some of the difficulties and challenges associated with Method 1 – analysis of samples.

**Staff Evaluation for Section 3.5.2.3:** The staff finds the GR guidance with respect to defining debris characteristics to be acceptable provided the method used is supplemented with the additional details outlined below.

It should be noted that conservatism with respect to head-loss potential includes both the aspects of transportability and the hydraulic properties of the material in a mixed debris bed. The four GR bullets for evaluating debris characteristics will be addressed in a parallel format that discusses the Method 1 and Method 2 approaches to each topic concurrently. Both methods first require that adequate surface samples be taken to characterize variability in the plant and that total masses in containment be estimated by multiplying the empirically determined concentration for each type of collection area ( $\text{g/ft}^2$ ) by the corresponding surface areas before summing to obtain the total inventory. Since the GR indicates that Method 2 – assume composition based on conservative values, is the preferred choice, it will be addressed first for each bullet provided.

First GR Bullet – use an appropriate fiber/particulate mix for the plant being evaluated.

•

Method 2 – Assume that fiber contributes 15% of the mass of the total estimated inventory. If abnormal qualified coating conditions indicate a dominant presence of paint chips compared to normal dust and dirt at a particular sampling location, that location should be characterized by measurement under Method 1. (see Appendix VII on Latent Debris for more specific information)

Method 1 – Characterize the fiber-to-particulate mass ratio in the plant by wet rinsing and manual separation of the fibers from the particulates followed by drying and weighing to obtain mass ratios for sample taken. If this option is chosen, HEPA filtration is recommended as the preferred collection method because of easier separation of the debris from the filter.

Second GR Bullet – Fiber density

- Fiber density: It is conservative to assume that all fiber exposed to water transports to the screen (unless special circumstances are noted as discussed)

earlier), but material buoyancy is not the primary contributing factor and the density should not be assigned equal to that of water.

Method 2 – Assume that latent fiber material has a mean density of  $1.5 \text{ g/cm}^3$ .

Method 1 – Immerse dry fiber samples of known mass in a graduated cylinder with a known quantity of water. Cover with plastic film to prevent evaporation and let stand for several days or heat gently to remove trapped air. Measure new volume of contents and determine fiber material density by displacement.

Third GR Bullet – Fiber density

- Particle density: It is appropriate to assume that latent particulates are primarily geophysical in origin being composed of soil, sand and dust, i.e., “dirt.”

Method 2- Assume latent particulate material has a nominal density of  $2.7 \text{ g/cm}^3$ .

Method 1 – Measure the particulate density by water displacement as described above for fiber.

Fourth GR Bullet – Particle Diameter

- Particle diameter: The principal use of particle diameter is in the estimation of hydraulic properties of the debris like the specific surface area. This information can also affect judgments regarding transportability and retention in a fibrous debris bed.

Method 2

- \* Assume that typical mixtures of latent particulate debris have a specific surface area of  $106,000 \text{ ft}^2/\text{ft}^3$  as defined for use in the NUREG/CR-6224 head-loss correlation.
- \* Assume that 22% of the particulate mass determined from the raw samples that is above the recirculation-pool flood level is nontransportable.
- \* Under conditions of low sump-screen flow  $<0.2 \text{ ft/s}$  and estimated particle-to-fiber mass ratios  $<3$ , assume that 7.5% of the latent particulate debris penetrates the sump screen and is not permanently deposited in the bed to contribute to head loss.

Method 1 – Dry sieve particulates into size fractions down to  $75\text{-}\mu\text{m}$  and characterize the mass distribution as a function of diameter. Assume that the fraction  $> 2\text{mm}$  is not transportable. Assume that 25% of the  $75\text{-}\mu\text{m}$  diameter mass fraction can penetrate the debris bed. Use scanning electron microscopy (SEM) on subsamples of the  $75\text{-}\mu\text{m}$  fraction to determine statistically the fraction of particles below  $10\text{-}\mu\text{m}$  diameter. Compare measured size distributions to literature reported determinations of latent debris size distribution and adjust the Method 2 specific surface area by ratios of estimated masses in each size bin.

Method 3 – Assume all particulate mass is composed of  $10\text{-}\mu\text{m}$  diameter grains. This approach is very conservative, especially when much of the mass may be composed of small paint chips, hardware, and visible sand grains. However, this assumption offers the convenience of consistency with baseline assumptions applied to failed coatings as mentioned in the GR.

Two additional factors needed that are not mentioned in the GR:

- The dry-bed accumulated density of latent fibers is needed for head-loss calculations. For fiberglass, this density is typically reported as the “as manufactured” density but there is no equivalent definition for latent fiber.

Method 2 – Assume the dry-bed bulk density for latent fiber is equal to that of fiberglass insulation ( $2.4 \text{ lbm/ft}^3 = 38.4 \text{ kg/m}^3$ ).

Method 1 – Using the dry fiber component obtained from the Method-1 measurement of fiber-to-particulate mass ratios, separate fibers and small flocks from a sample of known mass and drop them successively through several inches of air into a graduated container. Measure the volume after a bed has been formed by random settling and compute the bulk density of this configuration.

- The fiber specific surface area is also needed for head-loss calculations to compute the contributions to head loss of latent fiber in a mixed debris bed.

Method 2 – Assume the head loss properties of latent fiber are the same as reported in NUREG/CR-6224 for commercial fiberglass. Latent fiber will either be dominated by fiberglass present from the break location or it will form the substrate of a “thin-bed” particulate filter and be dominated by the particulate bed forming on top of the fiber. In either case, the exact properties of the latent fiber are dominated by another debris type, so the error associated with the assumption should be small.

Method 1 – Measure the hydraulic properties of latent fiber by inference using iterative comparisons of head-loss data and model predictions using the NUREG/CR-6224 head-loss correlation.

The NRC agrees with all of the cautionary notes provided in the GR regarding the difficulties of debris characterization except for the presumptive judgment of extreme expense and little benefit. While cost/benefit is an important practical consideration, the NRC never discourages well-documented testing to obtain site-specific information. For some of the more simple steps of the analysis, it may be an immediate benefit to characterize plant conditions more completely than the default assumptions permit. Improved particulate-to-fiber mass ratios, for example, may offer an immediate potential benefit because of the key role latent fiber plays in the assessment of vulnerability for thin-bed formation in a predominantly RMI-insulated plant.

#### 3.5.2.4 Determine Fraction of Surface Area Susceptible to Debris Accumulation

The guidance in this section of the GR is again offered in the form of a baseline approach, “... assume that the entire surface area is susceptible to debris accumulation.” and a proposed refinement that consists of estimating fractional surface areas susceptible to debris accumulation. The intent of the guidance in this section is to offer credit for cleanliness programs exercised in certain parts of containment.

**Staff Evaluation for Section 3.5.2.4:** The staff finds the GR guidance with respect to fractional surface area susceptible to debris accumulation acceptable with the provisions outline below:

To implement the baseline approach, it is presumed that the GR intended for a measurement to be made of the thickness of dust on a representative surface within

each inventory evaluation zone and that this thickness would be multiplied by the total relevant area in the zone to obtain the volume of debris. This approach is not considered reliable due to the difficulty and subjectivity of measuring a debris thickness as discussed in 3.5.2.2.1, and a conservative default inventory was offered as Option 1 in Section 3.5.2.1 of the SER as a simple characterization of build up.

Also discussed in section 3.5.2.1 of the SER was Option 2 for characterization of buildup. Although the discussion there is directly related to several categories of vertical surfaces, the same approach was suggested for horizontal surfaces at the end of Section 3.5.2.2.1, only over a larger set of surface types. Option 2 is based on simple surface collection activities, and it recommended that documentation and controls be established when periodically cleaned surfaces were used in the statistical survey to set the minimum surface concentration for a given surface type. As suggested here, an alternative approach is simply to exclude those areas under documented cleaning control from the surface inventory. Either approach is acceptable to the NRC with the following caveat: If areas are excluded from the surface inventory, documented cleaning procedures should be in place that are exercised before each restart. If periodic cleaning occurs less frequently, the sampling method is recommended to determine the minimum dust loading in those areas of a surface type that have been previously cleaned. The practical guidance offered as items 1 and 2 in this section of the GR are also acceptable to the staff.

An issue similar to accumulation susceptibility that may lead to a credit for reduced latent inventory is transport susceptibility. As recommended earlier in this SER, potential exposure to water should be assessed for each inventory evaluation zone. It is expected that most surfaces will be exposed to either direct spray, spray accumulation flow, or immersion in the recirculation pool, but some isolated areas may exist for which little or no water transport can occur (interior cabinets, elevated crawl spaces, locked rooms, etc). For these types of areas where latent debris is known or expected to exist, justification for exemptions from the total latent-debris inventory can be documented on a case-by-case basis.

#### 3.5.2.5 Calculate Total Quantity and Composition of Debris

The guidance in this section of the GR is based on the previous instruction for measurement of dust thickness on representative surfaces.

**Staff evaluation for Section 3.5.2.5:** The staff finds the general steps identified with respect to calculation acceptable provided that methods outlined previously in this SER are used in place of those specific items previously identified.

The process for integrating survey findings over all surface types has been alluded to several times in this SER review. The instructions provided in this section of the GR are concise and systematic. Given the revised approach to measurement of debris build up recommended by the staff, the total quantity of debris for each inventory evaluation zone and each surface type will be found by multiplying debris concentration (lbm/ft<sup>2</sup>) by the respective areas to obtain the total number of pounds in containment. Following the instructions in item 2 of the GR would yield a volume of debris that would then require conversion to mass using a bulk-averaged density that is ill defined and difficult to measure. No guidance was provided for determining this density.

### 3.5.3 Sample Calculation

The sample calculation presented in this section of the GR illustrates very well the concept and systematic process involved with defining categories of surfaces that reside within a given inventory evaluation zone, calculating areas, and summing debris inventories. Minor points of clarification are offered in the following sections.

#### 3.5.3.1 Calculate Horizontal Surface Area

This section illustrates the appropriate level of simplification for computing structural surface areas in containment.

**Staff Evaluation for Section 3.5.3.1:** Step 4 of the horizontal surface-area calculation discusses the calculation of additional horizontal surface areas contributed by equipment, piping, cable trays, etc. Where these items are large and obstruct floor areas computed in previous steps, the projected area of the item is effectively included twice. The duplicate area can either be subtracted from the inventory or cited as a conservatism to account for the complexity of the object in question, whichever is most appropriate.

The treatment given to the recirculation-sump cover as a projected area accounted for in the floor-area calculation is appropriate. However, the mention of recirculation sumps raises the important point of latent debris that may be found inside the sump itself. It is important that sump cavities be inspected and that foreign material be removed. While material found behind the screen would not technically be available to contribute to debris-bed formation and head loss across the screen, it would pose an immediate concern for degradation and blockage of downstream components.

#### 3.5.3.2 Calculate Quantity of Debris

The example calculation is consistent with guidance given in previous sections of the GR by assuming that a debris-layer thickness can be measure and that in situ densities can be determined; total latent-debris mass is then computed accordingly. Most importantly, the sample calculation correctly separates the fiber and particulate components of the debris aggregate. These fractions behave differently during transport, contribute separately to head loss, and introduce separate considerations regarding sump-screen vulnerability.

**Staff evaluation for Section 3.5.3.2:** The problems associated with direct measurement of debris thickness have been explained. If inventory analysis options involving sampling are pursued, it might be practical to conduct surveys like the one illustrated in this example problem before deciding where to collect actual samples. In this case additional comments should be collected during the survey walkdown regarding the qualitative amounts of debris loading to help select the candidate sampling locations.

## 3.6 DEBRIS TRANSPORT

### 3.6.1 Definition

Section 3.6 provides guidance for estimating debris that is transported from debris sources to the sump screen. The four major transport modes considered in the GR are blowdown, spray washdown, pool fill-up, and pool recirculation flow.

### 3.6.2 Discussion

Section 3.6.2 presents a generic transport logic tree used subsequently in the transport recommendations. In addition, three containment type categorizations are also defined. These categories are:

1. Highly compartmentalized containments defined as those containments that have distinct robust structures and compartments totally surrounding the major components of the RCS. For a main steam line break in a highly compartmentalized containment, the mostly un compartmentalized containment values should be used.
2. Mostly un compartmentalized containments defined as those containments that have partial robust structures surrounding the steam generators.
3. Ice condenser containments defined as all seven ice condenser plants, which lack lower containment compartmentalization.

**Staff Evaluation for Section 3.6.2:** The simple generic debris transport chart shown in GR Figure 3-2 is acceptable for a schematic representation of the GR baseline debris transport evaluation methodology. However, the distinction between the highly compartmentalized and mostly un compartmentalized containments has not been clearly defined. Therefore, if of the containment category in a plant specific analyses is not certain then the evaluation should assume the category that predicts the greater debris accumulation on the sump screens. The acceptance of the baseline guidance as a package is the subject of Section 3.8.

### 3.6.3 Debris Transport

The introduction to Section 3.6.3 introduces the NEI baseline concept for estimating debris trapped in inactive pool volumes defined as volumes located below the containment bottom floor (e.g., the cavity under the reactor vessel) that are not affected by drains from the upper part of the containment that may cause them to participate in the active volumes. All volumes at the containment bottom floor elevation are assumed to participate in the recirculation flow path from the containment sprays and break flow to the sump. The baseline model assumed no preferential direction for water to flow to the sump. Further, the baseline guidance assumes that all debris in the containment bottom floor is uniformly distributed throughout the entire volume of water in containment. This guidance then assumes that the debris transported to the inactive sumps is strictly based on the ratio of the volume of the inactive sumps to the total water volume in containment at the start of recirculation. The baseline guidance states that this assumption is conservative since it ignores the preferential sweeping of the debris on the containment floor to the inactive sumps by the thin sheets of high-velocity water. It was further noted that all small fine debris in active pools on the containment floor is transported to the sump during recirculation.

Subsections 3.6.3.1, 3.6.3.2, and 3.6.3.3 which address the highly compartmentalized, the mostly uncompartimentalized, and the ice condenser containments, respectively, primarily contain compartmental specific debris transport assumptions. These assumptions are summarized in Table 3-4 for the small fine debris generated within the ZOI. The baseline guidance recommends that all debris generated outside the ZOI be treated as small fine debris that subsequently transports to the sump screens (i.e., 100% washdown transport, 100% sump pool recirculation transport, and no transport into the inactive pools). The baseline guidance recommends the assumption that all of the large piece debris deposits onto the containment bottom floor where it stays.

**Table 3-4. Summary of Debris Transport Assumptions for Small Fines Debris from ZOI**

Transport Assumption	Fibrous Debris	RMI Debris	Other Debris
<b>Highly Compartmentalized Containments</b>			
Size Distribution Fraction	0.6	0.75	1
Fraction Ejected Upwards	0.25	0.25	0.25
Fraction Deposited on Bottom Floor	0.75	0.75	0.75
Washdown Transport Fraction	1	0	1
Transport into Inactive Pools	Volume Ratio	Volume Ratio	Volume Ratio
Sump Pool Recirculation Transport	1	1	1
<b>Mostly Uncompartimentalized Containments</b>			
Size Distribution Fraction	0.6	0.75	1
Fraction Ejected Upwards	0*	0	0
Fraction Deposited on Bottom Floor	1*	1	1
Washdown Transport Fraction	1	0	1
Transport into Inactive Pools	Volume Ratio	Volume Ratio	Volume Ratio
Sump Pool Recirculation Transport	1	1	1
<b>Ice Condenser Containments</b>			
Size Distribution Fraction	0.6	0.75	1
Fraction Ejected Upwards	0.1**	0.1**	0.1
Fraction Deposited on Bottom Floor	0.9	0.9	0.9
Washdown Transport Fraction	1	0	1
Transport into Inactive Pools	Volume Ratio	Volume Ratio	Volume Ratio
Sump Pool Recirculation Transport	1	1	1

\*Because this value was not actually specified in the baseline guidance (Section 3.6.3.2, fibrous blowdown transport), the table value was assumed to be the same as the stated RMI value.

\*\* Guidance assumes 100% ejected upwards of which 90% returns via ice melt to containment floor.

**Staff Evaluation for Section 3.6.3:** The staff's evaluation of this section was based on confirmatory research documented in Appendices IV and VI and the base of debris transport knowledge [NUREG/CR-6808]. The inactive pool debris entrapment model

does not represent the realities of debris transport. In the detailed volunteer plant debris blowdown/washdown transport analysis, (Appendix VI to this report), a majority of the small fine debris was determined to transport upwards in the containment where it deposited onto any number of surfaces. Only a few percent of the small fines would likely deposit directly onto the containment bottom floor where the debris would be subjected to pool formation flows into the inactive volumes. Note that in the volunteer plant, the openings into the bottom sump level floor consisted of two personnel access doorways, which are small compared to the large area that opens directly to the containment dome. The large opening was designed for pressure relief from HELB events in the steam generator compartments housing most of the RCS. A significant time delay would most certainly exist between the blowdown period and the time when major portions of the small fines would be transported down to the sump pool by the containment spray drainage. Therefore, the inactive pools would most likely fill (first few minutes) before a large portion of the debris could wash to the sump pool, hence the assumed volume ratio is non-conservative.

The baseline guidance assumes that the debris transported to the inactive sumps is strictly based on the ratio of the volume of the inactive sumps to the total water volume in containment at the start of recirculation. The baseline guidance states that this assumption is conservative because the debris transport methodology ignored the preferential sweeping of the debris on the containment floor to the inactive sumps by the thin sheets of high-velocity water. This basis does not reflect realistic debris transport. Observations made during the integrated tank tests [NUREG/CR-6773] show debris being directionally driven by sheeting flow wave front. Such transport could drive debris across the tank bottom (either away from or to the sump) unless the debris became otherwise trapped along the transport path. With this type of sheeting flow transport of fine debris, a sharp direction change, such as at an entrance into a hallway leading to the reactor cavity, could easily result in the debris being swept right past such an entrance because the debris was unable to alter direction with flow into the doorway. Since it is difficult to determine how sheeting flow would actually transport debris, the amount of conservatism achieved by ignoring the preferential transport of debris to the inactive volumes is difficult to quantify.

The baseline assumption that all debris in the containment bottom floor is uniformly distributed throughout the entire volume of water in containment also does not reflect reality, certainly not in the general sense of all PWRs. The volunteer plant detailed analysis of a line break within a steam generator compartment indicated that more of the blowdown-deposited debris on the bottom floor was likely retained within the affected steam generator compartment than being transported outside the compartment. Hence a substantial concentration of debris would initially be located in the affected steam generator compartment. Although the washdown debris would enter the sump pool at multiple locations with the containment spray drainage, the entry points would place the debris directly into the sump pool flow stream rather than into inactive pools or inactive or quieter portions of the sump pool.

The inactive pool debris entrapment model can predict unrealistically high fraction of debris moving into inactive pools for some plants. Therefore, the licensees should limit the fraction of debris moving into inactive pools to a maximum of 15% of the source unless shown otherwise by analysis as described in Appendix IV.

A review of Table 3-4 shows that the only distinguishing feature among the highly compartmentalized, mostly un compartmentalized, and ice condenser containments relative to the debris transport assumptions is the fraction of the debris assumed to deposit directly onto the containment bottom floor as a result of blowdown debris transport. For fibrous debris transport, however, this fraction becomes irrelevant because all the debris transported upwards is conservatively assumed to wash back down to the sump pool where the washdown debris is treated in the same manner as the blowdown floor deposited debris. In summary, for small fine fibrous debris transport (all three containment categories), the overall transport fraction to the sump screens is one (1.0) minus the fraction assumed to enter the inactive pools (based on a water volume ratio). The 100% washdown assumption for fibrous (and other) debris is conservative.

For small fine RMI debris transport, the fraction assumed ejected upwards (25%) is subsequently assumed to remain in the upper containment areas. In reality, some portion of the small fine RMI debris deposited in the upper reaches of the containment during blowdown would wash back down to the sump pool; therefore this baseline assumption is non-conservative in isolation. However, based on confirmatory debris transport research in Appendices IV and VI, this non-conservative transport assumption, in conjunction with the relatively high fractions of small fine blowdown deposited on the bottom floor (0.75, 1.0, or 0.9), represents a very conservative estimate of small fine RMI debris placed in the sump pool.

The baseline assumption that the recirculation phase pool transport is 100% for small fines is conservative, and removes a need to address the effects of the variety of pool geometries and flow velocities associated with the differences among the PWR containments. However, the baseline assumption of zero sump pool transport of the large piece debris is non-conservative for the plants with relatively fast pool velocities that are capable of moving large debris. The implication of this assumption is that absolutely no large piece debris would accumulate on the sump screens. Based on experimental results from testing performed at the University of New Mexico, the volunteer plant pool model demonstrated that large pieces will degrade and fibers will come out of the large flocks and be transported to the screen (NUREG/CR-6773). As stated in Appendix IV, the characteristic transport velocities must be compared to typical debris transport velocities to determine whether or not the baseline method should be modified to include the transport of large debris. Characteristic transport velocities can be sufficiently estimated using recirculation flow rates and nominal sump dimensions to determine if a potential exists that substantial portions of the large debris will transport. If substantial transport of large debris is reasonably possible and if such transport can alter the outcome of the NPSH margin evaluation, then analytical refinements are needed that evaluate large debris transport.

A conservative assumption recommended in the baseline guidance is that all debris generated outside the ZOI will be of small fine debris that subsequently transports to the sump screens (i.e., 100% washdown transport, 100% sump pool recirculation transport, and no transport into the inactive pools). This assumption removes a need to address the variability and uncertainties due to lack of data on the generation and transport of debris outside the ZOI, especially when considering the differences among the PWR containments.

**Staff Conclusions Regarding Section 3.6.3:** The staff concludes that two of the non-conservative transport assumptions in the baseline guidance are not realistic. These

assumptions are: (1) the assumption that the quantity of fine debris trapped in inactive pools, especially debris washed down from the upper levels of the containment, can be estimated simply by the ratio of the inactive pool volume to the total water volume, and (2) the large piece debris will not transport in the sump pool. In order to avoid prediction unrealistic results when using these assumptions the licensees should (1) limit the fraction of debris moving into inactive pools to a maximum of 15% of the source unless should otherwise by analysis and (2) evaluate large debris transport if characteristic transport velocities show that substantial transport of large debris is possible.

The baseline assumption that all debris in the containment bottom floor is uniformly distributed throughout the entire volume of water in containment is also not conservative. This assumption was made in the baseline guidance as justification for the inactive pool volume ratio but otherwise does not directly affect the acceptance of the baseline guidance due to the 100% recirculation pool transport assumption. However, should a plant subsequently perform a pool transport refinement, then this assumption would not apply and at that point alternative approaches such as those detailed in Appendix III would be required (see condition 8-XX).

### **3.6.4 Calculate Transport Factors**

A sample transport calculation is provided in Section 3.6.4 of the GR. For the sample calculation, it was assumed that the containment was highly compartmentalized with an inactive pool fraction of 30%, and that the ZOI insulation debris included NUKON™ and RMI debris. The unquantified logic chart shown in GR Figure 3-2 was applied to both the NUKON™ and RMI debris per the guidance outlined in GR Section 3.6.3.

Applying the chart to NUKON™ debris, the size distribution is 60% small fines and 40% large pieces that were assumed not to transport. Two transport pathways delivered small fines debris to the sump: (1) 75% of the debris was assumed directly deposited to the sump pool floor, and (2) the remaining 25% of the debris deposited in the upper containment but subsequently washed down to the sump pool after 30% of each case being sequestered in inactive pools. Therefore, 42% of the total NUKON™ debris was assumed to reach the sump with the remaining 58% assumed either trapped in the inactive pools (18%) or as large pieces (40%). Applying the chart to RMI debris, the size distribution is 75% small pieces and 25% large pieces that were assumed not to transport. Only one transport pathway delivered debris to the sump in which 75% of the debris assumed directly deposited to the sump pool floor. The 18.75% of the RMI assumed deposited in the upper containment was assumed to remain there and 30% of the small pieces assumed to reach the lower containment (56% was assumed trapped in the inactive pools). Therefore, 39% of the total (or 53 % of the small pieces) RMI debris was assumed to reach the sump. No large debris transport to the sump. The sample calculation acknowledges 100% transport of coatings debris, from both within and outside the ZOI; and all debris material outside the ZOI including latent debris. A list of all debris by type and size is provided and available for the subsequent sample head loss problem.

**Staff Evaluation for Section 3.6.4:** The sample problem is consistent with the baseline methodology discussed above and the specified transport assumptions. The sample problem illustrates the importance of the two non-conservative baseline debris transport

assumptions, i.e., the inactive pool assumption and the neglect of the large debris, which are described in Staff Evaluation for Section 3.6.3.

## **3.7 HEAD LOSS**

### **3.7.1 Introduction and Scope**

Section 3.7.1 consists of an introduction to the head loss guidance.

### **3.7.2 Inputs for Head Loss Evaluation**

#### **3.7.2.1 Sump Screen Design**

Section 3.7.2.1 briefly describes several aspects of sump screen design pertinent to estimating head losses across the screen. The aspects described include screen construction, screen orientation, screen mesh size, applicable screen area, flat screen versus alternate geometries such as stacked-disc strainers (circumscribed area versus actual screen area), and clean strainer head loss estimation.

**Staff Evaluation for Section 3.7.2.1:** The general guidance in this section is acceptable because it is consistent with general engineering practice

#### **3.7.2.2 Thermal-Hydraulic Conditions**

##### **3.7.2.2.1 Recirculation Pool Water Level**

Section 3.7.2.2.1 recommends using the minimum water level of the recirculation pool in estimating the head loss across the debris bed accumulated on the screen. The minimum water level will yield the smallest surface area for the water flow through the screens that are not completely submerged, as well as the lowest available NPSH to the ECCS pumps.

**Staff Evaluation for Section 3.7.2.2.1:** The staff concludes that the recommendation of using the minimum water level is the appropriate level. For partially submerged screens, the water level affects the wetted screen area, which affects both the water approach velocity used in the head loss calculation and the allowable head loss for the debris accumulation on the screen, which is governed by the pool static pressure head. For completely submerged screens, the static water height adds to the NPSH margin. The staff further notes that the determination of the minimum level must consider potential water hold up in the upper levels of the containment including water holdup due to potential debris blockage at water passages such as drains (e.g., refueling pool drains). The minimum level is not merely a conservative assumption but is required to ensure adequate NPSH margin when the pool is actually operated at that level.

##### **3.7.2.2.2 ECCS Flow Rate**

Section 3.7.2.2.2 recommends using the highest ECCS flow rate in calculating the head loss across a screen, i.e., the maximum pump flows as identified in current NPSH calculations. For multiple sump screens, the flow rate for the head loss calculation is the flow through each of the screens.

**Staff Evaluation for Section 3.7.2.2.2:** The staff concludes that the recommendation of using the maximum pump flows in the head loss calculations is the appropriate assumption although under certain conditions those pumps might be throttled back to a lesser flow rate. This maximum pump flow assumption removes the uncertainty associated with guaranteeing that a lesser flow rate will not be exceeded. The rate of flow through the screen along with the screen area is used to determine the velocity of flow through the screen, which is a primary input to the head loss calculation.

### 3.7.2.2.3 Temperature

Section 3.7.2.2.3 makes three recommendations for specifying the water temperature to be used in the head loss calculations.

1. The temperature at which the head loss is evaluated should be consistent with the temperature used for the NPSH evaluation.
2. The head loss is to be evaluated at of multiple times when different temperatures and flows exist during an accident.
3. The maximum expected temperature may be used for the NPSH analysis, whereas the lowest expected temperature during ECCS operation may be taken for the head loss analysis.

**Staff Evaluation for Section 3.7.2.2.3:** The water temperature determines the viscosity of the water, which affects head loss. A head loss correlation typically either includes the viscosity or is only valid for a distinct range of temperatures. The NPSH available at the pump inlet has to be greater than the NPSH required, which is specified by the pump manufacture, in order to stop cavitation of fluid that can seriously affect the pump performance. The NPSH available is defined as the static pressure head available at the pump inlet minus the frictional head loss at suction side minus the vapor pressure head. The water temperature has a mixed effect on NPSH available. A higher water temperature lowers the viscosity and therefore the frictional head loss across a sump screen. For pumps with fully-submerged sump screens lowering of the screen head loss increases the NPSH available by lowering the frictional head loss at suction side. For pumps with partially-submerged sump screens the lowering of the screen head loss increases the NPSH available by increasing the suction side water level and thus the static pressure head available at the pump inlet. A higher water temperature increases the vapor pressure and thus decreases the NPSH available. These effects act in reverse for a low water temperature. Given the two competing effects, a safe and conservative approach would be to assume a minimum water temperature for the head loss calculation but a maximum water temperature for the NPSH calculation, i.e., baseline guidance Recommendation 3. Recommendation 3 is a safe and valid method of specifying the water temperature.

It should be noted that the estimation of the minimum water temperature may require a different calculation than the typical plant estimation of the maximum water temperature for the design basis. It is conservative in the calculation of the maximum sump pool water temperature to neglect heat transfer processes or systems (e.g., a non-safety related heat removal systems) either to simplify the calculation or because a system cannot be relied upon to limit the temperature. But in a minimum water temperature calculation, all heat removal systems and processes must be included.

Recommendation 2 allows the time-dependency of the temperature to be evaluated, i.e., the evaluation of multiple times, temperatures, and flows during an accident. As the temperature varies during the accident, the same temperature is used in both the head loss calculation and the NPSH calculation with the resulting minimum NPSH margin being the determining factor. Staff concerns with the approach include:

1. Recommendation 2 appears to also recommend that the pump flow can vary with time as well, which is in direct conflict with Section 3.7.2.2.2, which states that the maximum pump flow should be used.
2. The debris in the time-dependent calculation must be assumed as the worst case debris accumulation because the debris transport evaluation capability is not sufficient to predict time-dependent accumulation.
3. If one calculation is used to estimate the pool temperature then that calculation should be sufficiently realistic to capture all important heat transport processes. The systems specified in the accident scenario and the specification of the accident scenario must address whether or not systems such as non-safety related heat removal systems are operating.

Recommendation 1 is obviously not a complete recommendation because it does not in any way specify a minimum temperature for the head loss calculation. A temperature consistent with the NPSH evaluation may not be consistent with a conservative head loss calculation.

**Staff Conclusions Regarding Section 3.7.2.2.3:** The staff concludes that Recommendation 3 for determining the pool temperatures is conservative and adequate if the minimum and maximum temperatures are properly estimated. Recommendation 2 is also a valid approach if properly evaluated with the provisions that the flow should remain that of the maximum pump flow, the debris bed should be the worst case debris accumulation throughout the time-dependent temperature transient, and the pool temperature is properly determined. Recommendation 1 is incomplete and unacceptable by itself.

#### 3.7.2.2.4 Debris Types, Quantities, and Characteristics

Section 3.7.2.2.4 provides a general discussion regarding the parameters needed to specify an accumulation of debris on the sump screen.

**Staff Evaluation for Section 3.7.2.2.4:** The staff notes that the list of important head loss parameters is incomplete. In addition to quantities specified as volumes or masses, the bulk and fiber densities are needed for fibrous debris; the particle density and limiting porosity are needed for the particulate; and the specific surface areas are needed for each debris bed component. Appendix V gives guidance on determining the specific surface areas.

#### 3.7.2.3 Head Loss Methodology

##### 3.7.2.3.1 General Theoretical/Empirical Formulas

#### 3.7.2.3.1.1 Fibrous Debris Beds with Particulate

Section 3.7.2.3.1.1 describes the NUREG/CR-6224 head loss correlation by providing the basic correlation equation and the supporting constituent equations for solidity (one minus the porosity). This section also discusses fibrous debris bed compression due to flow pressure as well as compression limiting factors.

The baseline guidance offers the following options for dealing with debris materials or combinations of materials for which the empirical head loss data do not exist:

1. Characterizing the material with scanning electron microscopy (SEM) analysis and the establishment of a size distribution.
2. Choosing an alternate material that conservatively represents the material in question, via similitude arguments.
3. Testing head loss of the particular material to establish a correlation or else validate an existing correlation for that material.
4. Using other data that may exist to establish head loss data for the material in question.

The section contains a discussion for estimating the specific surface area,  $S_v$ , from the constituent characteristic dimension (e.g., particle or fiber diameter). A formula is provided for determining  $S_v$  for a mixture of debris constituents that is based on volume averaging the squares of the constituent  $S_v$ . The baseline guidance states: "it is best to err on the low side for conservative values of  $S_v$ ." In addition, the guidance describes obtaining the aggregate density for both particulate and fibrous debris using a simple volume averaging procedure. Finally, a computational procedure is described for solving the correlation equations to obtain the head loss.

**Staff Evaluation for Section 3.7.2.3.1.1:** The GR options for obtaining head loss parameters for materials that have not been previously characterized are all valid methods of learning more about that material. Performing head loss testing (Option 3) that can be subsequently analyzed to determine appropriate head loss parameters is the best option since it provides results with the least uncertainty. The other three options will improve knowledge but can leave substantial uncertainty in the resultant head loss parameters that must be countered through the use of conservative safety factors.

Confirmatory research presented in Appendix V and head loss testing reports LA-UR-04-1227 and LA-UR-04-3970 illustrate the application of the NUREG/CR-6224 correlation to head loss data to determine applicable input parameters for the correlation.

The baseline adequately presents the concept of compression limiting whereby the compaction of the fiber and particulate effectively prevents further compression of the debris bed, i.e., limiting of the solidity of the debris bed. However, the computational procedure described in the GR for solving the correlation equations to obtain the head loss does not include a step for determining the limiting solidity and how to proceed with the calculation should the fibrous debris become limited in the iterative solution. The

reader is left with the impression that the limiting solidity is approximately 0.2 (i.e., limiting porosity of 0.8), which is correct for BWR iron oxide corrosion products. This impression is reinforced in the sample problem (Page 3-71) where the mixed bed solidity is set to 0.20 for a particulate that consists of latent and coating debris. Common sand, a likely component of latent debris has an approximate solidity of 0.60 (data available in common soil handbooks), which is greater than the GR implied limit of 0.2. The surrogate latent debris head loss testing documented in LA-UR-04-3970 tested common sand and verified this solidity. The correct value for the limiting solidity should be used with the NUREG/CR-6224 correlation because this limiting solidity governs the head loss when compression limiting occurs, as is the case with thin-bed debris accumulations.

The determination of the specific surface area for the debris bed is one of most important aspects of predicting the head loss. The head loss from the NUREG/CR-6224 correlation is directly dependent on  $S_v$ , in fact, the leading laminar term uses the  $S_v^2$ . For example, at lower flow velocities, if the  $S_v$  were underpredicted by a factor of 2, then the head loss could be under predicted by a factor of 4. The baseline guidance statement that: "it is best to err on the low side for conservative values of  $S_v$ ," should be clarified to indicate that it is the debris size that should be selected on the low side, not the value  $S_v$ . It is conservative to estimate  $S_v$  high, not low.

The baseline guidance for estimating  $S_v$  from the constituent characteristic size dimension (e.g., fiber or particle diameter) has been demonstrated to be unreliable particularly when a particulate is defined by a size distribution. The use of six divided by the diameter is reasonable when specifying  $S_v$  for the conservative all-one-size particulate (10 micron) postulated for coatings debris. However, it is unreasonable when a particulate distribution covers a wide range of sizes (e.g., iron oxide corrosion products ranges from 1 to 300 microns) typically described by 3 or 4 subgroups. The value of  $S_v$  calculated is sensitive to the value of the diameter which is used to represent the size group in the  $6/\text{diameter}$  formula. The natural tendency is to select the mean of the size group but the mean significantly under estimates the specific surface area because all particles in the group less than the mean make a substantially greater contribution to  $S_v$  than do the particles larger than the mean value. Selecting an appropriate value within the range is problematic because it depends upon the size distribution within the size group. A conservative solution to this problem is to use the minimum size of each size group. However, this approach can lead to large estimates of  $S_v$ , especially when the particles become very small. For example, assume the size group has a uniform distribution ranging from 5 to 100 microns. Using the 5 micron size results in a  $S_v$  of 366,000/ft which is conservative (but too large), whereas using the mean of 52.5 micron results in a  $S_v$  of only 34,800/ft which is much too small. Smaller particles in a debris bed cause greater head loss than do the larger particles. Confirmatory research presented in Appendix V show significant error in  $S_v$  calculated using simple geometric equations (e.g.,  $4/d$  for fibers and  $6/d$  for particles). compared to the one deduced using head loss data. Where the particulate for a specific material is defined by a size distribution, the licensees should use applicable head loss data to determine  $S_v$ .

The formula provided in the baseline for determining  $S_v$  for a mixture of debris constituents that is based on volume averaging the squares of  $S_v$  is adequate and conservative relative to the formula actually provided in the cited reference, NUREG/CR-6371.

**Staff Conclusions Regarding Section 3.7.2.3.1.1:** The staff agrees with the baseline that the NUREG/CR-6224 correlation is an appropriate method for estimating the head loss associated with a debris bed consisting of fibers and particulates.

#### 3.7.2.3.1.2 RMI Debris Beds

Section 3.7.2.3.1.2 provides a head loss correlation for estimating the head loss across a bed of RMI debris. This correlation and the values for the constant known as the interfoil gap thickness were extracted directly from NUREG/CR-6808.

**Staff Evaluation for Section 3.7.2.3.1.2:** The staff agrees with the baseline that the NUREG/CR-6808 is an appropriate method for estimating the head loss associated with a debris bed consisting of RMI. as documented in NUREG/CR-6808.

#### 3.7.2.3.1.3 Mixed Debris Beds (RMI, Fiber, and Particulates)

Section 3.7.2.3.1.3 provides guidance for mixed debris beds that include RMI, fibrous, and particulate debris. The baseline guidance recommends that the head loss for the fibrous/particulate debris and the RMI debris be estimated separately and then added together to obtain the head loss for the mixed debris bed.

**Staff Evaluation for Section 3.7.2.3.1.3:** NRC sponsored research found the test data for head loss for mixed debris beds to be bounded by the sum of the head loss of the individual constituents. However, it was noted that the mixed bed tests were not comprehensive in regards to all of the types and combinations of debris that may be possible. The staff concluded that the head loss associated with a mixed RMI and fiber debris bed should preferably be based on head loss measurements but can alternately be calculated as an algebraic sum of the fiber and RMI components after accurately accounting for the strainer geometry [NUREG/CR-6808]. A potential for forming a fiber/particulate thin-bed still needs to be performed even when mixed debris beds are possible because there is insufficient data to substantiate the conclusion that the presence of RMI debris can prevent the formation of a thin bed.

#### 3.7.2.3.1.4 Calcium Silicate Insulation

Section 3.7.2.3.1.4 discusses the calculation of head loss for debris beds containing calcium silicate insulation debris. It states: "Based on current information, the NUREG/CR-6224 correlation can be used according to the methods for fibrous debris beds with particulate if the application is limited to particulate mixtures containing up to about 20 percent calcium silicate by mass." The calcium silicate is treated as the particulate in the fiber/particulate debris bed. The guidance noted the NRC sponsored calcium silicate test report (issuance pending), which is now available as LA-UR-04-1227.

**Staff Evaluation for Section 3.7.2.3.1.4:** The staff concludes that the baseline guidance regarding the estimation of head loss for debris beds containing calcium silicate debris is not adequate. The staff recognizes that LA-UR-04-1227 was not available in time for it to be reviewed by industry and its results included in the baseline guidance. Therefore, the recommendations from LA-UR-04-1227 are summarized herein.

The staff recommended parameters for applying the NUREG/CR-6224 correlation to debris beds consisting of fibrous and calcium silicate debris are shown in Table 3-5. Note that the recommendations depend upon whether or not the thin-bed debris configuration is a potential concern. If the potential for a thin-bed debris configuration exists, then the application of the correlation must consider the higher specific surface area deduced from the tests where the high thin-bed head losses were encountered.

The reproducible thin-bed CalSil tests demonstrated that the potential thin-bed accumulation is realistic. Only a small quantity of fibers (or perhaps none) and fine CalSil particulate, which tends to remain in suspension, is needed to form a very uniform debris bed. The recommended specific surface area of 880,000/ft<sup>3</sup> is 10% higher than the experimentally deduced area, to prudently incorporate a 10% to 20% safety factor to account for (1) experimental uncertainties, such as instrumentation error; (2) an incomplete examination of the experimental test parameter space; and (3) the variance in the manufacture of calcium silicate insulation.

**Table 3-5. Recommended Conservative Calcium Silicate NUREG/CR-6224 Correlation Parameters**

Correlation Parameter	Recommended Head Loss Parameters	
	Thin-Bed Configuration	Mixed-Bed Configuration
Particle Density	115 lbm/ft <sup>3</sup>	115 lbm/ft <sup>3</sup>
Particulate Sludge Density	22 lbm/ft <sup>3</sup>	22 lbm/ft <sup>3</sup>
Particulate Specific Surface Area	880,000 ft <sup>2</sup> /ft <sup>3</sup>	600,000 ft <sup>2</sup> /ft <sup>3</sup>

The sump screen conditions, where it can be reasonably justified that the thin-bed configuration cannot form, include: (1) the advanced strainer designs, where test data has strongly indicated that thin-bed configurations would not uniformly form because of complex surface design; and (2) flow conditions insufficient for the required debris bed formation, which can be substantiated by applicable test data. Examples of advanced strainer designs include the stacked-disk strainers, where it has been generally accepted, based on testing of prototypical strainers, that a uniform thin-bed configuration will not form under potential debris loadings. An example of insufficient flow conditions include a maximum screen/strainer approach velocity of less than 0.1 ft/s and particulate-to-fiber mass ratios of less than 0.5—conditions for which a thin bed was not achieved in the calcium silicate head-loss tests because the filtration efficiency apparently was not sufficient to remove enough of the fine calcium silicate from the flow to form a granular debris bed. Beyond these conditions, a thin bed was actually formed during the tests or the tests did not cover that part of the parameter space; thus, it is not known if a thin bed can form.

The specific surface area for calcium silicate is not a fixed value as it is for hardened particulates such as BWR corrosion products. It was demonstrated that calcium silicate particles are somewhat “spongy,” with interior voids so that when compressed, the particulate deforms to fill interparticle spaces. A working theory that fits the experimental

results is that the compression forces water through smaller and smaller interior voids and increases the effective specific surface area of the calcium silicate particles. .

The three parameters recommended in Table 3-5 (i.e., particle density, particulate sludge density, and particulate specific surface area) are a parameter set and should be applied as a set. The experimental determination of the specific surface areas depended upon the specification of the debris densities. It is also important to note that the calcium silicate tested was obtained from only one manufacturer, and that these recommendations do not necessarily apply to all types of calcium silicate insulation debris.

Whether or not there is sufficient fiber to form a thin-bed has been generally based on the NUREG/CR-6224 recommendation that the quantity of fibrous debris available must be sufficient to form an accumulation 1/8-in thick on the screen. Tests conducted using only calcium silicate fragments have demonstrated that calcium silicate debris can accumulate without the aid of fibrous debris. However, tests conducted using only calcium silicate were not definitive enough to accurately determine the conditions under which a thin-bed can form without the presence of fibrous debris other than the fibers contained in the calcium silicate insulation.

**Staff Conclusions Regarding Section 3.7.2.3.1.4:** The staff concludes that the recommendations shown in Table -3-6 should be followed for debris beds containing calcium silicate debris unless other data becomes available that is more applicable to plant specific conditions. If it can be clearly demonstrated that a thin-bed configuration cannot be formed with calcium silicate debris, then the mixed bed configuration recommendations can be followed. Otherwise, the thin-bed configuration should be assumed. In determining whether or not enough fibrous debris is available, the determination that it may be possible to form a bed of calcium silicate debris without other supporting fiber should be factored into the analysis.

#### 3.7.2.3.1.5 Microporous Insulation

Section 3.7.2.3.1.5 acknowledges that microporous insulation (e.g., MinK and Microtherm) is a granular insulation that is in use in PWRs. For guidance, the baseline refers to insights gained in a very limited series of head loss experiments for which additional background is provided in the supplemental guidance (GR Section 4.2.5.2.2).

**Staff Evaluation for Section 3.7.2.3.1.5:** The staff concludes that guidance regarding the prediction of head loss for debris beds containing microporous insulation debris is largely missing from the baseline and therefore the baseline guidance for microporous insulation is not adequate for plant specific evaluations.

#### 3.7.2.3.1.6 Microporous and Fiber Debris

Section 3.7.2.3.1.6 provides limited guidance regarding the application of the NUREG/CR-6224 correlation to light loadings of microporous insulation debris on the screen, i.e., a particulate to fiber mass ratio less than 0.2.

For ratios larger than 0.2, the baseline guidance recommends the alternative of:

1. Removal of microporous or calcium silicate insulation until the particulate to fiber mass ratios drops below 0.2.
2. Seek an alternative head loss correlation to the NUREG/CR-6224 correlation.
3. Perform head loss experiments using plant-specific debris mixtures, sump screen configuration, and thermal-hydraulic conditions.

The baseline guidance in this section also discusses concerns for microporous or calcium silicate debris only (i.e., no additional fibers other than those integral to the microporous or calcium silicate debris). This guidance recommends the same three alternatives noted above for situations where a debris bed can be accumulated with these insulations without significant other fiber.

The baseline guidance addresses mixtures of granular insulation and RMI debris beds by referring to the superposition guidance presented in Section 3.7.2.3.1.3.

**Staff Evaluation for Section 3.7.2.3.1.6:** The staff concludes the following regarding the guidance presented in this section.

1. The baseline guidance is adequate for particulate-to-fiber mass ratios less than 0.2.
2. The alternatives for particulate-to-fiber mass ratios greater than 0.2 are adequate with the caveat relative to alternative 2 that the adequacy of the alternate correlation must be verified using applicable test data.
3. Since a debris bed formed of microporous debris without additional fibrous debris would be similar to a fibrous/microporous debris bed with a high particulate-to-fiber mass ratio, the adequacy of the alternatives is the same as for a debris bed with fibers and a particulate-to-fiber mass ratio greater than 0.2.
4. The acceptance of the baseline guidance for thin-beds containing microporous insulation types is also subject to the acceptance of the three alternatives.
5. The superposition guidance for mixtures of granular insulation and RMI debris is acceptable.

### 3.7.2.3.2 Methodology Application Considerations

#### 3.7.2.3.2.1 Total Sump Screen Head Loss

Section 3.7.2.3.2.1 recommends adding the clean strainer head loss to the debris bed head loss to get the total head loss across the screen.

**Staff Evaluation for Section 3.7.2.3.2.1:** The staff concludes this guidance is acceptable.

#### 3.7.2.3.2.2 Evaluation of Breaks with Different Combinations of Debris

Section 3.7.2.3.2.2 recommends that analysts evaluate a spectrum of breaks with different combinations of debris types to ensure the identification of the break with the mixture of debris on the screen that causes the highest head loss. The guidance notes that the limiting break is not necessarily the break that generates the largest total quantity of debris.

**Staff Evaluation for Section 3.7.2.3.2.2:** The staff concludes this guidance is acceptable.

#### 3.7.2.3.2.3 Thin Fibrous Beds

GR Section 3.7.2.3.2.3 recommends that the head loss associated with a thin-bed be calculated as a sensitivity analysis. To analyze a thin fiber bed, a fiber quantity sufficient to form a bed one-eighth-inch thick should be determined to be available and, if present, could be deposited on the sump screen. The head loss calculations are the same as described for fiber and particulate beds using the full value of particulate matter transported to the sump screen. The particulate matter includes the latent debris such as dirt, concrete dust, rust, inorganic zinc, epoxy fines, etc. The particulate layer is characterized by a very high sludge-to-fiber ratio; hence a limiting value for the compression is used. If under these conditions, the thin-bed head loss should exceed the NPSH margin, then the allowable particulate loading can be evaluated by reducing the particulate quantity until the calculated head loss is within the NPSH margin.

**Staff Evaluation for Section 3.7.2.3.2.3:** The staff agrees that the potential for developing a thin-bed head loss must be evaluated regardless of the composition of the potential containment debris. However, the staff believes that the thin-bed guidance would benefit from additional detailed guidance in several respects to ensure conservatism.

1. The appropriate density to apply to the fibrous debris in the determination of the quantity of debris needed to form a one-eighth-inch bed is the as-manufactured density. The one-eighth-inch minimum thickness has been based on the NUREG/CR-6224 (Appendix B, Page B-60) finding: *"The head loss model is applicable only to fiber bed thicknesses where uniform bed formation is expected. Typically, this is valid for fiber bed thicknesses larger than 0.125" (0.318 cm). Below this value, it appears the bed does not have the required structure to bridge the strainer holes and filter the sludge particles."* The NUREG/CR-6224 analysis used the as-manufactured density to specify the 'theoretical bed thickness', which is used to specify whether or not a one-eighth-inch thick bed exists. For NUKON™ debris, the accepted as-manufactured density has been 2.4 lb/ft<sup>3</sup>. For latent debris, the as-manufactured density lacks meaning since latent fibers can come from any number of sources; however, a recommendation of 2.4 lb/ft<sup>3</sup> was made in LA-UR-04-3970 that was based on the examination of latent fibers collected by volunteer plants.
2. For a thin-bed debris accumulation, the limiting bed compression specified as either the limiting porosity or limiting solidity becomes a controlling parameter in the NUREG/CR-6224 correlation, i.e., the bed porosity essentially approaches that of the granular materials. It is important that the limiting porosity is

correctly evaluated for the particular particulate or mixture of particulates in the debris bed. For example, the limiting porosity for BWR iron oxide corrosion products is about 0.8 (NUREG/CR-6224) but for common sand, it is more like 0.40 to 0.43 (standard handbook data). This issue was discussed in Section 3.7.2.3.1.1.

3. Because a number of uncertainties are associated with specifying the one-eighth-inch bed thickness criteria, the parameter values that go into the bed thickness determination need to be sufficiently conservative to compensate for uncertainties to ensure adequate NPSH margin. One consideration is the fineness of the fibrous debris accumulating on the screen. Tests have been conducted since the NUREG/CR-6224 study was completed where thin-beds have been formed that were somewhat thinner than one-eighth-inch (e.g., one-tenth-inch), principally because the bed was formed from suspended individual fibers rather than the shredded fiber debris used in the NUREG/CR-6224 testing. Another consideration is the fact that the one-eighth-inch criteria was based on NUKON™ debris and has not been actually determined for other type of fibrous debris. Still another consideration is the strong indication that calcium silicate (and perhaps similar materials) can form a debris bed without supporting fibers (other than the fibers integrated into the calcium silicate).
4. In determining the mass of allowable particulate on the sump screen that is needed to overcome the NPSH margin, the uncertainties associated with predicting this value should be noted. Specifically, the determination of the limiting porosity has a significant uncertainty due to inaccurate specifications of the densities of the particulate components or perhaps the mixing of constituents, and due to the involvement of fibers interlaced with the particulate.
5. Given these noted uncertainties, sufficient conservatism should be used in estimating the quantities of fibrous debris available to form a thin-bed to ensure compensation for these uncertainties. This point is particularly important for plants that do not have significant fibrous insulation (e.g., an all RMI plant) so that the main contribution to the fiber quantities on the sump screen comes from latent debris. In such cases the estimate of the latent fiber becomes a determining factor but substantial uncertainty is also associated with that estimate.

#### 3.7.2.3.2.4 Sump Screen Submergence

Section 3.7.2.3.2.4 described the applicable characterization for partially versus completely submerged sump screens. The limiting criterion for submerged screens occurs when the combined clean sump and debris bed head loss exceeds the NPSH margin. The limiting criterion for a partially submerged screen is when the debris bed accumulation on the screen reduces the flow to less than the flow requirements for the sump. An effective head loss across the debris, which is approximately equal to one-half of the pool height, is sufficient to prevent adequate water flow. The head loss estimate is applied to the submerged portion of the sump screen area.

**Staff Evaluation for Section 3.7.2.3.2.4:** The staff concludes that the baseline guidance in this section regarding partially and completely submerged sump screens is acceptable.

#### 3.7.2.3.2.5 Buoyant Debris

Section 3.7.2.3.2.5 addresses the conditions where buoyant debris could become a problem for strainer head loss. For fully submerged screens, buoyant debris is not considered a problem since it would not reach the sump screens. For partially submerged screens where buoyant debris is determined to reach the screen, the baseline guidance recommends that the effective area be reduced by the thickness of the buoyant debris layer times the length of the covered perimeter, to the extent that it fully envelopes the screen.

**Staff Evaluation for Section 3.7.2.3.2.5:** The staff agrees with the necessity of considering the potential for buoyant debris affecting sump screen head loss. The baseline guidance is acceptable with the exception that shallowly fully submerged sump screens could still draw buoyant debris down to the submerged screen. An analysis should be performed to determine the submerged depth needed to ensure buoyant debris cannot be drawn down onto the sump screen.

#### 3.7.2.3.3 Methodology Limitations and Other Considerations

##### 3.7.2.3.3.1 Flat Screen Assumption

Section 3.7.2.3.3.1 makes the point that head loss data obtained using a vertical pipe test section of a closed loop test apparatus with a horizontally mounted flat screen yielded conservative data for the development of the NUREG/CR-6224 correlation because all debris was forced onto a very small screen. Further, it states that in the alternative design screens, the direct application of the NUREG/CR-6224 correlation may yield overly conservative results and that for these alternate geometry screens, independent head loss correlations should be developed based on actual design configurations, debris loads, and test data to reduce conservatism.

**Staff Evaluation for Section 3.7.2.3.3.1:** The staff finds that the arguments in this section need the following clarification. The development and application of the NUREG/CR-6224 correlation is based on uniform and homogeneous debris beds. Applicable test data must therefore be measured on test debris beds that match these correlation assumptions. The vertical pipe closed-loop test apparatus generally meets these conditions provided the debris is introduced in such a manner that it settled uniformly on the test screen. The baseline statement that "all debris was forced onto a very small screen" does not reflect testing realities. The debris is allowed to settle uniformly but the important point is that the correlation is based on the bed thickness and composition as tested.

A very uniform debris bed is a realistic and a likely form of debris accumulation when debris accumulation is accomplished by filtering out suspended fibers. For example, during the conduct of the integrated tank tests [NUREG/CR-6773], the typical accumulation of fibrous debris was due primarily to suspended debris transport and resulted in uniform debris buildup on both horizontally and vertically oriented screens. Also consider the operational incidents at Perry [NUREG/CR-6808] where a coating of

fine dirt covered most of the surface of the strainers and at Limerick where a thin mat of material covered the strainer. The flat screen assumption is reality based and is not merely a conservative assumption, nor is it overly conservative.

While it is adequate to develop independent head loss correlations based on actual design configurations, debris loads, and test data for alternative screen designs, it should also be noted that the NUREG/CR-6224 correlation has been successfully applied to these designs without over conservatism. The application of the NUREG/CR-6224 correlation requires the selection of the appropriate screen area versus debris loading (i.e. total screen area, circumscribed area, or some area in between based on test data) but then so will any other successful correlation that models an alternate design from a clean screen to its fully loaded condition. The NUREG/CR-6224 correlation has been and can be applied to prototype alternate geometry screens/strainers to determine effective screen areas for specific debris loadings that can be subsequently used in plant specific evaluations.

#### 3.7.2.3.3.2 Non-Uniform Deposition on Sump Screen Surfaces

Section 3.7.2.3.3.2 discusses the conservatism of the assumption that the debris is uniformly distributed on the screen relative to potential non-conservative accumulation associated with vertical and inclined screens.

**Staff Evaluation for Section 3.7.2.3.3.2:** The staff agrees that it is conservative to assume uniform debris accumulation on all types and orientations of screens. However, it should be noted again that uniform debris accumulation is a realistic and likely form of accumulation whenever the accumulation is primarily due to fine suspended debris.

#### 3.7.2.3.3.3 Very Thin Fiber Beds

Section 3.7.2.3.3.2 discusses aspects where the fiber loading is less than that required to form a thin bed. It states that experiments have shown that very thin fibrous beds (with a thickness of less than one-eighth-inch) are characterized by large scale non-uniformities on the screen and negligible head losses. The baseline guidance recommends assuming a negligible head loss whenever the debris bed thickness is less one-eighth-inch.

**Staff Evaluation for Section 3.7.2.3.3.3:** The staff concludes that it is adequate to neglect the head loss associated with low density fiberglass insulation debris beds less than one-eighth-inch provided the concerns expressed in the staff's response to Section 3.7.2.3.2.3 regarding the determination of the thin bed thickness are adequately addressed. These concerns included using the appropriate density to determine the thickness for a given quantity of debris and the uncertainties associated with the original specification of one-eighth-inch as the threshold thickness. The uncertainties include the relative fineness of the insulation debris used to make the threshold thickness determination and the fact that the thickness determination was made only for NUKON™ debris and has not been directly determined for other types of insulation debris. An example where it is not appropriate to neglect the head loss for a debris bed less than one-eighth-inch thick is when there substantial calcium silicate debris is in the bed because there has been strong experimental indications that calcium silicate can form a debris bed without supporting fibers.

#### 3.7.2.3.4 Sample Calculations

Sample head loss calculations are provided in Section 3.7.2.3.4 of the GR. In the sample calculations, flat-plate strainer geometry, steady-state ECC flow conditions, and the final debris loadings are assumed. The debris sources were developed in the sample problem sections for debris generation (Section 3.4.3), latent debris (Table 3-4), and debris transport (Section 3.6). Sample head loss calculations were presented for a fiber/particulate debris bed, an RMI debris bed, a mixed RMI, fiber/particulate debris bed, and a thin-bed debris condition.

**Staff Evaluation for Section 3.7.2.3.4:** The sample problems are consistent with the baseline methodology discussed above and with the specified head loss calculational assumptions, with the exception that the sample problem used a fiber density of 175 lbs/ft<sup>3</sup> rather than the 159 lbs/ft<sup>3</sup> recommended in GR Table 3-2. However, the sample problems fail to clarify the differing volumes and densities associated with each constituent. For example in the fiber/particulate calculation, two volumes are provided for NUKON™ fibers without distinguishing the type of volume quoted: (1) 129 ft<sup>3</sup> for the bulk volume, and (2) 1.77 ft<sup>3</sup> for the material (solid) volume. The reader must take care to ensure the proper volumes and densities are used in the appropriate calculational steps.

In Section 3.7.2.3.1.1, the GR discusses maximum solidity for particulates as a material dependent property but then also leaves the reader with the impression that 20% is a reasonable limiting value for general use. The staff comments to this section pointed out that many particulates have maximum solidities much higher than 20%, e.g., common sand has an approximate solidity of 60%. Therefore, the general use of 20% is not appropriate. Rather, the maximum solidity should be determined for each particulate constituent and then the particulate constituent effective average must be determined. It should also be noted that the maximum solidity also depends upon the particulate size distribution. The sample head loss calculations, specifically the thin-bed calculation where the limit is applied, failed to treat material-specific maximum solidities. The failure to correctly treat the maximum solidities can lead to erroneous and non-conservative head loss predictions for pack limited debris beds.

### 3.8 ACCEPTANCE OF NEI BASELINE GUIDANCE

The purpose of the baseline evaluation methodology is to provide U.S.PWR licensees with a common and consistent approach for evaluating the susceptibility of containment sumps to blockage resulting from the effects of postulated LOCA events. The baseline evaluation methodology is the application of a conservative set of methods that help identify the dominant design factors for a given plant (GR Section 3) that could be subsequently followed by separate guidance on possible analytical refinements to the baseline approach (GR Section 4) and potential design/operational refinements (GR Section 5).

The baseline, however, goes beyond the scoping intent with the statement that "If a plant uses this method and guidance to determine that sufficient head loss margin exists for proper long-term Emergency Core Cooling (ECC) and Containment Spray (CS) function, no additional evaluation for head loss is required." Rather, the baseline methodology becomes an acceptance methodology for plant specific evaluations. Therefore, the NRC staff acceptance of the baseline evaluation methodology must be based on whether or

not any and all PWRs that determine an adequate head loss margin by applying the baseline evaluation methodology will actually have adequate sump performance capabilities to support long-term cooling functions.

The NRC staff acceptance depends upon providing high assurance that the baseline assumptions taken as whole and applied generically to any PWR will not result in a plant operating without adequate ECC or CS head loss margin. In addition, the staff's acceptance must consider how follow up analytical refinements will affect the baseline methodology retained in the final evaluation. Specifically, the acceptance of the baseline evaluation methodology as a package must balance conservative assumptions against non-conservative assumptions; therefore an analytical refinement that decreases the degree of conservatism on a particular assumption has the potential to alter the package balance such that the degree of conservatism is reduced, or even reversed to nonconservatism.

The primary difficulties with assessing whether or not the assumptions used in the baseline guidance result in the baseline guidance as a package being conservative with respect to estimating NPSH margin is that each assumption is variable with respect to the plant evaluated and the conservatism for each assumption cannot be quantified without actually performing a detailed evaluation. Without quantification for at least the more influential assumptions, it is difficult to judge the baseline package conservatism. For example, assuming that all unqualified coatings fail into 10 micron particles could be overly conservative for containments with large quantities of unqualified coatings. However, for plants with little unqualified coatings this assumption does not provide any extra conservatism to counter the non-conservative assumptions in the baseline guidance. The more influential assumptions with potential notable conservatism are summarized in Table 3-6 and the more influential assumptions that are clearly not conservative are summarized in Table 3-7.

**Table 3-7. Conservative Assumptions in the Baseline Evaluation Methodology**

No.	Baseline Guidance Assumption	Rationale for Assumption	Perceived Level of Conservatism
<b><i>Debris Generation Assumptions</i></b>			
1	All unqualified coatings in containment are assumed fail.	Compensate for lack of data, i.e., no basis for estimating failure of unqualified coatings.	Variable depending upon plant conditions, therefore the associated conservatism to the baseline package could range from essentially none to excessive.
2	All coatings debris (qualified and unqualified) assumed to become 10 micron particulate. The implication of the small particulate size is complete transport to sump screen and complete filtration.	Compensate for lack of data, i.e., no basis for estimating coatings debris size distributions.	Variable depending upon plant conditions, therefore the associated conservatism to the baseline package could range from minimal to excessive.

No.	Baseline Guidance Assumption	Rationale for Assumption	Perceived Level of Conservatism
3	100% destruction of materials for which suitable debris generation data is not available including all such materials inside the ZOI and unprotected materials outside the ZOI.	Compensate for lack of data, i.e., the fraction of the materials that becomes small fine debris cannot be ascertained without material-specific debris generation data.	Variable depending upon the types and quantities of such materials. Additionally, it depends upon the relative quantities of such materials compared to dominant insulation with known destruction characteristics. The associated conservatism to the baseline package could range from a minor correction to substantial.
<b>Debris Transport Assumptions</b>			
4	Washdown transport to the sump pool is 100% for fibrous debris and a large fraction of the blowdown transported debris is directed to the sump with the end result that all small fibrous debris fines transport to the sump pool.	Avoidance of complex analyses.	Variable depending upon containment design. Some containment designs could result in high washdown transport, e.g., the volunteer plant study (Appendix VI), while other may retain debris in the upper levels of the containment.
5	100% of small fines ZOI debris, not allocated to an inactive pool is transported to the sump screens.	Avoidance of complex analyses.	Variable depending upon the transport characteristics of the pool. Given a fast flowing pool, the transport could be high therefore this assumption would not necessarily be conservative. But for a slow pool, a substantial portion of the small fines debris could sink to the floor and not transport to the screen, i.e., substantial conservatism with this assumption.
6	All debris generated outside ZOI assumed to transport to sump screen.	Avoidance of complex analyses and compensation for lack of data.	Variable depending upon the types and quantities of such materials. The associated conservatism to the baseline package could range from a minor correction to substantial.



**Table 3-6. Non-Conservative Assumptions  
in the Baseline Evaluation Methodology**

No.	Baseline Guidance Assumption	Rationale for Assumption	Perceived Level of Non-Conservatism
<b><i>Debris Generation Assumptions</i></b>			
7	The adaptation of the BWROG URG destruction pressures to PWR LOCA jets.	Lack of BWR or PWR specific data. Similar application suggests the BWR data appropriate to PWRs.	Because a LWR LOCA jet is two-phase steam/water jet and the destruction pressures cited in the URG were determined using an air jet and due to limited experimental evidence from the OPG two-phase jets, the BWROG destruction pressures could be too high. The baseline methodology could underestimate debris quantities. Therefore, based on the study of this issue and testing, the staff position is to lower the debris destruction pressure by 40% in order to account for two-phase jet effects (see Section 3.4.2.2).
8	A spherical ZOI is truncated whenever the ZOI intersects a robust structure. The radius of the remaining ZOI is not increased to compensate for jet reflection effects.	Assumption that jet reflections off the robust structure would not extend further than the unrestrained sphere. This approach was used for resolving the BWR strainer issue.	Jet reflections off the robust structures would reinforce other components of the LOCA jet, thereby increasing the radius of the non-intercepted sphere. A major portion of the energy of the jet may be preserved. For a break located against a robust wall, it is conceivable that debris generation could be underestimated, relative to a truncated sphere by factor approaching 2.

No.	Baseline Guidance Assumption	Rationale for Assumption	Perceived Level of Non-Conservatism
9	The destruction pressures for coatings within the ZOI were based on high pressure water jet data rather than two-phase jets typical of a PWR LOCA.	Lack of applicable data.	The water jet data may not properly address thermal shock effects that spalled concrete in the HDR tests (NUREG-0897, Page C-2 and Figure C-5). The ZOI coatings debris quantities may be underestimated. Therefore, the staff recommends destruction pressures and ZOI for coatings be determined on a plant-specific basis, based on experimental data as described in Sections 3.4.2 and 3.4.3.
10	Default worse case paint thickness of 3 mil thickness for unqualified coatings outside ZOI	Default alternative when plant specific coating thickness data is not available.	Not worse case and the assumption was not been properly justified. Therefore, the staff recommends plant-specific justification of this thickness, or plant-specific evaluations to determine unqualified coating properties and thicknesses as described in Section 3.4.3.
<b>Debris Transport Assumptions</b>			
11	Debris transport into inactive pools based on the ratio of the inactive pool water volume to the total water volume in the sump pool. Implies a uniform distribution of debris throughout the water pools formed following the LOCA.	Assumptions of uniformly-distributed (as opposed to preferential) sweeping of debris on the containment floor into inactive pools by thin sheets of high-velocity water, and of 100% transport of small fines to the sump during recirculation.	Baseline assumption that debris entrapment in inactive pools (e.g., reactor cavity) based on ratio of water volumes is not realistic. Debris will not be uniformly distributed in the sump water and washdown transported debris likely to arrive in sump after inactive pools filled. Potentially very large non-conservatism that depends upon inactive pool volume relative to

No.	Baseline Guidance Assumption	Rationale for Assumption	Perceived Level of Non-Conservatism
			<p>total water volume. In addition, the same sheeting flow mechanism credited by the GR has the nonconservative result of sweeping debris preferentially to the screens.</p> <p>Therefore, the staff position is that licensees limit the ratio of debris transported to the inactive pools to 15% unless a higher fraction is adequately supported by analyses or experimental data (see Section 8.0).</p>
12	<p>Large piece debris (&gt; 4 in.) is assumed to not transport in sump pool, hence large piece debris accumulation on sump screen completely neglected.</p>	<p>Avoidance of complex analyses.</p>	<p>The impact of neglecting all large debris on the baseline conservatism depends upon pool transport characteristics and sump screen geometry. Little impact for a slowly flowing pool where detailed analyses would predict little large debris transport, but potentially a large impact for a fast flowing pool where substantial large debris could accumulate on the screen, or for geometries such as sump screens protected by gratings at floor level.</p>
<b>Head Loss Assumptions</b>			
13	<p>The baseline recommends using simple geometric formulas to use characteristic diameters for fibers and particles to determine specific surface areas needed for the NUREG/CR-6224 head loss correlation.</p>	<p>Lack of experimentally determined specific surface areas.</p>	<p>Confirmatory research has demonstrated that this approach is not reliable in that it has the potential to result in large underestimates of debris bed head loss.</p> <p>Therefore, the staff provides additional guidance in Appendix V</p>

No.	Baseline Guidance Assumption	Rationale for Assumption	Perceived Level of Non-Conservatism
			to deduce the specific surface areas from applicable head loss data through the application of the correlation.

The baseline methodology assumptions were apparently made for a variety of reasons. Worst case conditions were assumed in certain situations where there is nearly a complete lack of data required to support a more realistic evaluation. These assumptions primarily include the generation of debris such as the treatment of unqualified coatings where all unqualified coatings are assumed to fail and then form fine particulate debris that would readily transport and accumulate in a fibrous bed of debris. In reality, much if not most of this coatings debris would either remain attached to the surfaces or would form chip debris that may not transport so readily. In addition to the unqualified coatings, other materials both within and outside the ZOI were assumed to fail into 100% small fines debris. The difficulty with judging the impact of these assumptions is that a particular containment may not have much of these materials; therefore the relative conservatism associated with these types of assumptions cannot be quantified for PWR containments in general.

Other baseline assumptions were made so that complex debris transport analyses could be avoided. The baseline methodology does not recommend debris transport methods but does credit debris entrapment in inactive pools. Also, it does not consider washdown transport of RMI debris and does not consider the transport of large pieces of debris. Again, the conservatism and non-conservatism of these assumptions cannot be judged for PWR containments in general but only by plant specific analyses. Assuming all fine fibrous and particulate debris washes back down to the sump pool is conservative for all plants. However, neglecting the transport of large piece debris is not conservative for all plants. Judging whether or not a conservative assumption can compensate for a non-conservative assumption requires the consideration of plant specific features. The assumption that debris entrapment within inactive pools could be made on a simple water volume ratio is not realistic because it does not consider the timing of debris washdown relative to the fill up of the inactive pools, which would occur early in the sequence. The volunteer plant study estimated that a majority of the small fine debris was blown upwards in the containment where it subsequently would be subject to washdown processes. That study estimated a majority portion of the small fine debris returning to the sump pool but the analytical capabilities cannot determine the timing of the debris entrance into the pool. If the inactive pools filled before the small fine debris washed back to the sump, then only relatively minor quantities might become so trapped. Therefore, the inactive pool entrapment assumption is probably non-conservative.

As an illustration of the variability of these assumptions as applied to the fleet of PWR plants, consider the following hypothetical situations. Assume that the application of the baseline guidance to both Plants A and B results in the prediction of adequate NPSH margin. The importance of the key assumptions is summarized in Table 3-8. The containment of Plant A is characterized as having relatively large quantities of debris

with unknown debris generation characteristics and debris transport characteristics and the containment has debris transport characteristics that tend to entrap debris thereby preventing transport to the sump screens. The variability of the baseline assumptions would tend to overpredict debris generation and overpredict debris transport by substantial amounts. Therefore, if Plant A has sufficient NPSH margin evaluated using the baseline guidance, Plant A should then have an adequate NPSH margin with reasonable certainty. Plant B, however, would be characterized as having limited quantities of debris other than the ZOI insulation with reasonably well known destruction properties. Realistic debris transport fractions to the sump screen would be relatively high. Substantial larger debris transport would be expected with relatively minor quantities trapped in inactive pools. With hypothetical Plant B, there is a concern that the baseline evaluation could predict an adequate NPSH margin whereas an adequate margin may not actually exist if the uncertainties all lined up in a non-conservative fashion.

**Table 3-7. Baseline Guidance Application to Divergent Hypothetical Plants A and B**

<b>Assumption</b>	<b>Hypothetical Plant A</b>	<b>Hypothetical Plant B</b>
Unqualified Coatings (#1 and #2)	Large quantities of unqualified coatings	Little if any unqualified coatings
100% destruction of ZOI materials with unknown destruction pressures and unprotected materials outside ZOI (#3) and complete transport of the outside ZOI material (#6)	Large quantities of such materials.	Small quantities of such materials.
100% washdown transport for fibrous and particulate small fines debris (#4)	Containment design would likely retain substantial debris at the upper levels	Most debris would likely washdown to the sump pool.
100% pool transport for small fines debris not entrapped in inactive pools (#5)	Relative slow sump pool flow velocities results in significant small fines debris entrapment on sump pool floor.	Relative fast sump pool flow velocities results in little small fines debris entrapment on sump pool floor.
Debris entrapment in inactive pools (#11)	Inactive pool volumes are relatively small therefore debris entrapment in the inactive pools become minor consideration.	Inactive pool volumes are relatively large therefore debris entrapment in the inactive pools become substantial consideration.
Neglect large piece debris (#12)	Relative slow sump pool flow velocities results in little actual large piece debris transport.	Relative fast sump pool flow velocities results in substantial actual large piece debris transport.

It cannot be conclusively demonstrated with rigor that the application of the baseline evaluation methodology, as a package, to PWR plants in general can be relied upon to guarantee that any PWR predicting an adequate NPSH margin using the baseline will

truly have an adequate NSPH margin. However, a reasonable assessment of the methodology is that sufficient overall realistic conservatism exists in the baseline to accept its application with the use of acceptance qualifications or alternative guidance for specific outlier situations such as the one described below.

For example, consider a hypothetical plant that has extensive unqualified coatings but insufficient fibrous debris to form a fibrous debris accumulation sufficient to filter particles. Under the baseline methodology, all the coating debris would be in the form of 10 micron particles, which would be assumed to simply pass through the screens thereby not causing a significant head loss. But in a potential LOCA, the coating debris could fail in large quantities and possibly transport as chips that could accumulate on the screen without the aid of fibrous debris, and thus result in significant head loss.

This example raises two major concerns. First, the baseline guidance excludes transport and blockage of large piece debris. The staff position is that the sump screen blockage evaluation should address whether outlier scenarios such as these exist and evaluate any that are identified. If a plant's sump pool flow is relatively fast, then neglecting large piece debris could lead to substantially under estimated debris effects. Second, for debris characterization, a caution is needed regarding the determination of whether or not there is sufficient fiber to form a thin-bed. If this determination is a close call then all aspects of that determination become critical and must be examined to ensure that each of those aspects are realistic, with appropriate conservatism added before reaching the final conclusion that there is not sufficient fibrous material in containment to form a thin bed debris accumulation.

The results of supporting confirmatory research and information available in the knowledge base [NUREG/CR-6808] cause concern in several aspects of the baseline guidance acceptability. These concerns include:

- Concerns regarding two phase jet effects relative to data collected from air jet testing indicate a potential need to reduce the NEI recommended destruction pressures (which are based on air jet testing) unless over conservatism can be demonstrated in the analytical estimates for debris quantities.
- The baseline evaluation recommendation of truncating a ZOI whenever it intersects a robust structure without resizing the remaining ZOI to maintain jet volumes is not acceptable. Jet reflections from the robust structure will affect the remaining ZOI; therefore the remaining ZOI must be resized to maintain volume.
- The default coating thickness recommended by the baseline evaluation guidance are not worst case thickness. Only plant specific coating thickness evaluations can adequately assess not only the coating debris volumes but also the appropriate parameters for the head loss correlation, e.g., the particle densities.
- Because conservative estimates for the debris specific surface areas used in the NUREG/CR-6224 head loss correlation are critical to ensuring conservative estimates for the NSPH margins, the staff is concerned that the baseline evaluation methodology recommendations for estimating the areas using only the characteristic diameters will lead to non-conservative head loss predictions. Confirmatory research recommendations should be addressed.
- The baseline methodology neglects potential erosion of large piece debris by water flows by assuming all large piece debris remains in protective coverings,

which debris generation data clearly shows is not realistic. Even though such erosion is not expected to result in large quantities of additional fine debris, it should still be considered in the baseline evaluation if large portions of the large piece debris are physically located directly below large flows of fallings water.

In summary, the baseline evaluation methodology as a package cannot be given a blanket acceptance because: (1) non-conservative assumptions are recommended in the baseline guidance; (2) it is not possible to quantify the degree of conservatism or non-conservatism of each important assumption without performing detailed analyses for comparison; especially considering the diversity in the containment and RCS designs; and (3) confirmatory research has resulted in concerns associated with key aspects of the guidance. Therefore, the baseline evaluation methodology as modified in accordance with staff positions established in the preceding sections, is acceptable. If the baseline evaluation is based on planned design/operational changes, as opposed to current plant configuration, then acceptance of the evaluation is also based on the implementation of planned changes. The baseline evaluation guidance does not exempt a plant from concerns not explicitly addressed by the baseline, e.g., chemical effects and downstream effects.

Subsequent analytical refinements to the baseline evaluation must reconsider the non-conservative assumptions of the baseline evaluation; not merely reduce identified over-conservatisms. Supplemental NEI analytical refinements include recommendations for reducing the sump pool transport fractions by means of evaluating pool flow velocities and comparing those velocities with test data for threshold velocities for moving debris along the pool floor. If such analyzes are performed on small piece debris then those analyzes need to also treat large piece debris transport.

The sample problem developed in the baseline evaluation methodology may serve to illustrate the evaluation process but is not detailed enough to serve as a template for plant evaluations.

#### 4.0 ANALYTICAL REFINEMENTS

Few acceptable analytical refinements are provided in the GR. Some sections contain additional information to support the development of refinements. Some of this information is already in the baseline. For clarity, the NEI has presented the following table (Table 4-1) that lists the refinements offered in Section 4.0 of the GR.

**Table 4-1. Pressurized Water Reactor Sump Performance Evaluation Methodology Refinements Table**

No.	Section	Page	Topic	Description
1	4.2.1	4-1	Break Selection	This section identifies that plants may use Generic Letter 87-11, "Relaxation in Arbitrary Intermediate Pipe Rupture Requirements," consistent with their licensing basis, to select break locations for evaluating post-accident sump operability.
2	4.2.2.1	4-2	Debris Generation	This section identifies that plants may refine the Zone of Influence (ZOI) definition from a single all-encompassing region based on the material with the minimum destruction pressure by assigning multiple ZOIs to each break site. Each ZOI would correspond to the destruction pressure of one insulation species located near the break site.
3	4.2.2.1	4-3	Debris Generation	This section identifies that plants may refine the Zone of Influence (ZOI) definition by modeling two freely-expanding jets, each originating at one end of a postulated DEGB. The ZOI for a specific material would be evaluated as the region enclosed within the calculated isobar corresponding to a given destruction pressure of an insulation species located within the jet.
4	4.2.2.2	4-5	Debris Characteristics	This section provides additional refinements with respect to the characteristics of debris that might be generated from a postulated break. Specifically, the use of plant-specific or publicly available vendor-specific information, where applicable, is identified as source for refining debris sizes considered in the transport and blockage evaluation.
5	4.2.3	4-14	Latent Debris	This section identifies that plant-specific conditions (for example, cleanliness programs) may be used to support improvements to the latent debris source term.
6	4.2.4	4-14	Debris Transport	<p>This section identifies two refinements to evaluate debris transport.</p> <ul style="list-style-type: none"> <li>• The first refinement is the use of an open channel nodal network to evaluate bulk fluid movement about the containment.</li> <li>• The second refinement is the use of a Computational Fluid Dynamics (CFD) model to calculate a detailed flow field within the containment sump and assess debris transport.</li> </ul>

**Table 4-1. Pressurized Water Reactor Sump Performance Evaluation Methodology Refinements Table (Continued)**

No.	Section	Page	Topic	Description
7	4.2.4.1	4-14	Debris Transport	<p>This section provides guidance on the development of an open channel network model. Guidance is given on:</p> <ul style="list-style-type: none"> <li>• Use of the physical configuration of the containment geometry to define the model,</li> <li>• Development of boundary conditions based on sources and sinks of cooling water,</li> <li>• Defining hydraulic channels</li> <li>• Calculation of hydraulic losses in the channels, and,</li> <li>• Refinements to the channel pattern.</li> </ul> <p>A sample calculation is included for demonstration purposes.</p>
8	4.2.4.2	4-23	Debris Transport	<p>This section provides guidance on the development of detailed flow patterns in the containment pool using state-of-the-art 3D computational fluid dynamics (CFD) codes. Guidance is given on:</p> <ul style="list-style-type: none"> <li>• Selection of CFD software,</li> <li>• Building a CAD model of the containment to be used as input to the CFD model</li> <li>• Building the CFD model, including mesh generation and selection of material properties and boundary conditions,</li> <li>• Solution convergence considerations, and,</li> <li>• Use of computed results for evaluating debris transport.</li> </ul> <p>A sample calculation is included for demonstration purposes.</p>
9	Table 4-2	4-29	Debris Transport	<p>This table provides additional transport data for debris generated from common insulation materials. This information may be used in conjunction with either the Open Channel Nodal Network or CFD models to evaluate debris transport in the sump pool during operation of the ECCS in the recirculation mode.</p>
10	4.2.5.1	4-35	Head Loss	<p>This section identifies that no refinements for evaluating thin bed effects are offered beyond those already given in Section 3.7.2.3.2.3.</p>

**Table 4-1. Pressurized Water Reactor Sump Performance Evaluation Methodology Refinements Table (Continued)**

No.	Section	Page	Topic	Description
11	4.2.5.2	4-35	Head Loss	This section presents information that may be helpful in refining the head loss analysis as a whole including a brief background discussion on head loss correlation development. This section identifies the parameters to be considered when developing a head loss correlation. This discussion is given to identify the considerations to be accounted for when developing a design-specific head loss correlation for a sump screen.
12	4.2.5.2.1	4-37	Head Loss	This section presents a summary of early sump screen head loss testing. Included in the discussion is the method of test, a summary of the nature of the tests and the data obtained, and how the data were correlated. This is provided to facilitate understanding of the nature and complexity of head loss testing. Add statement regarding plant-specific basis.
13	4.2.5.2.2	4-39	Head Loss	<p>Several special head loss correlations are presented and discussed. Specifically:</p> <ul style="list-style-type: none"> <li>• An empirical correlation for fiber-only beds,</li> <li>• The US NRC NUREG/CR-6224 head loss model,</li> <li>• The US BWROG combined debris head loss correlation, and,</li> <li>• Correlations for head loss due to flow through reflective metallic insulation (RMI).</li> </ul> <p>The basis for, and considerations to be accounted for, in applying the RMI head loss equations are also listed.</p>
14	4.2.5.2.3	4-50	Head Loss	<p>This section presents information that may be useful in the development of correlations for alternate strainer designs. Two potential improvements identified for head loss modeling for alternate strainer designs are identified:</p> <ul style="list-style-type: none"> <li>• Accounting for geometry of the screen, if it varies significantly from a flat plate, and,</li> <li>• Non-uniform deposition of debris on the strainer, if appropriate and justifiable.</li> </ul>

**Table 4-1. Pressurized Water Reactor Sump Performance Evaluation Methodology Refinements Table (Continued)**

No.	Section	Page	Topic	Description
15	5.1	5-1	Debris Source Term	<p>This section identifies possible design and operational activities that may be undertaken to reduce the debris source term, such as:</p> <ul style="list-style-type: none"> <li>• Improved housekeeping and foreign materials exclusion (FME) programs</li> <li>• Insulation change-out,</li> <li>• Insulation modifications,</li> <li>• System and equipment modifications, and,</li> <li>• Modifications to protective coatings programs.</li> </ul>
16	5.2	5-4	Debris Transport	<p>This section identifies information that might be used for debris barriers that might mitigate debris transport about the containment. These barriers include:</p> <ul style="list-style-type: none"> <li>• Floor obstructions, and,</li> <li>• Debris racks.</li> </ul>
17	5.3	5-6	Screen Modifications	<p>This sections identifies options for sump screen modifications, including:</p> <ul style="list-style-type: none"> <li>• Passive strainer designs,</li> <li>• Backwash strainer designs, and,</li> <li>• Active strainer designs.</li> </ul> <p>In addition to the sump screen modification options, a list of considerations for each of the options is identified.</p>

For the purpose of this review, the staff provides its position on each of those analytical refinements recognized in this section of the GR for use by the industry. Any analytical refinement(s) proposed by a licensee in its plant-specific analysis of sump performance which is not addressed by the staff in this section of the SER, must be submitted to the staff for approval prior to its use.

#### **4.1 INTRODUCTION**

Section 4.1 defines four main analytical topics where analytical refinements to the baseline evaluation are offered in the GR. They are (1) break selection, (2) debris generation, (3) debris transport, and (4) head loss.

#### **4.2 METHOD DESCRIPTION**

Section 4.2 identifies three main analytical topics where refinements to the baseline evaluation is offered in Section 4.0, of the GR. They are (1) debris generation, (2) debris transport, and (3) head loss. It is stated that discussions on the other two topics, i.e., break selection and latent debris, are included for completeness.

##### **4.2.1 Break Selection**

Section 4.2.1 of the GR discusses an analytical refinement involving pipe break locations to be considered when performing PWR sump analyses. The proposed guidance suggests application of NRC Generic Letter 87-11, "Relaxation in Arbitrary Intermediate Pipe Rupture Requirements," (GL-87-11) to preclude arbitrary intermediate pipe break locations from consideration in PWR sump analyses. The refinement suggests consideration of only those break locations which are consistent with Branch Technical Position MEB 3-1, "Postulated Rupture Locations in Fluid System Piping Inside and Outside Containment," of NUREG-0800, "Standard Review Plan (SRP)," (SRP), Section 3.6.2, "Determination of Rupture Locations and Dynamic Effects Associated with the Postulated Rupture of Piping." Application of Branch Technical Position MEB 3-1 for PWR sump analyses is intended to focus attention on high stress and fatigue break locations, such as at the terminal ends of a piping system and intermediate pipe ruptures at locations of high stress.

**Staff Evaluation for Section 4.2.1:** The staff's evaluation of this section considered the proposed GR guidance in conjunction with existing, corresponding guidance on this subject. The staff's review considered the requirements of 10 CFR 50.46, the staff's evaluation and conclusions for a similar proposal from the boiling water reactor owners group (URG SER), the guidance provided in Regulatory Guide 1.82, "Water Sources for Long-Term Recirculation Cooling Following a Loss-of-Coolant Accident," (RG 1.82-3), and the Commission's staff requirements memorandum (SRM) regarding a proposed rulemaking to risk-inform requirements related to large break LOCA break size (SECY-04-0037).

GSI-191 and the concern of PWR sump blockage is directly associated with the long-term cooling acceptance criteria listed in 10 CFR 50.46 (b)(5). To ensure acceptable ECCS cooling capability, 10 CFR 50.46 requires that, "ECCS cooling performance must be calculated in accordance with an acceptable evaluation model and must be calculated for a number of postulated loss-of-coolant accidents of different sizes, locations, and other properties sufficient to provide assurance that the most severe

postulated loss-of-coolant accidents are calculated.” The staff notes that the worst breaks with respect to peak clad temperature and the other acceptance criteria of 10 CFR 50.46 may not necessarily be the limiting breaks for debris generation and sump head loss. When evaluating ECCS performance for compliance with 10 CFR 50.46, SRP Sections 6.3, “Emergency Core Cooling System,” and 15.6.5, “Loss-of-Coolant Accidents Resulting from Spectrum of Postulated Piping Breaks Within the Reactor Coolant Pressure Boundary,” are the appropriate SRP sections to consider. SRP Section 15.6.5 states that reviewers “evaluate whether the entire break spectrum (break size and location) has been addressed.” The proposed GR guidance to consider only break locations which are consistent with Branch Technical Position MEB 3-1 is not consistent with the requirements of 10 CFR 50.46.

NRC Regulatory Guide 1.82, Revision 3 (RG 1.82-3) provides NRC staff guidance regarding an appropriate spectrum of breaks to be considered when evaluating PWR sump performance. Specifically, regulatory position 1.3.2.3 of Regulatory Guide 1.82 states that a “sufficient number of breaks in each high-pressure system that relies on recirculation should be considered to reasonably bound variations in debris generation by the size, quantity, and type of debris.” As a minimum, the staff position is that the following postulated break locations should be considered: (a) Breaks in the hot leg, cold leg, intermediate leg, and, depending on the plant licensing basis, main steam and main feedwater lines with the largest amount of potential debris within the postulated zone of influence, (b) Large breaks with two or more different types of debris, including the breaks with the most variety of debris, within the expected zone of influence, (c) Breaks in areas with the most direct path to the sump, (d) Medium and large breaks with the largest potential particulate debris to insulation ratio by weight, and (e) Breaks that generate an amount of fibrous debris that, after its transport to the sump screen, creates a minimum uniform thin bed (1/8-inch layer of fiber) to filter particulate debris. The staff considers that Regulatory Guide 1.82 provides the complete scope of breaks which should be evaluated to ensure that the intent of 10 CFR 50.46 is satisfied. The proposed GR guidance to consider only break locations which are consistent with Branch Technical Position MEB 3-1 does not provide an adequate alternative to the guidance provided in Regulatory Guide 1.82, Revision 3 to demonstrate compliance with 10 CFR 50.46.

The staff previously reviewed a similar request to apply SRP Section 3.6.2 and Branch Technical Position MEB 3-1 for identifying break locations to be considered when evaluating ECCS strainer concerns in BWRs. As documented in the staff’s safety evaluation report for the BWR’s (URG SER), the staff rejected the BWROG proposal for two reasons. The first reason is that SRP Section 3.6.2 and Branch Technical Position MEB 3-1 do not provide guidance or acceptance criteria for demonstrating compliance with the requirements of 10 CFR 50.46. The staff noted that the only acceptance criterion specified in SRP Section 3.6.2 is compliance with General Design Criteria (GDC) 4. GDC 4 requires that licensees must protect structures, systems and components important to safety from the dynamic effects (e.g., pipe whip, direct steam jet impingement, etc.) and environmental effects (e.g., temperature, pressure, radiological effects) of postulated pipe ruptures. The staff communicated through Generic Letter 87-11, which transmitted the revised SRP Section 3.6.2 and Branch Technical Position MEB 3-1, that licensees could still provide an adequate and practical level of protection for compliance with GDC 4 by reducing the number of postulated pipe breaks and by physically protecting equipment important to safety from the postulated pipe breaks that have a relatively higher potential for failure (e.g., postulated failures at

high-stress and fatigue locations). As a result, when demonstrating compliance with GDC 4, licensees may analyze pipe breaks through the use of pipe stress analysis methodologies similar to that provided in SRP Section 3.6.2 and Branch Technical Position MEB 3-1. The staff considers SRP Section 3.6.2 and Branch Technical Position MEB 3-1 to be inappropriate for postulating break locations for the purpose of determining the extent of debris generated in order to comply with 10 CFR 50.46. The second reason given by the staff in rejecting the BWROG proposal was that the BWROG had not demonstrated that break locations selected consistent with SRP Section 3.6.2 and Branch Technical Position MEB 3-1 would bound the worst-case debris generation scenarios and, therefore, meet the intent of 10 CFR 50.46. The staff finds that this discussion also applies to the PWR's and the GR proposal.

Finally, in evaluating the GR proposal, the staff considered the current effort involving a proposed rulemaking to risk-inform requirements related to large break LOCA break size. For a risk-informed 10 CFR 50.46, the staff is revising the design basis LOCA break size, but does not plan on changing its current position regarding break locations which need to be considered for purposes of meeting the requirements of 10 CFR 50.46. The staff's intention is to ensure that GSI-191 resolution methodology be consistent with the 50.46 rulemaking effort.

Based on the above discussions, the staff concludes that it is inappropriate to cite SRP 3.6.2 and Branch Technical Position MEB 3-1 as methodology to be applied for determining break locations to be considered for PWR sump analyses. The staff concludes that the guidance regarding break locations, as described in GR Section 3.3 (and as amended in Section 3.3 of the staff's safety evaluation report) should be followed when performing PWR sump analyses. The staff's conclusion applies for the entire spectrum of pipe break sizes which are considered. When performing analyses described in Section 6 of the GR, "Alternate Evaluation," this conclusion applies for both Region I and Region II analyses.

## **4.2.2 Debris Generation**

### **4.2.2.1 Zone of Influence**

This section reiterates that, for the baseline calculation, the GR recommends the use of a spherical ZOI to encompass the effects of jet expansion resulting from impingement on structures and components. It notes that two refinements are to be presented for insulation materials, but none are offered relative to coatings.

**Staff Evaluation for Section 4.2.2.1:** The spherical zone is a practical convenience that accounts for multiple jet reflections and mutual interference of jets from opposing sides of a guillotine break. It is important to note that when the spherical volume is computed using an acceptable approximation for unimpeded free-jet expansion, the actual energy loss involved in multiple reflections is conservatively neglected to maximize the size of the ZOI. The staff concurs with the use of spherical ZOI as a practical approximation for jet-impingement damage zones.

#### **4.2.2.1.1 Method 1: Debris-Specific Spherical ZOIs**

Method 1 refines the evaluation of ZOI by recommending that multiple ZOIs be assigned to each break site, with each corresponding to the destruction pressure of one insulation

species located near the break site. Pressure isobars used to define the equivalent volume spherical ZOI pertinent to a particular insulation type are determined using the methodology of the ANSI/ANS 58.2-1988 standard. Destruction pressures for several insulation types were presented in Table 3-1 of the GR. That table provided the ratio of the ZOI radius to the break diameter for each insulation type listed. The Method 1 discussion notes that no changes to insulation destruction pressures are to be made to account for differences between dry and saturated steam jets. Robust barriers and the effects on the ZOI are to be treated as discussed in Section 3.4 of the GR.

Once the ZOI for each insulation type has been determined, the debris generated within each ZOI is calculated and the individual contributions are summed to arrive at a total debris source term.

**Staff Evaluation for Section 4.2.2.1.1:** The NRC agrees that the definition of multiple spherical ZOI at each break location that correspond to the damage pressures of potentially affected materials is an appropriate refinement for debris generation calculations. Furthermore, it is also appropriate to apply this refinement in a selective manner. For example, a separate well-characterized ZOI can be applied for coatings and all insulation types can be treated according to the baseline assumption of damage equivalent to the most vulnerable material in containment. This approach was illustrated in the Sample Calculation presented in Section 3.4.2.6. Target material inventories within their respective ZOI should be calculated as in accordance with the staff evaluation in Section 3.4 of this SER, including the treatment of robust barriers.

### **Definition of Spherical ZOI**

Application of the ANSI/ANS 58.2-1988 jet model was reviewed in Section 3.4 of the GR and in Appendix I of this report and was found to be an acceptable approach for computing volume-equivalent spherical ZOI. However, material-specific damage pressures that were experimentally determined using high-pressure air as a surrogate working fluid should be treated in a manner similar to that presented in Section 3.4.2.2 to account for potential differences between dry and saturated flashing steam jets. The listing of damage pressure provided in Table 3-1 of the GR implicitly acknowledges the potential for enhanced destruction by citing two-phase destruction tests for calcium silicate. The staff position to reduce destruction pressure by 40% for materials not tested under two-phase conditions is substantial; however, it is less than the decrease measured for calcium silicate.

Three additional refinements related to the application of the ANSI jet model can be developed on a case-by-case basis for selected breaks if it is advantageous to do so:

1. First, the application of worst-case thermal hydraulic conditions to every break location can be relaxed if there is supporting evidence to demonstrate that a particular break location or class of break locations exhibits substantially different conditions that can be conservatively calculated or measured. Maximum damage volumes are generally driven by increased pressure, but these volumes can exhibit a unexpected changes related to the degree of subcooling.. (See Appendix I).
2. Second, the assumption of equivalent maximum mass flux from both ends of a guillotine break can be relaxed if there are supporting calculations to

conservatively substantiate important differences between the thermal hydraulic conditions upstream in either direction. Damage volumes from each side would be calculated independently and then added similar to the way that damage volumes are doubled for the baseline analysis.

3. Third, some credit can be taken via conservative approximation for friction losses in lines leading to the break location if adequate documentation of roughness coefficients, and flow losses in piping components can be provided. This refinement will have the effect of reducing the effective total pressure at the exit plane below the stagnation pressure of the upstream system reservoir. The system stagnation enthalpy should be assumed constant.

It is expected (but not necessary) that these refinements would be pursued on a selective basis for break locations that are found to drive key decision points. For example, limiting breaks identified under the baseline assumptions might be found that impact vulnerable insulation types that are located in high-radiation areas. While replacement of vulnerable insulations with more robust material might be the desired mitigation option, these refinements might be effective in demonstrating that the material should be left in place. If these refinements are applied as described for the purpose of exempting specific targets, the corresponding assumed break locations should be located such that the flow-path distance between break and target is minimized. These refinements can be applied selectively in any combination, and they apply as well to the Method 2 refinement for direct jet impingement.

### **The ZOI and Robust Barriers**

Target material inventories within their respective ZOI or generic ZOI should be calculated as discussed in Section 3.4 of this SER, including the treatment of robust barriers. Section 3.4 does not allow simple truncation for robust barriers as proposed in the GR.

### **Evaluating Debris Generation Within the ZOI**

The NRC agrees that the contributions of each material type to the total debris inventory should be added to determine the debris source term available for transport as described in other sections of the GR and is an acceptable approach.

#### **4.2.2.1.2 Method 2: Direct jet Impingement Model**

This section of the GR offers the refinement of defining the ZOI by modeling two freely-expanding jets emanating from each broken pipe section as opposed to using the spherical ZOI approach presented in Section 3.4. The ANSI standard ANSI/ANS 58.2-1988 is recommended for determining the jet geometry. The specific procedures to be followed for determining jet geometry are summarized, and an example calculation is discussed. The results of the isobar mapping calculations and an example of a plotted isobar are presented in Appendix D of the GR. The treatment of robust barriers and the determination of overall debris generation are the same as for Method 1.

**Staff Evaluation for Section 4.2.2.1.2:** The NRC staff has reviewed this refinement and finds it acceptable. However, there may no longer be a compelling reason to

implement this refinement under the revised guidance of the SER. This refinement retains some spatial information inherent to the direction of the severed pipe. It implicitly assumes that the ends of the pipe are fully separated and fully offset, but yet, remain basically aligned in the original direction. The staff notes that there is no specific analysis of pipe-whip potential if this method is used. However, the spherical ZOI approximation carries similar inherent assumptions (basic alignment of pipe segments to create a spherical ZOI from opposing and interfering jets). Although not explicitly stated, the perceived advantage of this method under strict implementation of the GR would follow from truncation of a jet segment that impinges directly on a barrier like a wall or floor, as well as the economy associated with use of ZOI calculations that have already been performed for local dynamic effects (GDC4 analyses). The practice of ZOI truncation was reviewed in Section 3.4 and was judged to be nonconservative compared to the concept of ZOI volume conservation. In fact, the mapping of an independent directional jet segment within containment would be required for postulated sidewall ruptures if they are considered for analysis. Analysis of sidewall ruptures would carry the additional burden of investigating alternative jet directions. In lieu of mapping directional jet segments for sidewall ruptures, Section 6 of this Safety Evaluation reviews the use of directional (worst debris generation) hemispherical break geometry as an acceptable alternative to assuming a sphere for partial breaks in RCS main loop piping (non-DEGB).

The information provided in this section on ANSI jet modeling is identical to that provided in Section 3.4.2.1 and was reviewed previously. However, the staff would also like to emphasize the GR statement that this refinement requires a high degree of rigor in determining what stagnation pressure each insulation type is subjected to. The first task is to model unimpeded jet expansion using the ANSI standard and Appendix I of this SER for guidance, and the second task is to map relative spatial geometries of targets and the jet in the vicinity of the break location. It is also true, as stated in the GR, that isobar contours like those presented in Appendix D of the GR and Appendix I of the SER have rotational symmetry and can be rotated about the longitudinal axis to define the three-dimensional surface of equivalent damage potential, i.e. impingement pressure.

As a point of nomenclature consistency, there is a conceptual difference between the classical definition of stagnation pressure in a moving fluid as approximated by Bernoulli's Law and the pressures predicted by the ANSI model. The predicted pressures are referred to throughout the SER as impingement pressures because they represent nonisentropic stoppage of the fluid on the face of a target that should be slightly higher than the theoretical stagnation pressure at a freestream point in the flow field. Other limitations to this interpretation of the predicted jet pressures also apply as discussed in Appendix I.

It should be noted that the additional optional refinements discussed above as Method 1 refinements for debris-specific ZOI also apply to this Method 2. The choice of using an approximate spherical geometry or the more realistic geometry of a directed jet is largely independent of the thermal hydraulic assumptions used to compute a jet contour.

### **The ZOI and Robust Barriers**

Target material inventories within their respective ZOI or generic ZOI should be calculated as discussed in Section 3.4 of this SER, including the treatment of robust barriers. The isobar volume of interest should be mapped and conserved independently

for the jet on each side of the break. To be consistent with guidance in Section 3.4.2.3 of this SER, the total damage volume of the two jets should be preserved in a contiguous region rather than crediting overlapping reflections.

### **Evaluating Debris Generation Within the ZOI**

The guidance offered in this section is identical to that presented in Section 3.4.2.5 and has been reviewed previously. Additionally, the contributions of debris from both independently evaluated jets are added to represent the total debris source term.

#### **4.2.2.2 Debris Characteristics**

Section 4.2.2.2 provides additional information regarding the characteristics of debris following a postulated break. The section recommends using plant-specific or publicly available vendor-specific information, where applicable, for refining debris sizes considered in the transport and blockage evaluations. The section includes Table 4-1 that contains recommendations for destruction pressures, fabrication and material densities, and debris characteristic sizes. In addition to replicating data presented in baseline Tables 3-1 and 3-2, Table 4-1 includes recommendations for other materials as well.

**Staff Evaluation for Section 4.2.2.2:** The staff has the following concerns regarding the guidance provided in Section 4.2.2.2.

1. In Section 4.2.2.2.1 “Fibrous Insulation”, the guidance states “Not all generated fibrous debris needs to be assumed to be of a transportable size.” The reality is all debris not specifically attached to a structure can transport given a sufficient driving force. For example, an entire intact blanket of fibrous debris will move in a pool of water if the flow velocities are sufficiently fast. Sheeting flows during testing has shown the capability of moving intact RMI cassettes under certain conditions. The point is that all debris must be considered transportable until plant-specific analyses determine otherwise.
2. Reference 27 was cited in Section 4.2.2.2.2 “Reflective Metallic Insulation (RMI)” as a source of information for the debris size distribution for RMI debris. However, Reference 27 is a report on the testing of NUKON™ insulation and does not contain RMI information. Therefore, an appropriate debris size distribution for RMI debris is not available in the GR. Reference 27 is also inappropriately cited for evaluating coatings in Section 4.2.2.2.3, “Coatings”.
3. In Section 4.2.2.2.3.1, “Coatings within the ZOI”, the GR recommends using the properties of a multiple coating system that produces the post-accident debris with the most detrimental effects to the containment sump. However, the GR does not provide guidance regarding which types of properties (e.g., a light or heavy coating density) would produce the most detrimental effects. The most detrimental properties for debris transport may differ from those most detrimental to head loss. The staff is concerned that such ambiguity in the guidance could lead to improperly determined properties from a conservative standpoint and recommends that each component in a multiple coating system be evaluated separately with its applicable properties. Effective properties for multiple types of debris can then be determined. In a similar statement in

Section 4.2.2.2.3.2 “Coatings outside the ZOI”, assuming properties for unidentified non-DBA-qualified coatings systems used outside the ZOI should assume the most detrimental properties needs more supporting guidance regarding which types of properties are most detrimental.

4. In Section 4.2.2.2.4, the GR recommends assuming that all tape and stickers located in the ZOI are destroyed into small pieces and fibers. The positive aspect of the assumption is the subsequent transport to the sump screens would than be 100% of this debris. However, it is not a forgone conclusion that assuming the debris is destroyed into small pieces and fibers would cause a higher head loss than if this debris arrived at the screens intact, which is one of the potential realities, at least for non-soluble tapes, stickers, and tags. As intact debris, this debris could effectively interdict flow through covered portions of the screen thereby effectively reducing the size of the screen. Hence, the GR statement that it is conservative to assume that all debris created from tape and stickers is reduced into fine or small pieces or individual fibers is not supported. It is recommended that the head loss evaluation estimate the head loss by assuming each condition of the debris, and then use the higher head loss in the NPSH margin determination.
5. In Section 4.2.2.2.5 “Fire Barrier Materials”, fire barriers consist of many types of insulation and other materials including board materials, blanket materials, and foam materials. With a few exceptions, debris generation data does not exist for fire barrier materials that differ from the piping insulations tested. The GR recommends “For materials that are unique to fire barrier applications and do not have supporting test data, a destruction pressure equal to that of low-density fiberglass may be assumed.” While this guidance seems reasonable for fire barrier materials consisting of a low-density fiberglass or even a high-density fiberglass, it is not acceptable to apply data for low-density fiberglass to the variety of fire barrier materials, e.g., board and foam materials.

The staff did not independently verify all the data contained in GR Table 4-1 and has the following concerns:

1. Table 4-1 provides four seam orientation calcium silicate destruction pressures (i.e., 0°, 45°, 180°, and generic orientation) without additional guidance and the zero degree reference was not stated. Application of seam oriented destruction pressures requires orientation specific jet destruction models. As discussed in Appendix II, because substantial insulation damage occurred at a jet pressure of 24 psi in the OPG tests (45° orientation), the lowest pressure tested; the threshold pressure for destruction is actually less than 24 psi. The staff recommends using the recommendation in NUREG/CR-6808 of 20 psi for calcium silicate.
2. The destruction pressure recommended in Table 4-1 is 2.5 psi for blanketed and unjacketed Min-K whereas in the baseline Table 3-1 the GR recommendation is 4 psi. Hence, these two recommendations are in conflict. The staff recommends using a destruction pressure of 2.5 psi for blanketed unjacketed Min-K in the baseline as well as in the refinements. The GR recommended destruction pressure of 6 psi for blanketed jacketed Min-K with

SS bands and latch and strike locks does not specify the jacket construction. Unless a specific jacket construction can be correlated to test data whereby it can be shown that a pressure of 6 psi or greater is needed to compromise that specific jacket, then the lower destruction pressure of 2.5 psi should be used.

3. It is noted that several data are missing from Table 4-1 that will be required by the analyst. For example, the material density for Min-K is specified as NA but will be required when applying the GR recommended NUREG/CR-6224 head loss correlation.
4. Some data were assumed without justifying remarks, e.g., the destruction pressure for Microtherm was apparently set equal to that of Min-K. Some rationale should have been presented for this and other justifications.
5. The as-fabricated density of Kaowool is specified as 9.4 lbs/ft<sup>3</sup> in Table 4-1 but given as range of 3 to 12 lbs/ft<sup>3</sup> in baseline Table 3-2. If this density is a manufacturing variable, then the plant-specific as-applied density should be used. As illustrated in Appendix V, the head loss evaluation is very dependent upon this number.

#### **4.2.3 Latent Debris**

Although the GR does not identify any generic analytical refinements for quantifying latent debris in this section, other suggested by the staff in Section 3.5 for sampling plans could be viewed as refinements to a conservatively assumed baseline inventory. Other plant-specific improvements to the evaluation of the latent debris source term beyond those outlined in Section 3.5 require review by the staff. Specific details of an improved characterization plan do not require prior approval if the plan is designed to satisfy the objectives of estimating total plant-specific inventory of both fiber and particulate and characterizing the properties of this debris with respect to their hydraulic head-loss properties.

#### **4.2.4 Debris Transport**

Section 4.2.4 recommends two methods of analytical refinements for determining the flow characteristics of the sump pool for the purpose of predicting the transport of debris in the sump pool to the recirculation sump screens. These methods included the open channel flow network method (Section 4.2.4.1) and the three-dimensional computational fluid dynamics (CFD) method (Section 4.2.4.2). Aspects of the network method discussed included the following: the analytical approach, model input development, and the network solution. An example network model was superimposed onto a corresponding CFD result. No discussion was provided regarding the use of network predicted results to estimate debris transport within the sump pool. Aspects of the CFD method discussed included the following: the selection of software, the building of a CAD model, the CFD analysis, and the prediction of debris transport using the CFD results.

The debris transport discussion associated with the CFD modeling included a discussion of plotting velocity magnitude contours for the minimum bulk transport velocity at selected levels within the containment pool. After the area within this transport velocity

contour is determined, the debris within this area is assumed to transport to the sump screen.

The GR also includes Table 4-2, "Debris Transport Reference Table," that provides transport data such as the minimum velocities needed to transport debris.

**Staff Evaluation for Section 4.2.4:** Of the two methods of analytical refinements for transport of debris in the sump pool the staff identified the following challenges in using the open channel network method:

1. The implementation of the network method requires the adaptation of multiple correlations for estimating form loss coefficients and friction factors (correlations typical of piping pressure loss calculations). At each network node junction, a form loss coefficient is required that simulates flow for the connecting nodes. The complexity of the sump pool channel will require the analyst to make engineering judgment adaptations for the application of generic correlations and the complexity of the model input development can severely limit the detail of the model resulting in a rather coarse nodalization.

The coarseness of the network method, as illustrated by the example nodalization in GR Figure 4-4, limits the simulation of important aspects of the sump pool such as the complexity of the flow channel, obstacles to flow, and the complex distribution of containment spray drainage entering the pool. The example nodalization has ignored portions of the sump pool without providing a rationale for determining which portions of the pool do not need to be modeled.

2. The model coarseness forces the analyst to rely on predicted bulk velocities between coarse nodes and therefore cannot predict localized flow conditions that are capable of moving debris even if the bulk flow velocities indicate no movement of debris. An example of localized flow is vortices that could be completely internal to a network node. Testing [NUREG/CR-6773] has shown that vortices affect debris transport.
3. The network method is not capable of predicting sump pool turbulence or its effects on debris transport. Sump pool turbulence has been shown to affect debris suspension within the pool (e.g., water flows falling into the sump pool can suspend debris that would normally settle in calm water) and the rates of erosion (Section III.3.3.3) for certain types of debris (e.g., fiberglass insulation debris).
4. The network method is not capable of predicting pool characteristic during pool formation that affect the transport of debris during this period such as the initial spreading of water across the floor or the filling of inactive portions of the sump (e.g. reactor cavity).
5. The large number of input parameters associated with specifying a network nodalization model (e.g., inputs to form loss correlations) could make the performance of a quality sensitivity evaluation for those input values difficult.

Appendix C compares the results of the open channel network method to the results of CFD method. The staff concluded that the results do not agree in contrast to the assertion in the GR that the network and CFD results compare favorably. The difference in flow rates of less than 10% were calculated by dividing by the total recirculation flow but not on the differences between specific node junction flows. For example, the GR quoted error for Channel 156 is 7.7% (Table C-1) but the flow for the network method is in the opposite direction to that of the CFD analyses. If the difference for Channel 156 were calculated as the difference between the network and the CFD predicted flow rates divided by the CFD the result would have been 56% instead of 7.7%. In addition, the flows of the network and CFD methods are in the opposite direction.

The GR recommends adding 10% to the calculated channel flow rates but the staff recommends that the safety factor applied to the network calculated results be based benchmark analyses of the network methodology against experimental debris transport results and/or superior analytical methods. In addition, a method is still needed to perform the needed analysis that is well beyond the capabilities of the network method.

Regulatory Position 1.3.3.4 of Regulatory Guide 1.82, Revision 3, states the following:

An acceptable analytical approach to predict debris transport within the sump pool is to use computational fluid dynamics (CFD) simulations in combination with the experimental debris transport data. Examples of this approach are provided in NUREG/CR-6772 and NUREG/CR-6773. Alternative methods for debris transport analyses are also acceptable, provided they are supported by adequate validation of analytical techniques using experimental data to ensure that the debris transport estimates are conservative with respect to the quantities and types of debris transported to the sump screen.

Consistent with the above regulatory position the staff accepts the nodal network method as an alternative method to calculate debris transport onto the sump screens. However, the licensees need to support this method using experimental data to ensure that the debris transport estimates are conservative with respect to the quantities and types of debris transported to the sump screen.

The staff finds that the GR presentation regarding the CFD method and analysis is thorough. Specific staff comments include:

1. The GR suggests using turbulent turbine kinetic energy (TKE) profiles in the pool as a pool characteristic but fails to prescribe how this information would be useful in the debris transport analysis. The staff recommends a potential adaptation of a CFD method employed in the BWR drywell debris transport study (DDTS) [NUREG/CR-6369, Vol. 3] where the CFD code is also used to simulate applicable tests where debris settling was correlated to the CFD predicted turbulence indicators.
2. The GR discussions regarding the level of detail or analytical fineness to model does not adequately address potential plant features that can significantly affect sump pool hydraulics.. For example, the GR statement that "Obstructions less than 6 inches in diameter or the equivalent may be omitted," is too general a statement. If there is a single 6 inch obstacle, it might be argued that it can be

neglected but if there is a series or array of 6 inch objects, then the array may need to be modeled.

3. Other model development aspects, including the following, should be properly assessed before selecting modeling options: the type and size of calculational mesh, boundary conditions inflow and outflow options, and convergence criteria. Many of the modeling options depend upon the CFD code selected and the model development should properly select the best options for the plant-specific sump pool evaluation.

The GR recommends using a uniform distribution of debris on the sump floor, i.e., the sump pool debris transport fraction is equal to the floor area fraction where the velocity is greater than the minimum transport velocity (GR Section 4.2.4.2.5). This recommendation is not acceptable because the debris entrance into the pool is not uniform. The staff provided supplemental guidance in Appendices III and VI addressing sump pool debris transport and blowdown/washdown transport, respectively, in the volunteer plant. Appendix III demonstrated that the GR floor area transport model would underpredict the sump pool debris transport in the volunteer plant by a wide margin. Debris initially deposited onto the sump floor in the volunteer plant was preferentially deposited within or near the break compartment due to the partial confinement of debris in the break compartment and debris initially deposited in the upper levels of the containment would washdown with the drainage of the containment sprays entering the sump pool at discrete locations, typically in the faster areas of the pool. The licensees should use the debris transport methodologies presented in Appendices III and IV for refined analyses.

The GR did not address the debris size distributions. In the GR baseline, a two group size distribution was recommended where the small fines would completely transport to the sump screens and the large debris would not transport at all. Therefore, the sump pool debris transport refinement cannot be applied to small fines because at least a portion of this group must be treated as suspended fines with complete transport. A refinement can be applied to the large size group but in the baseline guidance this group is assumed to not transport. In order, to proceed with a sump pool analytical refinement, a better defined size distribution that addresses the key aspects of debris transport is required. In addition, if the analytical refinement is applied to the small debris, it must also be applied to the large debris that is neglected in the baseline methodology. The licensee should use the four size categories used in both Appendices III and VI for fibrous debris. This size distribution has: (1) fines that remain suspended, (2) small piece debris that transport along the pool floor, (3) large piece debris with the insulation exposed to potential erosion, and (4) large debris where the insulation is still protected by a covering thereby preventing further erosion.

GR Table 4-2, "Debris Transport Reference Table," provides useful data and references NRC published documents as the source of the data. However, one column in the table provides selected values for TKE energies required to suspend debris that are not in the referenced NRC published documents. Without knowing the basis for the TKE energies, these numbers cannot be reviewed or accepted. Typically, the determination of such numbers is done by applying a CFD code that has turbulence modeling capabilities to applicable debris transport experiments where debris settling is examined at different levels of turbulence, such that energy threshold values can be determined that allow

debris to settle. Because the turbulent energy models within CFD codes vary, the TKE numbers should be considered as code-dependent. As such, the energy model used in the code performing plant-specific evaluation should be the same or equivalent to the model used to determine the TKE threshold numbers. The staff has not assessed or accepted the TKE numbers presented in GR Table 4-2.

**Staff Conclusions Regarding Section 4.2.2:** Section 4.2.4 recommends the open channel flow network method and the three-dimensional computational fluid dynamics method for refining the analysis for transport of debris in the sump pool to the recirculation sump screens. Consistent with Regulatory Guide 1.82, Revision 3, the staff accepts (1) the CFD method and (2) the nodal network method as an alternative method to calculate debris transport onto the sump screens. However, the licensees using the nodal network method need to support it using experimental data to ensure that the debris transport estimates are conservative with respect to the quantities and types of debris transported to the sump screen. The GR recommended debris transport model in Section 4.2.2 that appears to assume using a uniform distribution of debris across the sump floor is not acceptable because the debris entrance into the pool is not uniform. Appendices III and VI provide additional staff guidance on adapting the debris transport methodologies for refined analyses.

#### **4.2.5 Head Loss**

The GR states that no head loss refinements are offered other than those given in Section 3.7.2.3.2.3. (See SER Section 3.7.2.3.2.3, "Thin Fibrous Beds," for the staff evaluation of that section.) The supporting Appendix E repeats the text found in Section 4.2.5, and provides tables that summarize available domestic and international head loss testing and results.

**Staff Evaluation for Section 4.2.5:** The staff did not identify any specific analytical refinement(s) offered in Section 4.2.5, or Appendix E.. Therefore, no evaluation is provided for analytical refinement(s) to the head loss analysis.

## 5.0 DESIGN AND ADMINISTRATIVE CONTROL REFINEMENTS

Industry representatives including the Nuclear Energy Institute (NEI), the Westinghouse Owners Group, and various participants from individual utilities have followed the development, research, and resolution process of GSI-191 for several years. Over this time, practical insights have been gained by the participants regarding the relative importance of each stage of the accident sequence to the overall assessment of recirculation-sump vulnerability. This section addresses the phenomenology associated with debris generation, debris transport, debris accumulation and head loss across beds of mixed composition. As the knowledge base of research data and plant survey information has improved, and as analytic methods have developed to address each aspect of the complex accident sequence, so too has the awareness of potential vulnerabilities grown. Recognition and understanding of the principle contributors to sump-screen vulnerabilities has initiated a discussion about possible mitigation strategies that seek to interdict the accident progression at one or more of the aforementioned stages.

Self assessment of recirculation sump vulnerability and the identification of site-specific contributing factors is a responsibility of each licensee, but this chapter attempts to share the broader industry perspective on possible improvements that a licensee can make to improve their sump-performance posture, regardless of their current plant condition.

Based on the findings of individual licensees, the range of mitigative actions pursued across the industry may range from status quo operation to sump-screen replacement. In many cases, though, new awareness of the issues involved with ensuring sump-screen performance will lead to at least procedural changes that help avoid unnecessary exposure to the risk of sump-screen blockage. With improved understanding of a problem comes a new perspective of common-sense regarding the simple things that can be done to improve safety as well as the detailed knowledge required to effect engineered solutions to a specific technical problem. This chapter provides insights at both levels. The discussion presented here may be sufficient for a given licensee to address any identified problems. For others it may motivate progress towards a site-specific solution of their own devising. It should also be recognized that successful management of sump-screen vulnerability may require a combination of the approaches presented in this chapter.

Given the diversity of possible responses to this issue and the variety of site-specific solutions that will be developed at varying degrees of complexity, the NRC cannot prematurely endorse any one mitigation strategy that is offered here. Assessments of relative effectiveness expressed in the GR are the opinion of the industry representatives. The staff believes that this information improves the practicality of the GR because licensees are immediately motivated to find workable solutions to any problems that are identified during their vulnerability assessments. Any necessary changes to plant configuration, technical specifications, operating procedures or other licensing basis changes should still consider the need for NRC staff review and approval. Licensees should consider existing regulatory processes, and if necessary, submit any required information for staff review. An important aspect of the existing review process is the need for applicable testing and analysis of any new equipment or materials that are incorporated into the ultimate resolution strategy. In this manner, the NRC can judge the effectiveness of the approaches chosen by each licensee. For these reasons, the staff review of Chapter 5 is limited. The staff found the technical

descriptions in this chapter to be acceptable as an introduction to the topic of mitigating sump-screen vulnerabilities.

## 5.1 DEBRIS SOURCE TERM

Five categories for design and operational refinements are examined in this section. Staff comments on each category are itemized below.

1. **Housekeeping and FME Programs:** The GR recommends that if housekeeping or FME programs are implemented or revised to reduce the latent/miscellaneous debris burden then appropriate procedures should be designed to ensure a high level of performance. The staff wishes to emphasize that such procedures and performance metrics, based on swipe sample analyses, for example, may be required if vulnerability assessments rely on periodic cleaning activities to maintain debris loadings below some minimum level of concern.
2. **Change-Out of Insulation:** Two additional comments are offered by the staff in addition to those itemized in the GR. First, it should be noted that while change out of problematic insulation types may address the issue of maximum debris loadings on the screen, it might not address the issue of minimum loadings required to form a thin filtration bed. To satisfy both concerns, a combination of strategies in addition to change out might be needed. Second, the large-scale removal of some insulation types may inadvertently increase the latent debris loading of residual insulation materials unless removal is performed carefully to minimize the spread of fine materials or effective plant cleaning routines are implemented after insulation removal to recover dispersed material.
3. **Modify Existing Insulation:** This may effectively address the issue of maximum debris loads on the screen without changing the minimum loadings required to form a thin filtration bed. To satisfy both concerns, a combination of strategies in addition to modification of existing insulation may be required.
4. **Modify Other Equipment or Systems:** The staff agrees that changes to noninsulation items should be considered in the context of the entire sump performance evaluation. Another example of beneficial change to equipment was suggested by the discussion of latent debris surveys that identify unique collections of particulate or fibrous material like filter housings that are vulnerable to water infiltration. If such sources can be sealed or protected from containment spray, then the internal inventory will not be released to the sump pool.
5. **Modify or Improve Coatings Program:** Under the conservative assumption that 100% of unqualified coatings will fail, the staff agrees that conversion to DBA qualified systems would reduce the source term contributed by failed coatings. However, coatings systems that are currently unqualified could be qualified through appropriate testing. Depending on the rigors of the ASTM testing standards, some of this testing might be accomplished in place to avoid destructive sample collection from existing surfaces and equipment. Additionally, the staff does not agree with recommendation number 5 is the statement that DBA-qualified coatings have very high destruction pressures.

This statement has not been proven for the simultaneous combination of high-temperature and high-pressure jet impingement. See Sections 3.4.4 and 4.2.2.2.3 for more discussion on acceptable coatings destruction pressures.

## **5.2 DEBRIS TRANSPORT OBSTRUCTIONS**

This section examines various options for redirecting or retarding the movement of debris towards the sump screen. The objective of these approaches is to trap or sequester debris so that it cannot reach the sump screen during recirculation. Transport velocities are highest during pool fill up when sheeting velocities can move large pieces of debris that are initially impacted on the floor near the break or washed to the floor by the break effluent. During this timeframe, flow direction is not preferentially towards the sump. As the containment pool fills, sheeting velocities decrease. With the onset of recirculation flow, debris transport with a preferential direction aligned towards the sump screen is established. Design of obstructions to provide a barrier to debris transport to the sump screens should consider all phases of pool fill and establishment of recirculation flow.

### **5.2.1 Floor Obstruction Design Considerations**

Careful thought must be given to the stability of the holding location with respect to turbulence introduced by cascading containment spray water. For example, if diversion baffles successfully collect debris during fill up in a drainage zone that is highly agitated by falling water, the net result may be to increase the fraction of individual fibers and fine material available for transport to the screen under low recirculation velocities. During initial fill up, curbs may be subjected to significant flow velocities, so heights would need to be designed accordingly in order to be effective. Removable structures like debris rakes and baffles may also experience significant hydrodynamic force loadings during fill up. The test data cited from GR reference 54 for the effectiveness of curbs is very rudimentary. Significant opportunity exists for optimizing curb designs to accomplish the complimentary objectives of debris capture and/or debris diversion.

#### **5.2.1.1 Test Results**

During pool fill up, flow directions are dictated by the location of the break and the containment geometry. During recirculation, there is a directed flow path towards the sump screens, but perhaps at lower bulk velocities. None of the data apply to turbulence induced from direct water splashing near the curbing. It is noted that curbs could be an especially important strategy for protecting horizontal sump screens from debris build up while the sump cavity is filling. To effectively design curbing a reasonable detailed understanding of water velocity and direction is needed during the phase of transport for which the curbs are intended to be effective. The staff also notes that while curbing may be effective at impeding the migration of larger debris along the floor, curbs do not address the problem of suspended fines. Thus, the overall effectiveness of curbing and debris racks (next section) will depend on the site-specific debris types that they were designed to mitigate.

### **5.2.2 Debris Obstruction Rack Design Considerations**

There is ample room for optimization of rack designs for trapping debris before it reaches the sump screen. One conceptual design that has been discussed involves two or more parallel racks placed across the flow path to act as weirs over which the water must flow while depositing larger debris in the spaces between racks. For this to be effective, the mesh size and height of the baffles would need to be optimized for the size of the debris and the depth of the pool in order to prevent obstruction of water flow. This design concept of interstitial capture between vertical risers might also be incorporated directly into a multilayered suction strainer where the outer layers serve initially to attract and capture debris leaving the inner layers clear to provide adequate water flow.

#### 5.2.2.1 Test Results

The test results cited from GR reference 55 focus on tumbling and sliding of debris along the floor. During pool fill, water velocities could be much higher than the incipient velocities listed in GR Table 5-1. The use of racks may effectively manage larger debris items moving along the floor, but would not stop the migration of individual suspended fines.

#### 5.2.2.2 Debris Rack Grating Size

In this section, the GR emphasizes several of the design considerations mentioned above in Section 5.2.2 of the SER.

### 5.3 SCREEN MODIFICATION

#### Staff Evaluation of Section 5.3:

This section of the GR provides guidance regarding potential sump screen designs and features. The relative effectiveness of curbs and debris racks depends on the characteristics of the debris that challenge the sump screen. While these design features may be effective at preventing the migration of large volumes of debris along the floor, they may not be effective at preventing transport of suspended fines. Therefore, depending on the dominant debris types at a site, licensees may determine that it may be more cost effective to modify screen configurations to manage the entire range of debris size. The GR considers the attributes of three generic design approaches that might licensees might pursue. These include passive strainers, backwash strainers, and active strainers.

The staff to emphasizes two performance objectives that should be addressed by a sump-screen design. First, the design should accommodate the maximum volume of debris that is predicted to arrive at the screen given full consideration of debris generation, containment transport and auxiliary mitigation systems like curbing that may be in place. Second, the design should address the possibility of thin-bed formation. When fibrous debris are expected as part of the limiting break condition, the screen should accommodate a large fraction of the expected fines (both from the ZOI and from potential pool degradation) as individual fibers with the potential to form a uniform layer. The difference between these objectives relates to the degree of uncertainty in debris transport methodology that the screen design should accommodate. While it is difficult to argue that debris will not transport (first objective), it is equally difficult to guarantee that it will transport (second objective). Thus, both extremes must be satisfied by the screen design.

### 5.3.1 Considerations for Passive Strainer Designs

The large appeal of passive strainers relates to their simplicity of maintenance and high reliability for an adequately tested design, both important considerations for safety-related equipment. While the GR accurately presents the general attributes of existing passive designs, the presentation is focused on applications of one-dimensional head-loss correlations that have traditionally lead to large strainer designs. Water velocity through the debris bed is an important factor in predicting head loss, so larger surface areas imply lower velocity for a given recirculation flow, and hence, lower head loss. The challenge with this approach is to achieve a large surface-to-volume ratio by using a convoluted screen geometry that traps debris while providing adequate recirculation flow and not taking up too much space in containment.

Given the requirement in some plants to address thin-bed formation for potentially large amounts of fine fibrous debris, large compact surface areas alone may not be sufficient. Two alternative design concepts may be effective, perhaps in combination with compact geometries that achieve large surface-to-volume ratios. Generically, these design concepts may be described as disrupting the formation of a uniform fiber layer by (a) using a complex porous filter structure to capture fiber, or (b) designing hydraulic flow paths that amplify velocity gradients across the flat surfaces of the strainer where fiber first approaches.

The first design concept can be imagined as a prefilter, made perhaps of crumpled wire cloth (~1-inch mesh) or similar material, that creates a very porous volumetric filter on the face of a standard sump screen for the purpose of capturing fibers with minimal head loss. Porosity and thickness of the prefilter section would require design optimization to accommodate a specific quantity and size of suspended fiber debris. The second concept utilizes small friction losses internal to the body of a convoluted filter structure that has many fins, fingers, plates or other protuberances on which to capture debris. Small internal friction losses can be enhanced and designed to create velocity gradients across the external surfaces of the filter. If properly designed, this feature might be effective at directing the build up of fiber in a controlled way that avoids uniform simultaneous coverage of the strainer face. This might be used to efficiently pack material on an essentially sacrificial surface while leaving other flow areas unobstructed. These concepts, and other innovations, share a common requirement for adequate design testing, but they may offer cost effective solutions to the drawbacks of large passive strainers presented in the GR.

### 5.3.2 Considerations for a Backwash Strainer Design

In addition to the practical considerations for a backwash strainer design offered in the GR, the NRC staff contributes the following observations. The staff agrees that backwash systems may be required to undergo design testing and possible surveillance testing to demonstrate that they will work as intended.

1. Any design that attempts to clear an existing debris blockage should give careful consideration to the problem of resuspension and redeposition of that debris. If the working fluid is applied too violently, a cloud of debris may temporarily disperse and then reform a bed on the screen. Testing may show that this is acceptable behavior that reduces the screen loading enough to be effective regardless of bed reformation.

2. It is stated implicitly in the GR that normal recirculation flow will be stopped during backflushing. This may raise concerns about restart reliability of the ECCS system. Some backflush designs might be able to operate effectively without interrupting ECCS flow. For example, a continuous water-jet curtain directed across the face of the screen might be effective at preventing debris buildup to unacceptable levels. This water flow might be provided as a side stream from the main ECCS system so that no additional pumps, actuators or valves need be qualified.
3. Debris beds, especially fiber-based mats, are effective filters of suspended particulate. If the entire debris mat is disturbed very quickly, the local concentration of material that can pass through the screen is suddenly very high. This may represent a unique challenge to downstream components that is not present during normal recirculation flow.
4. Most debris beds studied to date are held to the screen only by the pressure of the water flowing through them. They form no particular adhesive or mechanical attachment to the screen. Fibrous beds have been observed to slump or sluff off of the screen in contiguous mats. For designs where ECCS flow is interrupted, this behavior presents an opportunity for collecting or trapping the debris that loosens from the screen without dispersing it greatly. Debris racks, or bins might be designed to sequester the debris mats and minimize redeposition. Minimum-flow backflush systems in combination with inclined screens that provide gravity assist for the detachment might benefit the most from this behavior.
5. Item 5 in the GR suggests automated control systems to actuate the backwash cycle based on measurement of pressure drop or flow. For backwash systems that function intermittently upon actuation, some degree of information feedback and/or intervention might be given to operators to increase the flexibility and utility of the backflush system as a recovery alternative for potential sump blockage.

### **5.3.3 Considerations for an Active Strainer Design**

Active strainer concepts offer much greater design flexibility for addressing the challenges of debris accumulation in PWR recirculation pools. , Therefore, they offer some unique advantages over the other two generic screen designs. Several such advantages are presented as favorable technical considerations in the GR. One contradiction that the staff would point out relates to favorable technical consideration number 3, which offers the opinion that self-cleaning strainers may avoid uncertainties related to various debris generation and transport phenomenology. However, the same active strainer features that indicate success for some phenomena might also exacerbate problems for other phenomena. As an example, adhesive chemical corrosion byproducts might be smeared into a semi-impervious layer across the sump-screen mesh by a scraping device whereas the same debris might be dislodged by an optimized backflush system.

Active designs can carry a greater burden of proof for effectiveness and operability depending on their complexity, and the staff agrees with additional consideration number

1 that experimental studies would be needed to demonstrate the effectiveness of proposed active strainer designs. In general, many of the considerations for an active strainer design like power supply, control system reliability and functional reliability are similar to those presented in the GR for backwash systems.<sup>1</sup> Many of the staff observations are also similar. For example, active-strainers may be most effective when combined with mechanisms for debris collection and sequestration that over time reduce the local suspended debris concentration that poses a challenge to the strainer surface.

To maintain the generality of this discussion, the NRC prefers the terminology "active strainer" over the description of "self-cleaning." The GR accurately defines an active strainer as a design that incorporates active components to maintain flow to the sump, but there the generality of the presentation ends and discussions of self-cleaning mechanisms begin. Because there are no active strainer applications for either BWR suppression pools or PWR sumps, there should be no preconceptions imposed regarding typical active designs. Similarly, while continuous cleaning of the strainer surface area might be one desirable performance metric of an active design, it is not the only method of maintaining flow to the sump.

Another class of design solutions exists that periodically clean the strainer surface rather than continuously cleaning the surface. Consider, for example, a set of flat, parallel, inclined sump screens that are latched at the top corners and hinged at the bottom corners. When the outer face is loaded with debris, the latches are released and the screen swings to the floor, exposing a fresh screen for debris collection and trapping its debris inventory from further transport. Other more ingenious methods may be developed using gravity assisted debris detachment on downward inclined screen surfaces. Internal flows could be alternately switched between separate chambers of the strainer to permit detachment on one side while drawing flow from the other side. Flow baffles might be switched with actuation mechanisms and control logic systems or by simple rotation of a spindle based on hydraulic flow imbalance between the chambers. The success or failure of any innovative design concept depends on how completely it can satisfy the additional considerations presented in the GR, but once the commitment has been made to facing these design challenges, no restrictions should be placed on the options available for a successful plant-specific solution.

#### 5.3.4 Summary

In combination with staff comments provided in this SER, the NRC finds this chapter of the GR to be a useful and acceptable introduction to the variations in sump-screen design that may be pursued for sump modification by an individual licensee. The exact definitions of the generic categories and the particular label given to an innovative design are not as important as the generic attributes that have been defined in the GR. These attributes serve as a basis for comparing the technical challenges and benefits, and the potential programmatic costs of alternative design solutions. Any consideration of screen modifications should be made in the context of the comprehensive site-specific vulnerability assessment. Alternative combinations of source mitigation, design changes, and administrative control should be weighed against existing debris types, containment geometry constraints, and NPSH margins.

---

<sup>1</sup> In fact, after correcting a typographical error near the end, item 6 should read, "Margin must be available to initiate *active strainer mode* before sump blockage affects either ECC or CS operation."

## 6.0 ALTERNATE EVALUATION

### 6.1 BACKGROUND AND OVERVIEW

Section 6 of the GR describes an alternate evaluation methodology for demonstrating acceptable containment sump performance. The alternate evaluation methodology described in this section is shown as Option B in Figure 2-1 of the GR.

For the last several years, the NRC has recognized that probabilistic risk assessment (PRA) has evolved to the point that it can be used increasingly as a tool in regulatory decision making. Through its policy statement on PRA (ADAMS Accession number ML021980535), the Commission expressed its expectation that enhanced use of PRAs will improve the regulatory process in three ways: through safety decision making enhanced by the use of PRA insights; through more efficient use of agency resources; and through a reduction in unnecessary burdens on the licensees.

The NRC staff has considered the development of risk-informed approaches to the technical requirements specified in 10 CFR 50.46, and these considerations are documented in numerous communications between the Commission and the staff (SECY and Staff Requirements Memorandums (SRM)). The NRC Commissioners, in their March 31, 2003 SRM, directed the staff to undertake several rulemakings, one of which would develop a proposed rule to allow, as a voluntary alternative, a redefinition of the design basis LOCA break size. In a March 4, 2004 letter to NEI (SB, 2004), the staff stated that it would discuss, in public meetings, the use of current or planned work to risk-inform 10 CFR 50.46 as a suitable technical basis for defining a spectrum of break sizes for debris generation and containment sump strainer performance.

Specific to GSI-191, the Commission recently requested the staff to, "implement an aggressive, realistic plan to achieve resolution and implementation of actions related to PWR ECCS sump concerns." One such resolution path involves the LOCA break size used in PWR sump analyses. For example, it is well understood that the amount of debris generation to be expected following a LOCA is dependent on the break size, and generally that less debris would be generated with a smaller LOCA break size (although less debris generation may be worse in certain situations when considering debris type and break location). The staff is already working to risk-inform 10 CFR 50.46 to redefine the design-basis large break LOCA break size based on expected LOCA frequencies. A comparable approach for use in GSI-191 resolution would identify a "debris generation" break size which would be used to distinguish between customary and realistic design basis analyses. However, it is very important to note that an alternative approach for resolving GSI-191 would not redefine the design basis LOCA break size in advance of the 10 CFR 50.46 rulemaking effort. In developing an alternate approach for resolving GSI-191, the staff intends to remain at least as conservative as, and consistent with any forthcoming revision to 10 CFR 50.46.

On May 25, June 17 and June 29, 2004, the staff met with NEI, industry representatives and stakeholders, in category 2 meetings, to discuss alternate, realistic and risk-informed approaches for resolution of the PWR sump issue. Throughout these meetings, both NRC and NEI staff presented proposals and positions regarding technical and regulatory elements of alternative approaches.

These interactions between the staff, NEI, industry representatives and stakeholders yielded an alternative approach which includes both realistic and risk-informed elements. For such an approach, licensees would continue to perform design basis long-term cooling evaluations and satisfy design basis criteria for all LOCA break sizes up to a new "debris generation" break size that would be smaller than a double ended guillotine break (DEGB) of the largest pipe in the reactor coolant system (RCS). This analysis space is referred to as Region I in the GR. Long-term cooling must be assured for breaks between the new "debris generation" break size and the double-ended rupture of the largest pipe in the RCS, but the evaluation may be more realistic than a customary design basis evaluation, consistent with the small likelihood of the break occurring. For breaks larger than the "debris generation" break size, licensees could apply more realistic models and assumptions. This analysis space is referred to as Region II in the GR. Additionally, any physical modifications to plant equipment, or operator actions credited to demonstrate mitigative capability for these larger breaks (Region II) would not necessarily need to be safety-related or single-failure-proof. Changes to the existing facility designs, and credit for operator actions would require that risk evaluations be performed, consistent with Regulatory Guide 1.174. Licensees would need to ensure that the changes to the facility design would have sufficient reliability to provide reasonable assurance that they will perform their intended function.

While not a component of the 10 CFR 50.46 ECCS evaluation model, the calculation of sump performance is necessary to determine if the sump and the residual heat removal system are configured properly to provide enough flow to ensure long-term cooling, which is an acceptance criterion of 10 CFR 50.46. Therefore, the staff considers the modeling of sump performance as the validation of assumptions made in the ECCS evaluation model. Since the modeling of sump performance is a boundary calculation for the ECCS evaluation model, and acceptable sump performance is required for demonstrating long-term core cooling capability (10 CFR 50.46 (b)(5)), the requirements of 10 CFR 50.46 are applicable. Based on this, such an alternative approach might require plant-specific license amendment requests or exemption requests from the regulations, depending on each licensee's chosen resolution approach. Licensees could request, on a plant-specific basis, exemptions from the requirements associated with demonstrating long-term core cooling capability (10 CFR 50.46 (b)(5)). For example, exemptions from the requirements of 10 CFR 50.46 (d) would be required if a licensee chose to classify new equipment as non-safety related or non-single failure proof. For purposes of GSI-191 resolution, exemption requests would not be applicable to the other acceptance criteria of 10 CFR 50.46 (peak cladding temperature, maximum cladding oxidation, maximum hydrogen generation and coolable geometry), and would be submitted in accordance with existing NRC regulations (10 CFR 50.12). Additionally, license amendment requests may be needed for changes in analytical methodology or assumptions. Licensees would assess the need for license amendment requests in accordance with the requirements of 10 CFR 50.59.

NRC staff review and acceptance of such plant-specific license amendment or exemption requests would consider the following elements:

- Application of the principles of Regulatory Guide 1.174, "An Approach for Using Probabilistic Risk Assessment in Risk-Informed Decisions On Plant-Specific Changes to the Licensing Basis." (defense-in-depth, safety margins, delta Core Damage Frequency, delta Large Early Release Fraction)

- Consistency with NUREG-0800 (Standard Review Plan), Section 19, "Use of Probabilistic Risk Assessment in Plant-Specific, Risk-Informed Decisionmaking: General Guidance."
- Design-Basis, deterministic analyses necessary to verify compliance with 10 CFR 50.46 (b)(5) for break sizes up through "debris generation" break size.
- Acceptable mitigative capability up through the DEGB of the largest pipe in the RCS. The equipment needed for mitigative capability would have some functional reliability requirements, but would not necessarily need to be safety-related or single failure proof.

One key element of Regulatory Guide 1.174 involves assurance that defense-in-depth is maintained. Although a "debris generation" break size is selected to distinguish between customary and more realistic design basis analyses, the staff would require that licensees demonstrate acceptable mitigative capability for LOCA break sizes up through the DEGB of the largest pipe in the RCS. This philosophy is consistent with recent recommendations made by the Advisory Committee on Reactor Safeguards (ACRS) in their April 27, 2004, letter to the Chairman. Requiring that mitigative capability be maintained in a realistic and risk-informed evaluation of the PWR sump issue for all LOCA break sizes up through a DEGB of the largest RCS piping ensures that defense-in-depth is maintained.

## **6.2 ALTERNATE BREAK SIZE**

The alternate break size to be applied for alternate evaluation of sump performance is defined in the GR methodology as follows:

- A complete guillotine break of the largest line connected to the reactor coolant system loop piping.
- For main loop piping, a break size will be assumed to be that equivalent to a guillotine break of a 14-inch schedule 160 line. This equates to an effective break area of 196.6 square inches (assuming both sides of the break are pressurized).

In defining these break sizes, the alternate break size to be considered by each licensee for lines connected to the main loop piping is plant dependent, while the alternate break size to be applied to the main loop piping is identical for each licensee.

The GR also provides guidance for determining whether a double ended guillotine break needs to be considered in attached piping. If sufficient energy for debris generation exists on both sides of the break, a DEGB will be used. The GR criteria for determining whether sufficient energy exists are based on the postulated break distance from a normally closed isolation valve, and are as follows:

- 10 pipe inside diameters for large bore piping (i.e., greater than 2 inch diameter)
- 20 pipe diameters for small bore piping

If a normally closed isolation valve exists within this number of pipe diameters, than only a single ended break needs to be considered. These GR criteria are based on the low stored energy in the pipe section between the break and isolation valve with respect to significant debris generation.

Additionally, the GR provides guidance for consideration of the ongoing 10 CFR 50.46 rulemaking effort. The GR states that, "In using this GSI-191 alternate break size, it is recognized that when the 50.46 rule is finalized, licensees can re-perform the sump performance evaluations with the final break size specified in 50.46 and modify the plant design and operation. This would assure coherence in the implementation of 50.46."

**Staff Evaluation for Section 6.2:** The staff has reviewed the alternate break size proposals as described in the GR and finds them to be acceptable. The staff refers to the alternate break size as the "debris generation" break size (DGBS) and will do so throughout the following discussion.

The DGBS to distinguish between customary and more realistic design basis analyses is as follows:

1. All American Society of Mechanical Engineers (ASME) Code Class 1 PWR auxiliary piping (attached to RCS main loop piping) up to and including a double-ended guillotine break of any of these lines - design basis rules apply
2. RCS main loop piping (hot, cold and crossover piping) up to a size equivalent to the area of a DEGB of a 14 inch schedule 160 pipe (approximately 196.6 square inches) - design basis rules apply
3. Breaks in the RCS main loop piping (hot, cold and crossover piping) greater than the above size (approximately 196.6 square inches), and up to the DEGB - licensees must demonstrate mitigative capability, but design basis rules may not necessarily apply.

The technical basis for the staff's acceptance of the division of the pipe break spectrum for the purpose of evaluating debris generation is comprised of several factors. First, the staff considered recent information developed by the NRC's Office of Nuclear Regulatory Research (RES) regarding the frequency of RCS ruptures of various sizes. This information was developed by RES through an expert elicitation process as documented in SECY-04-0060, "Loss-of-Coolant Accident Break Frequencies for the Option III Risk-Informed Reevaluation of 10 CFR 50.46, Appendix K to 10 CFR Part 50, and General Design Criteria (GDC) 35." The RES study determined the frequency of primary pressure boundary failures under normal operational loading and transients. Although the results of the expert elicitation are not yet final, the preliminary results support the observation that the probability of a PWR primary piping system rupture is generally very low and that the break frequency decreases with increasing piping diameter. The selection of a break size equivalent to the area of a DEGB of a 14 inch schedule 160 pipe for RCS main loop piping is consistent with attached auxiliary piping sizes in PWRs, and is also consistent with the ongoing 10 CFR 50.46 rulemaking direction (at this time).

The staff also considered the fact that there is a substantial difference from a deterministic, "margins to failure" or "flaw tolerance" perspective between 30-to-42 inch

diameter PWR main coolant loop piping and the next largest ASME Code Class 1 attached auxiliary piping (generally the 12-to-14 inch diameter pressurizer surge line). This difference is evident, for example, in Leak-Before-Break (LBB) evaluations conducted in accordance with NUREG-1061, Volume 3, "Report of the U.S. Nuclear Regulatory Commission Piping Review Committee," wherein main coolant loop piping characteristically passes a LBB evaluation more easily than ASME Code Class 1 auxiliary piping systems. Finally, the staff considered the fact that certain ASME Code Class 1 auxiliary piping systems may be more susceptible to failure due to environmental conditions which are conducive to known degradation mechanisms and/or loading conditions which routinely apply significant stresses to the piping system. An example of both of these considerations would be a typical PWR pressurizer surge line in which Alloy 82/182 dissimilar metal welds are subjected to a high temperature operating environment known to abet primary water stress corrosion cracking and which is subjected to significant bending loads during startup/shutdown conditions due to the large temperature gradient between the pressurizer and the hot leg of the main coolant loop.

Based upon the considerations noted above, the staff considers that the division of the pipe break spectrum proposed for the purpose of evaluating debris generation to be acceptable based on operating experience, application of sound engineering judgment, and consideration of risk-informed principles. Licensees using the methods described in Section 6 can apply the defined DGBS for distinguishing between Region I and Region II analyses.

The staff has considered the GR guidance provided regarding the need to consider a DEGB in attached auxiliary piping. The GR provides criteria based on number of pipe diameters, pipe size and distance to a normally closed isolation valve for determining if sufficient energy for debris generation exists on both sides of the break. If a normally closed isolation valve exists within a specified number of pipe diameters from a postulated break location, than only a single ended break needs to be considered. The GR does not provide a technical basis for this criterion. To assess the acceptability of this proposal, the staff considered the fluid volumes available on each side of a DEGB which would fall within the criteria provided in the guidance. Considering that a break occurs at the maximum distance from a normally closed isolation valve, as allowed by the proposed criteria, the staff agrees that there would be an insignificant amount of energy available for destruction from the isolated side of the break when compared to the fluid volume and energy available on the unisolated side of the break. For example, considering a DEGB of a 1 foot diameter auxiliary pipe with a normally closed isolation valve 10 inside pipe diameters away, the fluid volume in the isolated piping portion is less than 10 cubic feet. This fluid volume is insignificant when compared to the RCS fluid volume, which is on the order of 10,000 cubic feet. The fluid and energy blowdown from the isolated side of the break will depressurize and void almost instantaneously, while the blowdown from the RCS side of the break would be significantly larger, on the order of minutes (the staff verified this through a simplified RELAP calculation). Based on this, and considering engineering judgement, the staff finds that the criteria proposed by NEI for evaluating whether a DEGB should be considered in auxiliary piping is acceptable. The staff's engineering judgment takes into consideration that (a) past experiments and analyses have confirmed that debris generation due to initial blast impulse (which would be from both sides of the postulated break) would be minimal, and (b) that debris generation is dominated by jet loading and/or jet erosion. As confirmed

by the staff's estimate, blowdown jet impacts would be dominated by the blowdown from the RCS side of the break.

The staff also considered the GR guidance regarding consideration of the ongoing 10 CFR 50.46 rulemaking effort. The staff agrees with the recommended guidance that licensees may re-perform the sump performance evaluations using the final break size specified by rulemaking, and modify the plant design and operation accordingly. This would assure consistency with a new 10 CFR 50.46. However, the guidance provided in the GR seems to imply that the final break size specified by the new 10 CFR 50.46 will be smaller than the DGBS defined above for GSI-191 debris generation purposes. Should the final design basis LOCA break size specified by a revised 10 CFR 50.46 be larger than the DGBS defined above for GSI-191 debris generation purposes, the staff expects that licensees using the alternate methodology of Section 6 would re-perform their sump performance evaluations considering the final break size specified by rulemaking, and modify the plant design and operation accordingly.

### **6.3 REGION I ANALYSIS**

The Region I analysis of recirculation sump performance includes evaluation of all break sizes up to and including the DGBS defined in Section 6.2. The majority of the analyses to be performed for the Region I break sizes are to be performed in the same manner as described in Sections 3, 4 and 5 of the GR. For Region I breaks, the GR states that a full range of break locations will be assessed to determine the limiting location considering both debris generation and debris transport. However, as discussed in Section 6.3.2, the GR refers to a Section 4 refinement proposing that Branch Technical Position MEB 3-1 (MEB 3-1) may be used to limit the break locations considered. Additionally, any design basis secondary side breaks (main steam line break, feedwater line break, etc.) which rely on sump recirculation will be analyzed in accordance with the Region I analyses.

With respect to break configuration, circumferential breaks will be assumed to result in pipe severance and separation amounting to at least one diameter lateral displacement of the ruptured piping sections unless physically limited by piping restraints and supports, or other plant structural members that can be shown through analysis to limit pipe movement to less than one diameter lateral displacement. For pipes with a larger diameter than the maximum break size, the maximum attainable break area would be modeled as a partial pipe break with an area equivalent to the DEGB of a pipe with the same diameter as the DGBS. The worst location of the break in terms of orientation around the break location must be considered.

One area where the Section 6.3 guidance differs from the guidance in the baseline analysis of section 3 involves the zone of influence (ZOI) to be considered for debris generation. The guidance in Section 3 regarding the ZOI presumes a DEGB, and for a DEGB, a spherical ZOI is conservatively postulated. A spherical ZOI is appropriate in the Region I analyses for any auxiliary piping attached to the RCS, since a DEGB of any such piping falls within Region I analysis. However, partial breaks of the RCS main loop piping are also included in Region I (breaks up to the DGBS), and would indicate a limited-displacement circumferential break or a longitudinal break, i.e., "split break." The GR proposes that the ZOI for such partial breaks in RCS main loop piping be accounted for by applying one of two methods:

- ZOI Based on a Hemisphere - The ZOI is simulated as a hemisphere radius determined by the destruction pressure of the insulation that would be affected by the postulated break. The break orientation needs to be simulated at various angles around the loop piping to determine maximum debris generation.
- ZOI Based on a Sphere - Because the worst-case break orientation can be difficult to determine, an alternative to assuming a hemispherical ZOI is to translate the hemispherical volume into an equivalent volume sphere.

The GR also states that the ZOI refinements discussed in Section 4 are available when performing Region I analyses.

The acceptance criteria for containment sump screen performance continues to be core cooling based on available NPSH equal to, or greater than, the required NPSH for all pumps required to operate for long term core cooling. The calculations of required and available NPSH are based on the models and assumptions currently used in design basis analyses of sump and core cooling recirculation performance. Additionally, the GR states that If containment spray is credited in the design basis analyses, the containment sump screen performance also includes NPSH margin for the minimum required containment spray.

The Region I analyses also consider the impact of the DGBS on event timings, thermal-hydraulic conditions and NPSH requirements. For example, use of the DGBS will affect key scenario events such as the timing of transfer from RWST injection to recirculation mode, the containment sump water properties (e.g., temperature), and containment back-pressure (if credited in the design basis analyses). The Region I evaluation will consider these revised timings and parameters as appropriate. The guidance also provides for the impact of operator actions to mitigate containment sump blockage, provided that the operator actions meet the criterion for consideration in design basis analyses. These considerations would include adequate time for operator action per design basis “rules”, proceduralized guidance, job-task-analysis, training and other requirements.

**Staff Evaluation for Section 6.3:** The staff has reviewed the Region I alternate evaluation methodology as described in the GR. The Region I analysis methods described in Section 6.3 are applicable for any break sizes equal to or smaller than the DGBS defined in Section 6.2. The Region I methodology therefore, applies to any ASME Code Class 1 auxiliary piping (attached to RCS main loop piping) up to and including a double-ended guillotine break of any of these lines, and RCS main loop piping (hot, cold and crossover piping) up to and including a size equivalent to the area of a DEGB of a 14 inch schedule 160 pipe. The majority of the Region I analyses are performed in the same manner as the methods described in Sections 3, 4 and 5 of the GR, and as such, those corresponding SER sections are applicable for Region I analysis. For example, the guidance in Sections 3 and 4 is to be used as part of the Region I analyses to determine the debris generation, transport and accumulation on the containment sump screens. The staff evaluation described here will focus on differences from Sections 3, 4 and 5 of the GR.

For Region I breaks, the GR states that a full range of break locations will be assessed to determine the limiting location considering both debris generation and debris transport. Additionally, as discussed in Section 6.3.2, the GR refers to a Section 4.2.1 refinement which proposes that Branch Technical Position MEB 3-1 may be used to limit the break locations considered. As documented in Section 4.2.1 of this SER, the staff concluded that it is inappropriate to cite SRP Section 3.6.2 and Branch Technical Position MEB 3-1 as methodology to be applied for determining break locations to be considered for PWR sump analyses. The staff concludes that for Region I breaks, which are considered as customary design basis analyses, a full range of break locations should be assessed to determine the limiting location considering both debris generation and debris transport. Section 4.2.1 of this SER provides further details regarding the staff's position.

The staff finds that the GR guidance is acceptable with respect to break configuration because the methodology assures that the limiting break location considering debris generation, debris transport and the worst location of the break in terms of orientation around the break location will be evaluated. This methodology provides reasonable assurance that the limiting break conditions for PWR sump analyses will be evaluated. Additionally, considering piping restraints and supports or other plant structural members that can be shown through analysis to limit pipe movement to less than one diameter lateral displacement may be acceptable to the staff; however, because the limiting break location and orientation must be evaluated, these locations may not produce the limiting conditions for sump analyses.

Regarding the ZOI to be considered for attached auxiliary piping breaks, the GR states that a spherical ZOI is postulated for breaks smaller than the DGBS for piping connected to the RCS main loop piping because a DEGB of this piping is postulated. For Region I partial pipe breaks, the GR proposes that one of two methods be applied, either a ZOI based on a hemisphere, or a ZOI based on translating the hemispherical volume into an equivalent volume sphere. The staff evaluated the GR with respect to the ZOI to be considered under these conditions and concludes that applying a hemispherical ZOI is acceptable for such partial breaks, and that when doing so, licensees would need to simulate various directions around the RCS main loop piping to determine the limiting break location. The staff does not accept the proposed approach of a ZOI based on translating the hemispherical volume into an equivalent volume sphere. The GR does not provide any technical justification for this approach except that it is a simplification because the worst-case break orientation can be difficult to determine. The staff does not have a technical basis for accepting a translation of the volumes, which would result in a different ZOI, and the staff has no basis to judge whether this would be conservative, nonconservative, or realistic. For simplification, the staff would accept application of a spherical ZOI with a radius equivalent to that of a ZOI based on a hemisphere.

The application the ZOI refinements for Region I analyses shall be in accordance with the staff's position as discussed in Section 4 of this SER.

For the Region I sump analyses, the acceptance criteria for containment sump screen performance continues to be core cooling based on available NPSH equal to, or greater than, the required NPSH for all pumps required to operate for long term core cooling. The calculations of required and available NPSH are based on the models and assumptions currently used in design basis analyses of sump and core cooling

recirculation performance, and therefore, the staff finds their continued application for Region I analyses to be acceptable. The staff agrees with the GR that the impact of the DGBS on event timings, thermal-hydraulic conditions and NPSH requirements, and crediting of operator actions for demonstrating that the acceptance criteria are satisfied, can be applied for Region I analyses consistent with customary design basis analysis procedures and requirements. Licensee analyses should consider, at a minimum, the following factors:

1. The accuracy of deterministic analyses performed to calculate DGBS event timings, T/H conditions and NPSH requirements, and their compliance with 10 CFR 50.46. Staff expects that licensees will document, and if necessary, provide to the staff detailed information regarding the analyses and the modeling assumptions. The GR guidance does not explicitly identify which phenomena and parameters will receive time dependent treatment and will be considered in-scope for estimating timing of events.
2. The experimental data used for estimating debris generation, transport and head loss buildup for breaks other than DEGB. In general most of the experimental data was obtained for jet conditions and transport flow rates prototypical of DEGB. For example, most of the debris generation data was obtained for jet durations typical of DEGB (10-30 several seconds). Direct use of such data for insulations where erosion is the dominant generation mechanism (e.g., calcium-silicate) may not be appropriate for DGBS breaks. Similar limitations on the applicability of available experimental data to DGBS exist for other phenomena as well, including debris transport and debris buildup – especially when operator actions are to be credited in the mix of the analyses being performed.
3. Also, due to uncertainties in various phenomena, the staff believes that it is difficult to judge when maximum head loss would occur (e.g., maximum debris accumulation and the minimum required NPSH may or may not occur simultaneously depending on operator actions). Considerable attention and a broad of spectrum of analyses should be devoted to establish that analyses are customary design basis analyses.
4. If credit is to be taken for containment overpressure, underlying analyses should conform with staff guidance for estimating minimum overpressure as suggested in Regulatory Guide 1.82, Revision 3.

The staff notes that there is a typographical error in the following sentence of Section 6.3.6 of the GR, “In addition, if containment spray is credited in the design basis analyses (containment pressure, radiological consequence, etc.), the containment sump screen performance also includes NPSH margin for operation of the minimum required containment spray.” The staff believes that this sentence should require that adequate NPSH margin be available for the maximum required containment spray, or to allow for an overestimate of the required containment spray.

#### **6.4 REGION II ANALYSIS**

The Region II analysis of recirculation sump performance includes evaluations of break sizes in the RCS main loop piping (hot, cold and crossover piping) greater than the DGBS specified in Section 6.2 (approximately 196.6 square inches) and up to a DEGB of the largest pipe in the RCS. Only RCS main loop piping is considered in Region II because all primary side attached auxiliary piping and secondary side breaks are fully addressed as part of the Region I analyses. Section 6.4.2 of the GR states that, “[I]f a licensee chooses to use an alternate break size smaller than the largest connected piping to the main coolant loop piping, as discussed in Section 6.2, then connected piping larger than the alternate break size would be addressed as part of the Region II evaluation.” The staff finds that this statement is not consistent with the alternate break size as defined in Section 6.2 and requires clarification. NEI and industry representatives informed the staff that this statement is included in the GR to allow for the possibility that the forthcoming 10 CFR 50.46 rulemaking would redefine the design basis LOCA break size to be smaller than the DGBS defined in Section 6.2. As discussed in Section 6.2 of this SER, the staff agrees with the recommended guidance that licensees may re-perform the sump performance evaluations using the final break size specified by rulemaking, and modify the plant design and operation accordingly. However, should the final design basis LOCA break size specified by the new 10 CFR 50.46 be larger than the DGBS defined in Section 6.2, the staff expects that licensees using the alternate methodology of Section 6 would re-perform their sump performance evaluations considering the final break size specified by rulemaking, and modify the plant design and operation accordingly.

Section 6.4.2 of the GR refers to a Section 4 refinement proposing that Branch Technical Position MEB 3-1 (MEB 3-1) may be used to limit the break locations considered. With respect to break configuration, the Region II analyses are limited to DEGB of the RCS main loop piping. These circumferential breaks are assumed to result in pipe severance and separation amounting to at least one diameter lateral displacement of the ruptured piping sections unless physically limited by piping restraints and supports, other plant structural members, or piping stiffness as may be demonstrated by analysis. The GR states that existing plant-specific dynamic loads analyses for postulated primary side breaks are utilized to assist the determination of the break configuration for Region II analyses.

The ZOI models and assumptions to be applied for Region II analyses are those as described in Sections 3 and 4 of the GR. There are a number of known conservatisms in the ZOI model presented in Sections 3 and 4. However, because development of a technically sound model to more realistically model the ZOI based on existing experimental and analytical data is quite complex and has not been initiated, the GR relies on the models described in Sections 3 and 4.

The guidance in Sections 3 and 4 of the GR is also applied to determine the debris generation, transport and accumulation on the containment sump screens for Region II evaluations. The models presented in Sections 3 and 4 are considered to be bounding models to assure that the debris generation, transport and accumulation are not under-predicted. There are known conservatisms in each portion of these evaluation models in Sections 3 and 4. However, development of more realistic models in these areas is difficult due to the limited amount of experimental and analytical information available, and this work has not yet been initiated.

The acceptance criteria for containment sump screen performance for Region II analyses are continued core and containment cooling. The applicable criteria to demonstrate retained mitigation capability for long-term cooling capability in Region II analyses are:

- Positive NPSH margin is maintained for the minimum number of ECCS pumps necessary to demonstrate adequate core cooling flow, and
- Demonstration of adequate containment cooling capability to provide assurance that the containment boundary remains intact.

The first criterion (Positive NPSH margin is maintained for the minimum number of ECCS pumps) can be met by ensuring NPSH margin is maintained for one or more moderate to high-capacity ECCS injection pumps. Additionally, for Region II analyses, the GR states that limited operation without NPSH margin is acceptable if it can be shown that the pumps can reasonably be expected to survive during the time period of inadequate available NPSH. Suggested technical justification for this would include vendor information in the form of test data or engineering judgment derived from tests and/or operational events.

The GR states that the second criterion (Demonstration of adequate containment cooling capability) can be met through credit taken for minimal heat removal pathways, including containment fan coolers, permitted by emergency procedures. Additionally, subatmospheric containment plants would not have to demonstrate that the containment remains below atmospheric pressure for the duration of the accident, if permitted by emergency procedures. The GR also states that, "exceeding nominal transient containment design pressure/temperature and environmental qualification (EQ) envelopes is allowed for Region II analysis, if reasonable assurance is provided that containment pressure boundary failure or vital equipment failure would not be expected."

The Region II analyses also consider more realistic modeling of debris generation, transport and accumulation on sump screens based on the timing of debris generation, and transport and accumulation in relation to the timing of the available and required NPSH. More realistic modeling of these items considers:

- debris generation, transport and accumulation is time dependent,
- available NPSH is time dependent, and
- the maximum debris accumulation and the minimum required NPSH may not occur simultaneously.

The GR also allows credit for operator actions and the operation of non-safety equipment.

**Staff Evaluation for Section 6.4:** The staff has reviewed the Region II alternate evaluation methodology as described in the GR. The Region II analysis methods described in Section 6.4 are applicable for any breaks in the RCS main loop piping (hot, cold and crossover piping) greater than the DGBS specified in Section 6.2 (approximately 196.6 square inches) and up to a DEGB of the largest pipe in the RCS.

For Region II break locations, Section 6.3.2 of the GR refers to a Section 4.2.1 refinement proposing that Branch Technical Position MEB 3-1 be used to limit the break locations considered. As documented in Section 4.2.1 of this SER, the staff concludes that it is inappropriate to cite SRP Section 3.6.2 and Branch Technical Position MEB 3-1 as methodology to be applied for determining break locations to be considered for PWR sump analyses. The staff concludes that for Region II breaks, a full range of break locations should be assessed to determine the limiting location considering both debris generation and debris transport. Section 4.2.1 of this SER provides further details regarding the staff's position.

The staff finds that the GR guidance is acceptable with respect to break configuration because the limiting break location considering debris generation, debris transport and resulting sump screen head loss will be evaluated. This methodology provides reasonable assurance that the limiting break conditions for PWR sump analyses will be evaluated. Additionally, considering piping restraints and supports or other plant structural members that can be shown through analysis to limit pipe movement to less than one diameter lateral displacement may be acceptable to the staff; however, because the limiting break location must be evaluated, these locations may not produce the limiting conditions for sump analyses.

Certain portions of the Region II analyses are performed in the same manner as the methods described in Sections 3 and 4 of the GR, and as such, those corresponding SER sections are applicable for Region II analyses. The guidance in Sections 3 and 4 is to be used as part of the Region II analyses with respect to ZOI models and assumptions, and for determining debris generation, transport and accumulation on the containment sump screens. There are known conservatisms in each of these models as described in Sections 3 and 4, and as such, the staff finds them to be acceptable for Region II analyses. Sections 3 and 4 of this SER provide further details regarding the staff's position and review of these models.

The GR proposed two acceptance criteria for the Region II analysis. These are:

- Positive NPSH margin is maintained for the minimum number of ECCS pumps necessary to demonstrate adequate core cooling.
- Demonstration of adequate containment cooling capability to provide assurance that the containment boundary remains intact.

The staff considers positive NPSH margin to mean that the available NPSH is greater than the required NPSH for each pump. The GR has not specified the amount of NPSH margin necessary. Since the staff has previously accepted the available NPSH equal to the required NPSH, that is, an NPSH margin of zero, this nonspecificity is acceptable for realistic and risk-informed Region II analyses. The determination of both the available and the required NPSH is addressed in Sections 6.4.7.1 and 6.4.7.2, respectively, of this safety evaluation report.

The GR does not specify what is meant by adequate core cooling. The staff interprets adequate core cooling to mean that the postulated accident consequences are within the scope of the emergency response guidelines (the basis for the plant specific emergency operating procedures). Significant cladding oxidation and/or loss of coolable geometry of the core have not occurred.

The GR does not specify what is meant by adequate containment cooling. The staff interprets adequate containment cooling to mean that the containment is in a safe and stable state and preventing risk-significant fission product releases. This will be further taken to mean that the containment has not failed structurally. The containment design pressure and the containment design temperature may be exceeded for analyses of breaks above the DGBS, as stated in this section of the GR. Licensees should determine, on a plant specific basis, whether exemption and/or license amendment requests are required if the containment design pressure and/or temperature is exceeded. Licensees should determine whether the containment leakage rate exceeds the value of  $L_a$  defined in 10 CFR Part 50, Appendix J and given in the plant's technical specifications. An exemption to this regulation and/or a license amendment request might be required if a licensee determines that this is the case.

The GR states that the second criterion can be met through credit taken for minimal heat removal pathways, including containment fan coolers, permitted by the emergency procedures. The staff finds that credit taken for minimal heat removal pathways permitted by the emergency procedures would be acceptable in a realistic and risk-informed Region II analysis. The staff expects that licensees will provide detailed information regarding plant equipment and/or operator actions credited in their Generic Letter responses. The staff will assess credit taken for minimal heat removal pathways as part of the Generic Letter response reviews and closeout process.

The GR also states that it is acceptable to exceed the "nominal" EQ envelopes. The staff finds that applying a more realistic EQ envelope could be acceptable in a realistic and risk-informed Region II analysis. For Region II analyses, the staff does not consider it necessary to comply with the guidance of NUREG-0588, Revision 1, which is the basis for the EQ analyses described in plant Updated Final Safety Analysis Reports (UFSARs). If any equipment exceeds the appropriate EQ envelope, the licensee should consider whether an exemption to 10 CFR 50.49 is required. The staff expects that licensees will provide detailed information with respect to exceeding nominal EQ profiles in their Generic Letter responses. The staff will assess the application of EQ envelopes as part of the Generic Letter response reviews and closeout process.

For the Region II evaluation, the GR criteria would allow limited ECCS and containment heat removal pump operation without NPSH margin. Licensees would need to demonstrate that the pumps can reasonably be expected to survive during the time of inadequate available NPSH margin. Technical justification for this conclusion should be based on test data or engineering judgment derived from tests and/or operating experience.

The GR points out that the guidance for determining adequate NPSH margin is currently provided in Regulatory Guide 1.1 (RG 1.1), which is the licensing basis for some operating reactors, and Regulatory Guide 1.82, Revision 3 (RG 1.82-3), which contains the current staff guidance. The GR suggests that it is not necessary to apply the conservative guidance provided in these Regulatory Guides when analyzing the consequences of breaks larger than the DGBS. The remainder of Section 6.4.7 provides guidance on an alternate, more realistic approach.

Section 6.4.7 discusses the application of Generic Letter (GL) 91-18 (GL 91-18) with respect to determination of realistic NPSH margin. The GR considers that a "nominal"

parameter value used in performing Region II analyses could be exceeded. For this situation, the GR proposes that operability assessments in accordance with GL 91-18 are not necessary. The GR establishes a time limit allowing the nominal value to be exceeded for a period of 30 days. LOCA analyses are typically carried out only to 30 days. The staff finds this proposal to be unacceptable because the Region II analyses remain within the design bases. Exceeding the nominal value of a parameter used the Region II analyses may result in decreasing the available NPSH to the degree that there is no longer positive margin for this design basis accident. Therefore, the staff concludes that the same conditions apply as would apply for a Region I analysis and the guidance in GL 91-18 should apply.

The GR discusses the realistic assumptions that may be applied in calculating the available NPSH for breaks larger than the DGBS. These are discussed in Section 6.4.7.1 for each of the factors which contribute to the available NPSH: suction elevation head, absolute pressure head, vapor pressure head, and friction and form head losses. The staff finds the GR discussion for Section 6.4.7.1 to be acceptable with one caveat. The discussion of friction losses notes that experience has shown that calculations of friction loss based on handbook values tend to overestimate the friction loss. The GR states that these values may be reduced based on engineering judgment or test results. For these calculations a more substantive basis than engineering judgment should be used. Engineering judgment is not a quantitative measure of conservatism. The staff will accept a reduction in head loss calculations based on accepted handbook values only if its basis is technically justified.

The required NPSH of a pump is measured by the pump vendor in accordance with applicable standards. It is usually based on a 3% drop in the pump total head (first stage for a multi-stage pump). This value has been selected as an easily recognized level of cavitation. It is not the level at which cavitation first appears. The GR states that, since total head is not necessarily a critical parameter for a centrifugal pump in the LOCA recirculation mode, the pump vendor may be able to provide relief in the amount of NPSH required to avoid pump damage rather than depend on the formal definition of required NPSH. The staff agrees. The staff has in the past accepted the pump vendor's technical judgment on pump capabilities. In this case, the conditions the pump will experience and the time period that the pump will experience these conditions must be well defined and evaluated by the pump vendor. In addition, staff believes that vendor's technical judgment should take into consideration the fact that recirculation water may include debris of different kinds and sizes (i.e., combined effects of debris ingestion and cavitation should be factored into decision making).

The GR states that accounting for the decrease in required NPSH with an increase in pumped liquid temperature as discussed in ANSI/HI 1.1-1.5-1994 (ANSI/HI 1.1-1.5) should not be used. The staff agrees. This is consistent with the guidance in Regulatory Guide 1.82, Revision 3.

The Calculational Method Section (Section 6.4.7.3) of the GR discusses assumptions that could be applied for more realistic available and required NPSH calculations. It is not clear what is meant by calculating required NPSH since required NPSH is typically measured and specified by the pump vendor. Licensees referencing the GR should clarify this. One of the items listed in this section states, "...Containment pressure head based on absolute pressure rather than vapor pressure." Rather than "absolute pressure," the term "pressure of the containment atmosphere," would be clearer. The

staff expects that licensees will provide detailed information regarding the application of more realistic analysis assumptions in their Generic Letter responses. The staff will assess these assumptions as part of the Generic Letter response reviews and closeout process. Additionally, application of certain assumptions may require plant-specific exemption and/or license amendment requests.

With respect to timing of events, the GR discusses the realistic modeling of debris generation, transport and accumulation on sump screens. One bullet in this section states that, "...the maximum debris accumulation and the minimum required NPSH may not occur simultaneously." It appears that this is referring to minimum available NPSH margin rather than minimum required NPSH. Other than this editorial comment, the staff agrees with the report's proposals in this section. The staff expects that licensees will provide detailed information regarding more realistic modeling of event timing in their Generic Letter responses. The staff will assess this modeling as part of the Generic Letter response reviews and closeout process.

The staff agrees with the GR's proposal of operator actions that may be credited to compensate for the effects of debris generation on the ECCS and the containment spray system. These actions will be assessed on a plant specific basis and would necessitate that risk calculations to be performed in accordance with Regulatory Guide 1.174.

The GR does not address the analytical methods to be used for performing the Region II analyses (e.g., computer codes and models). In particular, staff has reservations on how the models and methods described in Sections 3 and 4 could be adopted for these type of analyses. The staff will assess the adequacy of methods used during reviews of any plant-specific licensing submittals and plant-specific audits performed as part of the GSI-191 and Generic Letter closeout process. Part of staff's assessment would include: methods, models and data used to estimate event timings, T/H conditions, and how the debris phenomena treat calculational uncertainties. It is known that all aspects of debris phenomena (including, generation, transport and head loss) have large uncertainties. In lieu of explicitly treating these uncertainties, staff used engineering judgment to conclude that these uncertainties are typically small compared to conservatism introduced by DEGB type limiting analyses. Licensee evaluations performed under Region-II should be cognizant of such issues and address them explicitly. For example, considerable experimental evidence exists in support of increased head loss due to long-term operation. Very limited, if any, experiments are carried out to quantify such factor mechanistically. Instead traditional correlations developed using short-term tests, corrected based on engineering judgment, were used to account for long-term phenomena. In the past, staff accepted such approximations because of large margin-of-conservatism implicit in DEGB type analyses.

## **6.5 RISK INSIGHTS**

Section 6.5 of the NEI GR is provided to guide the determination of risk acceptability for cases in which a licensee relies on sump mitigation capability (including crediting operator actions) for the Region II Analysis (i.e., Section 6.4). In Section 6.5 of the NEI Evaluation Guidance, the acceptance guideline from Regulatory Guide (RG) 1.174 that is used to define an acceptably small increase in core damage frequency (CDF) is used to establish a target reliability for the sump mitigation capability. To further ensure the acceptability of this approach, the NEI Evaluation Guidance also uses a conservative value for the large break loss of coolant accident (LBLOCA) initiating event frequency,

which is taken from NUREG-1150. Thus, the NEI Evaluation Guidance provides a method by which a licensee can ensure that any increase in CDF resulting from plant modifications, operator actions, etc. that are credited in Section 6.4 will be small and meet the RG 1.174 acceptance guideline by demonstrating that the target reliability of the sump mitigation capability is achieved.

The target reliability is established by first calculating the increase in CDF as the combination of the LBLOCA initiating event frequency (LBLOCA:IEF) and the sump mitigation capability failure probability (SMC:FP). In this calculation there are a number of conservatisms used to make it simple and straightforward, including:

- The base case condition represents the condition in which the current sump meets the regulations without needing credit for mitigation capability and is assumed to not clog (i.e., the sump is perfect, with a clogging probability of 0).
- The mitigation condition case represents the condition in which the sump takes credit for mitigation capability and assumes if the mitigation capability fails the sump will clog (i.e., the sump always clogs if the mitigation capability fails, with a clogging probability of 1) and a clogged sump results in core damage (i.e., no credit for potential recovery actions).
- The calculation is performed for the entire LBLOCA break spectrum (i.e., all breaks greater than about 6 inches), while the NEI Evaluation Guidelines "Region II" alternate approach is only used for those break sizes greater than the "debris generation" break size, which is only a portion of the LBLOCA break spectrum (i.e., calculation assumes all LBLOCAs require mitigation, not just those greater than the "debris generation" break size).

Based on this approach, the calculation of the increase in CDF can be simplified to:

$$\Delta\text{CDF} = \text{LBLOCA:IEF} \times \text{SMC:FP}$$

Recognizing that the target reliability (TR) is the complement of the sump mitigation capability failure probability (SMC:FP) and resolving the equation results in:

$$\text{TR} = 1 - \text{SMC:FP} = 1 - [\Delta\text{CDF} / \text{LBLOCA:IEF}]$$

The RG 1.174 acceptance guideline for a small change in CDF is less than 1.0E-5/year. This is an appropriate acceptance guideline for plants where the total CDF can be reasonably shown to be less than 1.0E-4/year. The NEI Evaluation Guideline states that the 1.0E-4/year total CDF value bounds the population of PWRs. The staff accepts that this may be true. However, if a licensee's total CDF is greater than 1.0E-4/year, considering all modes and initiators, then that licensee should provide additional justification and meet an appropriately higher target reliability.

The value for the LBLOCA initiating event frequency from NUREG-1150 is 5.0E-4/reactor-year. It is recognized by the staff that this represents a generic bounding value of the LBLOCA frequency and is considerably greater (and thus conservative) than used in plant-specific probabilistic risk assessments (PRAs).

Substituting the above values into the equation for determining the target reliability results in a target reliability for the sump mitigation capability of 0.98 per demand (i.e., SMC:FP equals  $2.0E-2/\text{demand}$ ).

The staff understands that the reliability of the sump mitigation capability will be determined on a plant-specific basis and ensured with reasonable confidence to be equal to or greater than the above established target reliability. This determination will include evaluations of associated plant modifications as well as credited operator actions, including those modifications and actions credited in Section 6.4 that represent a change from current operations (e.g., crediting operator action to terminate or reduce containment spray flow to assure net positive suction head of the low head pumps).

The staff also accepts that passive components do not need to be considered in the reliability determination, as long as these passive components are demonstrated as being functional by design (e.g., enlarged sump screen areas) or failure is determined to be extremely unlikely (e.g., less than  $1.0E-5/\text{demand}$ ), even given challenges that passive components might see, such as jet forces or blowdown loads. However, if a measurable and inspectable reliability can be ascribed to a passive component (e.g., passive screen cleaning), then the reliability determination should include these features.

Consistent with the RG 1.174 principles of risk-informed decisionmaking, the impact of the proposed change should be monitored using performance measurement strategies. Therefore, an implementation and monitoring plan should be developed to ensure that the evaluation conducted to examine the impact of the proposed changes continues to reflect the actual reliability and availability of the SSCs and operator actions that have been evaluated. This will ensure that the conclusions that have been drawn from the evaluation remain valid. Thus, the staff expects licensees to propose, in their plant-specific submittals, a monitoring program that is consistent with RG 1.174 Section 2.3, which includes a means to adequately track the performance of equipment that, when degraded, can affect the conclusions of the licensee's evaluation (i.e., demonstration of the sump mitigative capability to meet its reliability target). The program should be capable of trending equipment performance after a change has been implemented to demonstrate that performance is consistent with that assumed in the traditional engineering and probabilistic analyses that were conducted to justify the change. This may include monitoring associated with non-safety-related SSCs if the analysis determines those SSCs to be relied upon to meet the sump mitigative capability target reliability. The program should also be structured such that feedback of information and corrective actions are accomplished in a timely manner and degradation in performance is detected and corrected before plant safety can be compromised.

In summary, the staff finds this portion of the alternate approach acceptable for use in the NEI Evaluation Guidelines "Region II" evaluations for the following reasons:

- The target reliability determination includes a number of conservative simplifications, including:
- It is performed for the entire LBLOCA break spectrum (i.e., all breaks greater than about 6 inches), while the NEI Evaluation Guidelines "Region II" alternate approach is only used for those break sizes greater than the "debris generation" break size, which is only a portion of the LBLOCA break spectrum.

- The base case condition is assumed not to be susceptible to clogging (i.e., the sump is perfect, with a clogging probability of 0).
- The mitigation condition case assumes if the mitigation capability fails the sump will clog (i.e., the sump always clogs if the mitigation capability fails, with a clogging probability of 1) and that a clogged sump results in core damage (i.e., no credit for potential recovery actions).
- The NUREG-1150 LBLOCA initiating event frequency of  $5.0E-4$ /reactor-year is expected to be much greater than the LBLOCA value derived from the on-going U.S. Nuclear Regulatory Commission (NRC) Office of Research (RES) expert elicitation process.
- The approach is consistent with RG 1.174 since it uses the acceptance guidelines that defines an acceptably small CDF increase in determining the target reliability of the sump mitigation capability.
- Licensees are required to implement a performance-monitoring program, consistent with Section 2.3 of RG 1.174 to ensure that the conclusions of the licensee's evaluation (i.e., demonstration that the sump mitigative capability meets the established target reliability) are maintained valid.

## 7.0 ADDITIONAL DESIGN CONSIDERATIONS

Four extenuating design considerations are discussed in this section of the GR that are related to the broad issue of recirculation-sump operability addressed under GSI-191. These topics are (1) structural analysis of the containment sump, (2) upstream effects that limit water flow, (3) downstream effects related to debris penetration of the screen, and (4) potential chemical effects that contribute to head loss either as an additional debris source or by modifying the hydraulic properties of pre-existing beds. Staff evaluations of the GR treatment of these topics follow in corresponding subsections of this SER. The NRC agrees that this list is complete when added to the balance of detail provided in the remainder of the GR, as modified by staff recommendations.

### 7.1 **SUMP STRUCTURAL ANALYSIS**

Consideration of sump structural analysis in the GR and in this SER is limited to the debris loads and the hydraulic loads imposed by water in the sump pool. Dynamic loads imposed on the sump structure and screen by break-jet impingement must be addressed in accordance with GDC 4, including provisions for exclusion of certain breaks from the design basis when analyses reviewed and approved by the NRC demonstrate that the probability of fluid system piping rupture is extremely low.

The GR does not provide detail in its presentation of criteria for sump screen performance and comparisons to predicted head loss. To clarify this information, the staff offers the following discussion. It is true that structural loads on a sump screen must be computed using the total pressure drop across the screen. The total pressure drop is the sum of the head loss computed or measured across the clean screen at a given volumetric flow rate in the absence of debris and the debris-induced head loss computed or measured under the same volumetric flow rate. Debris-bed head loss should be calculated for each postulated break scenario according to methods outlined in Sections 3.7 and 4.2.5 of the GR as amended by SER recommendations. The limiting conditions for sump screen structural analysis correspond to a break location and debris source term that induces the maximum total head loss at the sump screen after full consideration of transport and degradation mechanisms. This represents the minimum required performance criterion for judging recirculation-sump operability. In other words, the recirculation sump must be able to accommodate both the clean-screen head loss and the debris-induced head loss associated with the limiting break while providing adequate flow through both the ECCS injection pumps and the CS pumps if needed.

Licensing-basis calculations of NPSH margin already include the effects of flow resistance through the clean screen, so for comparison to this performance metric, it is sufficient to examine the debris-bed head loss separately. For a completely submerged sump screen, if the NPSH margin is smaller than the head loss induced by debris from the limiting break, then the licensing-basis margin has been exceeded and some form of mitigation, modification, or exemption is warranted. For a partially submerged sump screen, a potentially more restrictive condition may apply. In order to supply adequate water flow through the debris bed, the pressure drop cannot exceed one half of the pool depth in feet of water or the NPSH margin, whichever is smaller. This additional criterion arises because the containment pressure is equal on both sides of the debris bed and the static pressure of the pool is the only way to force water through the bed [RG 1.82-3].

Thus, different criteria may dictate the structural capacity of the sump screen for supporting water flow through a debris bed under recirculation velocities depending on screen geometry. For both submerged and exposed configurations, the screen must support a minimum of the clean-screen pressure drop and the pressure drop induced by debris from the limiting break. If a submerged screen is adequately designed, the debris component of head loss will be less than the licensing basis NPSH margin. This suggests that another rational criterion for minimum structural capacity might be the sum of the clean-screen head loss and the NPSH margin. For partially submerged configurations, the screen never has to support more than one half of the pool depth in equivalent average pressure, although additional design factors may be desired for any of these analyses. Other considerations like maximum water velocities during fill up and hydrodynamic loads during a seismic event may impose additional design constraints.

Practical information is provided about the origin of existing strainer designs that were built to accommodate a 50% blockage rule with essentially zero differential pressure. The staff agrees that potential bending and stretching of existing wire mesh may lead to gaps at the points of attachment between wire and framing structures. The staff further agrees that any modifications to existing sump-screen configurations should employ corrosion resistant materials that will not be affected by post-LOCA containment conditions. See the discussion in Section 7.4 of this SER regarding potential chemical effects.

As previously explained, the minimum structural design criterion for the sump screen can depend on the plant NPSH margin. The GR offers the very pragmatic advice that any increases in margin that are obtained through plant or procedural modifications will increase the differential pressure across the screen. When considering a screen modification, added structural design factors may be a relatively inexpensive way to retain operational flexibility that permits incremental improvements in NPSH margin over time.

The staff agrees that specialized structural components implemented for BWR strainer designs may not be necessary for the resolution of GSI-191 in PWRs. However, many of the same structural design considerations have been mentioned in the GR and each should be assessed for applicability.

## **7.2 UPSTREAM EFFECTS**

This section of the GR provides guidance on evaluating the flowpaths upstream of the containment sump for hold-up of inventory which could reduce flow to and possibly starve the sump. The GR identifies two parameters as being important to the evaluation of upstream effects, they are: (1) containment design and postulated break location; and (2) postulated break size and insulation materials in the ZOI. The GR states that the above two parameters provide a basis to evaluate hold-up or choke points in the flow field within containment upstream of the containment sump. The GR also advises that the containment condition assessment as described in NEI 02-01 provides guidance on this review.

The GR provides users of the document the following examples of locations to evaluate for hold-up of liquid upstream of the sump screen: (1) Narrowing of hallways or passages; (2) gates or screens that restrict access to areas of containment such as behind the bioshield or crane wall; and (3) refueling canal drain. The GR then states

that these areas of concern are generally applicable to all containments but advises licensees to evaluate their containment for possible holdup at unique geometric features, and to evaluate any plant-specific insulation installation.

**Staff Evaluation for Section 7.2:** The staff finds that the above mentioned items of the GR are appropriate as stated and offers the following amplification: Licensees should utilize the results of their debris assessments to estimate the potential for water inventory hold-up. Based on these assessments and the mapping of probable flow paths licensees should utilize methods provided in Chapter 5 of the GR (reducing the source term) for the additional purpose of reducing hold-up of blowdown inventory upstream of the sump. Licensees should evaluate the effect the placement of curbs and debris racks intended to holdup debris may have on the holdup of water en route to the sump.

**Staff Conclusions Regarding Section 7.2:** The staff finds that the GR provides adequate direction regarding the evaluation of holdup of inventory from the sump. The staff provides the above additional comments as an amplification to the GR.

### **7.3 DOWNSTREAM EFFECTS**

This section of the GR gives licensees guidance on evaluating the flow paths downstream of the containment sump for blockage due to entrained debris. The GR specifies three concerns to be addressed which are: (1) blockage of flow paths in equipment such as containment spray nozzles and tight-clearance valves; (2) wear and abrasion of surfaces such as pump running surfaces, and heat exchanger tubes and orifices; and (3) blockage of flow clearances through fuel assemblies. It is noted here that the NRC is currently conducting research in the area of debris bypass through sump screens and flow blockage of HPSI throttle valves, and that this SER may be supplemented with the results of this research in early CY 2005. The staff would then expect licensees to consider the supplemental information in evaluating their plants for downstream effects.

The GR identifies the starting point for the evaluation to be the flow clearance through the sump screen and states that the maximum size of particulate debris that will pass through the sump screen is determined by the flow clearance through it. The GR states that wear and abrasion of surfaces in the ECC and CS should be evaluated based on flow rates to which the surfaces will be subjected and the grittiness or abrasiveness of the ingested debris. The GR recognizes that the abrasiveness of debris is plant-specific. The GR also states that wear and abrasion of pumps due to ingestion of debris may have been addressed by the pump manufacturer and advises licensees to contact their vendor regarding the ability of the pump to perform with debris in the process fluid.

**Staff Evaluation for Section 7.3:** The GR states, "If passages and channels in the ECC and CS downstream of the sump screen are larger than the flow clearance through the sump screen, blockage of those passages and channels by ingested debris is not a concern." In addition, the GR states, "Similarly, wear and abrasion of surfaces in the ECC and CS should be evaluated based on flow rates to which the surfaces will be subjected..." The staff finds the GR statements do not fully address the potential safety impact of LOCA generated debris on components downstream of the containment sump. The following represents staff expectations on the review of the effects of debris on components and systems downstream of the containment sump following initiation of containment recirculation. (Refs. 68, 69)

The evaluation of GSI 191 should include a review of the effects of debris on pumps and rotating equipment, piping, valves and heat exchangers downstream of the containment sump related to emergency core cooling (ECC) and containment spray (CS) systems. In particular, any throttle valves installed in the ECC systems for flow balancing, e.g., HPSI throttle valves, should be evaluated for blockage potential. The evaluation should also address the effects of entrained debris on the reactor vessel and internal core components. (Refs. 2, 17)

In general, the downstream review must first define both long term and short term system operating lineups, conditions of operation, and mission times. Where more than one ECC or CS configuration is used during long and short term operation, each line-up shall be evaluated with respect to downstream effects. The definition of the design and license bases mission times form the premise from which the short and long term consequences will be determined and evaluated.

Once condition of operation and mission times are established, downstream process fluid conditions should be defined including assumed fiber content, hard materials, soft materials, and various sizes of material particulates. The staff has found that particles larger than the sump screen mesh size will pass through to downstream components. Debris may pass through due to its aspect ratio or because it is 'soft' and differential pressure across the screen pulls it through. No credit may be taken for 'thin bed' filtering effects. (Refs. 68, 69)

Evaluations of systems and components are to be based on the flow rates to which the wetted surfaces will be subjected and the grittiness or abrasiveness of the ingested debris. The abrasiveness of the debris is plant specific, as stated in the GR, and depends on the site-specific materials that may become latent or break-jet-generated debris.

Specific to pumps and rotating equipment, an evaluation should be performed to assess the condition and operability of the component during and following its required mission times. Consideration should be given to wear and abrasion of surfaces; for example, pump running surfaces, bushings, wear rings, etc. Tight clearance components or components where process water is used either to lubricate or cool should be identified and evaluated.

Dirt, dust, and other materials may combine or interact with fiber and cause a matting effect. This matting effect may significantly increase the rate of wear. Test data and operating experience has shown that hard faced components will wear under long-term exposure to post accident 'slurry' conditions. Soft surface materials such as brass, bronze, etc. will wear at much faster rates.

Component rotor dynamics changes and long-term effect on vibrations due to potential wear should be evaluated in the context of pump and rotating equipment operability and reliability. The evaluation should include the potential impact on pump internal loads to address such concerns as rotor and shaft cracking. (Refs. 68, 69)

As stated in the GR, pump manufacturers may have addressed wear and abrasion of pumps due to ingestion of debris. Licensees may consider requesting information and/or test data from the pump vendor regarding the ability of specific pumps to perform

with debris in the process fluid. Other sources of information available to licensees include information generated to support the closeout of USI A-43, "Containment Emergency Sump Performance," such as NUREG/CR-2792, "An Assessment of Residual Heat Removal and Containment Spray Pump Performance Under Air and Debris Ingesting Conditions."

The downstream effects evaluation should also consider system piping, containment spray nozzles and instrumentation tubing. Settling of dusts and fines in low flow / low fluid velocity areas may impact system operating characteristics and should be evaluated. The matting effect may cause blockages and should be addressed. The evaluation should include such tubing connections as provided for differential pressure from flow orifices, elbow taps, and venturis and reactor vessel / RCS leg connections for reactor vessel level and any potential to affect instrumentation necessary for continued long term operation.

Valve (Ref. 70) and heat exchanger wetted materials should be evaluated for susceptibility to wear, surface abrasion, and plugging. Wear may alter the system flow distribution by increasing flow down a path (decreasing resistance due to wear), thus starving another critical path. Or conversely, increased resistance due to plugging of a valve opening, orifice, or heat exchanger tube may cause wear to occur at another path that is taking the balance of the flow thus diverted from the blocked path.

Decreased heat exchanger performance due to plugging, blocking, plating of slurry materials or tube degradation should be evaluated with respect to overall system required hydraulic and heat removal capability.

An overall ECCS or CS system evaluation integrating limiting or worst case pump, valve, piping and heat exchanger conditions should be performed including the potential for reduced pump/system capacity due to internal bypass leakage or through external leakage. Internal leakage of pumps may be through inter-stage supply and discharge wear rings, shaft support and volute bushings, etc. (Refs. 68, 69) Piping systems design bypass flow may increase as bypass valve openings increase or as flow through a heat exchanger is diverted due to plugging or wear. External leakage may occur as a result of leakage through pump seal leak-off lines, from the failure of shaft sealing or bearing components, from the failure of valve packing or through leaks from instrument connections and any other potential fluid paths leading to fluid inventory loss.

Leakage past seals and rings due to wear from debris fines to areas outside containment should be evaluated with respect to fluid inventory and overall accident scenario design and license bases environmental and dose consequences.

Fluids present post LOCA during long and short term recirculation may flow through the reactor vessel and its internal components. The downstream effects evaluation should consider flow passage blockages such as associated with core grid supports, mixing vanes, and debris filters. The evaluation should also consider component binding such as reactor vessel vent valves in B&W designs.

If flow paths between upper downcomer and upper plenum / upper head (such as hot leg nozzle gaps and upper head cooling passages) have an influence on long term cooling, then the potential for plugging these paths should be addressed.

**Staff Conclusions Regarding Section 7.3:** The staff finds that the GR is non-conservative with respect to its statement that the maximum size of particulate debris that would pass through a sump screen is determined by the flow clearance through the sump screen. As stated above, the staff has seen evidence that particles larger than the flow openings in a screen will deform and flow through or orient axially and flow through. (Refs. 68, 69) Licensees should determine, based on their debris generation and transport calculations, what percentage of debris would likely pass through their sump screen and be available for blockage at the downstream locations discussed above.

The evaluation of downstream effects should include consideration of term of operating line-up (long or short), conditions of operation, and mission times as stated above.

Consideration should be given to wear and abrasion of pumps and rotating equipment as discussed above. (Refs. 68, 69) Licensee's downstream effects evaluations should consider system piping, containment spray nozzles, and instrumentation tubing as well. Valve and heat exchanger wetted surfaces should be evaluated for wear, abrasion, and plugging. Wear should be evaluated with respect to the potential to alter system flow distribution. Heat exchanger performance should be evaluated with respect to the potential for blockage or the plating of slurry materials. HPSI throttle valves should be specifically evaluated for their potential to plug and/or wear. (Ref. 70) ECCS and CS overall performance should be evaluated with respect to all conditions discussed above.

. Flow blockage such as associated with core grid supports, mixing vanes, and debris filters should be considered. Flow paths between upper downcomer and upper plenum / upper head should be evaluated for long term cooling degradation due to flow interruption from plugging.

As stated above, the staff concludes that the GR recommendations do not fully address the potential safety impact of LOCA generated debris on components downstream of the containment sump. Licensees should address the additional considerations detailed above in the staff's evaluation.

In order to effectively evaluate downstream effects, licensees may need to review equipment specifications, O&M (operations and maintenance) manuals, station drawings such as equipment, piping, isometrics, flow diagrams, etc. Review of previous physical walkdowns of piping and instrument systems may be necessary to verify low points where debris accumulation may occur, potential choke points or other areas of concern not readily verifiable from document reviews. Also Leakage past seals and rings due to wear from debris fines to areas outside containment should be evaluated with respect to license bases environmental and dose consequences Previously issued generic communications regarding downstream effects, HPSI throttle valve clogging, wear of HPI Pump, pipe line clogging, heat exchanger wear due to operation under abrasive or debris laden conditions should also be reviewed.

#### **7.4 CHEMICAL EFFECTS**

Section 7.4 of the GR introduces the potential problems of chemical reactions in the post-LOCA environment of PWR containments. The reaction products formed can contribute to blockage of the ECCS sump screens and increase the associated head loss across the screens. The GR notes that a test plan has been developed to study possible interactions among corrosion products and the resultant effects of those

products on sump filtration. The GR defers guidance for dealing with these effects until the testing is completed and the data has been appropriately evaluated.

For the purpose of this SER, the issue of chemical effects involves interactions between the post-LOCA PWR containment environment and containment materials that may produce corrosion products, gelatinous material, or other chemical reaction products capable of affecting sump screen head loss. A concern was raised by the Advisory Committee on Reactor Safeguards (ACRS) that an adequate technical basis should be developed to resolve the issues related to chemical reactions (ACRS letter dated 9/30/2003). A "gelatinous" material was observed in a water sample taken from the Three Mile Island (TMI) containment following the accident in 1979. (Oak Ridge National Laboratory Report Memorandum dated September 14, 1979). The relevance of the gelatinous material collected at TMI to the evaluation of potential post-LOCA chemical effects during the ECCS recirculation phase in plants today is uncertain for several reasons. The water sample containing a gelatinous material was collected from the TMI containment approximately 5 months after the accident, which is longer than the typical projected mission time for ECCS recirculation following a modern day PWR LOCA. The source of the water sample collected from the TMI containment was also unique in that some of the water in the TMI containment after the accident was introduced from the Susquehanna River.

A limited scope study was conducted at Los Alamos National Laboratory (LANL) to evaluate potential chemical effects occurring following a LOCA. This study was conducted to assess the potential for chemically induced corrosion products to impede ECCS performance. In some of these tests, metal nitrate salts were added to the test water in concentrations above their solubility limits in order to induce chemical precipitants and assess head loss effects. Although these LANL tests showed that gel formation, with a significant accompanying head loss across a fibrous bed was possible, no integrated testing was performed to demonstrate a progression from initial exposure of metal samples to formation of chemical interaction precipitation products. (LANL Report LA-UR-03-6415, ML033230260). In addition, the test conditions were not intended to be prototypical of a PWR post-LOCA environment. Therefore, a more comprehensive study has been initiated to address potential chemical effects.

An integrated chemical effects test program has been developed through a collaborative effort between the NRC and nuclear industry. The test objective is to characterize any chemical reaction products, including possible gelatinous material, that may develop in a representative plant post-LOCA PWR environment. Test conditions (e.g., pH, temperature, boron concentration) were selected to simulate representative, not necessarily bounding plant conditions. The initial sump conditions experienced during a large break LOCA will not be replicated in order to simplify the experimental test setup and equipment. Instead, the chemical reactions from corrosion and leaching products during the initial LOCA conditions were simulated using the OLI Systems Inc. Suite of Thermodynamic Equilibrium Programs (e.g., Environmental Simulation Program Version 6.6 and Stream Analyzer Version 1.2). The simulations varied the amount of key components, different pH moderators (i.e., sodium hydroxide versus trisodium phosphate), pH, temperature, and pressure and the results indicated large scale corrosion tests using a pressurized test loop were not necessary to capture the period immediately following the LOCA. Thermodynamic simulations and sensitivity analyses of key variables including corrosion products, were developed to rank species that have a potential for causing sump head loss through formation of precipitates. Validation of

the appropriate OLI Systems Inc. programs will be performed using available borated water literature and by comparing the Program's initial post-LOCA environment species predictions to results obtained in small scale (e.g., autoclave) corrosion tests in a representative initial post-LOCA environment.

Larger scale corrosion testing will be conducted using facilities at the University of New Mexico. Corrosion test coupon materials include zinc (galvanized steel and inorganic zinc based coatings), aluminum, copper, carbon steel, insulation, and concrete. Relative amounts of test materials were scaled according to plant data provided by the industry based on plant surveys. Test coupons will either be fully immersed or placed above the test loop water line but subjected to a fine spray to simulate exposure to containment spray. The relative distributions of each material were determined based on estimated percentages submerged or subjected to containment sprays following a plant LOCA. If gelatinous material is observed to develop, testing will be placed on hold and alternative courses of action considered (e.g., head loss tests). Initial testing is expected to begin in September 2004.

In order to address chemical effects on a plant specific basis, licensees will initially need to evaluate whether the chemical effects test parameters are sufficiently bounding for their plant specific conditions. If plant specific materials are not bounded by the chemical effects test parameters, licensees shall provide technical justification to use any results from the chemical effects tests in their plant specific evaluation. If chemical effects are observed during these tests, licensees will need to evaluate the sump screen head loss consequences of this effect in an integrated manner with other postulated post-LOCA effects. In addition, a licensee who chooses to modify their plant sump screens prior to the completion of chemical effects testing and analysis of the test results should consider potential chemical effects in order to ensure a second plant modification is not necessary should deleterious chemical effects be observed during testing.

## 8.0 CONDITIONS AND LIMITATIONS

The guidance in the GR and in this SER is offered for all licensees of domestic PWRs for the evaluation of ECCS sump performance. However, the following conditions and limitations apply to its use:

### **Debris Generation**

- 1) In the use of a spherical ZOI, truncation is judged to be nonconservative; therefore, the staff position is that calculated ZOI volumes be conserved within break compartments and adjacent rooms along the fluid expansion path.
- 2) The destruction pressures cited in the GR for determining ZOI radii are based on air jet data and could underestimate debris quantities for a two-phase jet, as discussed in Section 3.4.2.2 of this SER. Therefore the staff position is that destruction pressures based on air jet testing are to be lowered by 40% in order to account for two-phase jet effects.
- 3) The GR provides calculated and recommended values for ZOI radii for common PWR insulation and coatings materials in Table 3.1. The staff determined that the calculated values were non-conservative at higher destruction pressures but the recommended values are conservative. Therefore the staff position is that only the recommended values be used.
- 4) The staff agrees with the characterization of debris in GR Section 3.4.3; however, the staff position is that licensees apply insulation-specific debris size information if possible.

### **Protective Coatings**

- 5) Characterization of failed coatings with the value of 1000 psi as a destruction pressure, with corresponding ZOI of one pipe diameter is not sufficiently justified and may be nonconservative, as discussed in Section 3.4.2. Therefore, the staff position is that licensees should use a coatings ZOI equivalent to 10D or a ZOI determined by plant specific analysis, based on experimental data that correlate to plant materials over the range of temperatures and pressures of concern.
- 6) The alternative offered to plant-specific data in Section 3.4.3.4, for the determination of coatings thicknesses, may not be conservative, is not acceptable without adequate plant-specific justification.
- 7) For those plants that substantiate no formation of a fibrous thin bed, the assumptions and guidance provided in the GR may be nonconservative. Therefore, for any such plant, assumptions as to debris characterization, particularly for coatings characterization, must be conservative with regard to sump blockage. Consideration must be based upon the plant-specific environment and susceptibility to thin bed formation identified by the licensee. Specifically this includes the plant-specific consideration of larger sized chips, flakes, or other form of break-down which is realistically-conservative.

### **Latent Debris**

- 8) Periodic surveys that monitor changes in latent debris inventory are required to monitor the effectiveness of cleanliness programs for supporting the overall sump screen blockage vulnerability. The steps presented in the GR for direct assessment of dust thickness are considered by the staff to be impractical and unreliable, and thereby unacceptable. To provide more accurate results, statistical surface sampling must be performed in accordance with the guidance provided in this SER.
- 9) In addition to the three categories of miscellaneous debris discussed in the GR, the quantity, characteristics and location of any failed coatings must also be noted in the survey, to the extent available during plant specific walkdowns

### **Transport**

- 10) Those plants with configurations conducive to fast pool velocities should include large piece debris transport in their evaluations. The GR baseline methodology that assumes no transport of large debris to the sump screens is not adequate. A comparison of the characteristic transport velocities to typical debris transport velocities is needed to determine whether or not large piece debris transport is important.
- 11) Because (1) the method recommended for determining the quantity of fine debris trapped in inactive pools is over-simplified, (2) a survey of the fractions of inactive pool volumes to total sump pool water volumes is not available to better judge the potential industry wide impact of this assumption, and (3) the comparison of the baseline methodology and a detailed analysis for the volunteer plants was considerably different; a limit on this fraction is needed to limit the impact of this nonconservative methodology assumption. Therefore, the staff concludes that an upper limit on this ratio of 15% should be assumed unless a higher fraction is adequately supported by analyses or experimental data.
- 12) The baseline assumption that all debris in the containment bottom floor is uniformly distributed throughout the entire volume of water in containment is also not conservative. This assumption was made in the baseline guidance as justification for the inactive pool volume ratio but otherwise does not directly affect the acceptance of the baseline guidance due to the 100% recirculation pool transport assumption. However, should a plant subsequently perform a pool transport refinement, then this assumption would not apply and at that point alternative approaches such as those detailed in Appendix III would be required.

### **Alternative Evaluation**

- 13) For licensees applying the Alternate Evaluation methods described in Section 6 of the SER, the staff considered the GR guidance regarding consideration of the ongoing 10 CFR 50.46 rulemaking effort. The staff agrees with the recommended guidance that licensees may re-perform the sump performance evaluations using the final break size specified by rulemaking,

and modify the plant design and operation accordingly. This would assure consistency with a new 10 CFR 50.46. However, the guidance provided in the GR seems to imply that the final break size specified by the new 10 CFR 50.46 will be smaller than the DGBS defined above for GSI-191 debris generation purposes. Should the final design basis LOCA break size specified by the new 10 CFR 50.46 be larger than the DGBS defined in Section 6 for GSI-191 debris generation purposes, the staff requires that licensees using the alternate methodology of Section 6 re-perform their sump performance evaluations consistent with the final break size specified by rulemaking, and modify the plant design and operation accordingly.

#### **Downstream Effects**

- 14) Licensees should consider particles larger than the flow openings in a sump screen will deform and flow through or orient axially and flow through, and determine what percentage of debris would likely pass through their sump screen and be available for blockage at downstream locations.
- 15) Licensees should consider term of system operating line-up (short or long), conditions of operation, and mission times.
- 16) Licensees should consider wear and abrasion of pumps and rotating equipment, piping, spray nozzles, instrumentation tubing, and HPSI throttle valves. The potential for wear to alter system flow distribution and/or form plating of slurry materials (in heat exchangers) should be included.
- 17) Licensees should consider leakage past seals and rings due to wear from debris fines to areas outside containment, with respect to license basis dose consequences.
- 18) An overall ECCS or CS system evaluation should be performed considering the potential for reduced pump/system capacity due to internal bypass leakage or through external leakage.
- 19) Licensees should consider flow blockage associated with core grid supports, mixing vanes, and debris filter, and their effects on fuel rod temperature.

#### **Chemical Effects**

- 20) The staff has considered NEI's response and finds that chemical effects must be addressed on a plant-specific basis. Initially, licensees must evaluate whether the current chemical test parameters, which are available in the test plan for the joint NRC/Industry Integrated Chemical Effects Tests, are sufficiently bounding for their plant specific conditions. If they are not, then licensees must provide technical justification in order to use any of the results from the tests in their plant-specific evaluation. If chemical effects are observed during these tests, then licensees must evaluate the sump screen head loss consequences of this effect. A licensee who chooses to modify their sump screen before tests are complete should consider potential chemical effects in order to avoid additional screen modification should deleterious chemical effects be observed during testing.



## 9.0 CONCLUSION

The GR provides the PWR industry with an important tool for estimating the head loss across their ECCS sump screens based on the generation, transport, and accumulation of debris in containment to and on the sump screens. The NEI approach is to provide guidance and leave certain areas to be resolved on a plant-specific basis, as opposed to providing a detailed methodology that applies to all PWRs as a stand-alone document (as was done for BWRs with the URG), based on the argument of variability among PWRs. Little testing was done by NEI to support and justify assumptions made in the GR (as opposed to the approach by the BWROG to generate data that supports the URG). However, the NEI guidance provides historical data, considerations, and engineering judgments that can be used by the industry to develop those areas not fully addressed in the GR.

The iterative process used by NEI in this GR also creates some challenges in the overall review. Specifically, although this guidance has been characterized by NEI as extremely conservative, the iterative process allows for the reduction of conservatism in various areas (identified in each affected section of this evaluation) that could affect other areas of the analysis to produce larger reductions in overall conservatism than were expected. Therefore, characterization of the overall realistic-conservatism of this GR was difficult.

The approach taken by the staff was to evaluate each area of the GR, and in those areas where there was a lack of supporting data or where conservatism was questioned, provide alternative guidance based on the staff's engineering judgment and/or additional data generated in testing done mainly at LANL. This data is a result of testing specifically contracted by the NRC over the last five years as part of the GSI-191 resolution effort, and involves sump performance research which was completed but in a few cases not published, and is referenced (Ref x) and/or included as appendices in this document. Inclusion of this additional information is also intended to provide valuable insight to the industry in its effort toward evaluating plant-specific vulnerability to sump blockage and related issues.

The staff concludes that the combination of the guidance proposed by NEI with that alternative guidance offered by the staff in this SER, provides an acceptable evaluation methodology that establishes the necessary basis and provides the realistic-conservatism for an acceptable PWR guidance document. Key conclusions in each area of the analysis are documented below.

**Pipe Break Characterization:** The staff finds that the GR guidance is acceptable provided that two outstanding issues, listed below, are adequately addressed by each licensee:

- 1) The GR does not provide guidance for those plants that can substantiate no thin bed effect, which may impact head loss results and limiting break location.
- 2) For plants needing to evaluate secondary-side piping such as main steam and feedwater pipe breaks, break locations should be postulated in a manner consistent with the guidance in Section 3.3 of this SER.

To address these issues, the staff has provided enhanced guidance in Sections 3.3 and 3.4 of this SER, and in combination with the enhanced guidance offered in the SER, the staff finds this section to be acceptable.

**Debris Generation/Zone-Of-Influence:** The staff has reviewed the use of a spherical model sized in accordance with the ANSI/ANS standard, and finds this approach acceptable. The spherical geometry proposed encompasses a zone which considers multiple jet reflections at targets, offset between broken ends of a guillotine break, and pipe whip. The GR recommendation to truncate the spherical ZOI was judged to be nonconservative; therefore the staff position is that calculated ZOI volumes be conserved within break compartments and adjacent rooms along the fluid expansion path.

With regard to the destruction pressures cited for determining ZOI radii, data are referenced from the BWROG URG which were determined using an air jet. However a LOCA jet is a two-phase steam/water jet. Based on staff study of this difference and due to experimental evidence from two-phase jets, the destruction pressures based on air jets could be too high and thus could underestimate debris quantities. Therefore the staff position is that destruction pressures based on air jet testing are to be lowered by 40% in order to account for two-phase jet effects.

The confirmatory analysis performed by the staff (Appendix I) verifies the applicability of the ANSI/ANS standard for determining the size of this zone. Use of a ZOI model is identified as an acceptable approach for analyzing debris generation per RG 1.82, Rev. 3. (This approach was also used and approved by the staff in the BWR sump performance SER.)

The refinement offered in the GR to apply spherical ZOIs that correspond to material-specific destruction pressures for each material that may be affected in the vicinity of a break, is also acceptable.

The staff concurs with the characterization of debris in GR Section 3.4.3. Confirmatory analyses provided in Appendix II, verifies the acceptability of the size distributions recommended in the GR. However, the staff urges application of insulation-specific debris size information if possible.

**Protective Coatings:** Coating debris generation in the GR is treated separately from other debris types. The GR assumes that coating debris are generated from postulated failure (destruction) of both DBA-qualified and unqualified coatings within the ZOI and from postulated failure of all unqualified coatings outside the ZOI. For coatings, the GR recommends a ZOI destruction pressure of 1000 psi, with a corresponding ZOI radius of one pipe diameter. The GR assumes that all coating debris will fail to a particulate size equivalent to the basic material constituent.

The staff agrees with the approach taken with regard to characterization of coatings; however the staff considers there to be insufficient technical justification to support a value of 1000 psi as a destruction pressure, with corresponding ZOI of one pipe diameter. The staff position is that licensees should use a coatings ZOI equivalent to 10D or a ZOI determined by plant specific analysis, based on experimental data that correlate to plant materials over the range of temperatures and pressures of concern.

Note that an equivalent to ten pipe diameters was used for coatings characterization and was approved by the staff in the BWR sump performance SER.

Although Appendix A of the GR provides useful test data illustrating erosion effects of high-pressure water jets on coating systems, no test data are offered that combine both the effects of mechanical insult and elevated temperature in the same test, and no data appear to be available on the effects of very rapid thermal transients on coating performance. Therefore, the staff finds the results of the water jet testing to be inconclusive in this regard.

With regard to the characterization of coatings in Section 3.4.3.4 of the GR, an alternative offered to plant-specific data for the determination of coatings thicknesses is an equivalent IOZ thickness of 3 mils. Because this recommended value may be nonconservative and is unsubstantiated as is described in Section 3.4.3.4, the staff finds that this value of 3 mils not to be acceptable without adequate plant-specific justification for any coatings thicknesses used. Plant-specific evaluation of the unqualified coatings within containment is recommended to be performed to determine realistically-conservative coating properties, including thicknesses. Further, it is recommended that means be incorporated into the methodology to periodically assess the amount of unqualified coating identified and used in the sump analysis to ensure the quantity remains bounding and if nonconserveative changes in the amount of unqualified coating occur, that the impact of this change be evaluated.

Also, for those plants that substantiate no formation of a fibrous thin bed, the assumptions and guidance provided in the GR may be nonconservative. Therefore, for any such plant, assumptions as to debris characterization, particularly for coatings characterization, must be conservative with regard to sump blockage. Consideration must be based upon the plant-specific environment and susceptibility to thin bed formation identified by the licensee. Specifically, this includes the plant-specific consideration of larger sized chips, flakes, or other form of break-down which is realistically-conservative.

**Latent Debris:** The staff has reviewed the guidance provided for estimating the impact of latent debris and agrees that it is necessary to determine the types, quantities and locations of latent debris sources. The staff also agrees that it is not appropriate for licensees to claim that their existing foreign material exclusion (FME) programs have entirely eliminated miscellaneous debris. Results from plant specific walkdowns must be used to determine a conservative amount of latent debris in containment and to monitor cleanliness programs for compliance to committed estimates.

The staff further concludes that the guidance provided in the GR for consideration of effects of latent debris is informative and prescriptive, but treats certain attributes in an inconsistent manner, lacks consideration of a number of surfaces and unique phenomena that enhance dust collection, and relies on an impractical and imprecise method for estimating the volume of latent debris on surfaces. Alternate guidance is provided in this section of the SER for statistical sampling and sample analysis to allow licensees to more accurately determine the impact of latent debris on sump screen performance. This revised approach is based on generic characterization of actual PWR debris samples. If desired, a licensee could pursue plant-specific characterization as a refinement.

**Debris Transport:** The staff finds that the transport guidance for small fines is conservative and acceptable; however, neglect of the large pieces and the neglect of variability and uncertainties due to lack of data, are non-conservative. Therefore, for those plants with configurations conducive to fast pool velocities, consideration of large pieces of debris is necessary. Also, the method recommended for determining the quantity of fine debris trapped in inactive pools, is over-simplified, and therefore the acceptability of this method will be determined on a plant-specific basis depending on whether overall realistic-conservatism is maintained for this portion of the analysis.

**Head Loss:** Computation of head loss in the GR involves input of design characteristics and reflection of thermal-hydraulic conditions into a head loss correlation (NUREG/CR-6224), which is acceptable to the staff.

However, the staff finds that the following guidance is necessary in the consideration of fibrous thin bed formation:

- Use of the appropriate density in the determination of the quantity of debris needed to form a thin bed—i.e., the as-manufactured density.
- Careful evaluation of the limiting porosity for the particular particulate or mixture of particulates in the debris bed.
- Consideration of uncertainties in specifying a one-eighth-inch bed thickness criteria—e.g., the strong indication that calcium silicate can form a debris bed without supporting fibers.
- Consideration of other uncertainties—e.g., uncertainties associated with mixing of constituents, or uncertainties associated with latent debris data collection.

Additional guidance is offered by the staff in Sections 3.7.2.2 and 3.7.2.3 of this SER.

**Analytical Refinements:** Three analytical topics are identified in the GR to be included in this section—i.e., debris generation, debris transport, and head loss. A fourth, break selection, is addressed in Section 6.0.

For debris generation, the GR proposes use of debris-specific ZOI's versus use of the most conservative debris type applied to all. In addition, the GR proposes use of two freely-expanding jets emanating from each broken pipe section versus use of spherical ZOI. The staff finds both debris generation refinements to be acceptable.

For debris transport, two methods for computing flow velocities in a sump pool—i.e., the network method and the computational fluid dynamics method—are provided in the Analytical Refinements section of the GR. However, the staff finds insufficient guidance offered in either option to provide an acceptable alternative to the baseline approach. These refinements are thereby not acceptable.

For head loss, the only refinement cited by the GR is stated to be in GR Section 3.7.2.3.2.3, "Thin Fibrous Beds," where the need for consideration of fibrous thin bed formation, and the alternative consideration of latent debris as the primary contributor to this thin bed for all-RMI plants, are addressed. However, the staff addresses

consideration of thin fibrous beds in Section 3.4, "Debris Generation," of this SER pertaining to the baseline, rather than as a refinement.

Therefore, staff finds no specific refinement offered for the head loss analysis; and, if some analytical refinement is sought by the licensee in its plant-specific analysis with regard to head loss, then the licensee must submit the proposed refinement to the staff for review and approval prior to its use.

**Physical Refinements To Plant:** GR Section 5.0 provides guidance for refinements in the areas of debris source term, debris transport obstructions, and screen modifications.

The staff has reviewed the debris source term refinements involving primarily enhanced housekeeping programs, insulation and/or coatings modifications, and equipment modifications; and finds them to be acceptable. However, with regard to insulation change-out or modification, the staff emphasizes that although maximum debris loadings on the screen may be addressed with this refinement, minimum loadings required to form a thin-bed effect may not be. Also, on the coatings area, the statement that DBA-qualified coatings have very high destruction pressures, has not been proven (see sections 3.4.2, 3.4.2, and 4.2.2.2.3).

The staff agrees that debris consistent with the materials listed can be effectively trapped with the use of a debris transport obstructions in optimized locations where the local velocities are less than the test results presented. The staff finds the general statements in parts of this section to provide little specific information regarding the methods for determining proper debris transport obstruction design. However, the lack of specific implementation strategies and simplified concepts presented would require each plant to perform a plant specific evaluation of their proposed debris obstruction to determine their effectiveness and structural capability under post-accident conditions. To credit debris transport obstructions for trapping debris, plant specific documentation will also be required to demonstrate an appropriate correlation to the test results in terms of debris type and velocity limits.

With regard to screen modification, those discussed in the GR are found to be acceptable; however, licensees are not limited to those identified in this GR.

**Alternate Evaluation:** NEI has proposed an alternative evaluation approach which incorporates realistic and risk-informed elements to the PWR sump analysis as described in Section 6.0. The staff concludes that GR Section 6.0 provides an acceptable approach for evaluating PWR sump performance. Application of more realistic and risk-informed elements is technically justified based on the low likelihood of such breaks occurring.

**Sump Structural Analysis:** The GR does not provide detail in its presentation of criteria for sump screen performance and comparisons to predicted head loss. To clarify this, the staff notes that the ECCS sump must be able to accommodate both the clean screen head loss and the debris-induced head loss associated with the limiting break while providing adequate flow through both the ECCS injection pumps and the CS pumps if needed. For those structural design considerations mentioned in the GR, each should be assessed for applicability on a plant-specific basis.

**Upstream Effects:** The GR identifies certain hold-up or choke points which could reduce flow to and possibly cause blockage upstream of the sump. The staff finds the guidance with respect to upstream blockage to be acceptable.

**Downstream Effects:** This section provides guidance on the evaluation of entrained debris downstream of the sump causing downstream blockage. Because the GR provides limited guidance on how downstream effects should be evaluated, the staff provides the following alternative guidance with regard to downstream blockage:

- Licensees should consider particles larger than the flow openings in a sump screen will deform and flow through or orient axially and flow through, and determine what percentage of debris would likely pass through their sump screen and be available for blockage at downstream locations.
- Licensees should consider term of system operating line-up (short or long), conditions of operation, and mission times.
- Licensees should consider wear and abrasion of pumps and rotating equipment, piping, spray nozzles, instrumentation tubing, and HPSI throttle valves. The potential for wear to alter system flow distribution and/or form plating of slurry materials (in heat exchangers) should be included.
- Licensees should consider leakage past seals and rings due to wear from debris fines to areas outside containment, with respect to license basis dose consequences.
- An overall ECCS or CS system evaluation should be performed considering the potential for reduced pump/system capacity due to internal bypass leakage or through external leakage.
- Licensees should consider flow blockage associated with core grid supports, mixing vanes, and debris filter, and their effects on fuel rod temperature.

**Chemical Effects:** The staff has considered NEI's response and finds that chemical effects must be addressed on a plant-specific basis. Initially, licensees must evaluate whether the current chemical test parameters, which are available in the test plan for the joint NRC/Industry Integrated Chemical Effects Tests, are sufficiently bounding for their plant specific conditions. If they are not, then licensees must provide technical justification in order to use any of the results from the tests in their plant-specific evaluation. If chemical effects are observed during these tests, then licensees must evaluate the sump screen head loss consequences of this effect. A licensee who chooses to modify their sump screen before tests are complete should consider potential chemical effects in order to avoid additional screen modification should deleterious chemical effects be observed during testing.

**Overall Conclusion:** The staff has reviewed the GR and finds portions of the proposed guidance to be acceptable. For those areas found to need additional justification and/or modification due to inadequate detail, lack of supporting data, or lack of analysis to support the technical basis; the staff has provided identified conditions, limitations, and required modifications, including alternative guidance, to supplement the guidance in

the NEI submittal. The resultant combination of the NEI submittal and staff safety evaluation, provide an acceptable overall guidance methodology for the plant-specific evaluation of ECCS or CSS sump performance following all postulated accidents for which ECCS or CSS recirculation is required, with specific attention given to the potential for debris accumulation that could impede or prevent ECCS or CSS from performing its intended safety functions.

## 10.0 REFERENCES

- 1 NEI, 2004a Letter from A. R. Pietrangelo, NEI to J. H. Hannon, USNRC, ,  
"Pressurized Water Reactor Sump Performance Evaluation  
Methodology," Nuclear Energy Institute, May 28, 2004(proposed  
document number NEI 04-07) dated
- 2 GL-04-xx NRC Generic Letter 2004-XX, "Potential Impact of Debris Blockage  
on Emergency Recirculation During Design Basis Accidents at  
Pressurized-Water Reactors," dated August xx, 2004.
- 3 NEI, 2004b Letterfrom A. R. Pietrangelo, NEI xx to J. N. Hannon, USNRC xx,  
Transmittal of Baseline Evaluation Method Nuclear Energy  
Institute, dated April 19, 2004
- 4 NEI, 2003 Letter, , from A. R. Pietrangelo, NEI to xx,xx to J. N. Hannon,  
USNRC, xx Draft Transmittal of "PWR Containment Sump  
Evaluation Methodology," Nuclear Energy Institute, dated October  
31, 2003.
- 5 NRC, 2004a Letter, from S. C. Black, USNRC to A. R. Pietrangewlo, NEI ,  
Transmittal of NRC Preliminary Review of NEI Submittal of  
October 31, 2003, dated February 2, 2004
- 6 Mtg, 2004a Summary of Public Meeting Held March 23 and 24, 2004, Nuclear  
Regulatory Commission and Nuclear Energy Institute, to discuss  
PWR Containment Sump Evaluation Methodology and Requests  
for Additional Information, by Memorandum from J. G. Lamb,  
USNRC to L. Raghavan, USNRC, dated April 22, 2004
- 7 NEI, 2004c Letter, from A. R. Pietrangeo, NEI to J. N. Hannon, USNRC ,  
Nuclear Energy Institute Transmittal of Responses to Request for  
Additional Information of March 10, 2004, dated June 10, 2004.
- 8 NEI, 2004d Letter, from A. R. Pietrangelo, NEI to J. N. Hannon, USNRC,  
Nuclear Energy Institute Transmittal of Responses to Request for  
Additional Information of June 28, 2004, dated July 8, 2004.
- 9 NEI, 2004e Letter, from A. R. Pietrangelo, NEI to J. N. Hannon, USNRC,  
Nuclear Energy Institute Transmittal of Section 6, "Risk Informed  
Evaluation" of "PWR Containment Sump Evaluation Methodology,"  
dated July 13, 2004.
- 10 NUREG-0897 NUREG-0897, "Containment Emergency Sump Performance," US  
Nuclear Regulatory Commission, dated October 1985.
- 11 DG-1107 Draft Regulatory Guide DG-1107, "Water Sources for Long-Term  
Recirculation Cooling Following a Loss-of-Coolant Accident," U. S.  
Nuclear Regulatory Commission, Office of Nuclear Regulatory  
Research, transmitted December 2002.
- 12 NRCB, 1994 Bulletin 93-02, Supplement 1, "Debris Plugging of Emergency Core  
Cooling Suction Strainers," dated February 18, 1994
- 13 NRCB, 1995 Bulletin 95-02, "Unexpected Clogging of a Residual Heat Removal  
(RHR) Pump Strainer While Operating in Suppression Pool  
Cooling Mode," dated October 17, 1995;
- 14 NRCB, 1996 Bulletin 96-03, "Potential Plugging of Emergency Core Cooling  
Suction Strainers by Debris in Boiling-Water Reactors," dated May  
6, 1996
- 15 GL 85-22 NRC Generic Letter GL 85-22, "Potential for Loss of Post-LOCA  
Recirculation Capability Due to Insulation Debris Blockage," dated  
December 3, 1985

16 GSI 191 GSI-191, "Assessment of Debris Accumulation on PWR Sump Performance," dated xxxxx.

17 NRCB, 2003 NRC Bulletin 2003-01, "Potential Impact of Debris Blockage on Emergency Recirculation During Design-Basis Accidents at Pressurized-Water Reactors," dated June 9, 2003.

18 NUREG/CR-6762-1 NUREG/CR-6762, "GSI-191 Technical Assessment: Parametric Evaluations for Pressurized Water Reactor Recirculation Sump Performance," Vol. 1, dated August 2002.

19 NUREG/CR-6770 NUREG/CR-6770, "GSI-191: Thermal-Hydraulic Response of PWR Reactor Coolant System and Containments to Selected Accident Sequences," dated August 2002.

20 NUREG/CR-6762-3 NUREG/CR-6762, Vol. 3, "GSI-191 Technical Assessment: Development of Debris Generation Quantities in Support of the Parametric Evaluation," dated August 2002.

21 NUREG/CR-6762-4 NUREG/CR-6762, Vol. 4, "GSI-191 Technical Assessment: Development of Debris Transport Fractions in Support of the Parametric Evaluation," dated August 2002.

22 NUREG/CR-6224 NUREG/CR-6224, "Parametric Study of the Potential for BWR ECCS Strainer Blockage Due to LOCA Generated Debris," dated October 1995.

23 RG 1.82-3 Regulatory Guide (RG), Revision 3, "Water Sources for Long-Term Recirculation Cooling Following a Loss-of-Coolant Accident," dated November 2003

24 ANSI/ANS 58.2-1988 ANSI/ANS 58.2-1988, "American National Standard Design Basis for Protection of Light Water Nuclear Power Plants Against the Effects of Postulated Pipe Rupture," 1988.

25 NUREG/CR-6808 NUREG/CR-6808, "Knowledge Base for the Effect of Debris on Pressurized Water Reactor Emergency Core Cooling Sump Performance," U.S. Nuclear Regulatory Commission, February 2003.

26 URG SER Safety Evaluation by the Office of Nuclear Reactor Regulation Related to NRC Bulletin 96-03, Boiling Water Reactor Owners Group topical Report NEDO-32686, "Utility Resolution Guidance for ECCS Suction Strainer Blockage" (Docket No. Proj0691), dated August 20, 1998.

27 URG GE Nuclear Energy, "Utility Resolution Guide for ECCS Suction Strainer Blockage," by BWR Owners' Group, NEDO-32686-A, October 1998.

28 NUREG/CR-6369 NUREG/CR-6369, Vol 1: Drywall Debris Transport Study-Final Report; Vol 2: Drywell Debris Transport Study: Experimental Work-Final Report, February 1998.

29 NUREG/CR-6773 NUREG/CR-6773 (LA-UR-02-6786), "GSI-191: Integrated Debris-Transport Tests in Water Using Simulated Containment Floor Geometries," Los Alamos National Laboratory, December 2002.

30 CS, 2004a C. J. Shaffer, M. T. Leonard, B. C. Letellier, J. D. Madrid, A. K. Maji, K. Howe, A. Ghosh, and J. Garcia, "GSI-191: Experimental Studies of Loss-of-Coolant-Accident-Generated Debris Accumulation and Head Loss with Emphasis on the Effects of Calcium Silicate Insulation," Los Alamos National Laboratory report LA-UR-04-1227 (April 2004).

31 MD, 2004 Mei Ding, Amr Abdel-Fattah, Stewart Fischer, Bruce Letellier, Kerry

- Howe, Janet Garcia, and Clint Shaffer, "Characterization of Latent Debris from Pressurized-Water-Reactor Containment Buildings," Los Alamos National Laboratory report LA-UR-04-3970 (June 2004).
- 32 CS, 2004b Clinton J. Shaffer and Bruce C. Letellier, "GSI-191 Technical Study: Detailed Blowdown/Washdown Transport Analysis for Pressurized-Water-Reactor Volunteer Plant," Los Alamos National Laboratory report LA-UR-04-4338 (June 2004).
- 33 LA-UR-03-6415
- 34 GL-87-11 NRC Generic Letter 87-11, "Relaxation in Arbitrary Intermediate Pipe Rupture Requirements," dated June 19, 1987.
- 35 SRP NUREG-0800, "Standard Review Plan," U.S. Nuclear Regulatory Commission
- 36 SECY-04-0037 Memorandum from A. L. Vietti-Cook, to L. A. Reyes, "Staff Requirements - SECY-04-0037 - Issues Related to Proposed Rulemaking to Risk-Inform Requirements Related to Large Break Loss-of-Coolant Accident (LOCA) Break Size and Plans for Rulemaking on LOCA With Coincident Loss-of-Offsite Power," dated July 1, 2004.
- 37 Mtg, 2003e Summary of Public Meeting Held September 10, 2003, Nuclear Regulatory Commission and Stakeholders Concerning Generic Safety Issue 191, "Assessment of Debris Accumulation on PWR Sump Performance," (TAC No. MA6454) dated October 16, 2003.
- 38 Mtg, 2003d Summary of Public Meeting Held July 1, 2003, Nuclear Regulatory Commission and Stakeholders Concerning Generic Safety Issue 191, "Assessment of Debris Accumulation on PWR Sump Performance," (TAC No. MA6454) dated August 11, 2003.
- 39 Mtg, 2003c Summary of Public Meeting Held June 30, 2003, Nuclear Regulatory Commission and Stakeholders Concerning NRC Bulletin 2003-01, "Potential Impact of Debris Blockage on Emergency Sump Recirculation at Pressurized-Water Reactors," (TAC No. MA6454) dated August 12, 2003.
- 40 Mtg, 2003b Summary of Public Meeting Held April 29, 2003, Nuclear Regulatory Commission and Stakeholders Concerning Generic Safety Issue 191, "Assessment of Debris Accumulation on PWR Sump Performance," (TAC No. MA6454) dated May 15, 2003.
- 41 Mtg, 2003a Summary of Public Meeting Held March 5, 2003, Nuclear Regulatory Commission and Stakeholders Concerning Generic Safety Issue 191, "Assessment of Debris Accumulation on PWR Sump Performance," (TAC No. MA6454) dated April 24, 2003.  
Attachments:  
"Current Status and Plans Resolution of GSI-191," Accession Number ML031180084  
"Update of PWR Industry Plan to Address GSI-191," Accession Number ML031180102  
"NRC Comments on NEI Draft Evaluation Methodology Ground Rules," Accession Number ML031180095.  
"GSI-191: Analysis of Recovery Options," Accession Number ML031180119.  
"Debris Accumulation & CalSil Head Loss Testing – Findings &

- Preliminary Conclusions," Accession Number ML031180127.  
 "Volunteer Plant Containment Pool Flow Analysis," Accession Number ML031180140.  
 "Volunteer Plant (VP) ECCS Vulnerability Assessment," Accession Number ML031180154.
- 42 Mtg, 2003f Summary of Public Meeting Held December 12, 2003, Nuclear Regulatory Commission and Stakeholders Concerning Generic Safety Issue 191, "Assessment of Debris Accumulation on PWR Sump Performance," (TAC No. MA6454) dated December 12, 2003.
- 43 Mtg, 2002a Summary of Public Meeting Held March 28, 2002, Nuclear Regulatory Commission and Interested Stakeholders Concerning Generic Safety Issue 191, "Assessment of Debris Accumulation on PWR Sump Performance," (TAC No. MA6454), dated April 16, 2002.
- 44 Mtg, 2002b Summary of Public Meeting Held May 30, 2002, Nuclear Regulatory Commission and Interested Stakeholders Concerning Generic Safety Issue 191, "Assessment of Debris Accumulation on PWR Sump Performance," (TAC No. MA6454) dated June 6, 2002.
- 45 Mtg, 2002c Summary of Public Meeting Held July 2, 2002, Nuclear Regulatory Commission and Interested Stakeholders Concerning Generic Safety Issue 191, "Assessment of Debris Accumulation on PWR Sump Performance," (TAC No. MA6454) dated July 31, 2002.
- 46 Mtg, 2002d Summary of Public Meeting Held August 29, 2002, Nuclear Regulatory Commission and Stakeholders Concerning Generic Safety Issue 191, "Assessment of Debris Accumulation on PWR Sump Performance," (TAC No. MA6454) dated September 5, 2002.
- 47 Mtg, 2002e Summary of Public Meeting Held October 24, 2002, Nuclear Regulatory Commission, the Nuclear Energy Institute, and Interested Stakeholders Concerning Generic Safety Issue 191, "Assessment of Debris Accumulation on PWR Sump Performance," (TAC No. MA6454) dated October 31, 2002.
- 48 Mtg, 2002f Summary of Public Meeting Held December 12, 2002, Nuclear Regulatory Commission and Interested Stakeholders Concerning Generic Safety Issue 191, "Assessment of Debris Accumulation on PWR Sump Performance," (TAC No. MA6454) dated December 31, 2002.
- 49 Mtg, 2001 Summary of July 26-27, 2001, Meeting with Nuclear Energy Institute and Industry on ECCS Strainer Blockage in PWRs, dated August 14, 2001.
- 50 Rao, 2001 D. V. Rao, B. Letellier, C. Shaffer, S. Ashbaugh, and L. Bartlein, "GSI-191: Parametric Evaluations for Pressurized Water Reactor Recirculation Sump Performance," Draft Technical Letter Report, Los Alamos National Laboratory, July 2001.
- 51 NUREG/CR-6371 Shaffer, C., W. Bernahl, J. Brideau and D.V. Rao, BLOCKAGE 2.5 Reference Manual, NUREG/CR-6371, U.S. Nuclear Regulatory Commission, December 1996.
- 52 NEI, 2002a NEI 02-01, "Condition Assessment Guidelines: Debris Sources Inside PWR Containments," dated April 19, 2002.

- 53 NEI, 2002b "NEI Draft Evaluation Methodology Ground Rules" dated December 12, 2002.
- 54 Wkshp, 2003 NRC Presentations at NEI-Sponsored Public Workshop on Debris Impact on ECCS Recirculation, July 30-31, 2003, Baltimore, MD. [NRC ADAMS Accession No. ML032230372]
- 55 10 CFR Code of Federal Regulations, Title 10 "Energy"
- 56 SB, 2004 Letter from S. C. Black, USNRC, to A. Pietrangelo, NEI, "Nuclear Energy Institute's Proposals for Determining Limiting Pipe Break Size Used in Assessing Debris Generation Following a Design Basis LOCA (TAC NO. MC1154)," dated March 4, 2004.
- 57 RG 1.174 Regulatory Guide 1.174, "An Approach for Using Probabilistic Risk Assessment in Risk-Informed Decisions On Plant-Specific Changes to the Licensing Basis."
- 58 MEB 3-1 Branch Technical Position MEB 3-1, "Postulated Rupture Locations in Fluid System Piping Inside and Outside Containment," included in NUREG-0800, "Standard Review Plan (SRP)," (Reference 2), Section 3.6.2, "Determination of Rupture Locations and Dynamic Effects Associated with the Postulated Rupture of Piping."
- 59 NUREG-0588 NUREG-0588, "Interim Staff Position on Environmental Qualification of Safety-Related Electrical Equipment," Revision 1, July 1981.
- 60 RG 1.1 Regulatory Guide 1.1, "Net Positive Suction Head for Emergency Core Cooling and Containment Heat Removal System Pumps," November 2, 1970.
- 61 RG 1.82-3 Regulatory Guide 1.82, "Water Sources for Long-Term Recirculation Cooling Following a Loss-of-Coolant Accident," Revision 3, November 2003.
- 62 GL 91-18 Generic Letter 91-18, "Information to Licensees Regarding NRC Inspection Manual on Resolution of Degraded and Non-Conforming Conditions," Revision 1, October 8, 1997.
- 63 ANSI/HI 1.1-1.5 ANSI/HI 1.1-1.5 - 1994, "American National Standard for Centrifugal Pumps for Nomenclature, Definitions, Application and Operation."
- 64 OPG, 2001 Ontario Power Generation, "Jet Impact Tests—Preliminary Results and Their Applications," N-REP-34320-10000-R00, April 2001.
- 65 NIS96 National Institute of Standards and Technology, standard reference database 10, version 2.11, 1996.
- 66 WEI83 Weigand, G. G., et al., "Two-Phase Jet Loads," NUREG/CR-2913, Sandia National Laboratory (prepared for the U.S. Nuclear Regulatory Commission) January 1983.
- 67 DIN04 Ding, M., et al., "Characterization and Head-Loss Testing of Latent Debris from Pressurized-Water-Reactor Containment Buildings," prepared for the U.S. Nuclear Regulatory Commission by Los Alamos National Laboratory, LA-UR-04-3970, August 2004.

68 NUREG/CP-0152 Vol. 5 NUREG/CP-0152, Vol. 5, Proceedings of the Eighth NRC/ASME Symposium on Valve and Pump Testing, paper titled "Design, Testing and Implementation of Modifications to the Davis-Besse HPI Pumps for Debris Laden Water Operation" by Robert Coward and Stephen Kinsey, July 12, 2004, MPR Associates and Robert Schrauder, John O'neill and Stephen Osting, First Energy Nuclear Operating Company.

69 TIA 2003-04 Task Interface Agreement (TIA) No. 2003-04, Tac No. MC0584, Evaluation of Davis-Besse Modifications to the High Pressure Injection Pump and Associated Mock-up Testing dated February 11, 2004.

70 IN 96 – 27 NRC Information Notice 96-27, Potential Clogging of High Pressure Safety Injection Throttle Valves During Recirculation, May 1, 1966.

## Review of NEI Guidance Appendices

### Review of Appendix A, "Defining Coating Destruction Pressures and Coating Debris Sizes for DBA-Qualified and Acceptable Coatings in Pressurized Water Reactor (PWR) Containments"

The test program discussed in Appendix A is a nice starting point for assessing the necessary conditions to destroy qualified coatings and the resulting coating debris sizes. However, the aforementioned test program has several deficiencies and is far from producing quantitative results. These deficiencies are delineated below.

Unlike the test program discussed in Appendix A, testing should be done within an autoclave, wherein conditions can be controlled to simulate a LOCA and debris can be captured and characterized. The test program discussed in Appendix A approximated a break by a pressurized sprayer and found that any coating in close proximity to such a pipe break will be removed. However, a BWR testing program asserts that "the dynamic forces are what will cause a coating to detach and form debris ... It takes time for vapor pressure to build up within the coating film ... It also takes time for the hot moisture to soften and break the molecular bonds."<sup>1</sup> This same BWR report also asserts that "Hot water pressure washing is often carried out at pressures exceeding 2500 psi and at temperature of 200 °F to 250 °F. These cleaning methods will not remove sound IOZ or epoxy coatings." Additionally, this BWR report found "that coating failures which could generate debris would occur after six hours but within the first 4 days of the LOCA event." The test program discussed in Appendix A did not address any of the dynamic forces found in the BWR report to be responsible for coating failure. These BWR dynamic forces were identified as:

- Sustained (i.e., several hours), high (340 °F) temperature followed by an abrupt decrease in temperature of 90 °F, which causes thermal shock.
- Sustained exposure to steam.
- Elevated pressure (70 psi) followed by a series of abrupt decreases in pressure.
- Irradiation of test samples before testing to an accumulated dose of 1(10)<sup>9</sup> rads.
- Immersion in high purity water.

These forces exploit coating vulnerabilities related to aging (sustained heat and irradiation exacerbate the detrimental effects of oxygen), moisture absorption (silicate binders used in inorganic zinc coatings dissolve in hot water), and differences in epoxy and IOZ tensile strength (disbondment occurs during rapid pressure and temperature swings).

A LOCA in a PWR will not be the same as one in a BWR. However, there are several common LOCA features that adversely affect coatings:

---

<sup>1</sup> T. I. Aldinger, R. A. White, and R. A. Manley, "Performance of Containment Coatings During a Loss of Coolant Accident," Bechtel Power Corporation report (November 10, 1994).

- Abrupt changes in temperature.
- An initial rise to high (240 °F for a PWR) temperature.
- A drop to moderate (120 °F for a PWR) temperature when the ECCS is activated.
- Exposure to steam.
- Abrupt changes in pressure (100 psi for a PWR).
- Average coating will have accumulated a significant irradiation dose [ $\leq 1(10)^9$  rads].

Consequently, in addition to the erosion effects of a steam spray, a PWR testing program should also simulate the combined thermal and pressure shocks associated with the initiation of the LOCA and with the activation of the ECCS. Furthermore, “aged” coating specimens should be used that include the effects of prolonged exposure to oxygen and irradiation.

Recommendation: Adopt a testing program similar to that used for BWR coatings with the appropriate PWR-relevant modifications.

## **Review of Appendix B, "Example of a Latent Debris Survey"**

This Appendix in the GR provides a simplified example of a method for determining the amount of latent debris on containment surfaces. This Appendix does not contain new or unique information, and is not totally consistent with Section 3.5 of the GR where the detailed guidance for evaluating Latent Debris is contained. In the evaluation of Section 3.5, the staff provides a more comprehensive and accurate method for evaluation of Latent Debris. As such, a separate evaluation of this Appendix is not required.



## **Review of Appendix C, “Comparison of Nodal Network and CFD Analysis”**

The staff has reviewed the Appendix C comparison between the nodal network and CFD methods and finds that the conclusion of a “good comparison” is not supported by independent analysis and evaluations. The error values reported are computed by subtracting flow rates of the nodal network from the CFD and dividing by the total flow in the containment pool. The flows computed for the network sections are approximately 1000 gpm (order of magnitude). The total flow is 21,000 gpm, more than an order of magnitude larger than the individual flow rates, and almost 2 orders of magnitude larger than the flow difference between the two methods. The staff does not consider this approach to be a valid method for comparing nodal network results to those achieved with CFD analysis.

The staff finds that normalizing the flow error between the two methods by the total recirculation flow rate is incorrect, and minimizes the significance of the errors between the two methods. Particles/debris respond to local velocities, not normalized values. Comparison of the nodal values to the CFD values shows that there is quite a discrepancy in the associated local velocity values and discrepancies can also exist with respect to flow direction.

Also, in the information presented in the GR it is not clear how the flow channels were selected. In Figure 4-4 of the GR, the flow channels were determined by using the CFD analysis and essentially encapsulate the high velocity regions. Where the velocities are uniform across the channel, the comparison is fairly good in absolute terms, but not their “error” terms. When there is a gradient of velocity across the channel, the difference in the CFD versus nodal network velocity is quite large. Without the CFD analysis, the GR does not provide guidance for selecting the channel network. Even when the CFD results are known, the nodal network does not give a reasonable answer. The staff finds that relying on such a method for general use, where the flows are not known a priori is a difficult method to implement.

Appendix C does not provide a reference for the nodal analysis method used, nor is the method explicitly defined in the document. There is discussion about friction factors, having to choose a velocity for the Reynolds number assumed for the flow and needing to iterate to arrive at the correct velocity, but there are no equations or methodology outlined to follow. These conditions should be included and appropriate references cited for both the methodology and previously published applications to this type of flow problem.

Other issues the staff identified in Appendix C include:

A description of how the CFD flow rates were calculated for the nodal sections shown in Figure 4-4 is not provided.

Figure 4-4 is not a “composite” of the CFD results, it is exactly the case for a large local break in the lower right quadrant, not a composite of all break locations and flows.

On Page C-4 – the threshold velocities quoted are to initiate motion of debris, not to sustain motion. The velocity required to sustain the debris motion may in fact be much lower, i.e., starting vs. rolling friction.



This page is intentionally blank.

### Review of Appendix D, "Isobar Maps for Zone of Influence Determination"

The staff evaluation of GR Section 3.4.2.2 compared the ZOI isobars set forth in Appendix D of the GR with isobars independently calculated using the methodology of ANSI/ANS 58.2-1988. The comparison showed good agreement between the calculations for downrange behavior (Zone 3), but discrepancies exist in Zones 1 and 2. As indicated in Figure 3-1 of this SER, it appears that contour termination points on the centerline are not accurate and that the quadratic behavior of the Zone 2 isobar equations is not implemented correctly. These differences will have a negligible effect on volume integrals for jet pressures less than 20 psig, but may become more of a concern for higher pressures near the break. To quantify the magnitude of the difference, Table D-1 presents a comparison of ZOI radii computed from both methods. In particular, the GR approach may not have preserved the system stagnation pressure throughout the volume of the liquid core region as specified by the standard. However, in application of the calculated values as documented in Table 3-1 of the GR, the recommended value of 1.0 is provided for both the 1000 and 333 psig destruction pressures. The staff considers that using the recommended value of 1.0 is necessary for these pressures for a conservative treatment.

**Table D-1. Comparison of Computed Spherical ZOI Radii from Independent Evaluations of the ANSI Jet Model**

Impingement Pressure (psig)	ZOI Radius/Break Diameter	
	Guidance Report	SER Appendix I
1000	0.24	0.89 <sup>a</sup>
333	0.55	0.90
190	1.11	1.05
150	1.51	1.46
40	3.73	4.00
24	5.45	5.40
17	7.72	7.49
10	12.07	11.92
6	16.97	16.95
4	21.53	21.60

<sup>a</sup> The core volume at stagnation pressure P0 gives a minimum possible ZOI radius of 0.88 diameters.

This page is intentionally blank.

## **Review of Appendix E, “Additional Information Regarding Debris Head Loss”**

The GR Appendix E contains additional information regarding the estimation of head loss associated with debris beds. The supporting Appendix E repeats the text found in Section 4.2.5, and provides tables that summarize available domestic and international head loss testing and results. No head loss refinements are offered other than those given in Section 3.7.2.3.2.3. (See SER Section 3.7.2.3.2.3, “Thin Fibrous Beds,” for the staff evaluation of that section.)

## Confirmatory Appendices

### APPENDIX I: ANSI/ANS JET MODEL

#### I.1 INTRODUCTION

Debris generation is the first chronological step in the accident sequence for a postulated high-energy line break. In the idealized case of a double-ended guillotine break (DEGB), high-temperature, high-pressure reactor-cooling fluid may be ejected (from both sides of the broken pipe) that impinges on structures, equipment, piping, insulation, and coatings in the vicinity of the break. The degree of damage induced by the break jets is specific to the materials and structures involved, but the size and shape of the expanding jets and the forces imparted to surrounding objects depend on the thermodynamic conditions of the reactor at the location of the rupture. To maximize the volume of the damage zone, i.e., zone of influence (ZOI), it is conservative to consider free expansion of the break jet to ambient conditions with no perturbation, reflection, or truncation by adjacent structures. Spatial volumes of damage potential, as defined by empirical correlations of local jet pressure and observed damage, for example, can then be integrated over the free-jet conditions and remapped into convenient geometries, such as spheres or cones, that approximate the effects of congested reflection without crediting the associated shadowing, jet dispersion, and energy dissipation.

One reasonably accessible model that is available for computing pressure contours in an expanding jet is presented in Appendices B, C, and D of the American National Standards Institute (ANSI) guidance for the protection of nuclear power plants against the effects of pipe rupture [ANS88]. The ANSI model was used for the evaluation of potential damage volumes in the resolution of the boiling-water-reactor (BWR) strainer-blockage study [URG96, NRC98]. A similar approach suggested for this analysis by [ANS88] is a jet model developed at Sandia National Laboratories [WEI83]. Both the ANSI and the Sandia models were developed specifically for assessing structural loadings on relatively large targets near the jet centerline, so neither offers a true estimate of local pressures within a freely expanding jet. However, these models can be used with appropriate caution to learn a great deal about the spatial extent of and the thermodynamic conditions present within a high-energy jet.

This appendix presents the equation set needed to evaluate the ANSI model describing two-phase expansion of a jet from a broken high-energy line in a pressurized-water-reactor (PWR). To ensure a conservative review of the guidance report (GR), only the conditions related to full separation and full radial offset of a DEGB are developed. Alternative equations are presented in the standard for partial offsets and for longitudinal tears. This discussion is offered to resolve some of the confusion present in the notation of the standard and to provide a self-consistent basis for interpreting computational results relevant to PWR break conditions. The complexity of the jet model is somewhat beyond the scope of manual evaluation, but several investigators have performed successful spreadsheet calculations for discrete conditions. Routines developed in MATLAB and FORTRAN for evaluating the jet model are included at the end of this appendix as a further guide to implementation and for critical review; however, routines obtained from the National Institute of Standards and Technology (NIST) for evaluating thermodynamic state points are not provided.

## I.2 JET-MODEL FEATURES AND APPLICABILITY

Despite the apparent complexity of the equation set needed to evaluate the ANSI jet model, it is based on relatively few thermodynamic assumptions and limited comparisons with experimental observation. The bulk of the analytic detail supplies a geometric framework for interpolating jet pressures between assumed or observed transition points. Figure I-1 presents a sample calculation of jet pressure contours for a cold-leg DEGB. Although this calculation represents a relevant bound for evaluation of the GR, to be discussed later, the figure will be used first to introduce geometric features of the model.

The ANSI jet model subdivides the expanding jet into three zones that are delineated by dashed lines in Figure I-1. Zone 1 contains the core region, where it is assumed that liquid extrudes from the pipe under the same stagnation conditions as the upstream reservoir (interior red triangle). Zone 2 represents a zone of continued isentropic expansion, and Zone 3 represents a region of significant mixing with the environment, where the jet boundary is assumed to expand at a fixed, 10-degree, half angle. One group of equations from Appendix C of the standard defines the geometry of the jet envelope, and another group from Appendix D defines the behavior of internal pressure contours. Key geometry features that are determined by the thermodynamic conditions of the break include the length of the core region, the distance to the “asymptotic plane” between Zones 2 and 3, and the radii of the jet envelope at the transition planes between zones. At the asymptotic plane the centerline static pressure is assumed to approach the absolute ambient pressure outside of the jet.

Jet pressures provided by the ANSI model must be interpreted as local impingement gauge pressures. This is a property of the pressure field that is relevant to the interpretation of debris generation data; however, a subtle discrepancy exists between the ANSI model predictions and the desired local pressures. Because target materials may reside anywhere within the jet, fluid impingement can occur from a range of angles. Thus, idealized measurements or calculations of free-field impingement pressure should assume that the fluid stagnates (comes to rest) nonisentropically and parallel to the local flow direction. Note that a further subtlety appears here in the distinction between the classical definition of stagnation pressure that is related to the isentropic deceleration of flow along a streamline and the impingement pressure that includes entropy losses during impaction of a fluid on a physical test object. In general, impingement pressures will be higher than stagnation pressures, but the two terms may be used synonymously at times in this treatise.

In contrast to the desired local impingement pressure, the ANSI model appears to be concerned with total force loadings across relatively large objects placed near the jet centerline. It is stated in Appendix D of the standard that the pressure recovered on a target is related to the component of the flow perpendicular to the target and that, because of the diverging flow in an expanding jet, the pressure distribution on a large flat target will decrease in the radial direction. The pressure equations in the standard produce exactly this effect, and a brief allusion is made to a comparison of the predicted pressures with data taken across the face of large targets placed perpendicular to the jet. Further cautionary notes are given against applying the pressure equations to predict forces on small objects near the edges of the jet where flow velocities are clearly not parallel to the centerline.

These attributes of the model suggest that calculated pressures represent jet impingement conditions that would be experienced in a direction parallel to the midline only. Actual stream lines in a rapidly expanding jet must have a significant radial velocity component in order to create the characteristic envelope shown in Figure I-1, so in a sense, the predicted pressures represent only the longitudinal component of the local, momentum-dominated, total jet pressure. The implication of this interpretation is that true local impingement pressures as measured normal to realistic flow directions in the jet may be underestimated, particularly in Zones 1 and 2, where radial expansion is greatest.

Although a computed pressure isobar may be smaller in radius than that of the corresponding local impingement pressure that is desired for debris generation estimates, it may also be longer in the downstream direction. Comparative elongation of isobars from the jet model occurs because the entire mass flux ejected from the break is assumed to pass through the jet cross section at the asymptotic plane. Thus, the forward momentum of the jet is maximized in a manner that would be considered conservative for structural loading calculations. Unrealistic isobar elongation may also be predicted because the jet-centerline pressure equation for Zone 3 is inherently unbounded; that is, the centerline gauge pressure only falls to zero as the jet diameter grows infinitely large at infinite distance. It is impossible to quantify the net effect on isobar volume of these disparities between the ANSI model and the desired free-expansion impingement pressures without a complete understanding of the experimental measurements on which the model is based; however, the mathematical properties of the pressure equations are certain to exaggerate the length, and hence the volume, of low-pressure isobars.

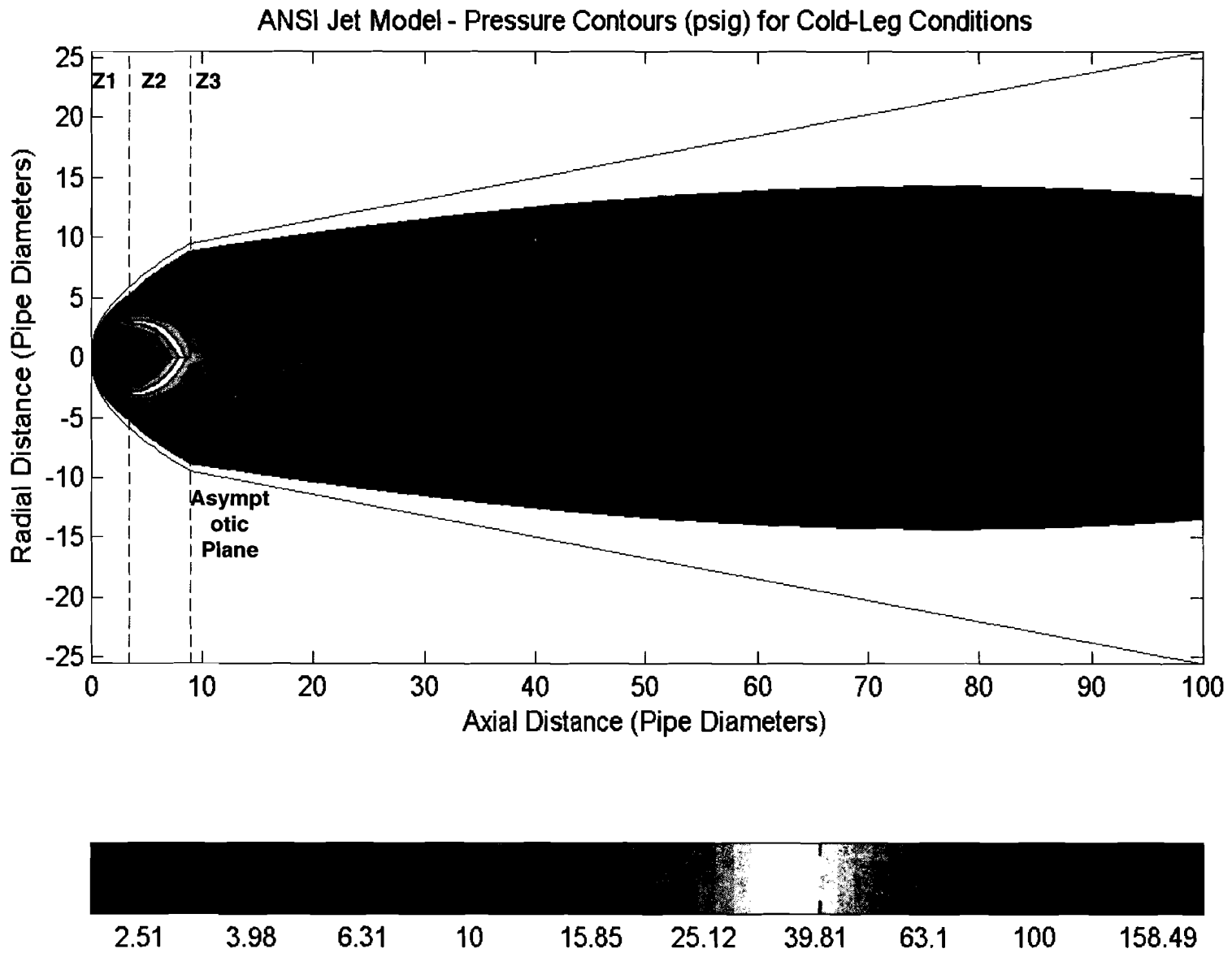


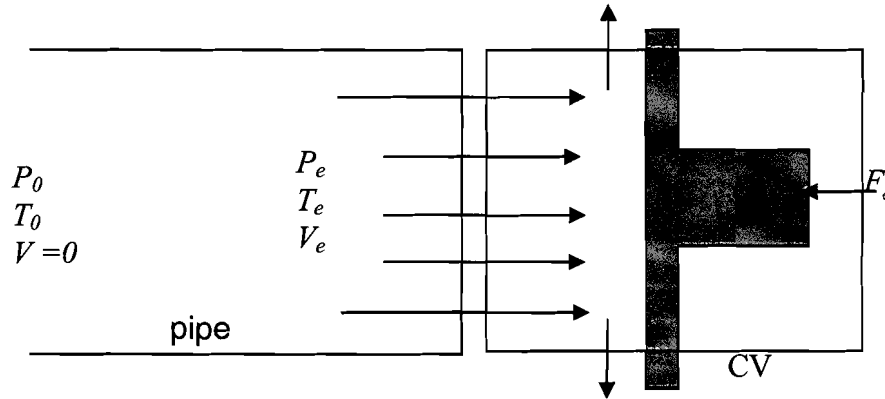
**Figure I-1. ANSI Jet-Model Stagnation Pressures for PWR Cold-Leg Break Conditions (530°F, 2250 psia)**

### I.3 JET-MODEL EQUATION SET

#### I.3.1 Fundamentals

Equations developed in the standard frequently refer to four distinct thermodynamic state points: (1) stagnation conditions of the fluid in the upstream reservoir denoted by subscript "0" (zero), (2) conditions at the exit plane of the pipe denoted by subscript "e", (3) conditions at any point in the jet denoted either with subscript "j" or with no subscript at all, and (4) conditions at the asymptotic plane denoted by subscript "a". These conventions are rigidly applied in the following development to resolve some notation inconsistencies found in the standard. Unless otherwise noted, pressures will refer to the absolute thermodynamic static pressure of the fluid. The first exception to this rule has already been mentioned—that is, the jet-pressure equations that define the local, gauge, longitudinal, impingement pressure.

**Figure I-2. Control-Volume Force Balance on a Rigid Plate near the Outlet**



One of the more fundamental relations in the model is actually presented near the end of the standard in Appendix D; it defines the total thrust (force) of the jet at the outlet. If a rigid plate were placed near the outlet, as shown in Figure I-2, the force balance on a control volume (CV) must consider both the static pressures and the rate of change of momentum acting on the boundary. If mass exits the control volume in a symmetric pattern at uniform velocity, the only possible force imbalance is in the x direction. The force on a plate near the exit is then

$$F_e = P_e A_e - P_{amb} A_e + \frac{1}{g_c} \frac{d}{dt} (m_e v_e) = (P_e - P_{amb}) A_e + \frac{1}{g_c} \left[ \left( \frac{d}{dt} m_e \right) v_e + m_e \left( \frac{d}{dt} v_e \right) \right], \quad (I-1)$$

where  $P_e$  is the fluid pressure at the exit plane,  $P_{amb}$  is the ambient pressure in containment,  $A_e$  is the area of the break, and  $m_e$  is the mass entering the control volume at velocity  $v_e$ . The force-to-mass conversion factor  $g_c$  equals  $32.2 \text{ lbm}\cdot\text{ft}/\text{lb}\cdot\text{s}^2$  in English units. Mass enters the control volume at constant velocity  $\left( \frac{d}{dt} v_e = 0 \right)$  at a rate

of  $\frac{d}{dt}m_e = \rho_e v_e A_e$ , where  $\rho_e$  is the fluid density at the exit. Thus, the total thrust generated at the exit plane is

$$F_e = (P_e - P_{amb})A_e + \frac{1}{g_c} \rho_e v_e^2 A_e. \quad \dots\dots\dots(1-2)$$

Substitution of  $G_e = \rho_e v_e$  for the critical mass flux crossing the exit plane yields

$$F_e = \left[ (P_e - P_{amb}) + \frac{G_e^2}{g_c \rho_e} \right] A_e, \quad \dots\dots\dots(1-3)$$

where the first term represents force applied by the static pressure of the fluid and the second term represents force imparted by the momentum of the fluid. The ambient pressure is often assumed to be zero to maximize the available jet thrust conservatively.

Division of Equation (1-2) or (1-3) by the exit area suggests an effective, or area-averaged, jet pressure of  $\bar{P}_e = F_e/A_e$ . This effective pressure will be greater than the classical stagnation pressure at the exit, which is defined by Bernoulli's equation as

$$P_e^{stag} = P_e^{static} + \frac{1}{2g_c} \rho_e v_e^2, \text{ because the derivation of Bernoulli's law requires that the fluid}$$

be brought to rest in an idealized, reversible manner. Jet impingement on a body is a highly anisentropic process. For an incompressible fluid, the static pressure at the exit equals the ambient pressure, and if friction losses in piping between the reservoir and the break can be neglected, the stagnation pressure at the exit equals the initial pressure. Under these conditions, Bernoulli's equation can be written as

$$\frac{1}{g_c} \rho_e v_e^2 = 2(P_0 - P_{amb}). \quad \dots\dots\dots (1-4)$$

Equations (1-2) and (1-3) are often simplified as  $F_e = C_T P_0 A_e$ , where  $P_0$  is the upstream stagnation pressure and  $C_T$  is the thrust coefficient defined by comparison to be

$$C_T = \frac{1}{P_0} \left[ \frac{1}{g_c} \rho_e v_e^2 + (P_e - P_{amb}) \right] = \frac{1}{P_0} \left[ \frac{G_e^2}{g_c \rho_e} + (P_e - P_{amb}) \right]. \quad \dots\dots\dots(1-5)$$

Equation (1-5) emphasizes that the correlation between upstream stagnation pressure and the thrust coefficient is determined by the fluid properties that exist at the exit plane. Several alternative models are available to describe the thermodynamic transitions occurring in a high-energy fluid that is expanding and accelerating, which, in turn, determine the exit density, and the critical mass flux. It is very important that the specification of  $C_T$  be consistent with the models used to evaluate  $G_e$  and  $\rho_e$ . It should be noted that the standard uses inconsistent notation for the thrust coefficient (ex.

$C_T, C_{T_e}, C_{T_e}^*$ ). All forms must refer to a single numeric value if the pressure equations are to be piecewise continuous between jet zones.

Under the conditions of zero friction loss and incompressible flow (solid liquid with no vapor fraction where  $P_e = P_{amb}$ ), Equation (I-4) can be substituted into Equation (I-5) to obtain a theoretical maximum value of  $C_T = 2.0$  when ambient pressure is neglected. By treating steam as a perfect gas under isentropic flow to obtain the exit velocity, Shapiro [SHA53] derives a lower theoretical limit of  $C_T = 1.26$ . Any numeric evaluation of Equation (I-5) using water property tables to derive  $G_e$  and  $\rho_e$  should be compared to these limits. Although it is clearly most conservative to apply the liquid limit for all state points, numerical evaluation of Equation (I-5) using water tables is sufficiently robust to permit this refinement. Recommendations for computing the thrust coefficient are discussed in Section I.4 later in this appendix, and convenient reference figures are provided.

### 1.3.2 Jet-Envelope Geometry

The shape and size of the jet envelope predicted by the ANSI model are dictated by the thermodynamic conditions upstream of the break. Except where noted, spatial distances are represented in dimensionless multiples of the broken-pipe inside diameter,  $D_e$ . Jet boundaries (and pressure contours) can be scaled in this manner because the equation set is linear with respect to pipe diameter. Linearity can be proven rigorously by factoring and eliminating terms of  $D_e$  in every equation. In general, because of potential nonlinearities, it is not sufficient to evaluate a complicated dimensional equation set at a unit value of a candidate scaling parameter and then to assume that the unit result can be multiplied by any desired value of that parameter. To recover physical quantities for a particular pipe size, dimensionless distances must be multiplied by  $D_e$ , dimensionless areas must be multiplied by  $D_e^2$ , etc.

The distance of extrusion by the jet core is

$$L_c = 0.26\sqrt{\Delta T_{sub}} + 0.5 \quad , \quad \dots\dots\dots(I-6)$$

where  $\Delta T_{sub}$  is the degree of subcooling (°F) upstream of the break location, i.e., the difference between the saturation temperature  $T_{sat}$  at the system pressure  $P_0$  and the system temperature  $T_0$ . The jet core is shown by the interior red triangle in Figure I-1. Note that  $L_c$  takes on a value of 0.5 for saturated or superheated conditions. Also, if  $L_c > L_a$ , the distance to the asymptotic plane defined below,  $L_c$  should be set to zero and the jet pressure should be assumed to be uniform across the break area at a value of  $\bar{P}_j = (F_e / A_e) / C_T$ , where the ratio  $F_e / A_e$  is computed from Equation (I-2) or (I-3). This can occur for low-pressure nonexpanding jets. A jet can be treated as nonexpanding when the initial temperature of a liquid reservoir is less than the

saturation temperature at  $P_{amb}$ , or the initial pressure of a gas reservoir is equal to ambient pressure,  $P_0 = P_{amb}$ .

The diameter of the jet at the exit plane is defined to be

$$D_{je} = \sqrt{C_T}, \quad \dots\dots\dots(1-7)$$

which is slightly larger than the diameter of the pipe because  $1.26 \leq C_T \leq 2.0$ .

The diameter of the jet at the asymptotic plane (Zone 2 to Zone 3 boundary) is defined by the relation

$$D_a^2 = \frac{G_e^2}{g_c \rho_a C_T P_0}, \quad \dots\dots\dots(1-8)$$

where  $\rho_a$  is the homogeneous fluid density at the centerline distance to this plane, which is given by

$$L_a = \frac{1}{2}(D_a - 1). \quad \dots\dots\dots(1-9)$$

Note that some care must be taken to keep pressure and mass flux dimensionally consistent in Equation (1-8). The density  $\rho_a$  is to be evaluated at a state point defined by the system enthalpy  $h_o$  and an asymptotic-plane static pressure defined by

$$P_a = \left\{ 1 - 0.5 \left( 1 - \frac{2P_{amb}}{P_0} \right) f(h_o) \right\} P_{amb}, \quad \dots\dots\dots(1-10)$$

where

$$f(h_o) = \sqrt{0.1 + \frac{h_o - h_f}{h_{fg}}} \text{ for } \frac{h_o - h_f}{h_{fg}} > -0.1, \text{ and } f(h_o) = 0 \text{ otherwise.} \quad (1-11)$$

Within the condition stated by Equation (1-11),  $h_f$  and  $h_g$  are the saturated fluid enthalpy and saturated vapor enthalpy at  $P_0$ , respectively, and  $h_{fg} = h_g - h_f$  is the heat of vaporization. Further conditions on Equation (1-10) are that if the ratio  $P_{amb} / P_0 > 1/2$ , it should be set equal to 1/2 and that, as a static pressure,  $P_a \geq 0$ .

The first criterion on  $f(h_o)$  simply checks whether the initial quality  $x_0 = \frac{h_o - h_f}{h_{fg}}$  is greater than negative 10%. When considered as a whole, these conditions imply that

$0 \leq P_a \leq P_{amb}$ . If the initial fluid is more than 10% subcooled, the jet static pressure equals ambient pressure at the asymptotic plane. If the jet is less than 10% subcooled, the jet static pressure at the asymptotic plane can be lower than ambient pressure. Equation (I-10) suggests that the asymptotic plane is placed at the distance where the jet static pressure approaches ambient pressure. The distance to this plane given by Equation (I-9) may simply have been chosen by geometric comparison with observed jets.

The state point defined by the asymptotic pressure  $P_a$  and the system enthalpy  $h_o$  may be a two-phase condition. In this case, it is necessary to evaluate the asymptotic density

$\rho_a$  using the quality  $x_a = \frac{h_o - h_{fa}}{h_{ga} - h_{fa}}$ , where  $h_{fa}$  and  $h_{ga}$  are the saturated fluid and

vapor enthalpies at  $P_a$ , respectively. Then  $\rho_a = \left[ \frac{x_a}{\rho_{ga}} + \frac{1-x_a}{\rho_{fa}} \right]^{-1}$ , where  $\rho_{fa}$  and  $\rho_{ga}$

are the saturated fluid and vapor densities at  $P_a$ , respectively. Automated steam tables generally give mixture densities directly for a two-phase state point, so this complication may be unnecessary.

The similarity of terms in Equation (I-8) to the force-balance equations derived in the previous section suggests a different interpretation for the asymptotic plane. For convenient reference, the jet diameter at the asymptotic plane is again given by

$$D_a^2 = \frac{G_e^2}{g_c \rho_a C_T P_o}, \quad \dots\dots\dots(I-12)$$

Given the discussion following Equation (I-3) and the definition of the thrust coefficient, the factors  $C_T P_o$  in Equation (I-12) are immediately recognized as  $\bar{P}_e = F_e / A_e$ , the average total jet pressure at the exit. If a relation similar to Equation (I-3) is written to describe the area-averaged pressure across the jet cross section at the asymptotic plane,

$$\bar{P}_a = \frac{F_a}{A_a} = \left[ (P_a - P_{amb}) + \frac{G_e^2}{g_c \rho_a} \right], \quad \dots\dots\dots(I-13)$$

then the term  $G_e^2 / g_c \rho_a$  in Equation (I-12) is recognized to be  $\bar{P}_a - (P_a - P_{amb})$ . If the static pressure at the asymptotic plane  $P_a$  is not much different than the ambient pressure  $P_{amb}$ , then Equation (I-12) reduces to the ratio of average pressures computed over the jet cross section at the asymptotic plane and over the jet cross section at the exit,

$$D_a^2 = \frac{F_a / A_a}{F_e / A_e} = \frac{\bar{P}_a}{\bar{P}_e}. \quad \dots\dots\dots(I-14)$$

Writing explicitly the definition of the dimensionless asymptotic-plane area as  $D_a^2 = \frac{A_a}{A_e}$

illustrates that the diameter of the jet given by Equation (I-8) has been chosen at the point where the ratio of average pressures approaches the ratio of cross sectional areas, and for this to be true, the total force across each area must be the same. Hence, the ANSI model implicitly assumes that the jet force available at the outlet is conserved across the jet cross section at the asymptotic plane. At this distance, the jet is presumed to begin interacting with the environment. This development also shows that the ANSI model projects the entire mass flux across the asymptotic plane rather than following more realistic stream lines across the jet boundary in Zones 1 and 2. Equation (I-8) is derived more rigorously in Section I-4 to further emphasize these points.

The remainder of the jet envelope is simply interpolated as a function of centerline distance  $L$  between the transition diameters discussed above. Within Zone 1, the diameter of the jet core is given by

$$D_c = \sqrt{C_T} \left( 1 - \frac{L}{L_c} \right) \quad \dots\dots\dots(I-15)$$

For Zone 1 and 2 ( $0 < L \leq L_a$ ), the jet diameter is given by

$$D_j^2 = \left[ 1 + \frac{L}{L_a} \left( \frac{D_a^2}{D_{je}^2} - 1 \right) \right] D_{je}^2 \quad \dots\dots\dots(I-16)$$

In Zone 3 ( $L > L_a$ ), the jet diameter expands at a 10-degree half angle beginning from the diameter at the asymptotic plane. The Zone-3 diameter is specified by

$$D_j^2 = \left[ 1 + \frac{2(L - L_a)}{D_a} \tan(10^\circ) \right]^2 D_a^2 \quad \dots\dots\dots(I-17)$$

### I.3.3 Jet Pressures

Pressure contours also appear to be interpolated from a limited number of geometric reference points, but the basis for this interpolation is not evident from the standard. It can be shown that all equations are piecewise continuous at the separation planes between zones; however, no effort was made to match first-derivative slopes. This deficiency admits the possibility of “kinks” in the contours, as observed in Figure I-1 across the boundary between Zones 2 and 3. Pressure contours in Zone 1 ( $0 \leq L \leq L_c$ ) depend on the following discriminant. If

---

\* This observation was derived from the jet equations and is not expounded as part of any derivation in the standard. It is simply an implication of the definitions.

$$D_j^2 + 2D_j D_c + 3D_c^2 \leq 6C_T, \quad \dots\dots\dots(1-18)$$

then the jet pressures are given as a function of radius ( $r_c < r \leq r_j$ ) for jet diameters  $D_j = 2r_j$  as

$$P_j = \left( \frac{D_j - 2r}{D_j - D_c} \right) \left[ 1 - \frac{2(D_j^2 + D_j D_c + D_c^2 - 3C_T)}{D_j^2 - D_c^2} \left( \frac{2r - D_c}{D_j - D_c} \right) \right] P_0. \quad \dots\dots\dots(1-19)$$

Otherwise,

$$P_j = \left( \frac{D_j - 2r}{D_j - D_c} \right)^2 \left[ \frac{6(C_T - D_c^2)}{(D_j - D_c)(D_j + 3D_c)} \right] P_0. \quad \dots\dots\dots(1-20)$$

It is important to note that the leading term ( $D_j - 2r$ ) vanishes in both Equation (1-19) and (1-20) as the radius approaches the jet envelope where the absolute pressure equals  $P_{amb}$ . Therefore, evaluations of  $P_j$  must be interpreted as gauge pressures. In

Equation (1-19), the term  $\left( \frac{2r - D_c}{D_j - D_c} \right)$  ensures that the jet pressure matches  $P_0$  on the boundary of the core. There is no similar constraint provided in Equation (1-20), so there will be a sharp discontinuity in pressure at the boundary of the jet core when this condition is invoked, as shown in Figure I-1. Equations (1-19) and (1-20) were not intended to be evaluated inside of the core region. Within the core, the system stagnation conditions are presumed to hold.

In Zones 2 and 3, jet pressures are parameterized in terms of the jet centerline pressure  $P_{jc}$ . In Zone 2 ( $L_c < L \leq L_a$ ),

$$P_{jc} = \left\{ F_c - \left( F_c - \frac{3C_T}{D_a^2} \right) \frac{L_a (L - L_c)}{L (L_a - L_c)} \right\} P_0, \quad \dots\dots\dots(1-21)$$

where the parameter  $F_c = 1.0$  if  $D_j^2 \leq 6C_T$  at distance  $L_c$  and  $F_c = 6C_T / D_j^2$  otherwise. When  $L = L_c$ , Equation (1-21) reduces to  $P_{jc} = F_c P_0$ . If  $F_c = 1.0$ , the centerline pressure will match the assumed pressure in the core region, but otherwise, there will again be a discontinuity. Given the centerline pressure, jet pressures in Zone 2 are specified by

$$P_j = \left( 1 - \frac{2r}{D_j} \right) \left\{ 1 - 2 \left( \frac{2r}{D_j} \right) \left[ 1 - \frac{3C_T}{D_j^2} \frac{P_0}{P_{jc}} \right] \right\} P_{jc}. \quad \dots\dots\dots(1-22)$$

It can be shown by integration that (I-22) is essentially a geometric rather than physical condition: it leads to full recovery of the jet force anywhere in Zone 2 regardless of the value assigned to the jet diameter. In Zone 3, centerline pressures are given by

$$P_{jc} = \frac{3C_T P_0}{D_a^2 \left[ 1 + \frac{2(L - L_a)}{D_a} \tan(10^\circ) \right]^2} \quad \dots\dots\dots(I-23)$$

and jet pressures are given by

$$P_j = \left( \frac{D_j - 2r}{D_j} \right) P_{jc}. \quad \dots\dots\dots(I-24)$$

Pressures on the transition between Zones 2 and 3 are piecewise continuous, including on the centerline.

### I.3.4 Pressure-Contour Characteristic Equations

Equations presented in the previous section can be used to evaluate longitudinal impingement pressures at any location in the jet. However, in the present forms, they are not particularly convenient for identifying geometric characteristics such as isobar boundaries. Similarly, when numerically computing volumes under a given isobar, it is convenient to know the downstream range of the contour, which always begins at  $L = 0$  and terminates in a cusp on the centerline at some distance  $L = L_c(P_j)$ . Relationships presented in this section are not developed in the ANSI standard; they are offered to facilitate some of the many practical details involved with implementing the standard.

Figure I-1 illustrates the typical behavior of jet-pressure isobars generated by the ANSI model. The isobars outlined in black represent lines of constant pressure that can be found by solving the pressure Equations (I-19), (I-20), (I-22), and (I-24) for the radii at a constant pressure  $P_j$ . Remember that the downstream distance  $L$  is implicitly specified by the jet diameter  $D_j$ . Each pressure equation can be reduced to a general quadratic expression for the radius of the form  $Ar^2 + Br + C = 0$ .

The coefficients from Equation (I-19) for Zone 1 are

$$A = 4H, \quad B = -2[1 + H(D_j + D_c)], \quad \text{and} \quad C = D_j + HD_j D_c + (D_c - D_j) \frac{P_j}{P_0}, \quad \dots\dots\dots(I-25)$$

where

$$H = 2 \frac{(D_j^2 + D_j D_c + D_c^2 - 3C_T)}{(D_j^2 - D_c^2)(D_j - D_c)}. \quad \dots\dots\dots(I-26)$$

The coefficients from Equation (I-20) for Zone 1 are

$$A = 4, B = -4D_j, \text{ and } C = D_j^2 - (D_j - D_c)^2 \frac{P_j}{P_0} I, \quad \dots\dots\dots(I-27)$$

where

$$I = \frac{6(C_T - D_c^2)}{(D_j - D_c)(D_j + 3D_c)}. \quad \dots\dots\dots(I-28)$$

A special case occurs in Zone 1 at  $L = 0$ , where  $D_j = D_c$  and  $r = D_j/2 = D_c/2$  for all  $P_j$ .

Equation (I-22) yields the following coefficients for Zone 2:

$$A = 8 \frac{J}{D_j^2}, B = -\left(\frac{2}{D_j} + \frac{4J}{D_j}\right), \text{ and } C = 1 - \frac{P_j}{P_{jc}}, \text{ where } J = \left(1 - \frac{3C_T P_0}{D_j^2 P_{jc}}\right). \quad \dots\dots\dots(I-29)$$

Finally, Equation (I-24) yields for Zone 3 the coefficients

$$A = 0, B = -2/D_j, \text{ and } C = 1 - \frac{P_j}{P_{jc}}. \quad \dots\dots\dots(I-30)$$

The analytic solution for radius in Zone 3 is

$$r = \frac{1}{2} D_j \left(1 - \frac{P_j}{P_{jc}}\right). \quad \dots\dots\dots(I-31)$$

The sharp tip of each contour shown in Figure I-1 is another nonphysical feature of the ANSI model that arises from lack of attention to matching spatial first derivatives. It might be expected that each isobar be smoothly bounded and have infinite slope at the terminal point, especially at very low pressures where the jet returns to ambient conditions. It is helpful to know the distance to the terminal point of each contour for iterative integration of spatial volumes. These points can be found by solving the centerline pressure Equations (I-21) and (I-23) for distances  $L_t$  corresponding to the desired pressure. Note that there are no terminal points in Zone 1 except for the jet core.

For Zone 2 from Equation (I-21) comes the relation

$$L_t = \frac{L_c}{1 - \frac{L_a - L_c}{RL_a} \left( F_c - \frac{P_j}{P_0} \right)}, \quad \dots\dots\dots(I-32)$$

where

$$R = F_c - \frac{3C_T}{D_a^2}, \quad \dots\dots\dots(I-33)$$

and for Zone 3 from Equation (I-23) comes the relation

$$L_t = \frac{1}{2} \left[ \left( \frac{3C_T P_0}{D_a^2 P_j} \right)^{1/2} - 1 \right] \frac{D_a}{\tan(10^\circ)} + L_a. \quad \dots\dots\dots(I-34)$$

One remaining practicality is the numerical integration of pressure isobars defined by Equations (25), (27), (29), and (31). If these equations are evaluated at a set of discrete distances  $L_i$ , the corresponding radii  $r_i$  define adjacent conical frusta with unique slopes as shown in Figure I-3. The analytic formula for the frustum of a cone is given by

$$V_i = \pi \left[ \frac{1}{3} m_i^2 L^3 + m_i (r_{i+1} - m_i L_{i+1}) L^2 + (m_i^2 L_{i+1}^2 - 2r_{i+1} m_i L_{i+1} + r_{i+1}^2) L \right]_{L_i}^{L_{i+1}} \quad \dots\dots\dots(I-35)$$

where the linear slope of the sides of the conical segment  $m = \frac{r_{i+1} - r_i}{L_{i+1} - L_i}$ . The total

volume under the isobar is approximated by the sum  $V_{isobar} = \sum V_i$  and can be refined to any desired accuracy by evaluating the pressure-isobar equations at finer resolution.

The total volume of an isobar should be multiplied by a factor of 2 when double-ended breaks of equivalent upstream pressure are being considered, and finally, converted to a volume-equivalent sphere by the formula

$$R_{sphere} = \left( \frac{3}{4\pi} V_{isobar} \right)^{1/3}. \quad \dots\dots\dots(I-36)$$

#### I.4 DERIVATION OF ASYMPTOTIC-PLANE AREA

To obtain Equation (I-8) for the jet diameter  $D_a$  at the asymptotic plane, force balances are applied to the two control volumes shown in Figure I-4 in a manner analogous to the derivation of the thrust force given by Equation (I-2). In the figure, a plate is positioned normal to the flow at the asymptotic plane. The force required to hold the plate in static equilibrium is notated  $F_e$ . The fluid deflected by the plate is assumed to exit the control

volume isotropically in a plane oriented parallel to the face of the plate. Exit flow is not represented in the figure.

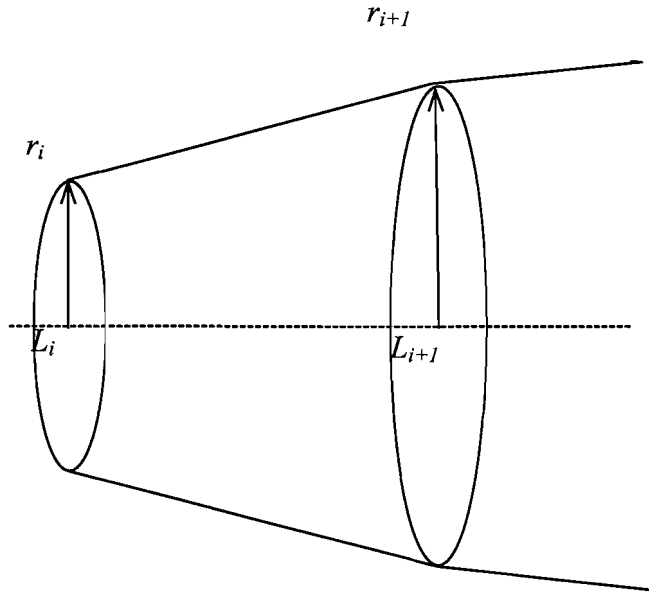


**Figure I-3. Linear Segmentation of Jet Cross Sections for Numerical Volume Integration**

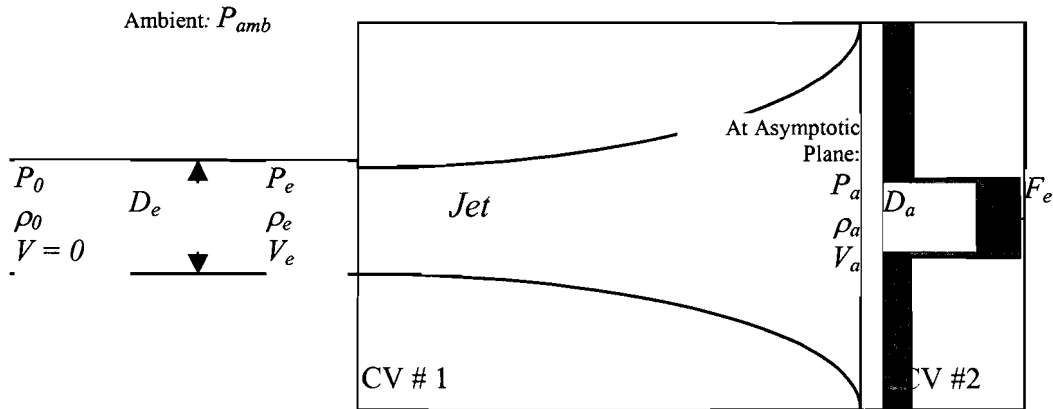


**Figure I-4. Control-Volume Force Balances on a Rigid Plate at the Asymptotic Plane**

It is assumed in Appendix C of the standard (p. 52) that the fluid does not begin to interact with the surrounding environment until after it crosses the asymptotic plane. Hence, no energy is supplied to or removed from the jet in the region described by the two control volumes in Figure (I-4). Therefore, the entire jet force is recovered, and the force balance for CV #1 is identical to that given by Equation (I-1).

The jet characteristics at the asymptotic plane – fluid density  $\rho_a$ , velocity  $v_a$ , and static pressure  $P_a$  – are not expected to be uniform, so to render the force balance for CV #2 tractable, these properties are assumed to be averaged over the jet cross section. The force balance in the direction of the jet flow for control volume #2 may hence be written as

$$F_e = (P_a - P_{amb})A_a + \frac{1}{g_c} \left( v_a \frac{d}{dt} m_a + m_a \frac{d}{dt} v_a \right), \quad \dots\dots\dots(I-37)$$

where  $A_a = \pi D_a^2 / 4$  is the jet area at the asymptotic plane and  $m_a$  is the mass of the fluid located within the control volume.

For steady flow,  $dv_a/dt = 0$ . The rate at which mass enters the control volume,  $dm_a/dt$ , is simply the total mass flow crossing the asymptotic plane and is given by

$$\frac{dm_a}{dt} = \rho_a v_a A_a. \quad \dots\dots\dots(I-38)$$

Hence, the force balance simplifies to

$$F_e = (P_a - P_{amb})A_a + \frac{1}{g_c} \rho_a v_a^2 A_a. \quad \dots\dots\dots(I-39)$$

Since no mass escapes the jet between the break location and the asymptotic plane, the mass flow rates at the break and at the asymptotic plane must be equal, i.e.,

$$\rho_a v_a A_a = \rho_e v_e A_e. \quad \dots\dots\dots(I-40)$$

This relation may be employed to eliminate  $v_a$  in the force balance.

As mentioned in the discussion following Equation (I-11), the static pressure at the asymptotic plane is generally taken to be equal to  $P_{amb}$ . Setting  $P_a$  equal to  $P_{amb}$  yields

$$F_e = \frac{1}{g_c} \frac{\rho_e^2 v_e^2 A_e^2}{\rho_a A_a}. \quad \dots\dots\dots(I-41)$$

Setting this evaluation of  $F_e$  equal to that obtained from the force balance on CV #1, Equation (I-2), gives the result

$$\frac{A_a}{A_e} = \frac{\rho_e^2 v_e^2}{g_c \rho_a} \cdot \frac{1}{(P_e - P_{amb}) + \frac{1}{g_c} \rho_e v_e^2} \quad \dots\dots\dots(I-42)$$

The second fraction in this equation is recognized by comparison with Equation (I-5) as being equal to  $1/(C_T P_0)$ . Making use of the mass flux definition  $G_e = \rho_e v_e$ , leads to the expression for the jet area at the asymptotic plane given in the standard,

$$\frac{A_a}{A_e} = \frac{G_e^2}{g_c \rho_a C_T P_0} \quad \dots\dots\dots(I-43)$$

The standard recommends that the density  $\rho_a$  at the asymptotic plane be evaluated using the local static pressure  $P_a$  and the system stagnation enthalpy  $h_0$  rather than the local static enthalpy  $h_a$ . Therefore, it is implicitly assumed that the dynamic enthalpy at the asymptotic plane,  $v_a^2/2$ , is small.

An inconsistency is noted here because  $P_a$  in the ANSI jet model – as governed by equation (I-10) – is not always equal to  $P_{amb}$ , yet the asymptotic plane area is always computed as if this were the case. For slightly subcooled, saturated, or two-phase upstream conditions, application of Equation (I-10) leads to a value for  $P_a$  that is less than  $P_{amb}$ . Although the physical reasoning behind Equation (I-10) is not documented in the standard, it appears to correct for cases in which the dynamic enthalpy is non-negligible. This development further confirms that only longitudinal pressures are being computed for  $P_{jet}$ , at least at the asymptotic plane, and probably everywhere within the jet envelope.

## I.5 CRITICAL FLOW MODELS

### I.5.1 Discharge Mass Flux

Results produced by the jet model are sensitive to the value assigned to the mass flux discharged from the break plane,  $G_e$  [lbm/ft<sup>2</sup>/s]. The area of the jet at the asymptotic plane  $A_a$  [ft<sup>2</sup>], i.e., the cross sectional area reached by the jet following free (isentropic) expansion, is proportional to  $G_e^2$ . Thus,  $G_e$  is indirectly specified via Figures C-4 and C-5 in the standard, which plot the ratio of the asymptotic area to the break plane area  $A_a/A_e$  for upstream conditions ranging from 50°F subcooled liquid to saturated vapor. Aside from difficulties inherent in recovering numerical values from coarsely resolved plots, use of these figures is not recommended for two reasons:

1. The range of upstream stagnation conditions covered by the plot – extending only to 50oF subcooling – is insufficient. Typical cold-leg conditions in a PWR might entail subcooling of 100oF or more.
2. The origin of the results is unclear. Which model was used to evaluate the relevant mass fluxes and thrust coefficients? Without this information, there can be no confidence that the rest of the model will be applied in a self-consistent manner.

Therefore, we strongly concur with the recommendation given in the standard (p. 57) that a two-phase critical flow model be employed to evaluate  $G_e$ . Two models that are in widespread use are cited: the homogeneous equilibrium model (HEM)<sup>†</sup> and the Henry-Fauske model [HEN71]. The standard provides a loose recommendation regarding the applicability of the models as a function of upstream stagnation properties: the HEM for saturated or two-phase and Henry-Fauske for subcooled conditions.

Several pitfalls await a naïve application of this guidance. To facilitate the exposition of these pitfalls, it is useful first to provide a simplified description of the physics inherent in each of the models.

Under the HEM, the phases are assumed to be in thermodynamic equilibrium and to remain well mixed. The relative velocity between the phases is therefore assumed to be zero. External heat transfer, wall roughness, and other interactions with the environment are neglected so that the expansion is isentropic.

Given these assumptions, the first law of thermodynamics is applied to the homogenized fluid. Combined with the definition of the mass flux, the first law yields an expression for  $G_e$  in terms of the mixture's static properties at the choked point. The critical mass flux is defined as the value of  $G_e$  that maximizes this expression. Numerical solution of the HEM is thus an iterative process, entailing a search over the space of static state points that preserve the upstream stagnation entropy.

The Henry-Fauske model preserves some of the assumptions made under the HEM, namely that the mass flux may be expressed as a function of the thermodynamic state at the throat, that the critical mass flux can be obtained by maximizing this function, and that the expansion is isentropic. However, Henry and Fauske argue that the assumptions of homogeneous mixing and thermodynamic equilibrium during the expansion are unrealistic given the short time scales involved. Rather, interphase mass transfer is constrained such that the quality  $x_t$  at the throat is equal to the upstream stagnation quality  $x_0$ . Heat transfer during the expansion is also assumed negligible; the liquid-phase temperature  $T_{ft}$  at the throat is held fixed at the upstream liquid temperature  $T_{f0}$ . The temperature of the vapor phase, if it is present, is allowed to vary. The heat- and mass-transfer rates at the throat are treated as significant, and expressions for these are developed assuming polytropic vapor behavior.

---

<sup>†</sup> For a discussion of practical considerations surrounding implementation of the HEM, as well as a tabulation of results for a wide range of upstream conditions, see Ref. [HAL80].

In practice, the Henry-Fauske model is implemented by solving a transcendental equation for the static pressure at the throat that maximizes mass flux. Both Henry-Fauske and the HEM are evaluated through iterative procedures, with thermodynamic properties being queried upon each iteration. Therefore, the models were coded as a series of FORTRAN subroutines, driven by a MATLAB control function, that directly couple with the FORTRAN implementation of the NIST/American Society of Mechanical Engineers (ASME) steam tables [HAR96] when fluid properties are required. The results obtained from the software were successfully validated against those presented in Refs. [Hal80] and [Hen71]. These programmed routines allow a thorough assessment of the practical ramifications of using each model within the ANSI jet-modeling framework.

The standard does not provide guidance with regard to critical flow modeling for superheated conditions. The simplest approach would be to treat the steam as an ideal gas and apply the appropriate equation of state. This treatment was attempted and found to be highly inadvisable for the slightly superheated states that are of most relevance to the present application. Two qualitative observations support this conclusion: first, when the upstream superheat is small the flow at the choked location is in fact two phase; second, slightly superheated high-pressure steam does not exhibit the typically assumed idealized properties (e.g., a specific heat ratio of 1.3) so that transitions evaluated using the ideal gas law would not preserve entropy. These considerations lead us to recommend that the HEM be used to treat the superheated state points that may arise in this application.

As mentioned above, the standard does provide guidance for two-phase and single-phase liquid stagnation state points. Specifically, it recommends the use of HEM for saturated and Henry-Fauske for subcooled upstream conditions. We believe that the Henry-Fauske model should, in fact, be employed for both of these regimes. This recommendation stems from several considerations, as outlined below.

Critical mass fluxes predicted by the HEM and Henry-Fauske models exhibit their most significant disagreement at precisely the transition point recommended in the standard, i.e., for saturated-liquid upstream conditions. Figure I-5 and Figure I-6 provide contour plots of  $G_e$  as obtained from the two models for subcooled vessel stagnation conditions. In figures showing flow properties for subcooled state points, the stagnation temperature is varied on the x axis and pressure on the y axis. The regions between contour lines of constant  $G_e$  are shaded for ease of delineation. Because the domain of validity of the flow models does not extend to superheated conditions, pressure and temperature combinations that lie within this regime are blanked out on the plots. Mass fluxes for saturated upstream conditions are shown in Figure I-7 and Figure I-8. In these plots,  $G_e$  is calculated at several saturated (temperature, pressure) state points as a function of the vessel quality.

Figure I-9 and Figure I-10 display the variation between the HEM and Henry-Fauske mass fluxes. It can be seen from these figures that discrepancies of 50% or more exist for saturated liquid upstream conditions and that significant variations persist for slightly subcooled and low-quality two-phase stagnation conditions. This disagreement follows from a variation in the assumptions regarding interphase mass transfer. Because the quality is held fixed under the Henry-Fauske model, the discharge is almost entirely in the liquid phase. Under the HEM, however, heat and mass transfer between the phases

is allowed and the discharge has a quality that is significantly greater than zero. This discharge possesses a lower density and higher velocity than that predicted by Henry-Fauske. It can be shown numerically that the HEM mass flux prediction will be lower than that of Henry-Fauske for the slightly subcooled, saturated liquid, and low-quality upstream conditions in which the HEM prediction of discharge quality is markedly higher than that of Henry-Fauske.

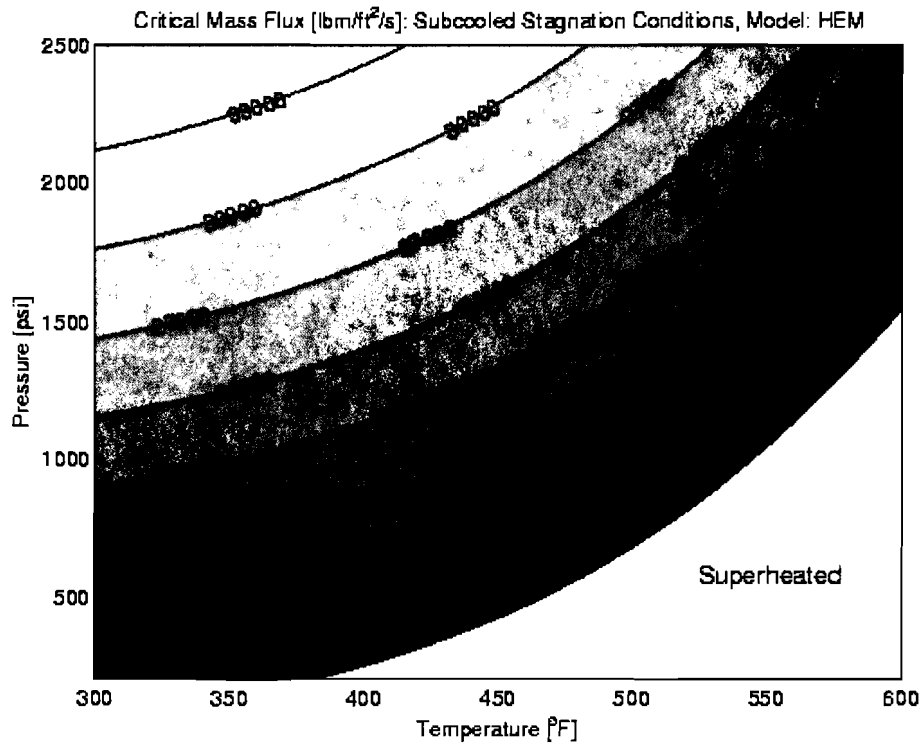


Figure I-5. HEM Critical Mass Flux, Subcooled Stagnation

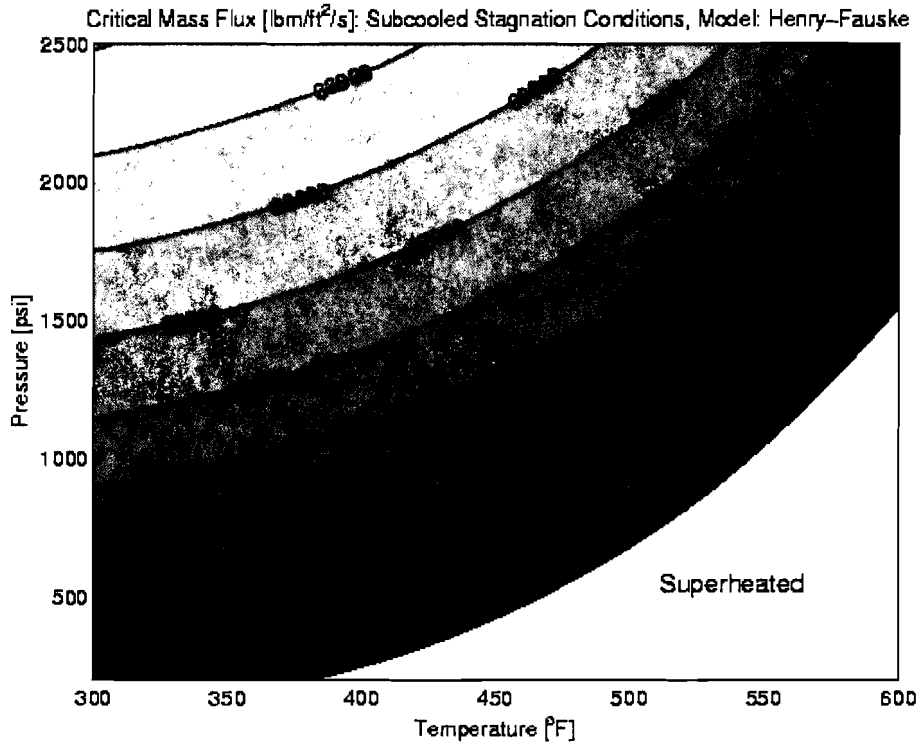


Figure I-6. Henry-Fauske Critical Mass Flux, Subcooled Stagnation

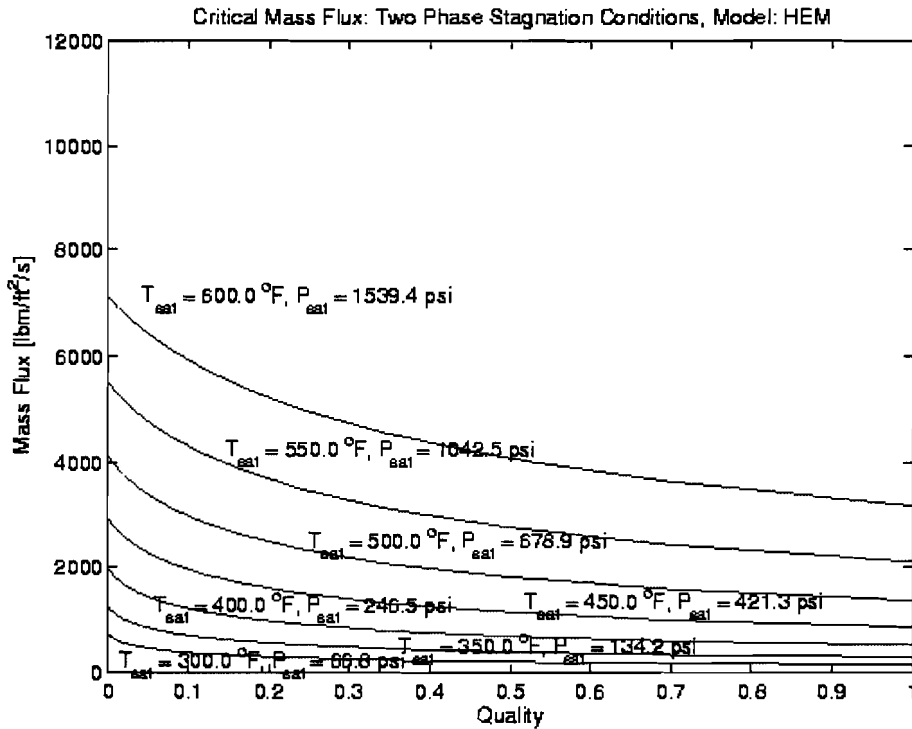
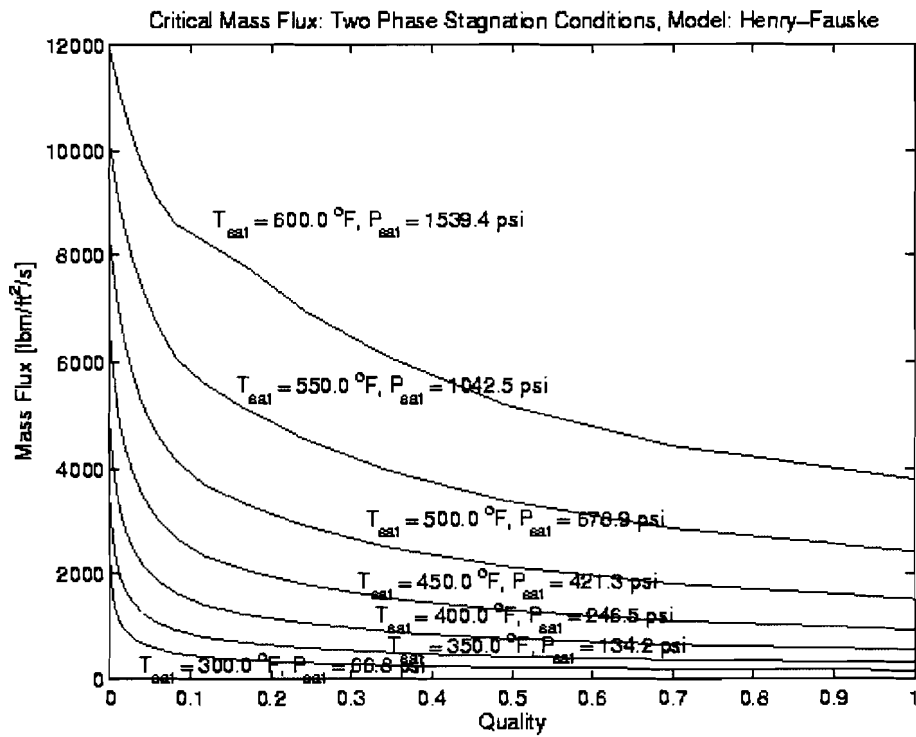
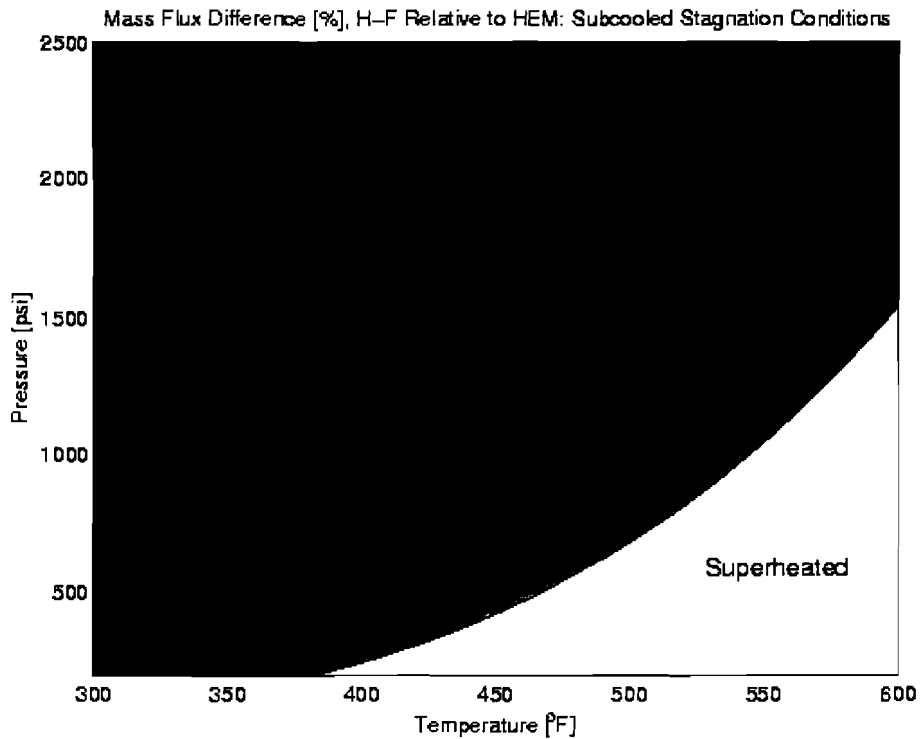


Figure I-7. HEM Critical Mass Flux, Saturated Stagnation



**Figure I-8. Henry-Fauske Critical Mass Flux, Saturated Stagnation**



**Figure I-9. Mass Flux Difference, Subcooled Stagnation**

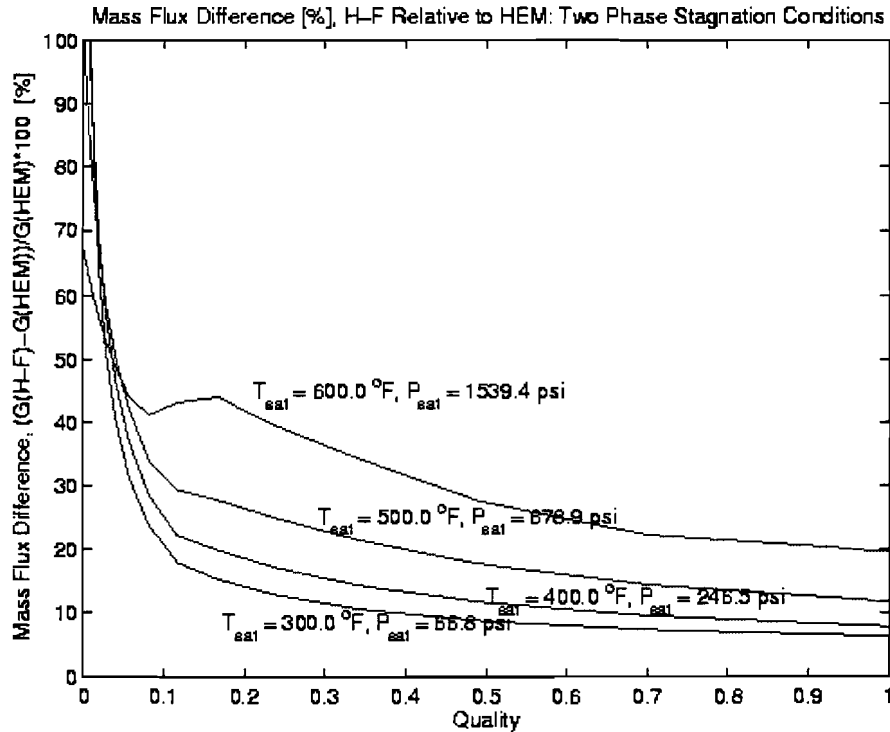


**Figure I-10. Mass Flux Difference, Saturated Stagnation**

If the advice of the standard is followed, then a significant discontinuity would be observed when the critical flow model transitions from the HEM to Henry-Fauske. The nature and magnitude of this discontinuity is explored further below. Although users of the jet model are in practice unlikely to observe this discontinuity, because during a blowdown, the transition might only occur after significant pressure drops, we see no compelling reason to preserve it. The issue then becomes one of selecting the model that offers the best fidelity to available data. The figures show that the HEM and Henry-Fauske offer comparable predictions for highly subcooled as well as high-quality two-phase conditions. This is to be expected because under these conditions, both models predict essentially monophasic fluid properties at the throat and the detailed treatment of the interphase heat- and mass-transfer rates offered by Henry-Fauske does not come into play. The benchmarking results reported in Ref. [Hen71] lead us to conclude that the Henry-Fauske model exhibits superior agreement to the data under low-quality two-phase and saturated liquid conditions. This alone is sufficient reason to adopt Henry-Fauske; further evidence may be found from an examination of a second major input to the ANSI jet model, the thrust coefficient.

### **1.5.2 Direct Evaluation of Thrust Coefficients**

The thrust coefficient  $C_T$  acts as a surrogate for the jet thrust force, which is not explicitly called for as an input to the ANSI model. This discussion will address only the steady-state thrust coefficient for frictionless, unrestricted flow, but its conclusions can be generalized to include those cases as well. Regardless of upstream conditions, the

thrust coefficient is used to correlate the thrust force  $T$ , upstream stagnation absolute pressure  $P_0$ , ambient pressure  $P_{amb}$ , and break area  $A_e$  by the expression

$$T = C_T(P_0 - P_{amb})A_e. \quad \dots\dots\dots(1-44)$$

Calculation of the thrust coefficient requires knowledge of local flow conditions at the break. Because these are unknown unless a critical flow model such as the HEM or Henry-Fauske is used to compute them, pp. 35 – 45 of the standard provide a series of correlations and figures that may be used as surrogates. Because both Henry-Fauske and the HEM were implemented for the current review, the results obtained from these models will be compared with the recommendations provided in the standard.

The thrust force may be computed by calculating the force that must be exerted to hold in static equilibrium a plate positioned normal to the flow directly at the break point. This thrust is given by

$$T = (P_e - P_{amb})A_e + \frac{1}{g_c} \rho_e v_e^2 A_e, \quad \dots\dots\dots(1-45)$$

where the static pressure  $P_e$ , fluid density  $\rho_e$ , and flow velocity  $v_e$  are evaluated at the exit. Combining the above equations yields an expression for the thrust coefficient:

$$C_T = \frac{1}{P_0 - P_{amb}} \left( \frac{1}{g_c} \rho_e v_e^2 + (P_e - P_{amb}) \right). \quad \dots\dots\dots(1-46)$$

Figure I-4 through Figure I-7 show thrust coefficients computed using pressures and fluid properties evaluated from the HEM and Henry-Fauske models. Regardless of the model, the value of  $C_T$  approaches 2.0 for incompressible, highly subcooled liquid and ~1.26 for saturated steam. These results agree with theory and are recommended for use in the standard.

For subcooled flashing upstream conditions, the standard on p. 42 recommends use of the curve fits presented by Webb [WEB76]. Based on an enthalpy normalization factor

$$h^* = \frac{h_0 - 180}{h_{sat} - 180}, \quad \dots\dots\dots(1-47)$$

where  $h_0$  [Btu/lbm] is the upstream stagnation enthalpy and  $h_{sat}$  [Btu/lbm] is the saturated water enthalpy at the stagnation pressure, the correlation is evaluated as

$$C_T = 2.0 - 0.861h^{*2} \text{ for } 0 \leq h^* < 0.75 \quad \dots\dots\dots(1-48)$$

and

$$C_T = 3.22 - 3.0h^* + 0.97h^{*2} \text{ for } 0.75 \leq h^* \leq 1.0. \quad \dots\dots\dots(1-49)$$

For saturated or superheated steam, the standard recommends a thrust coefficient of

$$C_T = 1.26 - P_{amb}/P_0 . \quad \dots\dots\dots(I-50)$$

For two-phase steam-water mixtures, the standard provides only a figure that does not address relevant PWR break conditions, and for nonflashing water jets with temperatures less than the saturation temperature at ambient pressure and pressures greater than ambient, the standard recommends that

$$C_T = \frac{2}{1 + fL/D} , \quad \dots\dots\dots(I-51)$$

where the Fanning friction factor  $f$  is normally assumed to be zero for conservatism. The ratio  $L/D$  represents a dimensionless flow-path length based on the characteristic length and diameter of the piping between the assumed thermodynamic reservoir and the break location.

Webb claims, and our calculations verify, that his correlations agree with values computed from the Henry-Fauske model to within 3% for upstream stagnation pressures ranging from 300 to 2400 psia. The standard does not clearly state this range of applicability. Webb's correlation is recommended when a computational implementation of a critical flow model is unavailable, but two inconsistencies require clarification.

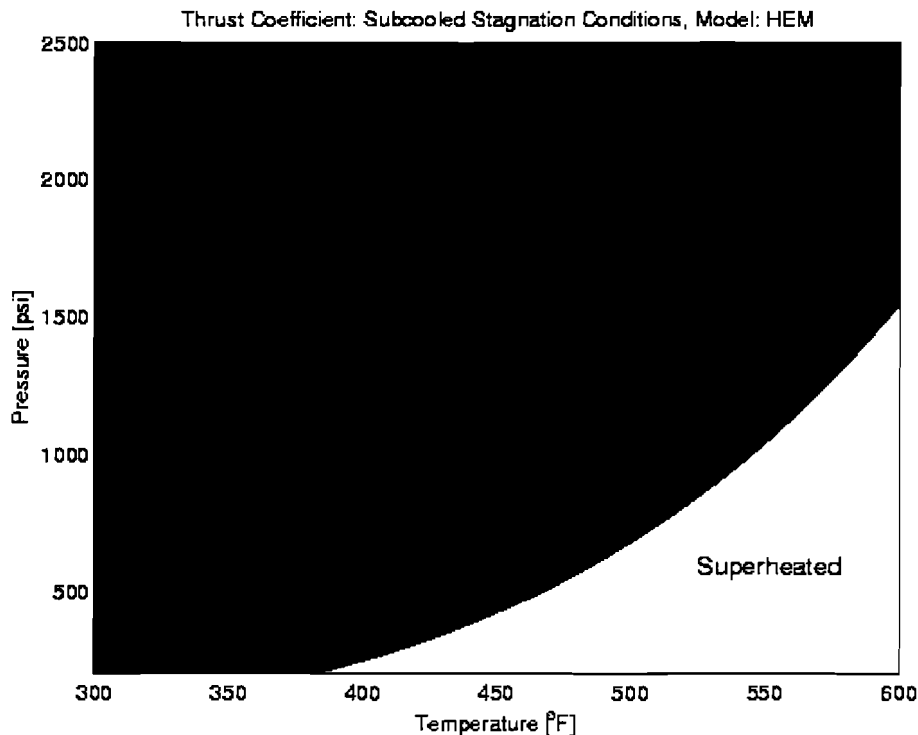


**Figure I-11. HEM Thrust Coefficient, Subcooled Stagnation**

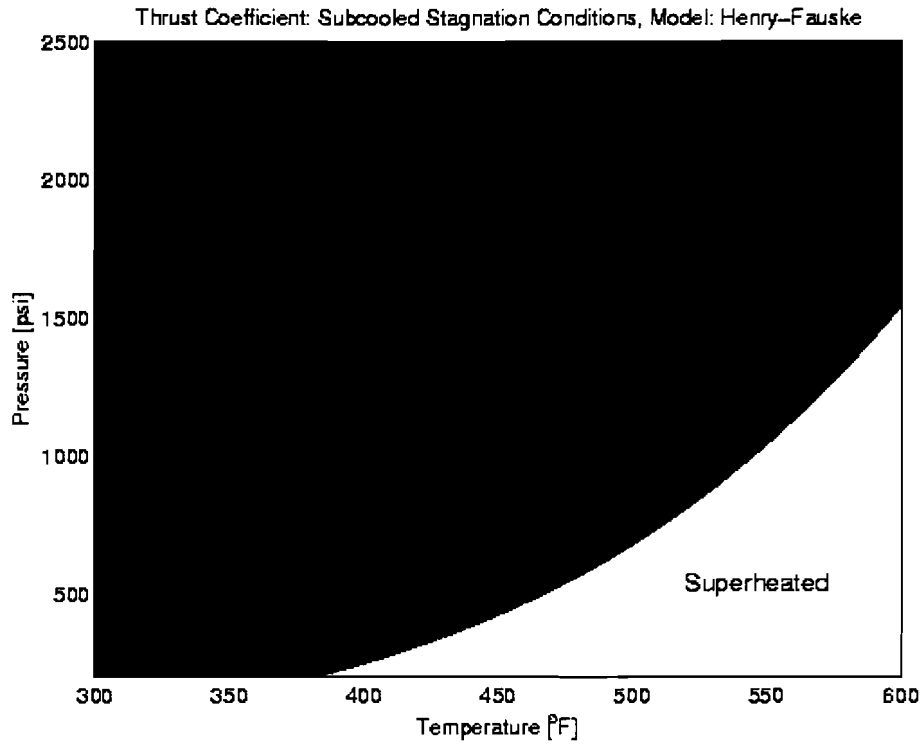


Figure I-12. Henry-Fauske Thrust Coefficient, Subcooled Stagnation

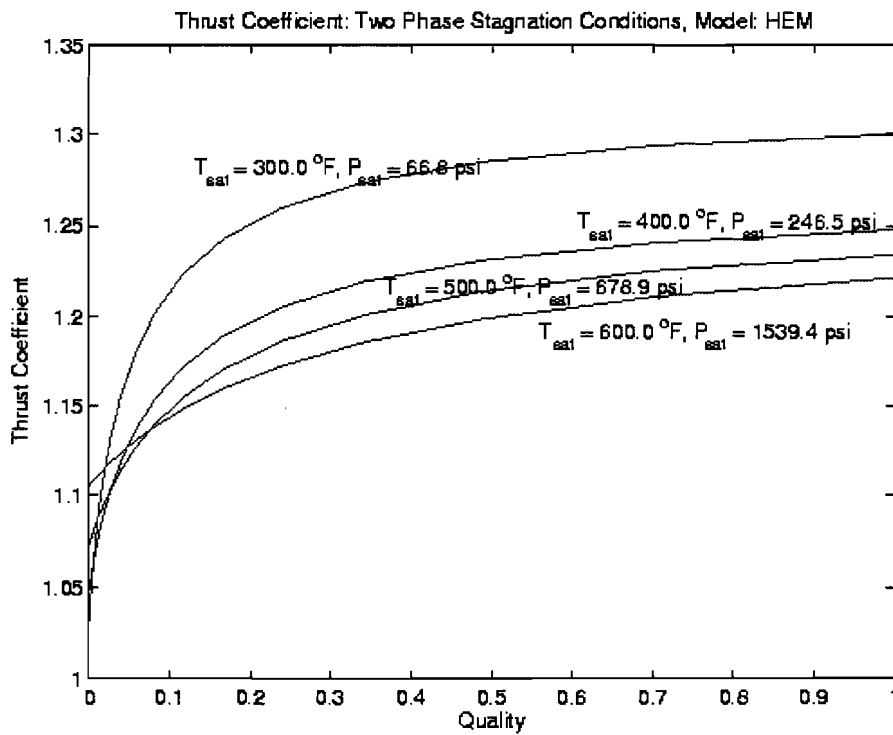
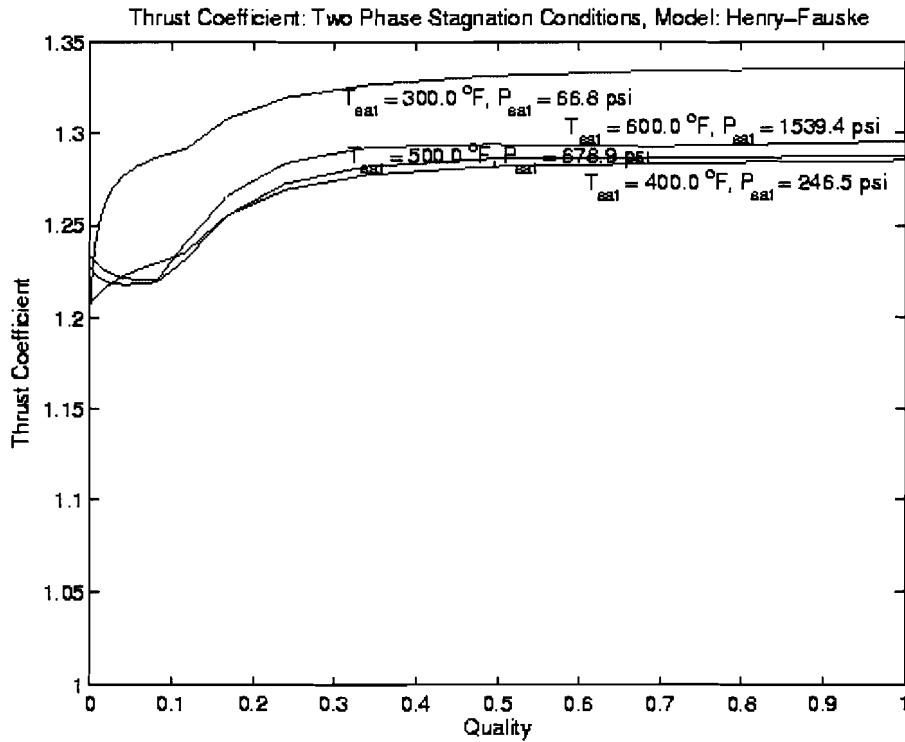


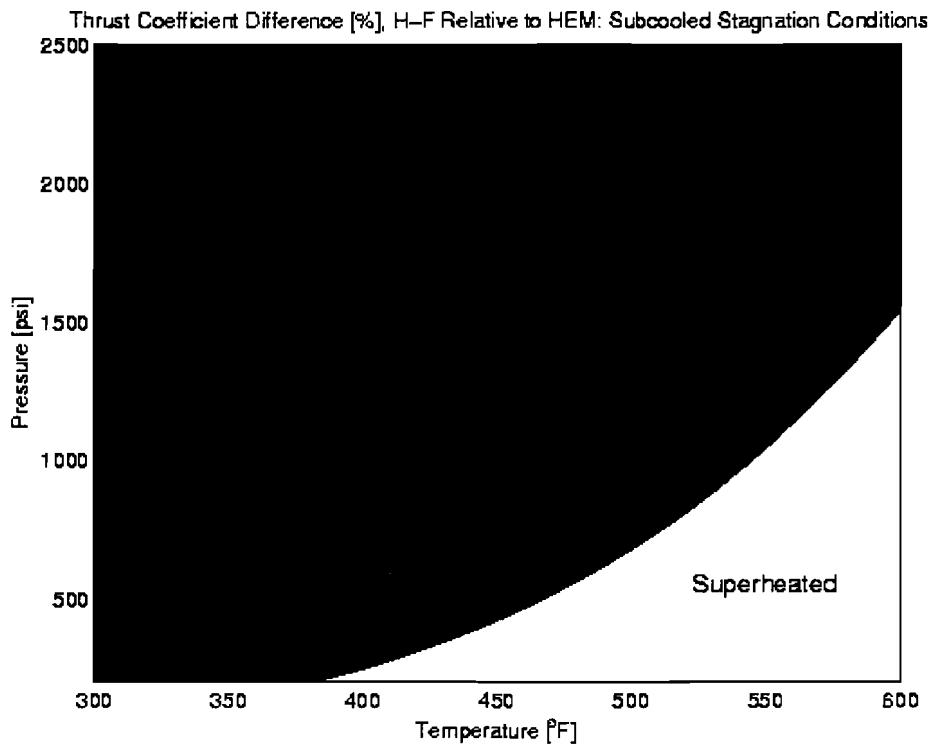
Figure I-13. HEM Thrust Coefficient, Saturated Stagnation



**Figure I-14. Henry-Fauske Thrust Coefficient, Saturated Stagnation**

In presenting Webb's model, the standard neglects to clarify the "180" figure against which the enthalpy is nondimensionalized. This is, in fact, the enthalpy of saturated water at atmospheric pressure, 14.7 psi. It may be justifiably claimed that, during a blowdown, the ambient containment pressure might vary from below atmospheric to significantly above atmospheric. Changes in  $P_{amb}$  cannot be accounted for by Webb's model; however,  $C_T$  evaluated from the force balance varies weakly with  $P_{amb}$ . This effect is not large: even for highly subcooled conditions at the lower end of the range of validity of Webb's correlation,  $P_0 = 300$  psia, neglecting  $P_{amb}$  altogether changes the thrust coefficient evaluated from the force balance by less than 5%.

The standard also places insufficient emphasis on the fact that Webb's correlation is obtained from calculations using the Henry-Fauske model. Because this is the case, employing HEM-derived mass fluxes with thrust coefficients obtained from this correlation propagates a significant inconsistency. Figure I-8 shows that significant deviation exists between thrust coefficients computed from the outlet conditions provided by the two critical flow models. The use of Henry-Fauske-derived thrust coefficients with HEM mass fluxes will result in overprediction of damage radii. This follows because the larger Henry-Fauske thrust coefficient implicitly imposes a higher flow density, velocity, and/or static pressure at the break plane.



### I.5.3 Effects of Flow Models on Jet Behavior

While the sensitivity of the jet pressure contour map in its entirety to variations in  $C_T$  is too complicated to permit analytic treatment, the effect of variation of  $C_T$  on conditions at the asymptotic plane can be used for illustration. Equation (I-43) shows that the jet area  $A_a$  at the asymptotic plane is inversely proportional to  $C_T$ . However, from conservation of mass, Equation (I-40), the average flow velocity at the asymptotic plane  $v_a$  is inversely proportional to  $A_a$  and, thus, directly proportional to  $C_T$ . This conclusion can be drawn because the average fluid density  $\rho_a$  at the asymptotic plane depends, in the ANSI formulation, only upon upstream stagnation conditions. The dynamic pressure of the fluid, which is proportional to the square of its velocity, thus varies as  $C_T^2$ . The results of decreased jet cross sectional area and increased velocity from the larger Henry-Fauske thrust coefficient will be a narrower, more penetrating jet and larger volume-equivalent radii at a given damage pressure.

In fact, it can be seen from Figure I-6 that the thrust coefficient for upstream conditions at or near saturation as derived from the HEM is significantly lower than the value of 1.26 recommended in Figure B-5 of the Standard. The inconsistency inherent in use of the 1.26 value with the HEM mass flux would again result in overprediction of volume-equivalent radii. This additional consideration strengthens our recommendation that the Henry-Fauske method be employed for all flow regimes when performing the calculations outlined in the standard.

As mentioned above, the critical mass flux  $G_e$  derived from the HEM will be smaller, significantly so for stagnation conditions lying near the liquid saturation line in  $(P, h)$  space, than that obtained from Henry-Fauske. Because this is the case, it is also useful to address the behavior at the asymptotic plane when  $G_e$  is varied with  $C_T$  being held constant. Following the same reasoning pursued above when the thrust coefficient was varied, we see that the jet area at the asymptotic plane varies as  $G_e^2$ . The average jet velocity at that location  $v_a$ , on the other hand, behaves as  $v_a = kG_e/A_a$  so that  $v_a \sim 1/G_e$ . Thus, a seemingly paradoxical conclusion is reached, namely that reducing the mass flux while holding the thrust coefficient constant increases the velocity at the asymptotic plane and might *increase* the volume-equivalent radii.

Although this thought experiment is not conclusive or comprehensive – the location of the asymptotic plane, for instance, also depends on  $G_e$  and  $C_T$  and has not been taken into account – numerical computations verify its conclusions. Table I-1 shows critical flow model results for five of the upstream conditions given in Table I-2. The conditions selected from that table are #8, PWR Hot Leg Initial; #1, PWR Cold Leg Initial; #2, PWR Cold-Leg Blowdown; #9, BWR Hot-Leg; and #11, Main Steam Line. All three PWR stagnation states are subcooled; the BWR state is two-phase with a quality of 0.15 and the steam line case is superheated by 35°F. In addition to the mass flux  $G_e$ , thrust coefficient  $C_T$  and discharge velocity  $v_e$  obtained, the volume-equivalent damage radii for the 10 and 150 psig contours are also shown. It might be intuitively expected that the Henry-Fauske model is the more conservative when calculating damage radii because it predicts critical mass fluxes and thrust coefficients that are greater than those of the HEM, but, as shown in the table, particularly for initial conditions nearing saturation, this is not the case.

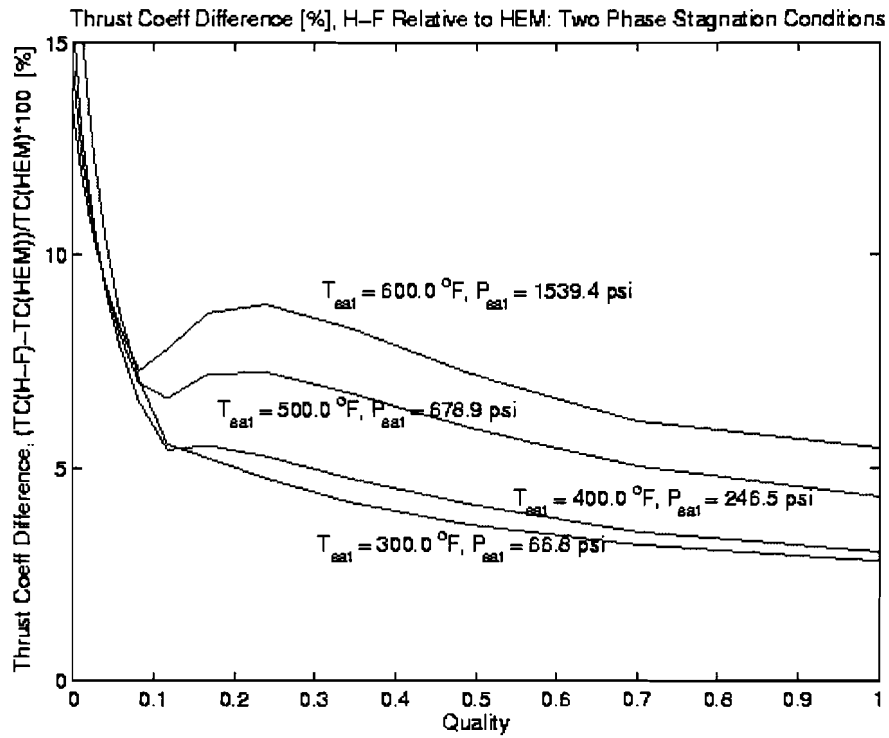


**Figure I-16. Thrust Coefficient Difference, Saturated Stagnation**

**Table I-1. Critical Flow Model Results and Their Effect on Volume-Equivalent Damage Radii**

	Critical Mass Flux $G_e$ [lbm/ft <sup>2</sup> /s]		Thrust Coefficient $C_T$ [--]			Break Flow Velocity $v_e$ [ft/s]		150-psig* Damage- Pressure Radius [pipe diameters]		10-psig* Damage- Pressure Radius [pipe diameters]	
	HEM	H-F	HEM	H-F	Webb**	HEM	H-F	HEM	H-F	HEM	H-F
1. Cold Leg Initial (2250 psia, 530 F)	24850	25330	1.62	1.64	1.63	522	527	1.48	1.48	12.00	12.04
2. Cold-Leg Blowdown (393 psia, 291 F)	13370	13390	1.88	1.89	1.90	232	232	0.96	0.96	4.42	4.43
8. Hot Leg Initial (2250 psia, 630 F)	11840	15400	1.17	1.28	1.28	296	382	1.60	1.59	11.14	11.07
9. BWR Hot Leg (1040 psia, 550 F, X = 0.15)	3920	5260	1.16	1.26	N/A	178	158	1.11	1.12	7.81	7.80
11. Main Steam Line (910 psia, 570 F)	1800	N/A	1.24	N/A	N/A	464	N/A	1.08	N/A	7.58	N/A

\* Damage-pressure radii are given as multiples of the break diameter. They are obtained by constructing spheres with volume equal to the volume enclosed by a given jet stagnation pressure contour. See Section I.3 for further elaboration.

\*\* Shown for purposes of comparison only; not used in damage-pressure-radius calculations given in this table.

## I.6 SAMPLE CALCULATIONS

The ANSI model presented in the previous sections for predicting stagnation pressures in an expanding jet was implemented in a MATLAB routine called ANSJet (see Attachment 1 to this appendix). This programming language was selected for convenient interface with steam-table routines available from NIST. Several cases relevant to both PWR initial break and blowdown conditions were evaluated. Two generic BWR state points were also evaluated, as were three cases applicable to steam line flow in secondary loops. Two of these relate to a single-pass Babcock & Wilcox steam generator discharging superheated (by ca. 35° F) steam; the third applies to a Combustion Engineering U-tube heat exchanger and is assumed to yield saturated steam. These conditions are defined in Table I-2 for later reference by case number. Note that Figure I-1 corresponds to the cold-leg initial break condition defined as Case #1.

**Table I-2. Comparative Calculation Set Using ANSI Jet Model**

Case #	Description	System Stagnation Conditions		
		$P_o$ (psia)	$T_o$ (°F)	Quality
1	cold leg initial <sup>1</sup>	2250	530	Subcooled
2	cold-leg blowdown <sup>1</sup>	393	291	Subcooled
3	cold-leg blowdown <sup>1</sup>	857	351	Subcooled
4	cold-leg blowdown <sup>1</sup>	1321	411	Subcooled
5	cold-leg blowdown <sup>1</sup>	1786	471	Subcooled
6	10% greater pressure than Case 1	2475	530	Subcooled
7	cold leg initial <sup>2</sup>	2250	540	Subcooled
8	hot leg initial <sup>3</sup>	2250	630	Subcooled
9	BWR hot leg <sup>4</sup>	1040	550	0.15
10	BWR cold leg <sup>4</sup>	1040	420	Subcooled
11	main steam line (MSL): Babcock & Wilcox (B&W) <sup>4</sup> – full power	910	570	Superheated
12	B&W MSL: design conditions <sup>4</sup>	1075	603	Superheated
13	MSL: Combustion Engr. Calvert Cliffs <sup>5</sup>	846	525	1.0

<sup>1</sup> From reference [RAO0]

<sup>2</sup> From reference [NEI04]

<sup>3</sup> From reference [DUD76]

<sup>4</sup> From reference [RAH92]

<sup>5</sup> From reference [LOB90]

Jet-pressure isobars for Cases 1 through 6 were integrated over a wide range of values and converted to equivalent spherical diameters. These results are presented in Fig. I-17. Recall that the ANSI-model stagnation pressure is being used as a correlation parameter that corresponds to observed damage in debris generation tests. Use of this

correlation is the reason that the Figure I-17 abscissa is labeled as “Damage Pressure.” Case 1 represents a previously studied hydraulic condition [RAO02] that will be used as the reference case. Reading from the figure, a damage pressure of 10 psig corresponds to an equivalent jet radius of approximately 12 pipe diameters. Note that equivalent radii climb sharply for damage pressures below 20 psig.

This set of calculations suggests that the state-point pressure of the jet dominates the determination of isobar volumes. Other cases that are not shown in Figure I-17 were bounded by Case 1. Case 7, the nominal PWR cold-leg condition recommended in the GR, was almost indistinguishable from Case 1. Case 8, a nominal hot-leg break condition, was also bounded by the reference case except at damage pressures greater than 120 psig. Hot-leg conditions are much closer to saturation (630°F vs. 653°F); therefore, the shapes of the pressure contours change near the core. Case 6 was run as a perturbation check for plants that may at times have higher operating pressures than the nominal value of 2250 psig. Although the pressure increase was 10% higher than the reference, the maximum deviation in spherical volume was only 8%; therefore, a linear adjustment for higher pressure would be conservative in the absence of a full jet-model analysis.

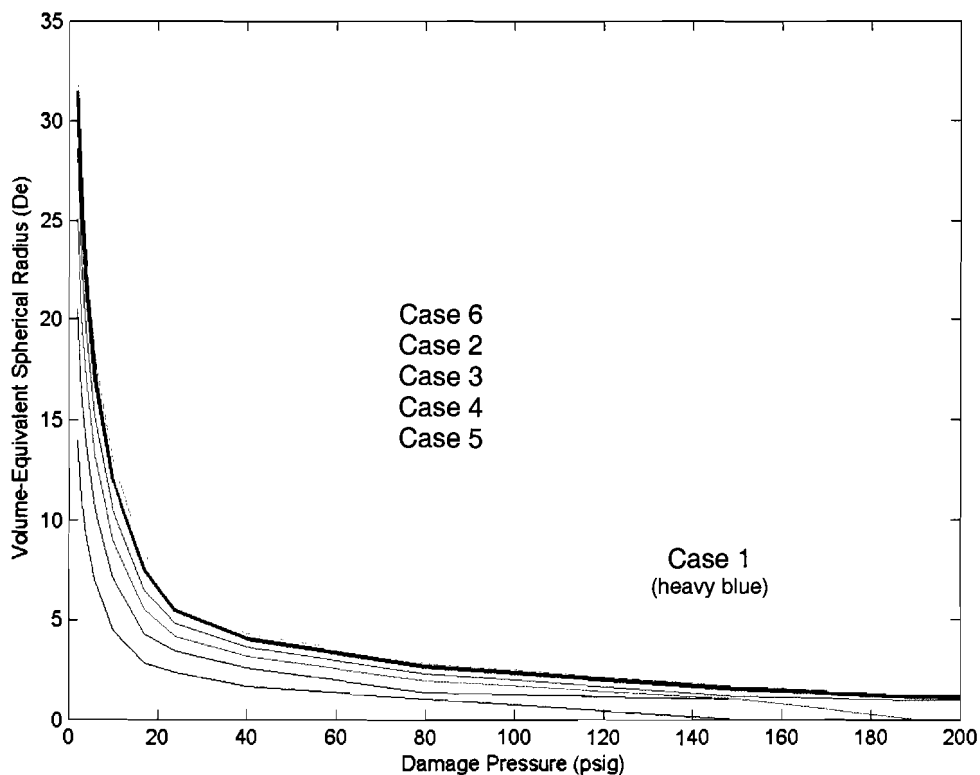


**Figure I-17. Comparison of ANSI Jet-Model Equivalent Spherical Radii for Six Initial Break Conditions**

The damage radii associated with the BWR hot-leg and cold-leg conditions of Cases 9 and 10 are shown in Figure I-18. Given the lower stagnation pressures pertinent to BWR coolant, the equivalent radii are, as expected, smaller than was the case for PWR

conditions at comparable values of damage pressure. The radii obtained for the three steam line cases are given in Figure I-19. Two of these, Cases 11 and 13, are specified as representative of full power operating conditions. The third, Case 12, is a design specification included to serve as a conservative bounding scenario. Given that the thrust coefficient is nearly invariant at a value near 1.26 for high-quality two-phase and superheated upstream conditions, it appears reasonable to expect damage radii in such regimes to respond linearly to variation in the stagnation pressure. A pressure contour plot for the steam line break condition is provided in Figure I-20. This figure compares to Figure I-1 for PWR cold-leg stagnation conditions. One of the subtle differences between these figures is the higher centerline pressure exhibited by the MSL case to axial distances of about 30 pipe diameters. The steam flow exhibits a narrower jet that is higher-velocity at the centerline, leading to a greater dynamic contribution to the stagnation pressure. Differences in the initial pressure should also be considered when visually comparing Figures I-1 and I-20.

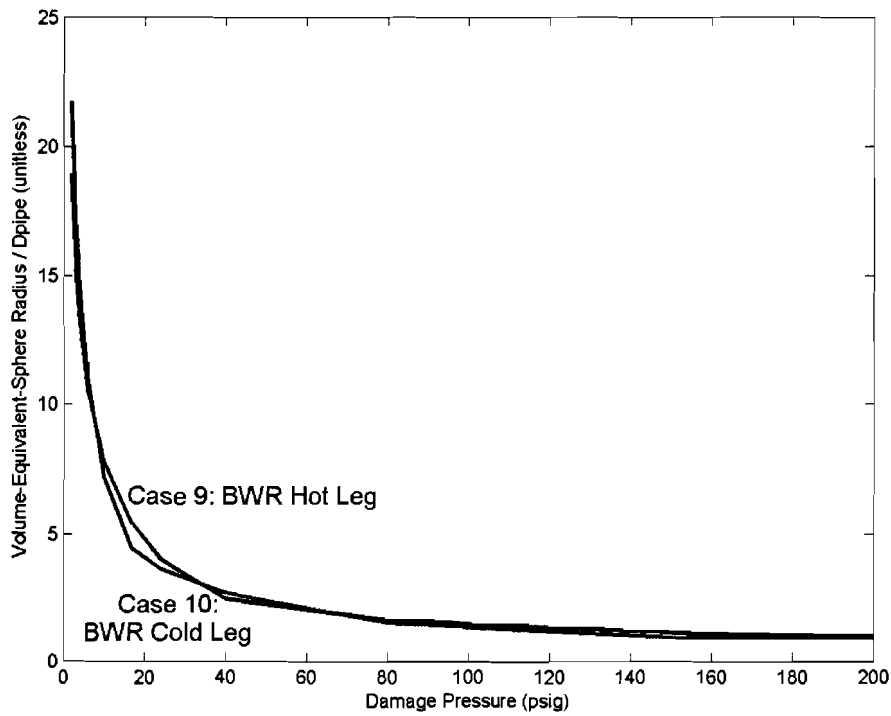


**Figure I-18. Comparison of ANSI Jet-Model Equivalent Spherical Radii for BWR Break Conditions**

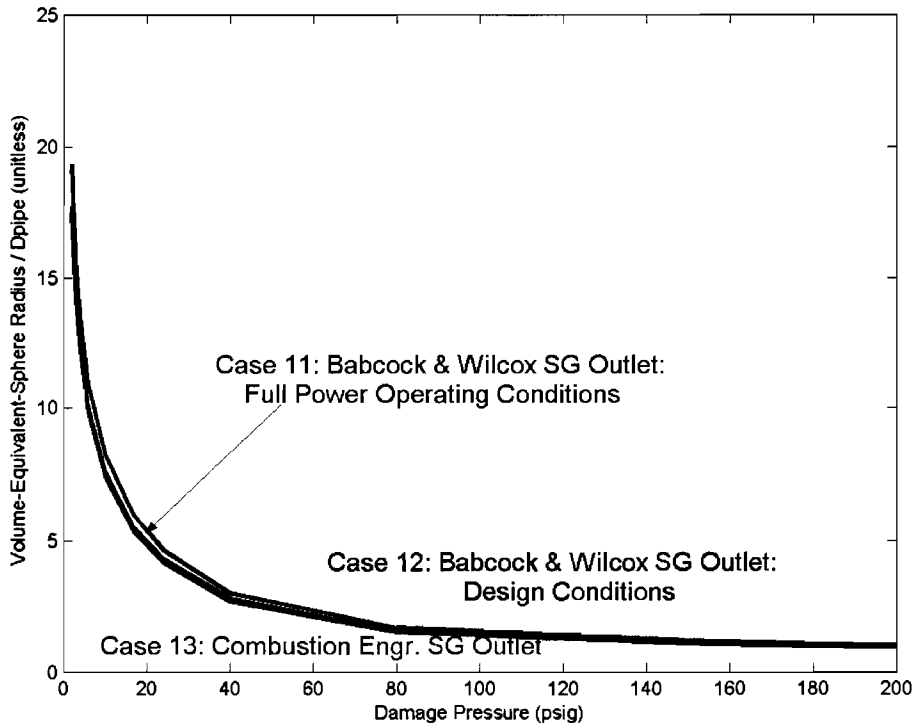


**Figure I-19. Comparison of ANSI Jet-Model Equivalent Spherical Radii for Main Steam Line Break Conditions**

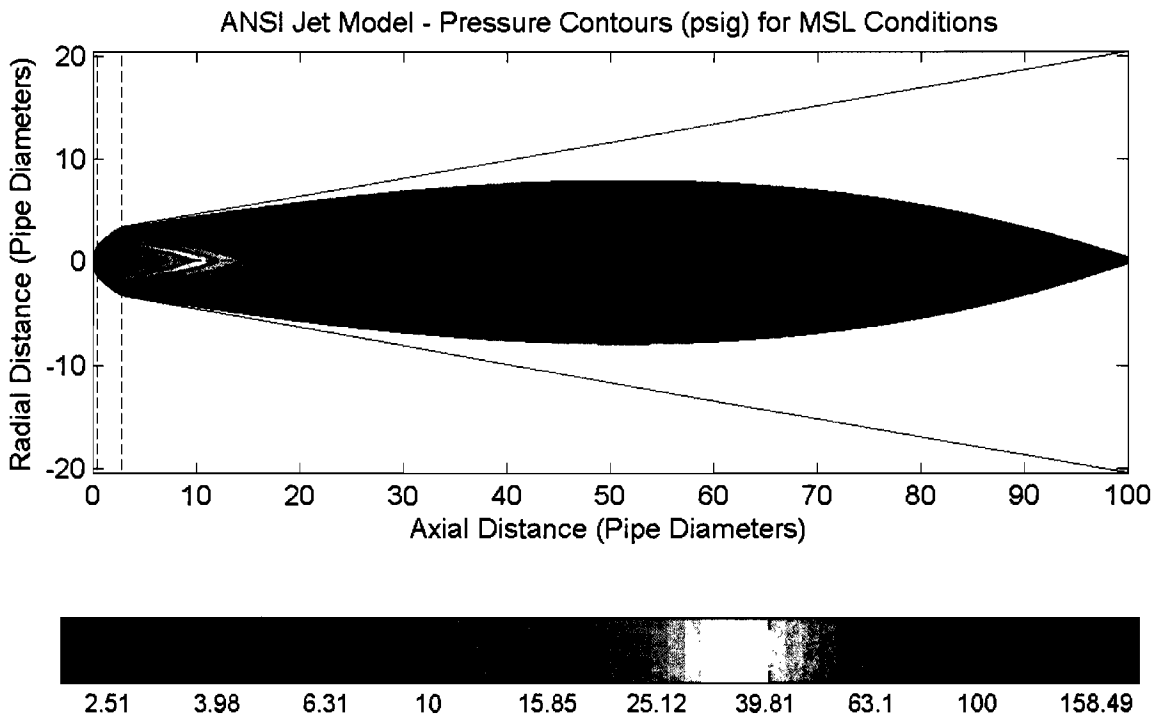


**Figure I-20. ANSI Jet-Model Stagnation Pressures for MSL Break Conditions (570°F, 910 psia)**

Other useful information can be extracted from the jet model in addition to equivalent spherical diameters derived from spatial volume integrals. Appendix D of the ANSI standard suggests that target temperatures can be estimated by evaluating a thermodynamic state point using the jet pressures  $P_j$  and the initial enthalpy  $h_0$ . Presuming that the model supplies realistic, nonisentropic impingement pressures (at least in the longitudinal direction), this approach will give the temperature of the stationary fluid striking the surface of a large target. Actual target temperatures might vary with internal heat conduction properties and external drag coefficients that affect aerodynamic heating, but it is instructive to compute this approximation nonetheless. Figure I-21 illustrates the isotherm plot corresponding to Case 1 for the reference cold-leg break.

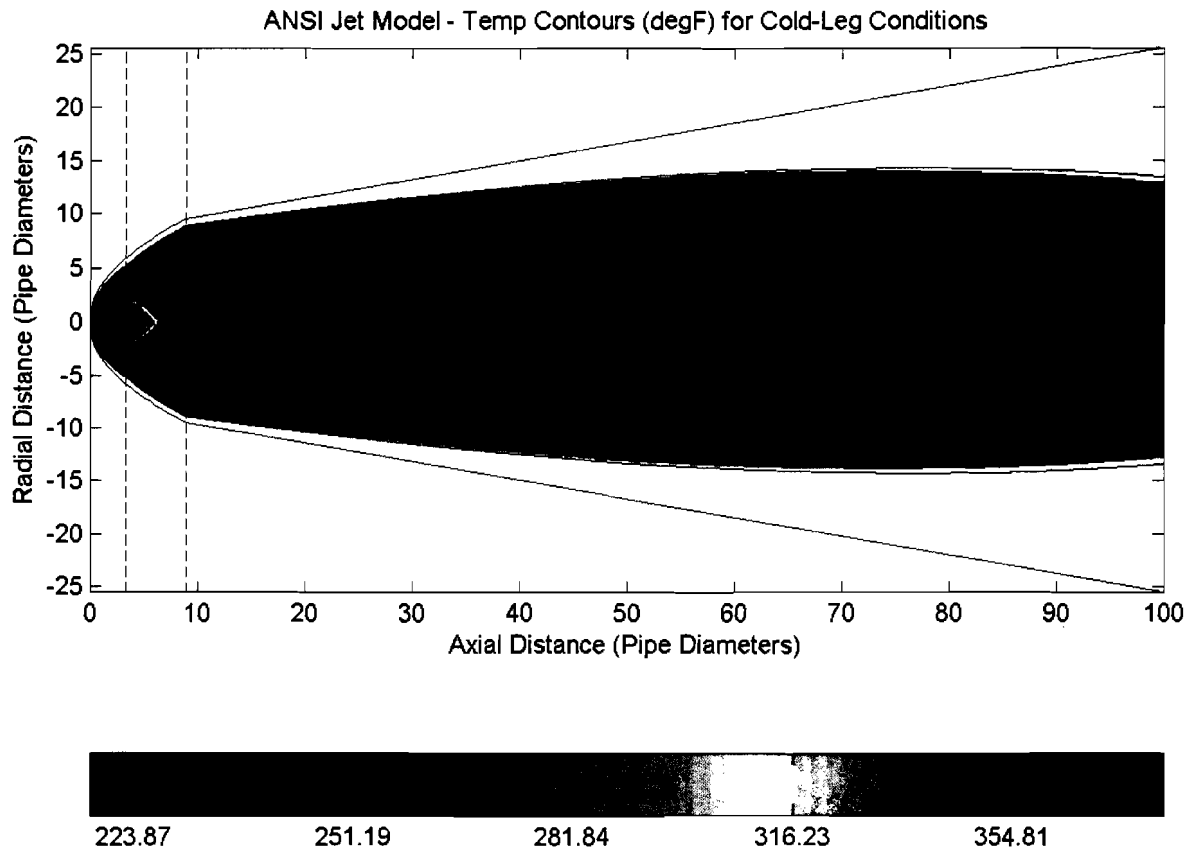


**Figure I-21. Isotherm Contours for the Reference Cold-Leg Break at 2250 psia and 530°F**

The somewhat surprising attribute of the isotherm map is how slowly the impingement temperature changes beyond the range of 10 to 15 pipe diameters downstream of the break. For potential debris-generation mechanisms that are suspected to have important thermal responses, this information can directly benefit both the specification of relevant test parameters and the interpretation of existing test data. For example, a test performed at 280°F that exhibits good damage resistance demonstrates substantially

less spatial vulnerability to high-temperature jets than a test performed at 220°F. As with pressure contours, isotherm volumes can also be mapped to equivalent spherical volumes, and because the ANSI model exhibits spatial monotonicity (uniformly increasing or decreasing in every direction) in all physical jet properties, there is a unique correspondence between pressure, temperature, and contour volume.

Another impingement-state parameter of interest is the fluid quality. There has been a long-standing debate regarding the potential for enhanced debris generation in the presence of entrained water droplets compared with that observed for high-quality steam and for air-jet surrogates. While the ANSI model cannot answer this concern, it may offer information on the spatial extent of the phenomena. Subject to the same interpretations and approximations as those discussed for impingement temperature, the jet quality can also be evaluated at  $P_0$  and  $h_0$ . Contours of equal two-phase steam quality are illustrated in Figure I-22 for the reference cold-leg break. Similar to temperature, the fluid quality changes slowly beyond a range of 10 to 15 pipe diameters and maintains a nominal value between 0.25 and 0.35. This range would be considered low-quality steam for turbine generator applications and might be viewed with concern for its potential erosion effects on stainless steel rotor blades. Certainly, the time regimes of jet impact and in-service steam components are drastically different, but the potential damage mechanisms are the same.

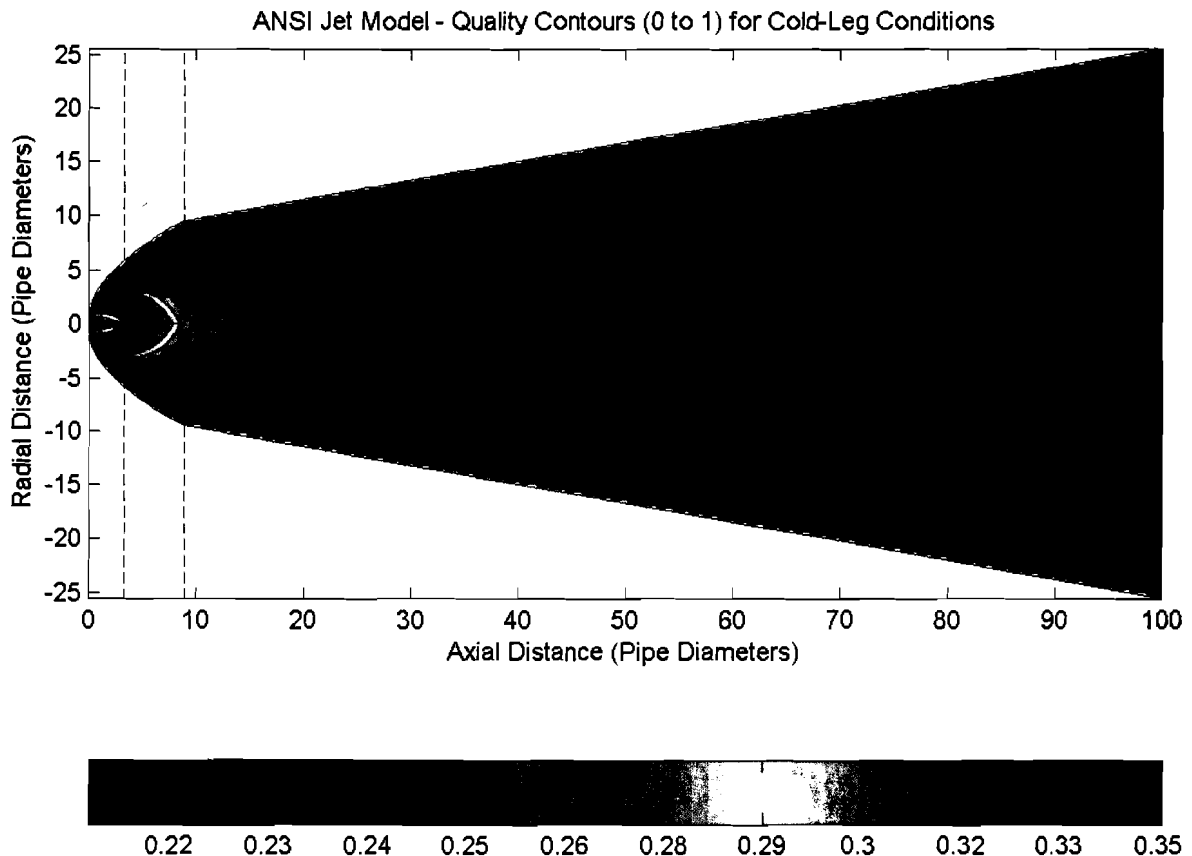


**Figure I-22. Contours of Equivalent Steam Quality for the Reference Cold-Leg Break at 2250 psia and 530°F**

The thermodynamic treatment of two-phase saturated conditions in the ANSI standard is inherently a homogeneous mass-mixture model. That is, the two-phase mixture is considered to be a single fluid with equivalent mass-weighted thermodynamic properties. This assumption, along with that of equal phase velocities in the jet, is justified by Lahey and Moody [LAH84]. Therefore, void fractions could be estimated from the local pressures and qualities. Under this assumption, it was found that the qualities shown in Figure I-19 would correspond to void fractions greater than 0.95 for all regions of the jet apart from the core. While Figure I-19 could be separated into the fluid and vapor mass fractions using the saturation properties and the definition of quality, the real issue of momentum transfer to a target could not be addressed with convincing accuracy. Theoretical treatments of two-phase transport introduce concepts of condensate nucleation, interphase velocities, droplet drag coefficients, and void fraction (space between droplets) that are difficult to measure experimentally. Pursuing this analysis with the present ANSI model would exceed the scope of its purpose and fidelity.

In summary, Table I-3 presents a set of concomitant values for pressure, temperature, quality and equivalent spherical radius that characterize the approximate impingement conditions in an expanding jet generated by a cold-leg break at 2250 psia and 530°F. With respect to equivalent spherical diameter, this reference case is observed to bound all break conditions of interest for a PWR accident analysis. Table I-4 lists intermediate parameter values computed by ANSJet for the reference break conditions. This information may be useful for comparisons of independent implementations of the jet model.

**Table I-3. Summary of Jet Properties for the Reference Cold-Leg Break**

$P_{jet}$ (psig)	$T_{jet}$ (°F)	$Q_{jet}$	$R_{sphere}$
2	218.7	0.35	31.5
3	221.8	0.34	25.4
4	224.6	0.34	21.6
6	230.0	0.34	17.0
10	239.6	0.33	11.9
17	253.7	0.32	7.5
24	265.5	0.31	5.4
40	287.0	0.29	4.0
80	324.2	0.26	2.6
150	366.1	0.21	1.5
190	384.0	0.20	1.1
2250	530.0	0.00	0.9

**Table I-4. Intermediate Parameters Computed by the ANSI Jet Routine for the Reference Cold-Leg Break Conditions**

Vessel Pressure	P0	[psia]	2250
Vessel Temp	T0	[deg F]	530
Vessel Quality	X0	[-]	-0.430084
Vessel Density	r0	[lbm/ft <sup>3</sup> ]	48.0879
Vessel Enthalpy	h0	[Btu/lbm]	522.455
Sat Temp at P0	Tsat	[deg F]	653.014
Liq Sat Enth at P0	hf	[Btu/lbm]	700.946
Vap Sat Enth at P0	hg	[Btu/lbm]	1115.96
Ambient Pressure	Pamb	[psia]	14.7
Pres at Asym Plane	Pa	[psia]	14.7
Dens at Pa, h0	rma	[lbm/ft <sup>3</sup> ]	0.105653
Computed Thrust Coeff	TC	[-]	1.64413
Crit Mass Flux	Ge	[lbm/ft <sup>2</sup> /s]	25329.2
Tsat at Pamb	Tsatamb	[deg F]	212.238
Liq Sat Enth at Pamb	hfamb	[Btu/lbm]	180.176
Vap Sat Enth at Pamb	hgamb	[Btu/lbm]	1150.28
Degrees Subcooling	delTsub	[deg F]	123.014

## I.7 SUMMARY CRITIQUE OF THE ANSI JET MODEL

Appendix I provides an exposition of the ANSI model and addresses several points where the model may be insufficiently clear or may suffer from an inconsistency. The major issues raised in the Appendix are summarized below; where applicable, recommendations for remediation are provided.

- The pressure distribution produced by the model exhibits a discontinuity across the boundary of the core. Within the core, the stagnation pressure is assumed to equal the upstream pressure  $P_0$ ; the discontinuity has been observed to reach an order of magnitude for certain upstream conditions.
- Although not explicitly stated in the model, the jet pressure distribution, which falls to zero in the far field, must be interpreted as representative of local impingement gauge pressures.
- The jet pressure at the centerline, however, remains nonzero for any finite value of the axial penetration distance. This exaggerates pressure isobar volumes and causes volume-equivalent spherical damage radii to approach infinity as the damage pressure goes to zero.
- The pressure distribution has evidently been formulated such that the thrust force is correctly recovered only for targets oriented normal to the flow direction at the orifice. Therefore, the model may not be a good approximation to free-field expansion: it may not accurately predict local conditions at points away from the jet centerline, where the flow velocity on such a normally-oriented plate would exhibit a significant tangential component. This concern is not

addressed by the application of a shape factor as outlined in Appendix D of the ANSI report.

- The above point has further ramifications for the applicability of the model to small targets. Since the stagnation pressure field produced by the model was developed to reproduce loadings on large flat targets, it is inaccurate to apply the stagnation pressures to small and/or non-flat objects. One could bound the true conditions by computing local static pressures as well; however, knowledge of the local velocity field and of the characteristics of the two-phase jet flow that are beyond the scope of the ANSI model would be required.
- A discontinuity in the slope of the isobars exists between Zones 2 and 3. This discontinuity is clearly evident in Figure I-1. The sharp terminal points of pressure isobars at the axial centerline also suggest that more attention could be given to the behavior of first spatial derivatives.
- The assumption of isentropic and/or isenthalpic expansion should be made with caution. For instance, stagnation conditions at the asymptotic plane are evaluated assuming isenthalpic behavior, implying no energy loss to the environment. In general, however, the isentropic assumption appears to be applied to the expanding jet. For a discussion of the limitations of these assumptions see Ref. [WIT02].
- Although it was analytically confirmed that all characteristic lengths in the problem scale linearly with the break diameter  $D_e$ , it is recommended that users implement the formulation of the model presented herein, as it has been nondimensionalized with respect to this quantity.
- The notation adopted by the standard for the thrust coefficient is evidently inconsistent:  $C_T$ ,  $C_{Te}$ , and  $C_{Te}^*$  all appear in the equations describing the pressure distribution for the various jet zones. These forms must all refer to a single numeric value if the pressure equations are to be piecewise continuous between zones.
- The ANSI model presents an expression for the jet area at the asymptotic plane that rests upon the assumption that the average flow static pressure at that location equals the ambient pressure  $P_{amb}$ . Elsewhere in the ANSI model, however, the asymptotic plane static pressure is assigned a value that may be less than  $P_{amb}$ .
- The standard advises users to implement a critical flow model, either the homogeneous equilibrium model (HEM) or the Henry-Fauske model, to obtain the jet mass flux  $G_e$ . Users not having such a model available may estimate  $G_e$  from Figure C-4 of the ANSI report; however this figure only covers stagnation conditions extending to 2000 psi and 50°F of subcooling, leaving certain states (e.g., cold leg conditions in many PWRs) unaddressed. Given the additional inaccuracies that may be introduced by reading from the figure, it

is strongly recommended that a critical flow model be implemented for use with the jet model.

- The standard recommends that Henry-Fauske critical flow model be used for subcooled vessel conditions and the HEM for saturated conditions. This would introduce a strong discontinuity as the liquid saturation point is crossed. Therefore, since Henry-Fauske is evidently in better agreement with the data for both subcooled and two-phase conditions, exclusive use of this model is recommended.
- An implied discontinuity exists across the break plane, as the ANSI model assumes that fluid in the core is in equilibrium at the upstream stagnation pressure and quality. This assumption contradicts aspects of both the HEM and Henry-Fauske models.
- The correlation recommended by the standard for use in calculating the thrust coefficient  $C_T$  for subcooled conditions applies only to Henry-Fauske derived mass fluxes. This is not made clear in the standard. Also left unclear is the assumption inherent in the correlation that ambient conditions are at standard pressure. Therefore, this correlation should not be used in conjunction with HEM mass fluxes, and users of the standard should bear in mind that the correlation is not strictly validated for ambient conditions deviating from those of the standard atmosphere. The error is small, though, for most upstream pressures of interest in the present analysis.
- No analytic correlation is provided by the standard for the thrust coefficient relevant to saturated steam-water mixtures. Within the standard, users may only consult Figure B-5 to visually gauge an approximate value. Another recourse would be to consult the thrust coefficient contour plots presented in this appendix, or better, implement a critical mass flux model to enable direct calculation of mass flux and thrust coefficient via the Henry-Fauske model.
- Users should be aware that one desired result of the model, volume-equivalent spherical damage-pressure radii, can behave nonintuitively as certain upstream conditions are varied. For instance, the PWR hot leg and cold leg results presented in Table I-1 of this appendix show that the flow from the hot leg break exhibits a lower mass flux and thrust coefficient than that from the cold leg. Nonetheless, the damage radii are roughly comparable, with radii for the hot leg break being greater than those of the cold leg for higher damage pressures and smaller for lower damage pressures. These results, which follow from variations in the flow velocity and density at the break, reinforce the importance of not eliminating lower-energy break points *a priori* when conducting ZOI analyses.

## I.8 REFERENCES

- [ANS88] "American National Standard: Design Basis for Protection of Light Water Nuclear Power Plants Against the Effects of Postulated Pipe Rupture," American Nuclear Society, ANSI/ANS-58.2-1988, October 1988.
- [DUD76] Duderstadt, J. J., Hamilton, L. J., *Nuclear Reactor Analysis*, Wiley and Sons, New York, New York (1976).
- [RAO02] Rao, D. V., Ross, K. W., Ashbaugh, S. G., "GSI-191: Thermal-Hydraulic Response of PWR Reactor Coolant System and Containments to Selected Accident Sequences," prepared for the U.S. Nuclear Regulatory Commission by Los Alamos National Laboratory, NUREG/CR-6770, LA-UR-01-5561 (August 2002).
- [NEI04] "Pressurized-Water-Reactor Sump Performance Evaluation Methodology," prepared by the Nuclear Energy Institute, May 28, 2004.
- [NRC98] "Safety Evaluation by the Office of Nuclear Reactor Regulation Related to NRC Bulletin 96-03, Boiling Water Reactor Owners Group Topical Report NEDO-32686," U.S. Nuclear Regulatory Commission, August 1998.
- [NRC03] Regulatory Guide 1.82, "Water Sources for Long-Term Recirculation Cooling Following a Loss-of-Coolant Accident," U.S. Nuclear Regulatory Commission, Office of Nuclear Regulatory Research, Rev. 3, August 2003.
- [URG96] NEDO-32686, Rev. 0, "Utility Resolution Guidance for ECCS Strainer Blockage," General Electric Nuclear Energy Company, Class 1, November 1996.
- [WEI83] Weigand, G. G. et al., "Two-Phase Jet Loads," NUREG/CR-2913, Sandia National Laboratory (prepared for the U.S. Nuclear Regulatory Commission), January 1983.
- [HAL80] D. G. HALL, D. G., L. S. CZAPARY, "Tables of Homogeneous Equilibrium Critical Flow Parameters for Water in SI Units," EG&G Idaho report EGG-2056 (1980).
- [HEN71] HENRY, R. E., FAUSKE, H. K., "The Two Phase Critical Flow of One-Component Mixtures in Nozzles, Orifices, and Short Tubes," *J. Heat Transfer*, p. 179, May 1971.
- [HAR96] HARVEY, A. H., PESKIN, A. P., KLEIN, S. A., "NIST/ASME Steam Properties: Formulation for General and Scientific Use," Version 2.11, 1996.
- [WEB76] S. W. Webb, "Evaluation of Subcooled Water Thrust Forces," *Nucl. Technology* 31, p. 48, October 1976.
- [LAH84] R. T. Lahey and F. J. Moody, *The Thermal-Hydraulics of a Boiling Water Nuclear Reactor*, 3rd ed., La Grande Park, IL: ANS Press, 1984: p. 381.

- [WIT02] Witlox, H. W. and Bowen, P. J., "Flashing Liquid Jets and Two-Phase Dispersion: A Review," United Kingdom Health and Safety Executive Contract Research Report 403/2002, p. 37 (2002).
- [RAH92] Rahn, F.J., Adamantiades, A. G., Kenton, J. E. and Braun, C., *A Guide to Nuclear Power Technology: A Resource for Decision Making*, Krieger, Malabar, Fla., 1992.
- [LOB90] Lobner, P., Donahoe, C. and Cavallin, C., "Overview and Comparison of US Commercial Nuclear Power Plants," prepared for the U.S. Nuclear Regulatory Commission by Science Applications International Corporation, NUREG/CR-5640, SAIC-89/1541, September 1990.

## Attachment 1 to APPENDIX I

```

CCCCCCCCCCCCCCCCCCCCCCCCCCCCCCCCCCCCCCCCCCCCCCCCCCCCCCCCCCCCCCCCCCCC
C      mexFunction
C      MATLAB-executable subroutine that serves as the jumping-off point
C      for calls to the ASME steam tables via the subroutines located in
C      INTPK.FOR and elsewhere.
C
C      The subroutine MUST be named mexFunction and it MUST contain the
C      four arguments
C      NLHS: number of elements contained in the array PLHS
C      PLHS: an array of pointers to the output values to be returned
C      to MATLAB by mexFunction. It is stored as an array of integer
C      memory references; MATLAB handles extraction of the outputs from
C      these references, but PLHS itself must be populated via the
C      mxCopyReal8ToPtr function (see below).
C      NRHS: number of elements contained in the array PRHS
C      PRHS: array of pointers to input values, as described above for
C      PLHS. The input values themselves are extracted by calling
C      mxCopyPtrToReal8.
C
C      For this application, the inputs in PRHS and outputs in PLHS are
C      organized as follows:
C
C      Say that there are y (Po,To,Xo) state points describing a blowdown
C      history. Po(y) [psia] is an array defining the pressures at these
C      points, To(y) [deg F] defines the pressures, and Xo(y) gives the
C      qualities. Only two of these would be specified for each state
C      point; mexFunction will return the third. During the subcooled
C      period, T and P would be given and mexFunction would populate
C      the quality by evaluating  $X = (h - h_f)/h_{fg}$ . Under saturated
C      conditions, either T or P would be given along with X and the model
C      would return the unspecified quantity as  $P = P_{sat}$  or  $T = T_{sat}$ .
C      Other outputs to be returned are
C
C      Tsat(y) [deg F], saturation temperature
C      Hf(y) [Btu/lbm], enthalpy of liquid phase at Tsat
C      Hg(y) [Btu/lbm], enthalpy of vapor phase at Tsat
C      Rhoo(y) [lbm/ft^3], fluid density
C      Ho(y) [Btu/lbm], fluid enthalpy
C
C      Note that for saturated fluid there are redundancies, e.g.,
C      To=Tsatsat and only three of Hf, Hg, Ho, X are needed.
C
C      Say that z pressure/temperature contours are to be evaluated.
C      The input would be an array Pj(z) of pressures. The temperatures
C      evaluated for the corresponding y state points would be stored in
C      the array Tj(y*z) indexed by  $T_j[y_i, z_j]=T_j[z*(y_i-1)+z_j]$ .
C
C      The critical mass flux Ge(y) [lbm/ft^2/s] is computed for each
C      state point, as is the thrust coefficient K (notated TC in the
C      code). This is evaluated using a force balance at the orifice,
C      with the mass flux and thermodynamic state at the orifice being
C      obtained from the model being implemented (the HEM, Henry-Fauske,
C      or the ideal gas law).
C
C      The pressure Pa(y) and density Rhoa(y) [lbm/ft^3] at the asymptotic
C      plane are also computed.
C
C      The Ge calculations are carried out using one of three models,
C      homogeneous equilibrium (HEM), Henry-Fauske (H-F), or the ideal gas
C      equations of state. The model used is governed by the value of the
C      USE_LOGIC integer input flag:
C
C      USE_LOGIC      Subcooled      Saturated      Superheated
C      0              HEM              HEM              HEM
C      1              H-F              H-F              HEM
C      2              HEM              HEM              Ideal Gas
C      3              H-F              H-F              Ideal Gas
C
C      Finally, the saturation temperature Tsat,amb at Pamb is computed,
C      as are the saturated liquid and vapor enthalpies Hf,amb and Hg,amb.
C
C      The input PRHS is thus

```

```

C
C CONCAT(Po, To, Xo, Pj, Pamb, y, z, USE_LOGIC)
C
C and the output PLHS is
C
C CONCAT(Po, To, Xo, Tsat, Hf, Hg, Rhoo, Ho, Pa, Rhoa, Ge, TC,
C Tj, Tsat,amb, Hf,amb, Hg,amb).
C
C AUTHOR: Erich Schneider
C DRAFTED: July 5, 2004
CCCCCCCCCCCCCCCCCCCCCCCCCCCCCCCCCCCCCCCCCCCCCCCCCCCCCCCCCCCC

```

```

SUBROUTINE mexFunction(NLHS, PLHS, NRHS, PRHS)

C Initialize and dimension other arguments to subroutines located in
C INTPK.FOR. See EXAM.FOR for another example.

```

```

IMPLICIT DOUBLE PRECISION (A-H,O-Z)
INCLUDE 'nprop.cmn'
DIMENSION IWORK(NPROP), IWANT(NPROP), PROPR(NPROP), PROPSI(NPROP)
DIMENSION WAVRI(NRIMAX), RI(NRIMAX), IRIFLG(NRIMAX)
DIMENSION IPCHK(5), IPFLG(5)
INTEGER mxGetM, mxGetN, mxGetPr
INTEGER NLHS, NRHS
INTEGER PLHS(*), PRHS(*)
INTEGER M, N, SIZE, IN_COUNT, OUT_COUNT, IY, IZ, I, J, MODE

INTEGER IN_PTR, OUT_PTR, USE_LOGIC, USE_MODEL

```

```

C number of outputs per state point. Currently 12: the three inputs
C P, T and X (recall that 2 are specified and this subroutine finds
C the third), Tsat, Hf, Hg, Rhoo, Ho, Pa, Rhoa, Ge, TC
PARAMETER (NUM_OUTPUTS = 12)

```

```

C Dimension input and output arrays given that no more than 50 state
C points and 50 contours may be accepted as inputs.
C This would be a lot more elegant if FORTRAN supported dynamic memory
C allocation, but that's the price one pays for a fast language!
PARAMETER (MAX_STATE_PTS=50, MAX_CONTOURS=50)

```

```

REAL*8 PAMB, TSATAMB, FOFHO, RATIO, MIX_PROP
REAL*8 HFAMB, HGAMB
REAL*8 IN_VALS(MAX_STATE_PTS*3+MAX_CONTOURS+4)
REAL*8 OUT_VALS(MAX_STATE_PTS*NUM_OUTPUTS+
& MAX_STATE_PTS*MAX_CONTOURS+1)
REAL*8 P0(MAX_STATE_PTS), T0(MAX_STATE_PTS), X0(MAX_STATE_PTS)
REAL*8 T_SAT(MAX_STATE_PTS), HF(MAX_STATE_PTS), HG(MAX_STATE_PTS)
REAL*8 RHO0(MAX_STATE_PTS), H0(MAX_STATE_PTS), PA(MAX_STATE_PTS)
REAL*8 RHOA(MAX_STATE_PTS), GE(MAX_STATE_PTS), PJ(MAX_CONTOURS)
REAL*8 TJ(MAX_STATE_PTS,MAX_CONTOURS), TC(MAX_STATE_PTS)

```

```

C Create array of reals from the array PRHS of pointers

M = mxGetM(PRHS(1))
N = mxGetN(PRHS(1))

SIZE = M*N

IN_PTR=mxGetPr(PRHS(1))

CALL mxCopyPtrToReal8(IN_PTR,IN_VALS,SIZE)

```

```

C Disassemble and parse input value array: get number of state points
C to be examined and number of P/T contours to be obtained for each
C state point. Note that at least one state point must exist for the
C contour calculation to take place. If this is not the case,
C the contour calculations will be skipped even if Pj input values
C are supplied.

```

```

IY=IN_VALS(SIZE-2)
IZ=IN_VALS(SIZE-1)

```

```

C Obtain value of integer USE_LOGIC flag
USE_LOGIC=IN_VALS(SIZE)

```

```

C Verify that user is not trying to evaluate more than MAX_STATE_PTS
C state points or more than MAX_CONTOURS contours.  If this is the
C case, return a soft landing

      IF (IY .GT. MAX_STATE_PTS) THEN
          CALL mexErrMsgTxt('Number of state points passed to QUERYST is greater
& than MAX_STATE_PTS.  Decrease number of points to be analyzed or
& increase MAX_STATE_PTS in QUERYST.for.')
      ENDIF
      IF (IZ .GT. MAX_CONTOURS) THEN
          CALL mexErrMsgTxt('Number of contour points passed to QUERYST is great
& er than MAX_CONTOURS.  Decrease number of points to be analyzed or
& increase MAX_CONTOURS in QUERYST.for.')
      ENDIF

      IN_COUNT=1
      OUT_COUNT=1

C Prepare IWANT vector to harvest enthalpies

      DO 110 I=1,NPROP
          IWANT(I) = 0
110  CONTINUE
      IWANT(6) = 1
      DO 111 I=1,5
          IPCHK(I) = 0
111  CONTINUE

C read P_amb and obtain Tsat and enthalpies at P_amb
      PAMB=IN_VALS(SIZE-3)
      CALL TSAT(PAMB, TSATAMB, RHOL, RHOV, IWORK, PROPR, IERR)

C Compute liquid and vapor enthalpies HF & HG
      CALL PROPS(IWANT, TSATAMB, RHOL, PROPSI, PROPR,0,I2PH,0,
& ISFLG,0, ICFLG, IPCHK, IPFLG, 0, 0, WAVRI, RI, IRIFLG)
      HFAMB = PROPSI(6)

      CALL PROPS(IWANT, TSATAMB, RHOV, PROPSI, PROPR,0,I2PH,0,
& ISFLG,0, ICFLG, IPCHK, IPFLG, 0, 0, WAVRI, RI, IRIFLG)
      HGAMB = PROPSI(6)

      IF (IY .GT. 0) THEN

C Read (P, T, X) values for IY state points
      DO 100 I=1,IY
          P0(I)=IN_VALS(I)
          T0(I)=IN_VALS(I+IY)
          X0(I)=IN_VALS(I+2*IY)
          GE(I)=0.
          TC(I)=0.

C Compute properties for this point: first check if fluid is saturated
C QUERYST.FOR treats the fluid as saturated if the input pressure is < 0,
C in which case the input quality should be in [0,1]

          IF ((P0(I) .LT. 0) .OR. (T0(I) .LT. 0)) THEN

C Saturated conditions with only one of P and T specified; calculate the other

              IF (P0(I) .LT. 0) THEN
                  T_SAT(I) = T0(I)
C Find saturation pressure
                  CALL PSAT(T0(I), PMPA, RHOL, RHOV, IWORK, PROPR,
& IERR)
                  P0(I) = PMPA
              ELSE IF (T0(I) .LT. 0) THEN
C Find saturation temperature
                  CALL TSAT(P0(I), TK, RHOL, RHOV, IWORK, PROPR,
& IERR)
                  T0(I) = TK
                  T_SAT(I) = T0(I)
              ENDIF

C Find mixture density
              RHO0(I) = MIX_PROP(X0(I), RHOL, RHOV)

C Compute liquid and vapor enthalpies HF & HG
              CALL PROPS(IWANT, T0(I), RHOL, PROPSI, PROPR,0,I2PH,0,

```

```

&          ISFLG,0, ICFLG, IPCHK, IPFLG, 0, 0, WAVRI, RI, IRIFLG)
          HF(I) = PROPSI(6)

          CALL PROPS(IWANT, T0(I), RHOV, PROPSI, PROPR,0,I2PH,0,
&          ISFLG,0, ICFLG, IPCHK, IPFLG, 0, 0, WAVRI, RI, IRIFLG)
          HG(I) = PROPSI(6)

C Compute mixture enthalpy
          H0(I) = MIX_PROP(X0(I), HF(I), HG(I))

          ELSE

C Find saturation temperature at P0
          CALL TSAT(P0(I), TK, RHOL, RHOV, IWORK, PROPR, IERR)
          T_SAT(I) = TK

C Obtain enthalpies at (Tsat, P0)
          CALL PROPS(IWANT, TK, RHOL, PROPSI, PROPR, 0, I2PH, 0,
&          ISFLG,0, ICFLG, IPCHK, IPFLG, 0, 0, WAVRI, RI, IRIFLG)
          HF(I) = PROPSI(6)
&          CALL PROPS(IWANT, TK, RHOV, PROPSI, PROPR, 0, I2PH, 0,
&          ISFLG,0, ICFLG, IPCHK, IPFLG, 0, 0, WAVRI, RI, IRIFLG)
          HG(I) = PROPSI(6)

C Find density and enthalpy at (T0, P0)
          CALL DENS0(DOUT, P0(I),T0(I), DPD, IWORK, PROPR, IERR)
          RHO0(I)=DOUT
&          CALL PROPS(IWANT,T0(I),DOUT,PROPSI, PROPR, 0, I2PH, 0,
&          ISFLG,0, ICFLG, IPCHK, IPFLG, 0, 0, WAVRI, RI, IRIFLG)
          H0(I) = PROPSI(6)

          X0(I) = (H0(I) - HF(I))/(HG(I) - HF(I))
          ENDIF

C Given the initial quality, determine the pressure at the asymptotic plane
          IF (X0(I) .GT. -0.1) THEN
              FOFH0 = SQRT(0.1 + X0(I))
          ELSE
              FOFH0 = 0.0
          ENDIF
          RATIO = PAMB/P0(I)
          IF (RATIO .GT. 0.5) THEN
              RATIO=0.5
          ENDIF

          PA(I) = (1. - 1./2.*(1.-2.*RATIO)*FOFH0)*PAMB

C Now find the density. Set MODE = 1 for HSSOLV (Inp: P, H, Out: T, rho)
          MODE = 1
          CALL HSSOLV(MODE, PA(I), H0(I), TPOUT, D1, DV, DL,
&          I2PH, Q, IWORK, PROPR, IERR)

C Format of result in HSSOLV dependent on phase of fluid as signified by I2PH
          IF ((I2PH .EQ. 2) .OR. (I2PH .EQ. 4)) THEN
              RHOA(I) = 1./MIX_PROP(Q, 1.0/DL, 1.0/DV)
          ELSE
              RHOA(I) = D1
          ENDIF

C The code block below sets USE_MODEL based upon user-specified USE_LOGIC
C and upstream stagnation conditions.

C Based upon the specification provided by the user, USE_MODEL is below
C assigned a value of zero (HEM), one (H-F) or two (ideal gas)
C prior to being passed to CRIT_MASS_FLUX. However: if USE_MODEL = 2 and
C upstream stagnation conditions are insufficiently superheated such that
C the ideal gas law yields a static state that is in the two-phase regime,
C CRIT_MASS_FLUX automatically defaults to the HEM. In general, since the
C HEM reduces to the ideal gas law as the superheating increases, USE_LOGIC
C = 2 and 3 should be avoided. This is doubly so since truly ideal gas-like
C behavior is not likely to be observed for any of the problems that are
C being studied with ANSIJET.

          IF (X0(I) .GT. 1.0) THEN
              IF ((USE_LOGIC .EQ. 2) .OR. (USE_LOGIC .EQ. 3)) THEN

```

```

                USE_MODEL = 2
            ELSE
                USE_MODEL = 0
            ENDIF
        ELSE
            IF ((USE_LOGIC .EQ. 0) .OR. (USE_LOGIC .EQ. 2)) THEN
                USE_MODEL = 0
            ELSE
                USE_MODEL = 1
            ENDIF
        ENDIF
        CALL CRIT_MASS_FLUX(GE(I),TC(I),PO(I),HO(I),PAMB,
&                USE_MODEL)
100        CONTINUE
            IN_COUNT=IY*3
            IF(IZ .GT. 0) THEN
C Read Pj values for IZ contours
                DO 101 J=1, IZ
                    PJ(J)=IN_VALS(IN_COUNT+J)
101                CONTINUE
C Compute Tj at each Pj value for every state point
                DO 102 I=1, IY
                    DO 103 J=1, IZ
C MODE = 1 -> HSSOLV expects P and H as inputs and returns T
                        MODE = 1
                        CALL HSSOLV(MODE, PJ(J), HO(I), TPOUT, D1, DV, DL,
&                                I2PH, Q, IWORK, PROPR, IERR)
                        TJ(I,J)=TPOUT
103                    CONTINUE
102                CONTINUE
            ENDIF
        ENDIF
C Create output array
        DO 104 I=1,IY
            OUT_VALS(I)=PO(I)
            OUT_VALS(I+IY)=T0(I)
            OUT_VALS(I+2*IY)=X0(I)
            OUT_VALS(I+3*IY)=T_SAT(I)
            OUT_VALS(I+4*IY)=HF(I)
            OUT_VALS(I+5*IY)=HG(I)
            OUT_VALS(I+6*IY)=RHO0(I)
            OUT_VALS(I+7*IY)=HO(I)
            OUT_VALS(I+8*IY)=PA(I)
            OUT_VALS(I+9*IY)=RHOA(I)
            OUT_VALS(I+10*IY)=GE(I)
            OUT_VALS(I+11*IY)=TC(I)
            DO 105 J=1,IZ
                OUT_VALS(NUM_OUTPUTS*IY+(I-1)*IZ+J)=TJ(I,J)
105            CONTINUE
104        CONTINUE
            OUT_VALS(NUM_OUTPUTS*IY+IZ*IY+1)=TSATAMB
            OUT_VALS(NUM_OUTPUTS*IY+IZ*IY+2)=HFAMB
            OUT_VALS(NUM_OUTPUTS*IY+IZ*IY+3)=HGAMB
C Create pointer to output array and size it
            SIZE=MAX_STATE_PTS+NUM_OUTPUTS+MAX_STATE_PTS*MAX_CONTOURS+3
            PLHS(1)=mxCreateDoubleMatrix(SIZE,1,0)
            OUT_PTR=mxGetPr(PLHS(1))
C Populate pointer to output for MATLAB use
            CALL mxCopyReal8ToPtr(OUT_VALS,OUT_PTR,SIZE)
            RETURN
        END
        FUNCTION MIX_PROP(QUALITY, PROP_F, PROP_G)
CCCCCCCCCCCCCCCCCCCCCCCCCCCCCCCCCCCCCCCCCCCCCCCCCCCCCCCCCCCCCCCCCCCC
C                                MIX_PROP                                C

```

```

C Given an input quality and phase properties at saturation, MIX_PROP C
C computes the value of the property for the mixture. Any mass- C
C specific property that has meaning for a two phase mixture C
C (1/density, enthalpy, etc.) may be computed. C
C C
C Inputs: C
C QUALITY Does not necessarily lie in [0,1] C
C PROP_F, PROP_G: saturation values of the property to be computed C
C C
C Output: C
C MIX_PROP = QUALITY*PROP_G + (1-QUALITY)*PROP_F C
C C
CCCCCCCCCCCCCCCCCCCCCCCCCCCCCCCCCCCCCCCCCCCCCCCCCCCCCCCCCCCC
      REAL*8 QUALITY, PROP_F, PROP_G, MIX_PROP
      MIX_PROP = QUALITY*PROP_G + (1.0-QUALITY)*PROP_F
      RETURN
      END
      SUBROUTINE CRIT_MASS_FLUX(G_CALC, TC_CALC, P0, H0,
& P_AMB, USE_MODEL)
CCCCCCCCCCCCCCCCCCCCCCCCCCCCCCCCCCCCCCCCCCCCCCCCCCCCCCCCCCCC
      CRIT_MASS_FLUX C
C Given a state point (P0, H0), derives the critical mass flow G C
C (kg/m^2-s) as per the homogeneous equil. method (see Hall & Czapary, C
C "Tables of Homogeneous Equilibrium Critical Flow Parameters for C
C Water In SI Units," EG&G Idaho Report EGG-2056,1980), or the method C
C of Henry and Fauske, "The Two-Phase Critical Flow of One-Component C
C Mixtures in Nozzles, Orifices, and Short Tubes," J. Heat Transfer C
C May 1971, p. 179, or the ideal gas equation of state. C
C C
C HEM Notes C
C C
C The HEM model maximizes the mass flux  $G = V/v$  ( $V$  = flow velocity C
C [m/s],  $v$  = specific volume [m^3/kg]). Applying the First Law, this C
C is equivalent to C
C  $G = 2(h_0 - h)^{1/2} / v$ , C
C where  $h_0$  is the stagnation enthalpy of the fluid, and  $h$  and  $v$  are C
C the enthalpy and specific volume to be adjusted isoentropically C
C such that  $G$  is maximized. The optimum or critical state at which C
C the tradeoff between decreased static enthalpy (and thus higher C
C velocity) and increased specific volume may be represented by a C
C critical pressure,  $p^*$ . It is convenient to optimize on the above C
C using  $p^*$  as the independent variable. C
C C
C The maximization method used is a golden-mean bisection after C
C Teukolsky et. al, "Numerical Recipes in Fortran." The algorithm C
C has been altered somewhat to take into account the nature of the C
C function  $G = f(p^*)$ : since  $f(p^*)$  is undefined for  $p^* > P_0$  and also C
C for very low values of  $p^*$ , some care must be taken in bracketing C
C the root. The algorithm generally converges within 50 iterations, C
C with 1% accuracy being obtained after about 20 evaluations of  $G$ . C
C C
C The algorithm may be tuned by adjusting the fractional tolerance C
C TOLER and the interval size STRETCH_FACTOR over which the root C
C bracketing algorithm searches. C
C C
C Henry-Fauske Notes C
C C
C The Henry-Fauske model also searches for the critical pressure  $p^*$  C
C for which the mass flux is maximized. However, the computational C
C technique is modified somewhat for the Henry-Fauske formulation as C
C it requires solution of a transcendental equation for  $p^*$ . The C
C equation only requires knowledge of upstream stagnation conditions C
C and is described in greater detail in subroutine HENRY_FAUSKE below. C
C C
C To use the same computational engine as that applied to the HEM C
C above, the Henry-Fauske formulation is recast as a maximization C
C problem by writing the transcendental equation for  $p^*$ , C
C  $f(p^*) = g(p^*)$ , C
C in a form amenable to solution via golden-mean maximization: C
C  $A = - (g(p^*) - f(p^*))^2$ , C

```

```

C where the problem becomes one of finding the value of p* that C
C maximizes A, with perfect convergence of course resulting in A = 0. C
C The quantity A is notated P_ROOT in the code below. C
C C
C The same considerations as described for the HEM above apply in C
C connection with root bracketing. Convergence slows for highly C
C subcooled upstream stagnation conditions. Under these conditions, C
C the quantity dG/dp* is very large in the vicinity of the root, and C
C the bracketing of the root becomes an increasingly difficult C
C problem. This is evidenced by the behavior of the equilibrium C
C quality at the throat (notated x_E in Henry and Fauske's paper), C
C which approaches zero for the p* that solves the model as upstream C
C subcooling increases. C
C C
C Ideal Gas Notes C
C C
C Application of the ideal gas equation of state is generally not C
C advisable since the ideal gas approximation is not a good one for C
C upstream stagnation conditions that are only slightly superheated. C
C In fact, it is possible for an evaluation using this method to C
C result in static (choked) conditions that in fact lie within the C
C two-phase regime. If the user has selected ideal gas evaluation C
C and this is found to occur, CRIT_MASS_FLUX defaults to the HEM for C
C G_e and thrust coefficient calculations. Since conditions of C
C interest for ANSIJET, e.g., main steam line break, are not greatly C
C superheated, it is recommended that users adopt the HEM instead C
C for all superheated evaluations of G_e. C
C C
C The HEM in fact reduces to the ideal gas eqn. for heavily C
C superheated conditions. This provides an additional reason to C
C adopt it. The only disadvantage to the HEM is that the method is C
C somewhat more computationally intensive. C
C C
C C
C EAS 7/7/04 C
C ***** MODIFICATIONS ***** C
C EAS 7/14/04: Fixed bug that caused code to use improperly C
C initialized values for GE C
C EAS 7/18/04: Deployed Henry-Fauske model solver; added switch to C
C allow user selection of model to use C
C EAS 7/28/04: Fixed root bracketing interval for H-F so that C
C routine will search the entire space of state points C
C allowed by the steam tables. C
C EAS 7/28/04: The model to be used is now an input from the MATLAB C
C function call. See MexFunction for documentation. C
C EAS 7/30/04: Changed to subroutine that computes thrust coeffs. C
C subsequent to critical mass flux calculations C
C EAS 8/17/04 Added ideal gas eqn. of state evaluation C
C C
CCCCCCCCCCCCCCCCCCCCCCCCCCCCCCCCCCCCCCCCCCCCCCCCCCCCCCCCCCCC

```

```

IMPLICIT DOUBLE PRECISION (A-H,O-Z)
INCLUDE 'nprop.cmn'
C Minimum temperature at which steam tables calculate thermo. properties
C Used for bounding of space in which root is to be sought
PARAMETER (T_MIN = 273.2)
DIMENSION IWORK(NPROP), IWANT(NPROP), PROPR(NPROP), PROPSI(NPROP)
DIMENSION WAVRI(NRIMAX), RI(NRIMAX), IRIFLG(NRIMAX)
DIMENSION IPCHK(5), IPFLG(5)
REAL*8 H0,P0,T0,S0,X0,STRETCH_FACTOR,P_HOLD,G_CALC,TC_CALC,R
REAL*8 G_HOLD, MIX_PROP, DENS, VG0, VF0, ROOT_HOLD, P_MIN,RHO_HOLD
REAL*8 T_HOLD
C 0 = HEM, 1 = Henry-Fauske
INTEGER USE_MODEL

C Bracketing triplet p_low=PSTAR(1), p_mid=PSTAR(2), p_hi=PSTAR(3)
C and values of G at each p*
REAL*8 PSTAR(3), GE(3), P_ROOT(3), RHO_T(3)

PARAMETER (GOLD = 1.618034, TOLER=1.0e-5)

C Get temperature T0 and density Rho0 corresponding to (P0, H0)
CALL HSSOLV(1, P0, H0, TPOUT, D1, DV, DL,
& I2PH, Q, IWORK, PROPR, IERR)

```

```

      IF ((I2PH .EQ. 2) .OR. (I2PH .EQ. 4)) THEN
C 2 phase stagnation conditions
      DENS = 1./MIX_PROP(Q, 1.0/DL, 1.0/DV)
      X0=Q
      VF0 = 1./DL
      VG0 = 1./DV
      ELSE IF (I2PH .EQ. -1) THEN
C Saturated / subcooled liquid stagnation
      DENS = D1
      X0= (1./DENS - 1./DL)/(1./DV-1./DL)
      VF0 = 1./DENS
      VG0 = 0.
      ELSE IF (I2PH .EQ. 1) THEN
C Saturated vapor stagnation
      DENS = D1
      X0= (1./DENS - 1./DL)/(1./DV-1./DL)
C Note: although the model functions without crashing for
C superheated vapor, this does not imply its validity!!
      VF0 = 1./DL
      VG0 = 1./DENS
      ENDIF
      T0=TPOUT

C Get entropy S0 corresponding to (T0, Rho0)
      DO 202 I=1,NPROP
          IWANT(I) = 0
202  CONTINUE
      IWANT(7) = 1

      CALL PROPS(IWANT,T0,DENS,PROPSI, PROPR, 1, I2PH, 0,
&ISFLG,0, ICFLG, IPCHK, IPFLG, 0, 0, WAVRI, RI, IRIFLG)
      S0 = PROPSI(7)

      IF (USE_MODEL .EQ. 2) THEN

C Using the ideal gas law for superheated steam:
C T_HOLD and RHO_HOLD will contain the static temperature and density
C at the throat. These are used to verify that the ideal gas law offers
C a reasonably valid model of the expansion.

      T_HOLD = T0
      RHO_HOLD = DENS

      IWANT(8) = 1
      IWANT(9) = 1

C Additional upstream properties are needed:
C Obtain ratio of specific heats, GAMMA = C_P/C_V. GAMMA ~ 1.3 for steam.
111  CALL PROPS(IWANT,T_HOLD,RHO_HOLD,PROPSI, PROPR, 1, I2PH, 0,
& ISFLG,0, ICFLG, IPCHK, IPFLG, 0, 0, WAVRI, RI, IRIFLG)

      IF ((I2PH .EQ. 2) .OR. (I2PH .EQ. 4)) THEN

C If this is true, static conditions at the exit are two-phase. The ideal
C gas equation of state is obviously not applicable. Break and evaluate
C using the HEM.

      USE_MODEL = 0
      GOTO 110
      ENDIF

      GAMMA = PROPSI(9)/PROPSI(8)
C Gas constant R = C_P - C_V [J/kg/K]
      R = 1000.*(PROPSI(9) - PROPSI(8))

C Compute the mass flux noting that P0 is stored in MPa and must be converted
C Hence G_CALC is has units [kg/m^2/s]
      G_CALC = (GAMMA/R*(2./((GAMMA+1.))**((GAMMA+1.)/(GAMMA-1.)))**
& 0.5 * P0 / T0**0.5 *1.e6
C Compute the static discharge density rho = G / V
      RHO_HOLD = G_CALC / (2.*GAMMA*R*T0/(GAMMA+1.))**0.5

C The static pressure at the exit is also needed to compute the thrust coeff:
C This pressure is given in MPa.

```

```

P_HOLD = P0 * (2./(GAMMA+1.))**(GAMMA/(GAMMA-1.))

C Obtain the static temperature, check for consistency, and recompute
C static properties to check validity of ideal gas law eqn. of state:
T_STAT = T0 * 2./(GAMMA + 1.)
IF ((T_HOLD - T_STAT)**2. .GT. .01) THEN
    T_HOLD = T_STAT

C Re-evaluate state equation to verify that the correct property values were
C used. If the fluid were behaving as a perfect gas this loop would not be
C necessary. Entropy, for instance, is not conserved between the stagnation and
C static states, although it is approximately constant through the expansion
C for highly superheated conditions.
    GOTO 111
ENDIF

C Success: the ideal gas law results for G, RHO and P will be used below
C to obtain the thrust coefficient (theoretically 1.26 for steam)

110    ENDIF

    IF(USE_MODEL. EQ. 0) THEN

C Using the HEM:
C Bracket the maximum. It is assumed that Ge(p*) is well-behaved in that
C there will be only one local maximum. Ge(p*=P0) = 0, so we sweep downward
C in p* until we have a triplet (p_low,p_mid,p_hi=P0) in which the root is
C bracketed.

        STRETCH_FACTOR=0.75
        GE(1)=1
        GE(2)=0
        PSTAR(1)=P0

C Increase P* interval to be searched for root until root is bracketed
200    IF (GE(1) .GT. GE(2)) THEN
            PSTAR(1)=PSTAR(1)*STRETCH_FACTOR
            PSTAR(3)=P0
            PSTAR(2)=PSTAR(1)+1./GOLD*(PSTAR(3)-PSTAR(1))
            GE(3)=0.
            CALL EVAL_G(GE(1), RHO_T(1), H0, PSTAR(1), S0)
            CALL EVAL_G(GE(2), RHO_T(2), H0, PSTAR(2), S0)
            IF(GE(2) .LT. TOLER) THEN
C If this is true, we've fallen into an area where both p_low and p_mid
C are undefined. Resize the bracketing interval and try again
                PSTAR(1)=PSTAR(1)/STRETCH_FACTOR
                STRETCH_FACTOR=SQRT(STRETCH_FACTOR)
                GE(1)=GE(2)+TOLER
            ENDIF
            GOTO 200
        ENDIF

201    IF((PSTAR(3)-PSTAR(1))/PSTAR(3) .GT. TOLER) THEN
C Check which interval of (p_low,p_mid), (p_mid,p_hi) is larger and bisection it
        IF(PSTAR(3)-PSTAR(2) .GT. PSTAR(2)-PSTAR(1)) THEN
C The p_mid to p_hi interval is larger; bisection this one
            P_HOLD=PSTAR(3)
            G_HOLD=GE(3)
            RHO_HOLD=RHO_T(3)
            PSTAR(3)=PSTAR(3)-1.0/GOLD*(PSTAR(3)-PSTAR(2))
            CALL EVAL_G(GE(3), RHO_T(3), H0, PSTAR(3), S0)
        ELSE
            P_HOLD=PSTAR(1)
            G_HOLD=GE(1)
            RHO_HOLD=RHO_T(1)
            PSTAR(1)=PSTAR(1)+1.0/GOLD*(PSTAR(2)-PSTAR(1))
            CALL EVAL_G(GE(1), RHO_T(1), H0, PSTAR(1), S0)
        ENDIF
        IF (GE(2) .LT. GE(1)) THEN
C G at p_mid is not as large as G at p_low. Shift bisection interval
C so that old p_mid is now p_hi
            PSTAR(3)=PSTAR(2)
            GE(3)=GE(2)
            RHO_T(3)=RHO_T(2)
            PSTAR(2)=PSTAR(1)

```

```

        GE(2)=GE(1)
        RHO_T(2)=RHO_T(1)
        PSTAR(1)=P_HOLD
        GE(1)=G_HOLD
        RHO_T(1)=RHO_HOLD
    ELSE IF (GE(2) .LT. GE(3)) THEN
C G at p_mid is not at large as G at p_hi. Shift bisection interval
C so that old p_mid is now p_low
        PSTAR(1)=PSTAR(2)
        GE(1)=GE(2)
        RHO_T(1)=RHO_T(2)
        PSTAR(2)=PSTAR(3)
        GE(2)=GE(3)
        RHO_T(2)=RHO_T(3)
        PSTAR(3)=P_HOLD
        GE(3)=G_HOLD
        RHO_T(3)=RHO_HOLD
    ELSE
C bisection interval is fine; continue
    ENDIF
    GOTO 201
ENDIF

C all done, interval size has decreased to specified tolerance.
    G_CALC=GE(2)
    RHO_HOLD=RHO_T(2)
    P_HOLD=PSTAR(2)
    ELSE IF (USE_MODEL .EQ. 1) THEN

C Using Henry - Fauske:
    GE(1)=0
    GE(2)=0
    GE(3)=0
    P_ROOT(1)=-1
    P_ROOT(2)=-1
    P_ROOT(3)=-1

C Bracketing the root and ensuring that the intermediate guess for the
C throat pressure PSTAR results in a larger P_ROOT than the other two
C guesses is a challenge, because the Henry-Fauske evaluation exhibits
C markedly different behavior in the subcooled region as compared to 2-
C phase initial conditions (observe discontinuities in the derivatives
C of the critical mass fluxes shown in Figs 12 through 14 of Henry &
C Fauske). Under subcooled initial conditions, some guesses for throat
C pressure may be invalid as they result in subcooled conditions at the
C throat (see subroutine HENRY_FAUSKE for more). Hence, bracket the root
C by starting with initial bounds of P_low ~ 0, P_high ~ P0. Evaluate
C RHS of 0 = P_ROOT at P_mid, P_low and P_high. If P_ROOT (P_low) is
C closer to zero than at P_mid, try again with P_hi now equal to P_mid.
C If P_ROOT (P_high) is closer to zero than at P_mid, pursue a similar
C strategy by setting P_low = P_hi. Repeat until the P_mid guess gives
C a root evaluation that is closer to zero than either P_low or P_hi.

        PSTAR(3)=P0 - TOLER

C Find the lowest saturation pressure at which steam tables can
C obtain the necessary thermo. properties. This will serve as a
C lower bound for throat pressure derived by the root-finding routine

        CALL PSAT(T_MIN, PMPA, RHOL, RHOV, IWORK, PROPR, IERR)
        PSTAR(1)=PMPA

196        PSTAR(2)=PSTAR(1)+1./GOLD*(PSTAR(3)-PSTAR(1))
        CALL HENRY_FAUSKE(H0, PSTAR(1), T0, S0, X0, P0,
&            VF0, VG0, P_ROOT(1), GE(1), RHO_T(1))
        CALL HENRY_FAUSKE(H0, PSTAR(2), T0, S0, X0, P0,
&            VF0, VG0, P_ROOT(2), GE(2), RHO_T(2))
        CALL HENRY_FAUSKE(H0, PSTAR(3), T0, S0, X0, P0,
&            VF0, VG0, P_ROOT(3), GE(3), RHO_T(3))
        IF (P_ROOT(2) .EQ. 0.0) THEN
            P_ROOT(2)=-1.
            P_ROOT(3)=-1.+TOLER
        ELSE IF (P_ROOT(3) .EQ. 0.0) THEN
            P_ROOT(3)=P_ROOT(2)-TOLER
        ENDIF
        IF (P_ROOT(2) .LT. P_ROOT(1)) THEN

```

```

        PSTAR(3)=PSTAR(2)
        GOTO 196
    ELSE IF(P_ROOT(2).LT. P_ROOT(3)) THEN
        PSTAR(1)=PSTAR(2)
        GOTO 196
    ENDIF
203    IF((PSTAR(3)-PSTAR(1))/PSTAR(3) .GT. TOLER) THEN
        IF(PSTAR(3)-PSTAR(2) .GT. PSTAR(2)-PSTAR(1)) THEN
C the p_mid to p_hi interval is larger; bisect this one
            P_HOLD=PSTAR(3)
            G_HOLD=GE(3)
            ROOT_HOLD=P_ROOT(3)
            RHO_HOLD=RHO_T(3)
            PSTAR(3)=PSTAR(3)-1.0/GOLD*(PSTAR(3)-PSTAR(2))
            CALL HENRY_FAUSKE(H0, PSTAR(3), T0, S0, X0, P0,
                & VF0, VG0, P_ROOT(3), GE(3), RHO_T(3))
            IF (P_ROOT(3) .EQ. 0.0) THEN
                P_ROOT(3)=P_ROOT(2)-TOLER
            ENDIF
        ELSE
            P_HOLD=PSTAR(1)
            G_HOLD=GE(1)
            ROOT_HOLD=P_ROOT(1)
            RHO_HOLD=RHO_T(1)
            PSTAR(1)=PSTAR(1)+1.0/GOLD*(PSTAR(2)-PSTAR(1))
            CALL HENRY_FAUSKE(H0, PSTAR(1), T0, S0, X0, P0,
                & VF0, VG0, P_ROOT(1), GE(1), RHO_T(1))
            IF (P_ROOT(1) .EQ. 0.0) THEN
                P_ROOT(1)=P_ROOT(2)-TOLER
            ENDIF
        ENDIF
        IF (P_ROOT(2) .LT. P_ROOT(1)) THEN
C RHS of 0 = f(PSTAR) as evaluated in HENRY_FAUSKE is farther from zero at
C p_mid than at p_low. Shift bisection interval so that old p_mid is now p_hi
            PSTAR(3)=PSTAR(2)
            GE(3)=GE(2)
            P_ROOT(3)=P_ROOT(2)
            RHO_T(3)=RHO_T(2)
            PSTAR(2)=PSTAR(1)
            P_ROOT(2)=P_ROOT(1)
            GE(2)=GE(1)
            RHO_T(2)=RHO_T(1)
            PSTAR(1)=P_HOLD
            GE(1)=G_HOLD
            P_ROOT(1)=ROOT_HOLD
            RHO_T(1)=RHO_HOLD
        ELSE IF(P_ROOT(2) .LT. P_ROOT(3)) THEN
C RHS of 0 = f(PSTAR) as evaluated in HENRY_FAUSKE is farther from zero at
C p_mid than at p_hi. Shift bisection interval so that old p_mid is now p_low
            PSTAR(1)=PSTAR(2)
            GE(1)=GE(2)
            P_ROOT(1)=P_ROOT(2)
            RHO_T(1)=RHO_T(2)
            PSTAR(2)=PSTAR(3)
            GE(2)=GE(3)
            P_ROOT(2)=P_ROOT(3)
            RHO_T(2)=RHO_T(3)
            PSTAR(3)=P_HOLD
            GE(3)=G_HOLD
            P_ROOT(3)=ROOT_HOLD
            RHO_T(3)=RHO_HOLD
        ELSE
C bisection interval is fine; continue
        ENDIF
        GOTO 203
    ENDIF
    G_CALC=GE(2)
    RHO_HOLD=RHO_T(2)
    P_HOLD=PSTAR(2)
ENDIF
IF(G_CALC .GT. 0) THEN
    TC_CALC = THRUST_COEFF(G_CALC, RHO_HOLD, P_AMB, P_HOLD, P0)
ELSE
    TC_CALC = 0.
ENDIF

```





```

C Orifice and short tube discharge coefficient as defined on p. 185
C of Henry and Fauske. This fudge factor modifies the critical pressure
C ratio and mass flow rate (see <EQ. 47>). It should be set to unity for
C subcooled flows; for two phase flow, if the flow regime may be considered
C compressible, it may be justified to take a lower value (0.84 is recommended
C in the paper). However, in the interest of conservatism it may be best
C to leave this set to 1.0 throughout.
      ORIFICE_C=1.0
C Define the throat to upstream pressure ratio as per <EQ. 34>
      ETA = PT/P0

C In H-F, liquid phase density at throat equal to upstream stagnation density
C See discussion preceding and following <EQ. 17>.
      VFT = VF0

C Vapor phase static density at throat (to be computed below if X0 > 0)
      VGT = 0

      DO 310 I=1,NPROP
          IWANT(I) = 0
310  CONTINUE
          IWANT(7) = 1
C Isochoric heat capacity, C_V
          IWANT(8) = 1

          CALL HSSOLV(2, PT, S0, TPOUT, D1, DV, DL,
&                I2PH, Q, IWORK, PROPR, IERR)

          TT = TPOUT
          IF ((I2PH .EQ. 2) .OR. (I2PH .EQ. 4)) THEN
              DENS = 1./MIX_PROP(Q, 1.0/DL, 1.0/DV)
          ELSE
              DENS = D1
          ENDIF
C Saturated liquid and vapor specific volumes at (PT,S0)
          VFE=1./DL
          VGE=1./DV

          CALL PROPS(IWANT,TT,1./VFE,PROPSI, PROPR, 1, I2PH, 0,
&                ISFLG,0, ICFLG, IPCHK, IPFLG, 0, 0, WAVRI, RI, IRIFLG)

C Obtain properties of saturated liquid at S0: heat capacity and entropy
          C_VF = PROPSI(8)
          SEF = PROPSI(7)

C Approximate pressure derivative of saturated liquid enthalpy by evaluating
C first the change in temperature and liquid density following from a
C change DP in PT with entropy held constant
          CALL HSSOLV(2, PT+DP, S0, TPOUT, D1, DV, DL,
&                I2PH, Q, IWORK, PROPR, IERR)
          PERTURBED_T = TPOUT
C evaluate saturated liquid enthalpy at this new temperature and density
          CALL PROPS(IWANT,PERTURBED_T,DL,PROPSI, PROPR, 1, I2PH, 0,
&                ISFLG,0, ICFLG, IPCHK, IPFLG, 0, 0, WAVRI, RI, IRIFLG)

C approximate the derivative by (S(PT+DP)- S(PT))/DP and convert from MPa to Pa
          DSDP = (PROPSI(7)-SEF)/DP*1.e-6

C Obtain entropy of saturated vapor at S0
          CALL PROPS(IWANT,TT,1./VGE,PROPSI, PROPR, 1, I2PH, 0,
&                ISFLG,0, ICFLG, IPCHK, IPFLG, 0, 0, WAVRI, RI, IRIFLG)

          SEG = PROPSI(7)

C Write the local equilibrium quality at the throat in terms of phase
C entropies at the throat. Represents quality that fluid would
C possess if phases were allowed to equilibrate <EQ. 23>
          XE = (S0 - SEF)/(SEG - SEF)

C Define the fudge factor correlating dX/dPT to dXE/dPT as per <EQ. 30>
          IF (XE .GT. 0.14) THEN
              N = 1.
          ELSE IF (XE .GT. 0) THEN
              N = XE/0.14
          ELSE

```

```

      N = 0.
ENDIF

      IF (X0 .GT. 0) THEN
C Isobaric heat capacity, C_p
      IWANT(9) = 1
      I2PH = 2
      FUDGE=0

124      CALL PROPS(IWANT,TT,1./VGE+FUDGE,PROPSI, PROPR, 1, I2PH, 0,
      & ISFLG,0, ICFLG, IPCHK, IPFLG, 0, 0, WAVRI, RI, IRIFLG)

C This loop is necessary because of apparent fluctuation
C in the least significant digit of the saturated vapor specific volume at P_E,
C VGE. If one calculates this volume using HSSOLV, then feeds it back into PROPS
C to obtain the isobaric heat capacity C_p of the vapor, an error *sometimes*
C results. C_p is not defined for a two-phase mixture; occasionally, the least
C significant digit of VGE varies such that PROPS believes the fluid being passed
C has quality very slightly less than 1.0. C_p, undefined in this regime, is
C returned as zero. Hence, if PROPS indicates that it believes the fluid is 2-phase,
C adjust the density very slightly to return to the vapor-only regime and try the
C calculation again:

      IF(I2PH .EQ. 2) THEN
          FUDGE=FUDGE-(1./VGE)*1.e-8
          GOTO 124
      ENDIF

C Isentropic exponent = C_p/C_V evaluated for saturated vapor at the throat
C (PROPS input arguments are T and sat vapor density at this state point)
      GAMMA = PROPSI(9)/PROPSI(8)
      C_PG=PROPSI(9)
      IWANT(8)=0
      IWANT(9)=0

C Finally, obtain liquid and vapor saturation enthalpies for upstream stagnation
C conditions. Arguments: stagnation temperature and saturated liquid and vapor
C densities
      CALL PROPS(IWANT,T0,1./VG0,PROPSI, PROPR, 1, I2PH, 0,
      & ISFLG,0, ICFLG, IPCHK, IPFLG, 0, 0, WAVRI, RI, IRIFLG)
      S0G = PROPSI(7)

      CALL PROPS(IWANT,T0,1./VF0,PROPSI, PROPR, 1, I2PH, 0,
      & ISFLG,0, ICFLG, IPCHK, IPFLG, 0, 0, WAVRI, RI, IRIFLG)
      S0F = PROPSI(7)

C Express the polytropic exponent at the throat. Recall that X_throat = X0 and
C the expansion is isentropic. <EQ. 19>
      POLYTROPIC = ((1.-X0)*C_VF/C_PG + 1)/((1.-X0)*C_VF/C_PG+
      & 1/GAMMA)

C The vapor specific volume at the throat obtained assuming polytropic behavior:
C See <EQS. 18, 19, 38>
      VGT = VG0*(ETA**(-1./GAMMA))

C Collecting terms into ALPHA_0 <EQ. 36>, ALPHA_T <EQ. 37> and BETA <EQ. 38>:
      ALPHA_0 = X0*VG0/((1.-X0)*VF0+X0*VG0)
      ALPHA_T = X0*VGT/((1.-X0)*VF0+X0*VGT)

      BETA = (1./POLYTROPIC+(1.-VF0/VGT)*((1.-X0)*N*PT*1.e6*DSDP/
      & (X0*(SEG-SEF)))-C_PG*(1./POLYTROPIC-1./GAMMA)/(S0G-S0F))

C Compute the RHS of <EQ. 33>
      GG = GAMMA/(GAMMA-1.)
      RHS = (((1.-ALPHA_0)*(1.-ETA)/ALPHA_0+GG)/
      & (1./(2.*BETA*ORIFICE_C*ORIFICE_C*
      & ALPHA_T*ALPHA_T)+GG))**(GG)

C To make this amenable to numerical solution via maximization, return the
C value -(RHS-ETA)^2, which will exhibit a maximum value of zero when the
C correct guess for the root, PT, is supplied.
      RHS = RHS-ETA
      ROOT=- (RHS*RHS)

C At last, evaluate the critical mass flux as a function of PT
      GCRIT=(X0*VGT/(POLYTROPIC*PT*1.e6)+(VGT-VF0)*((1.-X0)*N/(SEG-
      & SEF)*DSDP-(X0*C_PG*(1./POLYTROPIC-1./GAMMA)/(PT*1.e6*

```

```

&      (SOG-SOF))))**(-0.5)
      ELSE
C Subcooled upstream stagnation conditions
      IF (XE. GT. 0) THEN
C Pressure ratio guess was valid in that quality at the nozzle is nonzero
      GCRIT=((VGE-VF0)*N*DSDP/(SEG-SEF))**(-0.5)
      RHS = 1. - VF0*GCRIT*GCRIT/2/(P0*1.e6)/ORIFICE_C/ORIFICE_C
      RHS = RHS-ETA
      ROOT = -(RHS*RHS)
      ELSE
C Pressure ratio guess was not good, resulting in subcooled nozzle conditions.
C H-F does not function under these conditions -- see <EQ. 45> w/ N = 0.
C Return zero mass flux so that the root finder knows to discard this attempt.
      GCRIT = 0
      ENDIF
    ENDIF

C Return the fluid density at the throat to CRIT_MASS_FLUX for use in calculating
C the thrust coefficient. Specifying the mass flux and fluid density also
C specifies the velocity of the homogenized fluid.
    IF (GCRIT .GT. 0) THEN
      IF (X0. LE. 0) THEN
        RHO_T = 1./VFT
      ELSE IF (X0 .LE. 1) THEN
        RHO_T = 1./MIX_PROP(X0,VFT,VGT)
      ELSE
        RHO_T = 1./VGT
      ENDIF
    ELSE
      RHO_T = 0
    ENDIF
  END

  FUNCTION THRUST_COEFF(GE, RHO_T, P_AMB, PT, P0)

CCCCCCCCCCCCCCCCCCCCCCCCCCCCCCCCCCCCCCCCCCCCCCCCCCCCCCCCCCCCCCCCCCCC
C      THRUST_COEFF
C Calculates the thrust coefficient by
C
C      K = PT/P0*(1+G^2/RHO_T/PT),
C where
C P0 and PT are the stagnation and throat pressures [Pa_gauge]
C G is the mass flux [kg/m^2/s] as evaluated by H-F or the HEM,
C RHO_T is the fluid density [kg/m^3] at the throat
C
C      EAS 7/30/04 C
CCCCCCCCCCCCCCCCCCCCCCCCCCCCCCCCCCCCCCCCCCCCCCCCCCCCCCCCCCCCCCCCCCCC

    REAL*8 GE, RHO_T, P_AMB, PT, P0, THRUST_COEFF

    THRUST_COEFF=(PT-P_AMB)/(P0-P_AMB)*(1.0+GE*GE/
&  RHO_T/((PT-P_AMB)*1.e6))

    RETURN
  END

```

```

function [p,t,x,ts,hf,hg,d,h0,pa,da,ge,tc,tj,ta,hfa,hga] = ...
    GetProperties(pres, temp, qual, pdmg, pamb, use_model)

% Given N (pres, temp, qual) state points and M damage
% pressures, GetProperties invokes the NIST steam tables
% to obtain
% p[N] state point pressures    [psi]
% t[N] temperatures            [deg F]
% x[N] qualities                [-]
% ts[N] saturation temperatures [deg F]
% hf[N] liquid phase enthalpies at ts [Btu/lbm]
% hg[N] vapor phase enthalpies at ts [Btu/lbm]
% d[N] densities                [lbm/ft^3]
% h0[N] enthalpies              [Btu/lbm]
% pa[N] pressures at asymptotic plane [psi]
% da[N] densities at asymptotic plane [lbm/ft^3]
% ge[N] critical mass fluxes    [lbm/ft^2/s]
% tc[N] thrust coefficients     [-]
% tj[N][M] temperatures at pdmg[M] [deg F]
% ta saturation temp at ambient pres. [deg F]
% hfa liquid phase enthalpy at ta [Btu/lbm]
% hga vapor phase enthalpy at ta [Btu/lbm]
%
% EAS 7/12/04
%
% 7/28/04:
% To obtain the ge and tc, GetProperties uses the HEM or H-F according to
% the rule specified by the integer flag use_model. See ansijet.m and
% QUERYST.FOR for documentation regarding use_model.

n_outputs=12;

% define conversion factors for use in UnitConverter
pres_conv = [0 0 0 0 1 0];
temp_conv = [1 0 0 0 0 0];
enth_conv = [0 -1 0 1 0 0];
dens_conv = [0 1 -3 0 0 0];
mfix_conv = [0 1 -2 0 0 0];

% convert from english to SI units
pres=UnitConverter(pres,pres_conv);
temp=UnitConverter(temp,temp_conv);
pdmg=UnitConverter(pdmg,pres_conv);
pamb=UnitConverter(pamb,pres_conv);

% concatenate inputs. This is not strictly necessary
% since the mex routine can handle multiple input variables,
% but the functionality would be identical regardless
% the last two inputs should be the number of state points
% and the number of contours per state point

npts=size(pres);
npts=npts(:,2);

nconts=size(pdmg);
nconts=nconts(:,2);

mex_input=[pres temp qual pdmg pamb npts nconts use_model];

% call QUERYST.FOR via QUERYST.DLL
mex_output=queryst(mex_input);

% reconstruct outputs
for i=1 : npts
    p(i)=mex_output(i);
    t(i)=mex_output(i+npts);
    x(i)=mex_output(i+npts*2);
    ts(i)=mex_output(i+npts*3);
    hf(i)=mex_output(i+npts*4);

```

```

hg(i)=mex_output(i+npts*5);
d(i)=mex_output(i+npts*6);
h0(i)=mex_output(i+npts*7);
pa(i)=mex_output(i+npts*8);
da(i)=mex_output(i+npts*9);
ge(i)=mex_output(i+npts*10);
tc(i)=mex_output(i+npts*11);
for j=1 : nconts
    tj(i,j)=mex_output(npts*n_outputs+(i-1)*nconts+j);
end
end
ta=mex_output(npts*n_outputs+npts*nconts+1);
hfa=mex_output(npts*n_outputs+npts*nconts+2);
hga=mex_output(npts*n_outputs+npts*nconts+3);

% if no pressure / temperature contours were requested, create an empty
% dummy tj to avoid undefined variable contours later on
if(nconts==0)
    tj=[];
end

% convert back from SI to english units
p=UnitConverter(p,-pres_conv);
t=UnitConverter(t,-temp_conv);
ts=UnitConverter(ts,-temp_conv);
hf=UnitConverter(hf,-enth_conv);
hg=UnitConverter(hg,-enth_conv);
h0=UnitConverter(h0,-enth_conv);
pa=UnitConverter(pa,-pres_conv);
d=UnitConverter(d,-dens_conv);
da=UnitConverter(da,-dens_conv);
ge=UnitConverter(ge,-mflx_conv);
ta=UnitConverter(ta,-temp_conv);
tj=UnitConverter(tj,-temp_conv);
hga=UnitConverter(hga,-enth_conv);
hfa=UnitConverter(hfa,-enth_conv);
return

```

```

function conv_x = UnitConverter(x_o, dimension_array)

conv_factors = zeros(size(dimension_array));

% converts a quantity from the english unit system to SI
% or vice versa, returning the converted value as conv_x.
% x_o quantity (in english or SI units) to be converted
% default operation is english -> SI
% dimension_array of integers describing the english system
% unit to be converted to SI, viz:

% (1) temperature conversion F -> K
conv_factors(1)=5./9.;
% (1) can only take on the values 1 (F->K) and -1 (K->F).
% If (1) is nonzero, all other members of dimension_array
% will be ignored!
% (2) lbm -> kg
conv_factors(2)=0.45359237;
% (3) ft -> m
conv_factors(3)=0.3048;
% (4) Btu -> kJ
conv_factors(4)=1.05505585;
% (5) psi -> MPa
conv_factors(5)=0.00689475729;
% (6) deg F -> deg K
conv_factors(6)=5./9.;
%
% The value passed is the exponent of the unit to be converted.
% Example usage: to convert density [lbm/ft^3] to SI units,
% one would pass dimension_array = [0 1 -3 0 0 0].
% To convert [kg/m^3] back to [lbm/ft^3], one would simply
% obtain the inverse of the conversion factor applied previously
% by passing [0 -1 3 0 0 0].

result = x_o;
if dimension_array(1) == 1
    result = (result + 459.4) * conv_factors(1);
elseif dimension_array(1) == -1
    result = result / conv_factors(1) - 459.4;
else
    for i = 2:length(conv_factors)
        if dimension_array(i) ~= 0
            result = result * conv_factors(i)^dimension_array(i);
        end
    end
end
conv_x = result;

```

## APPENDIX II: CONFIRMATORY DEBRIS GENERATION ANALYSES

The Nuclear Energy Institute (NEI) guidance contains recommendations that will determine the quantities of insulation debris generated with the zone of influence (ZOI). These recommendations include the size of the ZOI based on the insulation destruction pressure and the fraction of the insulation located within the ZOI that subsequently is damaged into the small-fine-debris category. Confirmatory research was performed to ascertain whether the NEI recommendation would reliably result in conservative estimates for the volumes of debris generated within the ZOI. This appendix documents the confirmatory research estimates for the volumes of small fine debris. The confirmatory research for determining the size of the ZOI is the subject of Appendix I. Both the NEI guidance and the confirmatory research used the ANSI/ANS-58.2-1988 standard to calculate the jet isobar volumes with very similar results. The confirmatory research issues addressed herein include the following.

- The NEI guidance recommends the assumption that 60% of the fibrous and 75% of the reflective metal insulation (RMI) volume contained within the ZOI becomes small fine debris. Confirmatory research was performed that integrated the insulation damage versus jet pressures over the ZOI volume to determine the fraction of the insulation within the ZOI that would become small fine debris based on available debris generation data.
- The NEI guidance recommends adapting the debris-size distribution for NUKON™ to other types of fibrous insulation that have a destruction pressure higher than that of NUKON™. The size distribution confirmatory research provides partial justification that supports that NEI recommendation.
- The applicability of air-jet-determined destruction pressures to two-phase pressurized-water-reactor (PWR) loss-of-coolant-accident (LOCA) jets has been questioned. NUREG/CR-6762 (Vol. 3) noted that data from the Ontario Power Generation (OPG) two-phase debris generation tests indicated that the destruction pressure could be lower for a two-phase jet than for an air jet and that the resultant debris could be finer. Therefore, it may be prudent to apply a safety factor to accommodate the uncertainty. This confirmatory analysis estimates the volume fractions for small fine debris if an alternate lower destruction pressure were used than those in the NEI guidance.

### II.1 COMPARISON OF JET ISOBAR VOLUME CALCULATIONS

Three calculations of the jet isobar volumes were available for comparison.\* The calculations were the following.

- The volumes determined from the NEI guidance recommended values for ZOI radii versus the destruction pressures in NEI baseline guidance's Table 3-1. The destruction pressure represents the jet isobar pressure for each particular ZOI radii.
- The volumes determined from the confirmatory research (Appendix I) for the ZOI radii versus the jet pressure.

---

\* The volumes are actually presented in terms of the break diameter cubed ( $D^3$ ) corresponding to an equivalent spherical radius in terms of  $r/D$  (i.e.,  $4/3 \pi r^3/D^3$ ).

- The volumes determined from the boiling-water-reactor owners' group (BWROG) recommendation documented in their utility resolution guidance (URG). Although these volumes apply to a BWR steam jet rather than a PWR two-phase jet, the volumes are compared here to demonstrate the differences between PWR and BWR LOCA jets.

Both the NEI guidance and the confirmatory research volume calculations used the ANSI/ANS-58.2-1988 standard method, whereas the BWROG URG method used the computational-fluid-dynamics (CFD) code, NPARC, to evaluate the volumes. The equivalent spherical radii for these three methods are compared in Figure II-1.

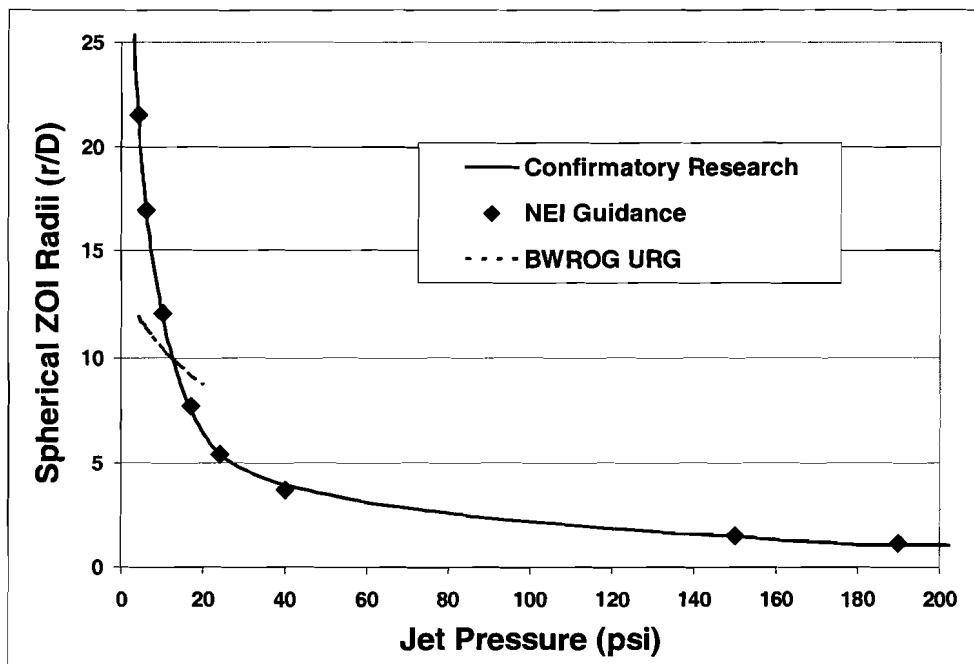


Figure VI-1. Comparison of Jet Isobar Volumes.

As shown, at the lower jet pressures, the pressure isobar volumes are much larger for the PWR two-phase LOCA jet than for the BWR steam jet. A principal reason for this difference is the higher energy associated with the higher pressure of a PWR reactor coolant system (RCS) than with a BWR RCS; however, another consideration is the accuracy of the ANSI/ANS-58.2-1988 standard at the lower pressures. For example, the validity of the assumption in the ANSI/ANS-58.2-1988 standard that the jet expands at a half angle of 10 degrees once the jet expansion has reached the asymptotic plane becomes more important at the lower expansion pressures. The accuracy of the debris volumes of insulations that damage significantly at the lower jet pressures is subject to the accuracy of this assumption. Note that the confirmatory research and NEI-recommended-equivalent spherical ZOI radii are in good agreement.

## II.2 METHOD OF DETERMINING ZOI DEBRIS-SIZE DISTRIBUTIONS

The volume of debris generated within a ZOI depends on the following three factors: (1) the size of the ZOI defined by the spherical radius, (2) the concentration of a particular insulation within the ZOI, and (3) the fraction of the ZOI insulation that is damaged into a particular debris-size

classification. The size distribution and spherical ZOI radius are interdependent. The threshold damage pressure and the jet volumes determine the size of the ZOI (Appendix I). The insulation concentration within a ZOI is determined by plant-specific information (i.e., the volume of a particular insulation within the ZOI divided by the volume of the ZOI).

Integration of experimental debris generation data is required to determine the fraction of the ZOI insulation that is damaged into a particular debris-size classification (e.g., NEI small fine debris). A generalized equation was offered in NUREG/CR-6808 for this integration. A slightly expanded version of this equation is

$$F_{ZOI} = \frac{3}{r_{ZOI}^3} \int_0^{r_{ZOI}} f_d(P_{jet}(r)) r^2 dr \quad ,$$

where

$F_{ZOI}$  = the fraction of the ZOI insulation type  $i$  that is damaged into a particular debris-size classification;

$f_d$  = the fraction of debris damaged into a particular debris size as a function of the jet pressure  $P_{jet}$ , which is a function of the spherical radius,  $r$ , within the ZOI; and

$r_{ZOI}$  = the outer radius of the ZOI.

Implicit in this integration is the assumption that the insulation is uniformly distributed within the ZOI, which may not be realistic. Because the functional information needed for this integration is not available in an equation form simple enough for a formal integration to proceed, the following simplification is used:

$$F_{ZOI} = \frac{1}{r_{ZOI}^3} \sum_j \left[ \frac{f_{fines}(P_{jet}(r_j)) + f_{fines}(P_{jet}(r_{j-1}))}{2} (r_j^3 - r_{j-1}^3) \right] \quad ,$$

where

$f_{fines}$  = the fraction of debris damaged into a particular debris size as a function of the jet pressure  $P_{jet}$  at a radius of  $r_j$ .

The spherical ZOI is first subdivided into numerous spherical shells ( $j$ ). The precision of the integration increases with the number of subdivisions. In a spreadsheet, the jet pressure is listed in increasing values and then the spherical radii are determined, followed by the damage fraction evaluated at each  $r_j$ . For the intervals, the average damage across the interval and the volume of the interval is determined. Multiplying the average interval damage by the interval volume, summing, and dividing by the total ZOI volume results in the debris fraction for the ZOI.

### II.3 EVALUATION OF DEBRIS SPECIFIC DAMAGE FRACTIONS AND POTENTIAL DEBRIS VOLUME

Potential debris volumes were calculated for fibrous, RMI, and particulate debris types and compared with the NEI baseline model to determine whether the baseline is conservative. The

potential volume of debris is defined as the fraction of the ZOI debris damaged into a particular debris size multiplied by the total volume of the sphere, as

$$V_{Potential} = F_{ZOI} \left( \frac{4}{3} \pi \right) r_{ZOI}^3 .$$

Note that to calculate the volume of small fine debris generated, the potential volume must be multiplied by the concentration of insulation ( $C_{insulation}$ ), i.e., the fraction of the ZOI actually occupied by the insulation, and by the pipe break diameter cubed. Again, it is assumed that the insulation type in question is uniformly distributed over the ZOI, regardless of the size of the ZOI, as

$$V_{Fines} = C_{Insulation} V_{Potential} D^3 .$$

### II.3.1 Fibrous Debris

The fibrous insulation types evaluated include NUKON™, Transco (Transco Products, Inc., or TPI), Temp-Mat, K-wool, and Knauf. Table II-1 shows the NEI-guidance-recommended destruction pressures and an alternate set of values used herein to test the sensitivity of the potential debris volumes to the destruction pressures.

**Table VI-1. Fibrous Insulation Destruction Pressures**

Insulation	NEI Recommendation	Alternate Lower Pressure
NUKON™	10 psi	6 psi
TPI	10 psi	6 psi
Knauf	10 psi	6 psi
Temp-Mat	17 psi	10 psi
K-wool	40 psi	17 psi

#### II.3.1.1 Low-Density Fiberglass (LDFG) Debris

A review of the air jet testing debris generation data, both the BWROG Air Jet Impact Testing (AJIT) data (BWROG URG) and the drywell debris transport study (DDTS) data [NUREG/CR-6369, 1999], demonstrates that NUKON™, TPI, and Knauf fiberglass insulations underwent similar damage. These insulations have approximately the same as-manufactured density (~2.4 lb/ft<sup>3</sup>), and their recommended minimum pressures for destruction are usually taken to be the same pressure. Therefore, these insulations have been grouped together as LDFG insulation.

The fractions for the small fines from the AJIT debris generation test data are plotted in Figure II-2 as a function of the jet centerline pressure for these three types of LDFG insulations. A curve was drawn through the data to continuously represent the damage for use in the damage integration over the ZOI. One set of seven data points was from tests (in the DDTS) that used a

\* NEI guidance considers TPI fiber blankets to behave similarly to NUKON™ blankets.

4-in. nozzle, whereas the remainder used a 3-in. nozzle. The 4-in. nozzle data from the DDTs generally shows more damage than do the 3-in. nozzle tests. The basic reason for the higher damage was that with the larger-diameter jet, more of the target insulation blanket was exposed to higher pressures. Note that the data were correlated by the estimated jet centerline pressure but that the pressure on the blanket decreased outward from the centerline. When the blanket was placed in close to the jet, the ends of the blanket were hit with substantially less force of flow than the centerline for which the data were correlated. For example, for the 3-in. nozzle data point for NUKON™ at a jet pressure of 20 psi, only ~7% of the insulation was damaged into small fine debris, whereas the TPI blankets in the 4-in. nozzle were totally destroyed at this pressure. Apparently, testing blanket destruction for insulations requiring a pressure higher than ~17 psi needs a jet nozzle larger than 3 in. For LDFG, any jet pressure larger than ~17 psi will totally destroy the blanket into small fine debris, whereas the NEI guidance cited an OPG two-phase jet test with 52% of the insulation damaged into small fine debris as their basis of conservatism.

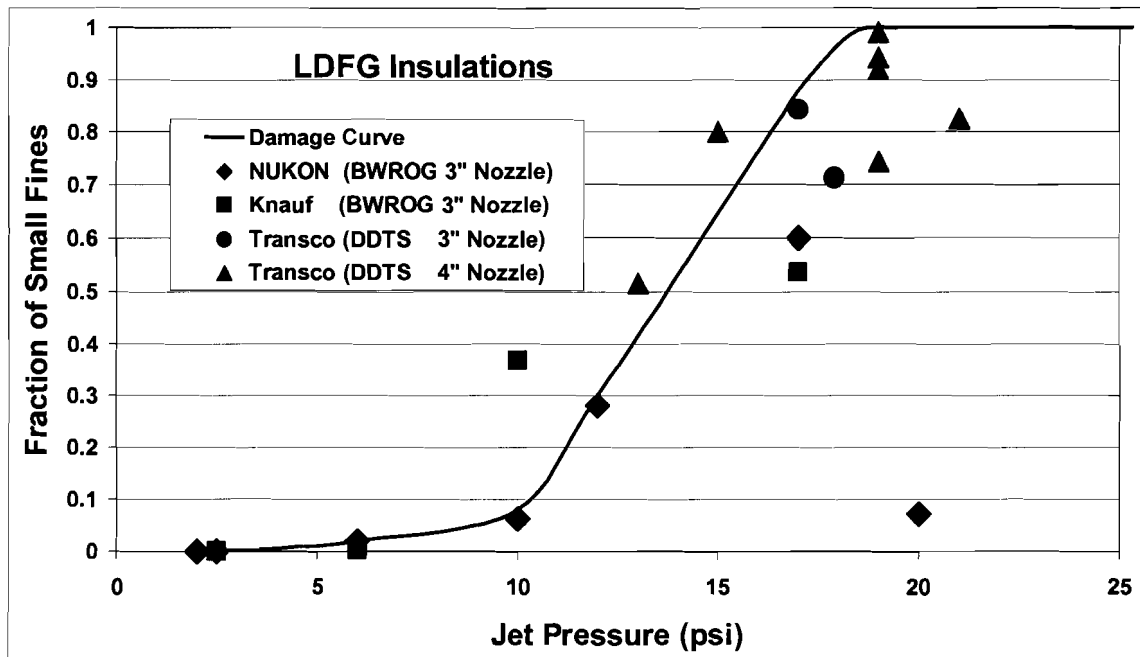


Figure VI-2. LDFG Damage Curve for Small Fine Debris.

Another significant point of discussion is that the threshold of damage for LDFG insulation has been specified as 10 psi, where Figure II-2 clearly shows damage at jet pressures <10 psi. Apparently, neglecting the tail of the damage curve was considered acceptable for the BWR strainer resolution because of the lesser BWR jet volumes at lower pressures, as shown in Figure II-1. However, the much larger jet volumes below 10 psi for the PWR jet shown in Figure II-1 make the neglect of the tail less acceptable.

The results of debris-size distribution integration over the ZOI are provided in Table II-2. A lower alternate damage pressure results in a larger equivalent spherical ZOI; however, a lesser fraction of the debris is damaged into small fine debris. The use of the alternate damage pressures over the NEI-recommended damage pressures for PWR analyses would result in

~16% more small fine debris. The potential debris volumes are compared in Figure II-3, along with an estimate using the baseline guidance. The baseline estimate is simply 60% of  $\frac{4}{3} \pi (12.1/D)^3$ . As shown, the baseline guidance appears to be conservative, but not overly so.

**Table VI-2. Results of Debris-Size Distribution Integration for LDFG Insulations**

Jet Pressure Isobar Volume Calculation	Radius of Sphere (r/D)	Fraction Small Fines	Potential Debris Volumes (V/D <sup>3</sup> )
<b>NEI-Recommended Damage Pressures</b>			
BWROG Steam Jet	10.4	0.83	3910
PWR Two-Phase Jet (Confirmatory)	11.9	0.53	3790
<b>Alternate Damage Pressures</b>			
BWROG Steam Jet	11.4	0.65	3980
PWR Two-Phase Jet (Confirmatory)	17.0	0.22	4410

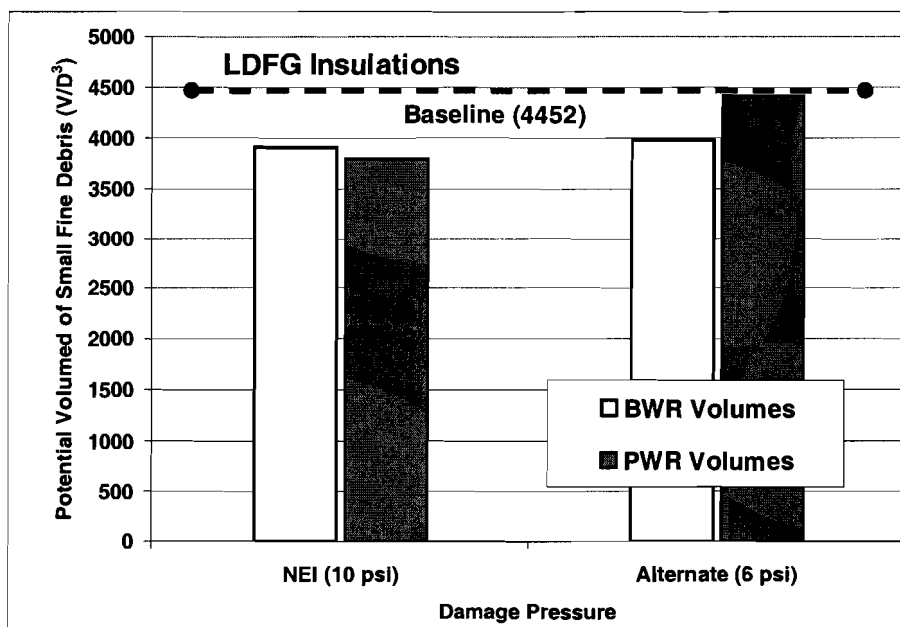


**Figure VI-3. Potential Volumes of Small Fines LDFG Debris.** fix y axis label (volumes)

The NEI baseline guidance completely neglects the transport of large debris to the sump screen; however, some plants will likely need to consider large debris transport as part of a more realistic evaluation. Therefore, the following equation is provided to estimate the volume of large debris generated within the ZOI:

$$V_{Large} = C_{Insulation} (1 - F_{ZOI}) \left( \frac{4}{3} \pi \right) r_{ZOI}^3 D^3 .$$

Also, plants that must perform more realistic evaluations may need to subdivide the baseline small-fine-debris class into fines and small-piece debris, where the fines (e.g., individual fibers) remain suspended in the pool and the small-piece debris sinks to the pool floor where the debris may or may not transport to the sump screen. The baseline guidance has the inherent assumption that all of its small fine debris essentially remains suspended.

During the debris generation tests conducted during the DDTs, 15% to 25% of the debris from a completely disintegrated TPI fiberglass blanket was classified as nonrecoverable. The nonrecoverable debris either exited the test chamber through a fine-mesh catch screen or deposited onto surfaces in such a fine form that it could not be collected by hand (it was collected by hosing off the surfaces). Therefore, it would be reasonable to assume that 25% of the baseline small fine debris (i.e.,  $F_{ZOI}$ ) is in the form of individual fibers and that the other 75% is in the form of small-piece debris.

### II.3.1.2 Temp-Mat Debris

Temp-Mat is much higher-density insulation (~11.8 lb/ft<sup>3</sup>) than the LDFG insulation and requires a significantly higher-pressure jet pressure to damage the insulation. The Temp-Mat insulation debris fractions for the small fine debris from the AJIT tests are shown in Figure II-4. This figure shows six data points for Temp-Mat, two of which were tests where no significant damage was noted. The test with the maximum damage had ~36% of the insulation damaged into small fine debris, with the remainder of the insulation forming large-piece debris. Unfortunately, no tests were conducted with jet pressures high enough to complete the damage curve to total destruction into small fine debris, as was done for the LDFG insulations. Therefore, a conservative extrapolation of the data is required to perform the debris generation integration over the equivalent ZOI sphere. The extrapolation used herein is shown as a dashed line in Figure II-4. The selection of the NEI-guidance damage pressure of 17 psi is also illustrated in Figure II-4, where it is seen that significant small fine debris is generated at jet pressures below 17 psi.

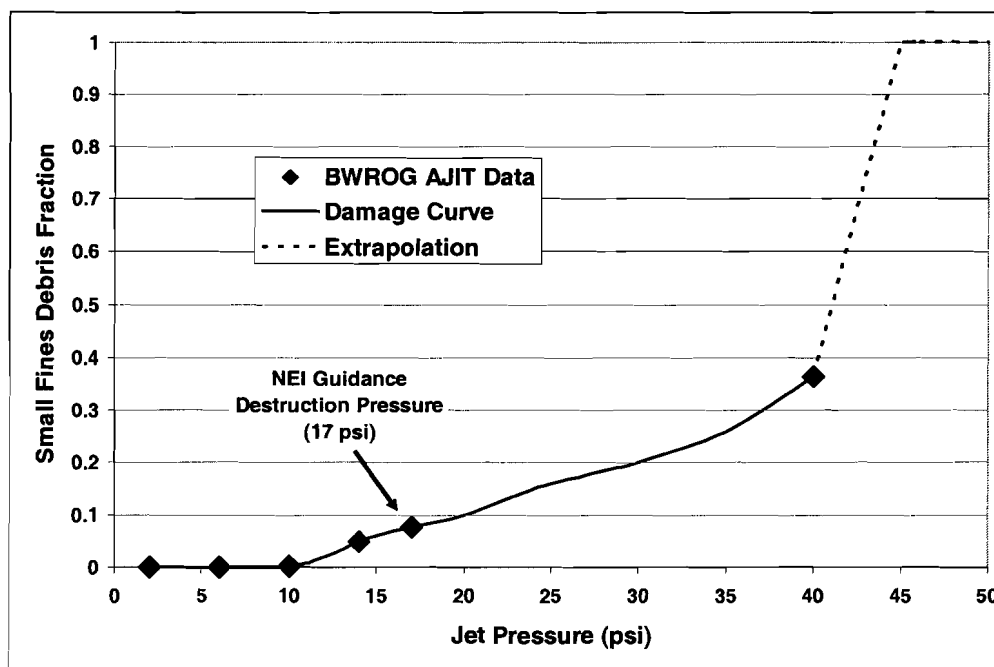


Figure VI-4. Temp-Mat Damage Curve for Small Fine Debris. fix x axis to “fine”

The results of the Temp-Mat debris-size distribution integration over the ZOI are provided in Table II-3. The potential debris volumes are compared in Figure II-5, along with an estimate using the baseline guidance [60% of  $4/3 \pi (7.8/D)^3$ ]. A lower alternate damage pressure results in a larger equivalent spherical ZOI; however, a lesser fraction of the debris is damaged into small fine debris. The use of the alternate damage pressures over the NEI-recommended damage pressures for PWR analyses would result in ~36% more estimated small fine debris. For Temp-Mat insulation, the baseline is conservative with respect to both the NEI-guidance damage pressure of 17 psi and the alternate pressure of 10 psi.

The debris-size estimate for Temp-Mat has more uncertainty associated with the estimate than does the similar calculation for LDFG, primarily because of more limited data. The negative uncertainties include the neglect of the damage curve tail by the NEI-recommended damage pressure (quantified using the alternate damage pressure) and the fact that the BWROG AJIT tests used the small 3-in. nozzle, which makes it difficult to subject the entire target blanket to the characteristic jet pressure (near the centerline pressure) when the blanket is located close to the nozzle. The positive uncertainty is the sharp extrapolation of the damage curve to 100% destruction at 45 psi. In this case, it is possible that the positive uncertainty overshadows the negative uncertainties.

**Table VI-3. Results of Debris-Size Distribution Integration for Temp-Mat Insulation**

<b>Jet Pressure Isobar Volume Calculation</b>	<b>Radius of Sphere(r/D)</b>	<b>Fraction Small Fines</b>	<b>Potential Debris Volumes (V/D<sup>3</sup>)</b>
<b><i>NEI Recommended Damage Pressures</i></b>			
PWR Two-Phase Jet (Confirmatory)	7.5	0.25	448
<b><i>Alternate Damage Pressures</i></b>			
PWR Two-Phase Jet (Confirmatory)	11.9	0.086	608

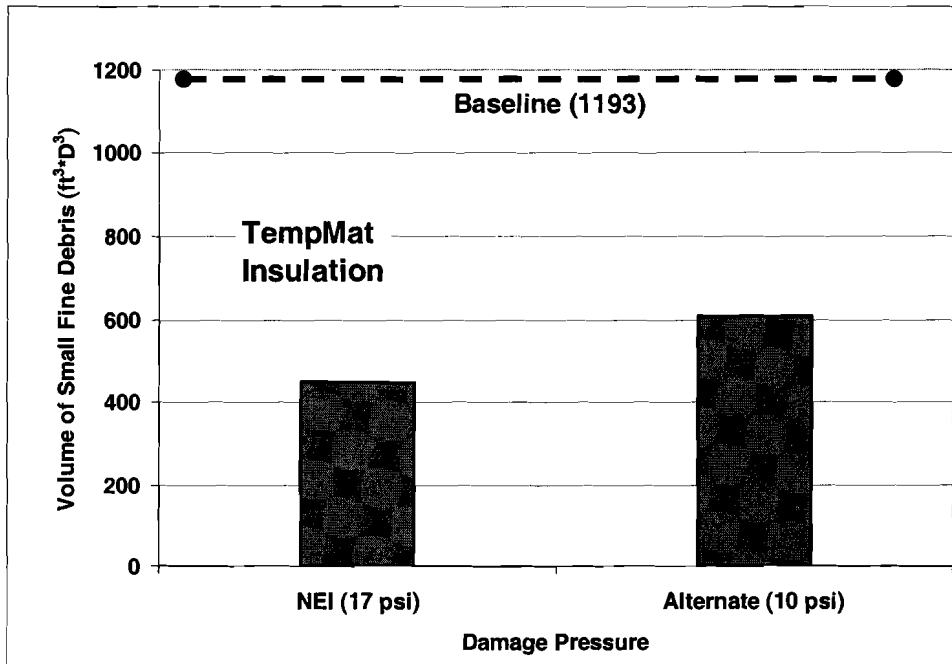


**Figure VI-5. Potential Volumes of Small Fine Temp-Mat Debris.**

### II.3.1.3K-wool Debris

K-wool is also higher-density insulation (~10 lb/ft<sup>3</sup>) than the LDFG insulation and requires an even higher-pressure jet pressure to damage the insulation. The NEI-recommended damage pressure for K-wool is 40 psi. The K-wool insulation debris fractions for the small fine debris from the AJIT tests are shown in Figure II-6. This figure shows only four data points for K-wool, two of which were tests where no significant damage was noted. The test with the maximum damage had ~7.1% of the insulation damaged into small fine debris, with much of the remainder of the insulation still contained in the blanket cover and still attached to the target mount. As with the Temp-Mat data, the K-wool damage curve is incomplete because the highest jet pressure tested was that of the NEI-recommended damage pressure. To perform the debris generation integration over the equivalent ZOI sphere, the test data were conservatively extrapolated, as shown in Figure II-6.

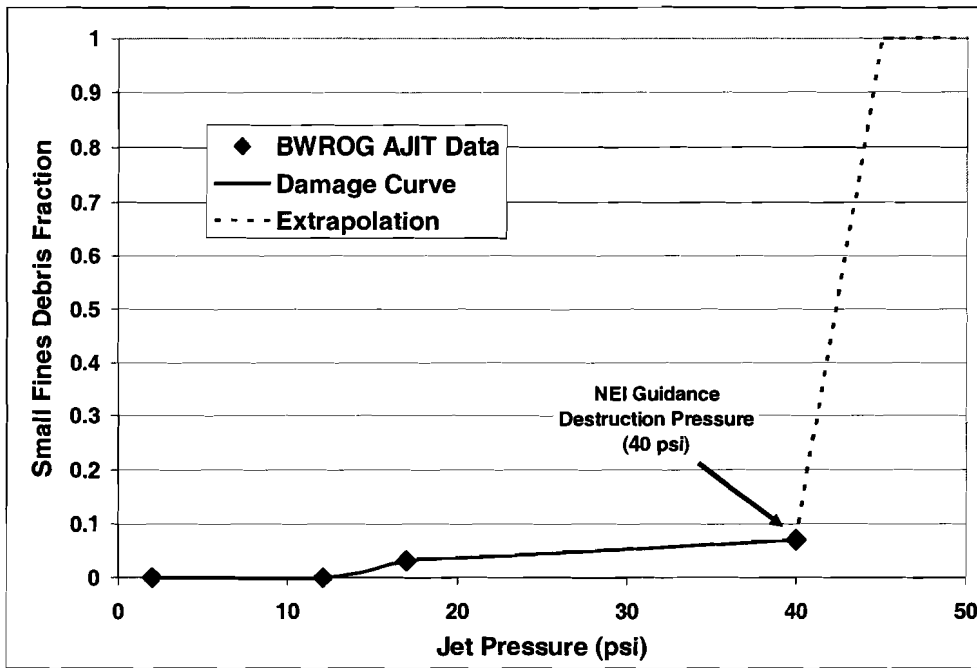


Figure VI-6. K-wool Damage Curve for Small Fine Debris. fix x axis label to “fine”

The results of the K-wool debris-size distribution integration over the ZOI are provided in Table II-4. The potential debris volumes are compared in Figure II-7, along with an estimate using the baseline guidance [60% of  $\frac{4}{3} \pi (3.8/D)^3$ ]. The difficulty with the K-wool integration is that there is no debris generation data for a jet pressure higher than the NEI-recommended destruction pressure of 40 psi. Therefore, to ensure conservative debris-size integration, it must necessarily be assumed that the insulation is completely destroyed at a pressure higher than 40 psi (the integration herein assumed 100% at 45 psi). However, this assumption may be overly conservative. For K-wool insulation, the baseline is not conservative with respect to either the NEI-guidance damage pressure of 40 psi or the alternate pressure of 17 psi.

Table VI-4. Results of Debris-Size Distribution Integration for K-wool Insulation

Jet Pressure Isobar Volume Calculation	Radius of Sphere(r/D)	Fraction Small Fines	Potential Debris Volumes (V/D <sup>3</sup> )
<b>NEI-Recommended Damage Pressures</b>			
PWR Two-Phase Jet (Confirmatory)	4.0	0.92	246
<b>Alternate Damage Pressures</b>			
PWR Two-Phase Jet (Confirmatory)	7.5	0.17	307

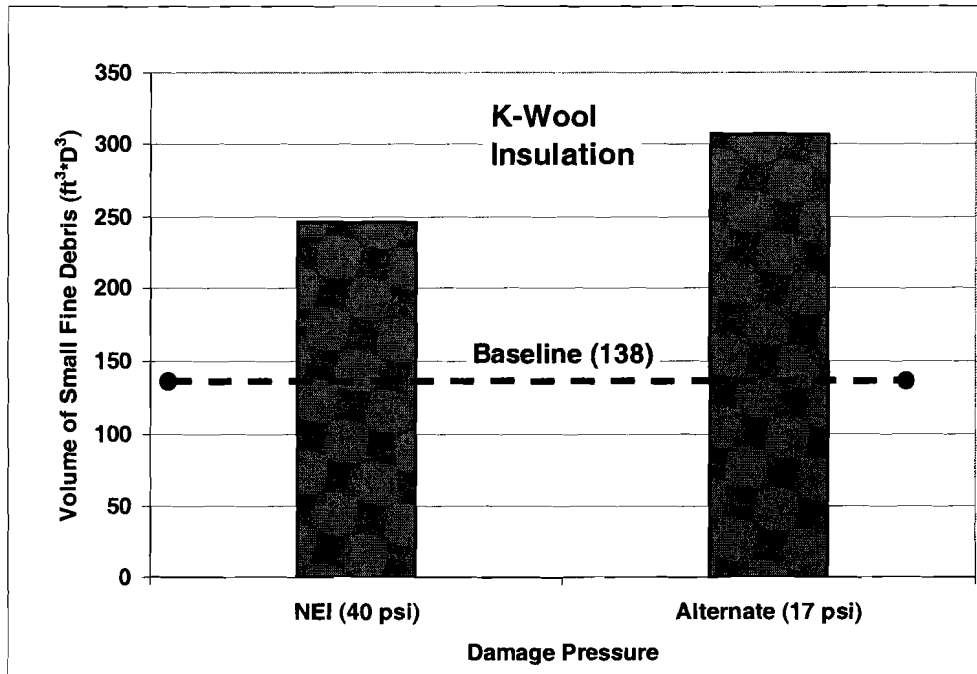


Figure VI-7. Potential Volumes of Small Fine K-wool Debris.

II.3.1.4 Correlation between Debris Size and Destruction Pressure

The NEI guidance contains the assumption that it is conservative to adapt the debris-size distribution for NUKON™ to other types of insulations that have a higher destruction pressure than NUKON™ (e.g., Temp-Mat and K-wool). This assumption is examined by comparing the debris generation data for LDFG, Temp-Mat, and K-wool, as shown in Figure II-8.

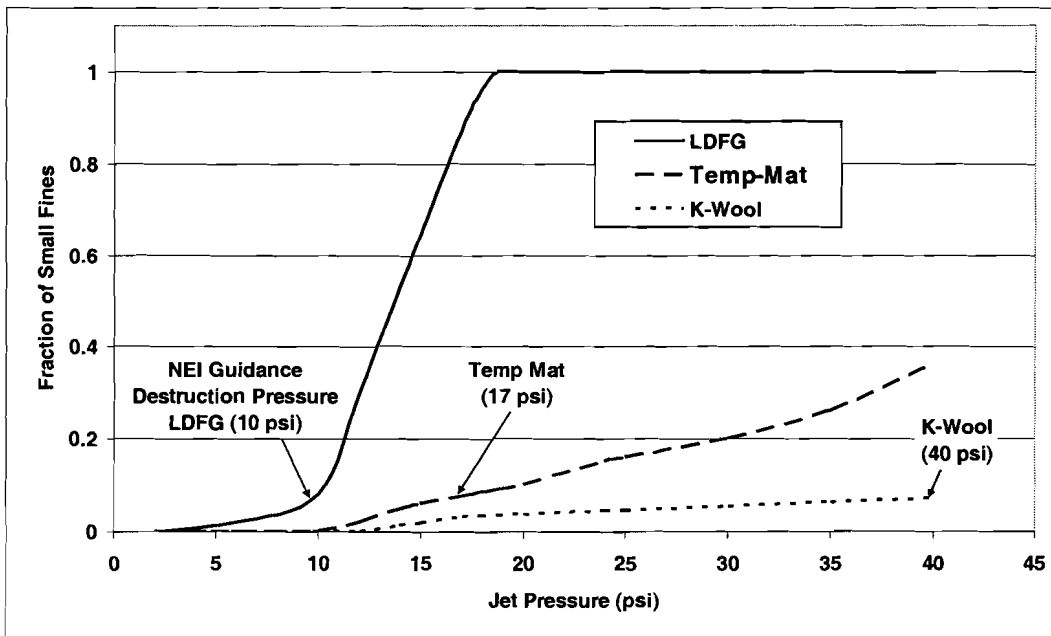


Figure VI-8. Comparison of Fibrous Insulation Damage Curves.

This damage curve comparison for LDFG, Temp-Mat, and K-wool does seem to support the concept that a higher destruction pressure results in the fractions of small fines being increasingly smaller as the destruction pressure increases. Certainly this is the case for Temp-Mat, where the baseline guidance is conservative relative to the integration herein where both the fractions of small fine debris and the potential debris volumes are smaller than the baseline guidance. Although this case is likely true for K-wool as well, it cannot be conclusively proven because of the complete lack of data beyond the NEI-recommended destruction pressure.

### II.3.2 RMI Debris

The NEI guidance contains recommendations for three types of RMI insulation:

1. DARMET<sup>®</sup> manufactured by Darchem Engineering, Ltd.;
2. RMI manufactured by TPI; and
3. Mirror<sup>®</sup> marketed by Diamond Power Specialty Company (DPSC).

The NEI recommends that 75% of the RMI insulation contained in the equivalent spherical ZOI should be assumed to be turned into small fine debris. Table II-5 shows the NEI-recommended destruction pressures and the corresponding NEI-recommended radii for those pressures. Note that the ZOI for DARMET<sup>®</sup> and TPI are quite small compared with the ZOI for DPSC Mirror<sup>®</sup>.

**Table VI-5. NEI-Recommended RMI Insulation Destruction Pressures and ZOI Radii**

RMI Insulation	Destruction Pressures (psi)	ZOI Radius (r/D)
DARMET <sup>®</sup>	190 psi	1.3
TPI	190 psi	1.3
DPSC Mirror <sup>®</sup>	4 psi	21.6

Nearly all the debris generation data used to justify the NEI recommendations came from the BWROG Air Jet Impact Testing (AJIT) data [BWROG URG]; therefore, the NEI recommendations must be anchored to the insulation types as tested. Besides the BWROG AJIT tests, a single Nuclear Regulatory Commission (NRC)-sponsored test<sup>‡</sup> was conducted using a stainless-steel DPSC Mirror<sup>®</sup> RMI cassette at the Siemens AG Power Generation Group (KWU) test facility in Karlstein am Main, Germany (1994 and 1995 **can't find these as references in this section**) [SEA-95-970-01-A:2, 1996]. The cassettes and their closures, as tested in the AJIT tests with the cassettes mounted perpendicular to the jet centerline,<sup>†</sup> are provided in Table II-6. All of the cassettes tested had stainless-steel sheaths.

<sup>‡</sup>The NRC-sponsored test involved a stainless-steel Mirror<sup>®</sup> cassette mounted directly on a device designed to simulate a double-ended guillotine break (DEGB) such that the discharge impinged on the inner surface of the RMI target as it would an insulation cassette surrounding a postulated pipe break. This NRC-sponsored test was performed with a high-pressure blast of two-phase water/steam flow from a pressurized vessel connected to a target mount by a blowdown line with a double-rupture disk. In this test, the cassette was completely destroyed into debris that can be considered small fine debris.

<sup>†</sup>Two tests were conducted, with the cassette mounted parallel to the jet centerline.

A review of the data indicates that the stainless-steel sheaths were not directly penetrated by the air jet; rather, the sheaths disassembled at the seams, such as with rivet failures. Those cassettes secured by stainless-steel bands in addition to latches and strikes generally remained relatively intact. The severity of the damage, in terms of the generation of small fine debris, depends on the degree or ease of disassembling the cassette. However, when considering large-piece debris, all detached cassettes, disassembled or not, become large-piece debris.

**Table VI-6. BWROG AJIT RMI Insulations Tested**

<b>Insulation</b>	<b>RMI Foils Tested</b>	<b>Cassette Closures</b>
DARMET <sup>®</sup>	Stainless-Steel Foils	Darchem Stainless-Steel Bands and CamLoc <sup>®</sup> Latches and Strikes
TPI	Aluminum Foils	Latch and Strike Closures
TPI	Stainless-Steel Foils	Latch and Strike Closures
DPSC Mirror <sup>®</sup>	Aluminum Foils	Latch and Strike Closures
DPSC Mirror <sup>®</sup>	Stainless-Steel Foils	Latch and Strike Closures
DPSC Mirror <sup>®</sup>	Stainless-Steel Foils	Latch and Strike Closures and Sure-Hold Band Closures

**II.3.2.1 DARMET<sup>®</sup>, Manufactured by Darchem Engineering, Ltd.**

The NEI-recommended destruction pressure of 190 psi for stainless-steel DARMET<sup>®</sup>, manufactured by Darchem Engineering, Ltd. and held in place by Darchem stainless-steel bands and CamLoc<sup>®</sup> latches and strikes, is based on two AJIT tests, Tests 25-1 and 25-2 with jet centerline pressures on target of 190 and 590 psi, respectively. In both of these tests, the cassettes, although deformed, remained intact and attached to the target mount. In effect, no debris was generated. This result indicates that a pressure greater than 590 psi is required to generate debris, with the exception of a cassette mounted over the break, where the jet would enter the inside of the cassette. This scenario would almost certainly result in complete destruction of that cassette. Another possible exception could be a jet approximately parallel to the cassette sheath that could penetrate through the ends—a configuration that has not been tested. It is apparent that the baseline recommendation of assuming 75% of this insulation within a 1.3/D spherical radius becomes small fine debris is conservative.

**II.3.2.2 RMI Manufactured by Transco Products, Inc.**

TPI manufactures stainless-steel and aluminum RMI insulation. The NEI guidance recommends a destruction pressure of 190 psi for the TPI RMI. The TPI cassettes tested included both aluminum and stainless-steel foils encased in stainless-steel sheaths secured with latches and strikes (no bands were used). Although the recommended destruction pressure is 190 psi, a small amount of fine debris was noted for jet pressures as low as 10 psi (Test 21-3). On the other hand, only small quantities of fine debris (i.e., <0.5%) were found for tests with jet pressures as high as 600 psi. Figure II-9 shows the debris generation fractions for TPI stainless-steel RMI small fines.

Table II-8 **Table II-7?** shows a comparison of potential debris volumes when estimated using the NEI baseline guidance and when acknowledging debris generation at jet pressures as low

as 10 psi. Recall that to get actual volumes of debris, the potential volumes must be multiplied by the insulation concentration and again by  $D^3$ . For the baseline estimate, the volume associated with a ZOI radius of  $1.3/D$  is multiplied by 75% to get the baseline potential volume. For the alternate estimate, the ZOI volume out to a jet pressure of 10 psi was multiplied by 0.5% to get the alternate potential volumes. The application of the alternate pressure results in approximately three times as much small fine debris as using the baseline guidance. However, even these quantities are not very large compared with such insulations as LDFG.

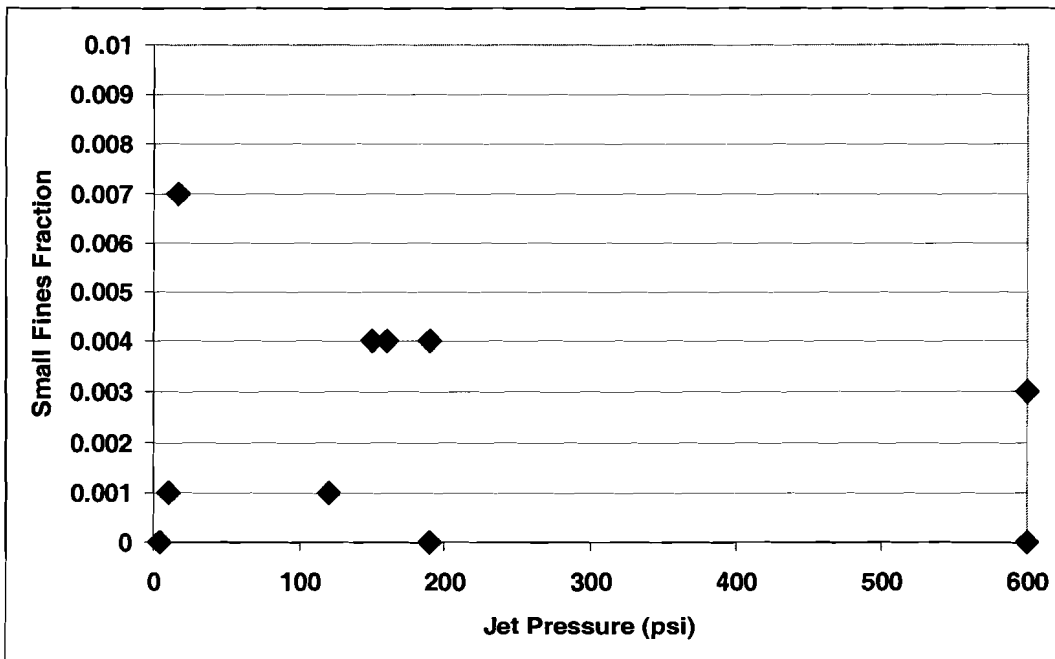


Figure VI-9. TPI Stainless-Steel RMI Small-Fine-Debris Fractions. fix y axis label (should be small-fine-debris fraction, not fines)

Table VI-7. Comparison of TPI Potential Debris Volumes

Guidance	Damage Pressure (psi)	Radius of ZOI (r/D)	Damage Fraction	Potential Volume of Debris ( $V/D^3$ )
<b>Confirmatory Recommended Jet Iso-bar Volumes</b>				
NEI Guidance	190	1.5	0.75	10.6
Alternate	10	11.9	0.005	35.3

However, if the transport of large-piece TPI RMI debris becomes necessary to the strainer blockage evaluation, the use of 190 psi to define the ZOI is totally inadequate. Although the TPI stainless-steel sheaths may effectively contain the foils, their latches and strikes do not effectively keep the cassettes attached to the mounts (or pipes). AJIT Test 21-2, with a jet pressure of only 4 psi, shows the two cassette half sections detached from the target mount, i.e., the cassettes become large-piece debris. At 4 psi, the ZOI radius would be  $\sim 21.6/D$ ;

therefore, numerous cassettes in various degrees of damage would be expected on the break-room floor. If the transport flow velocities were sufficient to move cassettes, then these cassettes could become a significant problem.

### II.3.2.3 DPSC Mirror<sup>®</sup>, Manufactured by Diamond Power Specialty Company

DPSC manufactures stainless-steel and aluminum RMI insulations marketed as Mirror<sup>®</sup> insulations. The Mirror<sup>®</sup> cassettes tested included both aluminum and stainless-steel foils encased in stainless-steel sheaths secured with latches and strikes with or without “Sure-Hold” bands. The NEI guidance recommends a destruction pressure of 4 psi for the DPSC Mirror<sup>®</sup> insulations. The apparent reason that Mirror<sup>®</sup> cassettes form debris at much lower pressures than does the TPI RMI is the construction of the sheaths, i.e., the cassette integrity depends on strength of the seams.

The debris fractions for the small fine debris from the AJIT tests are shown in Figure II-10. The small fine debris was correlated here as pieces <6 in., although the NEI guidance specified RMI small fines as <4 in.; therefore, a small measure of conservatism was added to the comparison. Figure II-10 shows six data points for Mirror<sup>®</sup>, with two of those tests generating very minor quantities of small fines. It should perhaps be noted that with the lower pressure test where the RMI cassette was exposed to a jet pressure of only 2 psi (AJIT Test 18-3), the cassette was still detached from the target mount, leaving two half cassettes on the chamber floor. The test with the largest quantity of small fine debris (AJIT Test 17-1) had only 10.6% of the foils turned into pieces <6 in., with the remaining foils becoming large-piece debris. The conservative extrapolation shown in Figure II-10 to complete the spherical ZOI debris fraction integration assumes complete destruction at a jet pressure of 130 psi. Note that in the single NRC-sponsored Mirror<sup>®</sup> debris generation test conducted at the KWU test facility, the test article was completely destroyed.

The results of the Mirror<sup>®</sup> debris-size distribution integration over the ZOI are provided in Table II-8. The potential debris volume of  $661/D^3$  is quite low compared with an estimate using the baseline guidance [75% of  $4/3 \pi (21.6/D)^3$ ] of  $31660/D^3$ . Although this insulation is damaged at jet pressures as low as 4 psi, a relatively small amount of small debris is formed at pressures less than ~120 psi, and when the debris damage data are applied to the larger ZOI radius of  $21.6/D$ , only a small fraction of the insulation in that sphere becomes small fine debris. For DPSC Mirror<sup>®</sup> RMI insulation, the NEI-baseline-guidance assumption that 75% of the insulation within a  $21.6/D$  ZOI sphere would become debris <4 in. in size (i.e.,  $31,660/D^3$ ) is overly conservative. However, the quantities of large-piece debris, including nearly intact cassettes, could be very large because even 2 psi can detach the cassettes, which could become very important in containments where the transport velocities are high enough to move this heavier debris significantly.

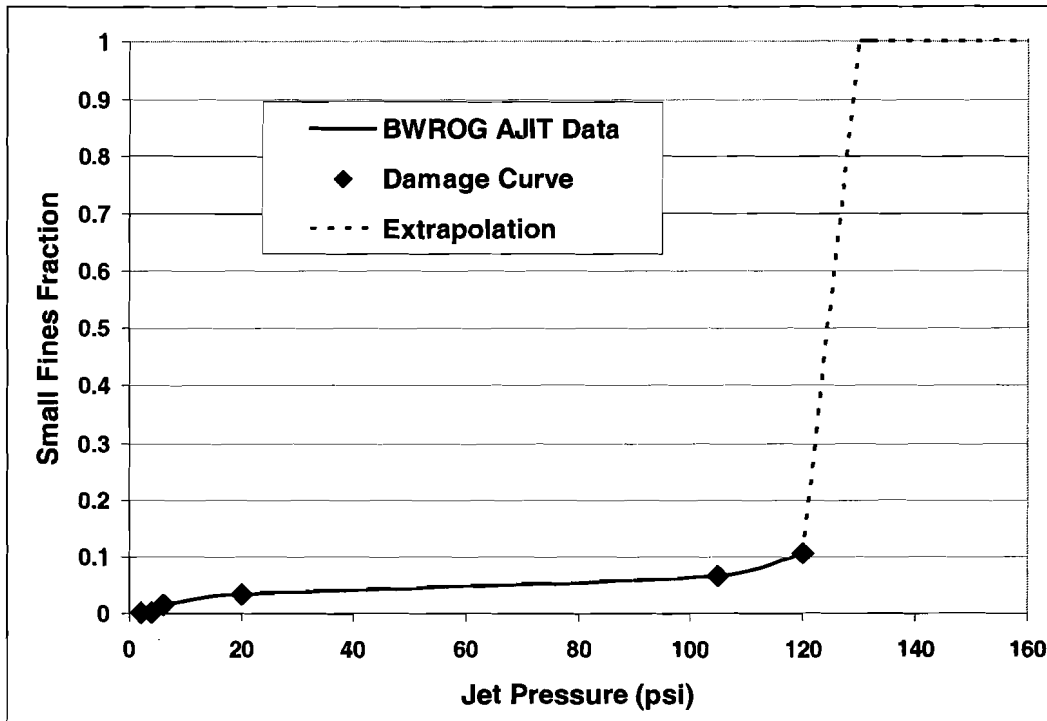


Figure VI-10. DPSC Mirror Damage Curve for Small Fine Debris.

Table VI-8. Results of Debris-Size Distribution Integration for DPSC Mirror<sup>®</sup> Insulation

Jet Pressure Isobar Volume Calculation	Radius of Sphere (r/D)	Fraction Small Fines	Potential Debris Volumes (V/D <sup>3</sup> )
<b>NEI-Recommended Damage Pressures</b>			
PWR Two-Phase Jet (Confirmatory)	21.6	0.016	658

### II.3.3 Particulate Insulation Debris

#### II.3.3.1 Min-K Debris

The NEI baseline guidance recommends the assumption that 100% of the Min-K insulation located inside a ZOI defined by the destruction pressure of 4 psi, corresponding to a radius of 21.6/D, becomes small fine debris. The basis for this recommendation apparently is the single Min-K BWROG AJIT debris generation test, Test 9-1. In this test, ~70% of the Min-K insulation became small fine debris. In fact, most of this debris was not recovered, apparently because it was too fine. Based on the extensive damage to this Min-K blanket at 4 psi, it does not seem reasonable to assume that the threshold of damage is 4 psi.

\* It was noted that a cloud of debris was observed to exit the test chamber through the exhaust screen and that the venting of the chamber to clear the dust required more than 15 minutes.

At jet pressures substantially higher than 4 psi, it seems likely that the Min-K would be totally destroyed. At jet pressures <4 psi, the damage to Min-K would continue but would decrease in severity until the pressure became insufficient to cause damage. However, that pressure is not known. It is unlikely that the NEI baseline guidance is conservative with respect to the Min-K blanket tested. On the other hand, Min-K insulation protected by a metal jacket secured with steel bands would most likely be substantially less damaged than theunjacketed blanket tested.

### II.3.3.2 Calcium Silicate Debris

The NEI baseline guidance recommends the assumption that 100% of the calcium silicate insulation located inside a ZOI defined by the destruction pressure of 24 psi (corresponding to a radius of 5.5/D) becomes small fine debris. The OPG debris generation tests [N-REP-34320-10000-R00] were cited to justify the 24-psi destruction pressure. The OPG tests involved impacting aluminum-jacketed calcium silicate insulation targets with a two-phase water/steam jet. The jacketing was secured with stainless-steel bands, and the jacketing seams were typically oriented at 45 degrees from the jet centerline—an orientation that appeared to maximize damage. The OPG data, illustrated in Figure II-11, only cover a limited range of damage pressures (~24 to 65 psi).

The damage curve shown in Figure II-12 was generated by summing all four debris categories in Figure II-11 to get the OPG debris fractions shown and then constructing a plausible curve through the data that was conservatively extrapolated at both ends. The results of the calcium silicate debris-size distribution integration over the ZOI are provided in Table II-9. The potential debris volumes are compared in Figure II-13, along with an estimate using the baseline guidance [100% of  $\frac{4}{3} \pi (5.45/D)^3$ ]. A lower alternate damage pressure results in a larger equivalent spherical ZOI, but a lesser fraction of the debris is damaged into small fine debris. The use of the alternate damage pressures over the NEI-recommended damage pressures for PWR analyses would result in ~43% more estimated small fine debris. For calcium silicate insulation, the baseline is conservative with respect to both the NEI guidance damage pressure of 24 psi and the alternate pressure of 20 psi.

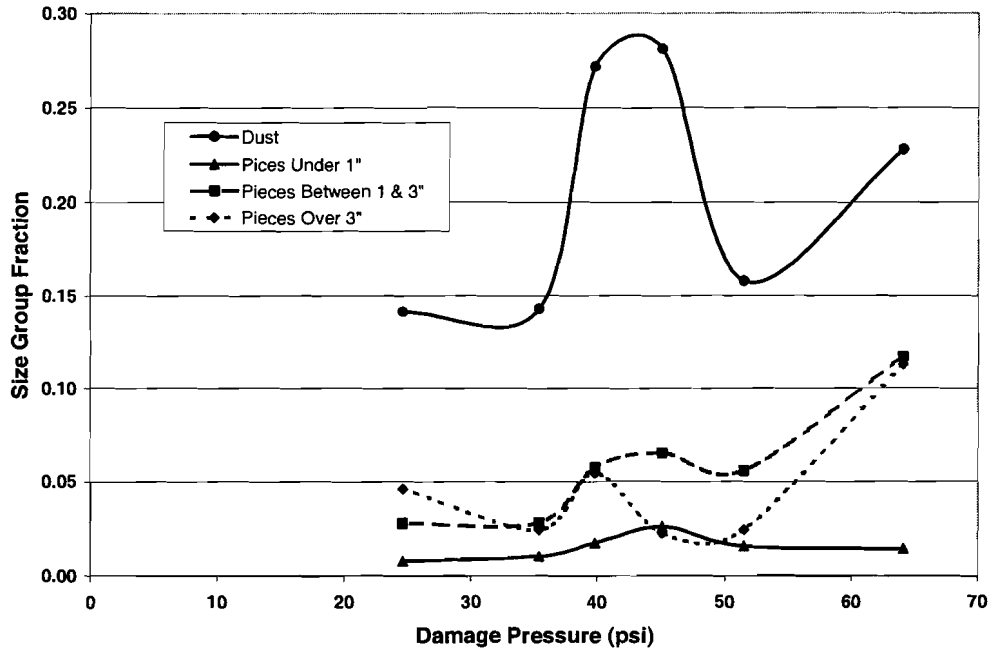


Figure VI-11. Debris-Size Distributions for OPG Calcium Silicate Tests.

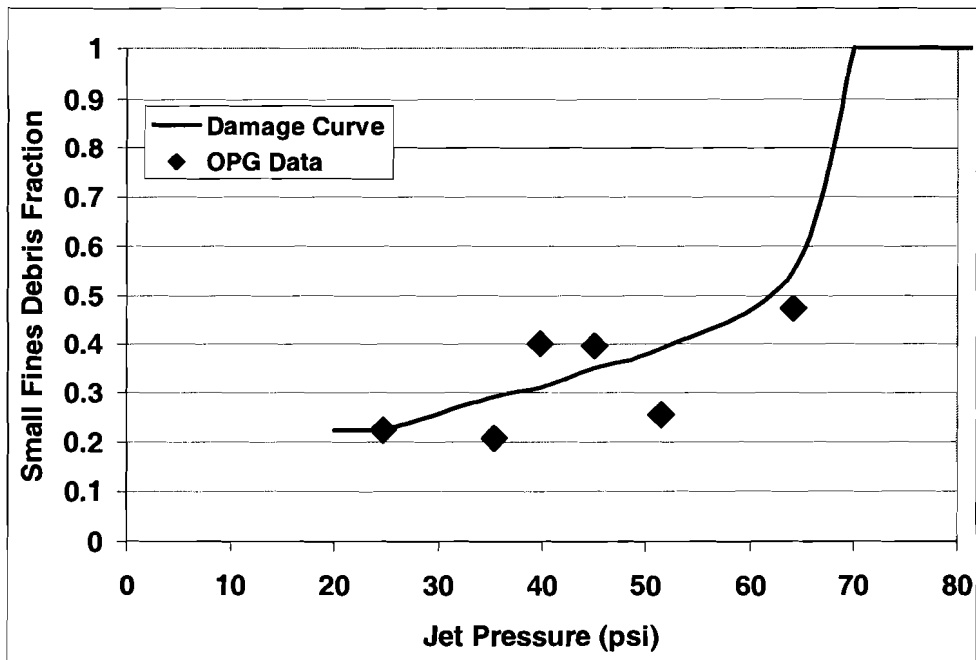
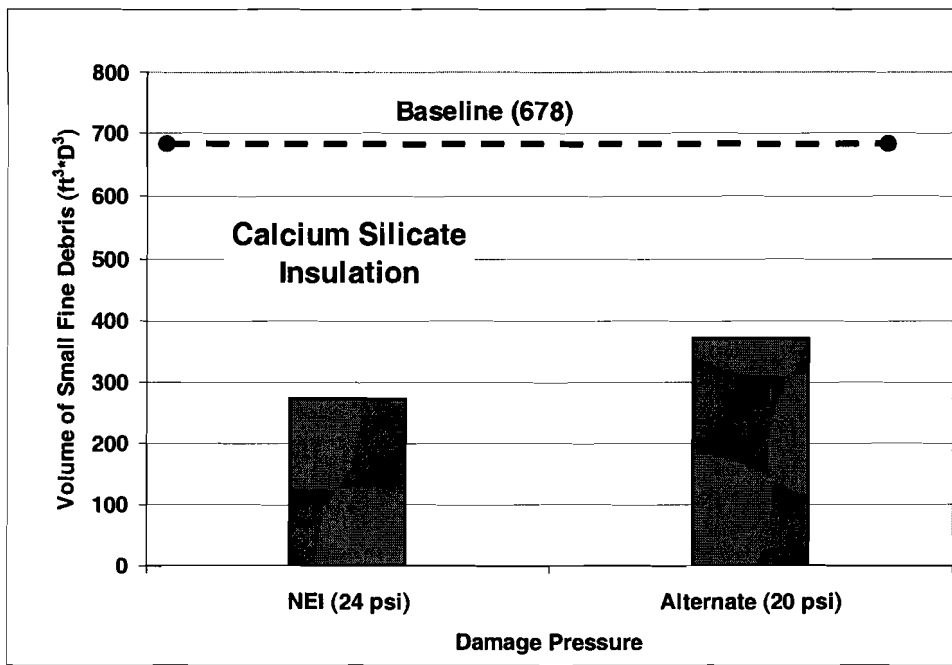


Figure VI-12. Calcium Silicate Damage Curve for Small Fine Debris.

**Table VI-9. Results of Debris-Size Distribution Integration for Calcium Silicate Insulation**

<b>Jet Pressure Isobar Volume Calculation</b>	<b>Radius of Sphere (r/D)</b>	<b>Fraction Small Fines</b>	<b>Potential Debris Volumes (V/D<sup>3</sup>)</b>
<b>NEI-Recommended Damage Pressures</b>			
PWR Two-Phase Jet (Confirmatory)	5.4	0.42	273
<b>Alternate Damage Pressures</b>			
PWR Two-Phase Jet (Confirmatory)	6.4	0.34	372



**Figure VI-13. Potential Volumes of Small Fine Calcium Silicate Debris.**

The BWROG AJIT tests also contain four tests of calcium silicate with aluminum jacketing secured by four 3/4-in. stainless steel bands; however, these tests indicated that a jet of 150 psi was needed to cause significant damage. The reason(s) that a much higher pressure was needed to cause significant damage in the AJIT calcium tests than in the OPG tests has not been determined but is likely due to the differences in jacketing thickness, seam orientation, and strength of the bands. Here the destruction pressure depends more on the pressure needed to remove the jacket and expose the insulation than on the pressure required to erode the calcium silicate.

## II.4 SUMMARY AND CONCLUSIONS

Confirmatory research was performed to ascertain whether the NEI recommendations for ZOI destruction pressures and debris fractions would reliably result in conservative estimates for the volumes of debris generated within the ZOI. Specifically, the NEI guidance recommends the assumption that 60% of the fibrous and 75% of the RMI insulation volume contained within the ZOI becomes small fine debris for ZOI radii defined by their recommended destruction pressures. The NEI guidance recommends adapting the debris-size distribution for NUKON™ to other types of fibrous insulation that have a destruction pressure higher than that of NUKON™.

Available debris generation data were used to define debris fractions versus jet pressure curves for the insulations examined. Difficulties encountered when correlating these data include aspects of protective jacketing and banding, as well as the variability in insulations. Before the insulation is subjected directly to jet flow forces, the flow must penetrate the protective coverings. Steel bands securing a metal jacket can require a rather high jet pressure to open the jacket before insulation debris is generated. The seam orientation affects the ease with which an edge of the jacket can be peeled back; it appeared that a seam orientation of ~45 degrees from the oncoming jet maximizes the potential for jacket opening. Another factor affecting the quality of debris generation data was the size of the jet nozzle relative to the insulation destruction pressure. If the target insulation had to be placed close to the nozzle to get the required destruction pressure, then the jet pressure became uneven along the length of the target; in fact, in some tests the target ends were likely located outside the influence of the jet. To test insulations with a higher destruction pressure, either larger nozzles or shorter targets are required. All of these considerations are factored into the evaluation of debris fractions.

ZOI debris fractions and insulation destruction pressures are interdependent; that is, the larger the ZOI, the smaller the fraction of the insulation within the ZOI that becomes small fine debris. Therefore, when the lower alternate pressure is used in the integration process, the resultant debris fraction will be less than that corresponding to the NEI-recommended destruction pressure.

The results and conclusions regarding relative conservatism of this confirmatory debris generation analyses are summarized in Table II-10 for the insulations examined. These results are relative to the NEI baseline guidance for the small-fine-debris-size category.

**Table VI-10. Summary Comparison of Confirmatory and Baseline Potential Debris Volumes**

<b>Insulation</b>	<b>Confirmatory Research Result</b>	<b>Relative Conservatism of Baseline Guidance</b>
<b><i>Fibrous Insulations</i></b>		
NUKON™	Baseline guidance results compare well with confirmatory results.	Baseline guidance for NUKON™ provides realistic results that are only slightly conservative.
Temp-Mat	Baseline results are approximately twice the confirmatory results (based on limited data).	Baseline guidance is conservative for Temp-Mat insulation.

<b>Insulation</b>	<b>Confirmatory Research Result</b>	<b>Relative Conservatism of Baseline Guidance</b>
K-wool	Baseline results are only about half that of the confirmatory results (based on limited data).	Baseline guidance is likely conservative for K-wool, despite the nonconservative comparison with confirmatory analysis. The poor nonconservative comparison is due to the extreme extrapolation of data required by the lack of data for pressures greater than the NEI destruction pressure. Still, conservatism cannot be proven with existing data.
<b>RMI Insulations</b>		
DARMET <sup>®</sup>	No confirmatory analysis for this insulation. Rather, a review of the debris generation data illustrated substantially less small fine debris than would be estimated using the baseline guidance methodology.	Baseline guidance is conservative for DARMET <sup>®</sup> insulation.
TPI	Baseline results account for only one-third of the confirmatory debris estimate, which includes the small quantities of debris generated at lower pressures but that are neglected when the baseline destruction pressure is used.	Baseline guidance is not conservative, but the quantities of this debris are relatively low; therefore, this nonconservative estimate is not a major issue.
DPSC Mirror <sup>®</sup>	Baseline results were almost 50 times that of the confirmatory result. The baseline minimum destruction pressure of 4 psi results in a very large ZOI volume, but the damage to the insulation is relatively minor at the lower pressures, thus the large differences in results.	Baseline guidance is conservative for Mirror <sup>®</sup> insulation.
<b>Particulate Insulations</b>		
Min-K	No confirmatory analysis for this insulation. Rather, the data from the single Min-K debris generation test were examined, i.e., approximately 2/3 of the insulation was turned into fine dust debris at a jet pressure of only 4 psi.	Baseline guidance is not conservative because the one test indicated that substantial damage would occur to Min-K insulation at significantly lower pressures than the destruction pressure of 4 psi and that the damage at 4 psi was extreme.
Calcium Silicate	Baseline results are approximately twice the confirmatory results, even when the lower jet pressure of 20 psi (recommended in NUREG/CR-6808) is considered instead of the baseline destruction pressure of 24 psi.	Baseline guidance appears to be conservative for calcium silicate insulation, but the debris generation data are not sufficient to determine the threshold jet pressure for generating small fine debris, i.e., the threshold destruction pressure could actually be less than the 20 psi alternate pressure used in the confirmatory analysis.

The following additional comments should be noted:

- The use of the alternate destruction pressure provides some quantification of the uncertainty associated with the selection of the destruction pressures. These uncertainties include the neglect of the tails of the debris damage curves and the uncertainty associated with the potential two-phase effect on debris generation relative to the available air-jet-generated data.
- A comparison of the NUKON™ results with the BWROG URG steam jet model illustrates that the neglect of the tails of the debris damage curve has a larger impact for PWRs than for BWRs (see Figure II-3).
- The NEI guidance recommendation that adapts the debris-size distribution for NUKON™ to other types of fibrous insulation that have a destruction pressure higher than that of NUKON™ has been partially supported (see Figure II-8), although it cannot be conclusively ensured.
- The ZOI for large debris generation in some cases does not correlate with the ZOI for small-fine-debris generation. A case in point is the analysis for TPI RMI, where most of the small fine debris would be generated inside jet pressures of 190 psi but large debris was generated (in the form of detached cassettes) at pressures as low as 4 psi. Therefore, rather larger quantities of large debris could be formed than were predicted using the baseline guidance ZOI sizes.
- It should be emphasized that the typical debris generation analyses were performed for insulations where the debris generation data were very limited. The data for the LDFG insulations (see Figure II-2) illustrate the potential variability in such data. Therefore, the limited debris generation data cause substantial uncertainty with debris generation estimations.

## II.5 REFERENCES

- [NUREG/CR-6762, Volume 3, 2002] C. J. Shaffer, D. V. Rao, and S. G. Ashbaugh, "GSI-191 Technical Assessment: Development of Debris-Generation Quantities in Support of the Parametric Evaluation," LA-UR-01-6640, NUREG/CR-6762, Volume 3, 2002.
- [NUREG/CR-6369, 1999] D. V. Rao, C. Shaffer, B. Carpenter, D. Cremer, J. Brideau, G. Hecker, M. Padmanabhan, and P. Stacey, "Drywell Debris Transport Study: Experimental Work," SEA97-3501-A:15, NUREG/CR-6369, Volume 2, September 1999.
- [NEDO-32686, Rev. 0, 1996] "Utility Resolution Guidance for ECCS Suction Strainer Blockage," BWROG, NEDO-32686, Rev. 0, November 1996. **not used in this section**
- [SEA-95-970-01-A:2, 1996] Gilbert Zigler et al., "Experimental Investigation of Head Loss and Sedimentation Characteristics of Reflective Metallic Insulation Debris," draft letter report prepared for the US Nuclear Regulatory Commission, SEA No. 95-970-01-A:2, May 1996.
- [N-REP-34320-10000-R00, 2001] Ontario Power Generation, "Jet Impact Tests—Preliminary Results and Their Applications," N-REP-34320-10000-R00, April 2001.



## **APPENDIX III: VOLUNTEER-PLANT CONTAINMENT POOL COMPUTATIONAL-FLUID-DYNAMICS ANALYSIS**

### **III.1 INTRODUCTION**

A three dimensional computational fluid dynamics (CFD) model was developed to analyze the flow patterns developed in the Nuclear Regulatory Commission's (NRC's) volunteer-plant reactor containment during loss-of-coolant accidents (LOCAs). The purpose of the CFD modeling was to assess the water velocities and flow patterns developed during sump pump operation to support estimates of subsequent LOCA-generated sump pool debris transport. Water sources to the sump pool included effluents from the LOCA break and containment spray drainage. The locations and flow rates of each of these water sources and the recirculation pumping rates determined the characteristics of the sump pool that subsequently determined whether, and what fraction of, the debris deposited into the pool could transport to the recirculation sump screens. Threshold transport velocities were determined by experiments conducted at the University of New Mexico (UNM) for debris from pressurized-water-reactor (PWR) insulating materials [NUREG/CR-6772]; therefore, these threshold velocities were used to set the velocity contours of the CFD flow diagrams to facilitate the determination of whether debris would likely transport. The CFD simulations are discussed in Section III.2.

A logic chart debris-transport model was developed to supplement the CFD analyses so that information from the CFD simulations could be used with the blowdown/washdown transport analyses documented in Appendix VI to determine estimates of debris transport to the recirculation sump screens. The pool velocity and turbulence characteristics determine areas of the pool where debris entrapment may occur. The flow streamlines can be used to determine whether debris entering the pool at a discrete location would likely pass through one of the potential entrapment locations. The debris transport process was decomposed using a logic chart approach to facilitate the individual transport steps—steps that could be determined analytically, experimentally, or simply judged. The subsequent quantification of the chart then provided an estimate of the overall sump pool debris transport. The debris transport estimates are discussed in Section III.3.

### **III.2 ANALYSIS OF THE CFD SIMULATION**

#### **III.2.1 Modeling Methodology, Assumptions, and Conditions Simulated**

The commercial CFD program Fluent™ was used to compute the volunteer-plant containment pool flows for large and small LOCA breaks. The containment geometry was available in Autocad™ format and was imported into the Fluent™ preprocessor and grid generator. As shown in Figure III.2-1, all of the structures, stairwells, and sumps were included in the model geometry, but the containment pool was modeled only to a depth of 6 ft. This is the maximum anticipated depth of water during steady-state operation of the spray system and sump pump operating in the recirculation mode.

The splash locations are shown in Figure III.2-2 and can be seen as the extruded volumes above the containment pool in Figure III.2-1. The splash locations and flow rates shown in Figure III.2-2 are explained in detail in Appendix VI. A few modifications to the splash locations and flow rates were made in the CFD model.

1. One of the four "yellow" floor drains from Level 832, with a total flow rate of 397 gpm in Figure III.2-2, is located on top of a wall. Thus, the adjacent yellow splash located in the corridor had double the individual flow rate. (Note: for all the Level 832 floor drains, the total mass flow was evenly distributed to all locations, with the exceptions noted here.)
2. The uniformly distributed "liner film flow" of 700 gpm and
3. The "Level 808 sprays" of 1080 gpm were neglected entirely.

Thirteen LOCA break conditions were simulated: eight large LOCA conditions (four break locations each considered with and without the spray flows) and five small LOCA conditions (four break locations without spray flows and one location with spray flows). Both large and small LOCA breaks were considered because each can cause the sump screens to become clogged in a different way. The large LOCA break and spray flows will result in a large pool depth and all of the screen surface area to be come wetted. The large LOCA break will likely generate more debris that can migrate to the sump screens causing an unacceptable head loss due to the amount of debris collected. The small LOCA break may not cause the spray systems to be activated, and could result in a water depth wetting only the lower portion of the sump screens. This has the potential of forming a thin bed debris mat over a small portion of the screen area resulting in an unacceptable head loss. If the spray flow systems are not activated, depending on break location, a larger portion of the pool flows do not have velocities in excess of the debris threshold velocities and do not participate in the recirculation flow. Therefore the debris generated in those regions does not migrate to the sump screens and provide information on areas to divert debris into during the break and pool fill up.

The four break locations considered correspond to a break occurring in one of the four quadrants [steam generator (SG) compartments] in Figure III.2-2. The total break flow was assumed to be 7400 and 1611 gpm for the large and small LOCA break flows, respectively. It was assumed that the upper two SG compartments were physically separate from the lower two compartments; thus, if the break were postulated to occur in the upper left quadrant, 75% of the break flow would be partitioned to the upper left and 25% to the upper right quadrants; none of the break flow was considered in the lower two quadrants. The 75%/25% partitioning was determined arbitrarily, but it seemed to be a realistic assumption. Additionally, a transient pool fill-up simulation was initiated for a large LOCA break in the upper-left quadrant. Only the break flows were simulated in the upper half of the SG compartments with the break flow partitioned as described above. It should be noted that the above apportionment of the flow represents an estimate of the volunteer plant break due to the steam generator compartment configuration. The steam generators are raised above the pool floor level and do not participate in the recirculation flow, thus the break flow enters the pool by flowing down the steam generator stairwells and thus the water sheets across the steam generator compartment and does not pool to any significant depth. Thus the 75/25% apportionment was assumed, but a thorough analysis of how the break flow would enter the pool would be required. These analyses would be required by each plant, using their expert knowledge of the containment configuration, thus the above apportionment is illustrative of the types of flows that would enter the pool.

Three boundary condition types were used in the simulation. All hard surfaces (walls, floors, etc.) were specified to be a no-slip wall condition. The spray system splash and LOCA break flows were specified as a mass flow inlet condition, and the sumps were set to a pressure outflow boundary condition. Because the break flow sheeting described

previously was not included, the break and spray flows present in the SG compartment were applied as a mass inflow boundary on a vertical surface at the exit of the SG entrance steps of each quadrant (i.e., a mass flow boundary condition located at the “door” of the SG entrance steps, for instance). The spray/splash mass flow boundary conditions were placed on the “top” of each extruded spray location, as shown in Figure III.2-1. This extruded volume was found to be easier to handle in Fluent™ than trying to set the boundary condition on the “top” of the pool surface.

The combination of mass inflow and pressure outflow satisfies the mass continuity condition without unnecessary complications due to numeric and other boundary condition errors. In theory, a mass outflow condition at the bottom of the sump could be specified, but there are numerical instabilities when that condition is prescribed. By using a pressure outflow condition at the sumps, the pressure is allowed to “float” to satisfy the incompressible continuity equation. In other words, the pressure at the bottom of the sump is adjusted by the code to balance the mass flow entering and exiting the pool. In this way the introduction of artificial pressure waves in the solution that can be created by specifying mass inflow and outflow conditions were avoided.

A second-order-accurate numerical method was used to solve the incompressible Navier-Stokes equations, in conjunction with a renormalized group-theory turbulent-kinetic-energy and dissipation (RNG  $\kappa$ - $\varepsilon$ ) turbulence closure. This closure was chosen because of its ability to treat swirling flows, but in practice, little difference was found between the RNG  $\kappa$ - $\varepsilon$  and the more traditional  $\kappa$ - $\varepsilon$  closure for these simulations. The pressure equation was solved using a PISO method, as described in the Fluent™ documentation. For the steady state pool flow analyses, the pool volume was assumed to be completely full of liquid water and initialized to zero velocity. The inflow boundary conditions were flowing from the start, and the solution was allowed to proceed until a steady-state condition was achieved. The normalized residuals of the continuity, momentum, and  $\kappa$  and  $\varepsilon$  equations were monitored until convergence was achieved, typically about 400 iterations. For the steady state pool flow analysis, an additional convergence criterion was to integrate the mass flow rate at the two sump pressure outflow boundaries and compare it with the mass inflow. A mass balance had to be achieved, in addition to a drop in the normalized residuals, for the simulation to be deemed converged.

### **III.2.2 Results and Discussion**

This section contains the results of the CFD simulations. These simulations illustrate what can be achieved with a CFD analysis of the containment pool flows. For application to a particular plant containment, a more rigorous set of simulations should be performed, including grid convergence tests (e.g., does doubling the number of grid points change the results significantly).

One figure of merit was to determine the fraction of the pool flow volume that produced velocities in excess of the debris migration threshold velocities. Based on the experimental measurements reported in NUREG/CR-6772, the RMI and fiber flock transport threshold velocities were determined to be 0.085 and 0.037 m/s, respectively. Note that only one debris transport threshold velocity for fiber and one for small RMI were used for the following analyses.

#### **III.2.2.1 Transient Containment Pool Fill-Up**

For this simulation, a volume-of-fluid (VOF) method was used. The containment pool was initially filled with air, and water was allowed to enter the pool from the SG entrance stairs. Only the break flows for a large LOCA break, located in the upper-left quadrant, were included. As noted in Section III.2.1, the break flow is partitioned such that 75% of the water leaves the upper-left SG compartment stairwell and 25% leaves the upper-right SG compartment stairwell. This condition corresponds to the time immediately after a break occurs and before the spray system is activated. All walls were treated as no-slip surfaces, and because the fill-up phase is being simulated, the sumps were also treated with no-slip surfaces instead of pressure outflow boundary conditions. The top boundary of the simulated pool was prescribed as a pressure outflow boundary condition instead of as a no-slip wall. This treatment allows the air to leave the domain as the water displaces it. The containment pressurization that occurs during a LOCA was not modeled because it has minimal effect on pool transport.

Figures III.2-4 through III.2-12 show the volume fraction of water, at a height of 0.01 m above the containment floor, as the containment pool fills at 0.34, 0.94, 11.4, 21.4, 31.4, 41.4, 51.4, 71.4, and 111.4 seconds after the water leaves the SG compartment stairwells. The color scheme shown corresponds to a red color for 100% water in the computational cell and blue for 100% air in the cell. Other colors indicate that the computational cell has both air and water partially filling the cell. From Figures III.2-4 to III.2-12, the areas that are first swept by the water can be seen, as well as how the containment pool fills. This simulation shows the areas that fill first and thus provides information needed to design systems to divert debris to areas of the pool that do not participate in recirculation flow. In general, the water leaves the SG compartment, flows out the doorway, and hits the circular outer wall. Then the water flows circumferentially around the containment until the two water streams meet near the sumps. Then the water starts to enter the areas between the upper and lower SG compartments. For this plant configuration, these two areas between the upper and lower SG compartments are the only “quiet” zones (i.e. flow velocities much lower than the debris threshold) in the pool when all break locations are considered in the subsequent steady-state pool flow analysis.

Figures III.2-13 through III.2-21 show the fluid velocity during the fill-up at the same set of time increments previously discussed for volume fractions. Note that when the water volume fraction and fluid velocity plots are compared, there is motion ahead of the water. This motion is the air moving in response to the approaching front of water. During fill-up, the water velocity near the front is in the range of 2–3 m/s, well in excess of the debris transport threshold velocities of 0.037 and 0.085 m/s for fiber and RMI, respectively.

#### III.2.2.2 Steady-State-Flow Analysis

To study the containment pool’s steady-state-flow dynamics, the simulated volume was considered to be completely full of water. In the case of a small LOCA break, the spray flows were not included; however, for the large LOCA break, spray flows were included in the simulations. With the simulated pool full of water, the break and spray flows were introduced as mass inflow boundary conditions and the sumps were set to a pressure outflow boundary condition. These simulations produced a simulated steady-state-flow condition for further debris transport analysis, which will be discussed in Section III.3.

Figures III.2-22 through III.2-29 show the steady-state-flow pattern developed for a small LOCA break condition, without spray flows, and Figures III.2-30 to III.2-37 show large LOCA break conditions, including spray flows. These figures show contours of water velocity at a height of 0.01 m above the containment floor and show a velocity range from 0 m/s up to the threshold velocity for fiber or RMI, 0.037 and 0.085 m/s, respectively. From these plots, the area enclosed by the threshold velocity contour can be computed, and by dividing by the entire available flow area in the containment, a percentage of area in excess of the threshold velocity may be computed. These percentages, or fractional areas in excess of the threshold velocity, are summarized in Table III.2-1 for both large and small LOCA break conditions.

Figures III.2-38 through III.2-47 show streamlines for origins near the splash locations for a large LOCA break at two different locations: an upper-left break and a lower-right break. A rake of particles was released from  $(-15 < X < -5, Y=10)$ , and also from  $(0 < X < 5, Y=15)$  and allowed to follow the flow. From these streamlines, debris trajectories can be determined and their fate postulated. Figures III.2-38 and III.2-39 show the streamlines superimposed on the background velocity map that were color coded using the fiber (0.037 m/s) and RMI (0.085 m/s) threshold velocity, respectively. An oblique view showing the three-dimensionality of the streamlines is shown in Figures III.2-41 and III.2-42, color coded according to the flow speed, using the fiber and RMI threshold velocity, respectively. Thus, it could be deduced that if the velocity (speed) along a particular streamline became smaller than the debris type threshold velocity, it would not be so likely to migrate to the sump screen. By using rakes and streamline analysis at potential debris entry locations, a method for determining whether the debris will transport to the sump screens could be developed.

A similar set of plots are shown in Figures III.2-42 through III.2-45 for the large LOCA break located in the lower-right quadrant. Notice that the streamline patterns are quite different for the lower-right break location when compared to the upper-left break location.

Shown in Figure III.2-46 is a vortex induced by the splash located in the upper-right quadrant in Figure III.2-42. Here the streamlines are color coded by velocity using the fiber velocity threshold. Because the water enters the pool from above and penetrates to the containment floor, a vortex with significant vertical motion is created. Figure III.2-47 shows the streamlines color coded by turbulent kinetic energy (TKE). This type of information would be useful in determining debris degradation mechanisms, particularly for fibrous debris. In Figures III.2-46 to III.2-47, the streamlines show the type of rotation that debris can encounter near the entry of a splash into the pool. The water flow produces vortices around the splash entry and could potentially shred debris into finer particles/pieces than those generated by the break itself. No attempt was made in this document to quantify the debris shredding mechanisms; rather, this document simply illustrates what can be gleaned from a CFD analysis of the pool dynamics.

**Table III.2-1 Percentage of Containment Pool Flow Area in Excess of the Debris Transport Threshold Velocity. Total Pool Area = 767.7 m<sup>2</sup>**

<b>Break Location</b>	<b>Break Size</b>	<b>RMI (%)</b>	<b>Fiber Flocks (%)</b>
Upper Right	Large	35	60
Upper Left	Large	30	54
Lower Left	Large	22	43

Break Location	Break Size	RMI (%)	Fiber Flocks (%)
Lower Right	Large	22	41
Upper Right	Small	5	31
Upper Left	Small	2	25
Lower Left	Small	5	14
Lower Right	Small	5	19



**Figure III.2-1. Volunteer plant geometry and flow region modeled. (Note: Splash Locations Are Shown Extruded above the Nominal Pool Depth.)**

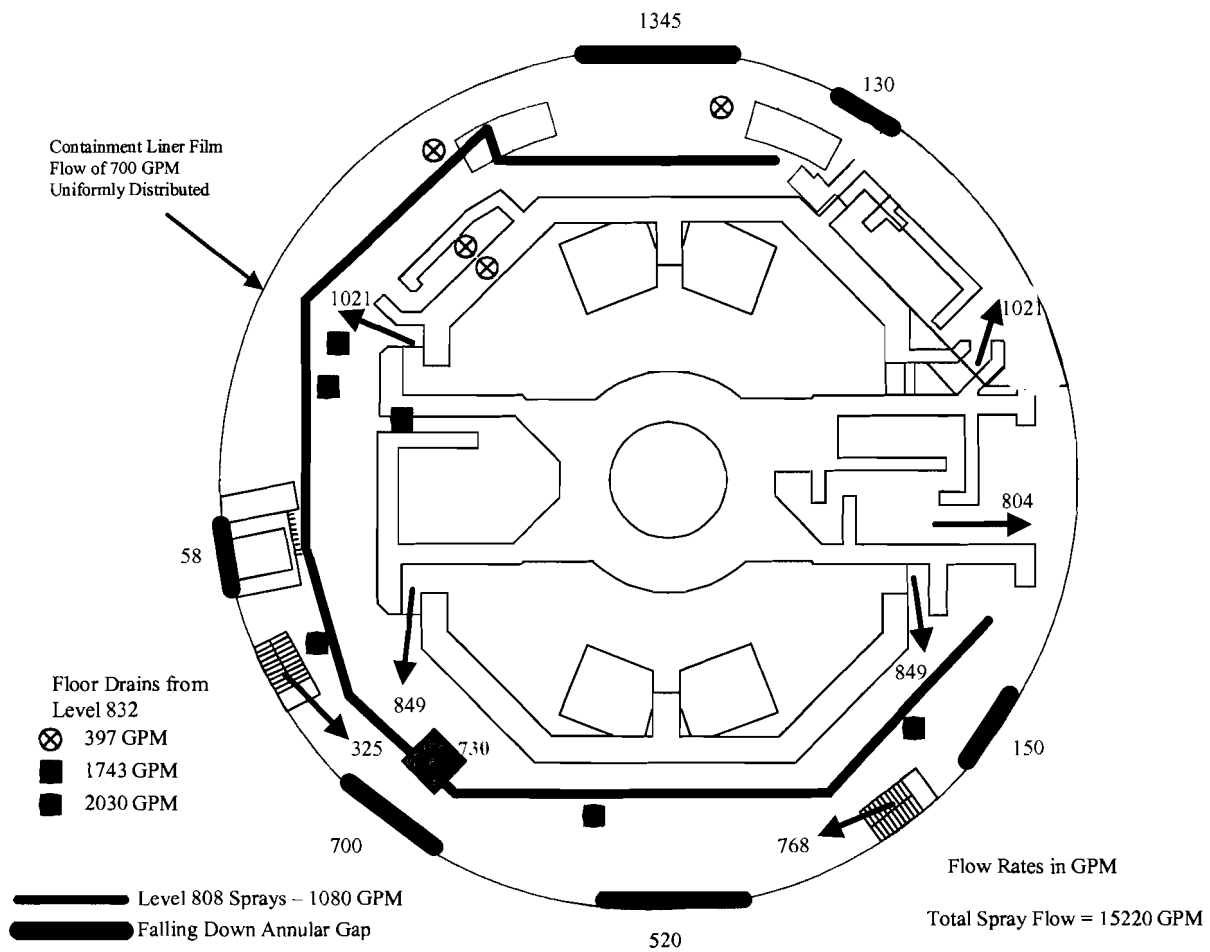


**Figure III.2-2. Spray Flow Rates (gpm) and Locations for the Volunteer-Plant Pool Flow Calculations.**

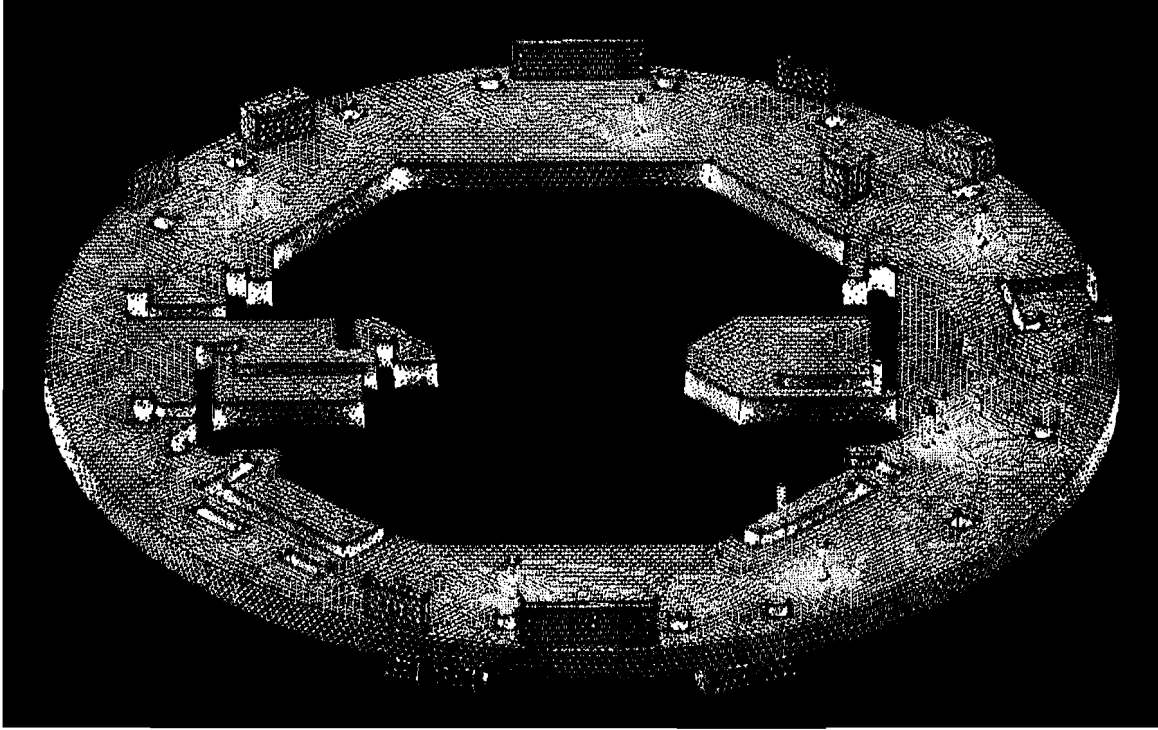


**Figure III.2-3. Unstructured Mesh Created for Containment Pool Flow Calculations.**

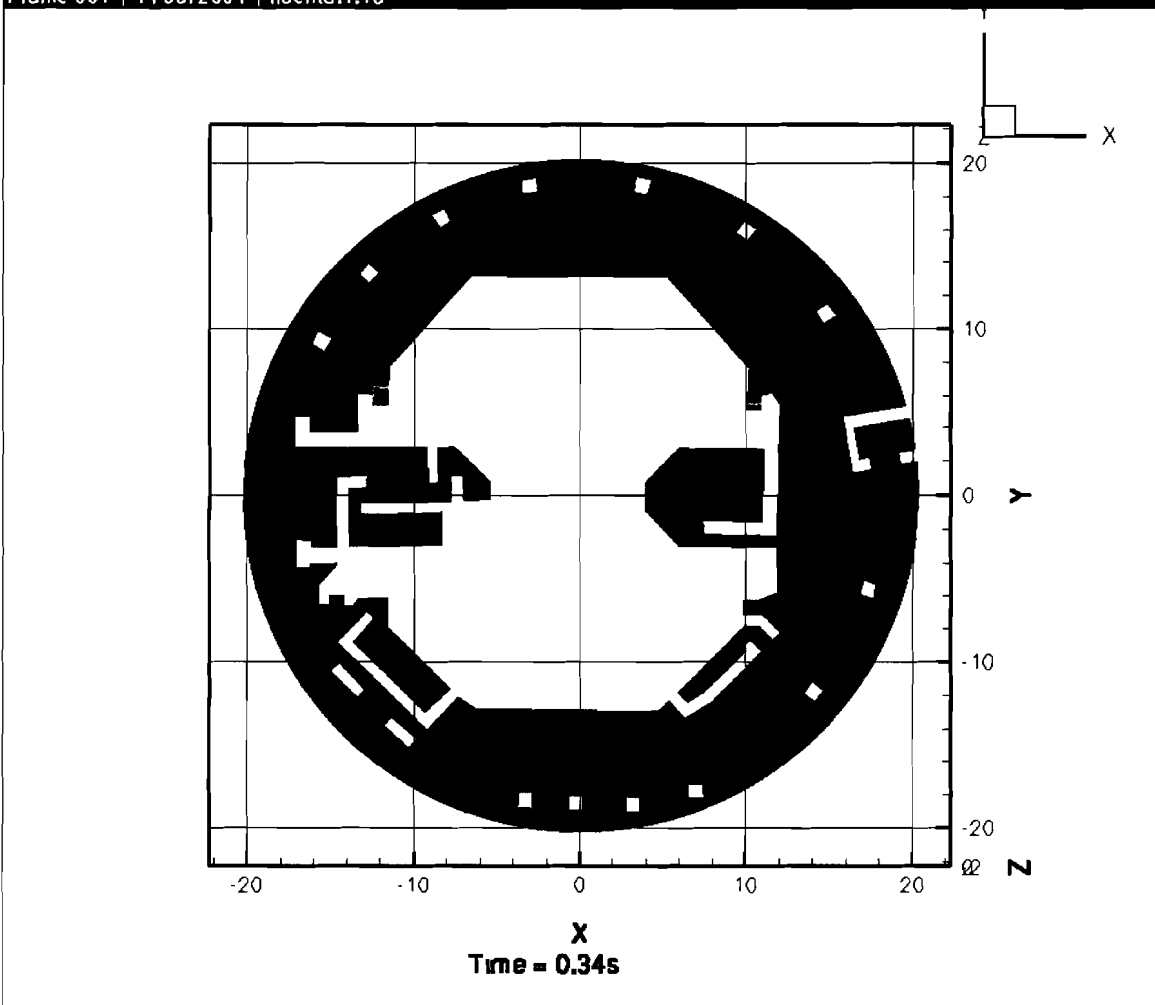


Figure III.2-4. Transient volume of fluid during the simulation of containment pool fill up. Computational cell volume fraction of water is shown at a height of 0.01m above the containment floor. Red is 100% water (0% air), blue 0% water (100% air). Time of the snapshot in seconds after the break flow is initiated is shown in the bottom of the figure.

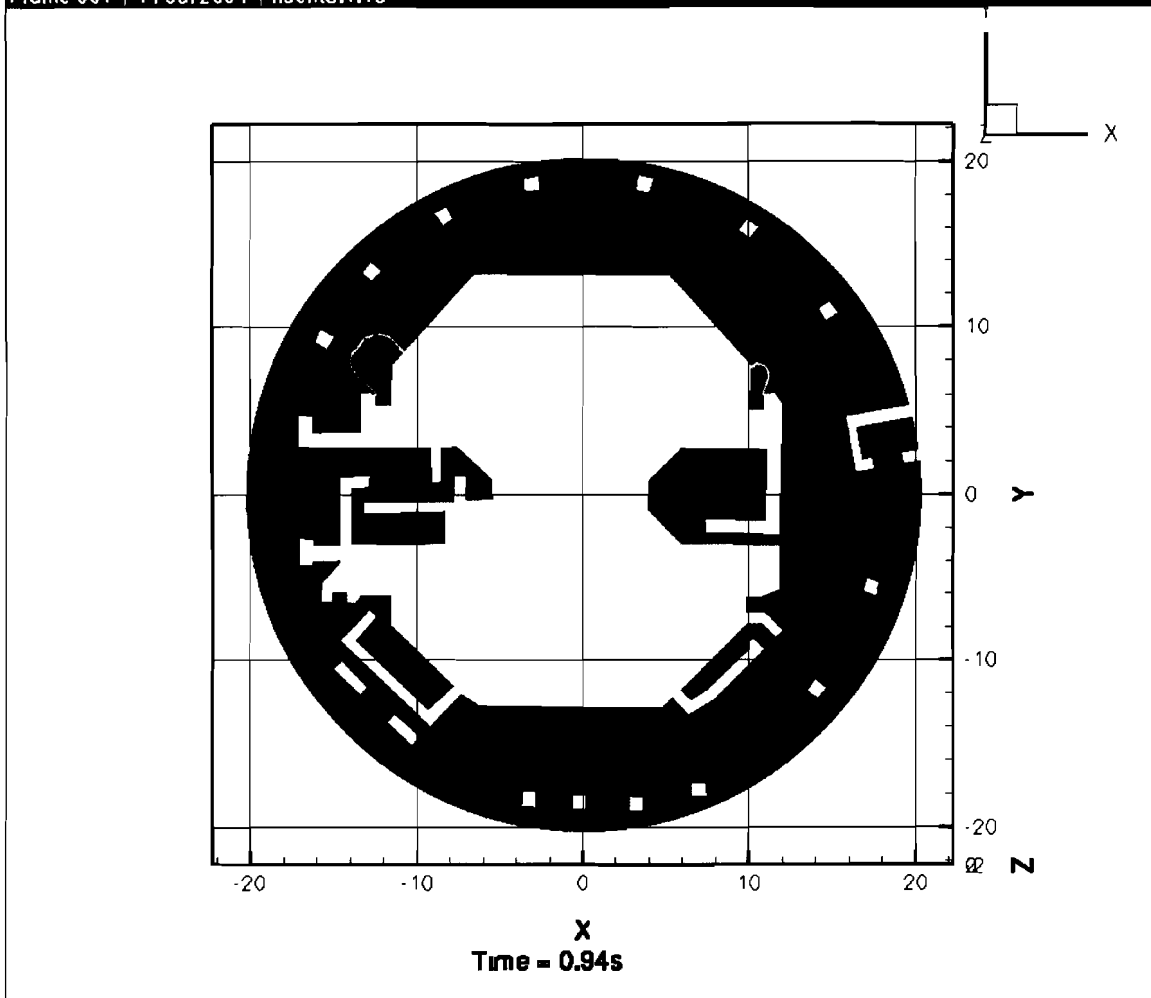


Figure III.2-5. Same as Figure III.2-4 for  $t = 0.94$  Seconds.

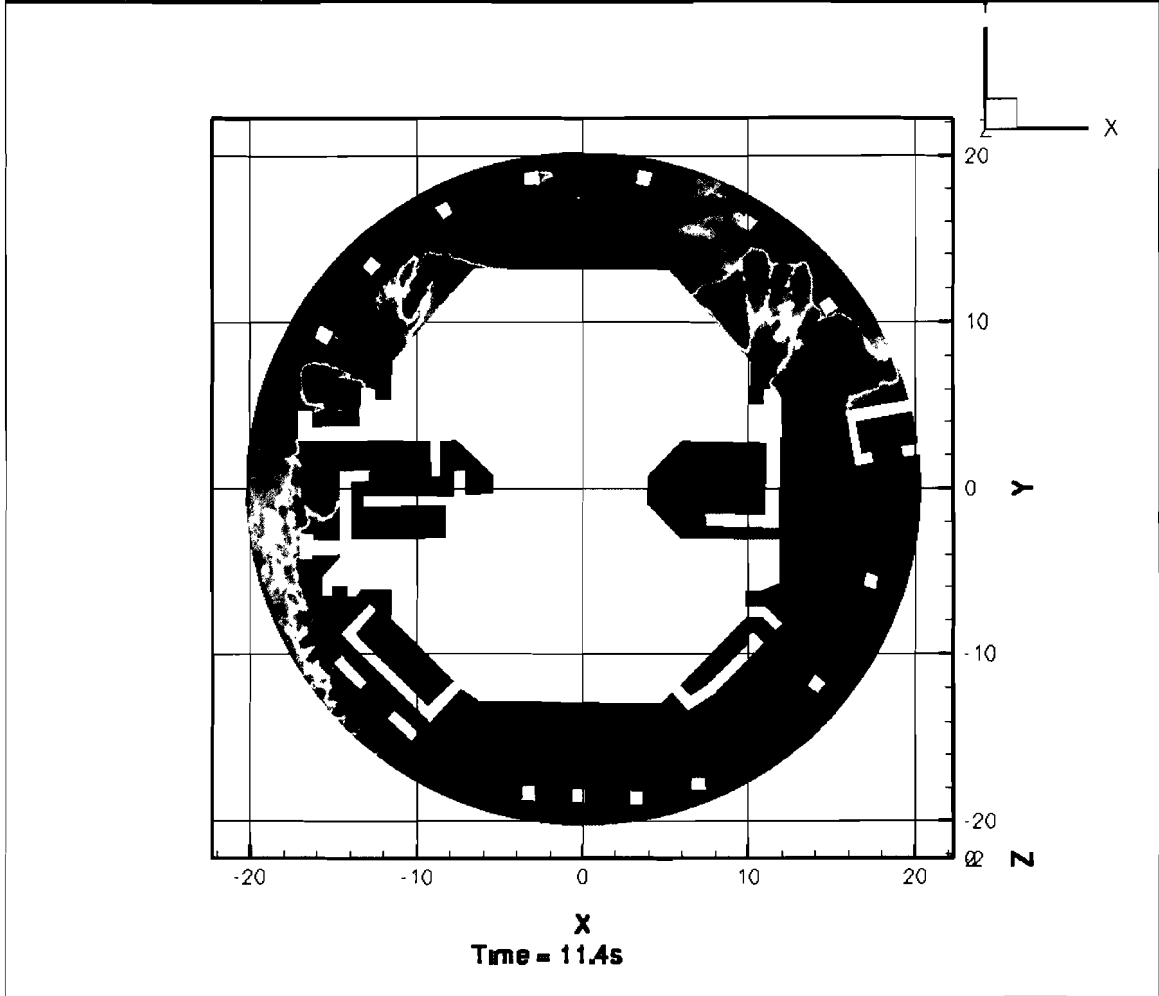


Figure III.2-6. Same as Figure III.2-4 for t = 11.4 Seconds.

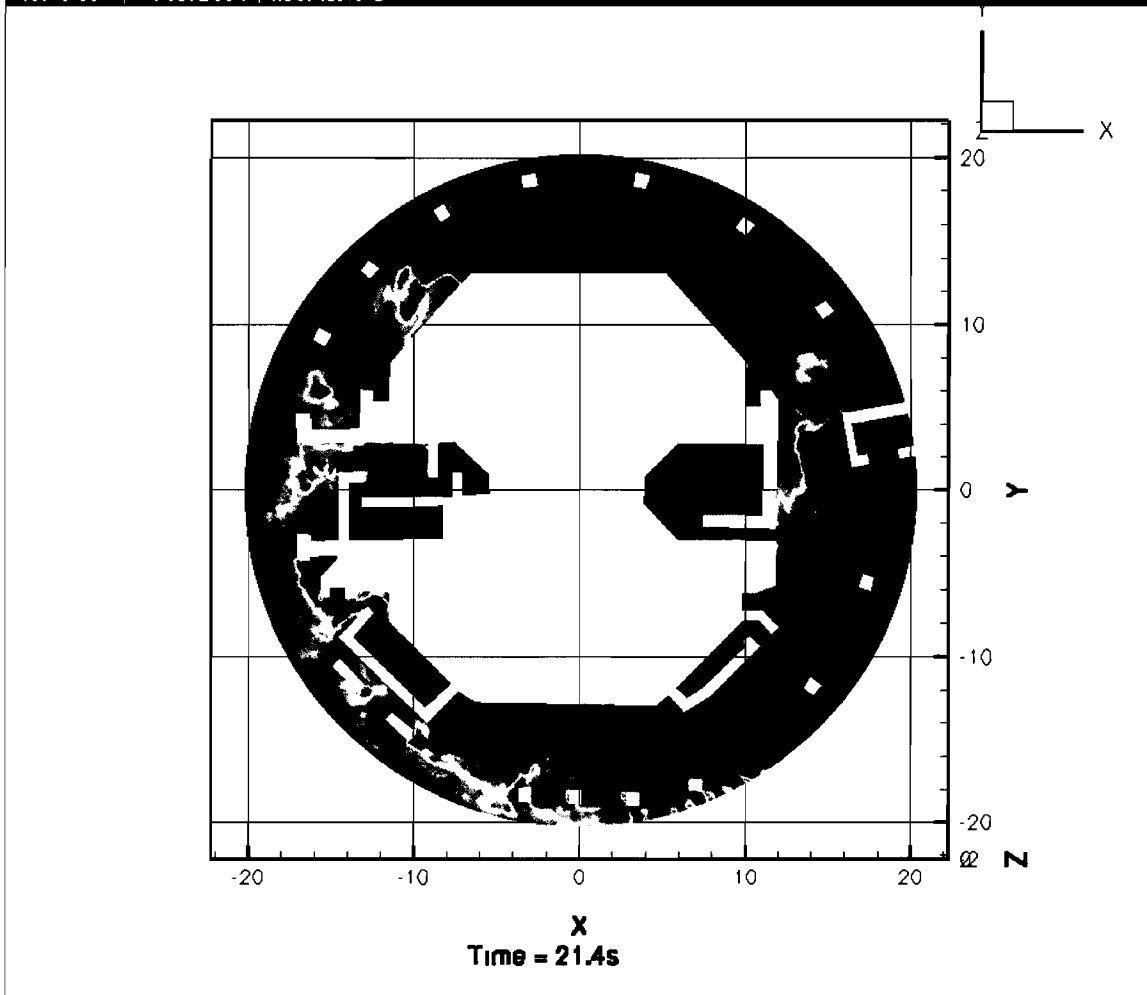


Figure III.2-7. Same as Figure III.2-4 for  $t = 21.4$  Seconds.

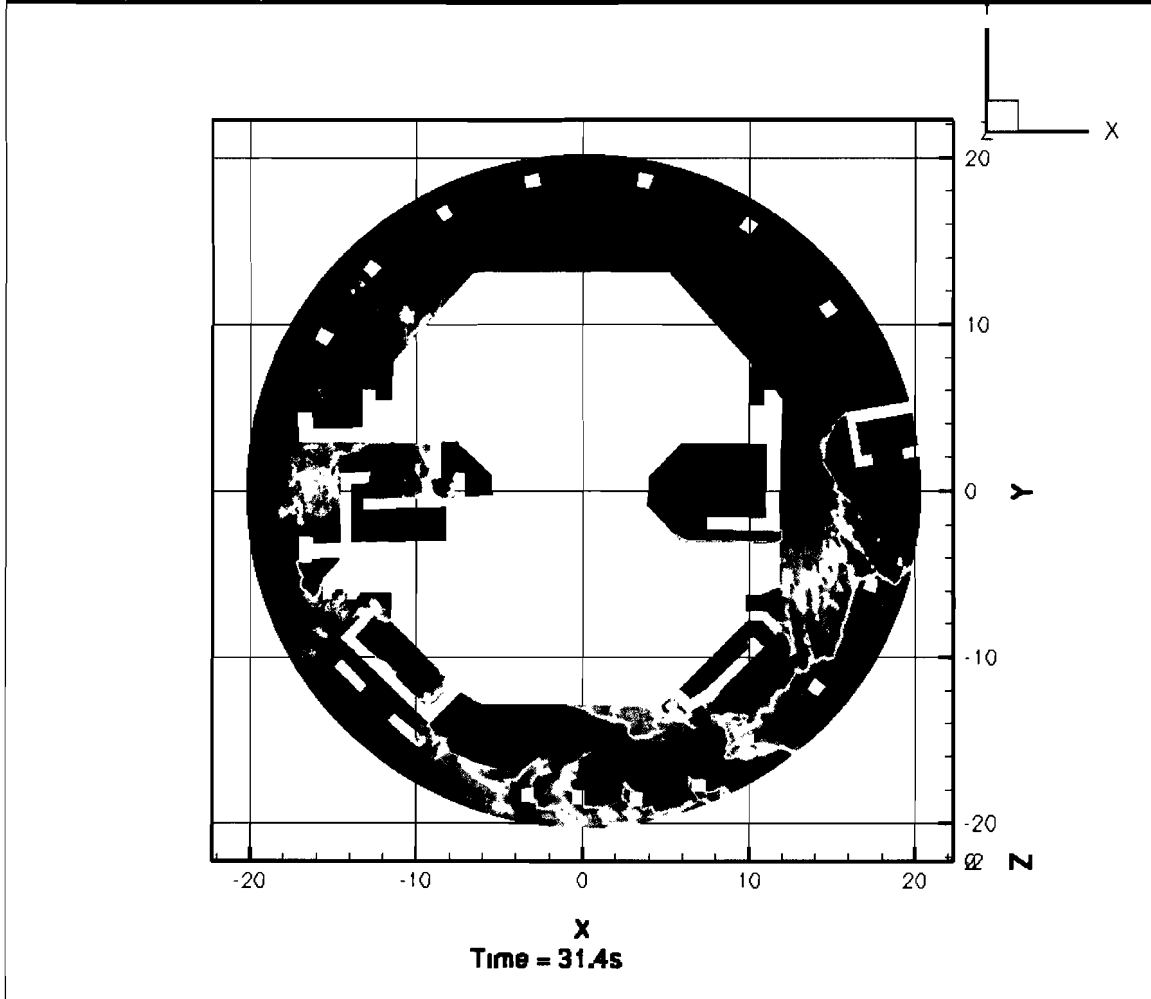


Figure III.2-8. Same as Figure III.2-4 for  $t = 31.4$  Seconds.

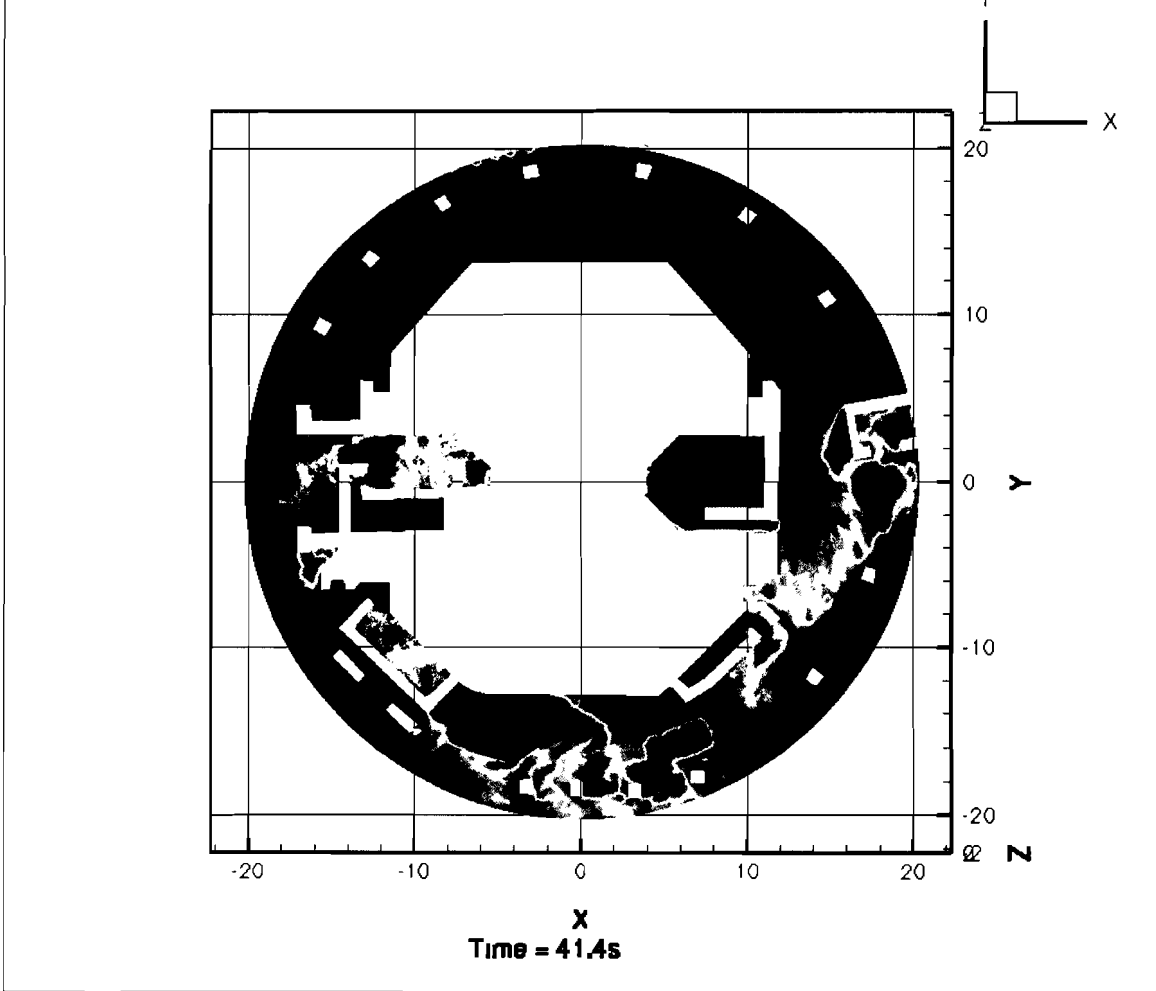


Figure III.2-9. Same as Figure III.2-4 for t = 41.4 Seconds.

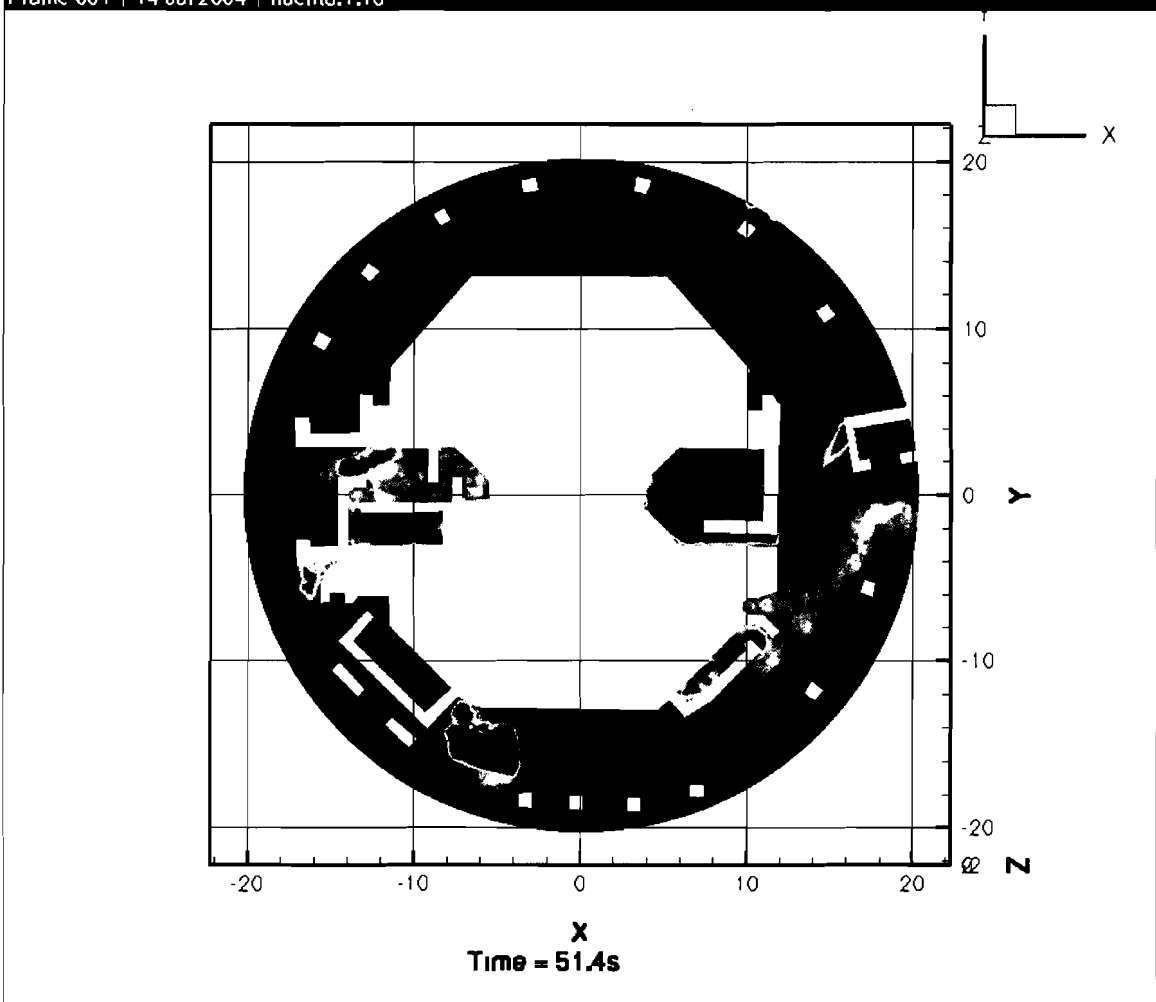


Figure III.2-10. Same as Figure III.2-4 for  $t = 51.4$  Seconds.

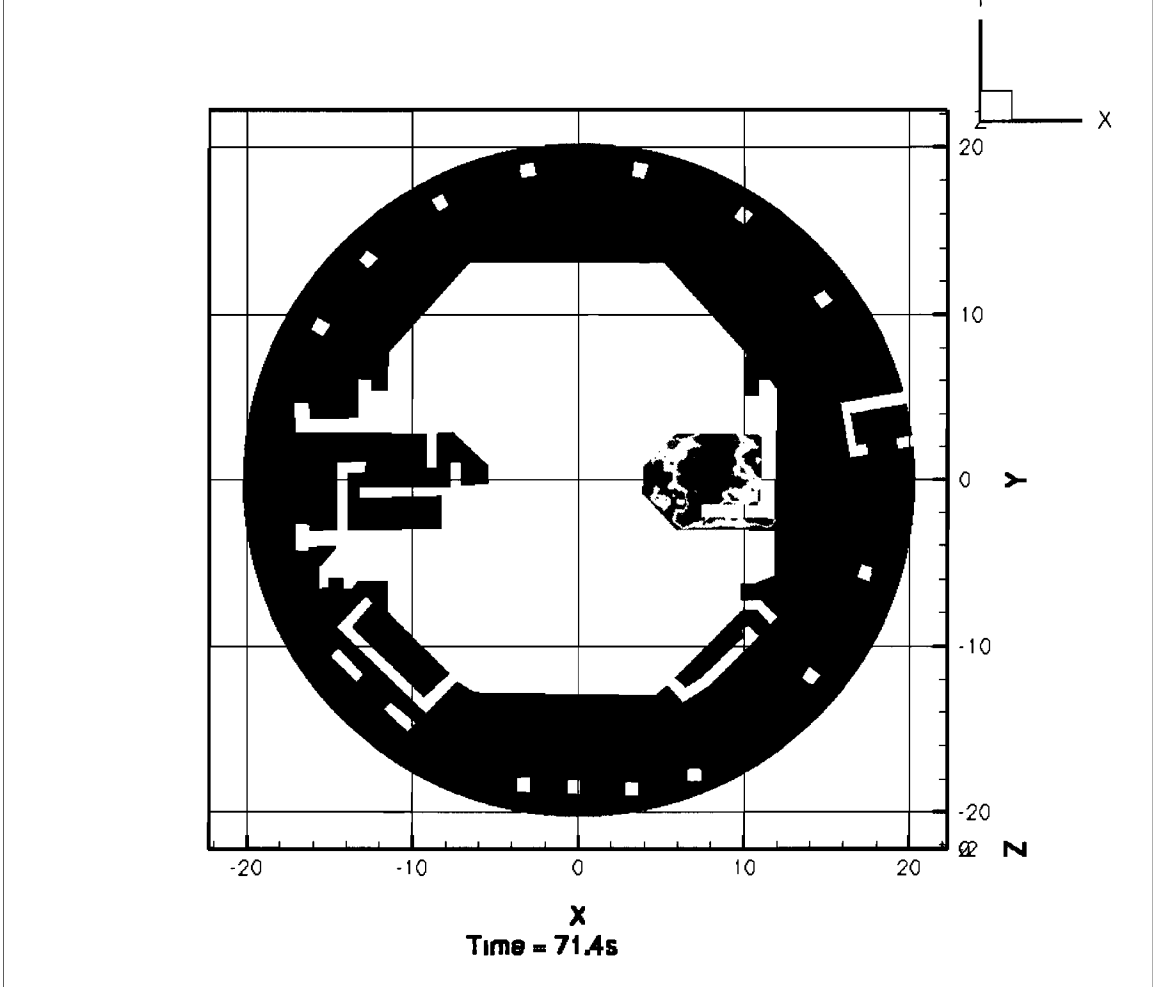


Figure III.2-11. Same as Figure III.2-4 for t = 71.4 Seconds.

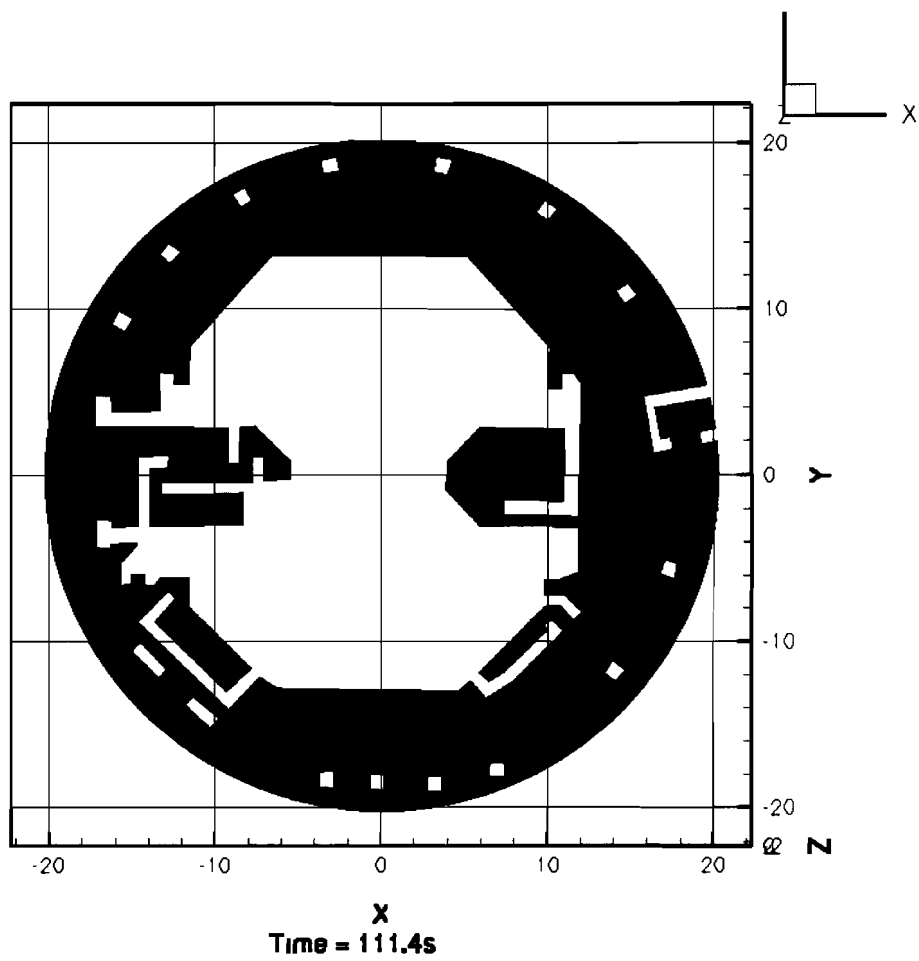
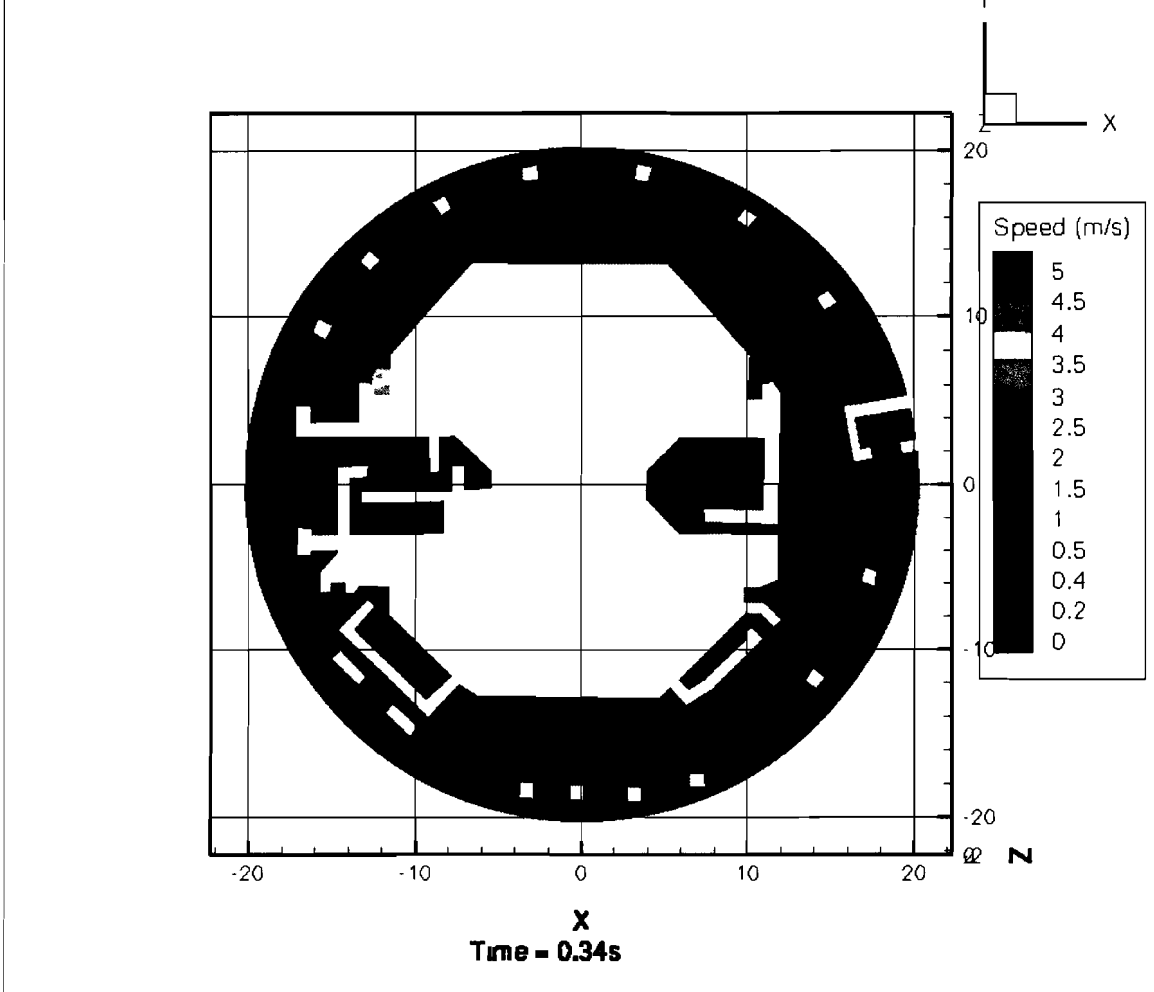


Figure III.2-12. Same as Figure III.2-4 for  $t = 111.4$  Seconds. Note That the Solid Red Color Indicates That the Cells Adjacent to the Floor Are Full of Water, Not That the Entire Pool Is Full of Water.



**Figure III.2-13. Transient VOF Simulation of Containment Pool Fill-Up. Contours of Fluid Velocity Are Shown. Time Snapshot Shown in the Figure Is Seconds after the Break Flow Is Initiated. Note That the Fluid Velocity May Be Water or Air; Figures Showing the Volume Fraction of Water (Figures III.2-4 to III.2-12) Should Be Used to Determine the Actual Water Velocity.**

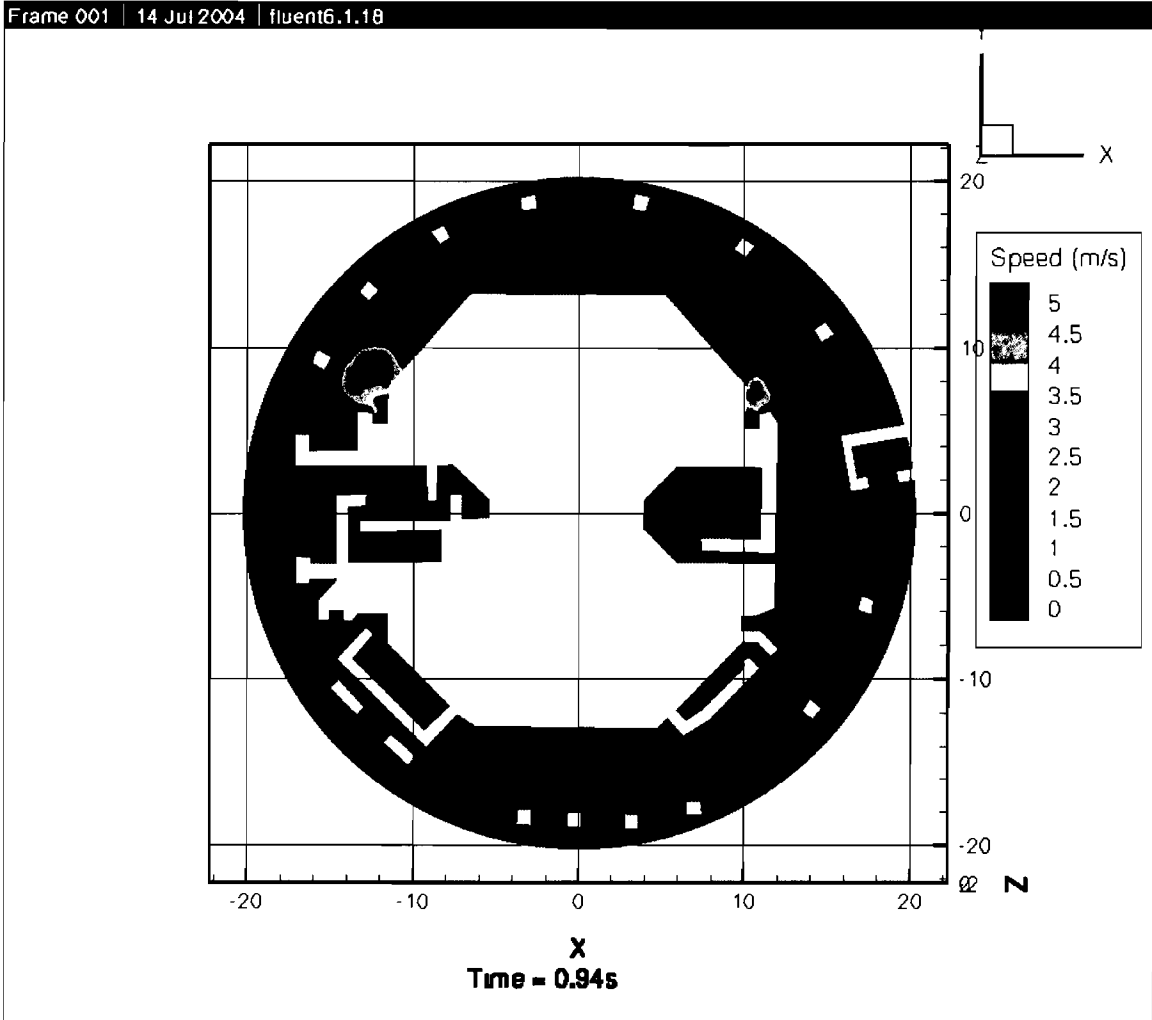


Figure III.2-14. Same as Figure III.2-13 for  $t = 0.94$  Seconds.

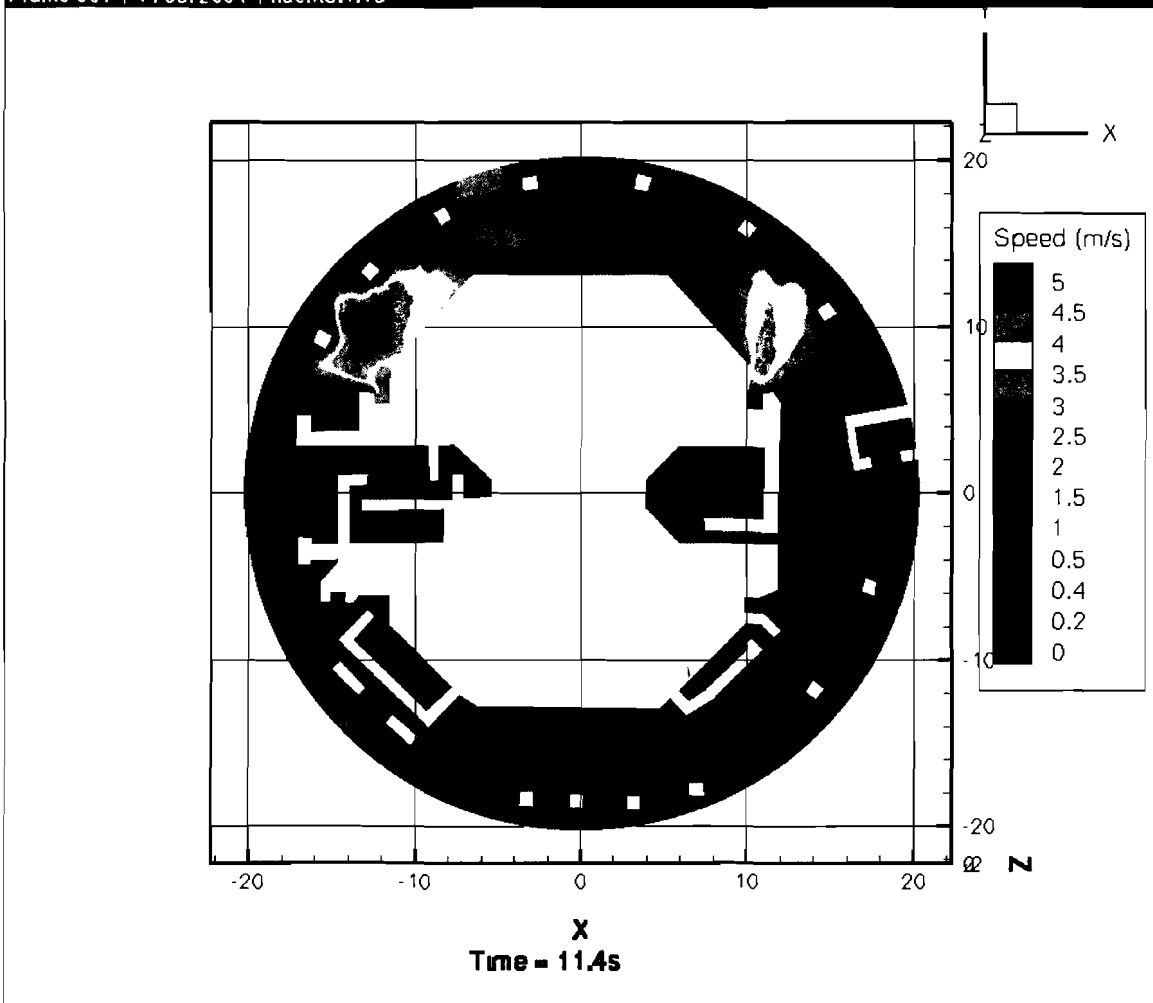


Figure III.2-15. Same as Figure III.2-13 for  $t = 11.4$  Seconds.

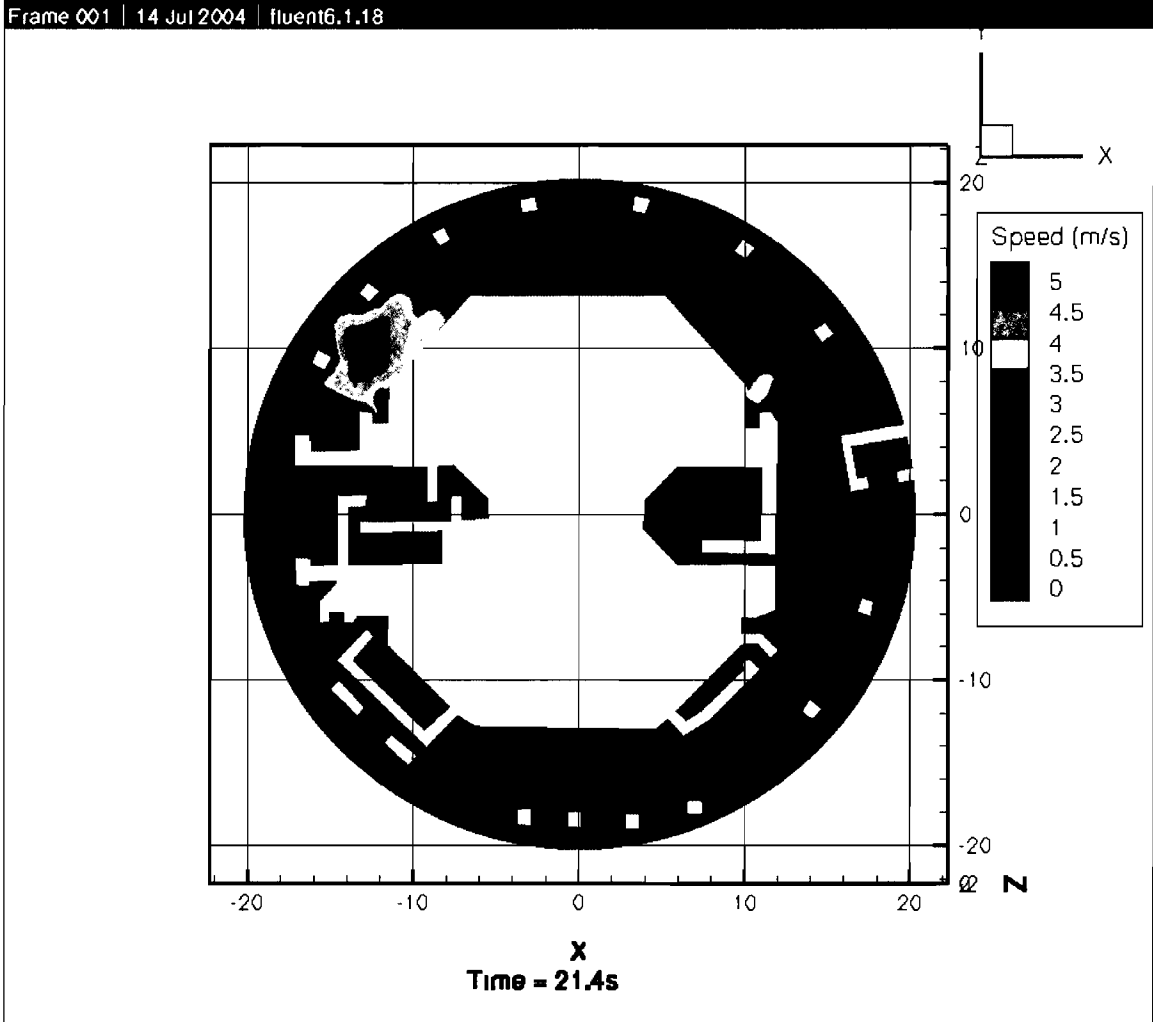


Figure III.2-16. Same as Figure III.2-13 for  $t = 21.4$  Seconds.

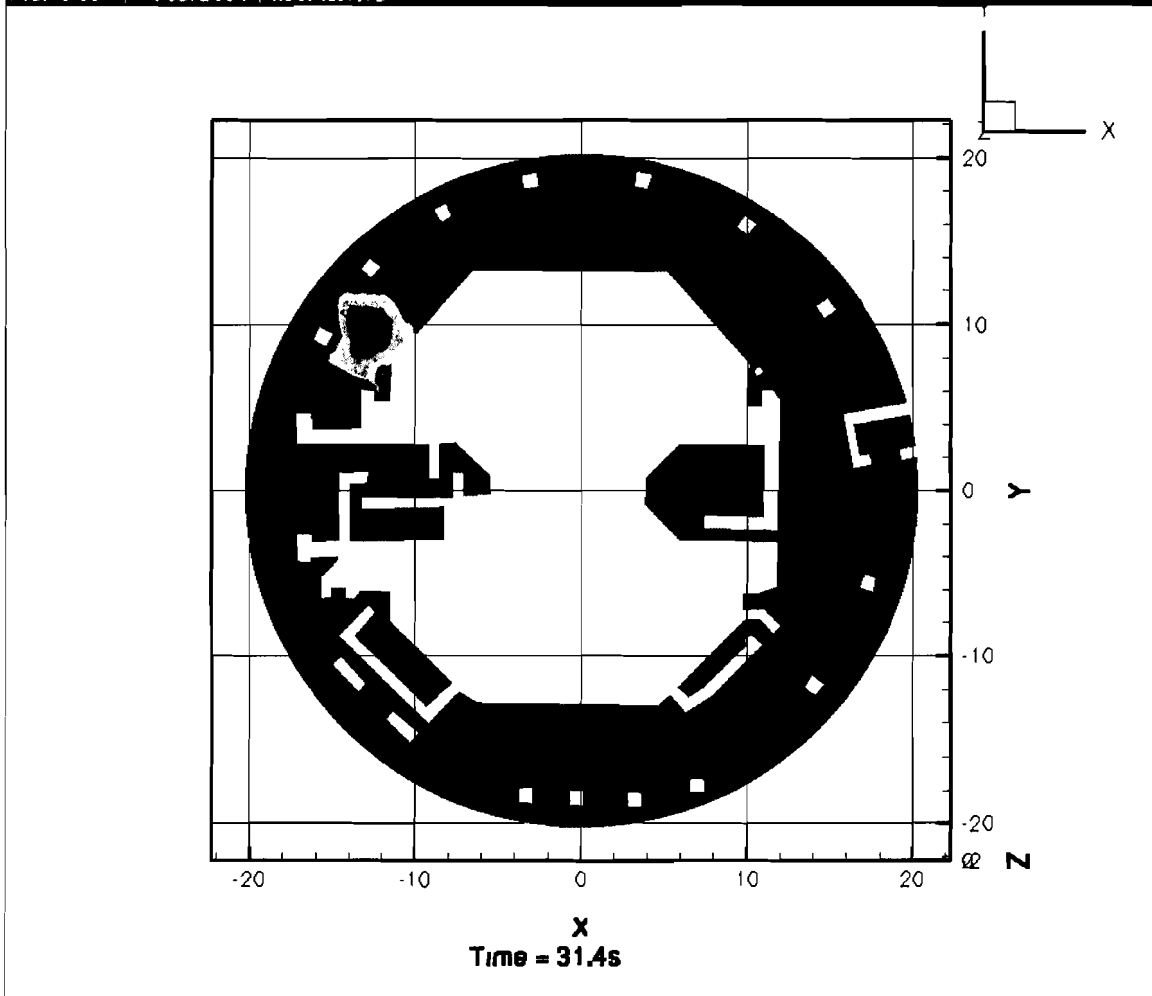


Figure III.2-17. Same as Figure III.2-13 for  $t = 31.4$  Seconds.

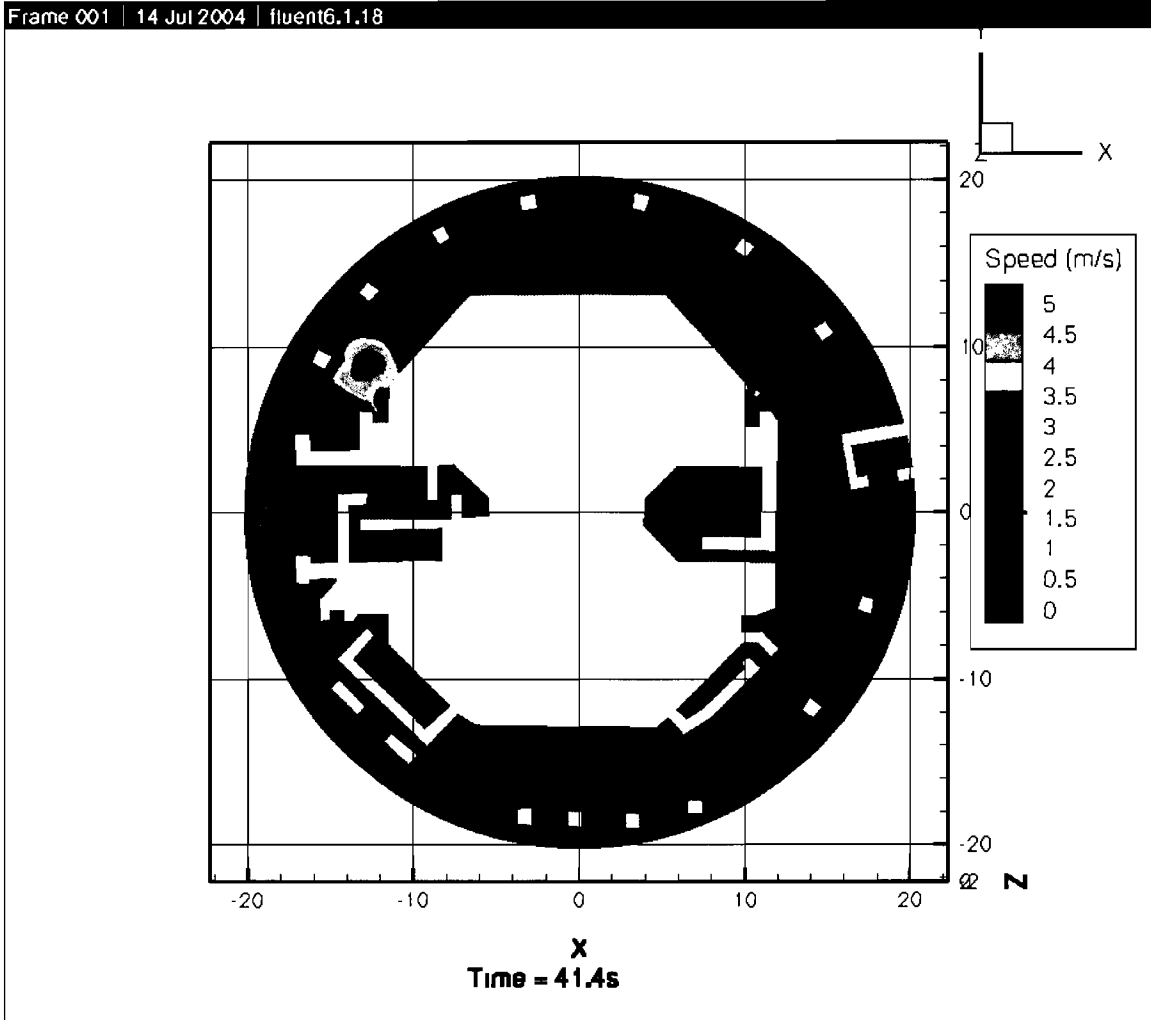


Figure III.2-18. Same as Figure III.2-13 for  $t = 41.4$  Seconds.

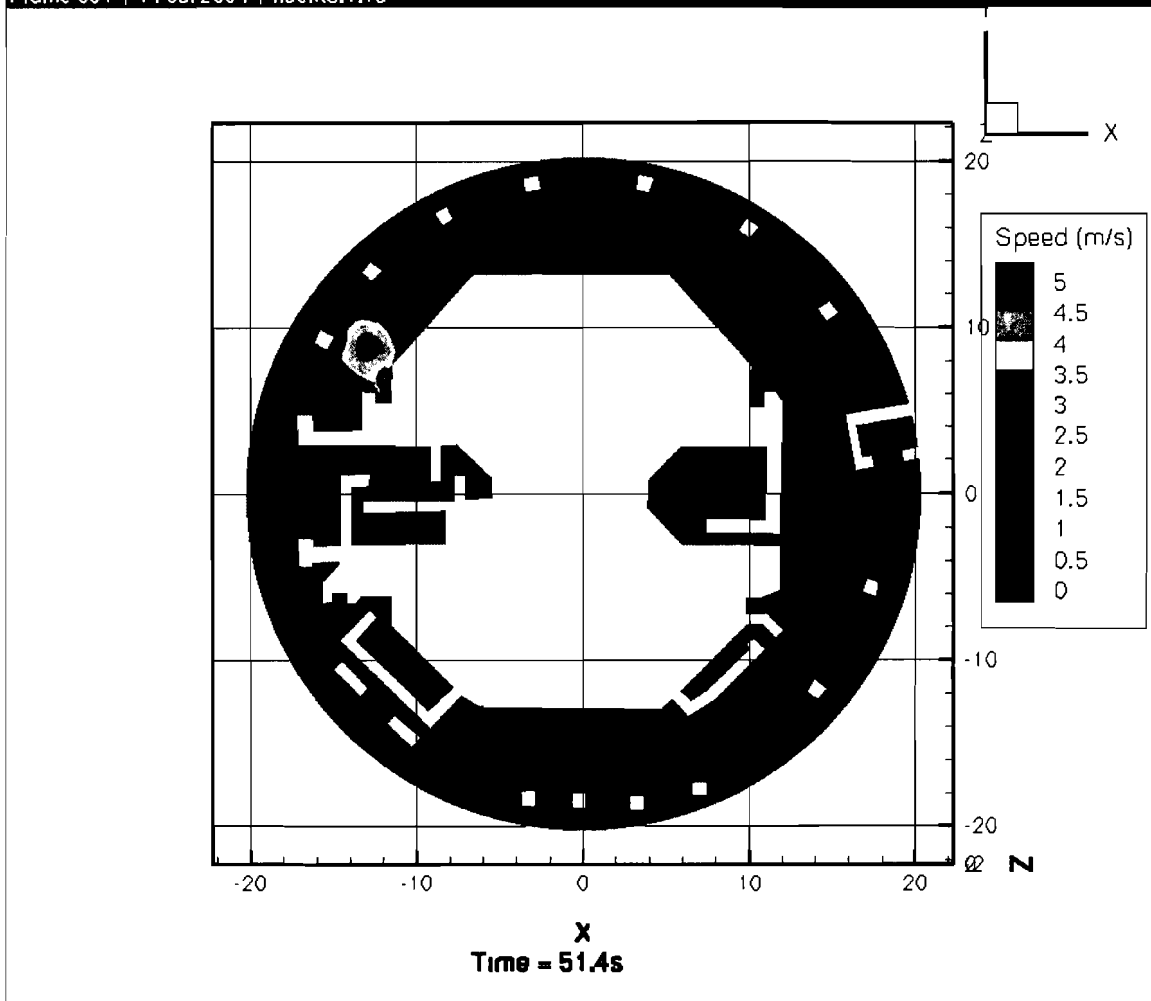


Figure III.2-19. Same as Figure III.2-13 for  $t = 51.4$  Seconds.

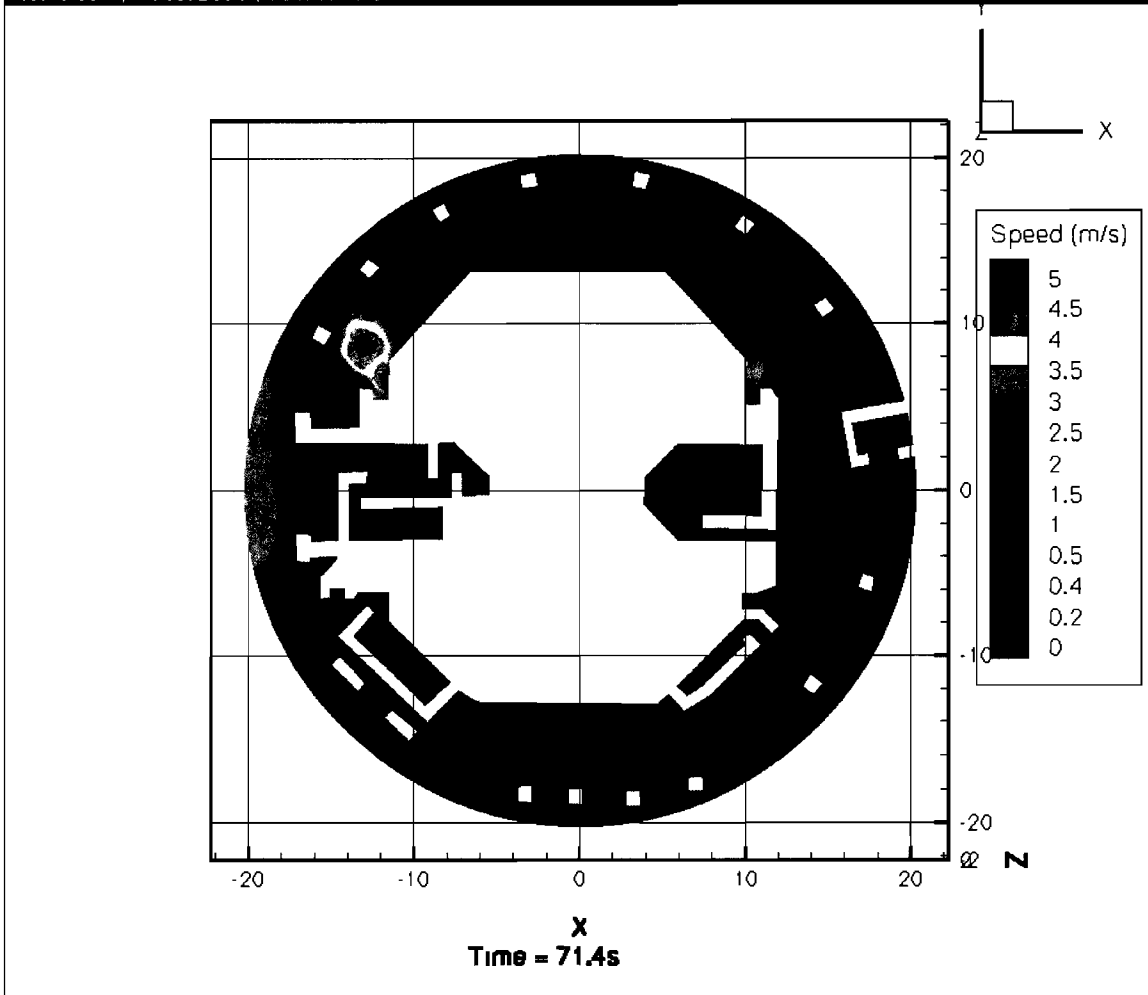


Figure III.2-20. Same as Figure III.2-13 for t = 71.4 Seconds.

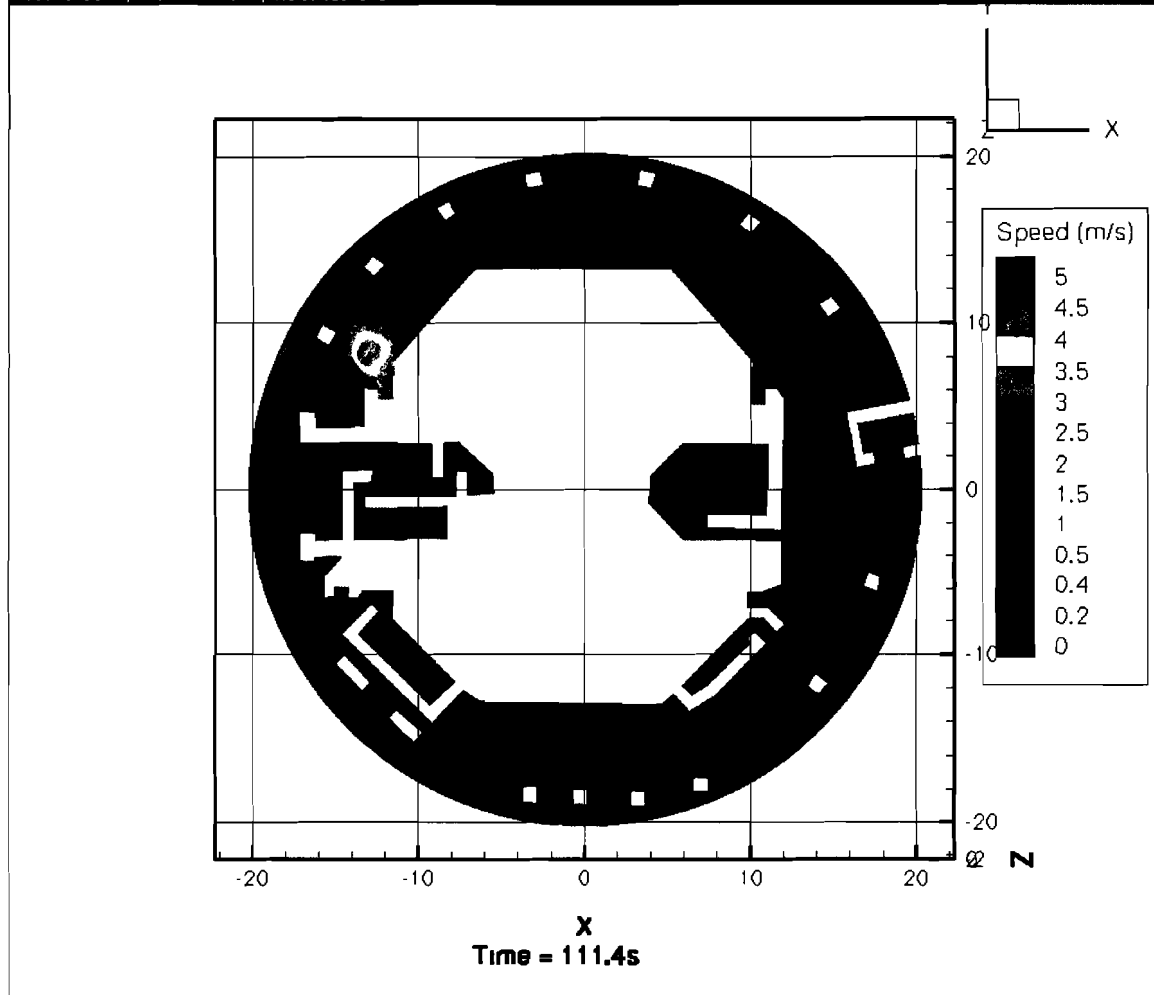
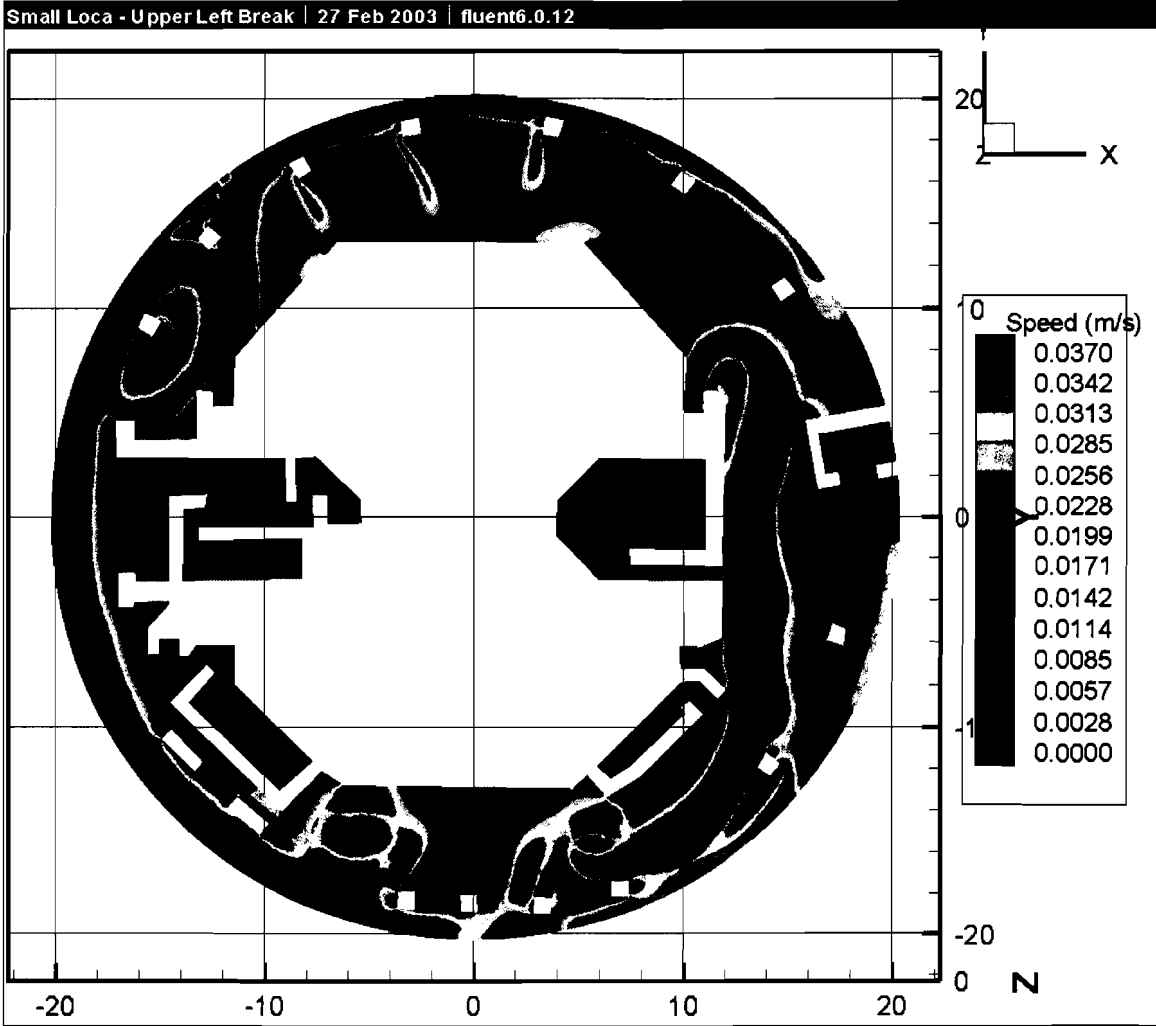


Figure III.2-21. Same as Figure III.2-13 for  $t = 111.4$  Seconds.



**Figure III.2-22. Small LOCA Break Located in the Upper-Left Quadrant. Speeds Greater Than or Equal to the Fiber Threshold (0.037 m/s) Are Colored RED.**

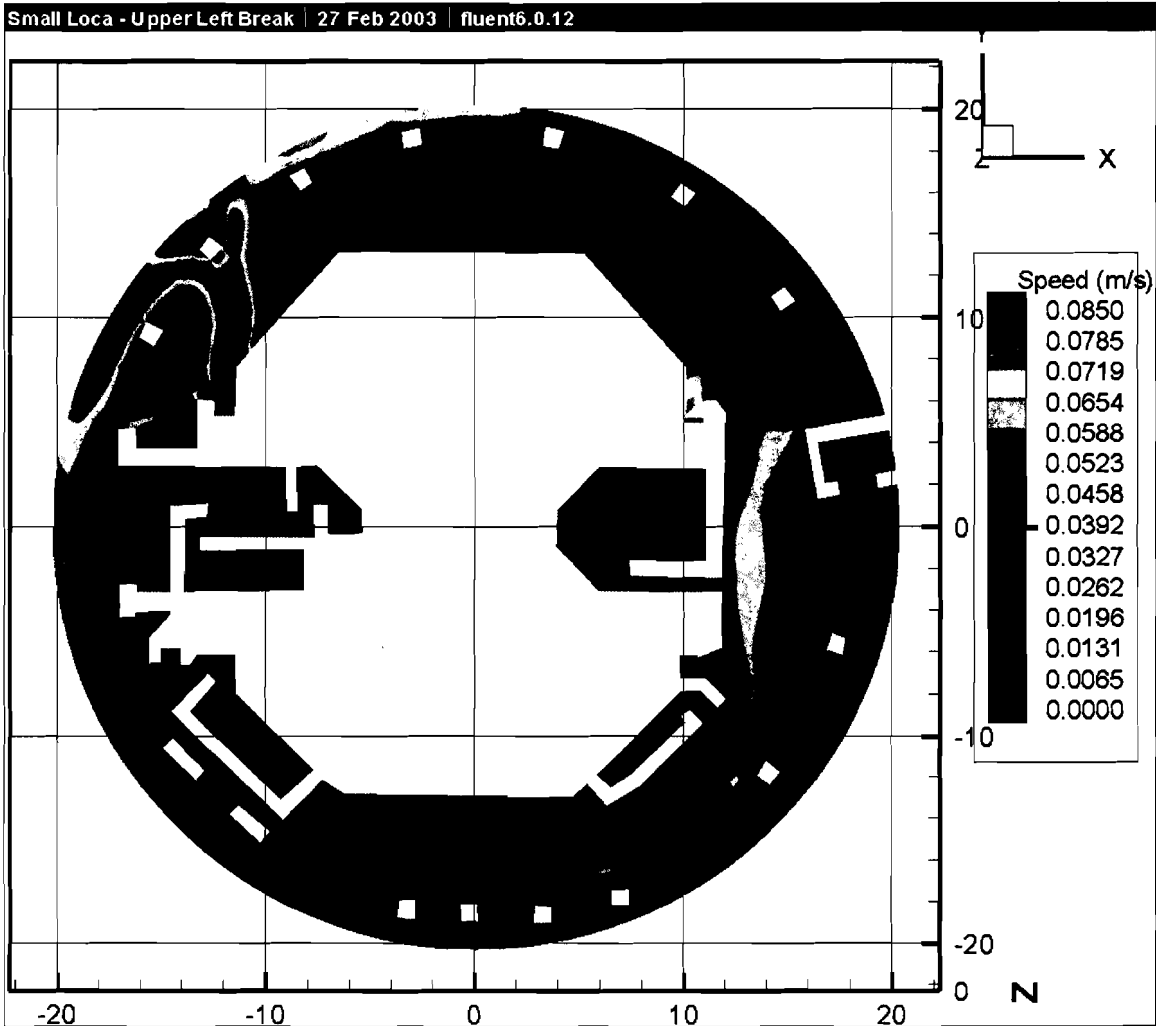


Figure III.2-23. Small LOCA Break Located in the Upper-Left Quadrant. Speeds Greater Than or Equal to the RMI Threshold (0.085 m/s) Are Colored RED.

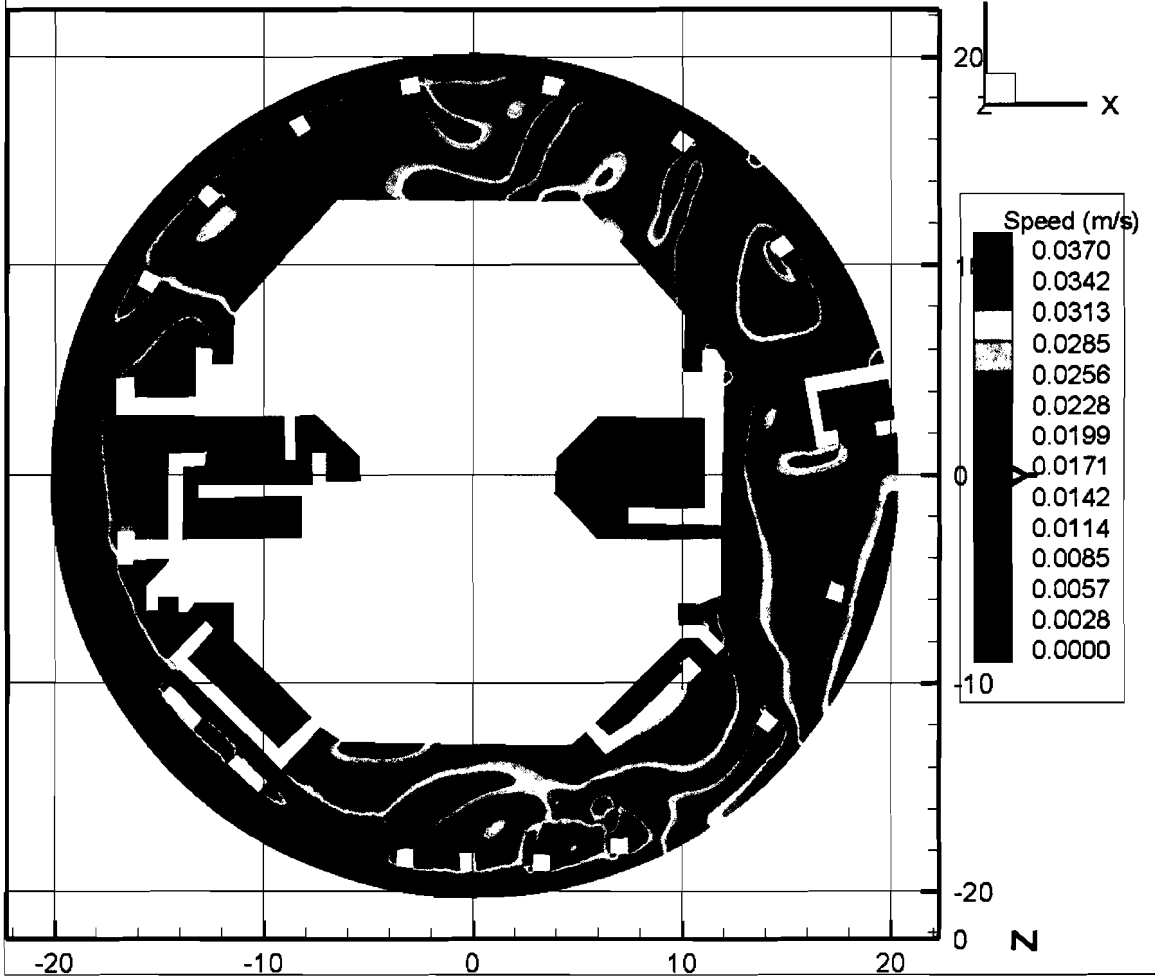
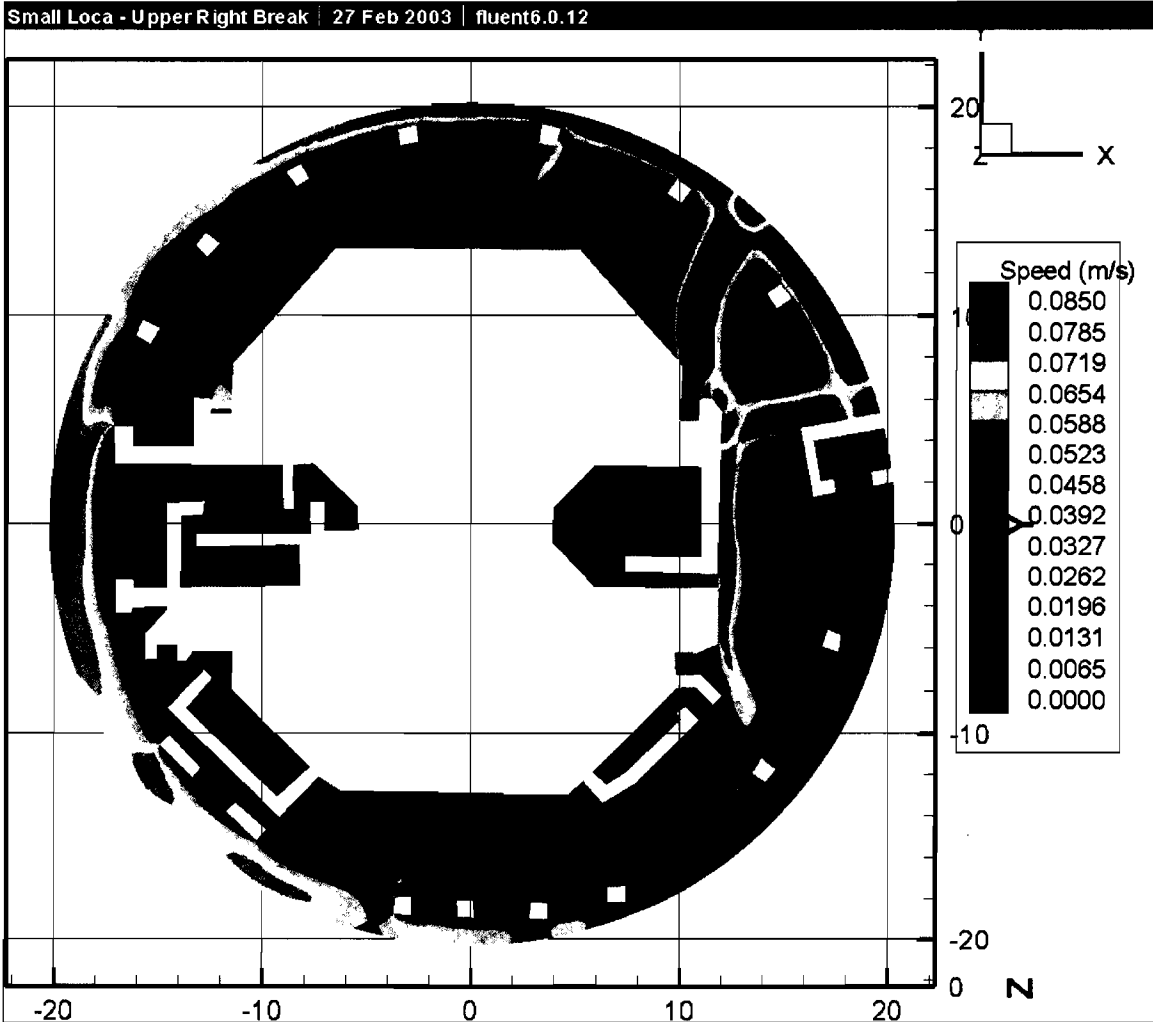
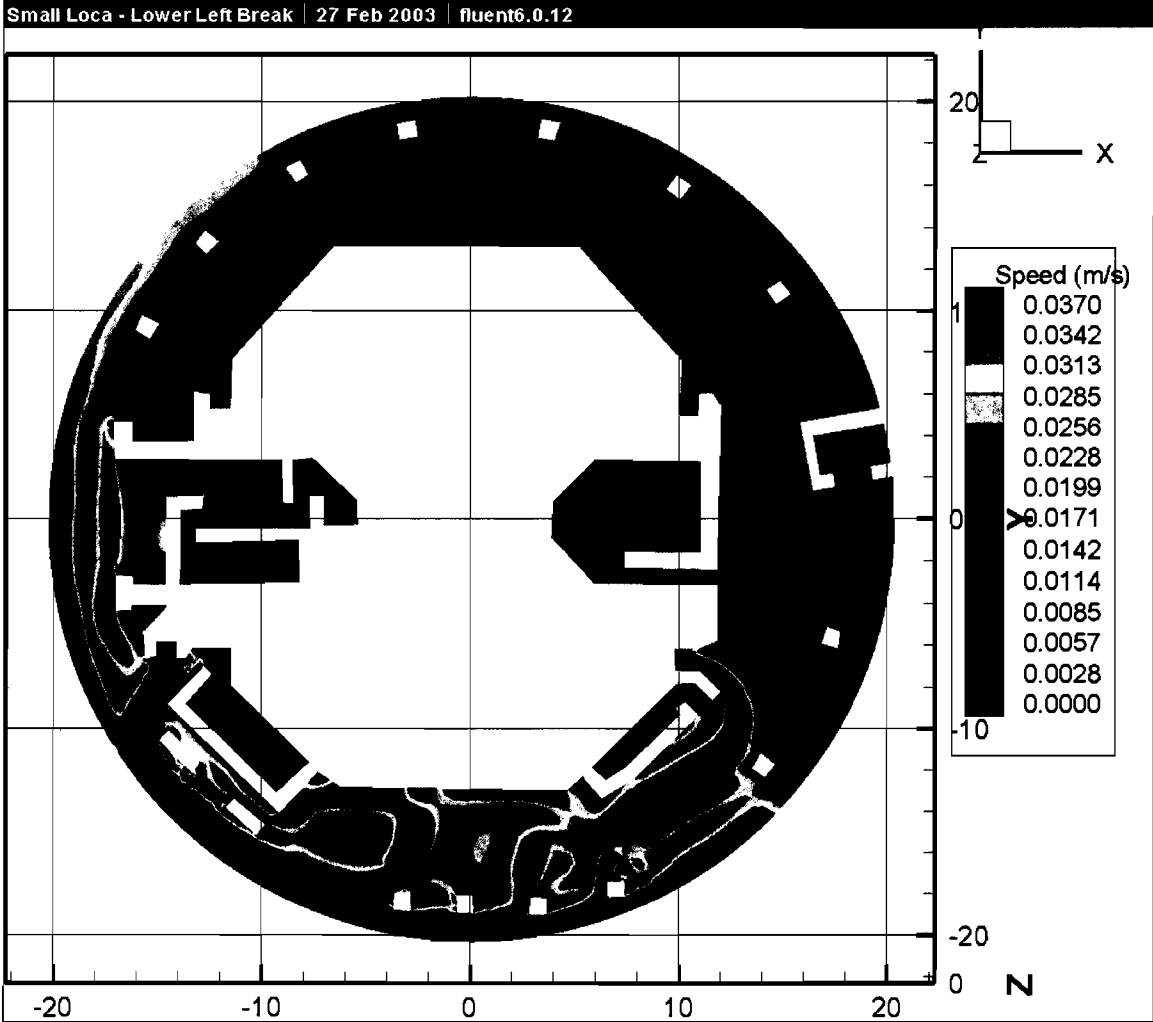


Figure III.2-24. Small LOCA Break Located in the Upper-Right Quadrant. Speeds Greater Than or Equal to the Fiber Threshold (0.037 m/s) Are Colored RED.



**Figure III.2-25. Small LOCA Break Located in the Upper-Right Quadrant. Speeds Greater Than or Equal to the RMI Threshold (0.085 m/s) Are Colored RED.**



**Figure III.2-26. Small LOCA Break Located in the Lower-Left Quadrant. Speeds Greater Than or Equal to the Fiber Threshold (0.037 m/s) Are Colored RED.**

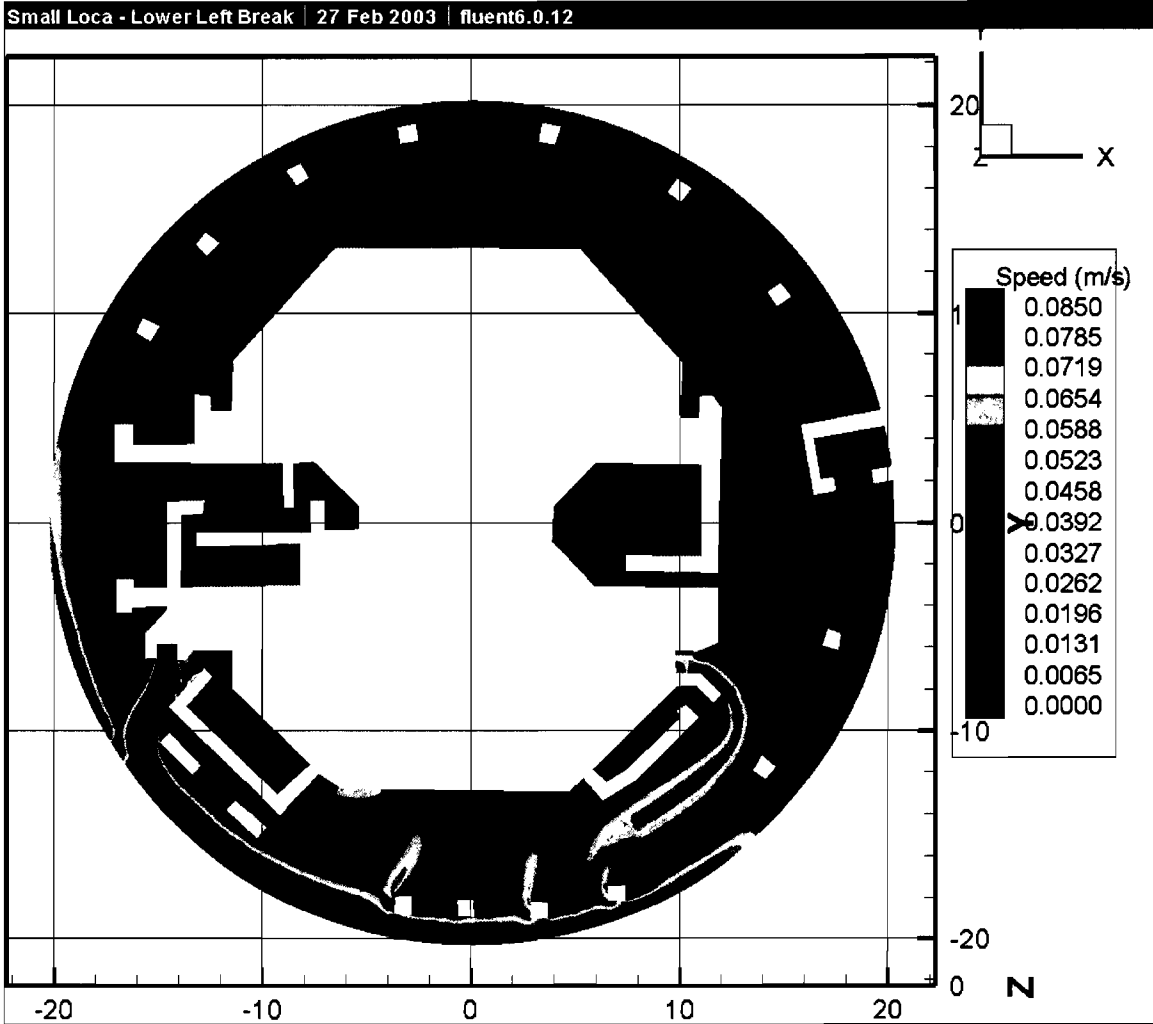


Figure III.2-27. Small LOCA Break Located in the Lower-Left Quadrant. Speeds Greater Than or Equal to the RMI Threshold (0.085 m/s) Are Colored RED.

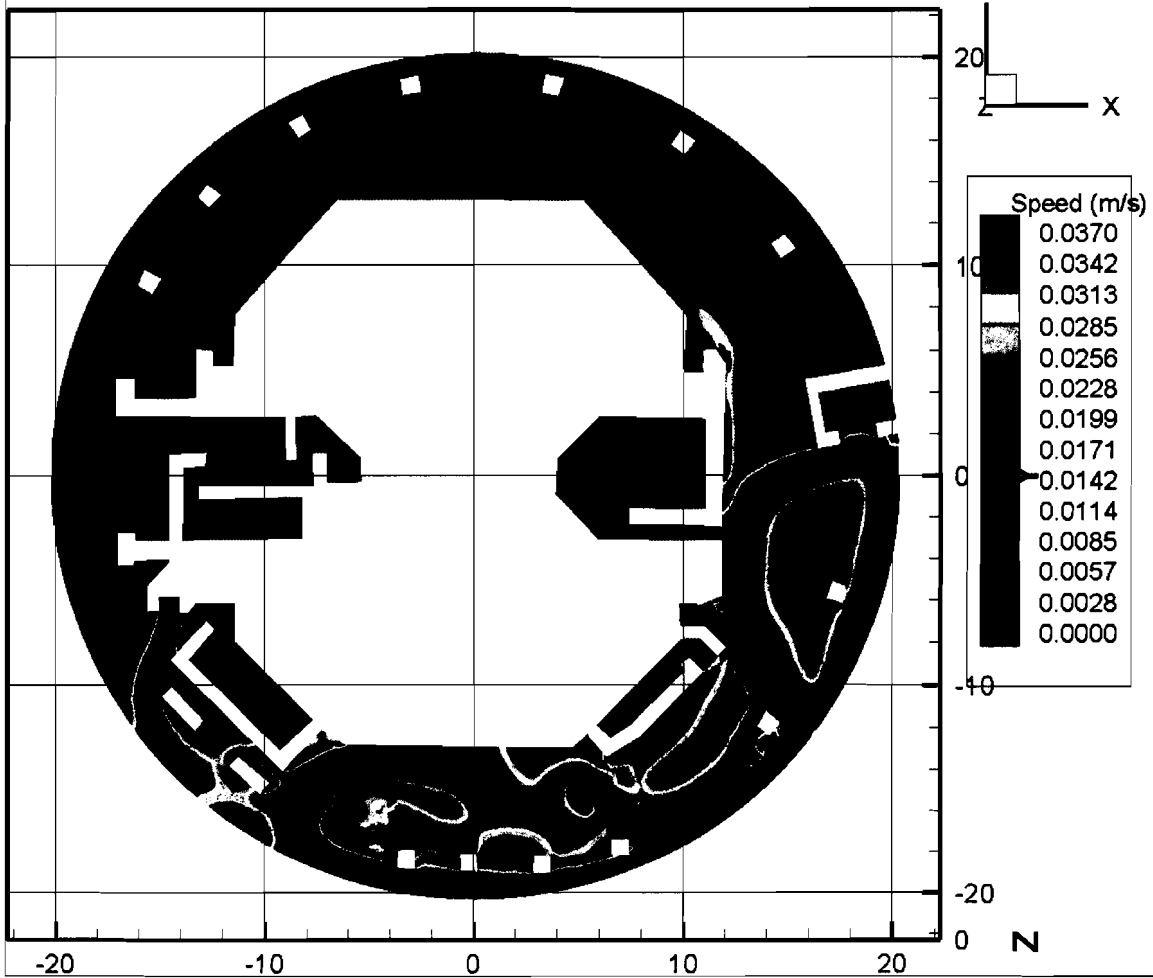


Figure III.2-28. Small LOCA Break Located in the Lower-Right Quadrant. Speeds Greater Than or Equal to the Fiber Threshold (0.037 m/s) Are Colored RED.

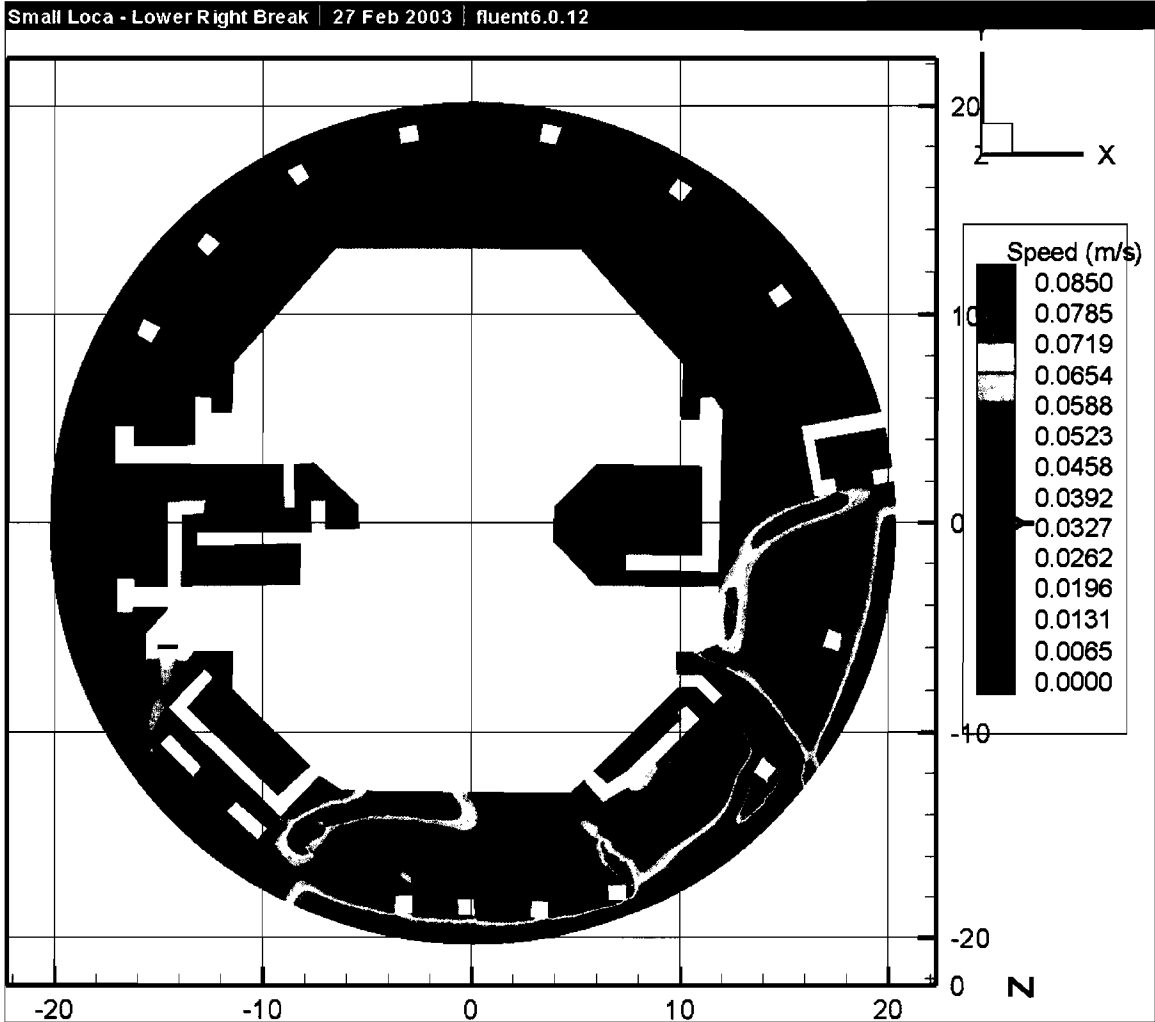


Figure III.2-29. Small LOCA Break Located in the Lower-Right Quadrant. Speeds Greater Than or Equal to the RMI Threshold (0.085 m/s) Are Colored RED.

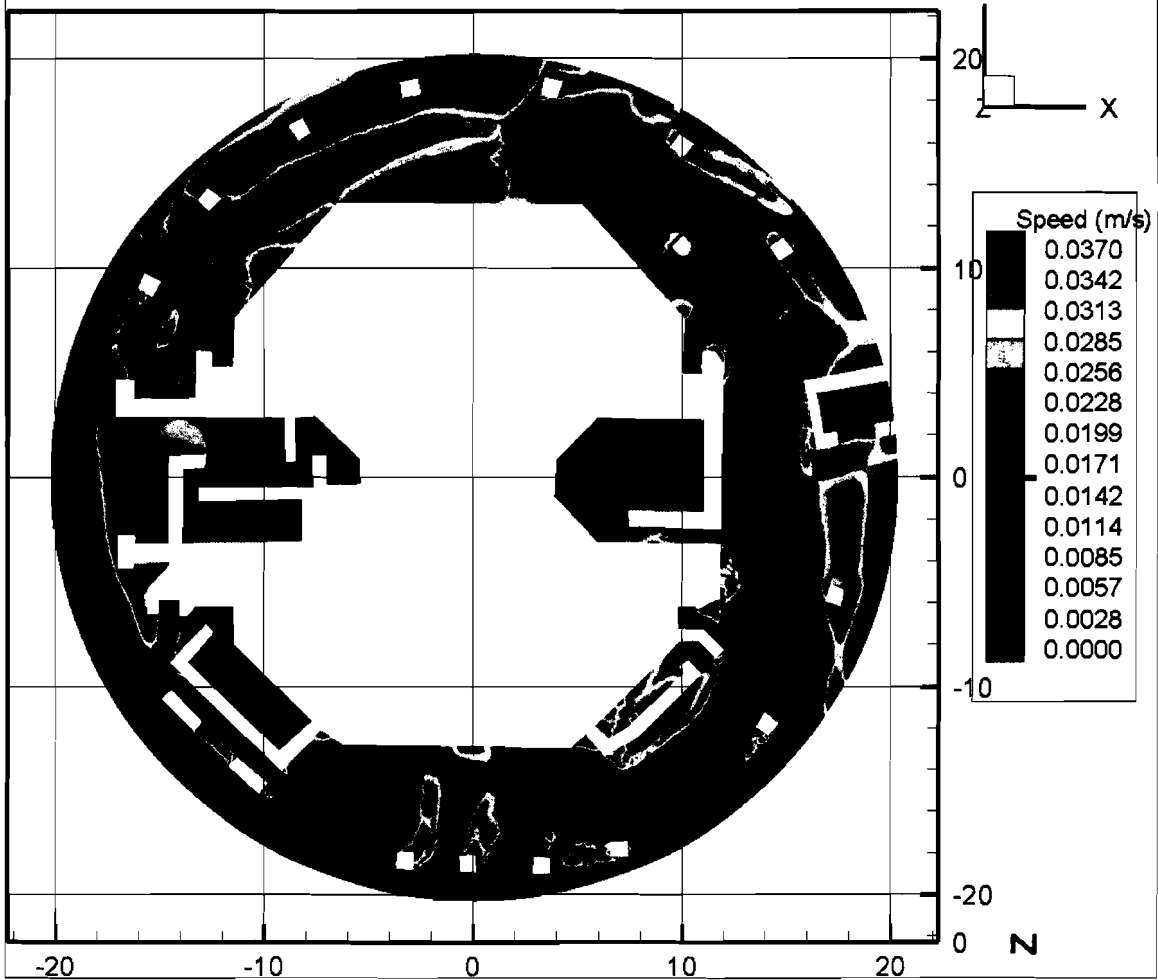


Figure III.2-30. Large LOCA Break Located in the Upper-Left Quadrant. Speeds Greater Than or Equal to the Fiber Threshold (0.037 m/s) Are Colored RED.

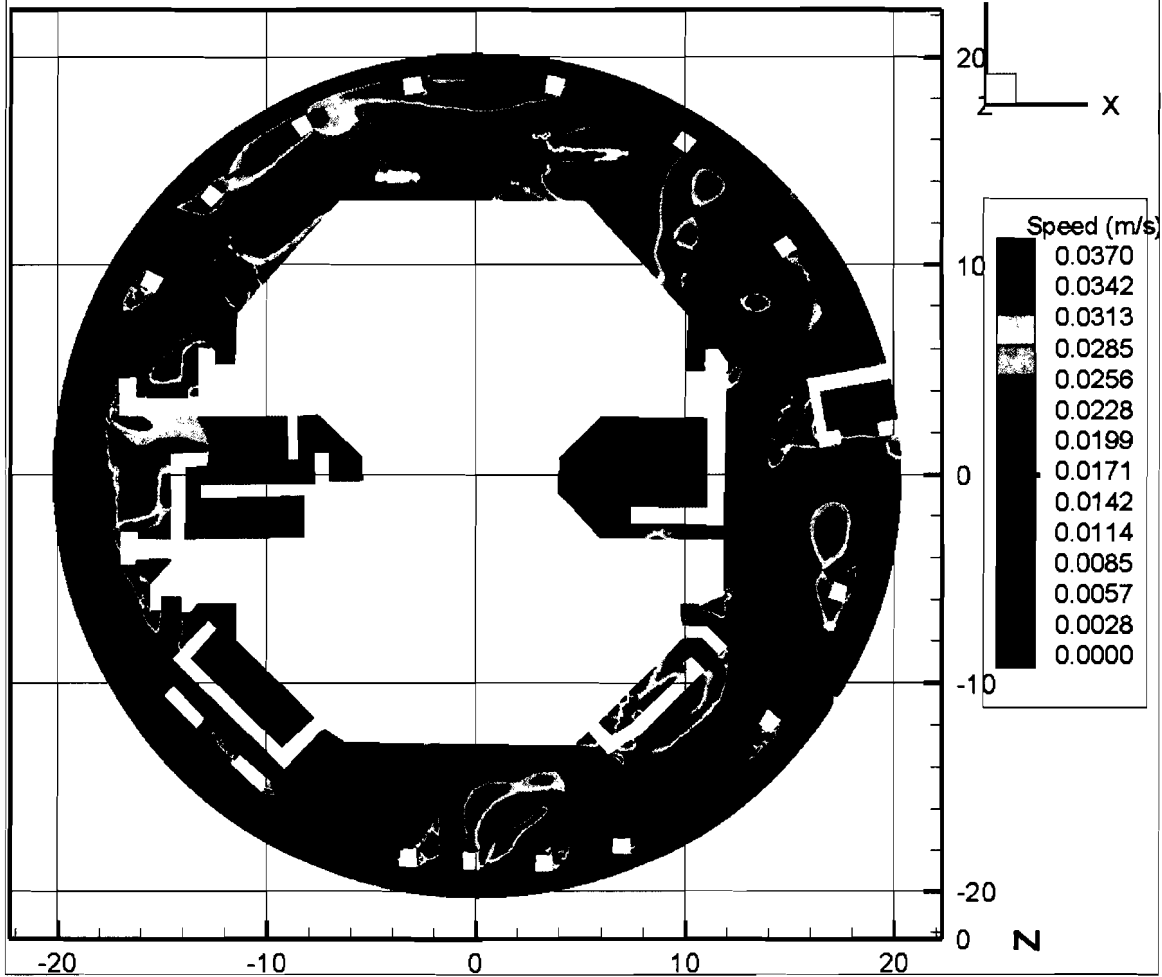
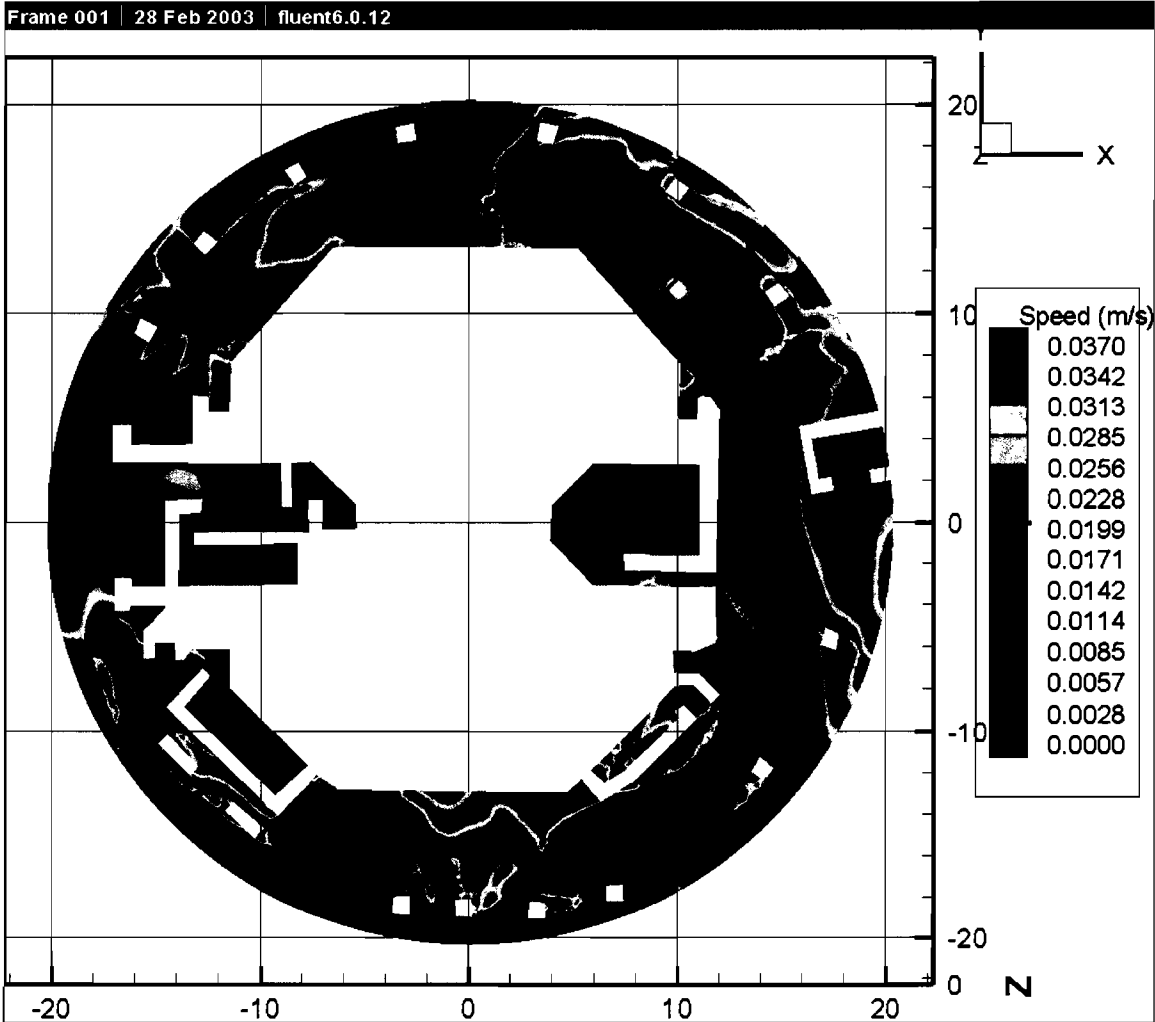


Figure III.2-31. Large LOCA Break Located in the Upper-Right Quadrant. Speeds Greater Than or Equal to the Fiber Threshold (0.037 m/s) Are Colored RED.



**Figure III.2-32. Large LOCA Break Located in the Lower-Left Quadrant. Speeds Greater Than or Equal to the Fiber Threshold (0.037 m/s) Are Colored RED.**

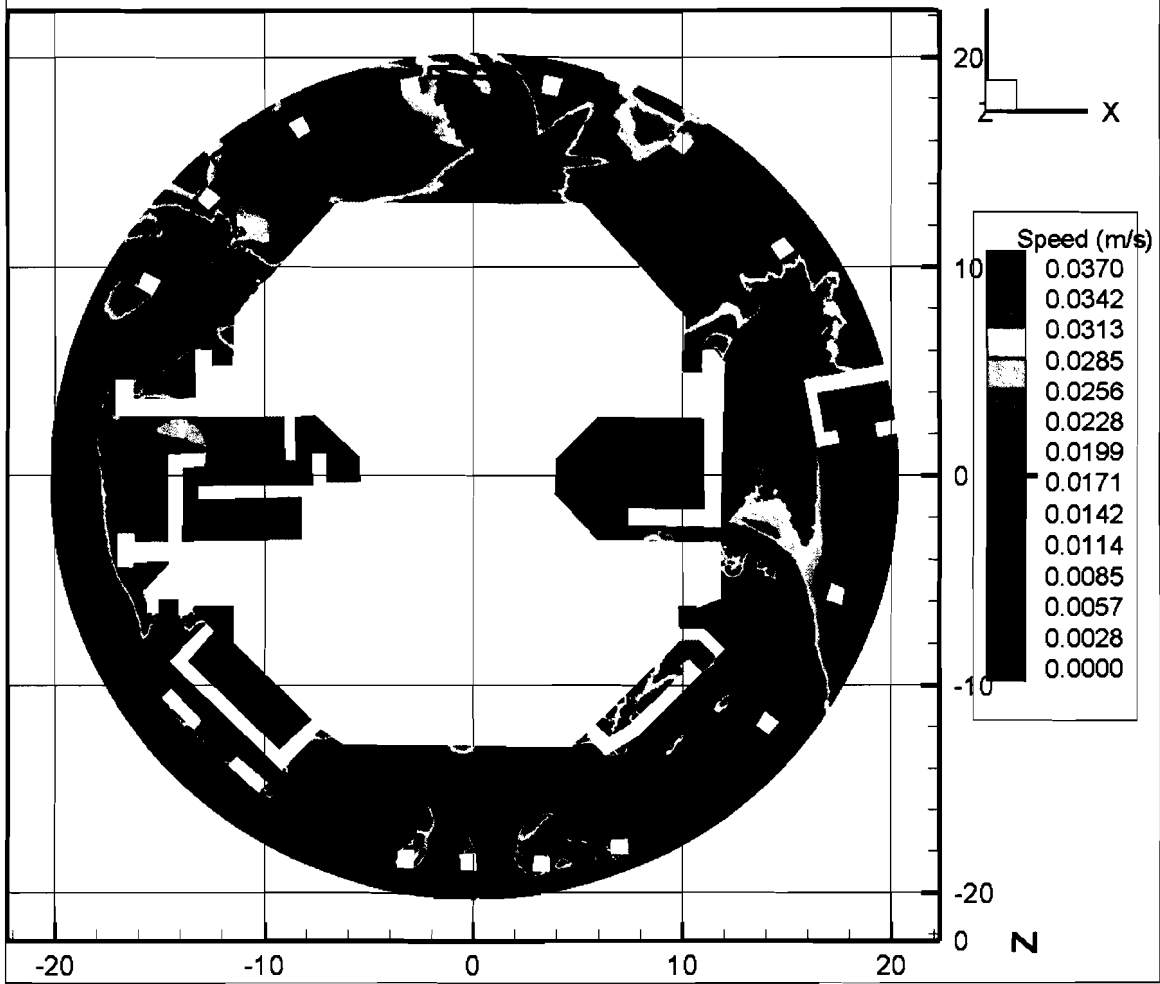


Figure III.2-33. Large LOCA Break Located in the Lower-Right Quadrant. Speeds Greater Than or Equal to the Fiber Threshold (0.037 m/s) Are Colored RED.

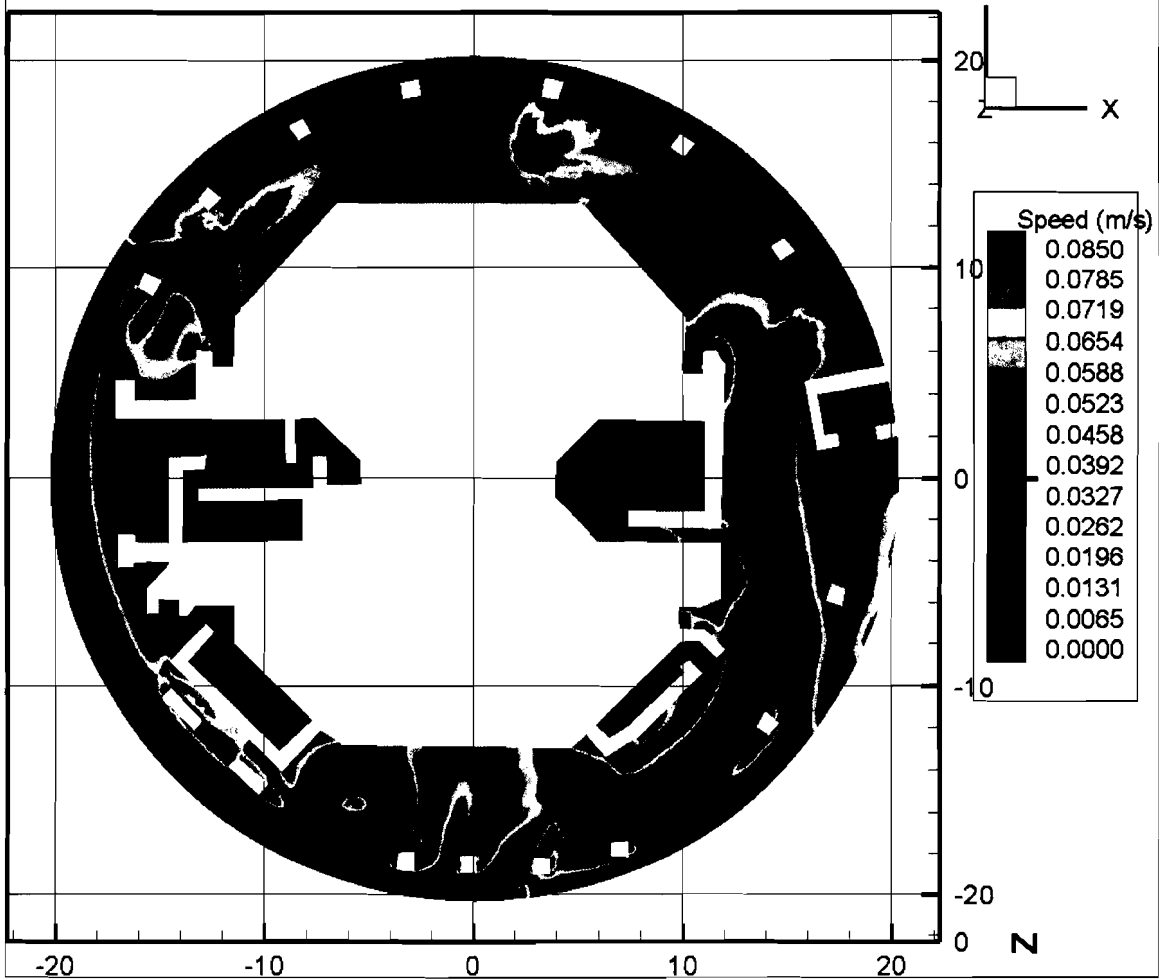


Figure III.2-34. Large LOCA Break Located in the Upper-Left Quadrant. Speeds Greater Than or Equal to the RMI Threshold (0.085 m/s) Are Colored RED.

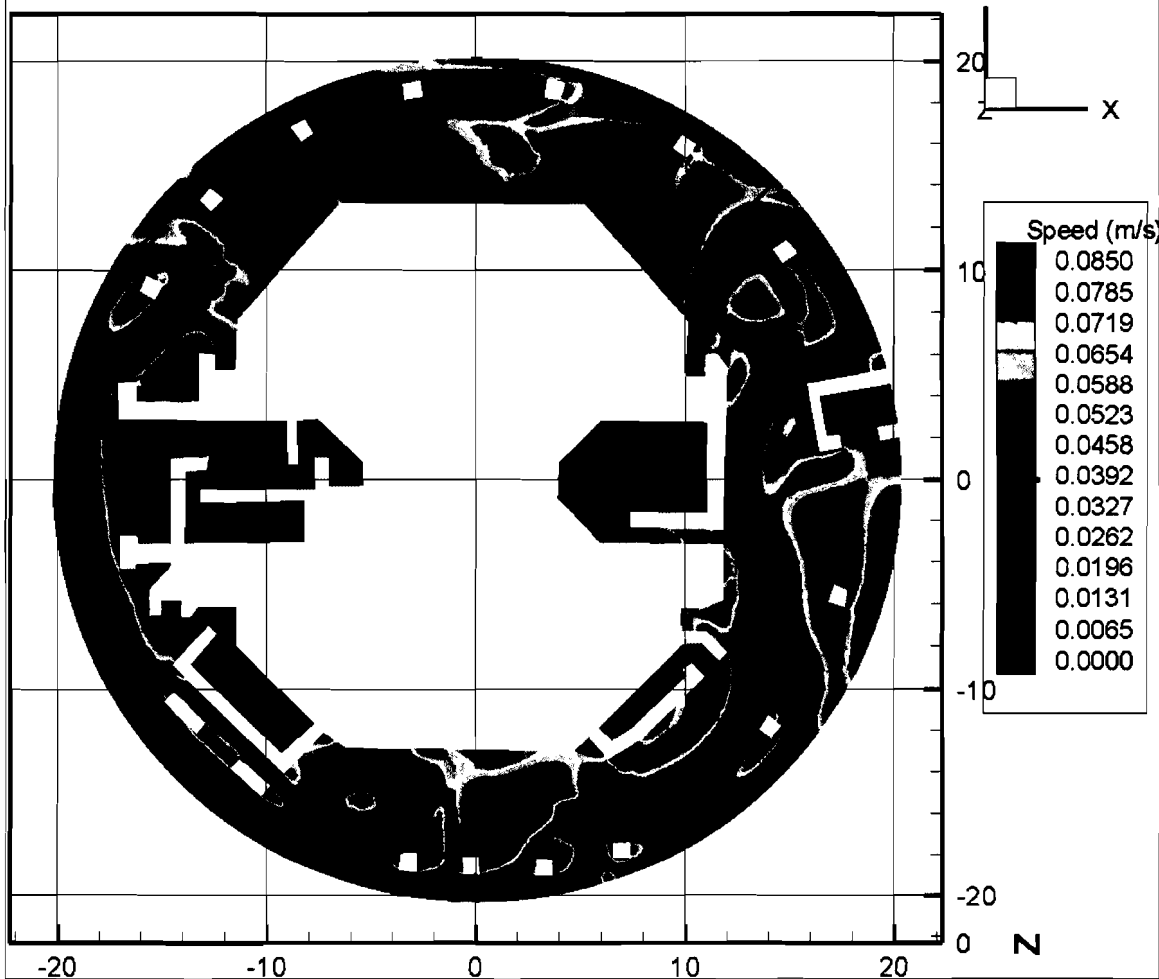


Figure III.2-35. Large LOCA Break Located in the Upper-Right Quadrant. Speeds Greater Than or Equal to the RMI Threshold (0.085 m/s) Are Colored RED.

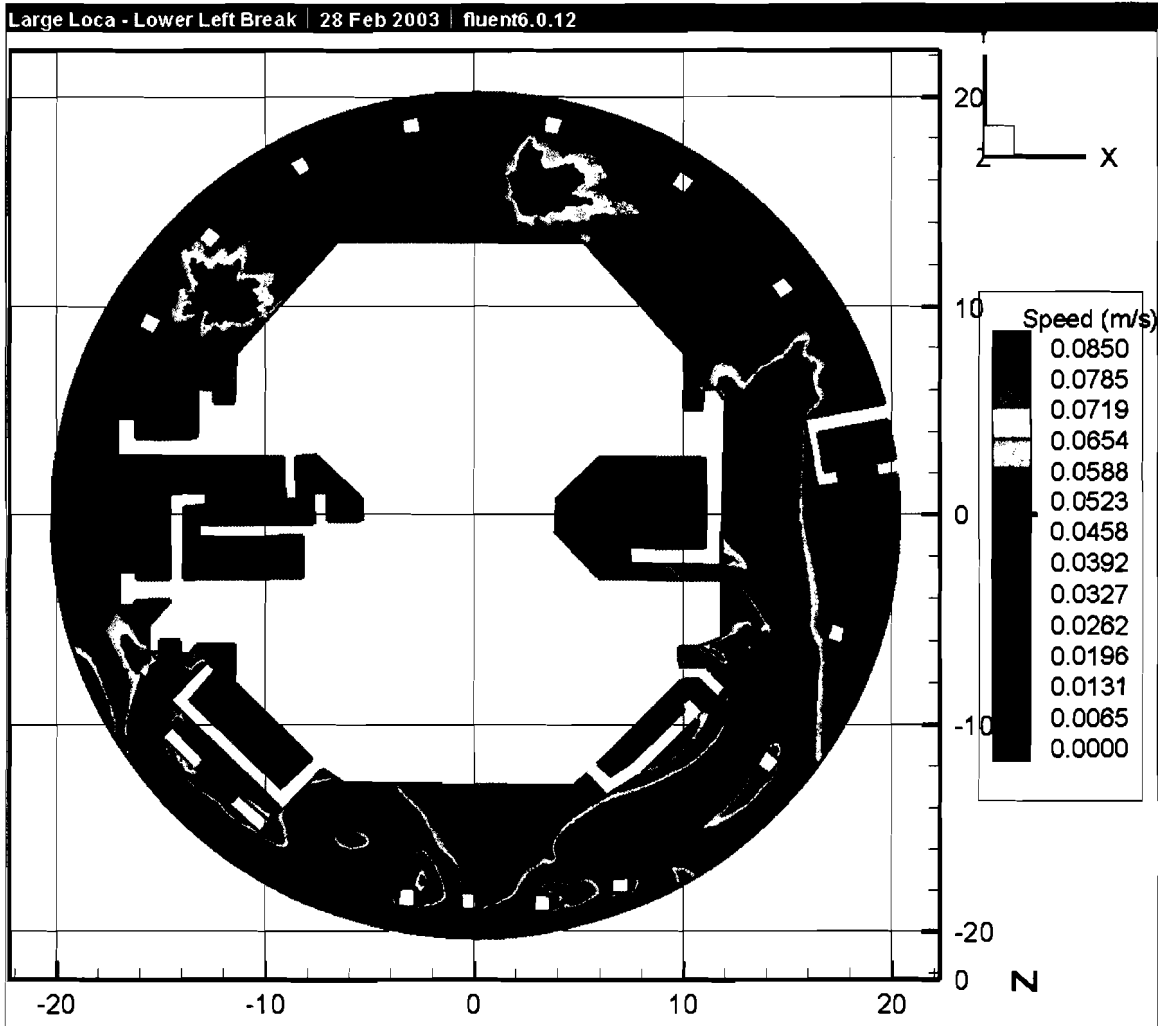


Figure III.2-36. Large LOCA Break Located in the Lower-Left Quadrant. Speeds Greater Than or Equal to the RMI Threshold (0.085 m/s) Are Colored RED.

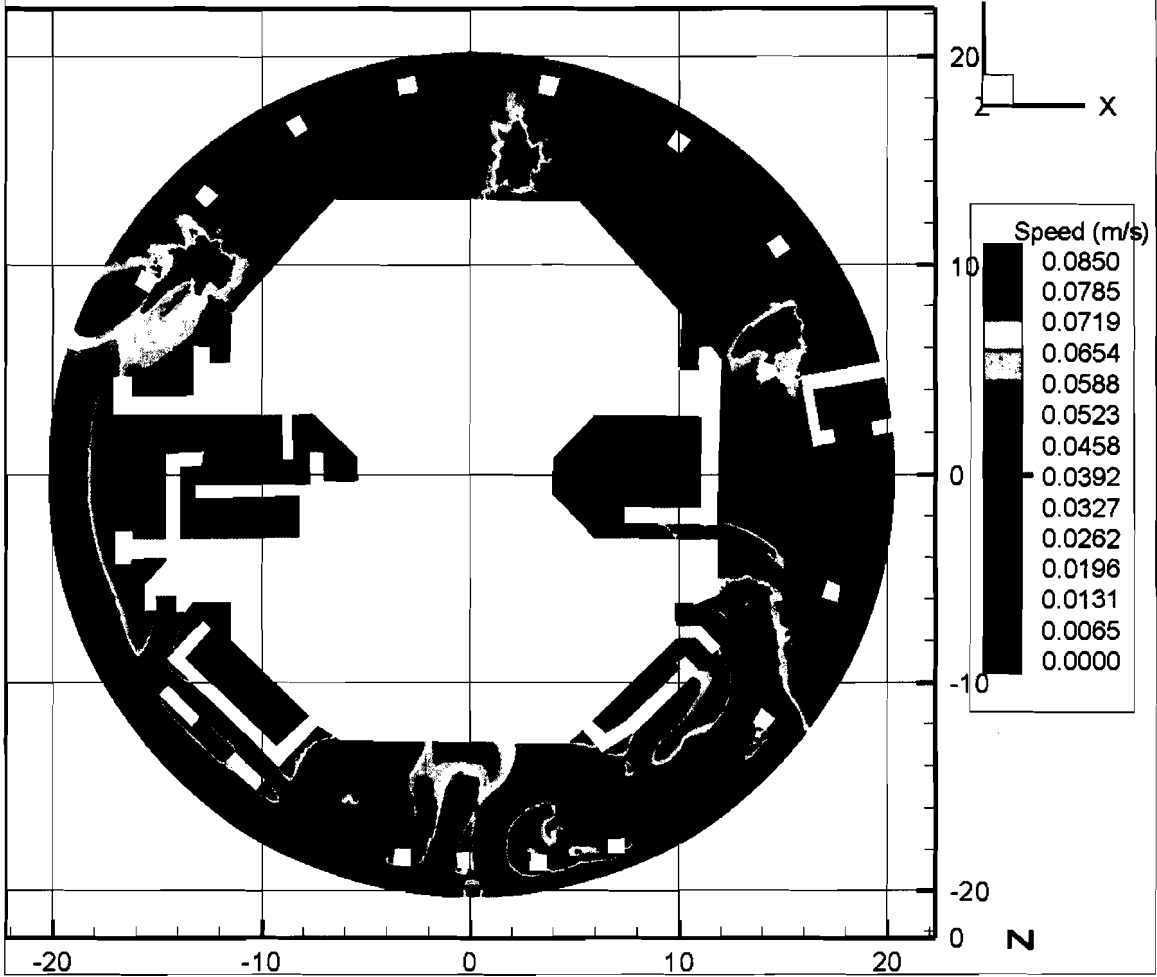
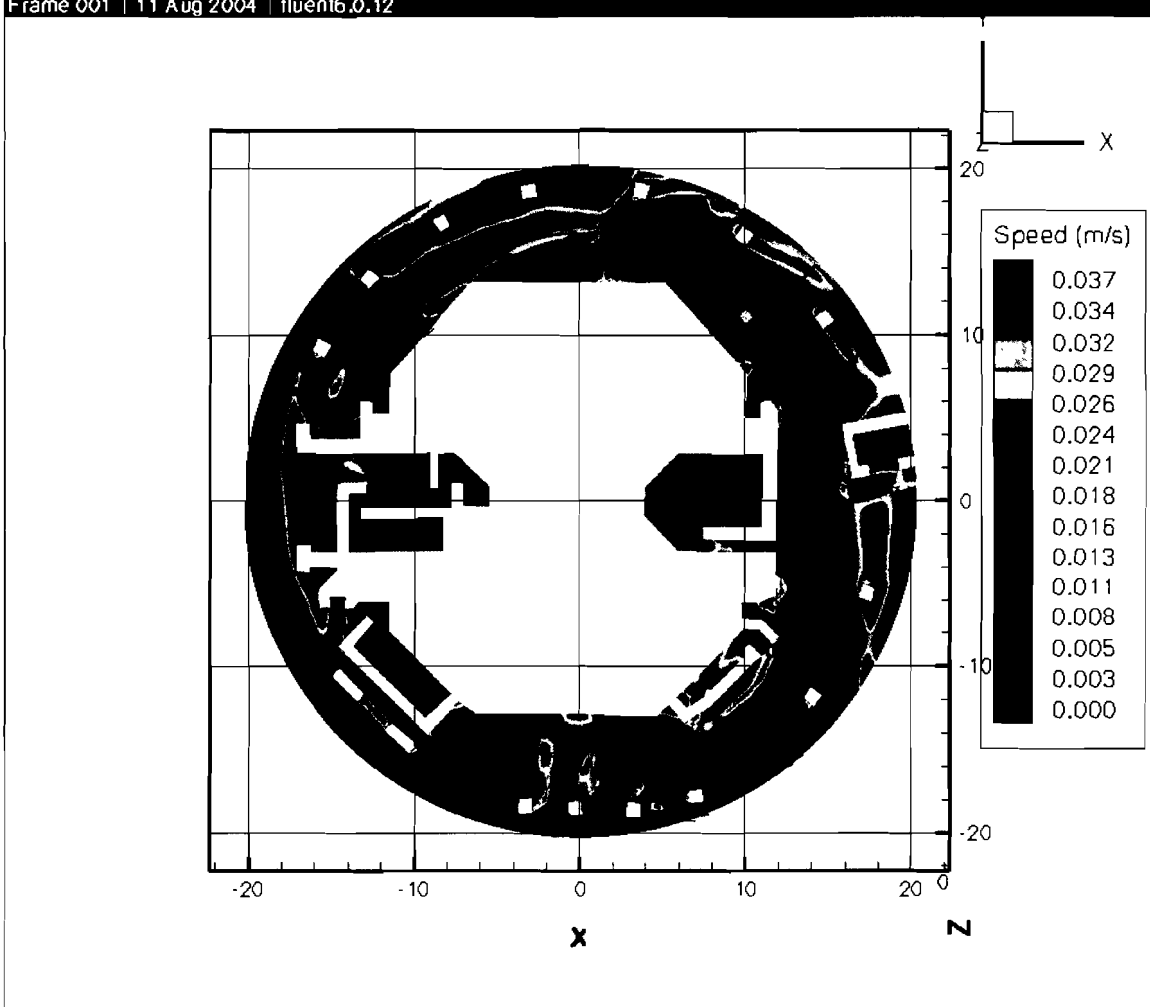
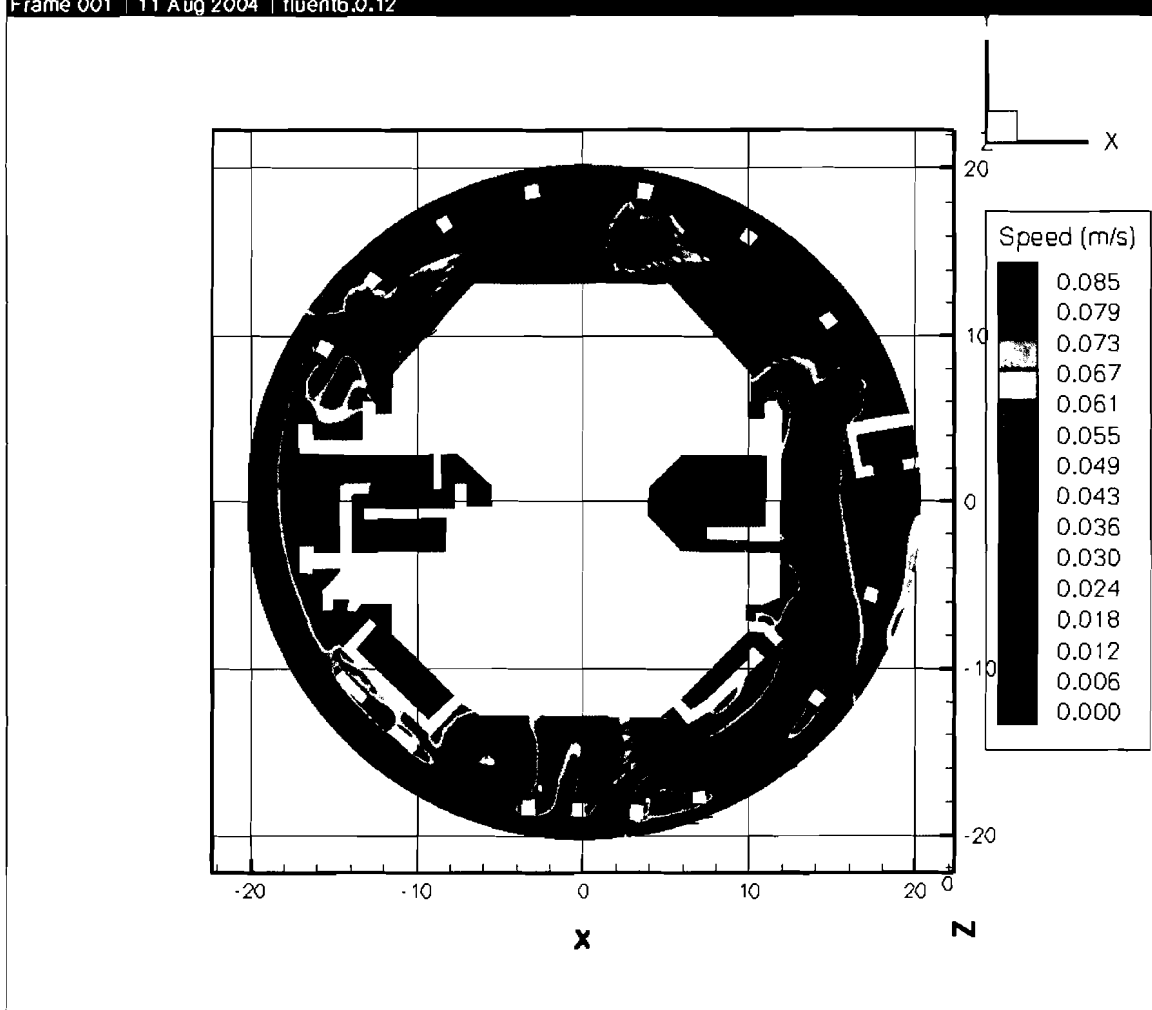


Figure III.2-37. Large LOCA Break Located in the Lower-Right Quadrant. Speeds Greater Than or Equal to the RMI Threshold (0.085 m/s) Are Colored RED.



**Figure III.2-38. Streamtraces across Two Splash Locations, Coordinates (-12,10) and (5,15), as Shown in the Figure, for a Large LOCA Break Located in the Upper-Left Quadrant. Speeds Greater Than or Equal to the Fiber Threshold (0.037 m/s) Are Colored RED.**



**Figure III.2-39. Streamtraces across Two Splash Locations, Coordinates (-12,10) and (5,15), as Shown in the Figure, for a Large LOCA Break Located in the Upper-Left Quadrant. Speeds Greater Than or Equal to the RMI Threshold (0.085 m/s) Are Colored RED.**

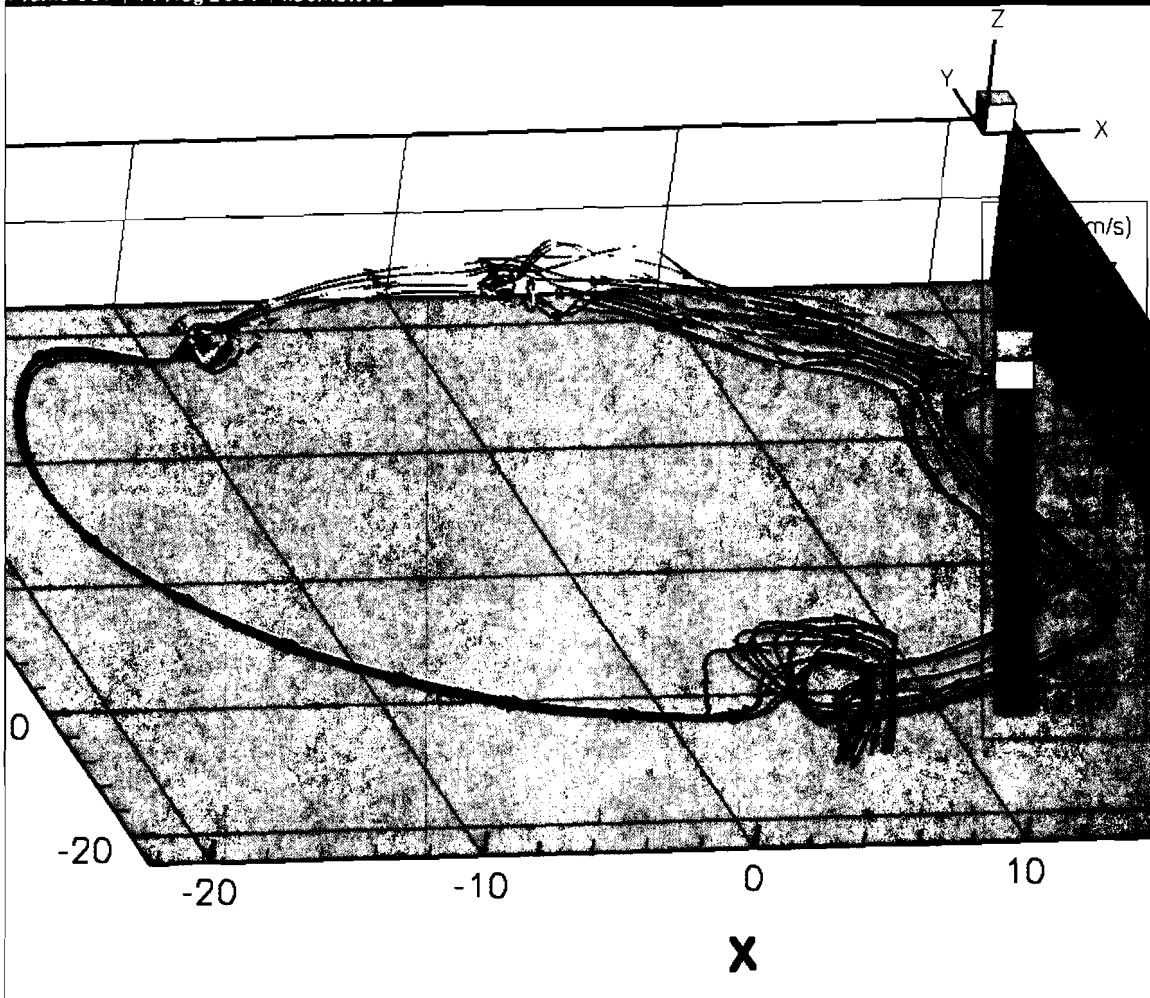


**Figure III.2-40. Oblique View of the Streamtraces, as Shown in Figure III.2-38 for the Fiber Threshold Velocity. Traces Are Color Coded to the Local Fluid Velocity. Speeds Greater Than or Equal to the Fiber Threshold (0.037 m/s) Are Colored RED.**

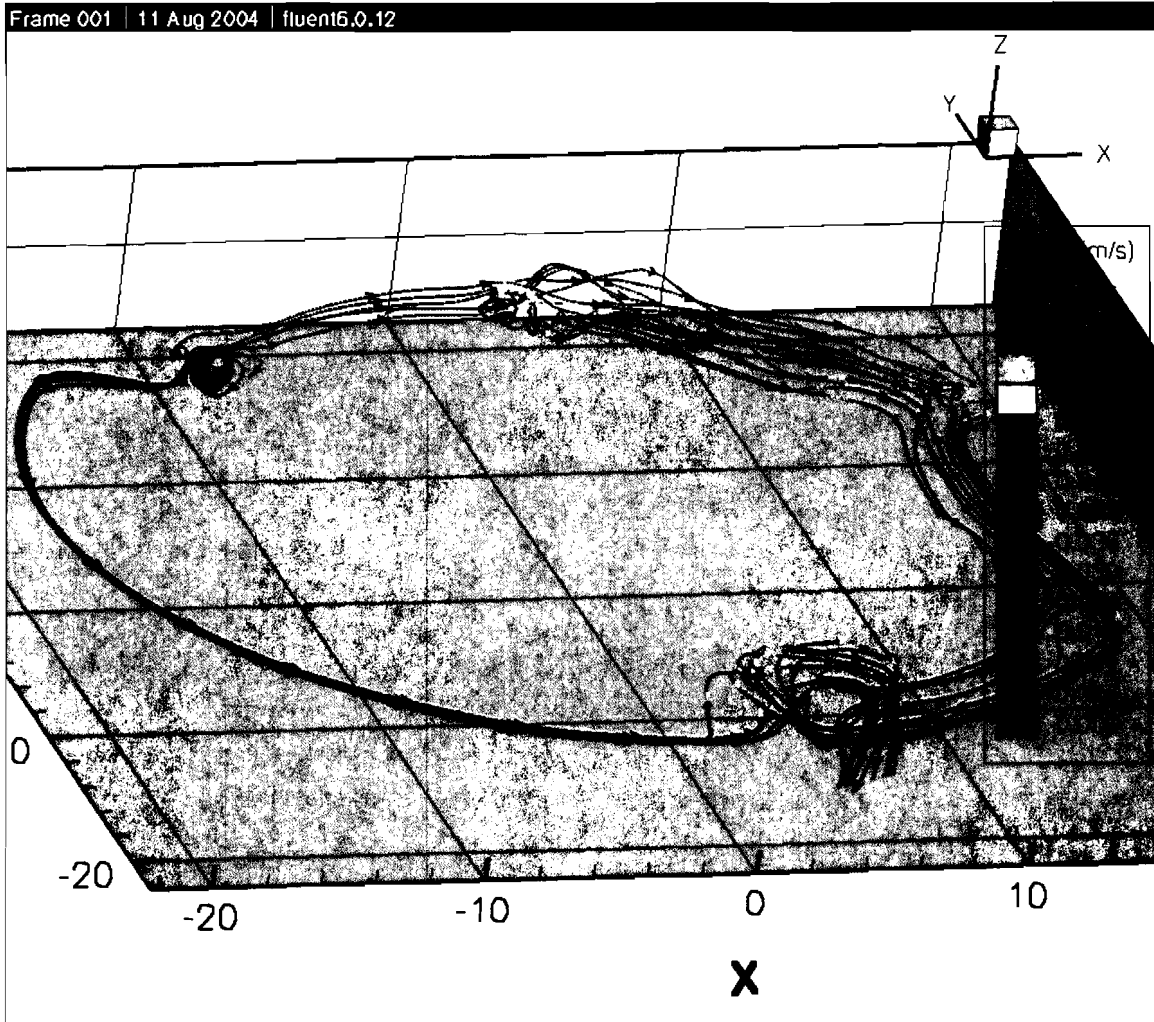


**Figure III.2-41. Oblique View of the Streamtraces Shown in Figure III.2-39 for the RMI Threshold Velocity. Traces are Color Coded to the Local Fluid Velocity. Speeds Greater Than or Equal to the RMI Threshold (0.085 m/s) Are Colored RED.**

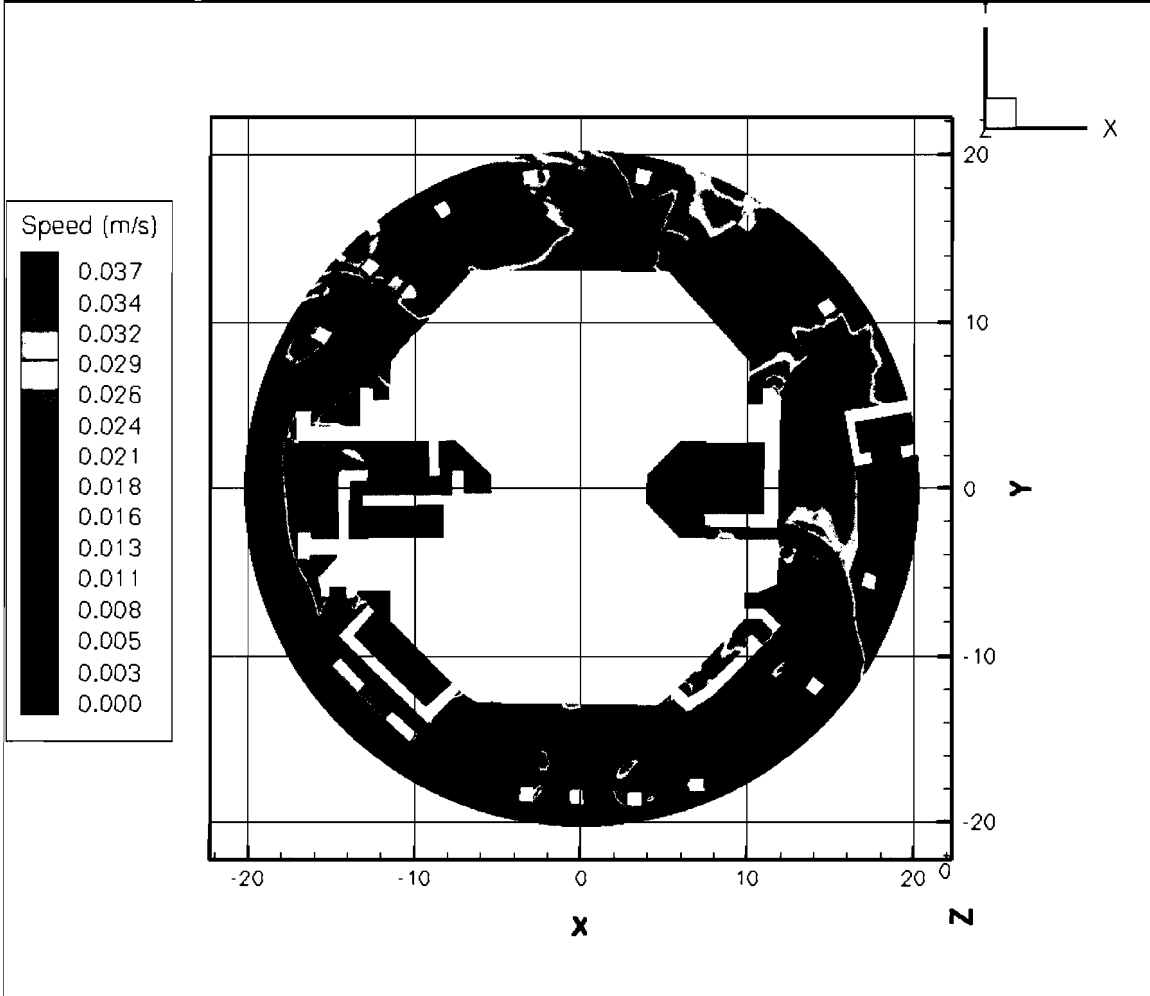


**Figure III.2-42. Streamtraces across Two Splash Locations, Coordinates (-12,10) and (5,15) as Shown in the Figure, for a Large LOCA Break Located in the Lower-Right Quadrant. Speeds Greater Than or Equal to the Fiber Threshold (0.037 m/s) Are Colored RED.**

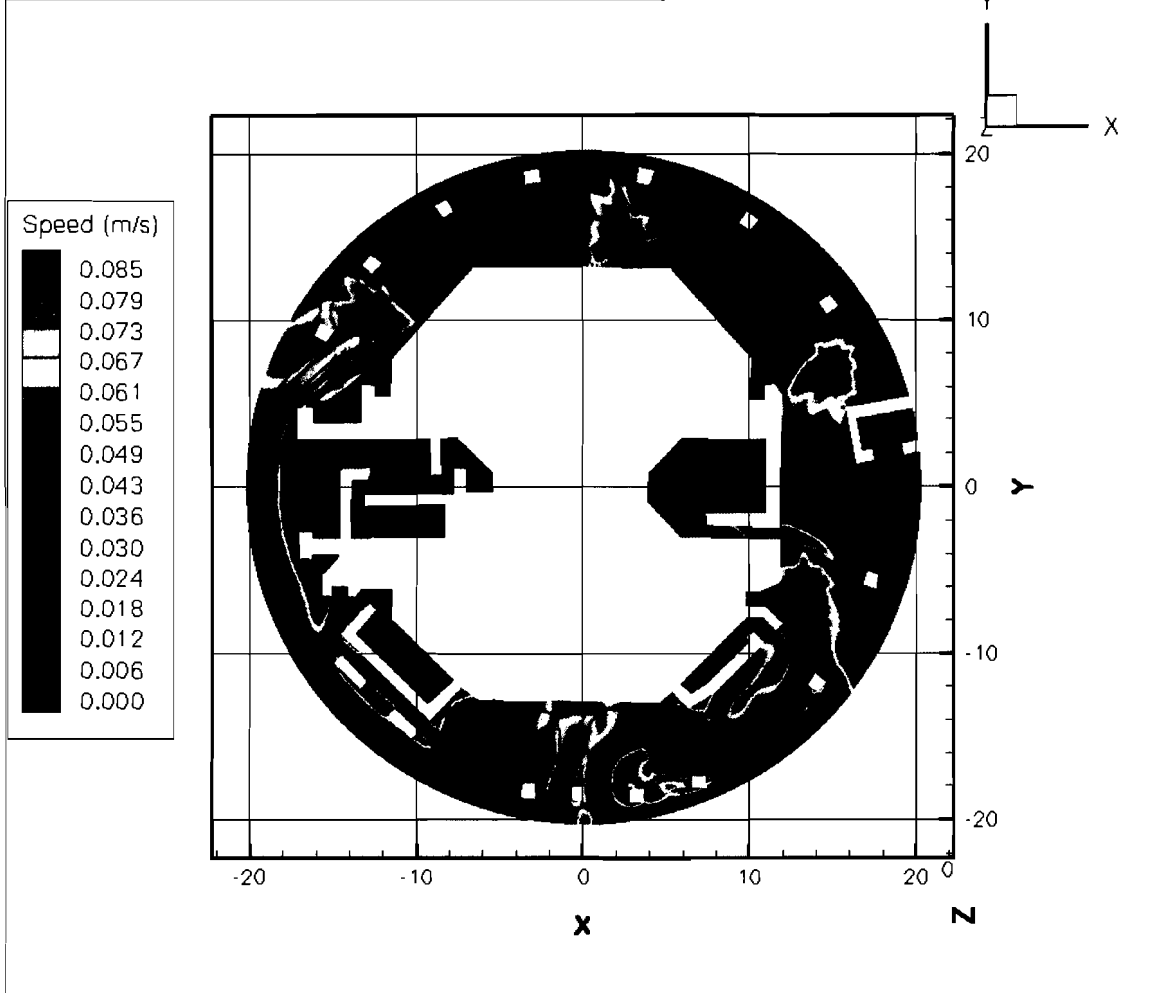


**Figure III.2-43. Streamtraces across Two Splash Locations, Coordinates (-12,10) and (5,15), as Shown in the Figure, for a Large LOCA Break Located in the Lower-Right Quadrant. Speeds Greater Than or Equal to the RMI Threshold (0.085 m/s) Are Colored RED.**

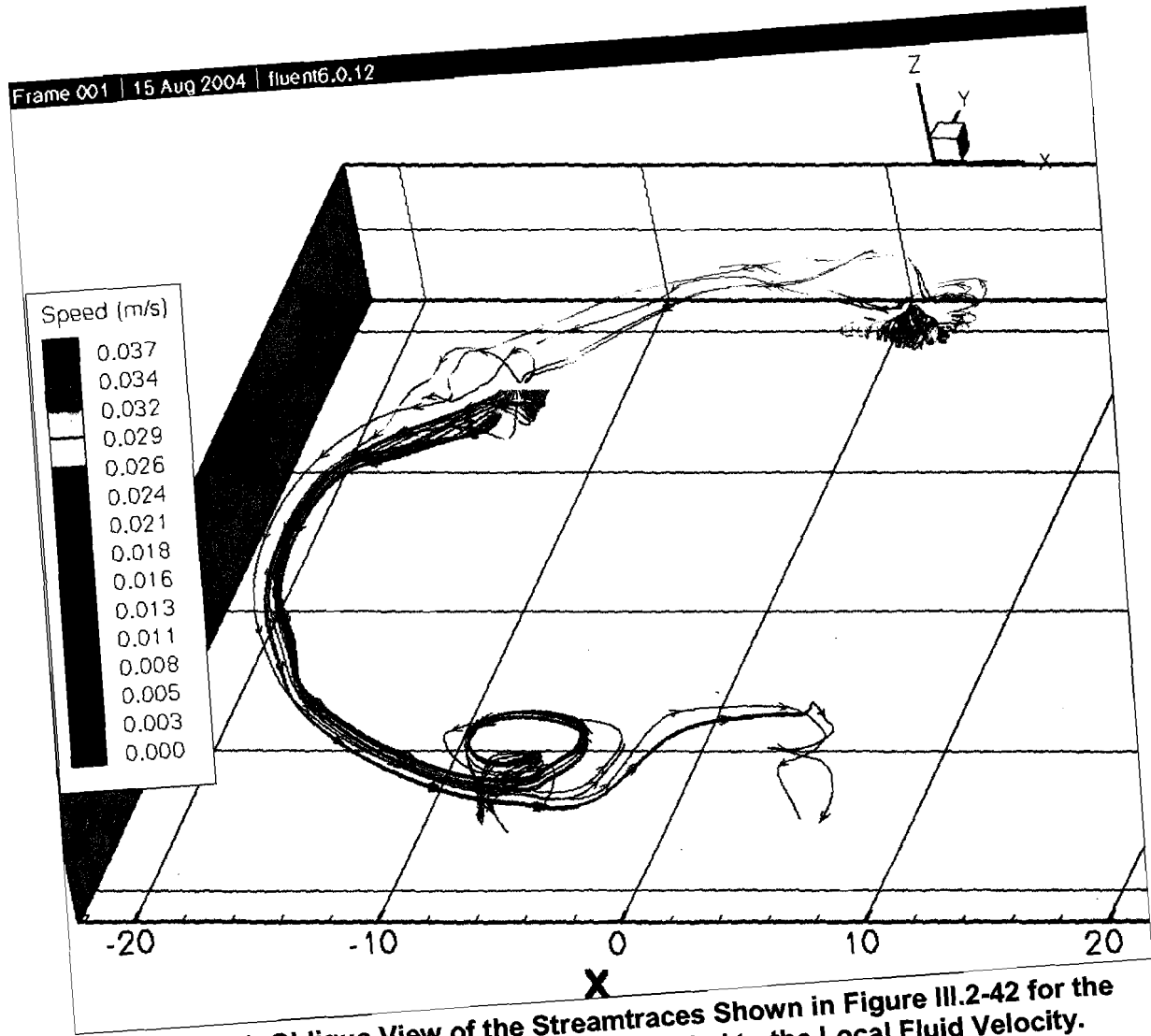
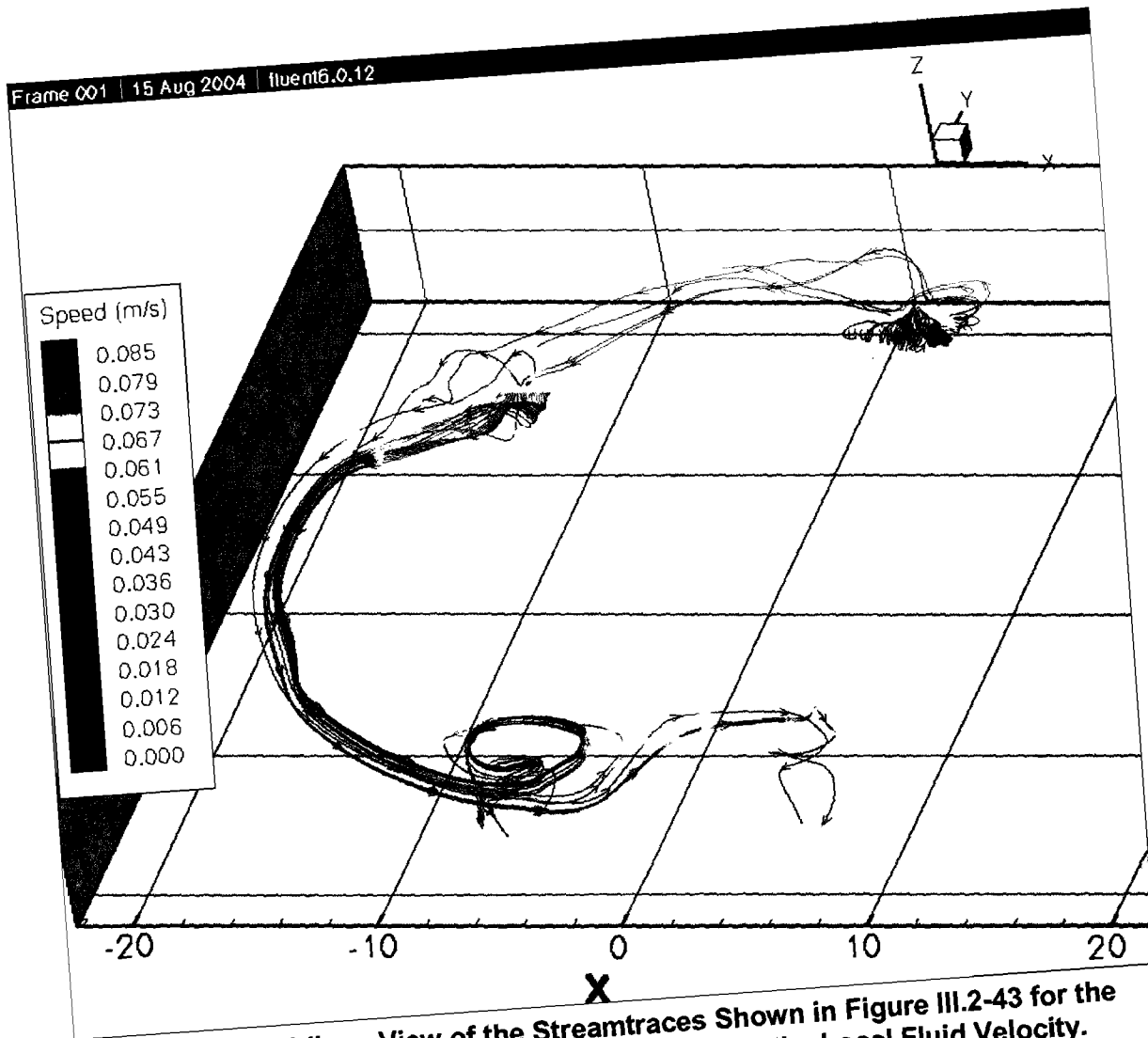
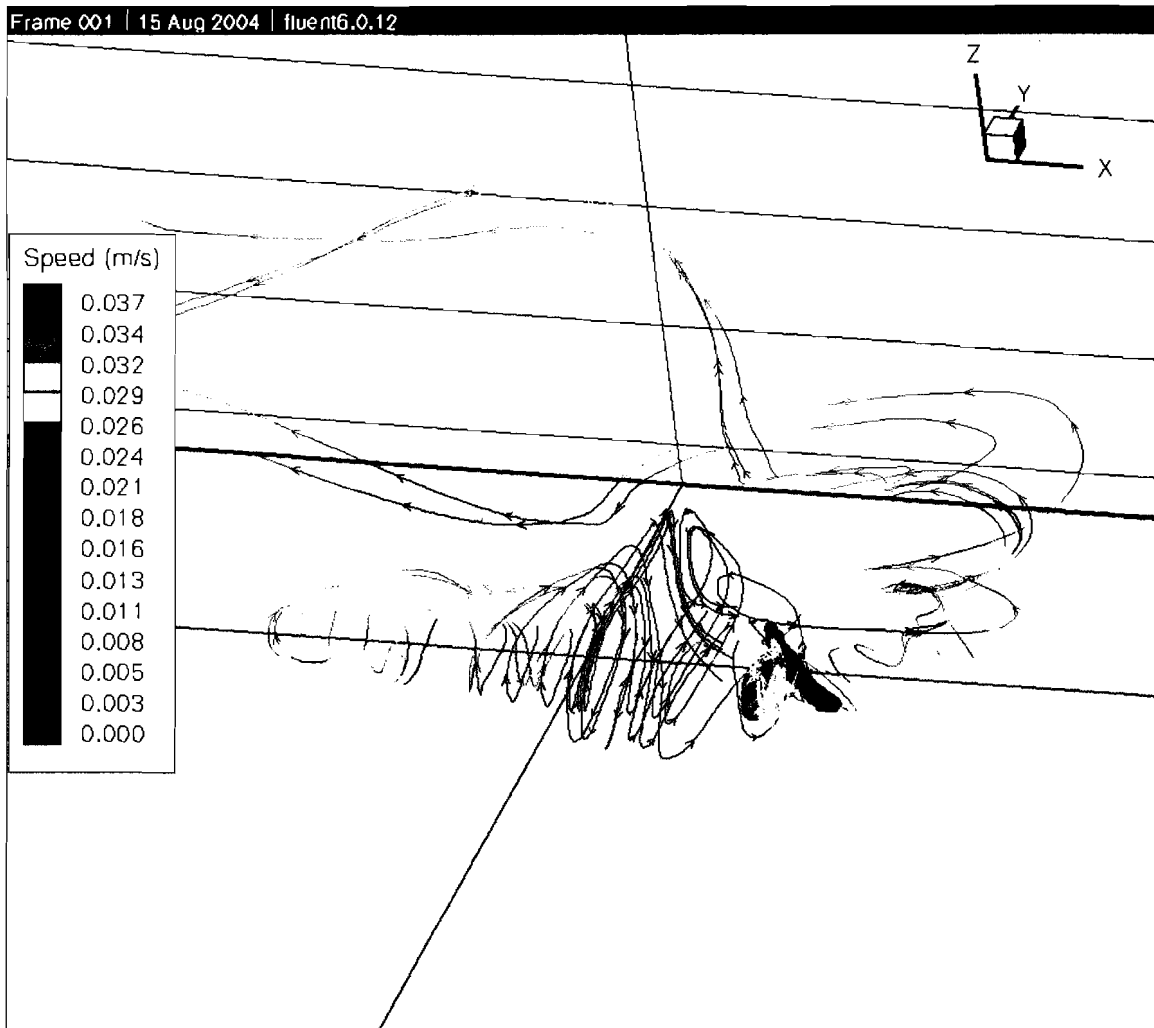


Figure III.2-44. Oblique View of the Streamtraces Shown in Figure III.2-42 for the Fiber Threshold Velocity. Traces Are Color Coded to the Local Fluid Velocity. Speeds Greater Than or Equal to the Fiber Threshold (0.037 m/s) Are Colored RED.



**Figure III.2-45. Oblique View of the Streamtraces Shown in Figure III.2-43 for the Fiber Threshold Velocity. Traces Are Color Coded to the Local Fluid Velocity. Speeds Greater Than or Equal to the RMI Threshold (0.085 m/s) Are Colored RED.**



**Figure III.2-46. Large LOCA Lower-Right Break, Zoom in at Upper-Right Splash Location Shown in Figures III.2-42 and III.2-43. Traces Are Color Coded to the Local Fluid Velocity. Speeds Greater Than or Equal to the Fiber Threshold (0.037 m/s) Are Colored RED.**

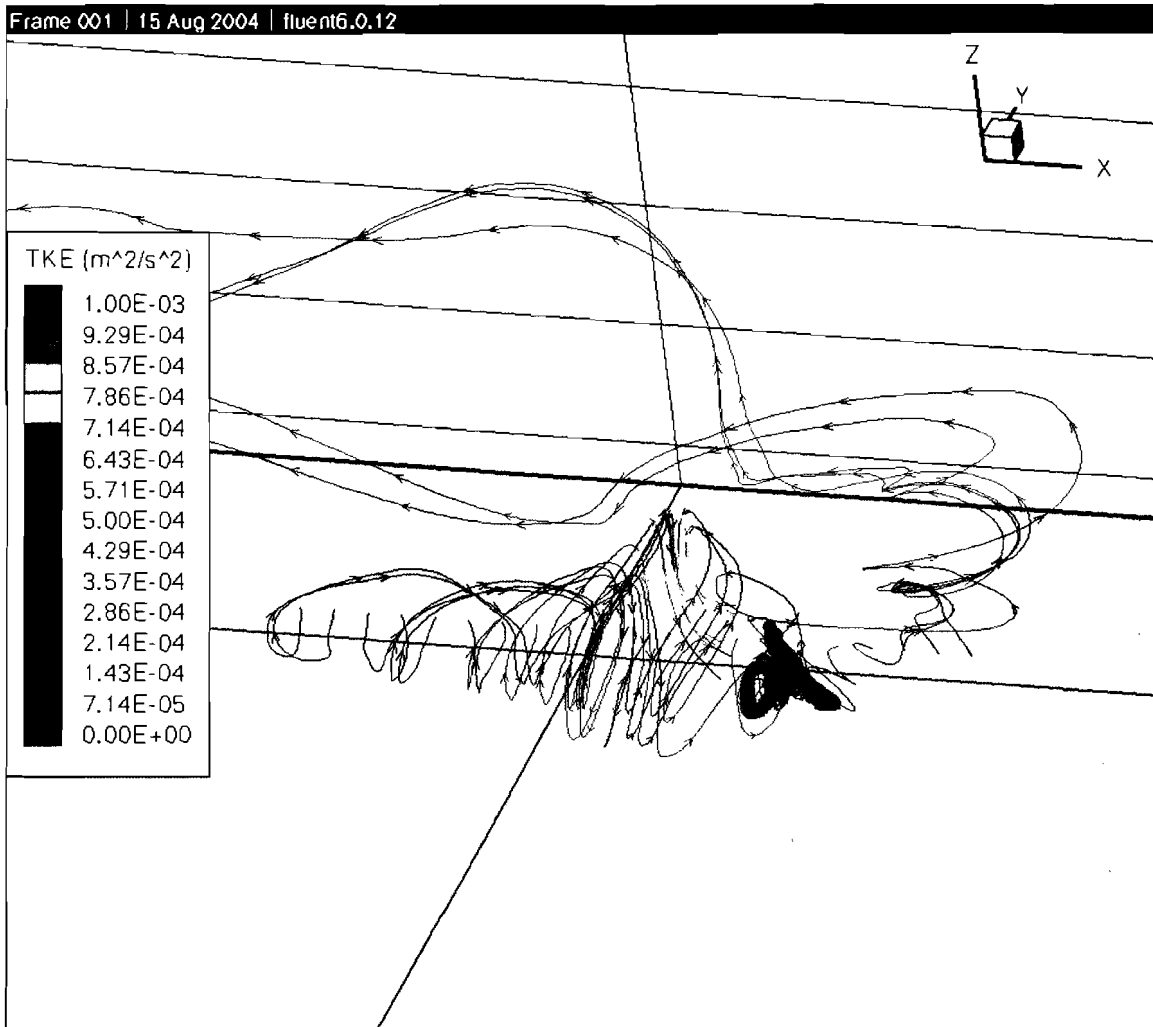


Figure III.2-47. Same as Figure III.2-46, with Streamlines Color Coded by TKE.

### III.3 SUMP POOL DEBRIS TRANSPORT

The CFD analyses characterized the flow conditions in the sump for a selection of LOCA accident scenarios. These conditions include flow velocity patterns, pool turbulence, and flow streamlines. The pool velocity and turbulence characteristics determine areas of the pool where debris entrapment may occur. The flow streamlines can be used to determine whether debris entering the pool at a discrete location would be likely to pass through one of the potential entrapment locations. The debris transport process was broken down using a logic chart approach to facilitate the individual transport steps—steps that could be determined analytically, experimentally, or simply judged. The subsequent quantification of the chart then provided an estimate of the overall sump pool debris transport.

### III.3.1 Debris Transport Logic Chart Methodology

Key to the evaluation of sump pool debris transport is “when” and “where” the debris enters the pool. The question of when debris enters the pool is basically separated into whether the debris was directly deposited onto the sump floor during the blowdown phase or entered the pool with the subsequent drainage of the containment sprays. To put the timing in perspective, the reactor cavity would likely fill in less than 12 minutes (e.g., a large LOCA break flow rate of 7400 GPM would fill the reactor cavity volume, estimated by the plant to be less than 12,000 ft<sup>3</sup>, in less than 12 minutes neglecting the contribution from the containment sprays), and the sump pool should reach a reasonable steady state in ~30 minutes. The entrance location for blowdown-deposited debris is a debris distribution on the floor that likely favors deposition nearer the location of the break. The question of where the debris enters the pool is decomposed into whether the debris is blown onto the break room floor (SG compartment housing the break) or the remainder of the sump floor, which is the lower-level annulus floor. Debris transport into the pool via the spray drainage would enter at the primary drainage locations. The debris transport analysis requires a distribution for where the washdown debris enters the sump pool. The spray drainage analysis in Appendix VI provides a distribution for drainage flows entering the sump pool. The assumption used in these analyses is that the distribution of washdown debris entering the pool mimics that of the spray water distribution for debris deposited outside the break compartment. Note that the blowdown deposition analyses determined substantial debris deposition within the break compartment that would subsequently wash directly to the break compartment floor; this deposition was considered in the debris introduction to the pool. The drainage from the containment sprays drained into the sump pool at many locations including floor drains, stairwells, an equipment hatch, the containment liner, overflow from upper levels into the annular gap, refueling pool drains, spray falling directly into the steam generator compartments and the containment spray trains location at the sump level. To simplify the analysis, the multiple drainage entrance locations into the sump pool were grouped into seven groups around the sump annulus. Figure III.3-1 shows this distribution in an event chart format. One of these charts is applied to each size category of each type of insulation. The distributions in the chart (moving from left to right) are the following:

1. the blowdown transport deposition distribution that splits the total debris among debris deposited in the upper level floors, the break compartment floor, and the remainder of the lower level (sump) floor;
2. the washdown transport distributions of whether the debris deposited in the upper levels would likely transport to the sump pool or remain in the upper levels;
3. the distribution of the locations where debris entrained in the containment spray drainage would enter the sump pool;
4. the distributions associated with sump pool formation debris transport;
5. the distributions associated with pool recirculation debris transport; and
6. the distributions associated with potential debris erosion.

Each transport path is assumed to transport debris to one of three destinations, which include (1) accumulation on the sump screens, (2) debris entrapped within the inactive

pools, and (3) debris otherwise entrapped at locations along the transport pathways. The fraction of the debris predicted to accumulate on the screens is then the transport fraction for the size and type of debris. The overall transport fraction by insulation type is obtained by applying the debris-size distributions to the size-specific transport fractions.

Debris Size	Blowdown Transport	Washdown Transport	Washdown Entry Location	Pool Fill Up Transport	Pool Recirculation Transport	Debris Erosion In Pool	Path	Fraction	Deposition Location			
FIBROUS DEBRIS	Deposited Above	Trapped Above					1		Not Transported			
							Erosion Products	2		Sump Screen		
								Remainder	3		Not Transported	
							Sump Area		Transport			Sump Screen
								Erosion Products		4		Sump Screen
							Stalled in Pool		Remainder	5		Not Transported
								SG #4		Transport	6	
							Erosion Products		Remainder		7	
								Stalled in Pool		Remainder	8	
							Eg. Room		Transport		9	
								Erosion Products		Remainder	10	
							Stalled in Pool		Remainder		11	
								SG #3 (Stairs)		Transport	12	
							Erosion Products		Remainder		13	
								Stalled in Pool		Remainder	14	
							Opposite Side		Transport		15	
								Erosion Products		Remainder	16	
							Stalled in Pool		Remainder		17	
								SG #2 (Elevator)		Transport	18	
							Erosion Products		Remainder		19	
								Stalled in Pool		Remainder	20	
							SG #1 (RV Cavity)		Transport		21	
								Erosion Products		Remainder	22	
							To Near Screen		Transport		23	
								Stalled in Pool		Remainder	24	
							Break Room Floor		Away From Screen		Transports	25
								Inactive		To Near Screen		26
							Erosion Products		Remainder		27	
								Stalled in Pool		Remainder	28	
							Sump Floor		Away From Screen		Transports	29
								Inactive		To Near Screen		30
Erosion Products	Remainder	31		Inactive Pools								

Figure III.3-1. Sump Pool Debris Transport Chart

### III.3.2 Blowdown/Washdown Debris Entry into the Sump Pool

The distributions for the blowdown and washdown phases of the transport analysis were obtained from the details of the volunteer blowdown/washdown debris transport analyses documented in Appendix VI; these distributions are shown in Table III.3-1.

The volunteer-plant fibrous debris was categorized as (1) fines, (2) small pieces, (3) large pieces, and (4) intact pieces. The fines and small pieces represent debris capable of passing through a typical grating during blowdown. The fines are generally the individual fibers that remain suspended in the sump pool, whereas the small-piece fibrous debris typically would readily sink to the pool floor in hot water. Thus, the fines and small pieces must be evaluated differently. The large-piece and intact-piece debris represents debris too large to pass through a grating, which is a process fundamental to blowdown debris transport evaluations. The difference between the large and intact piece debris is whether the fibrous insulation continues to be protected by covering material. With large-piece debris, the fibrous insulation is subject to erosion, whereas the intact-piece debris insulation is not. Another distinguishing difference is that the covering materials on the intact debris, which include nearly intact blankets, are more likely to snag onto structures, including gratings during blowdown transport such that it is less likely to fall back to a floor or wash off with the sprays. The guidance-report (GR) baseline small-fines category corresponds to the combination of the fines and small-piece debris in the volunteer-plant analyses, and the GR large-piece debris corresponds to the large- and intact-piece debris in the volunteer-plant analyses.

**Table III.3-1. Blowdown/Washdown Debris Transport Fractions**

Debris Size and Type	Debris Transport Fractions				
	Blowdown Transport			Washdown Transport	
	Deposited in Upper Levels	Deposited on Break Room Floor	Deposited on Sump Floor	Remains Trapped Above	Transports to Sump Pool
<b><i>Fibrous Debris</i></b>					
Fines	0.92	0.05	0.03	0.07	0.93
Small Pieces	0.92	0.05	0.03	0.37	0.63
Large Pieces	0.57	0.39	0.04	0.81	0.19
Intact Pieces	0.69	0.30	0.01	0.78	0.22
<b><i>RMI Debris</i></b>					
< 2-in.	0.47	0.50	0.03	0.38	0.62
2 to 6-in.	0.35	0.61	0.04	0.69	0.31
> 6-in.	0.22	0.77	0.01	0.68	0.32

The volunteer-plant RMI debris was categorized as (1) debris pieces less than 2-inches, (2) pieces between 2- and 6 -inch in size, and (3) pieces greater than 6 inches in size. The GR RMI size groups were subdivided at 4-inch rather than the 2- and 6-inch used for the volunteer plant analysis. However, the combination of the volunteer-plant analysis categories less than 6-inch is a reasonable representation of the GR small-fines category, leaving the pieces larger than 6-inch to represent the large-piece debris.

The debris washing down from the upper levels was assumed to enter the sump pool with the same distribution as the spray drainage. However, blowdown debris that was preferentially deposited in the steam generator (SG) compartment where the break (SG1) occurred and its adjacent SG compartment (SG4) would wash directly to the

floors of these compartments, regardless of the spray drainage fractions. For the volunteer plant, the spray drainage distribution, as shown in Table III.3-2, was obtained from the spray drainage analysis documented in Appendix VI. The location distributions for debris washing down from the upper levels are provided by debris size category in Table III.3.3 and III.3.4 for fibrous and RMI debris, respectively. Because the larger debris was preferentially trapped in SG1 and SG4, these washdown location fractions are larger.

**Table III.3-2. Spray Drainage Distribution into the Sump Pool**

No.	Location in Annular Sump	Spray Drainage Water Sources	Drainage Fraction
1	Annulus Section Containing Recirculation Sumps	Floor drains and annular gap sources	0.14
2	Vicinity of SG4 Access (Steam Generator Adjoining Break Room)	SG4 personnel access doorway and liner flow. Includes flow from a 6-in. refueling pool drain.	0.08
3	Vicinity of Interior Equipment Room Access (~90° from Sumps)	Refueling pool water drains into equipment room below refueling pools, then exits doorway into sump and liner flow.	0.06
4	Vicinity of SG3 Access	SG3 personnel access doorway, annular gap sources, and stairwell. Includes flow from a 6-in. refueling pool drain.	0.18
5	Annulus Section Directly Opposite Recirculation Sumps	Floor drains and annular gap sources.	0.09
6	Vicinity of SG2 Access	SG2 personnel access doorway, floor drains, upper-level equipment hatch, annular gap sources, and stairwell. Includes flow from a 6-in. refueling pool drain.	0.25
7	Vicinity of SG1 Access (Compartment with Break)	SG1 personnel access doorway, floor drains, and annular gap sources. Includes flow from a 6-in. refueling pool drain.	0.20

**Table III.3-3. Fibrous Debris Entrance Distributions to Sump Pool**

No.	Location in Annular Sump	Drainage Fraction	Fines Debris	Small-Piece Debris	Large-Piece Debris	Intact-Piece Debris
1	Sumps	0.14	0.09	0.09	0.01	0.01
2	SG4	0.08	0.17	0.17	0.28	0.22
3	Eq. Room	0.06	0.04	0.04	0	0
4	SG3	0.18	0.12	0.12	0.07	0.07
5	Opposite	0.09	0.06	0.06	0.01	0.01
6	SG2	0.25	0.16	0.16	0.07	0.07
7	SG1	0.20	0.36	0.36	0.56	0.62

**Table III.3-4. RMI Debris Entrance Distributions to Sump Pool**

No.	Location in Annular Sump	Drainage Fraction	<2-in. Debris	2- to 6-in. Debris	>6-in. Debris
1	Sumps	0.14	0.06	0.01	0.01
2	SG4	0.08	0.24	0.28	0.22
3	Eq. Room	0.06	0.02	0	0
4	SG3	0.18	0.06	0.07	0.07
5	Opposite	0.09	0.04	0.01	0.01
6	SG2	0.25	0.09	0.07	0.07
7	SG1	0.20	0.49	0.56	0.62

### III.3.3 Sump Pool Debris Transport Estimates

Debris transport in the sump pool was separated into the following three phases: (1) transport of floor deposited debris during the formation (fill-up) of the sump pool, (2) debris transport in an established sump during recirculation mode, and (3) long-term erosion of exposed fibrous debris in the sump pool.

#### III.3.3.1 Pool Formation Debris Transport

Based on observations taken during the integrated debris transport tests [NUREG/CR-6773], the primary driver for moving debris during pool formation, especially for the large debris, is the sheeting flow as the initial water from the break spreads across the sump floor. Debris initially deposited on the floor is pushed along with the wave front. As such, the movement of the debris has significant momentum that can carry the debris past the openings into interior spaces. Once the water depth becomes significant, further transport occurs due to the drag forces of the flow of water, and for larger debris that transport becomes substantially less dynamic than the sheeting flow transport. Individual fibers will move as suspended debris following the water flow.

In the volunteer plant, a majority of the debris initially deposited on the floor of the compartment containing the break (SG compartment 1 in this evaluation) would likely transport from that compartment onto the annular sump floor through either of the personnel access door for SG 1 or the door for SG 4. Because the break is in SG 1, considerably more flow would exit the door to SG 1 than to SG 4. In the scenario evaluated herein, the larger portion of the break room flow and therefore the debris (perhaps 75%) would flow through the personnel access door into the annulus on the side nearer the access for the reactor cavity (the flow distribution assumption was discussed in Section III.2.1). A smaller portion of the debris would exit the SG compartment through the access door into SG compartment 2. In the volunteer plant, nearly all of the essentially inactive pool is the water below the sump floor in the reactor cavity. All other quiescent regions would have sufficient water circulation that suspended fibers over time would circulate from those regions. When debris exits a SG compartment through a personnel access door due to the initial sheeting flow, the flow splits, with part going toward the recirculation sumps and part going in the opposite

direction. In the scenario analyzed, the part going away from the sump screens flowed past the narrow passageway into the room leading to the reactor cavity access hatch. For debris to follow water into this passageway, it must essentially make a 90° bend in a short distance. Therefore, it must be concluded that only a small fraction of debris moving with the dynamic wave front, especially larger debris, will make the 90° turn into the reactor cavity passageway.

With these concepts in mind, the pool transport distributions were judged as shown in Table III.3-4. Starting with the fines, it is assumed that 75% of the flow exits the SG1 compartment on the reactor cavity side, then that 60% of that flows in the direction of the reactor cavity, then that 50% of the flow makes the turn into reactor cavity passageway, which indicates that perhaps 25% of the fines initially on the break room floor goes into the reactor cavity on initial formation of the pool. Because these fibers are suspended, the remaining pool formation could increase this number to, for example, a conservative 40%. Then, the remaining amount is split 50%–50%, as toward the recirculation sump and away from the sump. With each fibrous debris category of increasing size, the fraction into the reactor cavity is decreased somewhat, with the even split maintained between the “toward” and “away” from the screen. With the heavier metallic debris, even the smaller pieces would transport less readily than the fiber pieces.

For debris initially deposited on the annular sump floor, a significant fraction of this debris could be located such that it would not be greatly affected by flow from the break compartment to the reactor cavity because the exit from the break compartment is near the entrance to the reactor cavity. However, larger debris deposition would also likely be preferential near the break compartment door. For lack of better justifications, the same distributions judged for debris initially deposited on the break room floor are assumed for debris initially deposited on the annular sump floor. In any case, only a few percent of the total debris is estimated to be deposited on the annular sump floor due to the relatively small doorway areas as compared with the upward area of the SG compartments.

**Table III.3-4. Pool Formation Debris Transport Distributions**

Debris Size and Type	Pool Formation Debris Transport Distributions					
	Floor of Break Room			Floor of Sump Pool		
	Toward Screen	Away from Screen	Into Inactive Pools	Toward Screen	Away from Screen	Into Inactive Pools
<b><i>Fibrous Debris</i></b>						
Fines	0.30	0.30	0.40	0.30	0.30	0.40
Small Pieces	0.35	0.35	0.30	0.35	0.35	0.30
Large Pieces	0.40	0.40	0.20	0.40	0.40	0.20
Intact Pieces	0.40	0.40	0.20	0.40	0.40	0.20
<b><i>RMI Debris</i></b>						
<2 in.	0.35	0.35	0.30	0.35	0.35	0.30
2 to 6 in.	0.40	0.40	0.20	0.40	0.40	0.20
>6 in.	0.50	0.50	0.00	0.50	0.50	0.00

### III.3.3.2 Recirculation Pool Debris Transport

Important aspects of sump pool debris transport were observed during the integrated debris transport tests [NUREG/CR-6773]. For low-density fiberglass debris, the fines (e.g., individual fibers) remain suspended and move with the flow of water, whereas the debris pieces of significant size readily saturate with water at the water temperatures typical of LOCA accidents and then sink to the pool floor, where further transport depends on the flow velocity and turbulence near the floor. For RMI debris, all debris sinks to the floor of the pool, with the occasional exception of a piece of debris that encapsulates an air pocket, keeping that piece buoyant.

The CFD analyses provide realistic descriptions of the floor-level flow conditions, which were described in Section III.2 as contours established so that the velocities higher than the experimental measured threshold are clearly indicated. The velocity contours illustrate the portion of the pool where debris would most likely readily move with the flow. In addition to velocity contours, the streamline plots provide a reasonable connecting pathway whereby a piece of debris would likely travel from its original location in the pool to the recirculation sumps. If a transport pathway passes through a slower portion of the pool, then debris moving along that pathway could stall and not transport to the recirculation sump. Otherwise, the transport is very likely.

The effects of pool turbulence are more difficult to quantify. Test observations have shown the occasional reentrainment of debris once stalled in relatively quiescent water. Water within quiescent regions typically tends to rotate, sending debris into the center of the vortex, where it becomes semi-trapped. However, that occasional pulsation can kick a piece of debris out of the vortex and back into the main stream. Although this behavior cannot be reasonably quantified, transport estimates should be enhanced to consider these effects.

A detailed transport analysis using the CFD predicted flow contours and flow streamlines would subdivide the sump pool floor into relatively fine subdivisions, where each subdivision would have a source term for debris depositing onto the pool floor at that location. Then the transport of the debris from each specific subdivision would be independently evaluated using a streamline generated from that subdivision to the recirculation sumps to illustrate where that debris would likely reside after movement ceases. Quantification of all the subdivision transport results would provide an overall sump pool transport fraction for each debris category. The transport results should then be adjusted to account for pool turbulence effects on debris, i.e., the threshold transport tumbling velocities reported in NUREG/CR-6772 were measured in very uniform and turbulence-dampened flows but turbulence is capable of moving debris where bulk flow will not. One method of accounting for turbulence effects would be to decrease the threshold velocities for transport.

In this analysis, the above detailed model description was simplified to only seven subdivisions for the sump floor. Even then, the available CFD streamlines did not form a complete set. Therefore, the individual pool transport fractions used to populate the transport charts were basically engineering judgments made while viewing the velocity profiles. The individual transport estimates are provided in Table III.3-5. The CFD flow velocity contours maps used to make these judgments are shown in Figures III.2-33 and III.2-37 for fibrous and RMI debris, respectively. A sampling of corresponding flow streamline plots are shown in Figures III.2-42 and III.2-43, for fibrous and RMI debris,

respectively. The transport fractions range from 100% transport for the suspended fibers and debris located nearer the recirculation sumps to 0% transport for the largest debris located on the opposite side of the containment.

### III.3.3.3 Sump Pool Debris Erosion

The only source of data for the erosion of fibrous debris in a sump pool was the integrated debris transport tests documented in NUREG/CR-6773. Four longer-term tests (3- to 5-hour durations) were conducted in this test program where debris accumulation on the simulated sump screen was collected after every 30 minutes.

Three sources of fibrous debris contributed to this accumulation: (1) small-piece debris tumbling or sliding along the floor, (2) suspended fibers initially introduced into the tank, and (3) fibers that had eroded from the small-piece debris residing on the floor of the tank. Late into these tests, most of the small-piece debris had already either transported to the screen or had come to relative rest in some quiescent location on the tank floor; therefore, its contribution should have been minimal near the end of the tests. Also, late in the tests, water recirculation should have substantially reduced the initially suspended fibers so that continued accumulation would fall off quite noticeably. Note that sufficient time had elapsed in each test for the water in the tank to be replaced (tank water volume divided by the simulated break flow) from 19 to 46 times during the course of the test. Because the continued accumulation tended to hold at a somewhat sustainable rate, it is likely that continued erosion was supporting the continued debris accumulation.

**Table III.3-5. Recirculation Pool (Steady-State) Debris Transport Fractions**

Location Where Debris Enters Sump Pool	Fraction of Debris Transported to Sump Screen						
	Fibrous Debris				RMI Debris		
	Fines	Small Pieces	Large Pieces	Intact Pieces	<2 in.	2 to 6 in.	>6 in.
<i>Debris Entering with Annular Sump Pool by Containment Spray Drainage (Debris Assumed to Enter Established Sump Pool)</i>							
Annulus Section Containing Recirculation Sumps	1	1	1	1	1	1	1
Vicinity of SG4 Access (SG Adjoining Break Room)	1	1	1	1	1	1	1
Vicinity of Interior Equipment Room Access (~90° from Sumps)	1	1	1	1	1	1	1
Vicinity of SG3 Access (Includes Inter-Level Stairwell)	1	0.5	0.4	0.3	0.3	0.2	0.1
Annulus Section Directly Opposite Recirculation Sumps	1	0.2	0.1	0	0.1	0	0

Vicinity of SG2 Access (Includes Inter-Level Stairwell and Hatch)	1	0.5	0.4	0.3	0.3	0.2	0.1
Vicinity of SG1 Access (Compartment with Break, Includes Multiple Floor Drains)	1	0.7	0.6	0.5	0.5	0.4	0.3
<i>Debris Directly Blowdown Deposited onto Sump Floor but Subsequently Relocated Away from Recirculation Sumps during Pool Formation (Section III.3.3.1)</i>							
Initially on Break Room Floor, Relocated Away from Recirculation Sumps	1	0.3	0.2	0.1	0.2	0.1	0
Initially Spread Around Annular Sump Floor, Relocated Away from Recirculation Sumps	1	0.3	0.2	0.1	0.2	0.1	0

Table III.3-6 shows the end of test debris accumulation rates for these longer-term tests. Although these tests were run several hours, as indicated in the table, the tests were of short duration compared with LOCA long-term recirculation times. One of the four tests was conducted with a shallower pool of 9-in. depth compared with the usual depth of 16 in. Note that the accumulation was about eight times more rapid for the shallow pool test than for the deeper tests. Also note that during the shallow pool test, the water recirculation in terms of water replacements (46) was significantly more frequent for the 9-in. test than for the 16-in. tests; thus, the initial suspended debris would have been more readily filtered from the tank. Therefore, most of the longer-term debris accumulation should have been due to the continued erosion of fibrous debris in the tank. Further, the erosion rate was greater in the shallow depth pool, which can most likely be attributed to the greater turbulence in the shallow pool relative to the deeper pools.

**Table III.3-6. Late-Term Debris Accumulation in Integrated Debris Transport Tests**

Test ID	Pool Depth (in.)	Test Duration (Hours)	Accumulation Rate near the End of the Test (Percent of Debris in Tank/hr)	Approximate Number of Water Replacements During the Test
LT1	16	4	0.4	26
LT2	9	4	2	46
LT3	16	3	0.3	19
LT4	16	5	0.3	32

In conclusion, the only applicable test data for long-term debris erosion in a sump pool strongly indicate a sustainable rate of erosion that is affected by the relative turbulence in the pool. It should also be noted that the small-piece debris residing on the floor of the pool, late term, was generally found in quiescent locations, not necessarily directly under the simulated break flow. It might also be noted that the turbulence associated with the

spray drainage was not simulated. Because the 16-in. depth more closely resembles the fully established volunteer-plant pool, the erosion rate of 0.3 percent of the current tank debris/hour is adapted for this analysis.

In the debris transport charts, the overall fraction of debris on the sump floor that erodes into fines is required. Using the long-term recirculation mission time of 30 days, analysis indicates that nearly 90% of the initial debris mass would become eroded if this erosion rate remained constant throughout the 30 days. This calculation took into account the steadily decreasing mass of debris the pool using the following equation.

$$f_{eroded} = 1 - (1 - rate)^{Number\ of\ Hours}$$

Therefore, in the debris transport charts, 90% of the small- and large-piece debris predicted to reside on the sump floor is assumed to erode into suspended fibers unless the debris is still enclosed in a protective cover.

There are substantial sources of uncertainty with this calculation:

1. The durations of the integral debris transport tests were 3 to 5 hours. This leaves the question "Does the erosion rate taper off with time?" In addition, it is not certain that all of the end-of-test debris accumulation was due to erosion products.
2. The test results include the usual variances in test data, such as flow and depth control, and debris collection.
3. Although the test series was designed to approximate the flow and turbulence characteristics of the volunteer plant sump pool, the tank characteristics may have been significantly different than what might occur at the plant. The difference in the erosion rates between the 9 and 16-inch pool depths in the integrated tests clearly illustrate the effect of pool turbulence on fibrous debris erosion.
4. The geometry of the volunteer plant sump pool is larger and more complex than the test tank used in the integrated tests.
5. Large piece debris was not tested in the long term tests.

The 90% debris eroded value is used for both the small and large piece debris, despite the uncertainties. With such limited data, the use of 90% is necessary to ensure conservatism in the overall transport results. It may be that this number can be relaxed once better erosion data is available.

### III.3.4 Quantification Results

The blowdown/washdown/pool transport estimates presented in Sections III.3.2 and III.3.3 were entered into debris transport charts shown generically in Figure III.3-1 and quantified to obtain overall transport fractions. A separate chart was created for each size category and for each type of debris. Figures III.3-2, III.3-3, III.3-4, and III.3-5 illustrate the transport processes for fibrous debris categories of fines, small pieces,

large pieces, and intact pieces, respectively. Figures III.3-6, III.3-7, and III.3-8 illustrate the transport processes for RMI debris categories of pieces <2 in., 2 to 6 in., and >6 in., respectively.

Debris Size	Blowdown Transport	Washdown Transport	Washdown Entry Location	Pool Fill Up Transport	Pool Recirculation Transport	Debris Erosion in Pool	Path	Fraction	Deposition Location
POOL TRANSPORT LOGIC CHART							1	6.440E-02	Not Transported
FIBROUS DEBRIS							2	0.000E+00	Sump Screen
Trapped Above							3	0.000E+00	Not Transported
0.07							4	0.000E+00	Sump Screen
Sump Area							5	0.000E+00	Not Transported
0.09							6	1.455E-01	Sump Screen
SG #4							7	0.000E+00	Sump Screen
0.17							8	0.000E+00	Not Transported
Eq. Room							9	3.422E-02	Sump Screen
0.04							10	0.000E+00	Sump Screen
SG #3 (Stairs)							11	0.000E+00	Not Transported
0.12							12	1.027E-01	Sump Screen
Opposite Side							13	0.000E+00	Sump Screen
0.06							14	0.000E+00	Not Transported
SG #2 (Elevator)							15	5.134E-02	Sump Screen
0.16							16	0.000E+00	Sump Screen
SG #1 (RV Cavity)							17	0.000E+00	Not Transported
0.36							18	1.369E-01	Sump Screen
Transports to Pool							19	0.000E+00	Sump Screen
0.93							20	0.000E+00	Not Transported
0.30							21	3.000E-01	Sump Screen
To Near Screen							22	1.500E-02	Sump Screen
0.30							23	0.000E+00	Sump Screen
Break Room Floor							24	0.000E+00	Not Transported
0.05							25	1.500E-02	Sump Screen
Away From Screen							26	2.000E-02	Inactive Pools
0.30							27	9.000E-03	Sump Screen
Inactive							28	0.000E+00	Sump Screen
0.40							29	0.000E+00	Not Transported
Sump Floor							30	9.000E-03	Sump Screen
0.03							31	1.200E-02	Inactive Pools
0.40								1.0000000	
Fines								0.06440	Not Transported
1.00								0.03200	Inactive Pools
								0.90360	Sump Screen

Figure III.3-2. Sump Pool Debris Transport Chart for Fine Fibrous Debris.







Debris Size	Blowdown Transport	Washdown Transport	Washdown Entry Location	Pool Fill Up Transport	Pool Recirculation Transport	Debris Erosion in Pool	Path	Fraction	Deposition Location			
POOL TRANSPORT LOGIC CHART RMI DEBRIS	Deposited Above 0.47	Trapped Above 0.38					1	1.786E-01	Not Transported			
							Stalled in Pool	Erosion Products	2	0.000E+00	Sump Screen	
								Remainder	3	0.000E+00	Not Transported	
							Sump Area	Transport	1.00	1.748E-02	Sump Screen	
									1.00	0.000E+00	Sump Screen	
							SG #4	Transport	0.00	0.000E+00	Not Transported	
									0.24	6.994E-02	Sump Screen	
							Eq. Room	Transport	0.00	0.000E+00	Sump Screen	
									0.02	5.828E-03	Sump Screen	
							SG #3 (Stairs)	Transport	0.70	1.224E-02	Not Transported	
									0.06	5.245E-03	Sump Screen	
							Opposite Side	Transport	0.90	1.049E-02	Not Transported	
									0.04	1.166E-03	Sump Screen	
							SG #2 (Elevator)	Transport	0.70	1.836E-02	Not Transported	
									0.09	7.868E-03	Sump Screen	
							SG #1 (RV Cavity)	Transport	0.50	7.139E-02	Not Transported	
									0.49	7.139E-02	Sump Screen	
							Pieces < 2"	Break Room Floor	Away From Screen	0.35	1.750E-01	Sump Screen
										0.50	0.000E+00	Sump Screen
							Sump Floor	Away From Screen	0.80	1.400E-01	Not Transported	
									0.35	3.500E-02	Sump Screen	
							Sump Floor	Inactive	0.20	1.500E-01	Inactive Pools	
									0.30	1.050E-02	Sump Screen	
							Sump Floor	Inactive	0.35	0.000E+00	Sump Screen	
									0.80	8.400E-03	Not Transported	
							Sump Floor	Inactive	0.35	2.100E-03	Sump Screen	
									0.20	9.000E-03	Inactive Pools	
							Sump Floor	Inactive	0.30	1.0000000		
									0.30	0.43948	Not Transported	
							Sump Floor	Inactive	0.30	0.15900	Inactive Pools	
									0.30	0.40152	Sump Screen	

Figure III.3-6. Sump-Pool-Debris Transport Chart for <2-in. RMI Debris.

Debris Size	Blowdown Transport	Washdown Transport	Washdown Entry Location	Pool Fill Up Transport	Pool Recirculation Transport	Debris Erosion in Pool	Path	Fraction	Deposition Location		
POOL TRANSPORT LOGIC CHART RMI DEBRIS	Deposited Above 0.35	Trapped Above 0.69					1	2.415E-01	Not Transported		
							Stalled in Pool	Erosion Products	2	0.000E+00	Sump Screen
								Remainder	3	0.000E+00	Not Transported
							Sump Area	Transport	1.00	1.085E-03	Sump Screen
								1.00			
							Stalled in Pool	Erosion Products	4	0.000E+00	Sump Screen
								Remainder	5	0.000E+00	Not Transported
							SG #4	Transport	1.00	3.038E-02	Sump Screen
								1.00			
							Stalled in Pool	Erosion Products	7	0.000E+00	Sump Screen
								Remainder	8	0.000E+00	Not Transported
							Eq. Room	Transport	1.00	0.000E+00	Sump Screen
								1.00			
							Stalled in Pool	Erosion Products	10	0.000E+00	Sump Screen
								Remainder	11	6.076E-03	Not Transported
							Tranports to Pool 0.31	SG #3 (Stairs)	1.00	1.519E-03	Sump Screen
								0.07			
							Stalled in Pool	Erosion Products	13	0.000E+00	Sump Screen
								Remainder	14	1.085E-03	Not Transported
							Opposite Side	Transport	1.00	0.000E+00	Sump Screen
								0.01			
							Stalled in Pool	Erosion Products	15	0.000E+00	Sump Screen
								Remainder	16	0.000E+00	Not Transported
							SG #2 (Elevator)	Transport	1.00	1.519E-03	Sump Screen
								0.07			
							Stalled in Pool	Erosion Products	19	0.000E+00	Sump Screen
								Remainder	20	3.646E-02	Not Transported
							SG #1 (RV Cavity)	Transport	1.00	2.430E-02	Sump Screen
								0.56			
							To Near Screen	0.40			
								0.40			
Stalled in Pool	Erosion Products	23	0.000E+00	Sump Screen							
	Remainder	24	2.196E-01	Not Transported							
Away From Screen	Transport	1.00	2.440E-02	Sump Screen							
	0.40										
Inactive	0.10										
	0.20										
To Near Screen	0.40										
	0.40										
Stalled in Pool	Erosion Products	28	0.000E+00	Sump Screen							
	Remainder	29	1.440E-02	Not Transported							
Away From Screen	Transport	1.00	1.600E-03	Sump Screen							
	0.40										
Inactive	0.10										
	0.20										
Break Room Floor	0.61										
	0.61										
Sump Floor	0.04										
	0.04										
Pieces 2-6"	1.00										
	1.00										
								0.52519	Not Transported		
								0.13000	Inactive Pools		
								0.34481	Sump Screen		

Figure III.3-7. Sump-Pool-Debris Transport Chart for 2- to 6-in. RMI Debris.

Debris Size	Blowdown Transport	Washdown Transport	Washdown Entry Location	Pool Fill Up Transport	Pool Recirculation Transport	Debris Erosion in Pool	Path	Fraction	Deposition Location					
POOL TRANSPORT LOGIC CHART RMI DEBRIS	Deposited Above 0.22	Trapped Above 0.68					1	1.49E-01	Not Transported					
							Erosion Products	2	0.00E+00	Sump Screen				
								Remainder	3	0.00E+00	Not Transported			
							Stalled in Pool		0.00	1.00	4	0.00E+00	Sump Screen	
								Transport	5		0.00E+00	Not Transported		
							Sump Area	0.01	SG #4	0.22	1.00	1.00	7.04E-04	Sump Screen
														6
							Stalled in Pool	0.00	Eq. Room	0.00	1.00	1.00	0.00E+00	Sump Screen
														8
							Transport	0.00	SG #3 (Stairs)	0.07	1.00	1.00	0.00E+00	Sump Screen
														9
							Stalled in Pool	0.00	Opposite Side	0.01	1.00	1.00	0.00E+00	Sump Screen
														10
							Erosion Products	0.00	SG #2 (Elevator)	0.07	0.90	1.00	4.43E-03	Not Transported
														11
							Remainder	0.00	SG #1 (RV Cavity)	0.62	0.90	1.00	4.92E-04	Sump Screen
														12
							Stalled in Pool	0.00	To Near Screen	0.50	0.10	1.00	0.00E+00	Sump Screen
														13
							Erosion Products	0.00	To Near Screen	0.50	0.00	1.00	0.00E+00	Sump Screen
														14
							Remainder	0.00	To Near Screen	0.50	0.00	1.00	0.00E+00	Sump Screen
														15
							Stalled in Pool	0.00	To Near Screen	0.50	0.90	1.00	4.43E-03	Not Transported
														16
							Erosion Products	0.00	To Near Screen	0.50	0.10	1.00	4.92E-04	Sump Screen
														17
							Remainder	0.00	To Near Screen	0.50	0.00	1.00	0.00E+00	Sump Screen
														18
							Stalled in Pool	0.00	To Near Screen	0.50	0.70	1.00	3.05E-02	Not Transported
														19
Erosion Products	0.00	To Near Screen	0.50	0.30	1.00	1.30E-02	Sump Screen							
							20	3.05E-02	Not Transported					
Remainder	0.00	To Near Screen	0.50	0.00	1.00	0.00E+00	Sump Screen							
							21	1.30E-02	Sump Screen					
Stalled in Pool	0.00	To Near Screen	0.50	0.00	1.00	3.85E-01	Sump Screen							
							22	3.85E-01	Sump Screen					
Erosion Products	0.00	To Near Screen	0.50	0.00	1.00	0.00E+00	Sump Screen							
							23	0.00E+00	Sump Screen					
Remainder	0.00	To Near Screen	0.50	1.00	1.00	3.85E-01	Not Transported							
							24	3.85E-01	Not Transported					
Stalled in Pool	0.00	To Near Screen	0.50	0.00	1.00	0.00E+00	Sump Screen							
							25	0.00E+00	Sump Screen					
Erosion Products	0.00	To Near Screen	0.50	0.00	1.00	0.00E+00	Inactive Pools							
							26	0.00E+00	Inactive Pools					
Remainder	0.00	To Near Screen	0.50	0.00	1.00	5.00E-03	Sump Screen							
							27	5.00E-03	Sump Screen					
Stalled in Pool	0.00	To Near Screen	0.50	0.00	1.00	0.00E+00	Sump Screen							
							28	0.00E+00	Sump Screen					
Erosion Products	0.00	To Near Screen	0.50	1.00	1.00	5.00E-03	Not Transported							
							29	5.00E-03	Not Transported					
Remainder	0.00	To Near Screen	0.50	0.00	1.00	0.00E+00	Sump Screen							
							30	0.00E+00	Sump Screen					
Stalled in Pool	0.00	To Near Screen	0.50	0.00	1.00	0.00E+00	Inactive Pools							
							31	0.00E+00	Inactive Pools					
1.000000														
0.57973								Not Transported						
0.00000								Inactive Pools						
0.42027								Sump Screen						

Figure III.3-8. Sump-Pool-Debris Transport Chart for >6-in. RMI Debris.

The quantified results by debris category and insulation type are shown in Table III.3-7, and the same results combined for each insulation type are shown in Table III.3-8. The analysis indicated that ~52% of the fibrous and ~42% of the RMI debris would accumulate on the recirculation screens for a large LOCA in steam-generator compartment 1 (SG1). The sump pool transport fractions for the small and large piece debris are quite high, 97 and 96%, respectively. The high fraction for debris eroded made a substantial contribution to these numbers. However, to put this assumption into perspective, if only 10% had been assumed for the erosion, the pool transport fractions would still have been 73 and 66%, respectively.

The RMI debris transport fractions were dominated by the large (> 6-inches) debris since 98.4% of the RMI was predicted to be in this category. It should be pointed out that this category includes quite large pieces including intact or nearly intact cassettes, which would required a faster flow to move the debris than 0.28 ft/s implemented into the CFD analyses.

**Table III.3-7. Quantified Category-Specific Sump-Pool-Debris Transport Results**

Debris Category	Category-Specific Debris Transport Fractions				
	Size Distribution	Entering Pool	Into Inactive Pools	Sump Pool Transport	Overall Transport
<b><i>Fibrous Debris</i></b>					
Fines	0.133	0.90	0.032	1	0.90
Small Pieces	0.397	0.64	0.024	0.97	0.62
Large Pieces	0.235	0.45	0.086	0.96	0.44
Intact Pieces	0.235	0.40	0.062	0.56	0.23
<b><i>RMI Debris</i></b>					
<2 in.	0.011	0.66	0.15	0.61	0.40
2 to 6 in.	0.005	0.63	0.13	0.55	0.35
>6 in.	0.984	0.85	0	0.49	0.42

**Table III.3-8. Quantified Insulation-Specific Sump-Pool-Debris Transport Results**

Debris Category	Insulation Specific Debris Transport Fractions			
	Entering Pool	Into Inactive Pools	Sump Pool Transport	Overall Transport
Fibrous	0.57	0.05	0.88	0.52
RMI	0.85	0.0024	0.50	0.42

The fractions of the sump pool floor where the floor level flow velocity was slower than the threshold velocities for debris (0.12 and 0.28 ft/s for fibrous and RMI debris, respectively) were calculated from the CFD results presented in Section III.2. The floor fractions corresponding to a large break in SG1 (lower-right quadrant in the CFD results) are 0.41 and 0.22 for fibrous and RMI debris, respectively. These floor area fractions are compared in Figure III.3-9 with the sump pool transport fractions by insulation type and size categories. In this scenario, if the debris was uniformly introduced into the pool across the pool cross sectional area and erosion was not significant, then the area fractions might be a reasonable indicator of the pool debris transport fractions. However, as shown, the area fractions are a poor indicator of debris transport when the debris is introduced into the pool in a more realistic and nonuniform manner and erosion is substantial. A uniform area fraction model can easily underpredict the pool debris transport by a factor of two or more.

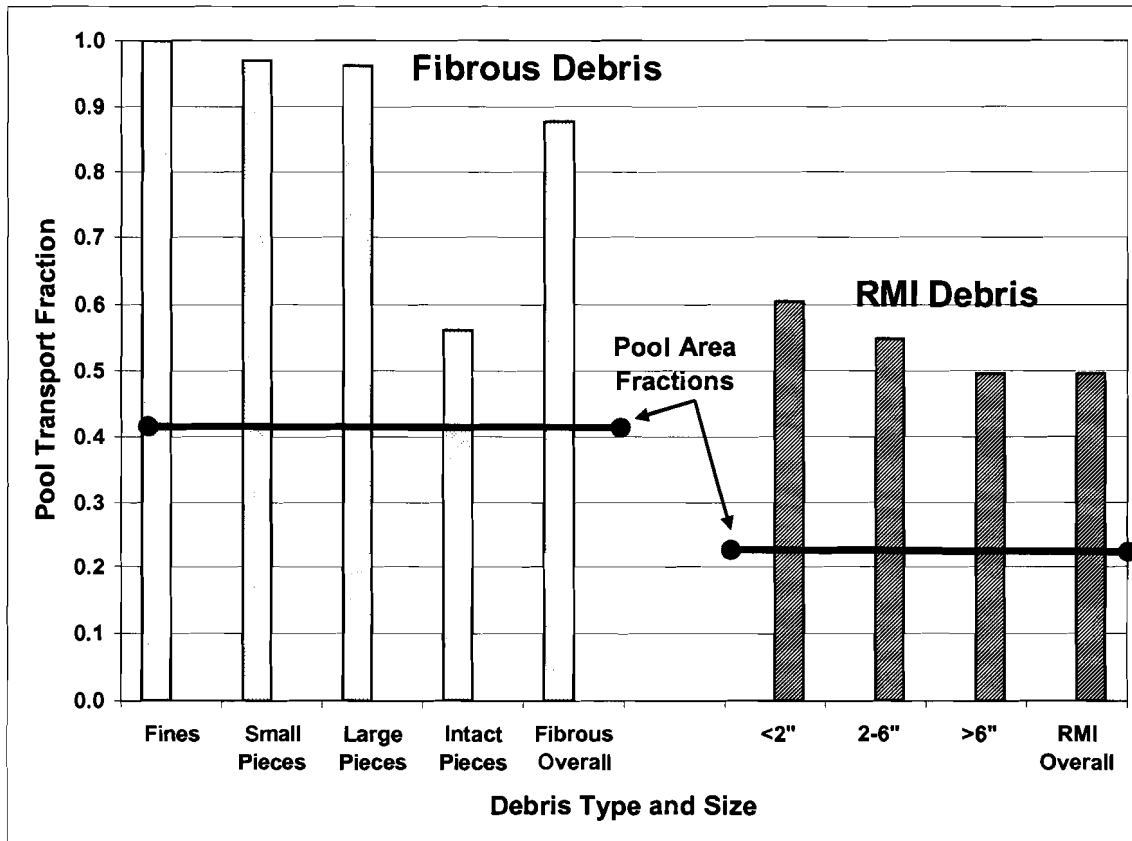


**Figure III.3-9. Comparison of Sump Pool Transport Fraction with Velocity Area Fractions.**

The transport of debris from its generation in the ZOI throughout the containment during the RCS depressurization phase, then the washdown transport by the containment sprays, and then its transport through the sump pool to the recirculation sump screens is a rather intractable problem. A logic chart method was used to decompose the overall transport problem into many smaller problems that were subsequently evaluated by either analysis or simply conservatively judged. As such, the results of the volunteer analyses contain many sources of uncertainties; however, these uncertain results are plausible results and show insight into the many aspects of debris transport that should be useful to subsequent evaluations. These sources of uncertainty regarding sump pool transport include (1) the timing and locations where debris enters the pool; (2) concerns regarding the effects of local pool turbulence that can move debris even when the bulk flow does not; (3) lack of data regarding erosion rates for debris that can decompose within the pool (e.g., fibrous debris); (4) the simplification of the analysis; and (5) the limited scenario space that can be realistically evaluated.

The debris transport results in this section pertain to a large LOCA in SG1. The same LOCA in another compartment could easily result in different transport results, which could be higher or lower than the scenario evaluated herein. In addition, the sump pool debris transport was evaluated herein using simplified nodalization, as discussed above.

A more detailed evaluation would likely refine these transport results significantly; however, the transport methodology has been demonstrated.

### **III.4 CONCLUSIONS AND RECOMMENDATIONS**

Section III.2 outlined a method for performing reactor containment pool flow dynamic analysis. A commercial CFD code was used to perform the simulations and assess the flow properties relevant to debris transport. From the simulations, flow area fractions in excess of debris transport threshold velocities were obtained. Transient containment pool fill-up simulations were performed that could potentially be used to design debris diversion systems to sequester debris into zones that do not participate in the flow when sump pumps are engaged.

Recommendations for future simulations include performing grid-mesh convergence studies, further analysis of debris degradation mechanisms, and flow diversion. The grid-mesh convergence studies are required to have a defensible CFD analysis. Additional constraints on the grid mesh, not used or presented in this document, should include clustering grid points near the mass flow injection locations (break and splash locations) and development of a proper boundary layer grid near the no-slip walls, particularly on the containment floor. With additional grid points near the floor, a near-wall velocity profile will be established. This near-wall velocity gradient and drag forces could have an impact on debris transport and should be thoroughly investigated as part of the grid refinement study. The debris degradation mechanisms should also be the subject of further study. Examples of degradation have been shown in this document, but no attempt to quantify the dynamics has been made at this time.

The transport of debris from its generation in the ZOI throughout the containment during the RCS depressurization phase, then the washdown transport by the containment sprays, and then its transport through the sump pool to the recirculation sump screens is a rather intractable problem. A logic chart method was used to separate the overall transport problem into many smaller problems that were subsequently evaluated by either analysis or engineering judgment. As such, the results of the volunteer analyses contain many source of uncertainties; however, these uncertain results are plausible results and show insight into the many aspects of debris transport that should be useful to subsequent evaluations. These sources of uncertainty regarding sump pool transport include (1) the timing and locations where debris enters the pool; (2) concerns regarding the effects of local pool turbulence that can move debris even when the bulk flow does not; (3) lack of data regarding erosion rates for debris that can decompose within the pool (e.g., fibrous debris); (4) the simplification of the analysis; and (5) the limited scenario space that can be realistically evaluated.

The debris transport results in this appendix pertain to one LOCA scenario: a large LOCA in SG1. The same LOCA in another compartment could easily result in different transport results that could be higher or lower than the scenario evaluated herein. In addition, the sump pool debris transport was evaluated herein using simplified nodalization, as discussed above. A more detailed evaluation would likely refine these transport results significantly; however, the transport methodology has been demonstrated.

### III.5 REFERENCES

[NUREG/CR-6772, 2001] D. V. Rao, B. C. Letellier, A. K. Maji, and B. Marshall, 2002, "GSI-191: Separate-Effects Characterization of Debris Transport in Water." NUREG/CR-6772, LA-UR-01-6882.

[NUREG/CR-6773, 2002] D. V. Rao, C. Shaffer, B. C. Letellier, A. K. Maji, and L. Bartlein, "GSI-191: Integrated Debris-Transport Tests in Water Using Simulated Containment Floor Geometries," NUREG/CR-6773, LA-UR-02-6786, December 2002.

## APPENDIX IV: DEBRIS TRANSPORT COMPARISON

The NEI GR baseline debris transport recommendations contain both conservative and nonconservative assumptions which were used to simplify the transport evaluation. To assess the effect of the nonconservative assumptions used in the baseline model, the baseline model was applied to the pressurized-water-reactor (PWR) volunteer plant, whereby those baseline results could be compared with the detailed debris transport evaluation performed for the volunteer plant. The comparison supported the review and acceptance of the NEI baseline evaluation methodology by illustrating that the baseline predicted conservative debris transport results for the volunteer plant. Insights gained from this comparison regarding debris entrapment in the inactive pool and the transport of large debris support staff imposed limitations on the acceptance of the baseline methodology.

Because the volunteer plant contains substantial quantities of both fibrous and reflective metal insulation (RMI), the baseline model was applied to both types of insulation debris. Detailed sump pool debris transport analyses were performed for the volunteer plant containment as documented in Appendix III. Detailed blowdown and washdown debris transport analyses were performed for the volunteer-plant containment documented in Appendix VI. Appendix IV (this appendix) compares the GR baseline analysis to the detailed analyses for the volunteer plant as documented in Appendices III and VI.

The comparison is based on the GR baseline two-group debris-size distributions, i.e., small fines and large-piece debris. The detailed analyses used a four-group distribution of fines, small pieces, large pieces, and intact pieces. The detailed four-group results were reduced to two groups by combining the fines and small-piece debris into the NEI small-fines group and combining the large-piece and the intact-piece groups into the NEI large-piece group. This approach was required to create a direct comparison.

The size distributions for both the NEI baseline results and the detailed analyses results were based on destruction pressures of 10 psi for the fibrous debris and 4 psi for the RMI debris. The respective size distributions were obtained from the research documented in Appendix II. The radii of the fibrous and RMI zone of influence (ZOI) for these pressures are 11.9 and 21.6 r/D, respectively (see Appendix I). In applying the baseline model to the volunteer plant, it was assumed that the containment was highly compartmentalized.

The baseline and detailed analyses results are compared by debris size in Tables IV.1 and IV.2 for fibrous and RMI debris, respectively. Table IV.3 compares the overall transport fractions, which combine the small fine debris and the large debris to obtain the total estimated screen accumulation. The respective debris-size distributions shown in Table IV.1 were used to calculate the overall transport results shown in Table IV.3. Note that the transport fractions in Tables IV.1 and IV.2 are pertinent only to the respective size categories.

**Table IV.1. Baseline Comparison with Detailed Volunteer-Plant Fibrous Transport Results**

Transport Phase	Debris Transport Fractions			
	Fine/Small Debris		Large-Piece Debris	
	Baseline	Detailed	Baseline	Detailed
Debris-Size Fraction	0.60	0.53	0.40	0.47
Blowdown Transport into Upward Levels	0.25	0.92	0	0.63
Blowdown Transport Directly to Sump Pool Floor	0.75	0.08	1	0.37
Washdown Transport from Upper Levels to Sump Pool	1	0.71	0	0.21
Total Debris Entering Pool	1	0.73	1	0.50
Entering Inactive Pool	0.14	0.03	N/A	0.07
Entering Active Sump Pool	0.86	0.70	1	0.43
Sump Pool Transport to Sump Screens	1	0.98	0	0.76
Fraction Accumulating on Sump Screens	0.86	0.69	0	0.33

**Table IV.2. Baseline Comparison with Detailed Volunteer-Plant RMI Transport Results**

Transport Phase	Debris Transport Fractions			
	Fine/Small Debris		Large-Piece Debris	
	Baseline	Detailed	Baseline	Detailed
Debris-Size Fraction	0.75	0.02	0.25	0.98
Blowdown Transport into Upward Levels	0.25	0.44	0	0.22
Blowdown Transport Directly to Sump Pool Floor	0.75	0.56	1	0.78
Washdown Transport from Upper Levels to Sump Pool	0	0.55	0	0.32
Total Debris Entering Pool	0.75	0.80	1	0.85
Entering Inactive Pool	0.11	0.15	N/A	0
Entering Active Sump Pool	0.64	0.65	1	0.85
Sump Pool Transport to Sump Screens	1	0.59	0	0.49
Fraction Accumulating on Sump Screens	0.64	0.39	0	0.42

**Table IV.3. Comparison of Overall Baseline and Detailed Analysis Transport Fractions**

Debris Type	Fraction of ZOI Insulation Debris Accumulated on Sump Screens	
	Baseline	Detailed
Fibrous Debris	0.52	0.52
RMI Debris	0.48	0.42

Substantial uncertainty exists in various aspects of the volunteer plant analyses that affect this comparison, which includes the following:

- Uncertainties in determining the debris generation size distributions.
- Uncertainties in specifying various aspects of the blowdown and washdown debris transport and deposition processes.
- Uncertainties in estimating the locations where debris enters the sump pool and when the debris enters with respect to the formation of the pool.

- Uncertainties in estimating the quantities of debris transported into the inactive pool regions.
- Uncertainties in estimating debris transport within an established sump pool.

The following points apply to the comparison of the fibrous debris transport:

1. The baseline recommendation for the debris-size distribution assumed 60% for the small fine debris, which is somewhat higher than the 53% determined from the integration of the air jet debris generation data (Appendix II). Although there is a potential that a two-phase steam/water jet could produce finer fibrous debris than a corresponding air jet, the baseline 60% small fines fraction for fibrous debris generated within the ZOI is accepted as conservative (note that the test data from the single available fibrous two-phase debris generation test is inconclusive in regards to this issue).
2. In the detailed analysis, most of the smaller fibrous debris was predicted to be deposited in the upper levels during blowdown debris transport, rather than directly on the sump floor as proposed in the baseline model. Because the transport of this upper-level debris to the sump pool by containment spray drainage (washdown) is delayed by a variable and indeterminate period of time, it must be postulated that relatively little of the debris reaches the sump floor in time to be entrained in the water flow filling the inactive pools (primarily the reactor cavity in the volunteer plant), which occurs relatively early in the accident sequence (<12 minutes). The detailed analyses predicted that at the end of the blowdown/washdown transport a significantly less amount of debris, compared to the baseline analyses, would enter the active sump pool.
3. The baseline model sump pool transport was 100% for small fines and 0% for large-piece debris. The baseline model predicted more small fine debris accumulation on the sump screens than did the detailed analyses. However, the detailed analyses predicted substantial accumulation of large-piece debris on the screens, whereas the baseline predicted none.
4. The baseline and detailed analyses both predicted that approximately 52% of the fibrous debris generated within the ZOI would accumulate on the sump screens. Although this comparison does not explicitly demonstrate that the baseline methodology is conservative relative to the detailed volunteer plant evaluation, detail-specific conservatisms built into various aspects of the blowdown/washdown and pool debris transport analyses still support the overall conclusion that the baseline methodology is conservative with respect to its application to the volunteer plant.

The following points apply to the comparison of the RMI debris transport:

1. The baseline recommends using more small fine RMI debris than was determined from the integration of the air jet debris generation data (Appendix II). The primary reason for the large difference is the large increase in ZOI volume predicted by the ANSI/ANS-58.2-1988 standard when that standard is applied to jet pressures as low as 4 psi. That is, although damage extends to 4 psi, only a small amount of small fine debris is generated over much of the ZOI volume. Most of the ZOI debris is large-piece debris.

2. The detailed analyses predicted lesser quantities of RMI debris than fibrous debris would deposit in the upper levels of the containment, although it was substantially more than the baseline model recommendation of 25%. A primary reason for this result was that so little blowdown debris transport data exist for RMI debris and thus the blowdown analyses conservatively assumed a large fraction of debris depositing directly on the sump floor. Both the detailed and baseline analyses predicted that approximately the same amount of debris would enter the active sump pool at the end of the blowdown/washdown transport.
3. The baseline model sump pool transport was 100% for small fines and 0% for large-piece debris. The baseline model predicted more small fine debris accumulation on the sump screens than did the detailed analyses. However, the detailed analyses predicted substantial accumulation of large-piece debris on the screens, whereas the baseline predicted none.
4. The baseline method predicted slightly more RMI debris accumulation on the sump screens than did the detailed analyses, i.e., 48% as compared with 42% of the debris generated.

## **CONCLUSIONS NUMBER AS HEADER?**

The application of the baseline methodology to the volunteer plant predicted approximately the same accumulation of fibrous debris and conservatively more RMI on the sump screen than did the detailed transport analyses. Although this comparison does not explicitly demonstrate that the baseline methodology is conservative relative to fibrous debris transport in the detailed volunteer plant evaluation, detail-specific conservatisms built into various aspects of the blowdown/washdown and pool debris transport analyses still support the overall conclusion that the baseline methodology is conservative with respect to its application to the volunteer plant. Even though the baseline and detailed evaluation arrived at the same fractions for sump screen debris accumulation, the intermediate steps disagreed. Due to the diversity among the PWR containment designs, this analysis does not conclusively demonstrate that the baseline methodology will be conservative for debris transport in all of the PWRs. In addition, substantial sources of uncertainty were noted in the detailed volunteer plant analyses.

Insights gained from this comparison regarding debris entrapment in the inactive pool and the transport of large debris support staff imposed limitations on the acceptance of the baseline methodology to prevent an outlier plant from demonstrating adequate NPSH margin using the baseline methodology where adequate NPSH margin might not exist in reality. The limitations resulted from the following two concerns that should be addressed before accepting baseline method results for plant-specific analyses.

First, if a plant baseline analysis estimates a relatively large fraction of the debris trapped in the inactive pools, as could be the case with a large reactor cavity volume and a shallow sump pool, then the baseline inactive pool fraction should be more limited than the current baseline model. Note that the detailed analyses reported herein predicted only approximately 3% of the small fibrous debris trapped in the inactive pool as compared with 14% using the baseline model. This comparison indicates for conservatism that the fraction of debris assumed to be trapped in the inactive pool should be limited to no more than ~15% unless a higher fraction is adequately supported by analyses or experimental data. The determination of a limiting fraction is difficult based on the available research. Given this comparison where the baseline predicted sump screen accumulation results comparable to the detailed analyses and the volunteer plant

inactive pool fraction was 14%, it seems reasonable to assume an inactive pool fraction limitation of about 14% would maintain acceptable baseline results. A limiting inactive pool fraction of 15% was recommended..

Second, if the characteristic sump pool transport velocities are relatively fast, such that large transport fractions for large debris are indicated, then the baseline method should be modified to include the transport of large debris, as well as the transport of the small fine debris. In the volunteer plant, for example, approximately 98% of the large RMI ZOI (based on a destruction pressure of 4 psi) was predicted to be debris larger than about 6 in., of which about 42% would be transported to the sump screens. If the transport fraction for the large RMI was increased to ~50% from 42%, then the volunteer transport analysis results would have predicted more total RMI accumulation than the GR baseline recommendation predicted. The characteristic transport velocities must be compared with typical debris transport velocities to determine whether the baseline method should be modified to include the transport of large debris. Characteristic transport velocities can be sufficiently estimated using recirculation flow rates and nominal sump dimensions to determine if a potential exists that substantial portions of the large debris will transport. If substantial transport of large debris is reasonably possible and if such transport can alter the outcome of the NPSH margin evaluation, then analytical refinements are needed that evaluate large debris transport.

## APPENDIX V: CONFIRMATORY HEAD-LOSS ANALYSES

Confirmatory research was performed to determine whether specific parameter assumptions made in the Nuclear Energy Institute (NEI) guidance report are conservative with respect to more realistic parameters. This research also provided additional insights into the estimation of head-loss parameters for the NUREG/CR-6224 head-loss correlation. Additional guidance is also provided for determining appropriate parameters for a mix of multiple fiber and particulate components.

### V.1 FIBROUS DEBRIS HEAD-LOSS PARAMETERS

A comparison of specific surface areas ( $S_v$ ) deduced from head-loss test data and the simple geometric correlation of four divided by the characteristic fiber diameter ( $4/d$ ) is presented for NUKON™ and Kaowool™ insulation debris. The test data used in both of these deductions are available in the BWROG head-loss tests documented in Volume 1 of the BWROG Utility Resolution Guidance (URG).

#### V.1.1 NUKON™ Fibrous Debris

The URG has three head-loss tests that used only NUKON™ insulation debris and used a type of strainer that behaved similarly to that of a flat-plate screen (i.e., a truncated cone strainer). These tests were numbered 2, 4, and 5 and used 8, 8, and 16 lb of NUKON™, respectively, and no particulate. The flow velocities through the bed varied from ~0.15 to 0.75 ft/s, resulting in a total of 15 head-loss data points. A specific surface area was deduced for each data point using the NUREG/CR-6224 head-loss correlation and using an as-manufactured density of 2.4 lb/ft<sup>3</sup> and a fiberglass material density of 175 lb/ft<sup>3</sup> (NUREG/CR-6224 study recommendations). The resultant  $S_v$  values are compared in Figure V-1.

The comparison was based on the debris bed compression as determined by the NUREG/CR-6224 correlation (the ratio of the compressed thickness divided by the uncompressed thickness), which is directly affected by the flow pressure (i.e., flow velocity). The average value for  $S_v$  was ~170,600/ft. The nominal diameter for NUKON™ fibers has been specified as 7.1 μm, which translates into an  $S_v$  of 171,710/ft. The NUREG/CR-6224 study recommended an  $S_v$  of 171,420/ft. For NUKON™ insulation debris, the  $S_v$  determined using four divided by the fiber diameter is in excellent agreement with the experimentally deduced value.

The NEI guidance has recommended using a material density of 159 lb/ft<sup>3</sup> rather than the NUREG/CR-6224 study value of 175 lb/ft<sup>3</sup>. Confirmatory analysis using the NUREG/CR-6224 correlation confirmed that it is conservative to use 159 lb/ft<sup>3</sup> rather than 175 lb/ft<sup>3</sup>, provided that the remaining head-loss parameters of 2.4 lb/ft<sup>3</sup> for the as-manufactured density and 171,000/ft for the specific surface area are maintained. The lower value for the material density estimates a slightly higher head loss than does the larger value.

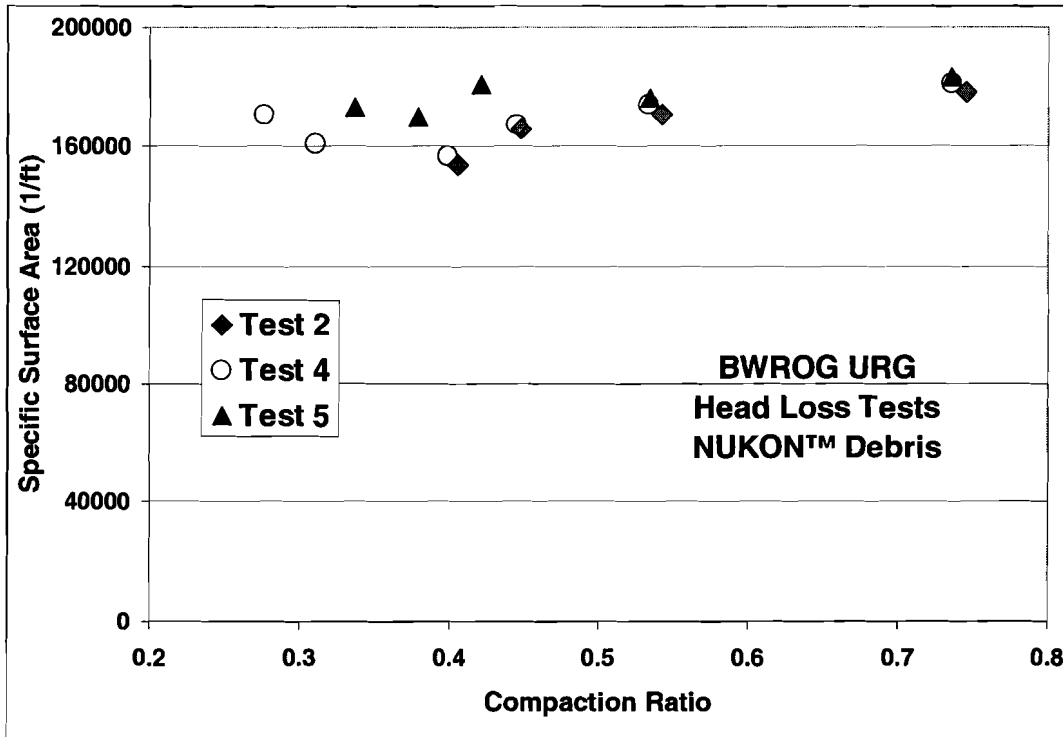


**Figure 0V-1. NUKON™ Specific Surface Area.**

Similarly, the NEI guidance recommended using 62.4-lb/ft<sup>3</sup> (1.0 g/cm<sup>3</sup>) for material density of latent fibers to enhance transport (neutral buoyancy). The latent debris characteristics test results [LA-UR-04-3970, 2004a] that analyzed latent debris collected in the containments of several volunteer plants show that the latent debris fibers had material densities ranging from 1.3 to 1.9 g/cm<sup>3</sup>. Again, confirmatory analyses verified that it is conservative from a head-loss prediction perspective to assume that the latent fiber material density is 1.0 g/cm<sup>3</sup> rather than 1.3 to 1.9 g/cm<sup>3</sup>, provided that the remaining head-loss parameters are appropriately specified.

### V.1.2 Kaowool™ Fibrous Debris

The URG has one valid head-loss test<sup>\*</sup> that used Kaowool™ insulation debris and used a type of strainer that behaved similarly to that of a flat-plate screen (i.e., a truncated cone strainer). Test J13 initially had added 12 lb of Kaowool™, then later added 5 lb of iron oxide corrosion products (CPs), and then subsequently added another 5 lb of CP. The flow velocities through the bed varied from ~0.31 to 0.62 ft/s, resulting in a total of nine head-loss data points (three data points without particulate). A specific surface area was deduced for each data point using the NUREG/CR-6224 head-loss correlation, with the NUREG/CR-6224 study recommended parameters for the corrosion products used as input.<sup>†</sup> The recommended fiber material density for Kaowool™ is 160 lb/ft<sup>3</sup>.

<sup>\*</sup> Test J12 also used Kaowool, but the quantities of corrosion products so overwhelmed the debris bed that if all of the corrosion products had filtered from the flow, the granular bed, not counting the Kaowool, would have been nearly 2 in. thick. In any case, the head-loss contribution due to Kaowool was so overshadowed by the corrosion products that the test was not valid for determining the specific surface area for Kaowool.

<sup>†</sup> The NUREG/CR-6224-recommended parameters are 183,000/ft for the specific surface area, 324 lb/ft<sup>3</sup> for the particulate material density, and 65 lb/ft<sup>3</sup> for the granular packing-limit density.

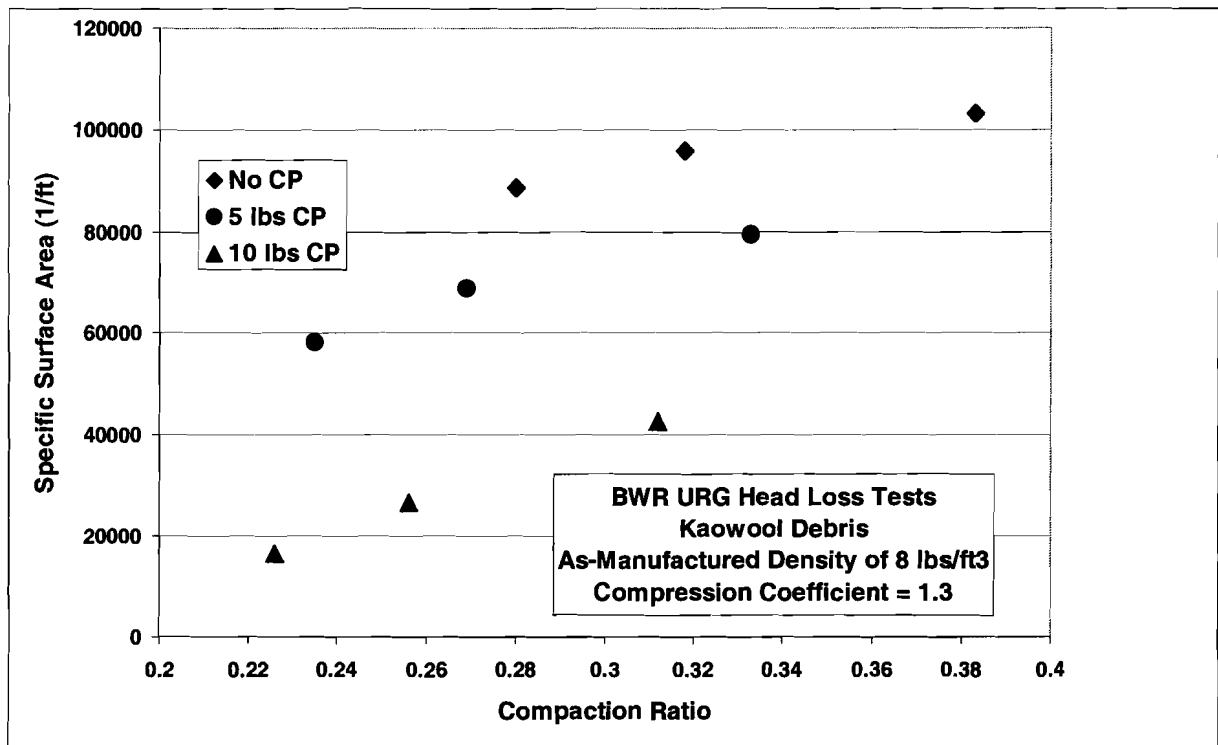


**Figure V-2. Kaowool Specific Surface Area Assuming Base Parameters**

The NEI guidance recommends an as-manufactured density of Kaowool™ ranging from 3 to 12 lb/ft<sup>3</sup>, whereas the URG recommended a value of 8 lb/ft<sup>3</sup>, apparently a midrange value. First, the Sv values were deduced from Test J13 data by assuming an as-manufactured density of 8 lb/ft<sup>3</sup> and the same bed compression correlation that was so successful for NUKON™. These resultant Sv values are compared in Figure V-2. The values of Sv, as shown, are very scattered, ranging from 16,000 to 103,000/ft. All in all, the NUREG/CR-6224 correlation does not work well with these input parameters. Noting that the as-manufactured density cited in the guidance report (GR) ranged from 3 to 12 lb/ft<sup>3</sup>, it was subsequently determined that a smaller value of the density would reduce the scatter in the resultant Sv values. Further, it was discovered that stiffening the compression function also reduced the scatter. A second comparison of the deduced Sv values was developed assuming an as-manufactured density of 4 lb/ft<sup>3</sup> and a leading compression coefficient of 0.5 (rather than the standard 1.3). The results are shown in Figure V-3. The comparison in Figure V-3 has the deduced values in good agreement, with an average value of 165,500/ft.

The nominal diameter for Kaowool™ fibers has been specified as 2.7 to 3.0 μm in the NEI guidance, which translates into an Sv of 406,400 to 451,500/ft using the four-divided-by-the-diameter formula. Although using such high values for Sv is conservative, the simple formula is not even close to the experimentally deduced value of 165,500. The application of an Sv of 406,400/ft would substantially overpredict the results of Test J13.

The coefficient of the NUREG/CR-6224 compression correlation is an important issue. The standard coefficient of 1.3 was developed and validated essentially using NUKON™; therefore, the validation of other fibrous insulation must assess the validity of this value for the insulation

under consideration. It is noted that the baseline guidance in the GR considers this point by including the constant K (Equation 3.7.2-4 in Section 3.7.2.3.1.1 of the baseline guidance with a default value of 1 for K). For Kaowool™, a K = 0.385 and a Sv of 165,500/ft in the NUREG/CR-6224 correlation predicts URG Test J13 results reasonably well.

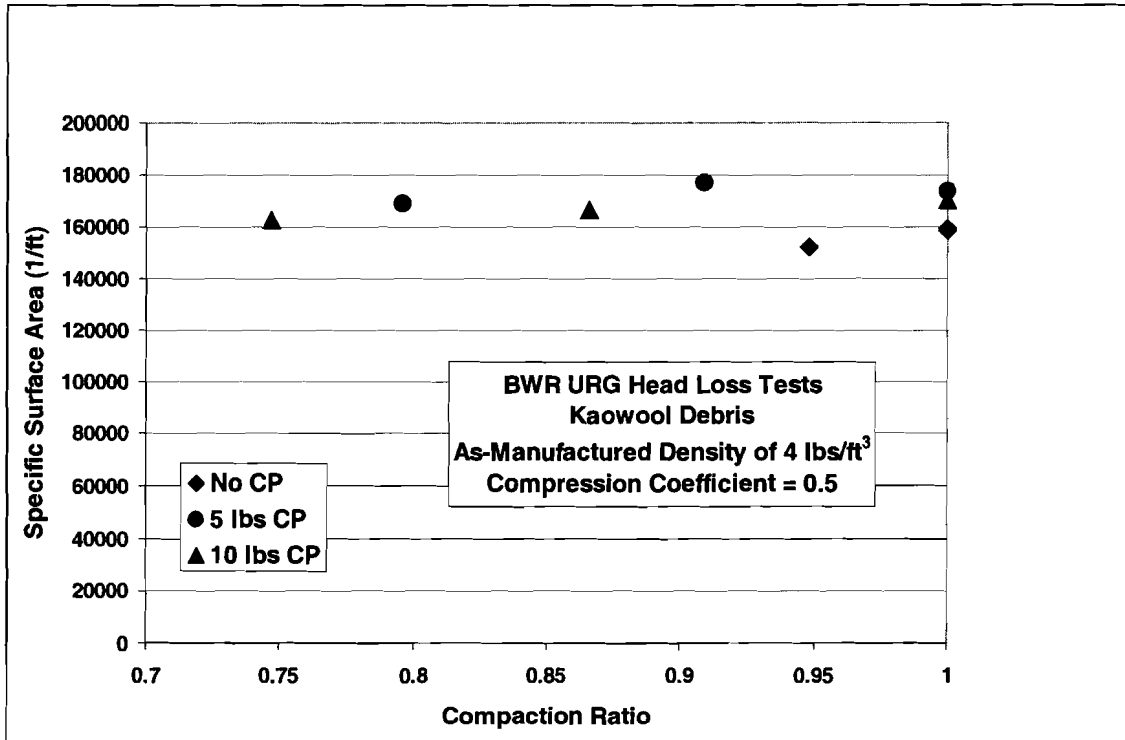


Figure V-3. Kaowool™ Specific Surface Area Using Modified Parameters.

### V.1.3 Comparison of Fibrous Debris

The specific surface areas are compared in Figure V-4 for areas determined using the four-divided-by-the-fiber-diameter formula and the two experimentally deduced values presented herein for NUKON™ and Kaowool™. The following points are made:

1. The coefficient(s) for the compression correlation also have a role in the application of the NUREG/CR-6224 correlation to the various types of fibrous debris.
2. The 4/d formula was formerly validated using NUKON™, but not necessarily for other types of fibrous insulations.
3. The 4/d formula is not reliable and should not be applied indiscriminately. It should not be assumed that because this formula overpredicts Kaowool™ head losses that it will be conservative for untested types of fibrous debris. The only reliable method of determining the specific surface area of a particular insulation material is deduction from applicable test data.

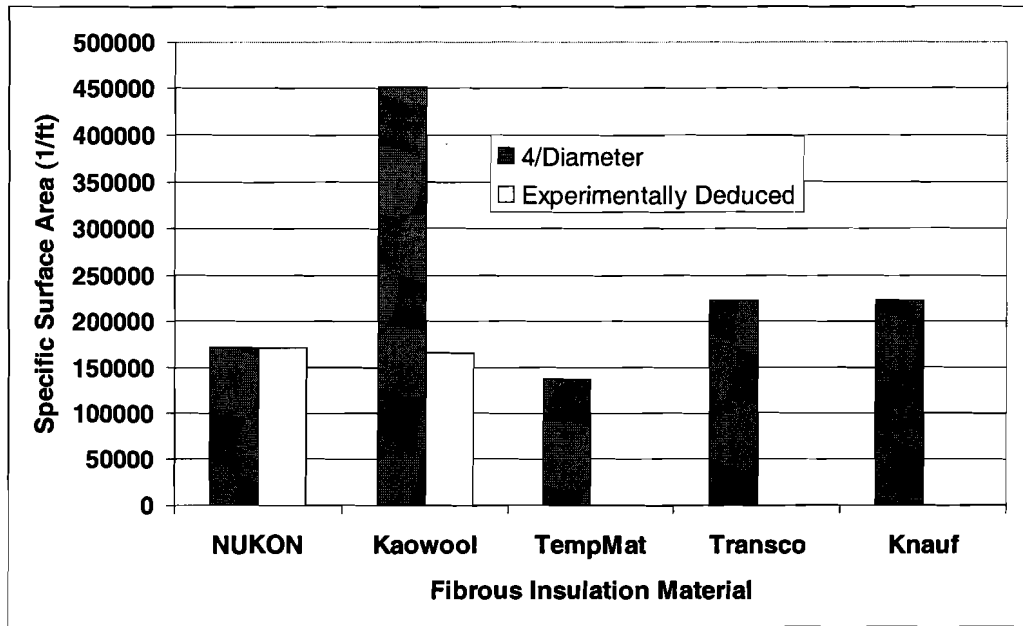


Figure 0-4. Comparison of Fibrous Insulation Specific Surface Areas.

## V.2 PARTICULATE DEBRIS HEAD-LOSS PARAMETERS

In Section 3.7.2.3.1.1 of the GR, the NEI guidance recommends using the simple formula of six divided by the characteristic particle diameter to determine the specific surface areas for particulate debris. The following confirmatory analyses provide insights into this relationship and experimentally deduced values for particulate  $S_v$ .

### V.2.1 Iron Oxide Corrosion Products

During the resolution of the BWR strainer blockage issue, the iron oxide CPs that accumulate in a boiling-water-reactor (BWR) suppression pool were the primary particulate in the head-loss calculations. The BWR sludge (CP) is characterized by the size distribution shown in Table V-1.

The NUREG/CR-6224 correlation recommends a specific surface area of 183,000/ft for head-loss estimates with CP, which has been validated by comparison with test data. Using the midrange diameters from Table V-1 to estimate the  $S_v$  for the CP distribution using the  $6/d$  formula, the  $S_v$  estimate becomes 48,400/ft (almost a factor of four less than the NUREG/CR-6224 recommendation). Note that a factor-of-4 error in the  $S_v$  can result in a factor as large as 16 in error in the head loss at low flow velocities.

If the minimum value of the range is used (assuming a minimum particle size of 2  $\mu\text{m}$  for the 0- to 5- $\mu\text{m}$  size group), then an  $S_v$  of ~290,000/ft is calculated (~58% higher than the recommended validated area). The smaller particles have more effect on the particulate  $S_v$  than do the larger particles, which is why the midrange diameters are not a valid representation of the distribution. Using the smallest diameters of each group is conservative but can result in

large estimates of  $S_v$ . Further, these examples illustrate that it is difficult to determine where in a size range is an appropriate diameter for the  $S_v$  determination using  $6/d$ .\*

**Table V-1. Size Distribution of BWR Suppression Pool Iron Oxide Corrosion Products<sup>†</sup>**

Size Range (µm)	Percent by Number of Particles	Percent by Weight
0–5	81%	0.3%
5–10	14%	1.5%
10–75	5%	98.2%

An example of how the  $6/d$  formula works over a particle-size grouping is illustrated in Figure V-5, where  $6/d$  is plotted for particle diameters ranging from 5 to 75 µm (typical distribution grouping). If it is assumed that particles are uniformly distributed (by weight) across this size range (which is not necessarily a valid assumption), then the average  $6/d$  corresponds to a diameter of 25.8 µm, whereas the midrange diameter is 40 µm. Because this simple arithmetic relationship arrives at differing conclusions, depending on the range specification, this method cannot be used reliably in a general sense, even if the uniform distribution assumption is valid.

In summary, the only reliable method of determining the  $S_v$  for a particulate, unless the particulate-size distribution is known in much greater detail than has been typically specified to date, is to deduce  $S_v$  from valid head-loss test data. It is conservative to use the lower diameter of each size group but this can lead to large estimates of the  $S_v$ . However, this method is valid when applicable head-loss data are lacking. Another difficulty is the determination of the smallest particles in the distribution. Although most particulates will have sub-micron particles in the distribution, fiber debris beds may not filter such small particles or certainly the efficiency of filtration could be rather low and is difficult to determine.

\* Similar results were obtained when  $6/d$  was applied to concrete dust head-loss test data during NRC-sponsored tests documented in LA-UR-04-1227.

<sup>†</sup> The NEI guidance (Table 4-3) and NUREG/CR-6224 (Table E-2) both have the percentages in the center column of this table listed as percentages by weight. However, the BWROG URG (Table 7) lists this column as percentages by the number of particles, as shown here. Because the data originated from the BWROG and the numbers only seem to make sense as the number of particles, it is assumed here that the URG is the correct source. Therefore, it is believed that the heading was mislabeled in NUREG/CR-6224 from which the NEI adapted the data for the guidance. In any case, it is conservative to assume that 81% of the particulate by weight is <5 microns because this assumption leads to very high specific-surface-area estimates.

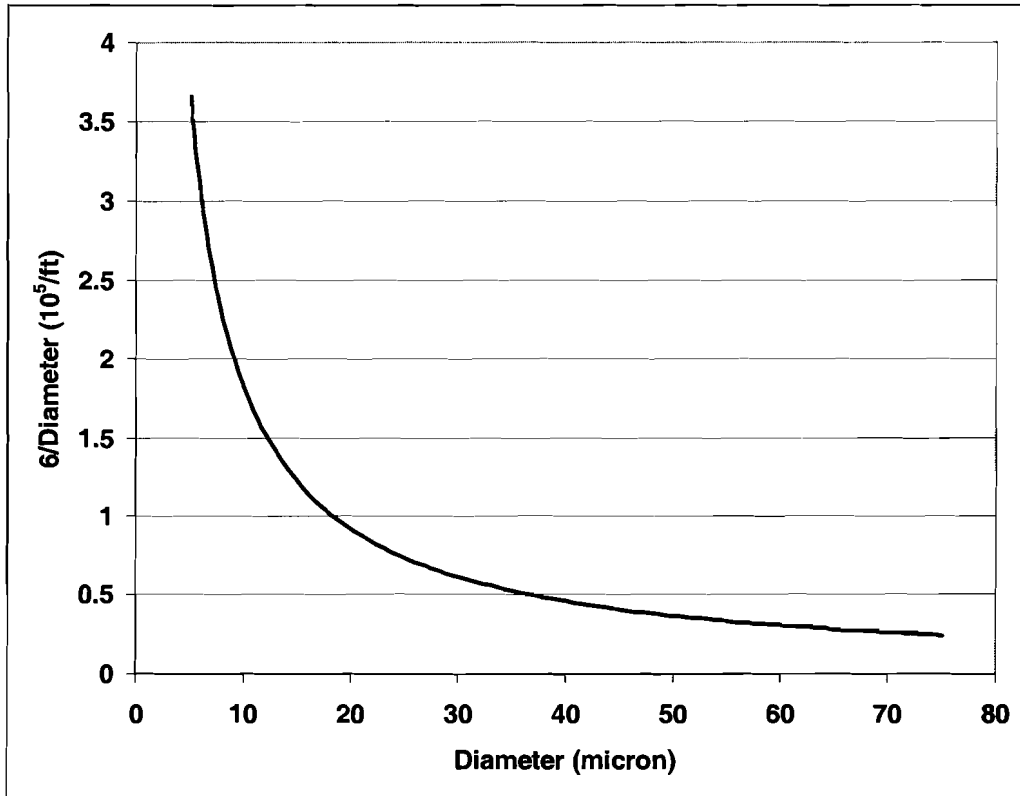


**Figure V-5. Example of Sv Variance with Particle Diameter.**

## V.2.2 Latent Debris

The characteristics of latent debris collected from inside containments of several nuclear plants have been determined by Los Alamos National Laboratory (LANL) [LA-UR-04-3970, 2004a]. These characteristics included properties of material composition and hydraulic flow properties (e.g., specific gravities and characteristic dimensions). Based on these characteristic properties, surrogate latent particulate debris was formulated for testing in the closed-circulation head-loss simulation loop operated by the Civil Engineering Department at the University of New Mexico (UNM).<sup>†</sup> Applying the NUREG/CR-6224 head-loss correlation to the test data for the surrogate latent debris resulted in parameter recommendations for the application of the correlation to plant latent debris. Those recommendations are summarized below, together with insights gained from the surrogate latent debris data reduction. The test apparatus and base test procedures are described in detail in the calcium silicate debris test report [LA-UR-04-1227, 2004b].

The plant debris characteristics pertinent to the specification of a recipe to create a suitable latent particulate surrogate include the particulate specific gravity and the particulate-size distribution. The particulate-size distribution, shown in Table V-2, was used as a recipe for the

\* A surrogate was required to provide the quantities of debris needed for head-loss testing. The latent debris collected in containment required the special handling associated with radioactive materials.

<sup>†</sup>NUKON™ insulation debris was selected to form the fiber bed to filter the surrogate particulate from the flow because of its well-established head-loss properties.

particulate. The surrogate particulate debris tested at UNM was constructed from common sand and soil (referred to as dirt) with the sand used for the two larger size groups and the dirt for the <75- $\mu\text{m}$ -size group. The specific gravity of the latent debris characterized at LANL varied but is well represented as a specific gravity of 2.7, and both the sand and dirt used to formulate the surrogate were found to have a specific gravity near 2.7. The dirt had a clay component that tended to disintegrate, in part, in water, thereby adding substantial particulate <10  $\mu\text{m}$  to accommodate the LANL finding that substantial very fine debris was collected in the filters. Both granular (thin-bed) and nongranular debris beds were tested.

**Table V-2. Surrogate Particulate Size Distribution**

Size Range ( $\mu\text{m}$ )	Fraction
500 to 2000	0.277
75 to 500	0.352
< 75	0.371

Tests were conducted using the individual size groupings for the 75- to 500- $\mu\text{m}$  sand and the <75- $\mu\text{m}$  dirt (without the other groups present) to determine specifically the head-loss characteristics of these individual size groupings; then the latent debris recipe was tested with all three size groups represented according to the recipe. The largest size group (500  $\mu\text{m}$  to 2 mm) was not individually tested because of its relatively minor impact on the recipe head loss; its small specific surface area was estimated using the 6/d equation. For the other two size groups, the specific surface area was deduced from the head-loss data. The bulk densities of the three components were estimated by measuring the bulk volume in a calibrated beaker for a weighted mass of particulate. Given the particle specific gravity and the bulk densities, the granular debris bed porosities were estimated. The test results for the surrogate latent particulate debris are summarized in Table V-3.

**Table V-3. Summary of Test Results**

Particulate ( $\mu\text{m}$ )	Bulk Density (lbm/ft <sup>3</sup> )	Limiting Granular Porosity	Limiting Granular Solidity	Specific Surface Area (ft <sup>-1</sup> )
500 to 2000 (Sand)	104	0.38	0.62	2000
75 to 500 (Sand)	99	0.41	0.59	10,800
<75 (Dirt)	39	0.77	0.23	285,000
Recipe	63 to 75	0.62 to 0.55	0.38 to 0.45	106,000

A range of numbers is shown for the bulk density and limiting granular porosity and solidity due to the uncertainty associated with filtration of the very fine dirt from the water flow, i.e., how much of the dirt introduced into the test loop actually resided in the debris bed. Test-loop water turbidity measurements clearly showed that significant, sometimes substantial quantities of the fine dirt were not filtered from the flow by the fibrous bed. If there is a minimum particle size for effective filtration, it is most certainly significantly <10  $\mu\text{m}$  and likely less than a few microns. Table V-3 presents nominal estimates for the specific surface area for each component; however, there is significant uncertainty in determining these numbers. The primary uncertainty

associates with the less than 75 microns particulate was the filtration efficiency of the finer particles. Assessing the uncertainties in the turbidity resulted in the conclusion that between 30% and 45% of the particulate remained in solution, which corresponded to a range of about 250,000/ft to 340,000/ft in the specific surface area when the correlation was applied. For the two larger particulate size groups (75 to 500 microns and 500 to 2000 microns), the uncertainties were analytically estimated using the  $6/diameter$  formula where the diameter was ranged from the smallest diameter particles up to 25% of the range. These estimated uncertainties are compared in Figure V-6.

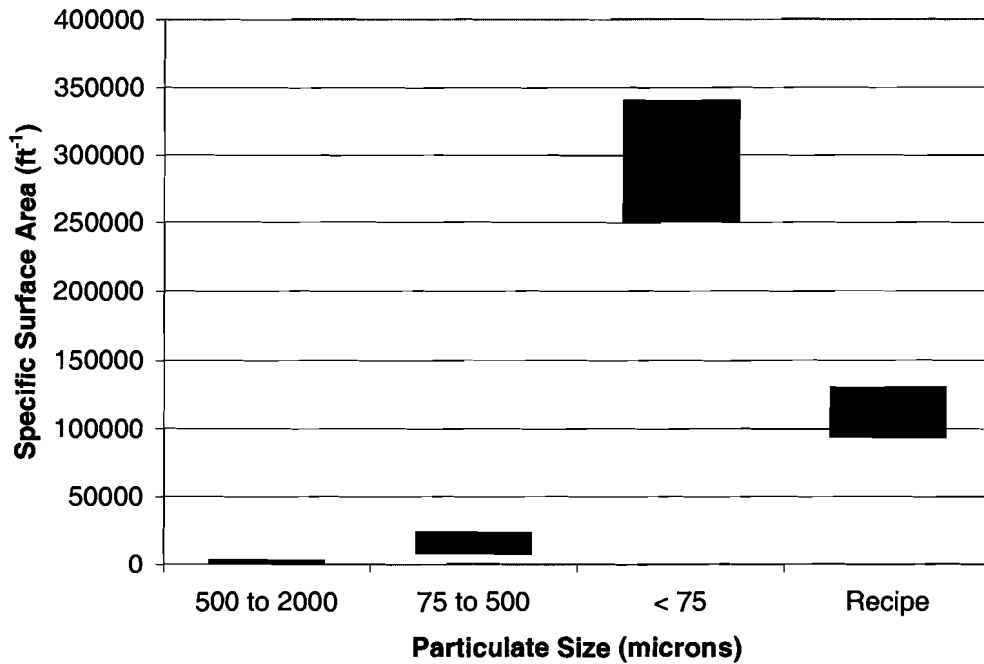


**Figure V-6. Comparison of Component and Recipe Specific-Surface-Area Ranges.**

Key points that can be deduced from the foregoing discussions relative to latent debris are the following:

1. The head loss through granular (thin-bed) debris is controlled by the limiting porosity (solidity), which depends on the composition of the debris. Solidity certainly is not a fixed number, as is indicated in the presentation of the NEI guidance as a solidity of 0.2. Handbooks on soils show many materials with limiting porosity  $<0.8$ , e.g., common sand is  $\sim 0.40$  to  $0.43$  and was experimentally verified in the LANL tests.
2. The major contributors to the head loss are the increasingly smaller particles ( $<75 \mu\text{m}$ ), as illustrated by the  $6/d$  formula, until the particles become too small for filtration. However, it is difficult to determine some limiting particle diameter that will not filter.
3. It is difficult to formulate specific recommendations for the appropriate parameters to use in the NUREG/CR-6224 correlation for pressurized-water-reactor (PWR)-containment latent particulate because the latent debris composition will vary from plant to plant and because the latent debris transported to the sump screen will also be plant specific because of such differences as flow velocities. In addition, the uncertainties associated with whether the surrogate recipe suitably represents actual containment latent debris further compound the problem of developing recommended characteristics for latent debris. More important than specific recommendations are the methods for ascertaining appropriate head-loss parameters once the plant has assessed latent debris accumulation on the sump screen.
4. The surrogate latent particulate debris head-loss tests effectively demonstrate the necessity of characterizing the latent particulate so that appropriate parameters can be estimated. For example, if the entire mass of the latent debris is assumed to be deposited onto the sump screen, then a lower specific surface area, such as the recipe in these tests, can be applied. However, if transport analyses are used to limit the transport of latent particulate to only the fine particulate, then the appropriate specific surface area would be more like that of the fine dirt in these tests. The same consideration also applies to the limiting packing density.
5. It is recommended that plant latent debris estimates be separated into as many particle size groupings as reasonably possible and then that subsequent transport analysis be applied to each group to determine the particulate makeup on the sump screen.
6. Wherever possible, specific surface areas should be determined for each size group based on test data. When the areas must be estimated from the particle diameters, the appropriate diameter is clearly not the mean or average diameter of the size group but a diameter closer to the minimum diameter of the group. The minimum diameter should normally result in a conservative specific surface area.
7. The use of the simple geometric relationship of  $6/d$  to estimate the specific surface areas for particulate is not reliable because the appropriate diameter within the range is not known. This point is illustrated in Table V-4, where values for  $S_v$  are estimated using both the mid-range and minimum diameters for each size group in the surrogate latent particulate recipe; these values are compared to the  $S_v$  deduced from the experimental head loss and the particle diameters that correspond to the experimental  $S_v$ . This minimum diameter in the size range estimates a conservative  $S_v$ ; however, that number could be unacceptably large if the minimum size for the smallest particles is not well known. The use of mid-range diameters is unacceptable because this

approach excessively underpredicts Sv values for plant-specific evaluations. . If the specific surface areas corresponding to the minimum particle diameters in each size grouping range are unacceptable, then head loss test data is required to determine a specific surface area for the particulate size distribution in question.

8. The NEI guidance recommends the use of 100 lb/ft<sup>3</sup> for the material density of latent particulate, whereas LA-UR-04-3970 indicates a density of ~168 lb/ft<sup>3</sup> (specific gravity of ~2.7). The use of the lighter density of 100 lb/ft<sup>3</sup> is conservative relative to a heavier density of 168 lb/ft<sup>3</sup>, for example, if the other head-loss parameters are appropriately specified.

**Table V-4. Comparison of Specific Surface Area Estimation Methods**

Particulate Size (µm)	Analysis			Experimental Sv	
	Mid-Range Diameter (µm)	Sv = 6/d Mid-Range Sv (ft <sup>-1</sup> )	Sv = 6/d Mid-Range Sv (ft <sup>-1</sup> )	Sv Deduced from Experimental Head-Loss Data (ft <sup>-1</sup> )	6/Sv Experiment (µm)
500 to 2000 (Sand)	1250	1460	3660	2000	914
75 to 500 (Sand)	287.5	6360	24,380	10,800	169
<75 (Dirt)	37.5	48,770	914,000*	285,000	6.4
Recipe	88.2	20,740	349,000	106,000	17.3

\* Assuming a 2-µm minimum particle size.

### V.3 FORMULAS FOR MIXING MULTIPLE FIBER AND PARTICULATE COMPONENTS

Most head-loss testing has been performed with a single type of fibrous debris, e.g., NUKON™, and particulates such as CPs. However, plant-specific analyses may well postulate debris beds containing more than one type of fiber and several types of particulate. The application of the NUREG/CR-6224 correlation requires the head-loss properties for the mixture to be estimated from the individual species properties.

#### V.3.1 Mixture of Specific Surface Areas

The equation for the mixture of the specific surface areas simply multiplies each area by the species volume and sums these products to get the total surface area, which is then divided by the total volume to get the mixture-average specific surface area. Such an equation was recommended in NUREG/CR-6371. Section 3.7.2.3.1.1 of the NEI guidance on the mixing equation recommends using the square of the specific surface area rather than the linear

\* The NEI guidance refers to NUREG/CR-6371 as the source of their recommendation; however, NUREG/CR-6371 recommends using the linear, not the square of the area in the mixing. The NEI source for the squaring equation has not been provided for review.

relationship The following equation for the mixing is set up to accommodate the linear ( $n = 1$ ), the square ( $n = 2$ ), or any other exponent. Performing example mixing evaluations demonstrated that using the square results in larger values for the mixture of specific surface areas than does using the linear relationship; therefore, it is conservative to use the square of the specific surface area in the mixing rather than the linear.

$$Sv_{Mixture} = \left[ \frac{\sum_i \frac{m_i}{\rho_i} Sv_i^n}{\sum_i \frac{m_i}{\rho_i}} \right]^{\frac{1}{n}},$$

where

- $Sv$  = the specific surface area for component  $i$  or for the mixture,
- $m_i$  = the mass of component  $i$ ,
- $\rho_i$  = the material (solid) density of the particles in component  $i$ , and
- $n$  = the weighting exponent.

For the surrogate latent particulate debris, mixing the three constituents to get the recipe test result seemed to work best using an  $n = 4/3$  (assuming that ~40% of the fine dirt did not filter from the flow). Because of the substantial uncertainties associated with head-loss predictions, it is prudent to include a safety factor; therefore, the NEI recommendation of using the square of the specific surface area in the mixing equation is a good recommendation.

### V.3.2 Mixture Densities

The equation for the mixture of densities (bulk, material, or granular) simply adds all of the species masses and then divides by the total of the species volumes as

$$\rho_{Mixture} = \frac{\sum_i m_i}{\sum_i \frac{m_i}{\rho_i}},$$

where

- $\rho_i$  = the density of the particles in component  $i$  and
- $m_i$  = the mass of component  $i$ .

This density mixing equation can be reduced to the following, even simpler form:

$$\frac{1}{\rho_{Mixture}} = \sum_i \frac{f_i}{\rho_i},$$

where

$f_i$  = the mass fraction of component  $i$ .

#### V.4 REFERENCES FOR APPENDIX V

[NEDO-32686-A, 1998] GE Nuclear Energy, "Utility Resolution Guide for ECCS Suction Strainer Blockage," prepared by the BWR Owners' Group, NEDO-32686-A, October 1998.**not referenced in this section**

[NUREG/CR-6224, 1995] NUREG/CR-6224, "Parametric Study of the Potential for BWR ECCS Strainer Blockage due to LOCA Generated Debris," October 1995.

[NUREG/CR-6371, 1996] C. Shaffer, C., W. Bernahl, J. Brideau, and D. V. Rao, BLOCKAGE 2.5 Reference Manual, NUREG/CR-6371, US Nuclear Regulatory Commission, December 1996.

[LA-UR-04-3970, 2004a] Mei Ding, Amr Abdel-Fattah, Stewart Fischer, Bruce Letellier, Kerry Howe, Janet Garcia, and Clint Shaffer, "Characterization of Latent Debris from Pressurized-Water-Reactor Containment Buildings," Los Alamos National Laboratory report LA-UR-04-3970 (June 2004).

[LA-UR-04-1227, 2004b] C. J. Shaffer, M. T. Leonard, B. C. Letellier, J. D. Madrid, A. K. Maji, K. Howe, A. Ghosh, and J. Garcia, "GSI-191: Experimental Studies of Loss-of-Coolant-Accident-Generated Debris Accumulation and Head Loss with Emphasis on the Effects of Calcium Silicate Insulation," Los Alamos National Laboratory report LA-UR-04-1227 (April 2004).

This page is intentionally blank.

## APPENDIX VI: DETAILED BLOWDOWN/WASHDOWN TRANSPORT ANALYSIS FOR PRESSURIZED-WATER-REACTOR VOLUNTEER PLANT

### VI.1 INTRODUCTION

In the event of a loss-of-coolant accident (LOCA) within the containment of a pressurized-water reactor (PWR), piping thermal insulation and other materials in the vicinity of the break will be dislodged by break-jet impingement. A fraction of this fragmented and dislodged insulation and other materials, such as chips of paint, paint particulates, and concrete dust, will be transported to the containment floor by the steam/water flows induced by the break and by the containment sprays (CSs). Some of this debris eventually will be transported to and will accumulate on the recirculation sump suction screens. Debris accumulation on the sump screen may challenge the sump's ability to provide adequate, long-term cooling water to the emergency core-cooling system (ECCS) and to the CS pumps. The Generic Safety Issue (GSI)-191 study titled "Assessment of Debris Accumulation on PWR Sump Performance" addresses the issue of debris generation, transport, and accumulation on the PWR sump screen and its subsequent impact on ECCS performance. The purpose of the GSI-191 study is to determine whether debris accumulation in containment following a postulated LOCA would prevent or impede the performance of the ECCS. Los Alamos National Laboratory (LANL) has been supporting the United States (US) Nuclear Regulatory Commission (NRC) in the resolution of GSI-191.

Analytical studies were performed and small-scale experimental programs [NUREG/CR-6772, 2002, NUREG/CR-6773, 2002] were conducted to support the resolution of GSI-191. A parametric evaluation of the US PWR plants demonstrated that potential sump-screen blockage was a plausible concern for operating PWRs [NUREG/CR-6762, Vol. 2, 2002]. As part of the GSI-191 study, a US PWR plant was volunteered and selected for a detailed analysis to develop and demonstrate a methodology for estimating the debris-transport fractions within PWR containments using plant-specific data. This report documents the blowdown and washdown transport portion of the study, describes the methodology, and provides an estimate for the transport of debris from its points of origin to the sump pool. The transport analysis consisted of (1) blowdown debris transport, where the effluences from a high-energy pipe break would destroy insulation near the break and then transport that debris throughout the containment; and (2) washdown debris transport caused by the operation of the CSs. Along the debris-transport pathways, substantial quantities of debris came into contact with containment structures and equipment where that debris could be retained, thereby preventing further transport. The blowdown/washdown debris-transport analysis provides the source term for the subsequent sump-pool debris-transport analysis.

The volunteer plant has a large, dry, cylindrical containment with a hemispherical dome constructed of steel-lined reinforced concrete and having a free volume of ~3 million ft<sup>3</sup>. The nuclear steam supply system is a Westinghouse reactor with four steam generators (SGs). Each of the SGs is housed in a separate compartment that vents upward into the dome. Approximately two-thirds of the free space within the containment is located in the upper dome region, which is relatively free of equipment. The lower part of the containment is compartmentalized. The internal structures are supported independently so that a circumferential gap exists between the internal structures and the steel containment liner. Numerous pathways, including the circumferential gap, interconnect the lower compartments. The CS system has spray train headers at four different levels; however, ~70% of the spray nozzles are located in the upper dome. Some spaces in the lower levels are not sprayed by the spray system; therefore, areas of significant size exist where debris washdown by the sprays

would not occur. The sprays activate when the containment pressure exceeds 18.2 psig. If the sprays do not activate, debris washdown likely would be minimal. The insulation composition for the volunteer plant is ~13% fiberglass, 86% reflective metal insulation (RMI), and 1% Min-K insulation. For the purposes of this study, it was assumed that the fiberglass insulation was one of the low-density fiberglass (LDFG) types. For plant-specific analyses, these transport results for fibrous debris may have to be adjusted to compensate if the fiberglass insulation makeup is determined to be significantly different.

The effluences from a high-energy pipe break not only would destroy insulation near the break but also would transport that debris throughout the containment (i.e., blowdown debris transport). Substantial amounts of this airborne debris would come into contact with containment structures and equipment and would be deposited onto these surfaces. As depressurization flows slow, debris would settle gravitationally onto equipment and floors. If pressurization of the containment were to occur, the CSs would activate to suppress pressurization. These sprays would tend to wash out remaining airborne debris (except in areas not covered by the sprays), and the impact of these sprays onto surfaces and the subsequent drainage of the accumulated water would wash deposited debris downward toward the sump pool (i.e., washdown debris transport). In addition, CSs could degrade certain types of insulation debris further through the process of erosion, thereby creating even more of the fine transportable debris.

An assessment of the likelihood of blocking the recirculation sump screens requires an estimate of the debris transport from the containment to the sump pool.<sup>†</sup> The debris transport within the sump pool is analyzed separately from this analysis, but the sump pool analysis requires the quantities of debris and the entry locations and timing as input to that analysis. An objective of this analysis was to develop and demonstrate an effective methodology for estimating the transport of debris from the debris point of origin in the containment down to the sump pool, thereby providing the source term to the sump-pool debris-transport analysis. Applying the methodology to the volunteer plant generated plausible debris-transport fractions for that plant.

The analyses herein considered only one break location: a LOCA located in one of the SG compartments, which is a probable location for that plant because most of the primary system piping is located in these compartments.

Neither the debris-size distributions nor the overall transport fractions in this report are valid for plant-specific evaluations because these fractions were calculated using LOCA-generated debris-size distributions that did not account properly for PWR jet characteristics. Boiling-water-reactor (BWR) jet characteristics were substituted for PWR jet characteristics because the PWR jet analyses had not yet been performed. When the PWR jet characteristics do become available, the overall transport fractions can be recalculated easily using PWR LOCA-generated debris-size characteristics.

The basic concepts of this methodology are applicable to the assessment of the debris transport within other PWR plants, as well; however, that application depends on the plant-specific aspects of each plant. The complexity of a plant-specific methodology could vary significantly from one plant to the next.

---

\* The terms "airborne" and "airflow" are used loosely with regard to gas flows, which actually consist of both air and steam.

† The simplest and most conservative assessment would be to assume 100% transport to the sump pool.

## VI.2 DEBRIS-TRANSPORT PHENOMENOLOGY

The transport of debris within a PWR would be influenced both by the spectrum of physical processes and phenomena and by the features of a particular containment design. Because of the violent nature of flows following a LOCA, insulation destruction and subsequent debris transport are rather chaotic processes. For example, a piece of debris could be deposited directly near the sump screen or it could take a much more tortuous path, first going to the dome and then being washed back down to the sump by the sprays. Conversely, a piece of debris could be trapped in any number of locations. Aspects of debris-transport analysis include the characterization of the accident, the design and configuration of the plant, the generation of debris by the break flows, and both air- and water-borne debris dynamics.

Long-term recirculation cooling must operate according to the range of possible accident scenarios. A comprehensive debris-transport study should consider an appropriate selection of these scenarios, as well as all engineered safety features and plant-operating procedures. The maximum debris transport to the screen likely will be determined by a small subset of accident scenarios, but this scenario subset should be determined systematically. Many important debris-transport parameters will be dependent on the accident scenarios. These parameters include the timing of specific phases of the accident (i.e., blowdown, injection, and recirculation phases) and pumping flow rates. The blowdown phase refers to primary-system depressurization. The injection phase corresponds to ECCS injection into the primary system, a process that subsequently establishes the sump pool. The recirculation phase refers to long-term ECCS recirculation.

Many features in nuclear-power-plant containments significantly affect the transport of insulation debris. The dominant break flows will move from the break location toward the pressure suppression system (i.e., the suppression pool in BWR plants and the upper regions of the compartment in PWR plants). Structures such as gratings are placed in the paths of these dominant flows and likely would capture substantial quantities of debris. The lower-compartment geometry—such as the open floor area, ledges, structures, and obstacles—defines the shape and depth of the sump pool and is important in determining the potential for debris to settle in the pool. Furthermore, the relative locations of the sump, LOCA break, and drainage paths from the upper regions to the sump pool are important in determining pool turbulence, which in turn determines whether debris can settle in the pool.

Transport of debris is strongly dependent on the characteristics of the debris that has formed. These characteristics include the types of debris (insulation type, coatings, dust, etc.) and the size distribution and form of the debris. Each type of debris has its own set of physical properties, such as densities, specific surface areas, buoyancy (including dry, wet, or partially wet), and settling velocities in water. Several distinct types of insulation are used in PWR plants [NUREG/CR-6762, Vol. 2, 2002]. The size and form of the debris, in turn, depends on the method of debris formation (e.g., jet impingement, erosion, aging, and latent accumulation). The size and form of the debris affect whether the debris passes through a screen, as well as the transport of the debris to the screen. For example, fibrous debris may consist of individual fibers or of large sections of an insulation blanket and all sizes within these two extremes.

The complete range of thermal-hydraulic processes affects the transport of insulation debris, and the containment thermal-hydraulic response to a LOCA includes most forms of thermal-hydraulic processes. Debris transport is affected by a full spectrum of physical processes, including particle deposition and resuspension for airborne transport and both settling and resuspension within calm and turbulent water pools for both buoyant and nonbuoyant debris.

The dominant debris-capture mechanism in a rapidly moving flow likely would be inertial capture; however, in slower flows, the dominant process likely would be gravitational settling. Much of the debris deposited onto structures likely would be washed off by the CSs or possibly by condensate drainage. Other debris on structures could be subject to erosion.

A panel of experts was convened to identify and rank the important phenomena, processes, and systems in regard to PWR debris transport [LA-UR-99-3371, 1999]. The insights gained from the work of this panel were factored into the analysis methodology. Additionally, all of the experimental and analytical research performed to resolve the BWR strainer-blockage issue was accessed for this analysis [LA-UR-01-1595, 2001; NUREG/CR-6369-1, 1999; NUREG/CR-6369-2, 1999; NUREG/CR-6369-3, 1999]. A summary was published on the base of knowledge for the effect of debris on PWR ECC sump performance [NUREG/CR-6808, 2003].

## **VI.3 METHODOLOGY**

### **VI.3.1 Overall Description**

Transport of LOCA-generated debris from its point of origin to the PWR sump pool is a complex process involving many physical processes and complex plant-specific geometry. To evaluate the blowdown and washdown debris transport within the drywell of a BWR plant, the NRC developed a methodology that accomplished the objectives of the drywell-debris-transport study (DDTS) [NUREG/CR-6369-1, 1999; NUREG/CR-6369-2, 1999; NUREG/CR-6369-3, 1999]. The methodology used herein was based on the BWR methodology.

The BWR methodology separated the overall transport problem into many smaller problems that were either amenable to the solution or that could be judged conservatively. The breakdown of the problem was organized using logic charts that were similar to well-known event-tree analyses. For some solution steps, sufficient data were available to solve that step reasonably. For other steps, insufficient data were available; therefore, the solution had to be found using engineering judgment that was applied after the available knowledge base was reviewed. Judgments were tempered to the desired level of conservatism called for in that particular analysis (sometimes assuming the worst case for a particular step). The result of each specific analysis was a transport fraction, defined as the fraction of insulation contained within the pipe-break destructive zone of influence (ZOI) that subsequently was damaged or destroyed by a LOCA and was eventually transported to the suppression pool. Certainly, the degree of refinement that is feasible depends on available resources and time restraints. Also, the conservatism in the estimates for each step in the divided problem may be compounded when the final transport fraction is quantified.

The PWR debris-transport methodology necessarily will differ from the BWR transport methodology because of differences in plant designs. These differences include the basic transport pathways, dominant capture mechanisms, and the timing of the accident sequence events. The dominant transport pathway for a PWR is different from the dominant pathway for a BWR. In a BWR, where pressure suppression would be due to steam condensation in the suppression pool, the debris initially would be transported directly to the suppression pool, where the ECCS strainers operate. In PWR containments, which are designed to suppress pressurization by channeling break effluences<sup>\*</sup> to the relatively large free volume of PWR containments, debris likely would be blown away from the sump area initially. Because one-half

---

<sup>\*</sup>In an ice-condenser plant, the break effluences would be channeled through the ice banks to condense steam.

to three-quarters of the containment free volume typically is located in the upper regions of the containment that includes the dome, it is justified to assume that a significant fraction of the small debris is blown directly into the upper regions, where the debris will settle onto floor surfaces or structures. Although debris blown into the upper regions then could be washed back down to the compartment sump area by the CSs, the washdown pathway can be tortuous and could certainly result in substantial debris entrapment.

The dominant debris-capture locations are different in a PWR than in a BWR. In many typical PWRs, the likely dominant locations are the upper regions of the containment, the ice condensers in an ice-condenser plant, the refueling pool, an outer annulus pool, and the sump pool. In the volunteer-plant containments, dominant locations for debris capture may not exist; rather, the debris likely would be blown throughout the entire containment. Gratings in a PWR could play a substantially different role versus the gratings played in the BWR methodology because the debris likely would be blown up through a grating as opposed to down through a grating. Debris trapped underneath a grating would be less likely to remain there than debris trapped on top of a grating.

Debris transport during the washdown phase would be caused by the water drainages of break recirculation overflow, the CSs, and condensate. The most important of these drainages would be the drainage of the activated CSs because the sprays usually cover a majority of the containment free volume, whereas the break overflow would wash only surfaces directly below the break. In a PWR, the break overflow could impinge on piping and equipment before reaching the containment sump floor, thereby washing debris from these surfaces, as well as potentially dispersing the flow. In a BWR, the break overflow for a majority of postulated breaks would pass down through at least one grating, where the flows would erode larger debris trapped on the gratings directly below the break—a situation less likely in a PWR. Although condensate drainage could transport debris from surfaces, the quantities of debris transported would likely be much less than the quantities transported by spray drainage.

The following methodology was designed specifically to analyze debris transport within the volunteer-plant containments; however, it is also directly applicable to several other containment designs, and it can be modified to tailor the methodology to any other PWR design. The best method for a particular plant will depend on the complexity of the containment design. If the containment has definitive upper and lower compartments that are separated by relatively few and narrow pathways, the analysis may be used to track debris transports in a manner similar to the DDTs analysis. Using an ice-condenser plant as an example, the containments were designed specifically to channel break flow through the ice banks to the dome region. This generally means that the connecting flow pathways between the lower and upper containments include the ice banks, small air-circulation return pathways, (needed to establish post-blowdown air circulation through the ice banks), and refueling-pool drains. Debris capture through the ice banks could be substantial. In addition, a large fraction of the small and fine debris would be blown into the dome region, where substantial quantities could be retained, even with the CSs operating.

The analysis here would focus on debris capture in the ice banks during blowdown and on debris retention in the upper compartment during the spray washdown process to identify debris transported from the lower containment and not likely to return there. Some plants would have a flooded outer annulus in which debris deposited in that pool would be less likely to transport from that pool to the sump pool. A conservative estimate of the maximum debris quantities that would be expected to transport to the sump pool can be made by subtracting masses of debris retained at various locations from the generation totals.

The design of the volunteer-plant containments is more complex than an ice-condenser design, from a debris-transport point of view; that is, the lower and upper regions of the containment are less well defined and are connected by several different pathways, thereby making it difficult to determine the motion of air and steam flows and the transport of debris. Certainly, system-level codes such as MELCOR can model the progression of break flows throughout the containment; however, the input model for the volunteer plant would have to be rather detailed to follow the flows through all of the lower levels in the containment. The modeling detail must include all of the levels and rooms and separate sprayed areas from non-sprayed areas. The model would need to simulate all of the connecting flow pathways, such as stairwells, equipment hatches, and doorways. A detailed thermal-hydraulics analysis was not performed for the volunteer-plant analysis.

The transport and deposition of insulation debris cannot be simulated realistically using a thermal-hydraulics computer code that incorporates aerosol transport models. The primary mode of debris capture during the violent primary-system depressurization is inertial capture. The available models for inertial capture are based on data taken for rather simple geometries (e.g., a bend in a pipe). Inertial capture in the complex geometry of containments cannot be modeled reasonably using current codes. However, inertial capture can be determined in specific parts of the containment. For example, at the volunteer plant, the personnel access doors between an SG compartment and the sump annulus have at least one 90° bend. A LOCA, particularly a large LOCA, in an SG compartment would result in depressurization flows that would carry insulation debris through these doors with the flow. As the flow underwent the sharp bend, some types of debris would be deposited by inertia on the wall at the bend. The tests conducted at the Colorado Engineering Experiment Station, Inc. (CEESI) demonstrated an average inertial capture fraction for fibrous debris of 17% at such a bend if the surface were wetted, and analysis has shown that surfaces within the containment likely would build a filmy layer of condensation rapidly. Because the CSs do not impinge on these wall surfaces, the debris would remain attached to those surfaces. In this situation, small amounts of debris can be removed from the equation, thereby lowering the transport fraction. Perhaps many of these types of definable captures can add up to a significant reduction in the transport fraction. Again, the size of that reduction would depend somewhat on both the geometry/conditions and the depth of the analysis.

The basic idea of the mechanics of this methodology is to look for such reductions systematically. The demonstration of this methodology in this volunteer-plant analysis assumed a large LOCA occurred inside SG compartment number 1 (SG1) of the containment. Figure IX-1 illustrates this methodology in the general sense. The idea is first to estimate the blowdown dispersal of the debris until all of the debris is associated with some surface area. Then the likelihood of debris remaining on each of these surfaces during washdown is estimated or judged. For example, debris deposited onto a surface that has been impacted by the CSs is much more likely to transport than debris deposited onto surfaces that have been wetted only by condensate.

As with the DDTS, the debris for transport must first be categorized according to type and size according to transport properties so that the transport of each type of debris can be analyzed independently. All insulation located within the break-region ZOI is assumed to be damaged to some extent. These categories and their properties are the subject of Section VI.3.2.

The containment free volume in the volunteer plant was subdivided into many regions based on geometry and the locations of the CSs. The volume region containing the postulated LOCA was

analyzed separately and first. For SG1, a MELCOR simulation of only the break compartment was used to determine the distribution of flows exiting that compartment (i.e., the fraction of flow going upward into the dome as opposed to the fraction entering the lower levels through personnel access doors). Debris capture within SG1 was based on such considerations as flows through gratings and flows making sharp bends (see Section VI.3.3.1). In each region, debris capture would deposit debris onto the “floor” or “other” surfaces, based on surface areas and judgment regarding whether debris was deposited by settling or by another mechanism. Floor surfaces were treated separately because these surfaces would collect and drain spray water differently from vertical surfaces, for example, and because debris that gravitationally settles would deposit onto horizontal surfaces. These surfaces were divided further according to their exposure to spray and condensate moisture. All surfaces would collect condensate. The sprays would impact some surfaces directly, and others simply would be washed by the process of spray drainage. Debris entrained by spray-drainage water could become captured a second time as the drainage fell from one level to another.

Because the chart illustrated in Figure IX-1 would become unreasonably large if it were developed for the entire volunteer-plant containment, another approach was used. The process was handled using an equation-format model (described in Figure IX-1), with the input entered into data arrays.

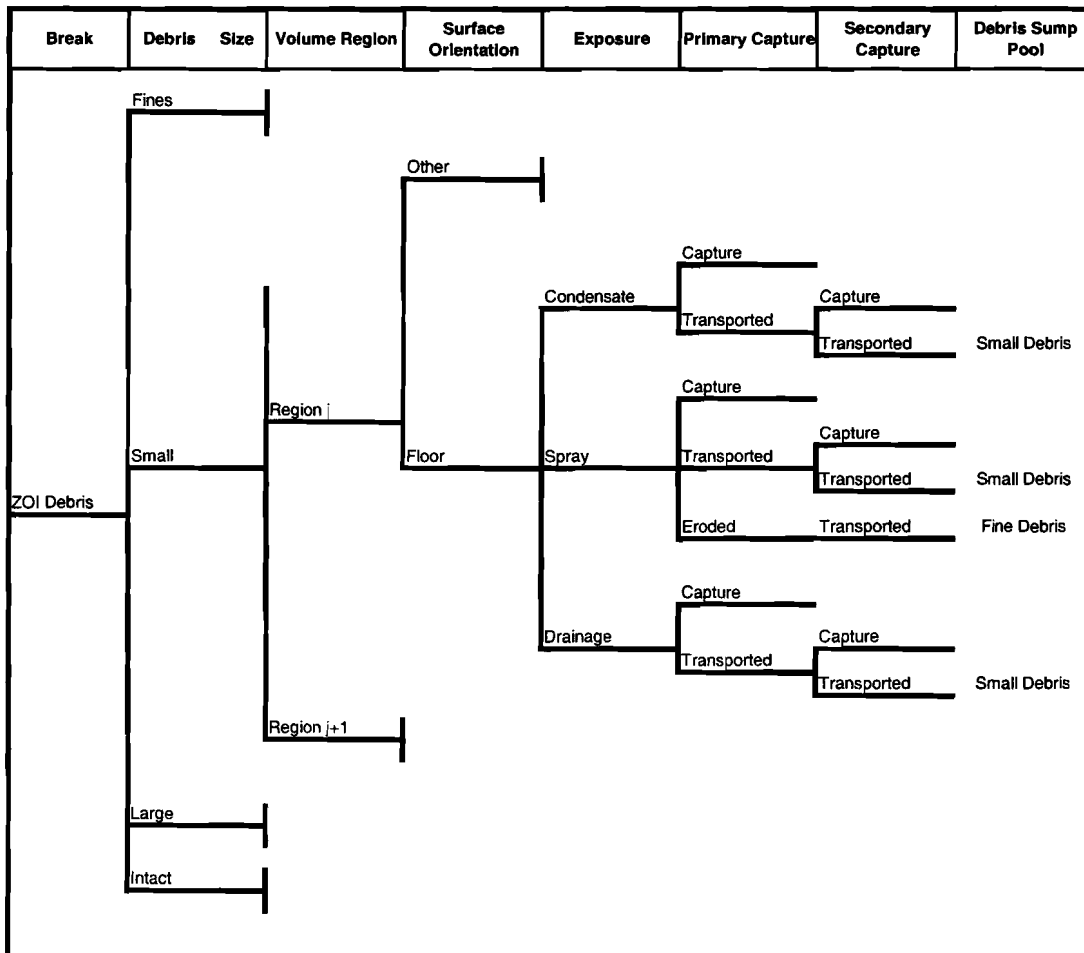


Figure IX-1. Example of a Section of a Debris-Transport Chart.

### VI.3.2 Debris-Size Categorization

The types of insulation used inside the volunteer-plant containments include fiberglass insulation, RMI, and stainless-steel-encapsulated Min-K insulation at ~13.4%, 85.7%, and 0.9%, respectively [NUREG/CR-6762, Vol. 2, 2002]. Although a majority of the insulation within these containments is RMI, the fibrous insulation more likely would cause blockage of the sump. First of all, the RMI debris would transport less easily than the fibrous debris (i.e., it takes a faster flow of water to move RMI debris than it does for fibrous debris). In addition, it takes substantially more RMI debris on the sump screens to block the flow effectively through the screens than it does for fibrous debris. Although the Min-K debris, in combination with the fibrous debris, could create substantial head losses on the screen, the inventory of the Min-K in the containments is relatively low. Therefore, the primary focus in this analysis was on the transport of fibrous debris, with the transport of RMI and Min-K estimated more crudely.

The difficulties associated with determining debris-size distributions to represent the LOCA-generated debris are (1) the limited debris-generation data and (2) the need to determine the characteristics of the LOCA jet (i.e., the size of the ZOI and volumes within specific pressure isobars). The limitations in the debris-generation data must be handled by skewing the integration of size fractions conservatively over the ZOI toward the smaller debris sizes; the more limited the data, the more conservative the integration. The determination of the jet characteristics for a PWR jet is a relatively straightforward analysis; but those characteristics unfortunately were not yet available for use in this report. Because, debris-size distributions are necessary to determine estimates for the overall transport of debris to the sump pool, assumptions were made to provide distributions that were suitable to illustrate the transport methodology. Therefore:

**Neither the debris-size distributions nor the overall transport fractions in this report are valid for plant-specific evaluations.**

However, the transport fractions for specific debris-size classes are considered to be valid for the volunteer plant.

#### VI.3.2.1 Fibrous Insulation Debris-Size Categorization

All insulation located within the break-region ZOI is assumed to be damaged to some extent. The damage could range from slight damage (insulation erosion occurring through a rip in the blanket cover) that leaves the blanket attached to its piping to the total destruction of a blanket (with its insulation reduced to small or very fine debris). For the purposes of this analysis, all of the insulation within the ZOI was considered to be debris. The fibrous debris was categorized into one of four categories based on transport properties so that the transport of each type of debris could be analyzed independently. These categories and their properties are shown in Table IX-1.

The primary difference between the two smaller and two larger categories was whether the debris was likely to pass through a grating that is typical of those found in nuclear power plants. This criterion also was used in the DDTs analysis. Thus, fines and small pieces pass through gratings but large and intact pieces do not. The fines and small pieces are much more

---

\*The type (or types) of fiberglass insulation used in the volunteer-plant containments has yet to be determined. This analysis assumes that the fiberglass is LDFG.

transportable than the large debris. The fines were then distinguished from the small pieces because the fines would tend to remain in suspension in the sump pool, even under relatively quiescent conditions, whereas the small pieces would tend to sink. Furthermore, the fines tended to transport slightly more as an aerosol in the containment-air/steam flows and were slower to settle than the small pieces when airflow turbulence decreased. The CEESI tests illustrated that when an LDFG blanket was completely destroyed, 15% to 25% of the insulation was in the form of very fine debris (i.e., debris too fine to collect readily by hand).

The distinguishing difference between the large and intact debris was whether the blanket covering was still protecting the fibrous insulation. The primary reason for this distinction was whether the CSs could further erode the insulation material.

**Table IX-1. Debris-Size Categories and Their Capture and Retention Properties**

<b>Fraction Variable</b>	<b>Size</b>	<b>Description</b>	<b>Airborne Behavior</b>	<b>Waterborne Behavior</b>	<b>Debris-Capture Mechanisms</b>	<b>Requirements for Crediting Retention</b>
$D_F$	Fines	Individual fibers or small groups of fibers.	Readily moves with airflows and slow to settle out of air, even after completion of blowdown.	Easily remains suspended in water, even relatively quiescent water.	Inertial impaction Diffusiophoresis Diffusion Gravitational settling Spray washout	Must be deposited onto surface that is not subsequently subjected to CSs or to spray drainage. Natural-circulation airflow likely will transport residual airborne debris into a sprayed region. Retention in quiescent pools without significant flow through the pool may be possible.
$D_S$	Small Pieces	Pieces of debris that easily pass through gratings.	Readily moves with depressurization airflows and tends to settle out when airflows slow.	Readily sinks in hot water, then transports along the floor when flow velocities and pool turbulence are sufficient. Subject to subsequent erosion by flow water and by turbulent pool agitation.	Inertial impaction Gravitational settling Spray washout	Must be deposited onto surface that is not subsequently subjected to high rates of CSs or to substantial drainage of spray water. Retention in quiescent pools (e.g., reactor cavity). Subject to subsequent erosion.
$D_L$	Large Pieces	Pieces of debris that do not easily pass through gratings.	Transports with dynamic depressurization flows but generally is stopped by gratings.	Readily sinks in hot water and can transport along the floor at faster flow velocities. Subject to subsequent erosion by flow water and by turbulent pool agitation.	Trapped by structures (e.g., gratings) Gravitational settling	Must be either firmly captured by structure or on a floor where spray drainage and/or pool flow velocities are not sufficient to move the object. Subject to subsequent erosion.

Fraction Variable	Size	Description	Airborne Behavior	Waterborne Behavior	Debris-Capture Mechanisms	Requirements for Crediting Retention
$D_i$	Intact	Damaged but relatively intact pillows.	Transports with dynamic depressurization flows, stopped by a grating, or may even remain attached to its piping.	Readily sinks in hot water and can transport along the floor at faster flow velocities. Assumed to be still encased in its cover, thereby not subject to significant subsequent erosion by flow water and by turbulent pool agitation.	Trapped by structures (e.g., gratings) Gravitational settling Not detached from piping	Must be either firmly captured by structure or on a floor where spray drainage and/or pool flow velocities are not sufficient to move the object. Intact debris subsequently would not erode because of its encasement.

The volume (or mass) distribution,  $D_i$ , of the four categories of insulation debris was estimated first. This estimate assumed that the fibrous insulation within the ZOI was uniformly distributed and that the distribution must add up to one, as

$$\sum_{i=1}^{N_{types}} D_i = 1 \quad ,$$

where

$D_i$  = the fraction of total debris that is type  $i$ .

The volume of each category of debris is simply the distribution fraction multiplied by the total volume of insulation within the ZOI. In debris-transport analysis, volumes of fibrous debris have been used interchangeably with mass on the basis that the density is that of the undamaged (as fabricated) insulation. Certainly the density would be altered by the destruction of the insulation and again when the debris became water saturated. For example, the physical volume of debris on the screen must include the actual density of the debris on the screen as

$$V_i = D_i V_{ZOI} \quad ,$$

where

$V_i$  = the volume of debris of type  $i$  and

$V_{ZOI}$  = the total volume of insulation contained within the ZOI.

The estimation of the debris-size distribution must be based on experimental data. When sufficient data are available, the following analytical model illustrates how the fraction of fine and small debris can be estimated from that data. Using the spherical ZOI destruction model, the fraction of the ZOI insulation that becomes type- $i$  debris is given by the following integration:

$$F_i = \frac{3}{r_{ZOI}^3} \int_0^{r_{ZOI}} g_i(r) r^2 dr \quad ,$$

where

$F_i$  = the fraction of debris of type  $i$ ;

$g_i(r)$  = the radial destruction distribution for debris of type  $i$ ;

$r$  = the radius from the break in the spherical ZOI model; and

$r_{ZOI}$  = the outer radius of the ZOI.

Typical test data provide an estimate of the damage to insulation samples at selected distances from the test jet nozzle (i.e., the size distribution of the resultant debris). The jet pressure at the target is determined from test pressure measurements, suitable analytical models, or both. Thus, the size distribution as a function of the jet pressure is obtained. The volume associated with a particular level of destruction is determined by estimating the volume within a particular

pressure isobar within the jet [i.e., any insulation located within this pressure isobar would be damaged to the extent (or greater) associated with that pressure]. The isobar volumes then are converted to the equivalent spherical volumes; thus, the debris-size distribution is associated with the spherical radius (i.e.,  $g_i(r)$ ). The distribution would be specific to a particular kind of insulation, jacketing, jacketing seam orientation, and banding.

To demonstrate the transport methodology completely, it was assumed that the fibrous insulation used in the volunteer-plant containments was LDFG insulation, for which significant data are available to predict the LOCA-generated size distribution. The most extensive debris-generation data for LDFG insulation are the data from the BWR Owners' Group (BWROG) air-jet impact tests (AJITs) [NEDO-32686, 1996]. These data, combined with the jet characteristics of a PWR LOCA, could result in a realistic LOCA size distribution; however, the PWR jet characteristics were not available at the time of this writing.

The development of a suitable size distribution for the purposes of demonstrating this methodology follows. For fibrous debris, the BWROG correlated the fraction of the original insulation that became fine debris with the distance from the jet nozzle and then crudely estimated the ZOI destruction fractions for specific types of insulation. The fine debris in the BWROG analysis correlates with the combined fine and small debris of Table IX-1.

For the NUKON™ insulation debris—both jacketed and unjacketed insulation—the BWROG recommended in its Utility Resolution Guidance (URG) the assumption that 23% of the insulation within the ZOI be considered in the strainer head-loss evaluations during the resolution of the BWR strainer blockage issue. Applying this recommendation to this analysis means that 23% of the ZOI would be distributed between the fine and small debris and that the remaining 77% would be distributed between the large and intact debris. The NRC reviewed the BWROG recommendations and documented its findings in a safety evaluation report (SER) [NRC-SER-URG, 1998]. Although the NRC had some reservations regarding the BWROG's method for determining the debris fractions, the NRC believed the debris fractions to be conservative primarily because the blanket seams were arranged in the AJITs to maximize the destruction of the blankets.

Whereas the BWROG's recommendations were based on AJITs, more recent testing using two-phase jet impact testing indicated the need for somewhat higher small-debris fractions than did the AJIT data (refer to the staff evaluation of GR, Section 3.4.2.2 in this report, for the evaluation of the two-phase jet concern). Ontario Power Generation (OPG) of Canada conducted these debris-generation tests [OPG, 2001]. A comparison of the AJIT and the OPG tests was discussed in a report [NUREG/CR-6762, Vol. 3, 2002] that was supporting the PWR parametric evaluation [NUREG/CR-6762, Vol. 1, 2002]. This comparison illustrated the potential for more small debris to be generated by a two-phase jet than was supported by the AJIT data. For the parametric evaluation, the qualitative conclusion of comparing these two sets of test data was that the small debris fraction should be increased from the BWROG's recommendation. An engineering judgment was used to increase the recommended destruction fraction for small debris from 23% to 33%. The remaining 67% of the insulation would be assumed to be large debris either exposed or enclosed in its covering material.

For this analysis, the small-debris fraction of 33% that was used in the parametric evaluation was split to accommodate the fine- and small-debris categories of this analysis. The analysis of the AJIT testing performed at CEESI to support the DDTs determined that whenever entire blankets were completely destroyed, 15% to 25% of the insulation was too fine to collect by

hand.\* Complete destruction here means that nearly all of the insulation was either fine or small pieces. In any case, the 15% to 25% of the blanket (an average of 20%) can be considered fine debris for the purposes of this analysis. For this analysis, it was assumed that 20% of the 33%-small-debris fraction was fine debris (i.e.,  $0.2 \times 0.33 = 0.066$ ). Therefore, 7% of the ZOI insulation was estimated to be destroyed into fine debris, leaving 26% for the small-piece debris.

In a similar manner, the parametric evaluation of the 67%-large-debris fraction was split in this analysis to accommodate the large and intact debris categories. In DDTS analysis, based on the AJIT data, 40% of the blanket insulation was assumed to remain covered. The DDTS assumption of 40% was accepted for the covered (intact) debris fraction for this analysis. However, that number had to be adjusted downward to account for the increase in the small-debris fraction from 23% to 33% (i.e.,  $0.67/0.77 \times 0.4 = 0.35$ ). Therefore, 35% of the ZOI insulation was considered to be intact debris, leaving 32% for the exposed large-piece debris. The debris category distribution for fibrous debris assumed in this analysis is summarized in Table IX-2.

**Table IX-2. Fibrous-Debris-Category Distribution**

Category	Category Percentage
Fines	7%
Small Pieces	26%
Large Pieces	32%
Intact	35%

#### VI.3.2.2 RMI Insulation Debris-Size Categorization

In the volunteer-plant containments, the RMI insulation is made of stainless steel. TPI manufactured the insulation around the reactor vessel. Diamond Power Specialty Company (DPSC) manufactured all of the other RMI inside the containments and marketed it as DPSC MIRROR™ insulation. Furthermore, the insulation panels generally are held in place simply by buckling the panels together (i.e., an absence of bands on most panels). Because the reactor vessel insulation is shielded from a postulated jet impingement for the most part, LOCA-generated RMI debris would consist primarily of the DPSC type. The threshold jet-impingement pressure required to damage DPSC MIRROR™ insulation with standard bands was estimated by the BWROG [NEDO-32686, 1996] and accepted by the NRC [NRC-SER-URG, 1998] as 4 psi; these data should be applicable to the volunteer-plant RMI. Therefore, some debris could be formed from any insulation subjected to a differential of 4 psi or greater, but the extent of damage would depend on the magnitude of the pressure. Insulation that is closer to the break would be destroyed completely and form small pieces of debris, whereas insulation farther from the break may remain nearly intact. A size distribution is needed for the transport analysis. Data from two experimental programs provide limited information on the extent of destruction that

\* This debris either was blown through the fine-mesh screen at the end of the test chamber and lost from the facility or was deposited onto surfaces inside the chamber in such a dispersed manner that it could be collected only by hosing down the walls and structures.

would occur in this type of RMI insulation. These programs were (1) the Siemens Karlstein tests [SEA-95-970-01-A:2, 1996], and (2) the BWROG AJIT [NEDO-32686, 1996].

Swedish Nuclear Utilities conducted metallic insulation jet impact tests at the Siemens AG Power Generation Group (KWU) test facility in Karlstein am Main, Germany (1994 and 1995 can't find these in references). During this test program, the US NRC conducted a single RMI debris-generation test to obtain debris-generation data and debris samples that are representative of RMI used in US plants. The NRC test sample was provided by the DPSC. The NRC-sponsored test was performed with a high-pressure blast of two-phase water/steam flow from a pressurized vessel connected to a target mount by a blowdown line with a double-rupture disk. The target was mounted directly on a device designed to simulate a double-ended guillotine break (DEGB) such that the discharge impinged the inner surface of the RMI target as it would an insulation cassette surrounding a postulated pipe break. Most of the RMI debris was recovered and analyzed with respect to size distribution. The overall size distribution for the total recovered debris mass is shown in Figure IX-2, and a photograph of the recovered RMI debris is shown in Figure IX-3. This debris sample is likely typical of debris formed from the RMI cassettes nearest the break.

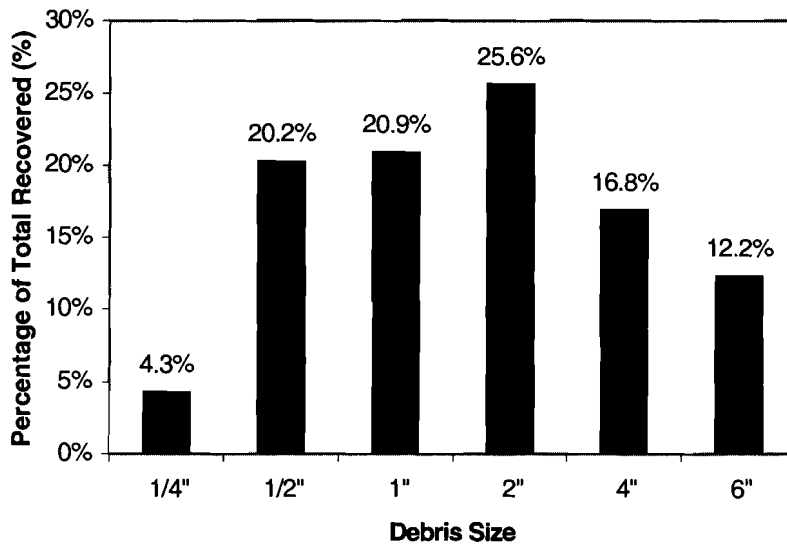


Figure IX-2. Size Distribution of Recovered RMI Debris.



**Figure IX-3. RMI Debris Observed in Siemens Steam-Jet Impact Tests.**

The BWROG-sponsored tests conducted at CEESI examined the failure characteristics of various types of insulation materials when subjected to jet impingement forces. CEESI has compressed-air facilities that provided choked nozzle airflow. This airflow was directed at insulation samples mounted inside a test chamber that did not pressurize significantly but retained most of the insulation debris for subsequent analysis. The variety of insulation materials tested included samples of the stainless-steel DPSC MIRROR™ insulation. The test samples were mounted at various distances from the nozzle, thereby subjecting similar samples to varying damage pressures. In this manner, the test data were used to estimate the threshold pressure required to damage this type of insulation. The data also provided information regarding the size distribution of the resulting debris. The formation of debris was dependent on the separation of the outer sheath, which in turn depended on the type, number, and placement of the supporting bands. The data used herein were for stainless-steel DPSC MIRROR™ cassettes mounted either with standard bands or without bands; therefore, these data are conservative with respect to data for cassettes mounted with even stronger banding. The recorded debris-generation data separated the quantities of debris into several distinct size groupings. For this transport analysis, the debris was grouped into three size groups: (1) debris generally smaller than 2 in. in size, (2) debris larger than 2 in. but smaller than 6 in., and (3) all RMI pieces larger than 6 in. (including both debris and relatively intact insulation cassettes). Figure IX-4 shows the fractions of the collected debris for the two finer groups as a function of the damage pressure on the cassette; all other insulation either remained relatively intact or formed debris larger than ~6 in.

The BWROG data describe the damage to stainless-steel DPSC MIRROR™ insulation (standard banding) when subjected to jet pressures of up to 120 psi. The NRC-sponsored Siemens test demonstrates the complete destruction of stainless-steel DPSC MIRROR™ insulation when impacted by the highest jet pressure near the break. A gap exists in the data between 120 psi and the higher pressure near the jet. The damage to the RMI within the ZOI was estimated using the spherical equivalent volume method in conjunction with BWR-specific data (i.e., volumes with specific pressure isobars). The BWROG analysis that was provided to the utilities [NEDO-32686, 1996] was used to convert jet isobar volumes to equivalent spherical volumes. Furthermore, the outer radius of the equivalent sphere was assumed to be 12D (i.e., 12 times the diameter of the pipe break), which corresponds to an insulation destruction pressure of 4 psi for a BWR radial offset DEGB. **The resultant size distribution can demonstrate the overall transport methodology fully but is not suitable for PWR plant-**

**specific analyses.** The BWROG data were applied when the impact pressure was <120 psi; the Siemens data were conservatively applied when the impact pressure was >130 psi (insulation totally destroyed), and a linear extrapolation was applied between 120 and 130 psi. The data shown in Figure IX-2 indicates that when the insulation is totally destroyed, ~70% of the debris would be <~2 in. in size and the remaining 30% would be between 2 and 6 in. in size.

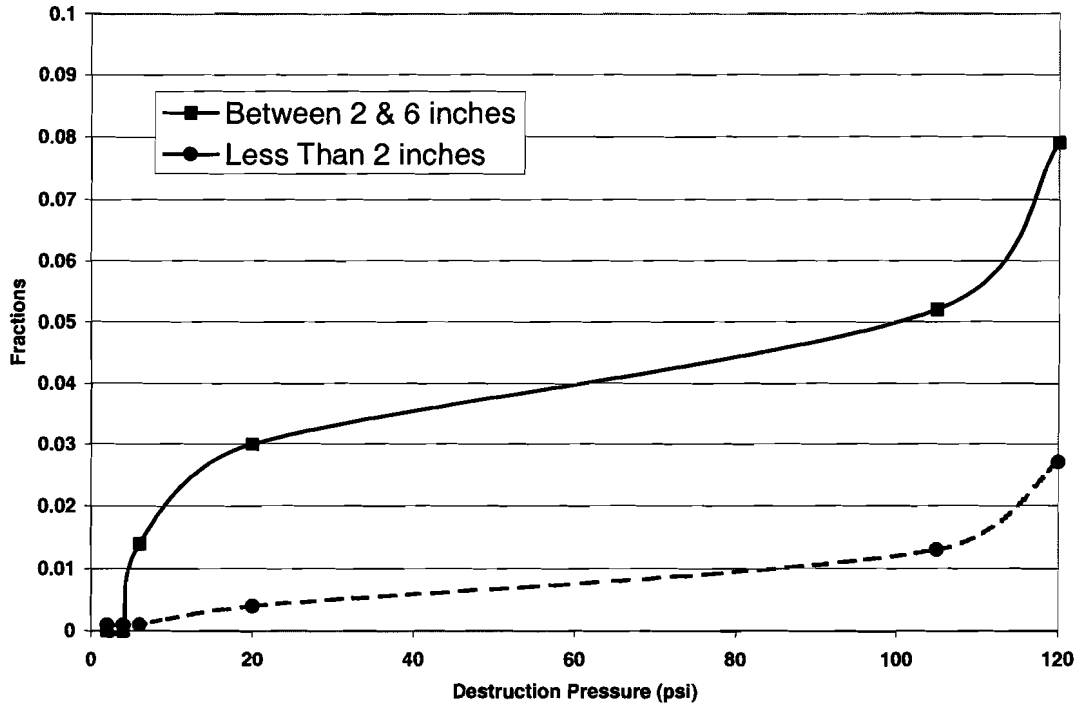


**Figure IX-4. Relative Damage of Stainless-Steel DPSC MIRROR™ Insulation.**

Because of variability and uncertainty in debris-generation estimates, as well as the use of BWR-specific jet characteristics, it is prudent to enhance the fractions for the finer groups of debris, noting that the smaller debris would transport more easily than would the larger debris. One uncertainty is the fact that the BWROG data were generated using an air jet, whereas the postulated accident would involve a two-phase steam/water jet; the comparison of two-phase and air test data has indicated that a two-phase jet could generate finer debris than could an air jet. To make the debris-generation estimates more conservative to compensate for variability and uncertainty in the estimates, the fractions for the two fines size groups were increased by 50%. The spherical volume damage estimates with and without the 50% increase are shown in Table IX-3.

**Table IX-3. RMI Debris Category Distribution**

Category	Category Percentage	
	Integration Result	Conservative Estimate
<2 in.	14%	21%
Between 2 and 6 in.	8%	12%
>6 in.	78%	67%

### VI.3.2.3 Min-K Insulation Debris-Size Categorization

In locations where insulation thickness was a specific concern, such as pipe-whip-restraint locations, fully encapsulated Min-K insulation was used instead of the usual RMI insulation. Containment-wide, ~0.9% of the insulation is Min-K. Although the potential quantities of Min-K debris would be substantially smaller than corresponding quantities of fibrous or RMI debris, a small amount of Min-K particulate debris could contribute more significantly than RMI debris to sump-screen head loss. In particular, Min-K debris dust would contribute to the particulate load in the debris bed when combined with the fibrous debris on the screens. Min-K is a thermo-ceramic insulation (also referred to as a particulate insulation) that is made of microporous material. The particulate insulations include calcium silicate, asbestos, Unibestos, Microtherm, and gypsum board. Test data have demonstrated that microporous particulate, combined with fibrous debris, creates a debris bed that can cause relatively high head losses across that bed. This head loss is over and above the corresponding head loss associated with more ordinary particulate, such as corrosion products. The most notable of the particulate insulation types has been calcium silicate.

Limited debris-generation data exist for the microporous insulations, and most of the available data were obtained for calcium silicate. No debris-generation data were available for Min-K insulation. The primary source of calcium silicate debris-generation data are test data from tests conducted by the OPG [NUREG/CR-6762, Vol. 3, 2002]. These tests involved impacting aluminum-jacketed calcium silicate insulation targets with a two-phase water/steam jet. The size distribution data are shown in Figure IX-5.

Even if it is assumed that Min-K behaves similarly to calcium silicate with regard to debris generation, the OPG data cover only a limited range of damage pressures. Integrating the damage over the spherical ZOI requires a conservative extrapolation to a full range of pressures. The ZOI for Min-K corresponds to a destruction pressure of 4 psi, based on the BWROG guidance to utilities. At high pressures, the conservative extrapolation should assume that complete destruction of the insulation occurs (i.e., all of the insulation is pulverized to dust). At lower pressures, the damage fractions of the lowest pressures tested would be extended out to the ZOI boundary. This crude conservative extrapolation indicates that about half of the insulation should be considered dust. In addition to the conservative extrapolation, the debris-generation fraction is conservative with respect to the jacket seam angle relative to the jet. The seams in the test data shown in Figure IX-5 were oriented toward maximum damage. In reality, the seams within the ZOI likely would be distributed more randomly with respect to the jet; therefore, many of the jackets would provide more protection for the Min-K than is indicated by the OPG data. On the other hand, applying data for calcium silicate to Min-K insulation introduces substantial uncertainty.

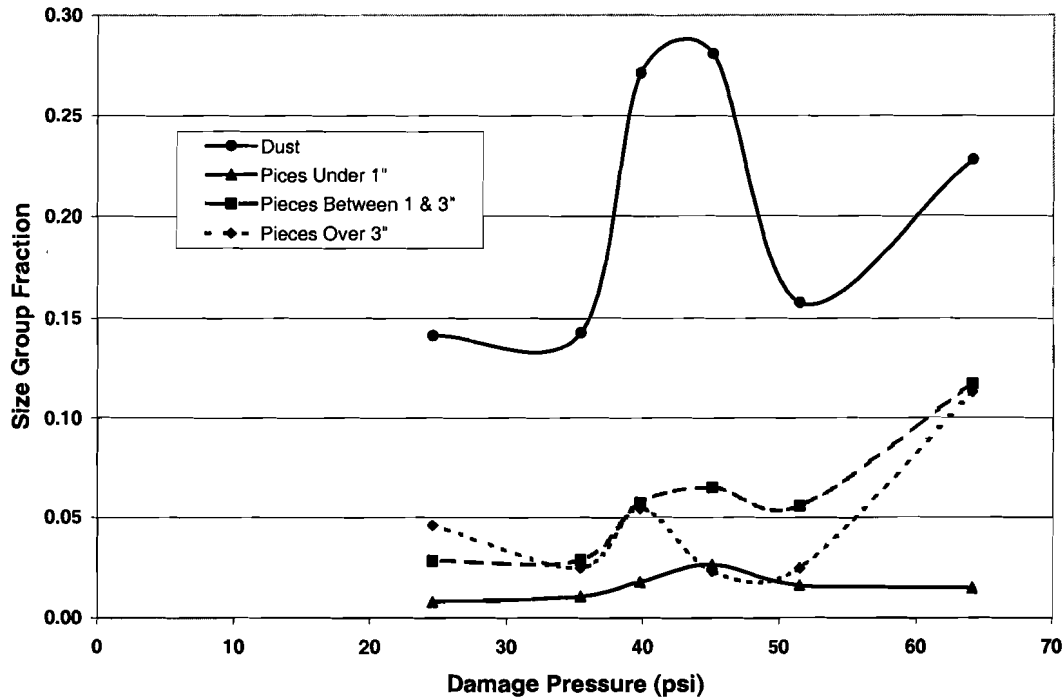


**Figure IX-5. Debris-Size Distributions for OPG Calcium Silicate Tests.**

Another source of uncertainty is the location of the minimal quantities of Min-K insulation with respect to the break. A key assumption of the ZOI integration is a uniform distribution of insulation within the ZOI. However, with so little Min-K insulation inside the volunteer-plant containments, all damaged Min-K insulation could be located preferentially near or far from the break. Therefore, all Min-K insulation could be destroyed totally or only slightly damaged. Another source of uncertainty that has not been assessed experimentally is the subsequent erosion of the Min-K debris by the CSs. In light of these uncertainties, it is conservative and prudent to assume that all of the Min-K insulation inside a ZOI would be pulverized to dust.

### VI.3.3 Blowdown Debris Transport

The break region, SG1, would be the source of all insulation debris and would be subject to the most violent of the containment flows, and the primary debris capture mechanism in this region would be inertial capture. For these reasons, the transport of debris within the region of the pipe break likely should be solved separately from that of the rest of the containment. The methodology is described for fibrous-debris transport but also was applied to RMI debris in a similar manner.

#### VI.3.3.1 Break-Region Dispersion and Capture

The first step in determining the dispersal of debris near the debris-generation source was to determine the distribution of the break flow from the region—specifically, the fractions of the flow directed to the dome versus other locations. This determination was accomplished using the containment thermal-hydraulics code MELCOR. The containment was designed to force reactor-coolant-system (RCS) break effluents upward through the open tops of the SG

compartments and into the dome. Figure IX-6 shows the nodalization diagram for the break-region MELCOR calculation.

The LOCA-generated debris that was not captured within the region of the break would be carried away from the break region by the break flows. The primary capture mechanism near the break would be inertial capture or entrapment by a structure such as a grating. The break-region flow that occurred immediately after the initiation of the break would be much too violent to allow debris simply to settle to the floor of the region.

The inertial capture of fine and small debris occurs when a flow changes directions, such as flows through the doorways from the SG compartments into the sump-level annular space. These flows must make at least one 90° bend through these doorways, and these surfaces would be wetted by steam condensation as well as by the liquid portion of the break effluence. Debris-transport experiments conducted at CEESI [NUREG/CR-6369-2, 1999] demonstrated an average capture fraction of 17% for fine debris and small debris that make a 90° bend at a wetted surface. Other bends in the flow would occur as the break effluents interacted with equipment and walls.

The platform gratings within the SG compartments would capture substantial debris, even though the gratings do not extend across the entire compartment. The CEESI debris-transport tests demonstrated that an average of 28% of the fine and small debris was captured when the airflow passed through the first wetted grating that it encountered and that an average of 24% was captured at the second grating. By definition, the large and intact debris would be trapped completely by a grating. In addition, equipment such as beams and pipes was shown to capture fine and small debris. In the CEESI tests, the structural maze in the test section captured an average of 9% of the debris passing through the maze.

To evaluate the transport and capture within the break region, the evaluation must be separated into many smaller problems that are amenable to resolution. This separation can be accomplished using a logic-chart approach that is similar to the approach developed for the resolution of the BWR-strainer-blockage issue [NUREG/CR-6369-1, 1999]. The chart for a LOCA in the volunteer-plant SG1 is shown in Figure IX-7 and is based on the MELCOR nodalization diagram in Figure IX-6. This chart tracks the progress of small debris from the pipe break (Volume V12) until the debris is assumed to be captured or is transported beyond the compartment. Because SGs 1 and 4 are joined at two locations, the compartments were combined into one model (i.e., a LOCA in SG1 will discharge to the containment through SG4 as well).

The questions across the top of the chart, shown in Figure IX-7, alternate among volume capture, flow split, and junction capture as the debris-transport process progresses through the nodalization scheme. The nodalization scheme was constructed to place the gratings at junction boundaries. The first chart question (header) after the initiator asks how much debris would be captured in Volume V12, where the LOCA was postulated to occur. The evaluation of this question involves simply estimating the fraction of small debris that was deposited by inertia near the pipe break; the remainder of the debris would be assumed to transport beyond this volume. The next question in the chart concerns a flow split (i.e., the distribution of the break flow going upward or downward from the break). The flow split is actually a debris split (i.e., how much debris goes in each direction). For fine- and small-piece debris, it is reasonable to assume that the debris split is approximated by the flow split. For large and intact-piece debris, the debris split may differ from the flow split, depending on the geometry. The third question concerns the amount of the debris captured at the flow junction between two volumes. The two

junctions in the third question represent gratings that extend partly across the compartment at two levels. The fourth question starts the cycle over again for the next set of volumes in the sequence.

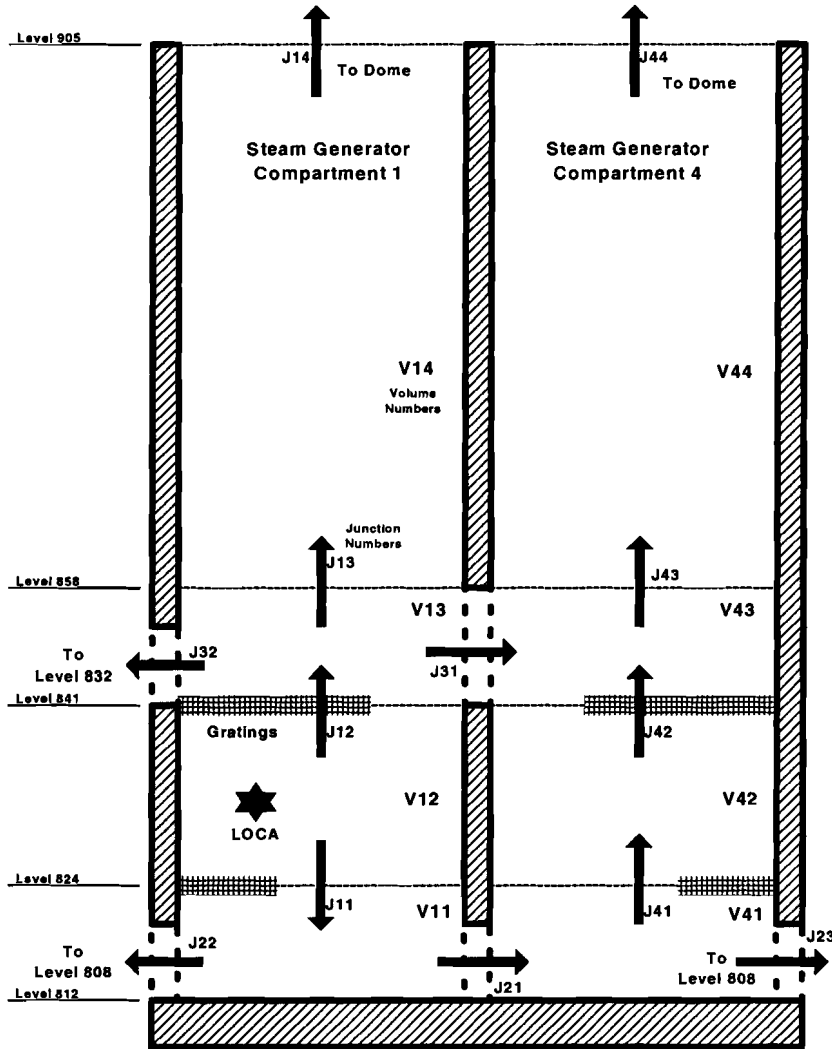


**Figure IX-6. Break-Region Nodalization.**

Once the distributions are inserted into the chart and the results are quantified, the results will indicate the distribution of captured debris within the compartments, as well as the debris transport from the compartments. The chart also will indicate where the debris that is transported from the SG compartments goes (e.g., to the dome or to the lower levels through access doorways).

Break & Size	Volume Capture	Flow Split	Junct Capture	Volume Capture	Flow Split	Junct Capture	Volume Capture	Flow Split	Junct Capture	Volume Capture	Flow Split	Junct Capture	Volume Capture	Flow Split	Junct Capture	Volume Capture	Flow Split	Junct Capture	Dispersion Location
1	2	3	4	5	6	7	8	9	10	11	12	13	14	15	16	17	18	19	
																			1 Expelled To Dome
																			2 SG1 L905 Grating
																			3 Volume 14
																			4 Expelled To Dome
																			5 SG4 L905 Grating
																			6 Volume 44
																			7 Volume 43
																			8 Expelled to L832
																			9 Doorway Bend
																			10 Volume 13
																			11 SG1 L841 Grating
																			12 Expelled to Dome
																			13 SG4 L905 Grating
																			14 Volume 44
																			15 Volume 43
																			16 SG4 L841 Grating
																			17 Volume 42
																			18 SG4 L824 Grating
																			19 Expelled to L808
																			20 Doorway Bend
																			21 Volume 41
																			22 Expelled to L808
																			23 Doorway Bend
																			24 Volume 11
																			25 SG1 L824 Grating
																			26 Volume 12

Figure IX-7. Chart for the Structure of Break-Region Debris-Transport.

### VI.3.3.2 Dispersion and Capture throughout the Containment

The debris dispersion model used to evaluate debris transport within the volunteer-plant containments estimated dispersion throughout the containment first by free volume and then by surface orientation within a volume region. Dispersion distributions were based first on actual volumes and areas and then were adjusted using weighting factors that were based on engineering judgment.

#### VI.3.3.2.1 Dispersion by Region

As the containment pressurizes following a LOCA, break flows carrying debris would enter all free volume within the containment. Larger debris would tend to settle out of the break flows as the flow slowed down after leaving the break region. However, the fine and smaller debris more likely would remain entrained so that fine and small debris would be distributed more uniformly throughout the containment. Certainly, the distribution would not be completely uniform because of debris being captured along the way, which is the reason for the weighting factors.

First, the containment free volume was subdivided into volume regions. This subdivision was based on geometry (i.e., floor levels and walls) and on the location of CSs. Specifically, areas where deposited debris likely would not be entrained by the CSs were separated from areas that were impacted by the sprays. Some areas that were not actually sprayed still could be washed by the drainage of spray water as the water worked its way down through the containment structures. Areas where debris could be deposited without subsequently being washed downward by the sprays and the spray drainage could reduce the estimated transport fractions.

The total free volume of the containment is the sum of the free volumes for all of the volume regions. The volunteer-plant containment free volume was subdivided into a total of 24 volume regions ( $J = 24$ ) as

$$V_{cont} = \sum_{j=1}^J V_{C_j} \quad ,$$

where

- $V_{cont}$  = the total free volume of the containment;
- $V_{C_j}$  = the free volume in containment region  $j$ ; and
- $J$  = the number of volume regions.

The following equations define the dispersion model;

$$V_{i,j} = F_{i,j} D_i V_{ZOI} \quad ,$$

where

- $V_{i,j}$  = the volume of debris-type  $i$  located in region  $j$ ;
- $F_{i,j}$  = the fraction of debris-type  $i$  deposited in region  $j$  during blowdown;

- $D_i$  = the fraction of total debris-type  $i$ ; and  
 $V_{ZOI}$  = the total volume of insulation contained within the ZOI.

For fibrous debris, the numbering system is  $i = 1, 2, 3,$  and  $4$  for fines, small pieces, large pieces, and intact debris, respectively.

The volume dispersion distribution must add up to one, as

$$\sum_{j=1}^J F_{i,j} = 1 \text{ (for each } i \text{)} .$$

The break region was designated as Region 1 (i.e.,  $j = 1$  and  $F_{i,1} = F_{i,break}$ ), and the methodology for the break-region dispersion fraction was provided in Section VI.3.3.1. The remaining distribution fractions were estimated using the following volume and engineering judgment weighted distribution:

$$F'_{i,j(j \neq 1)} = (1 - F'_{i,break}) \frac{wc_{i,j} Vc_j}{\sum_{j=2}^J wc_{i,j} Vc_j} ,$$

where

$wc_{i,j}$  = the weighting factor based on engineering judgment.

If all of the  $wc_{i,j}$  were set to one, then the distribution would be simply a volume-weighted distribution.

For large and intact pieces, many of these weighting values  $wc_{i,j}$  were set to zero to reflect the fact that large and intact debris likely would not transport into many of the lower-level volume regions. It is anticipated that most of the large and intact debris would reside in the break-region volume, sump-pool volume, containment-dome volume, or refueling area.

The substantial quantities of debris transported into the dome subsequently would tend to either fall out of the atmosphere or be washed out by the CSs. About half of this debris would be deposited onto the Level 905 floors that are associated with the dome. However, the other half would fall below this level, thereby entering other volume regions. The volume distribution function  $F'_{i,j}$  is modified as follows to account for debris fallout between regions:

$$F_{i,j} = F'_{i,j} + T_j F'_{i,2} ,$$

where

$T_j$  = the fraction of debris (type independent) located in the dome that subsequently falls or washes to region  $j$ .

The values of  $T_j$  are based on the opening areas into regions below the dome (e.g., the cross-sectional area of the SG compartments divided by the total cross-sectional area of the containment provides the values for debris that is falling into an SG compartment). The value for a region receiving no debris from dome fallout would be zero. Note that the dome volume region was designated Region 2; therefore, the value for region 2 (i.e.,  $T_2$ ) must be negative to remove debris from Region 2:

$$T_2 = - \sum_{j=1}^J T_{j(j \neq 2)} \quad .$$

#### VI.3.3.2.2 Dispersion by Surface Orientation and Exposure

Once the debris was dispersed to a volume region, it was assumed to have been deposited within that region. Some residual fine debris could remain airborne in regions that are not impacted by the sprays; however, the total quantity of this residual airborne debris was not expected to be significant.

The surface area within each volume region was subdivided into six subsections. These subsections reflect both the differing surface orientations and their exposure to moisture. The floors were separated from all of the other surfaces because the floors would receive the gravitationally settled debris and the other surfaces could be flooded partially by spray drainage. The spray water would not accumulate on the other surfaces, which include the walls, ceilings, and equipment.

Three surface exposures or moisture conditions were considered in the analysis: surfaces wetted directly by the CSs, surfaces not directly sprayed but washed by spray drainage (most likely floor surfaces), and surfaces wetted only by steam condensation. All surfaces likely would be wetted by condensation. The surface exposure determined how likely debris that was deposited onto that particular surface subsequently would be transported by the flow of water.

These areas were described by the following three-dimensional array:

$$A_{j,k,l} = \text{area for volume region } j, \text{ orientation } k, \text{ and exposure } l.$$

All of the area within a particular volume region then would be

$$A_j = \sum_{k=1}^2 \sum_{l=1}^3 A_{j,k,l} \quad .$$

The numbering system is  $k = 1$  and  $2$  for "floor" and "other" surfaces, respectively, and  $l = 1, 2,$  and  $3,$  for condensate, spray, and drainage exposures, respectively.

The surface-area distribution fractions were estimated using the following area and engineering judgment weighted distribution:

$$f_{i,j,k,l} = \frac{w_{i,j,k,l} A_{j,k,l}}{\sum_{k=1}^2 \sum_{l=1}^3 w_{i,j,k,l} A_{j,k,l}} ,$$

where

- $f_{i,j,k,l}$  = the fraction of debris-type  $i$  deposited within volume region  $j$  that was deposited onto surface  $k, l$ ; and  
 $w_{i,j,k,l}$  = the weighting factor based on engineering judgment for debris-type  $i$  deposited within volume region  $j$  that was deposited onto surface  $k, l$ .

An equivalent expression for  $f_{i,j,k,l}$  is

$$f_{i,j,k,l} = \frac{w_{i,j,k,l} g_{j,k,l}}{\sum_{k=1}^2 \sum_{l=1}^3 w_{i,j,k,l} g_{j,k,l}} ,$$

where

$$g_{j,k,l} = \frac{A_{j,k,l}}{A_j} .$$

The fractions summed within a particular volume region and for a particular debris type must add up to one:

$$\sum_{k=1}^2 \sum_{l=1}^3 f_{i,j,k,l} = 1 .$$

If all of the  $w_{i,j,k,l}$  were set to one, then the distribution would be simply an area-weighted distribution. If all the  $w_{i,j,k,l}$  were set to zero for  $k = 2$  ("other" surfaces), then all of the debris would be deposited on the floor, as likely would be the case for the large and intact debris. It is anticipated that most of the large and intact debris would reside on the floors in the break-region volume, sump pool volume, containment dome volume, or refueling area. In the SG compartment, much of the large debris stopped on the underside of a grating could fall back down after the depressurization flows subsided.

The volume of debris on a particular surface is expressed by

$$V_{i,j,k,l} = f_{i,j,k,l} F_{i,j} D_i V_{ZOT} .$$

### VI.3.4 Washdown Debris Transport

Debris that is deposited throughout the containment subsequently would be subject to potential washdown by the CSs, the drainage of the spray water to the sump pool, and (to a lesser extent) the drainage of condensate. Debris on surfaces that would be hit directly by CS would

be much more likely to transport with the flow of water than would debris on a surface that is wetted merely by condensation. The transport of debris entrained in spray water drainage is less easy to characterize. If the drainage flows were substantial and rapidly moving, the debris likely would transport with the water. However, at some locations, the drainage flow could slow and be shallow enough for the debris to remain in place. As drainage water dropped from one level to another, as it would through the floor drains, the impact of the water on the next lower level could splatter sufficiently to transport debris beyond the main flow of the drainage, thereby essentially capturing the debris a second time. In addition, the flow of water could erode the debris further, generating more of the very fine debris. These considerations must be factored into the analysis. The washdown processes are illustrated schematically in Figure IX-8.

The drainage of spray water from the location of the spray heads down to the sump pool was evaluated. This evaluation, reported in Appendix A **Appendix I?**, provided insights for the transport analysis, such as identifying areas that were not impacted by the CSs, the water drainage pathways, likely locations for drainage water to pool, and locations where drainage water plummets from one level to the next.

#### VI.3.4.1 Debris Erosion during Washdown

Experiments conducted in support of the DDTS analysis demonstrated that insulation debris could be eroded further by the flow of water. The primary concern of the DDTS analysis was LDFG debris that was deposited directly below the pipe break and therefore was inundated by the break overflow. Debris erosion in this case was substantial (i.e., ~9%/h at full flow). Debris erosion due to the impact of the sprays and spray drainage flows was certainly possible but was found to be much less significant. The DDTS study concluded that <1% of the LDFG was eroded because of the CSs. Debris erosion occurring because of condensation and condensate flow was neglected. Debris with its insulation still in its cover was not expected to erode further. For RMI debris, erosion was not a consideration. However, for a microporous insulation such as calcium silicate or Min-K, the washdown erosion has not been determined; it would be expected to be substantial and could potentially erode this type of debris completely into fine silt.

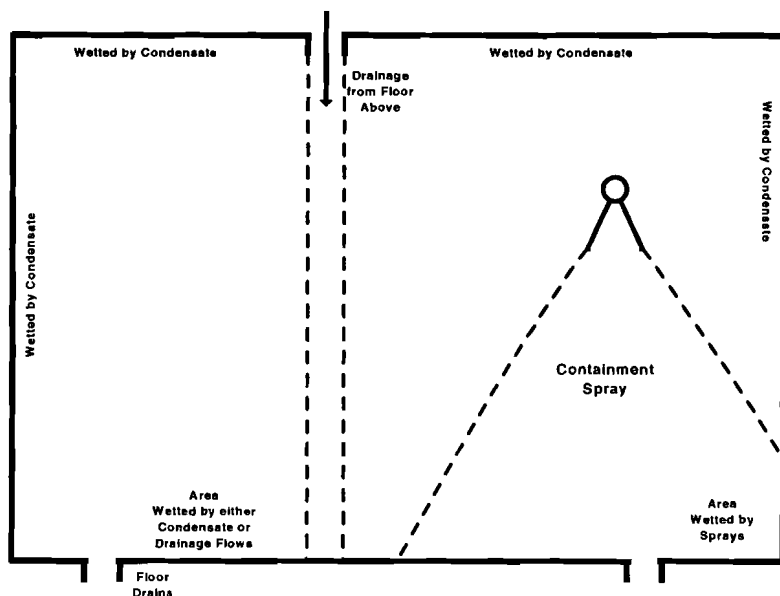


Figure IX-8. Schematic of Debris-Washdown Processes.

Because the byproduct of the erosion process is more of the very fine and easily transportable debris, the process must be evaluated. All erosion products were assumed to transport to the sump pool. Recall that this debris would remain suspended in the sump pool until filtered from the flow at the sump screens. Therefore, even a small amount of erosion could contribute significantly toward the likelihood of screen blockage.

The only erosion process evaluated herein was the erosion of debris that was impacted directly by the CSs. Erosion caused by break overflow was deferred to the degeneration of debris due to sump pool turbulence associated with the plummeting of the break flow into the pool. This assumption neglects the erosion of any large debris that is deposited on top of the lower grating in SG1 and impacted directly by the break overflow; however, this quantity of debris was not considered to be substantial. Most of the debris that is located directly below the break likely would be pushed away from the break and into the sump pool. Note that the floors of the SG compartments are 4 ft above the floor of the sump pool. At switchover, the SG floor would not be flooded but that at the maximum pool height, that pool would have a depth of 0.7 ft in the SG compartment.

The assumed fractions of fibrous debris that were eroded are summarized in Table IX-4. It was assumed that condensate drainage would not cause further erosion of debris and that intact or covered debris would not erode further. Erosion does not apply to fine debris because that debris is already fine. About 1% of the small- and large-piece debris that was directly impacted by the sprays was considered to have eroded. This amount of erosion was considered to be conservative because the DDTs concluded that the erosion was <1%. No erosion of the intact debris was assumed because the canvas cover likely would protect the insulation.

**Table IX-4. Total Erosion Fractions for Fibrous Debris**

Exposure	Fines	Small	Large	Intact
Condensate	N/A	0	0	0
Sprays	N/A	1%	1%	0

To estimate the volume of debris that was eroded, the volume of debris that was impacted by the sprays first must be estimated. The latter estimate can be made using the data arrays that were already established in this methodology. These volumes for small and large debris, respectively, are estimated using the following two equations:

$$V_{spr_2} = \sum_{j=1}^J \sum_{k=1}^2 f_{2,j,k,2} F_{2,j} D_2 V_{ZOI}$$

and

$$V_{spr_3} = \sum_{j=1}^J \sum_{k=1}^2 f_{3,j,k,2} F_{3,j} D_3 V_{ZOI} \cdot$$

The volumes that are eroded ( $E_2$  and  $E_3$  for small and large debris, respectively) are simply 1% of the debris volumes impacted by the sprays, given as

$$E_2 = e_{spr} V_{spr} r_2$$

and

$$E_3 = e_{spr} V_{spr} r_3 \quad ,$$

where the spray erosion fraction  $e_{spr}$  is 0.01.

#### VI.3.4.2 Capture Retention during Washdown

The retention of debris during washdown must be estimated for the debris deposited on each surface (i.e., the fraction of debris that remains on each surface). These estimates, based on experimental data and engineering judgment, were assigned somewhat generically. For surfaces that would be washed only by condensate drainage, nearly all deposited fine and small debris likely would remain there. The DDTs assumed that only 1% of the fibrous debris would be washed away in the more realistic central estimate of that study (a value of 10% was assumed for the upper-bound estimate). When the 1% assumption was applied, all of the surfaces that drained only condensate would have a retention fraction of 0.99 with respect to fibrous debris.

For surfaces that were hit directly by sprays, the DDTs assumed 50% and 100% for the central- and upper-bound estimates for small fibrous debris. Large and intact debris likely would not be washed down to the sump pool (retention fractions of 1). For surfaces that were not sprayed directly but subsequently drain accumulated spray water, such as floors close to spray areas, the retention fractions were much less clear. These fractions likely would vary with location and drainage flow rates and therefore must be area location specific, with more retention for small pieces than for fine debris.

The retention fraction for a specific volume region is expressed as

$$R_{i,j} = \sum_{k=1}^2 \sum_{l=1}^3 f_{i,j,k,l} r_{i,j,k,l} \quad ,$$

where

$R_{i,j}$  = the fraction of debris-type  $i$  retained in region  $j$ ; and

$r_{i,j,k,l}$  = the fraction of debris-type  $i$  retained, on surface  $k$ ,  $l$ , in region  $j$ .

These volume region retention fractions  $R_{i,j}$  do not account for the quantities that are eroded from the captured pieces of debris. To complete the erosion model, the volumes of eroded debris that came from debris that remained captured versus debris that transported to the sump pool were estimated. Therefore, the debris that remained captured during the washdown process is estimated using the following two equations for small- and large-piece debris, respectively:

$$Rspr_2 = \sum_{j=1}^J \sum_{k=1}^2 r_{2,j,k,2} f_{2,j,k,2} F_{2,j} D_2 V_{Z01}$$

and

$$Rspr_3 = \sum_{j=1}^J \sum_{k=1}^2 r_{3,j,k,2} f_{3,j,k,2} F_{3,j} D_3 V_{Z01} .$$

Therefore, the volumes of eroded debris associated with the debris that remained captured are expressed as

$$ER_2 = e_{spr} Rspr_2$$

and

$$ER_3 = e_{spr} Rspr_3 .$$

Debris transported from its original volume region still could be captured at a lower elevation. This secondary capture was neglected in this analysis.

### VI.3.5 Debris Volumes Introduced to the Sump Pool

The primary result of the blowdown/washdown transport analysis is the volume that is transported to the sump pool by debris category. The volumes of debris transported to the pool are given by

$$V_{i,pool} = \left[ 1 - \sum_{j=1}^J R_{i,j} F_{i,j} \right] D_i V_{Z01} + Ve_i ,$$

where

$V_{i,pool}$  = the volume of debris-type  $i$  transported to the sump pool and

$Ve_i$  = the volumes of eroded debris transferring from small- and large-debris categories to the fine-debris category.

The erosion translation array is given by

$$Ve_i = \begin{bmatrix} +(E_2 + E_3) \\ -(E_2 - ER_2) \\ -(E_3 - ER_3) \\ 0 \end{bmatrix} .$$

This array adds the eroded product ( $E_2 + E_3$ ) to the fine-debris category and subtracts the eroded volume from the noncaptured small- and large-debris categories ( $E_i - ER_i$ ).

The total debris that transports to the pool is

$$V_{pool} = \sum_{i=1}^4 V_{i,pool} \quad .$$

This model does not track debris transport in sufficient detail to determine where the debris would enter the sump pool. It was assumed simply that the debris would be mixed uniformly with flows entering the pool.

### VI.3.6 Transport Fractions

The overall debris-transport fraction now can be estimated as

$$TF_{ZOI} = \frac{V_{pool}}{V_{ZOI}} \quad ,$$

where

$TF_{ZOI}$  = the fraction of insulation that is located in the ZOI and subsequently is transported to the sump pool.

The transport fractions for each individual debris category can be estimated as

$$TF_i = \frac{V_{i,pool}}{D_i V_{ZOI}} \quad ,$$

where

$TF_i$  = the fraction of debris-type  $i$  that is generated within the ZOI and subsequently is transported to the sump pool.

Note that the translation of erosion products from the small- and large-debris categories to the fine-debris category has been incorporated into the transport fractions.

## VI.4 DEBRIS-TRANSPORT ANALYSIS

When the methodology presented in Section VI.3 was used, plausible estimates were developed for the transport of insulation debris within the volunteer-plant containments. Because of the complexity of the analysis and the limited available data, substantial uncertainty exists in these estimates. Engineering judgment that was used to fill gaps in the data was tempered conservatively. Despite the uncertainty, the transport analysis illustrated trends, as well as plausible estimates of the fractions of the debris that was generated and subsequently could transport to the sump pool.

### VI.4.1 Fibrous Insulation Debris Transport

As discussed in Section VI.3.2, the insulation that is used in the volunteer-plant containments consists of fibrous, RMI, and Min-K insulation at ~13.4%, 85.7%, and 0.9%, respectively. The

majority of the available debris-transport data was obtained for LDFG insulation debris, specifically experimental data taken for the DDTS [NUREG/CR-6369-2, 1999]. Although a majority of the insulation within these containments is RMI, the fibrous insulation debris, in combination with particulate, is expected to be a larger challenge to the operation of the recirculation sump screens. Therefore, the debris transport for the fibrous debris was analyzed first. Even with the available transport data for LDFG debris, the transport analysis required the application of conservatively tempered engineering judgment.

#### VI.4.1.1 Fibrous Blowdown Debris Transport

The first consideration in performing the dispersion estimate for the fibrous blowdown insulation debris was the dispersion and deposition within the break region (assumed to be a break in SG1), where deposition likely resulted from inertial impaction. The dispersion through the remainder of the containment was subsequently estimated.

##### VI.4.1.1.1 Break-Region Blowdown Debris Deposition

The effluences from the break would carry insulation debris with the flows into the upper-containment dome through the large opening at the top of the SG compartment and into lower compartments through the compartment access doorways. Along the way, substantial portions of that debris likely would be inertially deposited or otherwise entrapped onto structures. In general, the break-region flow immediately after the initiation of the break would be much too violent to allow debris simply to settle to the floor of the region.

##### VI.4.1.1.1.1 Characterize Break Flows within Break Region

The thermal-hydraulic MELCOR code was used to determine the distribution of the break effluents from the SG compartment. When a break in SG1 was postulated, it was determined that most of the break effluent would be directed upward toward the large upper dome. Because of the large openings connecting SG1 to SG4, the venting to the dome would occur through both SG compartments. Effluents venting into lower-level compartments (surrounding the two SGs) by way of open access doorways would flow at much lower rates than the upward flows to the dome. The nodalization of the two SG compartments is shown in Figure IX-6, where the break was postulated to occur in Volume V12. Break effluents that are typical of three break sizes were assumed: large-break (LB) LOCA, medium-break (MB) LOCA, and small-break (SB) LOCA. The results of the MELCOR simulations are summarized in Table IX-5, where the distributions from a particular control volume are shown by the connecting junction. For example, given an LB LOCA scenario, ~80% of the flow from Volume V12, where the break was postulated, went upward through Junction J12, with the remainder going downward through Junction J11. Note that the flow splits were somewhat transient and that the results in Table IX-5 are reasonable approximations of the transients over the time where most debris transport would occur. LB LOCA and MB LOCA flows were reasonably steady over the transport period, but SB LOCA flows were not steady because of transition into natural circulation after ~6 s.

Inertial debris deposition is dependent on the flow velocities transporting the debris. The MELCOR calculations predicted transient flow velocities for each flow junction and each size of break. The general ranges of these velocities are provided in Table IX-6. The velocities are in the general range as the test velocities for which the debris-capture data were measured in the DDTS.

**Table IX-5. Break Effluent Flow Splits**

Break Size	Flows Exiting Volume V <sub>i</sub> through Junction J <sub>j</sub>								
	V12		V11		V41		V13		
	J11	J12	J21	J22	J23	J41	J13	J31	J32
LB LOCA	20%	80%	70%	30%	5%	95%	62%	33%	5%
MB LOCA	20%	80%	70%	30%	14%	86%	62%	33%	5%
SB LOCA	15%	85%	80%	20%	30%	70%	66%	28%	6%

**Table IX-6. Characteristic Velocities in SG1**

Postulated Break Size	Characteristic Velocities	
	m/s	ft/s
LB LOCA	25–200	80–660
MB LOCA	5–45	15–150
SB LOCA	1–8	5–25

VI.4.1.1.1.2 Debris-Transport Distributions from Volumes

The very fine debris would transport more like an aerosol in that the particles would disperse within the flow and follow the flow. Portions of this debris would be deposited onto structures along the transport pathways, primarily because of inertial deposition at bends in the flow. However, with larger debris, the tendency would be greater for the debris not to follow the flow through sharp bends in the flow and larger debris would more likely be trapped by a structure such as a grating. In addition, gravitational settling as the flow velocities slow would be more effective for larger debris than smaller debris. For example, following an LB LOCA in an SG compartment, a large, nearly intact insulation pillow could travel upward with the main flow to the containment dome unless an obstacle, such as a grating, impeded that pillow. However, this pillow would be much less likely to follow the flow through a connecting doorway to the next SG compartment.

Assumptions based on engineering judgments that were tempered by experimental observations were required to reach a solution. The assumptions provide a reasonable crude approximation of debris transport from a volume when there is a split in the flow. These assumptions are the following.

- The fine and small fibrous debris would be well dispersed within the flow and would transport uniformly with the flow; therefore, the debris-transport junction distributions for fines and small debris are the same as the junction flow distributions in Table IX-5.
- Large and intact debris would not make the turn to exit SG1 at Level 832 (Junctions J31 and J32). In addition to the turn, most of this debris that was moving toward these exits would be stopped by the gratings that cover ~45% of the cross-sectional area of the compartment that is nearest those exits.

- Large and intact debris entering SG4 at the floor level (Level 812) would be much less likely to follow the flow through the 90° bend and subsequently transport upward through SG4. Debris entering Volume V41 that is not captured in Volume V41 would exit by either Junction V23 or V41. For large and intact debris, the flow fractions for Junction V41 were reduced by one-half and two-thirds, respectively (engineering judgment).

Applying these assumptions to the transport of the large and intact debris through the node junctions resulted in the junction transport distributions that are shown in Table IX-7 and Table IX-8.

**Table IX-7. Large-Debris-Transport Junction Distributions**

Break	V12		V11		V41		V13		
	J11	J12	J21	J22	J23	J41	J13	J31	J32
LB LOCA	20%	80%	70%	30%	52%	48%	100%	0%	0%
MB LOCA	20%	80%	70%	30%	57%	43%	100%	0%	0%
SB LOCA	15%	85%	80%	20%	65%	35%	100%	0%	0%

**Table IX-8. Intact-Debris-Transport Junction Distributions**

Break	V12		V11		V41		V13		
	J11	J12	J21	J22	J23	J41	J13	J31	J32
LB LOCA	20%	80%	70%	30%	68%	32%	100%	0%	0%
MB LOCA	20%	80%	70%	30%	71%	29%	100%	0%	0%
SB LOCA	15%	85%	80%	20%	77%	23%	100%	0%	0%

#### VI.4.1.1.1.3 Capture Fractions at Junctions

Debris-transport data from the Army Research Laboratory (ARL) and the CEESI tests that were conducted to support the DDTS [NUREG/CR-6369-2, 1999] provide average capture fractions for LDFG debris that is passing through typical gratings and around typical structures, such as piping and beams, and for debris making a 90° bend. These structures and the bend were wetted during the tests; the data do not apply to dry structures. These data are assumed to apply in general to the volunteer-plant containments because it is expected that the containment surface would be wetted rapidly by steam condensation, as well as liquid break effluent, and because the range of predicted flow velocities (Table IX-6) are in general agreement with the flow velocities of the tests. The flow velocities ranged from 25 to 150 ft/s for the ARL tests and from 35 to 60 ft/s for the CEESI tests. The debris capture was most applicable to MB LOCAs and perhaps least applicable to SB LOCAs.

Fine and small fibrous debris could be captured inertially onto wetted surfaces whenever the break flow changed direction, such as flows through the doorways from the SG compartments into the sump-level annular space. These flows must make at least one 90° bend through those entrances. Debris-transport experiments that were conducted at CEESI demonstrated an average capture fraction of 17% for fine and small debris that were making a 90° bend. These surfaces would be wetted because of steam condensation and the liquid portion of the break

\*Based on analyses performed for the DDTS [NUREG/CR-6369-3, 1999].

effluence. Other flow bends likely would occur within the violent three-dimensional flows near the break. The platform gratings within the SG compartments would capture substantial amounts of debris, even though the gratings do not extend across the entire compartment. The CEESI debris-transport tests demonstrated that an average of 28% of the fine and small LDFG debris was captured when the airflow passed through the first wetted grating encountered and that an average of 24% was captured at the second grating. The large and intact debris, by definition, would be trapped completely by a grating. In addition, equipment (such as beams and pipes) was shown to capture fine and small debris. In the CEESI tests, the structural maze in the test section captured an average of 9% of the debris passing through the maze.

Grating Capture: In the volunteer plant, partial gratings exist at three levels in each of the SG compartments. The gratings extend out over ~22%, 45%, and 15% of the SG cross-sectional area at plant elevations 824, 841, and 905 ft, respectively. If it is assumed that 28% of small and fine fibrous debris and 100% of the large and intact debris are captured from the flow by a grating as the flow passes through the grating, the capture fractions for model junctions that contain a grating are provided in Table IX-9.

**Table IX-9. Grating Capture Fractions at Model Junctions**

Grating Level	Model Junctions	Fine and Small Debris		Large and Intact Debris	
		Unit Area Capture Fraction	Junction Capture Fraction	Unit Area Capture Fraction	Junction Capture Fraction
Level 905	J14 and J44	0.28	0.04	1.0	0.15
Level 841	J12 and J42	0.28	0.13	1.0	0.45
Level 824	J11 and J 41	0.28	0.06	1.0	0.22

Doorway Capture: Depressurization flows also would exit the SGs by way of the SG access doorways at Levels 808 and 832. Flows traveling through these pathways would carry debris directly into the lower levels of the containment; in fact, some of the debris likely would be deposited near the recirculation sumps. Because these doorways were designed with at least one 90° bend, debris would be deposited inertially onto wetted surfaces at each bend in the flow. Furthermore, because the CSs would not impact these vertical surfaces, the debris likely would remain on the surfaces once it was captured there. The CEESI data showed an average of 17% debris capture at its 90° bend for debris that was small enough to already have passed through a grating (i.e., fines and small debris). It was assumed that 17% of fine and small debris that was transported from the SG break region through the Level 808 and Level 832 doorways to the bulk containment would be captured at a bend (one bend assumed). No comparable data exist for the large and intact debris; however, the larger debris would be much less likely to stick to a wall once it impacted inertially against the wall. Because of a lack of appropriate data, it was assumed conservatively that no large or intact debris would be captured at these doorways.

\* These fractions were estimated from plant drawings.

#### VI.4.1.1.1.4 Capture Fractions within Volumes

As illustrated in Figure IX-7, debris would be captured on structures within the model nodes, as well as the node junctions. As the break effluents flowed around and through the structural and equipment congestion within the SG compartment, debris would be driven inertially onto surfaces where some portion of it would remain captured. The structures include the pumps; SGs; and associated piping, beams, equipment stands, cabling, etc. The chaotic nature of the flows as the break jet is deflected off structures and wall surfaces could create a multitude of bends in the flow that could deposit debris inertially onto wall surfaces and irregular wall features. In the CEESI tests, ~9% of the fine and small debris was deposited onto wetted structures as the debris passed through a test structural assembly and 17% was captured onto a wetted surface at a sharp 90° bend in flow. Estimates of the amounts of debris captured within a node volume were based on this CEESI test data and on conservatively tempered engineering judgment. It is likely conservative to capture more debris within the SG than to transport the debris throughout the containment because washdown within the SG should be relatively greater than some other areas of the containment and because debris washed off the SG structures can go directly to the sump pool.

Applying a number of engineering judgments in conjunction with the CEESI data resulted in estimates for the capture of debris within each volume of the break-region debris-transport model. These estimates, along with the associated assumptions, are provided in Table IX-10.

**Table IX-10. Fractions of Debris Captured within Each Volume**

SG1				SG4			
Volume	Fines and Small Pieces	Large Pieces	Intact Pieces	Volume	Fines and Small Pieces	Large Pieces	Intact Pieces
V14	1% (A)	2% (A)	5% (A)	V44	1% (A)	2% (A)	5% (A)
V13	1% (A)	2% (A)	5% (A)	V43	1% (A)	2% (A)	5% (A)
V12	14% (C)	30% (E)	50% (F)	V42	9% (B)	15% (E)	30% (G)
V11	26% (D)	40% (E)	80% (H)	V41	14% (C)	25% (E)	80% (H)
<b>Assumptions</b>							
A. Volumes contain minimal structures and no significant flow bends; therefore, a minimal amount of capture occurs. It is somewhat more likely that large debris would be captured than small debris and more likely that intact debris would be captured than large debris.							
B. Structures are equivalent to one CEESI structural test assembly (9%), and no significant flow bends exist.							
C. Structures are equivalent to one CEESI structural test assembly (9%), and significant flow bending that is less than a sharp 90° bend exists (5%).							
D. Structures are equivalent to one CEESI structural test assembly (9%), and significant flow bending that is equivalent to a sharp 90° bend exists (17%).							
E. Large debris is more likely to be captured than small debris, and 50% more large debris is captured than small debris.							

F. Intact debris is much more likely to snag on equipment than the large debris. In addition, some insulation within the ZOI likely could remain attached to piping.

G. Intact debris is much more likely to snag on equipment than the large debris.

H. The congestion of equipment and cables near the floor is expected to trap most of the intact debris as the flow makes a 90° bend near the floor. Intact debris is less likely to follow the distribution of flow than is smaller debris.

#### VI.4.1.1.1.5 Break-Region Debris-Transport Quantification

The logic chart shown in Figure IX-7 and discussed in Section VI.3.3.1 was used to quantify the various flow splits and capture and to estimate the debris deposition within and from SG1. These charts divide the evaluation into many smaller problems that are amenable to resolution—an approach that was adapted from the resolution of the BWR strainer-blockage issue [NUREG/CR-6369-1, 1999]. This chart tracks the progress either of small debris from the pipe break (Volume V12) until the debris is assumed to be captured or until the debris is transported beyond the compartment. Charts were quantified for each of the three LOCA sizes (i.e., small, medium, and large) and for three classifications of fibrous debris (i.e., fines and small pieces, large pieces, and intact pieces). Note that there was no basis to treat the fines and small pieces differently. The data that were used to quantify the charts are discussed in Sections VI.4.1.1.1.1 through VI.4.1.1.1.4. As an example, the chart for the transport of fines and small debris following an LB LOCA is shown in Figure IX-9.

The overall results of the break-region quantification are shown in Table IX-11. The results for the three break sizes were averaged into a single set of results. This was done because the differences among the three size groups were substantially less than the substantial uncertainties associated with these analyses. The charts also provided information regarding the distribution of debris captured with the SGs, as well as the debris driven from the SGs.

**Table IX-11. Distribution of Debris Captured and Exiting Break Region**

Location	Debris Category		
	Fines and Small Pieces	Large Pieces	Intact Pieces
Captured within SGs 1 and 4	0.36	0.70	0.82
Expelled to Dome	0.58	0.26	0.17
Expelled to Level 832	0.03	0	0
Expelled to Level 808	0.03	0.04	0.01

Debris	Volume Capture	Flow Split	Junct Capture	Volume Capture	Flow Split	Junct Capture	Volume Capture	Flow Split	Junct Capture	Volume Capture	Flow Split	Junct Capture	Volume Capture	Flow Split	Junct Capture	Volume Capture	Flow Split	Junct Capture	Volume Capture	Flow Split	Junct Capture	Location	Fraction
1	2	3	4	5	6	7	8	9	10	11	12	13	14	15	16	17	18	19					
Large LOCA Fines & Small Pieces	Pass J14 To Dome																			1	Dome	3.492E-01	
	Exit V14 To Dome																			2	Grating	1.455E-02	
	To V14 Pass J13																			3	V14	3.674E-03	
	Exit V13																			4	Dome	1.840E-01	
	Exit V44 To Dome																			5	Grating	7.666E-03	
	Exit V43 To V44 Pass J43																			8	V44	1.936E-03	
	To V43 Pass J31																			7	V43	1.955E-03	
	Pass J32 To L832																			8	L832	2.459E-02	
	To L832																			9	Door	5.037E-03	
	To V13																			10	V13	5.986E-03	
	Pass J12																			11	Grating	8.944E-02	
	Exit V12																			12	Dome	4.791E-02	
	Exit V44 To Dome																			13	Grating	1.996E-03	
	Exit V43 To V44 Pass J43																			14	V44	5.041E-04	
	Pass J42																			15	V43	5.092E-04	
	Exit V42 To V43																			16	Grating	7.609E-03	
	Pass J41																			17	V42	5.789E-03	
	Exit V41																			18	Grating	4.105E-03	
	To V41 Pass J21																			19	L808	2.989E-03	
	To L808																			20	Door	6.122E-04	
	Exit V11																			21	V41	1.173E-02	
	Pass J22 To L808																			22	L808	2.979E-02	
	To L808																			23	Door	6.102E-03	
	Pass J11																			24	V11	4.204E-02	
	To V11																			25	Grating	1.032E-02	
	Captured																			26	V12	1.400E-01	
Total	1																						

Figure IX-9. Break-Region LB LOCA Transport Chart for Fines and Small Debris.

#### VI.4.1.1.2 Dispersion throughout Remainder of Containment

The debris dispersion model that was presented in Section VI.3.3.2 was used to evaluate debris transport within the volunteer-plant containments by estimating dispersion throughout the containment first by free volume and then by surface orientation within a volume region.

##### VI.4.1.1.2.1 Dispersion by Volume Region

The containment free volume was subdivided into volume regions that were based on geometry, such as floor levels and walls, and on the location of CSs. Specifically, areas where deposited debris likely would not be washed down by the CSs were separated from areas that were impacted by the sprays. The volunteer-plant free volume was subdivided into 24 distinct regions of free volume, as shown in Table IX-12. The volumes of each region were estimated from plant drawings.

**Table IX-12. Subdivision of Containment Free Volume**

No.	Volume Region	Volume (ft <sup>3</sup> )	Volume Fraction V <sub>cj</sub>
1	SG1&4	76600	0.02570
2	Dome - Above 905.75-ft	1992060	0.66848
3	L873 - MS	39300	0.01319
4	Head Lay-Down - L871.5	17120	0.00574
5	Below Head Platform	5750	0.00193
6	Refueling A	45340	0.01521
7	Refueling B	53860	0.01807
8	Refueling C	48660	0.01633
9	Refueling D	47960	0.01609
10	SG2&3	76600	0.02570
11	Pressurizer	11250	0.00378
12	L860 Annulus - Section 1	34100	0.01144
13	L860 Annulus - Section 2	54580	0.01832
14	L860 Annulus - Section 3	94310	0.03165
15	L851 - FW	25800	0.00866
16	Accumulator Section	31500	0.01057
17	L832 Annulus - Section 1	37250	0.01250
18	L832 Annulus - Section 2	33940	0.01139
19	L832 Annulus - Section 3	69890	0.02345
20	L808 Annulus - Section 1	61650	0.02069
21	L808 Annulus - Section 2	30830	0.01035
22	L808 Annulus - Section 3	61650	0.02069
23	Reactor Cavity	25000	0.00839
24	Equipment Room L808	5000	0.00168
Containment Total		2980000	1.00000

Key aspects of the region subdivision follow. The first region, designated SG1 and 4, is the SG compartment 1 where the break was postulated and its connected neighboring SG compartment, SG4. Debris dispersion and deposition in these SG compartments was predicted

in Section VI.4.1.1.1. The second region represents the free volume above the highest floor (i.e., the dome region), which is approximately two-thirds of the entire containment free volume. As shown in Figure IX-10, the lower floor levels were subdivided azimuthally into three sectors to better distinguish the areas with CSs from areas without the sprays. The refueling pool area was subdivided into four regions to reflect the three different pools and the reactor-vessel (RV) head area [i.e., (A) storage pool for RV upper internals, (B) RV area, (C) storage pool for RV lower internals, and (D) pool for fuel transfer and storage].

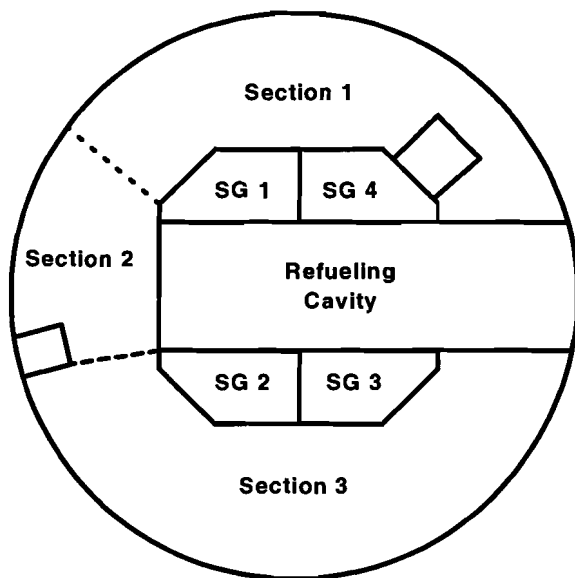


**Figure IX-10. Volume Region Sector Model**

Debris, particularly the larger debris, would not distribute uniformly throughout the free volume. The methodology presented in Section VI.3.3.2.1 applies weighting factors ( $w_{C_{i,j}}$ ) to the free-volume distribution to estimate the distribution of debris throughout the containment (i.e., the distribution of the debris among the 24 volume regions) by debris type. The very fine debris likely would transport somewhat uniformly with the depressurization flows, which would penetrate all free space within the containment as the containment pressurized. The transient nature of debris generation would also introduce nonuniformities into the dispersion of the fine debris. Because no rationale was found to weight the distribution of the fine and small debris away from that of a uniform free-volume distribution outside the break region, all weighting factors were assumed to be one for fine and small fibrous debris.

For the largest debris, specifically the large-piece and intact-piece classifications, the debris that is ejected from the SG compartments into the dome region likely would fall back to the floors and structures of the higher levels. The settling of debris that was ejected into the dome atmosphere was proportioned onto the upper floors according to the distribution of floor area (e.g., the cross-sectional area of a SG compartment divided by the cross-sectional area of the overall containment determined the fraction of settling debris that would fall into that compartment). The largest debris likely would not enter lower compartment volumes, except for debris ejected into the sump-level annulus via personnel access doorways. The assumed weighting factors for the large and intact debris were specified to preference the deposition of larger debris onto the uppermost floors and into the sump-level annulus. The large-piece debris

was assumed to transport somewhat more easily than the intact-piece debris. The assumed weighting factors and the dome fallout fractions are shown in Table IX-13.

**Table IX-13. Volume Region Weighting Factors**

No.	Volume Region	Dome Fallout Fraction $T_j$	Volume Weighting Factors			
			Fines $w_{c1,j}$	Small Pieces $w_{c2,j}$	Large Pieces $w_{c3,j}$	Intact Pieces $w_{c4,j}$
1	SG1&4	0.0951	1	1	1	1
2	Dome - Above 905.75-ft	0	1	1	1	1
3	L873 - MS	0.0555	1	1	0.5	0.3
4	Head Lay-Down - L871.5	0.0349	1	1	0.8	0.5
5	Below Head Platform	0	1	1	0.3	0
6	Refueling A	0.0495	1	1	0.8	0.5
7	Refueling B	0.0579	1	1	0.8	0.5
8	Refueling C	0.0505	1	1	0.8	0.5
9	Refueling D	0.0596	1	1	0.8	0.5
10	SG2&3	0.0978	1	1	0.5	0.3
11	Pressurizer	0	1	1	0	0
12	L860 Annulus - Section 1	0.0092	1	1	0.3	0
13	L860 Annulus - Section 2	0.0052	1	1	0.3	0
14	L860 Annulus - Section 3	0.0241	1	1	0.3	0
15	L851 - FW	0	1	1	0	0
16	Accumulator Section	0.0060	1	1	0.8	0.5
17	L832 Annulus - Section 1	0	1	1	0	0
18	L832 Annulus - Section 2	0	1	1	0	0
19	L832 Annulus - Section 3	0	1	1	0	0
20	L808 Annulus - Section 1	0	1	1	1	1
21	L808 Annulus - Section 2	0	1	1	1	1
22	L808 Annulus - Section 3	0	1	1	0.3	0
23	Reactor Cavity	0	1	1	0	0
24	Equipment Room L808	0	1	1	0	0
Total		0.5453				

The results of the blowdown distribution by groups of volume regions are illustrated in Figure IX-11. In this estimate, the largest portion of the debris was deposited inside the SG compartments, where the break was postulated because of inertial deposition that occurred as the fast-moving flows drove the debris into and through equipment and structures. This was particularly true for the larger debris, which could not pass through the gratings. The upper-level floors (871-, 873-, and 905-ft levels) received substantial debris falling or settling out of the dome atmosphere. The regions above the refueling pools received debris that was driven into those volumes, as well as debris falling or settling from the dome atmosphere; this comment also applies to the opposite SG compartments, SGs 2 and 3. The pressurizer compartment received only small amounts of fine and small debris and no larger debris because the compartment has a roof that prevents debris from falling into the compartment and is relatively small. The lower levels receive relatively small quantities of mostly large-piece debris because

of their remoteness from the dome. Most of the debris entering Levels 832 and 808 was debris that was expelled from the SG compartments by way of the personnel access doorways; therefore, this debris would likely be located near those doors.

CSs would impact most of the deposited debris; these surface areas include the four SG compartments, the upper floor surfaces, and the refueling area. Regions that were not impacted by the sprays included the pressurizer compartment and certain portions of the lower levels. This observation suggests that a large fraction of the more transportable debris would transport to the sump pool.

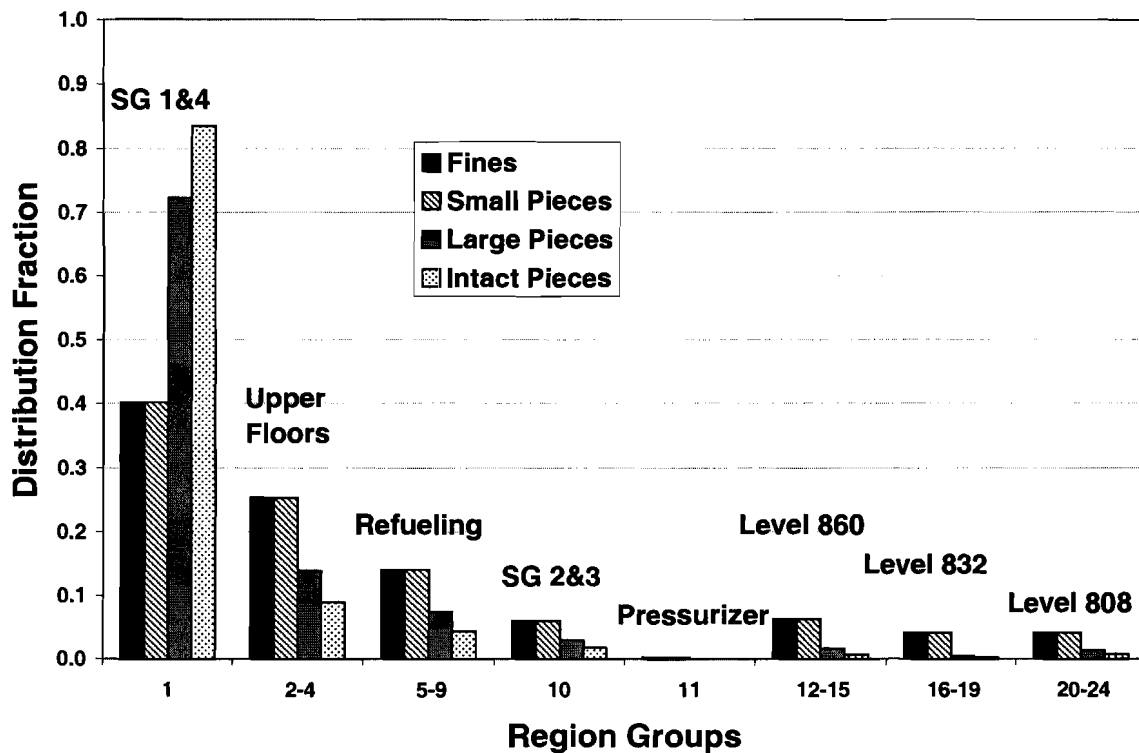


Figure IX-11. Blowdown Distribution by Region Groups.

#### VI.4.1.1.2.2 Dispersion by Surface Orientation and Surface Wetness

Once the debris dispersion prediction placed each type of debris within the 24 volume regions, the debris was dispersed further by surface area classification, i.e., orientation and exposure to moisture. The surface orientation was either “floor area” or “other” area; the distinction was that gravitational settling preferentially deposited debris onto the floor. The surface exposure to moisture included surfaces that were impacted directly by the CSs, surfaces subjected to spray drainage but not sprayed directly, and the remaining surfaces, which would be wetted by condensation. In this manner, the surface area within each volume region was subdivided into six surface groupings. This subdivision was based on both engineering drawings and engineering judgment. The drawings provided basic geometric information such as floor areas; however, engineering judgment, in addition to drawings, was required to estimate fractions of

surfaces that were sprayed directly or covered by spray drainage. The estimated area distribution fractions are shown in Table IX-14.

The floor fraction is an estimate of the total surface area that would receive gravitationally settling debris. This estimate includes upward-facing equipment, as well as the floor (the equipment and piping was assumed to have the same floor fraction as the wall, floor, and ceiling surfaces). The condensate, spray, and drainage fractions represent the fraction of each orientation with this type of exposure. With these fractions, the surface areas and area ratios (i.e.,  $A_{j,k,l}$  and  $g_{j,k,l}$ ) are determined. For example, the floor fraction for a given region multiplied by the spray  $g_{j,k,l}$  are fractions for that region's floor multiplied by the total surface area of the region yields the floor surface area that was sprayed directly by the sprays.

**Table IX-14. Regional Areas Fractions**

No.	Volume Region	Floor Fraction	Floor Surface Area			Other Surface Area		
			Condensate Fraction	Spray Fraction	Drainage Fraction	Condensate Fraction	Spray Fraction	Drainage Fraction
1	SG1&4	0.07	0	1	0	0.1	0.5	0.4
2	Dome - Above 905.75-ft	0.09	0	1	0	0	1	0
3	L873 - MS	0.17	0.2	0.6	0.2	0.9	0.1	0
4	Head Lay-Down - L871.5	0.61	0	1	0	0	0	1
5	Below Head Platform	0.30	0.6	0.1	0.3	0	0	1
6	Refueling A	0.37	0	1	0	0	0	1
7	Refueling B	0.41	0	1	0	0	0	1
8	Refueling C	0.55	0	1	0	0	0	1
9	Refueling D	0.68	0	1	0	0	0	1
10	SG2&3	0.07	0	1	0	0.1	0.5	0.4
11	Pressurizer	0.04	1	0	0	1	0	0
12	L860 Annulus - Section 1	0.10	0.9	0.1	0	1	0	0
13	L860 Annulus - Section 2	0.19	0.1	0.6	0.3	0.6	0.1	0.3
14	L860 Annulus - Section 3	0.19	0.1	0.6	0.3	0.6	0.1	0.3
15	L851 - FW	0.19	0.8	0	0.2	1	0	0
16	Accumulator Section	0.13	0	0.5	0.5	0.5	0	0.5
17	L832 Annulus - Section 1	0.18	0.9	0	0.1	0.7	0	0.3
18	L832 Annulus - Section 2	0.15	0.4	0	0.6	0.6	0	0.4
19	L832 Annulus - Section 3	0.17	0.3	0.5	0.2	0.6	0	0.4
20	L808 Annulus - Section 1	0.18	0	0	1	0.7	0.3	0
21	L808 Annulus - Section 2	0.18	0	0	1	0.7	0.3	0
22	L808 Annulus - Section 3	0.19	0	0	1	0.7	0.3	0
23	Reactor Cavity	0.13	0	0	1	1	0	0
24	Equipment Room L808	0.21	0	0	1	1	0	0

Next, the area weighting factors ( $w_{i,j,k,l}$ ) were estimated, which preference debris toward one surface over another. The dominant preferential debris deposition (and the only preference that can be estimated realistically) is gravitational debris that settles to the floor surfaces. The weighting factors for the non-floor surfaces ( $k = 2$ ) were set first to 1 (i.e.,  $w_{i,j,2,l} = 1$ ), and then the weighting factors for the floor surfaces within each volume region were estimated for each debris type such that the weighting factors preferentially forced debris deposition onto the floor surfaces. The floor weighting factor estimates used the following equation, where the weighting factor is a function of two physical variables that can be estimated more readily. These variables are the fraction of the surface area that is floor area (a geometric determination) and the fraction

of the debris that is deposited onto the floor (an engineering judgment and computational determination):

$$W_{floor} = \left( \frac{d_{floor}}{1-d_{floor}} \right) \left( \frac{1-g_{floor}}{g_{floor}} \right) ,$$

where

- $w_{floor}$  = the weighting factor for debris deposited onto the floor inside a volume;
- $d_{floor}$  = the fraction of the debris deposited within a volume that was on the floor; and
- $g_{floor}$  = the fraction of the volume surface area that is floor area.

The determination of the floor-area fraction ( $g_{floor}$ ) is a straightforward estimate of the floor area divided by the total surface area in a volume region (listed in Table IX-14). In actuality, the surface-area estimate includes the areas associated with equipment and piping because debris can settle onto equipment and piping, as well as onto floors. To reduce the complexity of the area estimates, it was assumed that the area fractions for the equipment and piping were the same as the area fractions for the wall, ceiling, and floor surfaces. Because of this assumption and other geometrical assumptions, these area fractions have an inherent uncertainty associated with the estimates; however, this uncertainty should be significantly smaller than some of the other transport uncertainties.

Debris deposition processes other than gravitational settling, such as diffusiophoresis (condensation-driven deposition), do not depend on surface orientation for these processes; the weighting factors all would be set to 1. Driven debris could be deposited inertially onto any surface or could snag on an obstacle. Heavy, inertially deposited debris subsequently may fall to the floor, but substantially smaller debris likely would remain pasted onto the surface. Even heavy debris can remain on a nonhorizontal surface if the piece were physically snagged. Vertically moving debris eventually would settle onto a surface that is sufficiently horizontal to retain the debris. The fraction of debris deposition onto the floor is highly dependent on the size of the debris.

The estimate of the fraction of the debris that was deposited onto the floor depended greatly on conservative judgments; therefore, the fraction introduced substantial uncertainty into the transport estimates. The engineering judgments accounted for the geometry of the region under consideration, including the relative structural congestion. It was conservative to place the debris on the floor as opposed to other surfaces because more of the debris that was deposited on the floor would be subjected to spray washdown on the floor than on other surfaces. For the SG compartments where the pipe break was postulated (SGs 1 and 4), debris deposition data from the logic charts were used to estimate debris on the floor of these compartments. This estimate included larger debris that was trapped on the underside of gratings and that would likely fall back once the depressurization flow subsided. It was assumed that debris that fell or settled from the dome atmosphere into lower-level regions would fall or settle onto a floor surface.

A typical judgment estimate for fractions of debris that had been driven into an enclosure and that would subsequently settle to the floor was 0.4, 0.7, 0.99, and 0.99 of the fines, small pieces, large pieces, and intact pieces, respectively. For fine debris, the floor deposition fraction was

two to three times the floor area fraction, thereby allowing a substantial settling of the very fine debris, even though diffusion processes would deposit the fine debris onto any surface. The floor fraction for small-piece debris was substantially higher than for the fine debris. Large and intact debris would fall to a horizontal surface unless it snagged on an obstacle. The floor fraction was set to 0.99 to place the large debris on the floor; however, some pieces could have snagged on an obstacle before reaching the floor.

For the far-side SG compartments (SGs 2 and 3) and the pressurizer compartment, the floor-debris deposition fractions acknowledged that the debris would have to travel downward in the compartment and through a variety of structures, including gratings, before reaching the floor; the fractions were reduced for these compartments. For instance, the gratings would catch much of the large debris before it could reach the floor. For open regions, such as the refueling pool regions, where a small amount of equipment and piping is located and the region is not enclosed completely by walls, the floor-debris fractions were increased substantially.

Once the weighting factors were estimated, the final deposition of the debris was determined both as a function of the region and by the surface orientation and its exposure to moisture. Figure IX-12 and Figure IX-13 illustrate the dispersion patterns in the containment according to surface orientation and surface wetness.

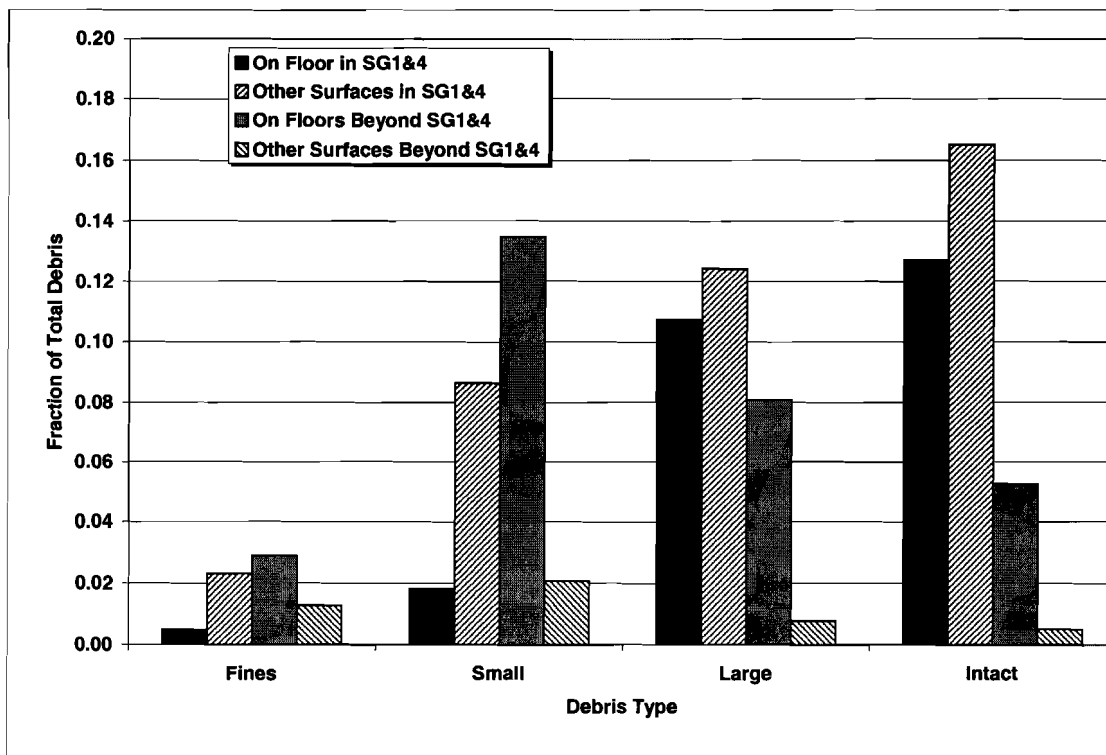
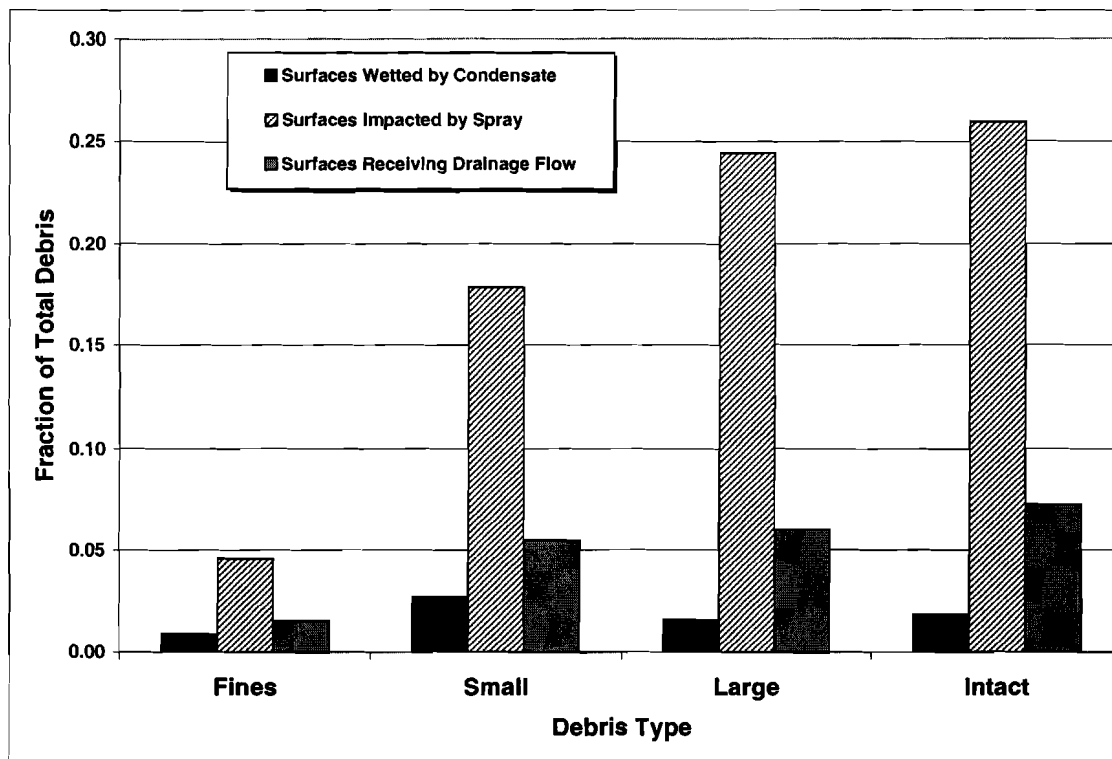


Figure IX-12. Blowdown Debris Dispersion by Surface Orientation.



**Figure IX-13. Blowdown Debris Dispersion by Surface Wetting.**

In Figure IX-12, all of the LOCA-generated debris is distributed fractionally according to surface orientation (floor surfaces or other surfaces), whether the debris was captured within the break region (SGs 1 and 4), and debris type. This distribution reflects the debris-generation size distribution of Table IX-2 and the break-region capture fractions of Table IX-11. For the fines and small-piece debris, the largest fractions corresponded to floor surfaces outside or beyond the break region; debris preferentially settled onto the floors. Most of the debris that was captured within the break region was located on other structures that correspond to equipment, piping, and gratings within those SG compartments. For the larger debris, the majority of the debris was trapped within the break region by the congestion of structures. Nearly half of this debris either was deposited onto the floor of the break region or was assumed to fall to the floor after the break flows subsided. Most large debris that was ejected from the break region was predicted to fall out onto floor surfaces; therefore, small amounts of large debris were found on other structures outside of the break region.

In Figure IX-13, all of the LOCA-generated debris is distributed fractionally according to the surface wetting condition (condensate, sprayed, or spray drainage) and by debris type. Only relatively small quantities of debris were predicted to reside at locations where the debris would not be washed downward by the CSs or by the spray drainage. Conservatively speaking, the sprays falling from the upper dome would wash a majority of the surfaces within the SG compartments, as well as all of the upper floor surfaces and the refueling pool areas.

Although there is a relatively high degree of uncertainty with these blowdown transport results, the trends generally make sense. Because so little debris is protected from the CSs, these trends indicate a relatively high transport of debris to the sump pool.

#### VI.4.1.2 Fibrous Washdown Debris Transport

The CSs and condensation of steam throughout the containment and subsequent drainage to the sump pool would entrain substantial debris that was deposited onto the various surfaces and would transport the debris to the sump pool. In addition, these processes would degrade the fibrous insulation debris to some extent further, thereby creating more of the very fine, readily transportable debris.

##### VI.4.1.2.1 Surface Retention of Deposited Debris

The fraction of debris that stays on a specific surface, as opposed to being washed away, is referred to as the retention fraction. The fraction transported from a specific surface would then be 1 minus the retention fraction. Estimates of the retention fractions were essentially engineering judgments that were based on experience with small-scale testing during the DDTS. These experiments did not examine specifically the flow requirement needed to remove a piece of debris from a specified type of surface. Most of these tests dealt with either debris generation or airborne debris transport. One set of tests examined the erosion that was associated with fibrous debris inundated by water flow. During the conduct of these tests, experience with the handling of the debris provided some understanding regarding the ease or difficulty of forcing a piece of debris to move. These findings are summarized in Table IX-15. The estimated transport and corresponding retention fractions are shown in Table IX-16 and Table IX-17, respectively.

Debris transport due to condensate drainage would be expected to affect only the smaller debris. As condensation builds on a surface, it forms a thin film that subsequently drains and typically forms small rivulets of flow. This flow usually would move around significantly sized pieces of debris. Individual fibers could be entrained in the flow, or the fiber simply could be pushed to the sides of the rivulets. Some fine and small-piece debris certainly would transport, but the quantities of small debris transporting were estimated to be a small portion of the total. The DDTS's central estimate (realistic yet conservative) assumed that 1% of small debris transported (the extreme upper bound was 10%) but no large debris. The DDTS did not separate fines from small pieces. For this estimate, increasing the 1% to 2% for small-piece debris and increasing the 1% to 5% for the fines increased the level of conservatism. The larger debris was assumed not to transport because of condensate runoff.

**Table IX-15. Fibrous-Debris Washdown Transport Trends**

Debris Type	Surfaces Wetted by Condensate	Surfaces Either Sprayed or Receiving Drainage Flow	
		Without Intervening Floor Drains	With Intervening Floor Drains
Fines	Minority Transport	Nearly Complete Transport	
Small Pieces	Minority Transport	Majority Transport	
Large Pieces	No Significant Transport	Medium Transport	No Significant Transport
Intact Pieces	No Significant Transport	Minority Transport	No Significant Transport

**Table IX-16. Estimated Fibrous-Debris Washdown Transport Percentages**

Debris Type	Surfaces Wetted by Condensate	Surfaces Either Sprayed or Receiving Drainage Flow	
		Without Intervening Floor Drains	With Intervening Floor Drains
Fines	5%	99%	
Small Pieces	2%	70%	
Large Pieces	0%	50%	0%
Intact Pieces	0%	20%	0%

**Table IX-17. Estimated Fibrous-Debris Washdown Retention Fractions**

Debris Type	Surfaces Wetted by Condensate	Surfaces Either Sprayed or Receiving Drainage Flow	
		Without Intervening Floor Drains	With Intervening Floor Drains
Fines	0.95	0.01	
Small Pieces	0.98	0.3	
Large Pieces	1	0.5	1
Intact Pieces	1	0.8	1

Whenever fine and small-piece debris would be subjected to the substantial flows of the impacting CSs or the subsequent drainage of the sprays, the flow likely would entrain nearly all of the fine debris and a majority of the small debris. Test experience indicates that the CSs would wash fines from surfaces easily and carry those fines with the drainage to the sump pool. However, some of this fine debris would be pushed into relatively protected spots, corners, crevices, etc., where the debris would remain. Surfaces that were impacted directly by sprays and drained surfaces were grouped together for washdown transport because of the lack of information that was required to treat these two surface types differently. It was assumed that 99% of the fines would be transported from surfaces that were impacted by the sprays or drainage and that the other 1% experienced something less than total transport.

CSs also would wash substantial small-piece debris off structures, walls, and floors. The DDTS's central estimate was 50% (realistic yet conservative), with an extreme upper bound of 100%. Substantial quantities of debris likely would become trapped at locations that were protected from full spray flow due to the complex arrangements of containment equipment, piping, etc. It was assumed that 70% of the small debris would transport from surfaces that were impacted directly either by the CSs or by the subsequent drainage. This assumption adds additional conservatism to the DDTS's central estimate without becoming excessively conservative.

The 70% estimate was supported further by a simple floor-water drainage calculation, in which a uniform spray was applied to a floor area at a rate of flow corresponding to the containment-dome spray Trains A and B. A floor-area estimate indicates that ~800 ft<sup>2</sup> would be drained by

each floor drain. A plant calculation estimated that the floor-water hold-up depth would be ~1.5 in. The separate-effect characterization of debris transport in water tests [NUREG/CR-6772, 2002] shows that a turbulent flow velocity as low as ~0.06 ft/s can cause a small piece of debris to tumble or slide along the floor. If circular drainage geometry is assumed, the transport estimate indicates that 30% to 40% of the floor area would not have sufficient flow velocity to transport small-piece debris. This calculation did not consider the effect of structures on the transport, which would create locations for debris entrapment. Therefore, the 70% estimate is a reasonable number for small-debris transport by the CSs.

For the large and intact pieces of debris, the surfaces were split into two additional categories based on whether the transport of the debris would encounter floor drain holes that would prevent further transport. A typical floor drain is ~6 1/2 in. in diameter and has a coarse grating that would stop any debris that is larger than ~3 in. square. A few floor drains have a relatively fine mesh screen over the hole. Floor surfaces are sloped to channel water to the drains. Large debris deposited onto the upper floors likely would have to pass through more than one of these floor drains to reach the sump. Large debris settling into the refueling pools would also have to pass through drains to reach the sump, some of which have a screen cover. The two largest of the refueling drains are nominal 6-in. drains without any cover or grating and are open during normal operation. Although a piece of large debris could pass through this 6-in. drain, the amount of debris would not be enough to treat these drains separately. It was assumed that these drains would stop further transport of large and intact debris.

Conversely, large and intact debris that is deposited at locations such as the SG compartments would not encounter any drain holes as the debris transports toward the sump pool. CSs would wash substantial quantities of large-piece debris off structures, walls, and floors. A portion of the large debris would be trapped on top of gratings and would not transport. Other large pieces would snag onto structures such that the sprays would not dislodge them. Substantial quantities of debris likely would become trapped at locations that are protected from full spray flow due to the complexities of containment equipment, piping, etc. Because large debris would transport less easily than small debris, it was assumed that 50% of the large debris was transported. The intact debris would be less likely to transport than the large-piece debris. Based on DDTs experience, the intact pieces of debris were significantly more likely to snag on structures than the large pieces, and substantial quantities of intact debris were likely to remain attached to the original piping. It was assumed that 20% of the intact debris would transport.

#### VI.4.1.2.2 Erosion of Debris by CSs

Experiments conducted in support of the DDTs analysis illustrated that insulation debris could be eroded further by the flow of water. Some debris erosion could occur because of the impact of the sprays and spray drainage flows, but the amount of erosion would not be great. The DDTs concluded that <1% of the fibrous debris eroded as a result of CS operation. Debris erosion caused by condensation and condensate flow was neglected. Debris containing insulation that is still in its cover would not be expected to erode further. The erosion of debris caused by the plummeting of the break flow into the sump pool is considered as part of the sump-pool transport analysis.

It was assumed that condensate drainage would not cause further erosion of fibrous debris and that intact or covered debris would not erode further. Erosion does not apply to fine debris because the debris is already fine. It was assumed that 1% of the small- and large-piece debris that was impacted directly by the sprays would erode. It was assumed that intact pieces of debris could not erode because its canvas cover would protect the fibrous materials.

### VI.4.1.3 Quantification of Fibrous-Debris Transport

The transport of fibrous debris was quantified using the models presented in Section VI.3 and the input presented in Section VI.4.1. The quantified transport results are presented in Table IX-18. The table shows the transport fractions for each size category, as well as the overall transport fraction. It also shows the fractions of the total ZOI insulation that entered the pool, which were normalized to provide a size distribution for the debris entering the pool. About 57% of the ZOI fibrous insulation was predicted to transport to the sump pool, and nearly half of that would be the relatively transportable sizes. The transport fraction for the fines includes the erosion products from the predicted erosion of the small and large pieces of debris. The quantity of erosion products was approximately equal to 6% of the original generated fines.

**Table IX-18. Fibrous-Debris-Transport Results**

<b>Debris Size Category</b>	<b>Category Generation Fraction</b>	<b>Size Category Transport Fraction</b>	<b>Fraction of ZOI Insulation</b>	<b>Distribution Entering Sump Pool</b>
Fines	0.07	0.93	0.07	0.12
Small Pieces	0.26	0.66	0.17	0.30
Large Pieces	0.32	0.54	0.17	0.30
Intact Pieces	0.35	0.46	0.16	0.28
All Debris	1.00	0.57	0.57	1.00

### VI.4.2 RMI Debris Transport

Roughly 85.7% of the insulation in the volunteer-plant containment is RMI. The debris-transport methodology discussed in Section VI.3 applies to RMI debris, as well as fibrous debris. Unfortunately, unlike the fibrous insulation, very little useful airborne transport data for RMI debris exist. Specifically, the capture fractions for the capture of RMI debris passing through structures such as gratings and of RMI debris inertially impacting surfaces have not been measured. Only secondary experience associated with RMI debris-generation experiments is applicable in this study. For RMI debris washdown, the pool transport velocities are available. Small-scale experiments suggest that RMI debris transports less easily than would the fibrous debris, primarily because the RMI debris is heavier. In addition, it would take substantially more RMI debris on the sump screen to block flow effectively through the screen than it would fibrous debris.

#### VI.4.2.1 RMI Blowdown Debris Transport

The capture fractions for RMI debris are likely much different from the corresponding fractions for fibrous debris. For fibrous debris, the capture fractions were very dependent on surface wetting; when the surfaces were dry, debris capture was minimal. For RMI, surface wetting may not be important. For instance, it seems likely that the capture of RMI on a grating depends on the foil folding over a bar in such a manner that it remains in place. Capture may depend on the debris remaining stuck on a structure. The amount of RMI debris that was captured by a grating could be significantly less than the amount of fibrous insulation; conversely, it could be substantially greater. Furthermore, the ability of flows to transport large cassette-like RMI debris

is not known. Therefore, application of the Section VI.3 methodology required very conservative assumptions to compensate for the nearly complete lack of data.

#### VI.4.2.1.1 Break-Region Blowdown Debris Transport

It is conservative to overestimate the retention of debris within the SG compartments because subsequent debris washdown is more likely if the debris were in the SGs as opposed to being dispersed throughout the containment. Because the capture rates for RMI debris passing through a grating have not been determined, it was conservatively assumed that 100% of all RMI debris impacting a grating was stopped by that grating from further forward transport. Debris stopped on the underside of a grating likely could fall back once depressurization flows subside. Because the gratings do not extend completely across the SG compartments, substantial debris still could be propelled upward into the containment dome.

Likewise, the inertial capture of RMI debris by miscellaneous structures—such as pipes, beams, or vessels—or by inertial impaction whenever the flow makes a sharp bend—has not been determined. For instance, it would seem less likely that a piece of RMI debris would stick to a wall than would a small piece of fibrous debris. The fibrous-debris capture fractions for miscellaneous structures and sharp bends were applied to the RMI debris to conservatively overpredict the retention of RMI debris within the SG compartments. Applying these assumptions to the logic charts, which are similar to Figure IX-7, results in the conservative SG capture fractions shown in Table IX-19. The values for 2- to 6-in. and the larger-than-6-in. debris categories in Table IX-19 correspond to the values for the fibrous large- and intact-category values (shown in Table IX-11): a result of similar assumptions. The assumption that the gratings capture all of the RMI debris, even the smallest pieces, predicts substantially more RMI retention within the SG compartments than likely would occur in reality. The predicted over-conservative retention was necessitated by the lack of RMI transport data.

**Table IX-19. Fractional Distribution of Debris Captured and Exiting Break Region**

Location	RMI Debris Category		
	<2-in. Pieces	2- to 6-in. Pieces	>6-in. Pieces
Captured within SGs 1 and 4	0.64	0.70	0.82
Expelled to Dome	0.32	0.26	0.17
Expelled to Level 832	0.01	0	0
Expelled to Level 808	0.03	0.04	0.01

#### VI.4.2.1.2 Dispersion Throughout the Remainder of Containment

The 24-region subdivision of the containment free volume that was used in the fibrous-debris-transport estimate (Table IX-12) also was used for the RMI debris-transport estimate. The volume weighting factors that were estimated for fibrous-debris transport (Table IX-13) also were applied to the RMI debris because no rationale was found to weight the distributions otherwise. For RMI debris, no fine debris was postulated (i.e., even the smaller pieces of RMI debris should sink readily in water, as opposed to fibrous fines, which tend to remain in suspension). The predicted dispersion of RMI debris was judged to place more debris into

locations where it subsequently would be predicted to transport with the CS drainage to the sump pool. The results of the blowdown dispersion by groups of volume regions are illustrated in Figure IX-14. As modeled, a majority of the debris was retained in the break region (SGs 1 and 4). In reality, it is likely that much more of the smaller debris would be blown free of the break region and into the upper dome region, where subsequent washdown to the sump pool would be substantially less than it would be if the debris were kept within the break region. However, the lack of RMI debris-transport data necessitated the conservative assumptions leading to these results.

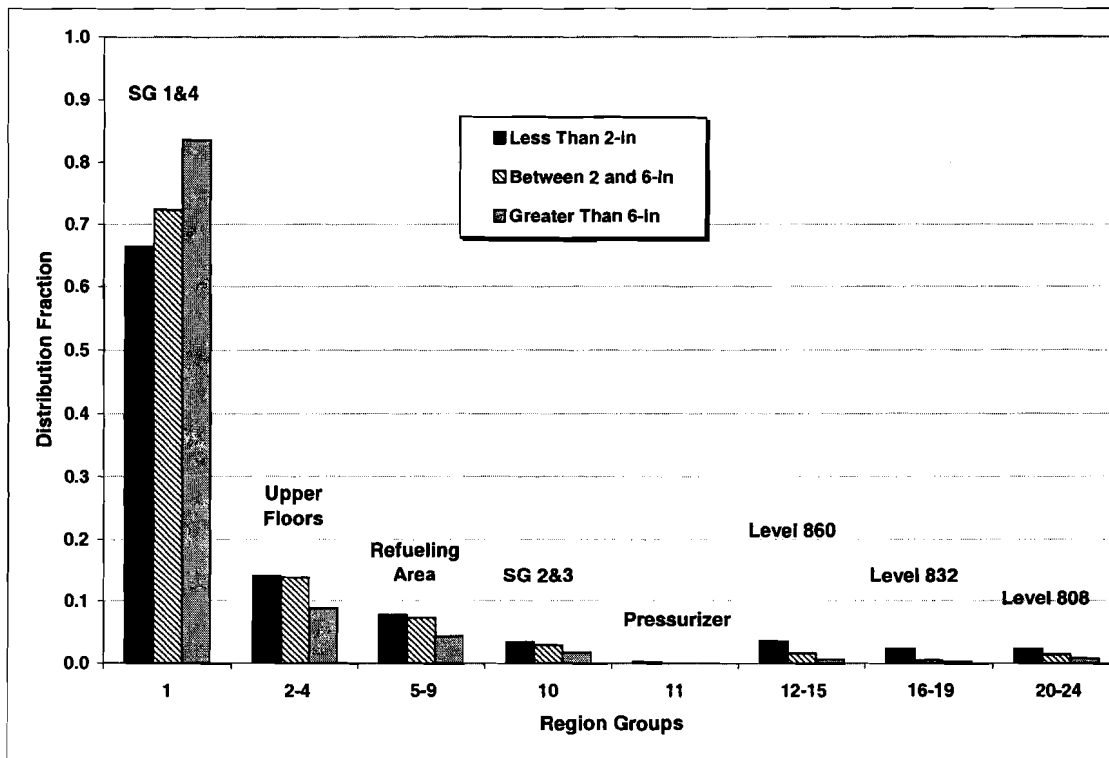


Figure IX-14. RMI Blowdown Distribution by Region Groups.

#### VI.4.2.1.3 Dispersion by Surface Orientation and Surface Wetness

A review of photos that were taken of RMI debris following RMI debris-generation tests indicates that RMI debris would reside preferentially on the floor surfaces [NEDO-32686, 1996, LA-UR-01-1595, 2001], although some RMI debris was caught on structures. However, the structures in these debris-generation tests were dry; therefore, it is not known if surface wetness would cause RMI to stick to wetted surfaces. Still, it is conservative to place the debris on the floors, where the subsequent washdown would be more effective. Therefore, the various surface-area-weighting factors were set to place most of the RMI debris on the volume region floors. It was assumed that 99% of the RMI debris would reside on the floor. The surface-area fractions shown in Table IX-14 apply to RMI debris as well as to fibrous debris. In these assumptions, ~99% of the RMI debris following blowdown was located where it either was impacted directly by the sprays or was located in the path of the spray drainage, leaving only 1% on surfaces that were wetted by condensation only.

#### VI.4.2.2 RMI Washdown Debris Transport

The RMI debris surface-retention fractions (i.e., the fraction that was not washed away) were estimated based primarily on engineering judgments and RMI pool debris-transport data. Small-scale testing of the transport of RMI debris in a pool of water demonstrated the ease or difficulty of forcing a piece of debris to move in a pool of water. Debris transport in a flowing layer of water that resides on a floor is similar to the transport of the debris in an established pool of water. Perceptions regarding the transport of RMI debris in nonpool situations are summarized in Table IX-20. The estimated transport and corresponding retention fractions are shown in Table IX-21 and Table IX-22, respectively.

**Table IX-20. RMI-Debris-Washdown Transport Trends**

Debris Type	Surfaces Wetted by Condensate	Surfaces Either Sprayed or Receiving Drainage Flow	
		Without Intervening Floor Drains	With Intervening Floor Drains
<2 in.	Minority Transport	Medium Transport	
2 to 6 in.	No Significant Transport	Medium Transport	No Significant Transport
>6 in.	No Significant Transport	Minority Transport	No Significant Transport

**Table IX-21. Estimated RMI-Debris-Washdown Transport Percentages**

Debris Type	Surfaces Wetted by Condensate	Surfaces Either Sprayed or Receiving Drainage Flow	
		Without Intervening Floor Drains	With Intervening Floor Drains
<2 in.	1%	40%	
2 to 6 in.	0%	30%	0%
>6 in.	0%	10%	0%

**Table IX-22. Estimated RMI-Debris-Washdown Retention Percentages**

Debris Type	Surfaces Wetted by Condensate	Surfaces Either Sprayed or Receiving Drainage Flow	
		Without Intervening Floor Drains	With Intervening Floor Drains
<2 in.	99%	60%	
2 to 6 in.	1%	70%	1%
>6 in.	1%	90%	1%

All debris that was deposited onto the SG compartment floors and the sump-level floors automatically was assumed to have entered the sump pool; this assumption was not indicated in the tables. This assumption primarily affected the debris that was deposited onto the break-region floor during either blowdown or washdown. The actual movement of this debris from the SG compartment floor into the outer annulus would be driven by the falling and spreading break flow; this would generally be expected to be a relatively high level of transport.

Debris transport resulting from condensate drainage would be expected to affect only the smaller debris. As condensation builds on a surface, it forms a thin film that subsequently drains and typically forms small rivulets of flow. This flow usually would not move around significantly sized pieces of debris. Significant transport of RMI debris does not seem likely; however, it is possible that some of the smaller debris could move with the condensate flow until the condensate flow linked up with more substantial water drainage. It was assumed that 1% of the debris that was <2 in. and subjected only to condensate drainage ultimately would transport to the sump pool. Furthermore, it was assumed that none of the debris that was >2 in. would transport to the sump pool.

Whenever pieces of debris <2 in. were subjected to substantial flows from impacting the CSs or from the subsequent drainage of the sprays, the flow likely would entrain a substantial portion of that debris. The evaluation of the transport of the smaller RMI debris that was exposed to sprays and/or spray drainage was based on a floor-pool drain velocity estimate and on the pool debris-transport threshold velocities. The drainage-flow velocity calculation assumed that a uniform spray was applied to an upper-level floor area corresponding to the containment-dome spray Trains A and B. A floor-area estimate indicated that ~800 ft<sup>2</sup> of floor area would be drained by each floor drain. A plant calculation estimated that the floor-water hold-up depth would be ~1.5 in. The separate-effect characterization of debris transport in water tests [NUREG/CR-6772, 2002] showed that a turbulent flow velocity of ~0.2 ft/s would be required to cause small stainless-steel RMI debris to tumble or slide along the floor. If it is assumed that circular drainage geometry exists, the transport estimate indicates that 60% to 80% of the floor area would not have sufficient flow velocity to transport small stainless-steel RMI debris, depending on the assumed thickness of the water layer. This conclusion resulted in the 40% transport estimate shown in Table IX-21. Because this calculation did not consider the effect of structures on the transport, which would create locations for debris entrapment, the 40% transport estimate is a reasonable number for the transport of RMI debris that is <2 in. by the CSs.

As was done for fibrous debris, pieces of RMI debris that were >2 in. were assumed not to pass through floor drains or refueling-pool drains. At locations where the larger debris would not encounter floor or refueling drains, 30% of the 2- to 6-in. debris and 10% of the >6-in. debris were assumed to transport. The corresponding fibrous-debris-transport number simply was reduced based on engineering judgment to account for the fact the RMI debris transports less easily than does fibrous debris. In any case, these two estimates affected only a relatively minor portion of the total debris.

Debris erosion of any significance would not happen to stainless-steel RMI debris; therefore, no erosion of the RMI debris by the CSs was considered in this study.

### VI.4.2.3 Quantification of RMI Debris Transport

The transport of fibrous debris was quantified using the models presented in Section VI.3 and the input presented in Section VI.4.2. The quantified transport results are presented in Table IX-23. The table shows the transport fractions for each size category, as well as the overall transport fraction. It also shows the fractions of the total ZOI insulation that entered the pool. These fractions then were normalized to provide a size distribution for the debris entering the pool. Approximately 83% of the ZOI RMI was predicted to transport to the sump pool, but only ~20% of that amount was pieces <2 in.

**Table IX-23. Fractional RMI Debris-Transport Results**

<b>Debris-Size Category</b>	<b>Category Generation Fraction</b>	<b>Size Category Transport Fraction</b>	<b>Fraction of ZOI Insulation</b>	<b>Distribution Entering Sump Pool</b>
<2 in.	0.21	0.82	0.17	0.21
2 to 6 in.	0.12	0.76	0.09	0.11
>6 in.	0.67	0.85	0.57	0.68
All Debris	1.00	0.83	0.83	1.00

### VI.4.3 Min-K Insulation Debris Transport

Less than 1% of the insulation in the volunteer-plant containment is Min-K insulation, a form of insulation referred to as microporous or particulate insulation. Although the transport methodology discussed in Section VI.3 also applies to Min-K insulation, a nearly complete lack of airborne transport data for this type of insulation exist, as well as debris-generation data, which were discussed in Section VI.3.2.3. Because of the lack of data for the generation of debris from Min-K insulation, the unknown erosion characteristics of this insulation, and the sparseness of the insulation within the containment (i.e., leads to a potential spatial nonuniform distribution), it was conservatively assumed that all Min-K located within the ZOI would be pulverized into a fine, highly transportable dust. If larger pieces of Min-K debris were inundated by the CSs, these pieces simply could dissolve into fine silt and transport with the spray drainage; however, this outcome is yet to be proven. Although <1% of the containment insulation is Min-K, this type of particulate debris could affect the sump-screen head losses significantly.

A conservative transport fraction for Min-K dust must be relatively high, and it seems likely that this fraction would be similar to the fraction for the transport of fibrous fines without the addition of erosion products, which was ~0.87. That is, the transport of fibrous fines generated from the ZOI to the sump pool was ~87%. (Note that the 93% value that was shown in Table IX-18 included erosion products.) Because the bulk of the 13% of fine fibers that did not transport was located on surfaces wetted only by condensate, it seems likely that a similar result would occur for the Min-K. For this study, it was assumed that 90% of the Min-K dust would transport to the sump pool.

## VI.5 BLOWDOWN/WASHDOWN CONCLUSION

A methodology was developed that considers both transport phenomenology and plant features and that divides the overall complex transport problem into many smaller problems that either are amenable to solution by combining experimental data with analysis or that can be judged conservatively based on the foundation of debris-transport knowledge. The quantification of the methodology results in predicted transport fractions that are both conservative and plausible. The overall transport results are shown in Table IX-24. These transport fractions represent the fractions of the insulation by type that was initially located within the ZOI and that subsequently would transport to the sump pool. Detailed results, including size distribution information, are discussed in Sections VI.3 and VI.4.

**Table IX-24. Overall Transport Results**

<b>Insulation Type</b>	<b>Overall Transport Fraction*</b>	<b>Debris-Size Distribution</b>
Fibrous	57%	Table IX-18
RMI	83%	Table IX-23
Min-K	90%	All Dust

\* Overall percentages are for demonstration only.

The overall transport fractions listed in Table IX-24 serve for demonstration purposes but are not valid for plant-specific evaluations because these fractions were calculated using LOCA-generated debris-size distributions that did not account properly for PWR jet characteristics. BWR jet characteristics were substituted for PWR jet characteristics because the PWR jet analyses had not been performed yet. When the PWR jet characteristics become available, it will be a simple matter to recalculate the overall transport fractions using PWR LOCA-generated debris-size characteristics.

**Neither the debris-size distributions nor the overall transport fractions in this report are valid for plant-specific evaluations.**

The transport fractions for each debris-size category are considered to be conservative for the LDFG insulation in the volunteer plant (but not necessarily for containments of other design). The fibrous-debris-transport analysis contained herein was based on LDFG insulation and may require adjusting for any high-density fiberglass insulation or mineral wool that may also be in the plant.

For the volunteer plant, a high percentage of the fine LOCA-generated debris most likely would transport to the sump pool via the spray drainage flows. The transport fractions tended to decrease as the debris size increased. A majority of the larger debris that was predicted to transport to the sump pool was stopped in the SG compartments that were associated with the break, where subsequent CS drainage was assumed to be readily capable of moving the debris downward to the pool.

The transport of the RMI and Min-K debris was skewed more conservatively toward larger transport fractions than was the fibrous debris because of the lack of transport data. Realistically speaking, the RMI might be expected to transport less readily than would the fibrous debris because it is heavier. However, a larger fraction of the RMI debris could be trapped in the break region (SG compartments), where it could be transported subsequently into the sump pool and thus the need to skew the transport fractions conservatively. A similar discussion applies to the Min-K because of the lack of LOCA debris-generation data, lack of erosion data, and the potential nonuniform placement of Min-K in the ZOI. Therefore, most of the Min-K must be conservatively assumed to transport to the sump pool as a fine dust or silt.

Conservative engineering judgments were made in this analysis at various steps along the way. The degree of conservatism that was associated with these judgments was intended to ensure conservative final results without straying too far from realistic behavior. The judgments were not intended to be upper bounding. For example, the erosion of LDFG by CSs was assessed in the DDTs as being <1%. In reality, the erosion may be significantly <1%. The 1% value was assumed to be conservative but not far from reality. In addition, many conservative judgments tend to compound as the analysis progresses.

The analyses herein considered only one break location (SG1), although they considered a range of break sizes at that location. Plant-specific analyses must consider a range of break locations. For the volunteer plant, LOCAs can occur within an SG compartment, which is likely the most probable location. A break in the same SG but at a different level likely would have a result similar to the one analyzed because most of the break effluent still would flow to the containment dome. A break in an SG compartment different from SG1 most likely would have a similar result, except that the debris would tend to enter the sump pool at different locations. A break outside the SG compartments, such as in a main steam line, would behave differently than a break inside an SG compartment and probably should be analyzed separately. A break in the pressurizer certainly would be different because that compartment does not vent directly to the containment dome as with the SG compartments (i.e., no major upper openings exist). Therefore, a larger fraction of the debris might be driven out of the pressurizer compartment directly into the sump area, but the total quantity of debris might be substantially less than a primary-loop piping break. Neither a pressurizer-line break nor a main steam-line break was analyzed herein.

In performing blowdown/washdown analyses, it is important that

- the debris-size categories match the characteristics of the debris-transport behavior;
- the break region is analyzed in substantial detail because so much of the debris capture is likely to occur in this region;
- the debris capture along the primary exits from the break region also should be analyzed in substantial detail;
- CS drainage patterns should be determined to support the washdown analysis and to indicate where the debris would enter the sump pool and how the spray drainage would impact sump pool turbulence; and
- vulnerable spray-drainage pathways, where potential debris blockage might occur, should be identified.

## VI.6 REFERENCES

1. [NUREG/CR-6772, 2002] D. V. Rao, B. C. Letellier, A. K. Maji, and B. Marshall, "GSI-191: Separate-Effects Characterization of Debris Transport in Water," NUREG/CR-6772, LA-UR-01-6882, August 2002.
2. [NUREG/CR-6773, 2002] D. V. Rao, C. Shaffer, B. C. Letellier, A. K. Maji, and L. Bartlein, "GSI-191: Integrated Debris-Transport Tests in Water Using Simulated Containment Floor Geometries," NUREG/CR-6773, LA-UR-02-6786, December 2002.
3. [NUREG/CR-6762, Vol. 2, 2002] D. V. Rao, B. Letellier, K. W. Ross, L. Bartlein, and M. T. Leonard, "GSI-191 Technical Assessment: Summary and Analysis of US Pressurized Water Reactor Industry Survey Response and Responses to GL 97-04," Volume 2, LA-UR-01-1800, Los Alamos National Laboratory, August 2002.
4. [LA-UR-99-3371, 1999] B. E. Boyack, T. S. Andreychek, P. Griffith, F. E. Haskin, and J. Tills, "PWR Debris Transport in Dry Ambient Containments—Phenomena Identification and Ranking Tables (PIRTs)," LA-UR-99-3371, Revision 2, December 14, 1999.
5. [LA-UR-01-1595, 2001] D. V. Rao, Clinton J. Shaffer, and Robert Elliott, "BWR ECCS Strainer Blockage Issue: Summary of Research and Resolution Actions," prepared for the US Nuclear Regulatory Commission, Los Alamos National Laboratory, LA-UR-01-1595, March 21, 2001.
6. [NUREG/CR-6369-1, 1999] D. V. Rao, C. Shaffer, and E. Haskin, "Drywell Debris Transport Study," NUREG/CR-6369, Volume 1, SEA97-3501-A:14, September 1999.
7. [NUREG/CR-6369-2, 1999] D. V. Rao, C. Shaffer, B. Carpenter, D. Cremer, J. Brideau, G. Hecker, M. Padmanabhan, and P. Stacey, "Drywell Debris Transport Study: Experimental Work," NUREG/CR-6369, Volume 2, SEA97-3501-A:15, September 1999.
8. [NUREG/CR-6369-3, 1999] C. Shaffer, D. V. Rao, and J. Brideau, "Drywell Debris Transport Study: Computational Work," NUREG/CR-6369, Volume 3, SEA97-3501-A:17, September 1999.
9. [NUREG/CR-6808, 2003] C. J. Shaffer, D. V. Rao, M. T. Leonard, and K. W. Ross, "Knowledge Base for the Effect of Debris on Pressurized Water Reactor Emergency Core Cooling Sump Performance," NUREG/CR-6808, LA-UR-03-0880, February 2003.
10. [NEDO-32686, 1996], "Utility Resolution Guidance for ECCS Suction Strainer Blockage," BWROG, NEDO-32686, Rev. 0, November 1996.
11. [NRC-SER-URG, 1998], "Safety Evaluation by the Office of Nuclear Reactor Regulation Related to NRC Bulletin 96-03 Boiling Water Reactor Owners Group Topical Report NEDO-32686, 'Utility Resolution Guidance for ECCS Suction Strainer Blockage,'" Docket No. PROJ0691, August 20, 1998.
12. [OPG, 2001] John Russell, "Jet Impact Tests—Preliminary Results and Their Application," N-REP-34320-10000, Revision R00, April 18, 2001.

13. [NUREG/CR-6762, Vol. 3, 2002] D. V. Rao, C. J. Shaffer, and S. G. Ashbaugh, "GSI-191 Technical Assessment: Development of Debris-Generation Quantities in Support of the Parametric Evaluation," LA-UR-01-6640, Los Alamos National Laboratory, August 2002.
14. [NUREG/CR-6762, Vol. 1, 2002] D. V. Rao, B. C. Letellier, C. Shaffer, S. Ashbaugh, and L. S. Bertlein, "GSI-191 Technical Assessment: Parametric Evaluations for Pressurized Water Reactor Recirculation Sump Performance," LA-UR-01-4083, Los Alamos National Laboratory, August 2002.
15. [SEA-95-970-01-A:2, 1996] Gilbert Zigler et al., "Experimental Investigation of Head Loss and Sedimentation Characteristics of Reflective Metallic Insulation Debris," draft letter report, prepared for the US Nuclear Regulatory Commission, SEA No. 95-970-01-A:2, May 1996.

**Attachment 1 to APPENDIX VI:**

**VOLUNTEER-PLANT SPRAY-WATER DRAINAGE ANALYSIS**

**INTRODUCTION** numbered headings throughout attachment?

A postulated LOCA in the volunteer plant would distribute insulation debris throughout the containment, whereby the subsequent drainage of spray water following the LOCA would transport portions of this insulation debris toward the recirculation sump screens. A best estimate of how the water would drain to the sump was performed to support subsequent debris-transport calculations. The analysis will help to identify spaces and surfaces where insulation debris likely would not be washed away by sprays or drainage flow (e.g., an area that was not impacted by sprays and has too little drainage flow to transport debris). The analysis will help to determine how the drainage water enters the sump pool, which in turn will affect debris transport within that pool.

**SYSTEM DESCRIPTIONS**

The CS systems in the volunteer plant consist of two independent trains (Trains A and B), with headers located in four containment regions. Spray nozzles are located in one of four regions of the containment:

- Region A—Containment dome spraying down toward Level 905;
- Region B—Below Level 905 spraying Level 860;
- Region C—Below Level 860 spraying Level 832; and
- Region D—Below Level 832 spraying Level 808.

The specifications are shown in Table 1 consistently number by section? e.g., VI-1?for both trains in Unit 1, combined. Spray Train B has one more nozzle in the dome than Train A; therefore, the flows that are associated with single train operations constitute essentially half of the flows shown for both trains. Unit 1 has seven more nozzles than Unit 2. The drainage estimate performed for Unit 1 is applicable also to Unit 2.

**Table 1. Unit 1 Spray Nozzle Summary**

<b>Spray Region</b>	<b>Number of Nozzles</b>	<b>Nozzle Flow (gpm)</b>	<b>Region Flow (gpm)</b>
A	545	20	10,900
B	134	20	2680
C	28	20	560
D	54	20	1080
Total	761	20	15,220

The containment was designed to drain the spray water down to the containment recirculation sumps. Furthermore, the containment apparently was designed to minimize water holdup, thereby maximizing the depth of the sump pool. Several features of the containment determine the primary drainage pathways in the containment. These features include the following.

Floor Drains—A primary means of draining spray water is the floor drains that drain water from one floor directly down to the next floor. A typical drain, which is ~6 1/2 in. in diameter, is shown in Figure 1. **consistently number by section? e.g., VI-1?**At the top of this figure, another type of drain is shown that drains directly to the containment sump. Floor surfaces are sloped to channel water into the drains.

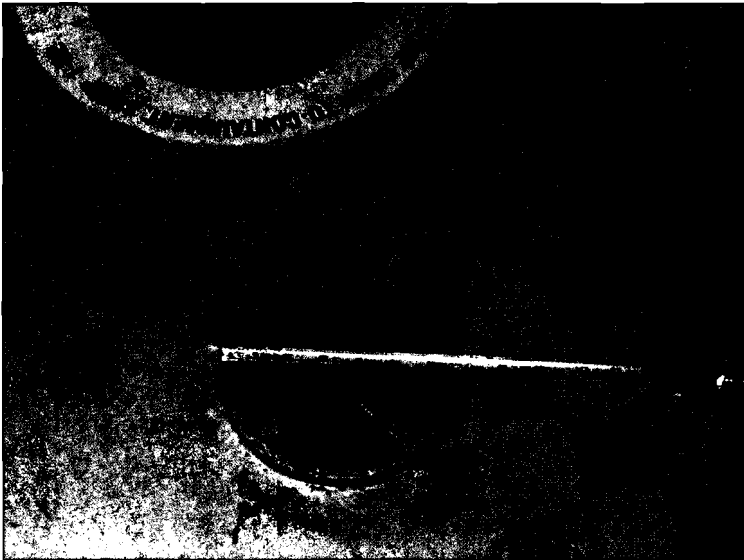


**Figure 1. Typical Floor Drain.**

Water Barriers—Water drainage is controlled by water barriers (curbs)—both concrete and metallic types—that are placed around floor-area perimeters to prevent water from draining from those perimeters. However, these barriers do not cover the entire perimeter of a floor. Gaps exist in the barriers at locations such as the areas around walkways and ladders. In many places, water can flow from a floor perimeter onto another floor, into the gap between the internal structures and the outer wall, into an SG compartment, into a stairwell, etc. A typical curb is shown in Figure 2. Figure 3 shows another curb next to an SG compartment that illustrates a discontinuity in a curb.

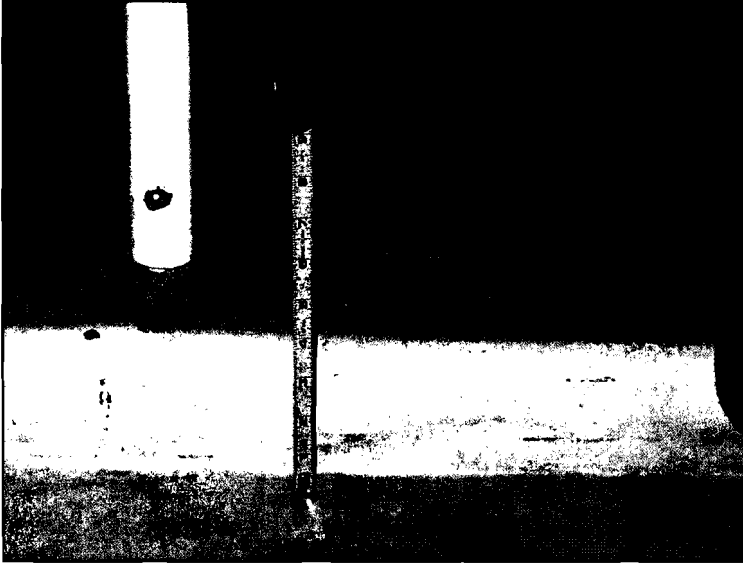


**Figure 2. Typical Concrete Curb.**



**Figure 3. Gap in Concrete Curb Surrounding an SG Compartment.**

Refueling Pool Drains—A substantial portion of the dome sprays will fall into the refueling cavity and accumulate in the three pool areas of the cavity. During normal operation, the pool drains are open, allowing spray water to drain down to the sump. The pool drains consist of 4-in. and 6-in. sizes. Figure 4 shows the drains in the pool that are used to store the reactor vessel lower internals during refueling. A 4-in. drain with a cover screen (with holes ~1/4 to 1/2 in. in diameter) is shown near the center of the photo. Two 6-in. drains also are shown in the upper-right (cover off) and lower-right corners (cover in place). These 6-in. drains are closed off with blind flanges during refueling and are uncovered during normal operations. The 4-in. drains drain down into the labyrinth of rooms on Level 808, which is located directly below the refueling pools. The two 6-in. drains drain to SGs 3 and 4. The pool that is used to store and transfer fuel is drained to Level 808 by a single 4-in. drain. The pool that is used to store reactor vessel

upper internals during refueling has a single 4-in. drain, which drains into the pool that stores the lower internals.



**Figure 4. Refueling Pool Drains.**

Floor Gratings—Water drainage between floors also occurs through the floor gratings that cover several open areas in the floors (e.g., the equipment-transfer floor hatches).

Stairwells—At several staircases, water can drain from one floor to the next. Two primary staircases extend all the way from sump Level 808 up to the top floor at Level 905.

#### **APPROACH number as heading?**

A review of containment drawings and plant documents led to many general observations.\*

- Little, if any, water is expected to drain down the elevator shaft by way of the elevator doors. The elevator shaft was not treated as a wetted drain perimeter in the plant's minimum pool calculation, and the floors generally slope away from elevator. Furthermore, elevator doors may prevent water entry into the elevator shaft.
- The pressurizer compartment should remain essentially dry. A roof covers the compartment so that sprays do not enter this compartment. Drains and sloping floors generally prevent water flow into this compartment at other entrances.
- Water entering the SG compartments consists of dome-spray droplets falling directly into those compartments. Droplets falling onto the wall-tops and floor that are located between or near the SG compartments likely will flow into the SG compartments. Also, the two 6-in. refueling-pool drains flow directly into the SG compartments.

---

\*The most useful drawings were floor layouts that showed floor slopes, water barriers, and floor drains. The most useful document was a plant calculation of the minimum sump-pool height.

- Water entering the stairwells consists of spray droplets falling directly into stairwells and of some water overflowing a floor perimeter.
- Water entering the refueling cavity consists of spray droplets falling directly into the cavity. This water includes droplets that are falling onto walkways surrounding the refueling pool and that subsequently would flow into the pool.
- Water entering the gap between the inner containment structure and the containment outer wall consists of spray droplets impinging the outer containment wall and subsequently flowing down the liner and of water from gaps in the water barriers along the floor perimeters.
- Substantial quantities of water are intended to drain from one floor to the next by way of the floor drains between the floors.

Because of the complexity of the water drainage, many simplifying assumptions and engineering judgments were necessary. The primary assumptions include the following.

- All spray systems were active (only one possible spray scenario was evaluated).<sup>\*</sup>
- No blockage of drain flows by debris was postulated.<sup>†</sup>
- Dome spray droplets fall vertically and distribute uniformly across the containment cross section before encountering any containment structure. Distribution was based on cross-sectional areas.
- Crosswalks on Level 905 that are directly between the refueling cavity and the SG compartments drain into those compartments.<sup>‡</sup>
- Refueling cavity walkways on Level 860 drain into pools.
- Levels 873 and 851 do not have floor drains (floor drains not shown in drawing).
- Water draining onto Level 849 from Level 860 subsequently drains to Level 832.
- Water drains that drain directly to a containment sump (e.g., the one shown in the upper portion of Figure 1) are neglected. These specialized drains were not delineated in the drawings and are assumed to be substantially fewer in number than the main floor drains.

Engineering judgments were necessary where insufficient data were available to estimate drainage accurately.

The calculational approach included the following steps:

- the locations of all spray nozzles were identified;

---

<sup>\*</sup>The scenario where one train operates and one train is inactive can be estimated by dividing all flows for both trains by a factor of 2.

<sup>†</sup>Insulation debris could block a floor drain or a refueling pool drain.

- the dome spray impacting and running down the containment liner was estimated;
- the main floor areas on Levels 808, 832, 860, and 905 were nodalized into three sections for each floor;
- the locations where the spray droplets would settle were identified; and
- the drainage process was tracked from the uppermost surfaces down to Level 808.

The dome spray nozzles, arranged around four rings for each of the two trains, are aimed in four different directions. Some of the nozzles apparently are aimed to spray the dome liner. A portion of this spray impacting the liner subsequently should drain down the liner itself. The number of nozzles aimed in each of the four directions was tabulated for each ring. Then the spray impact and runoff was judged for each ring location. Of the 10,900-gpm total dome spray flow, 700 gpm was estimated to flow down the liner.

Figure 5 illustrates the subdivision of the main floors. Section 1 includes the side of the containment where the main steam and feedwater lines penetrate the containment. Drainage on this side would be distinctly different from the remainder of the containment. Section 2 includes unique features such as Level 849 and Level 832; sprays do not extend into this section. Section 3 includes the remainder of the floors.

To estimate the distribution of settled dome spray water, the containment cross-sectional area was estimated for each section of floor, refueling cavity, SG compartment, open area, etc. It was assumed that the spray droplets would fall uniformly onto these areas. Once the settled flows were determined, the drainage from floor to floor was estimated, starting with the uppermost floor surface. For each floor section, a drainage distribution was estimated, based on floor sloping relative to drainage pathways.

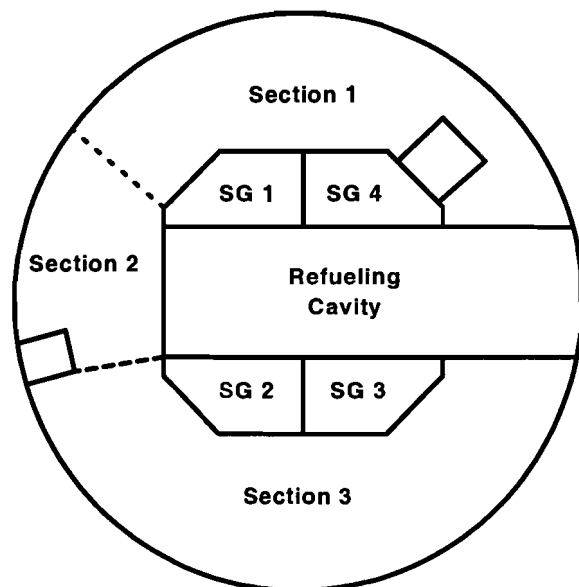


**Figure 5. Schematic of Floor Sections.**

The overall spray drainage is shown in Figure 6. The dashed lines represent spray droplets falling onto a surface\* (the arrow head indicates the surface receiving the droplets). The numbers indicate flow rates in gallons per minute. The solid lines indicate water draining from one surface to another or water falling into and through a stairwell or the outer wall gap. A diagram illustrating where the water enters the Level 808 sump pool is shown in Figure 7.

---

\* The surfaces are not drawn to scale.

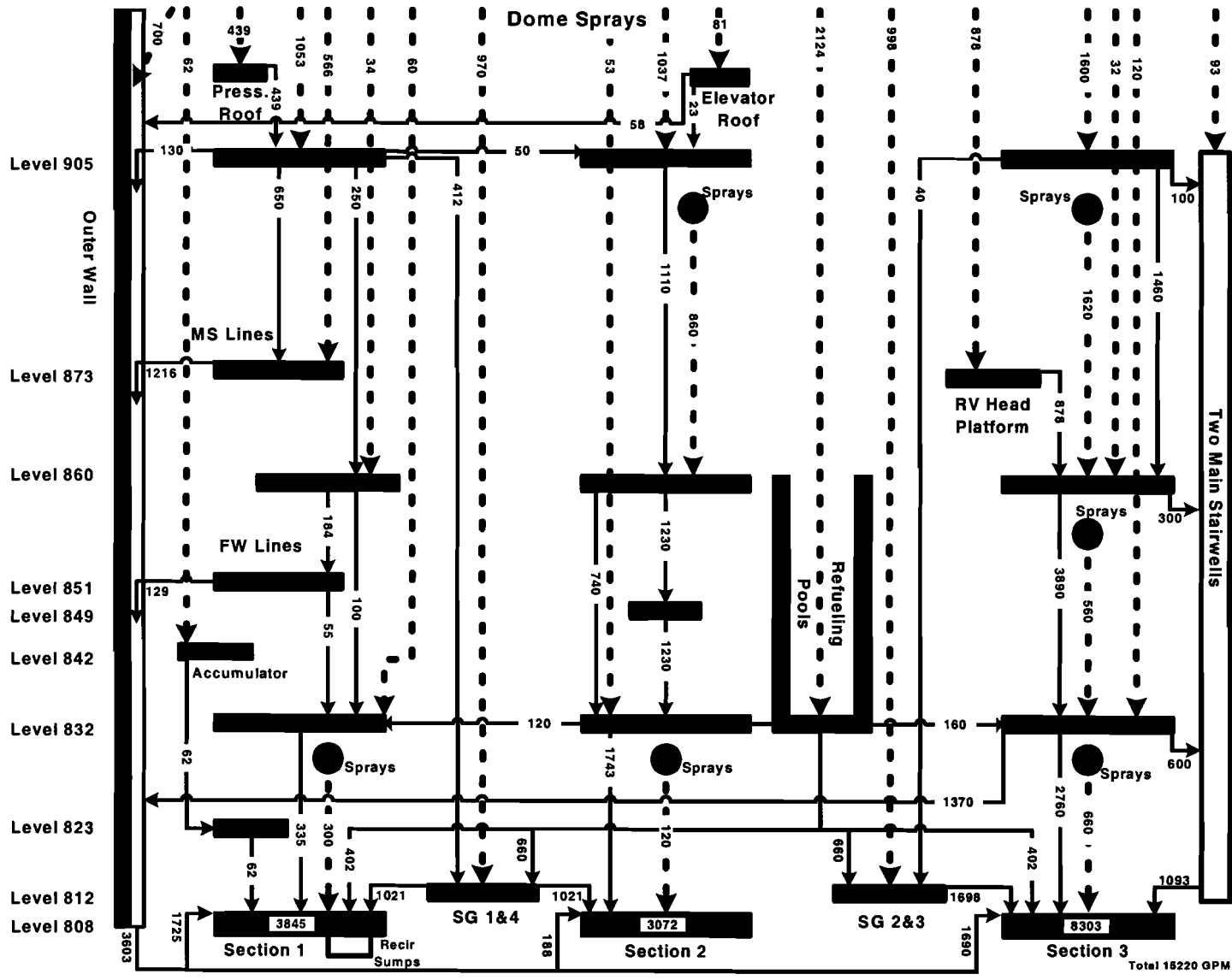


Figure 6. Spray-Water Drainage Schematic.

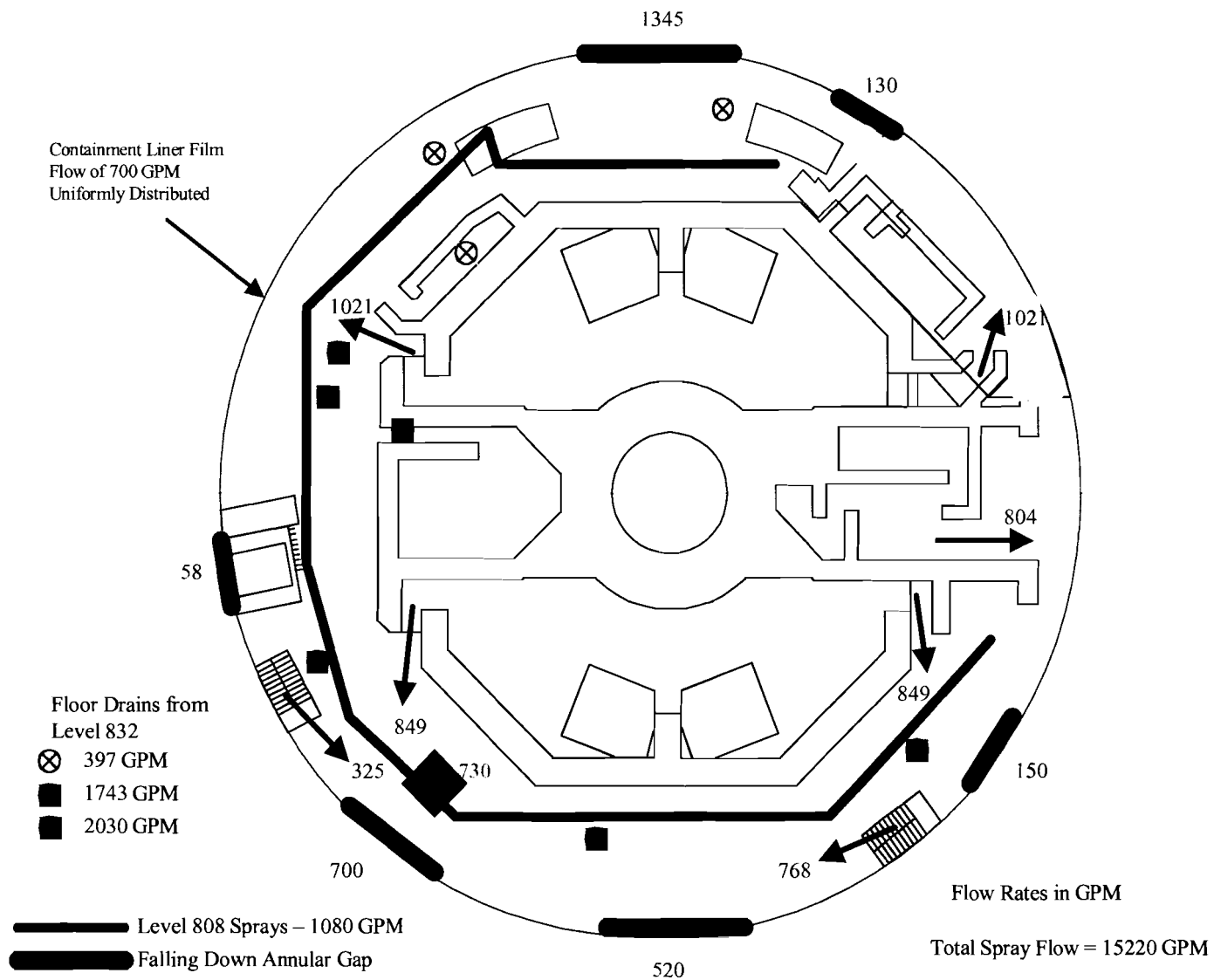


Figure 7. Spray-Water Drainage to Level 808 Sump Pool.



# Union of Concerned Scientists

Citizens and Scientists for Environmental Solutions

October 12, 2004

Dr. Mario V. Bonaca, Chairman  
Dr. Graham B. Wallis, Vice Chairman  
Advisory Committee on Reactor Safeguards  
United States Nuclear Regulatory Commission  
Washington, DC 20555-0001

EEB 23

**SUBJECT: TWO MISSING PIECES OF THE DIALOGUE ABOUT GSI-191,  
"ASSESSMENT OF DEBRIS ACCUMULATION ON PWR SUMP  
PERFORMANCE"**

Dear Chairmen Bonaca and Wallis:

As Chairmen of the Advisory Committee on Reactor Safeguards and its Subcommittee on Thermal Hydraulics, you have led a series of meetings where representatives of the Nuclear Regulatory Commission staff and industry discussed proposals to remedy Generic Safety Issue 191, "Assessment of Debris Accumulation on PWR Sump Performance." The June 22-23 Subcommittee and the October 7<sup>th</sup> full Committee meetings probed the matter in considerable detail and asked many questions that must be answered before this important issue is resolved.

We believe two topics have been omitted from the dialogue about the resolution of GSI-191. We do not feel the topics have been intentionally ignored by any party to the dialogue. We suspect that the enormity and complexity of the GSI-191 resolution consumes so much attention that these topics have been overlooked. But we feel both of these topics are so closely related to the GSI resolution that their inclusion in the dialogue can actually facilitate, rather than impede, progress towards resolution.

The first topic involves continued operation of PWRs until GSI-191 is resolved. Many of the questions posed by ACRS members about various aspects of the GSI-191 resolution plans also apply to the situation at the PWRs today. For example, the thin-bed effect and the validity of the assumption about homogeneous debris loading on the sump screens apply to the current designs as much as they do to the final design configuration. Issues such as these that question whether the proposed resolution path is adequate should be accompanied by questions whether the justification for continued operation remains adequate. Absent such questions, opportunities to supplement/revise/enhance interim compensatory measures may be lost. These questions also seem relevant when debating the pros and cons of acting upon the available knowledge base or waiting for additional research to fill in more of the gaps.

The second topic involves the correction to the containment sump screen problem at the Davis-Besse nuclear plant. Among the problems that FirstEnergy had to correct prior to obtaining NRC approval to restart Davis-Besse was the containment sump problem. Many of the questions still being debated – such as debris generation, debris transport, debris loading, and impact on net positive suction head – were answered by FirstEnergy last year. The NRC reviewed the answers, found them acceptable, and allowed Davis-Besse to restart. We are not suggesting that the Davis-Besse fix is a template that all other PWRs must follow, but it seems to us that there are lessons learned at Davis-Besse that can better inform the GSI-191 dialogue. Davis-Besse seems remembered only for what it did wrong, not for what it may have done right.

Washington Office: 1707 H Street NW Suite 600 • Washington DC 20006-3919 • 202-223-6133 • FAX: 202-223-6162  
Cambridge Headquarters: Two Brattle Street • Cambridge MA 02238-9105 • 617-547-5552 • FAX: 617-864-9405  
California Office: 2397 Shattuck Avenue Suite 107 • Berkeley CA 94704-3187 • FAX: 510-843-3785

**DO NOT REMOVE FROM ACRS OFFICE COPY**

GT-9990407

We hope these two topics will be explicitly included in the GSI-191 dialogue in the future. We feel their inclusion would constructively supplement the extensive dialogue to date.

Sincerely,

A handwritten signature in black ink, reading "David Lochbaum". The signature is written in a cursive style with a large, prominent "D" and "L".

David Lochbaum  
Nuclear Safety Engineer  
Washington Office

## APPENDIX VII: Characterization of PWR Latent Debris

The United States (US) Nuclear Regulatory Commission (NRC) has recently initiated a study conducted through Los Alamos National Laboratory (LANL) and the University of New Mexico (UNM) to characterize latent debris samples collected at five individual volunteer plants. The focus of this work is to study physical attributes of dust and dirt, such as particulate-to-fiber mass ratio, size distributions of particulate, material and bulk densities, and hydraulic parameters, including the specific surface area. Because of variations in plant collection methods and sampling schemes, it is not possible to make estimates of total latent-debris inventories. This appendix documents preliminary results of that study that are relevant to the supplementary guidance provided by the staff in Section 3.5 of the safety evaluation report (SER).

A total of five sets of samples were received at LANL for analysis, but only four were totally characterized. The fifth set was not characterized fully because it was dominated by paint chips generated from pressure washing and was therefore deemed to be unrepresentative of pressurized-water-reactor (PWR) containment debris. Material property data collected for the latent-debris samples establish the basis for preparation of a particulate-debris simulant that is suitable for large-scale head-loss testing at UNM. The objective of head-loss testing is to quantify the hydraulic properties of latent debris that are needed for the proper application of the NUREG/CR-6224 debris-bed head-loss correlation.

The experimental scope for sample characterization was as follows.

1. The debris was removed from its shipping container and transferred to plastic laboratory containers for gamma-spectrum counting.
2. The "fiber" and "particle" fractions were separated from the remaining (or "other") debris items by manual manipulation, sieving, and water rinsing.
3. Particulate size distributions were obtained by graduated sieving.
4. The weight of fine particles attached to swiping (masslin) need to correct throughout SER cloth or filter paper was determined by mass balance and comparisons of clean collection media to soiled collection media.
5. The fiber thickness/diameter was determined by scanning electron microscopy (SEM) and microphotographic statistics.
6. The material and bulk densities of fibers were estimated by mass measurement combined with volume estimates obtained from water displacement and direct measurement in graduated columns, respectively.
7. Particle surface area and density measurements were taken using state-of-the-art nitrogen adsorption techniques.
8. Scanning electron microscope/energy-dispersive spectroscopy (EDS) methods were used to characterize the chemical composition of representative particulate and fiber samples.

Figure VII-1 illustrates a typical variety of composition and proportion between particulate, fiber, and other larger pieces that are assumed to have minimal transport potential. All plants submitted multiple samples ranging from a few grams to several thousand grams that exhibited similar characteristics. For some plants, the samples had to be combined to obtain meaningful measurements; for others, each individual sample could be fully characterized.

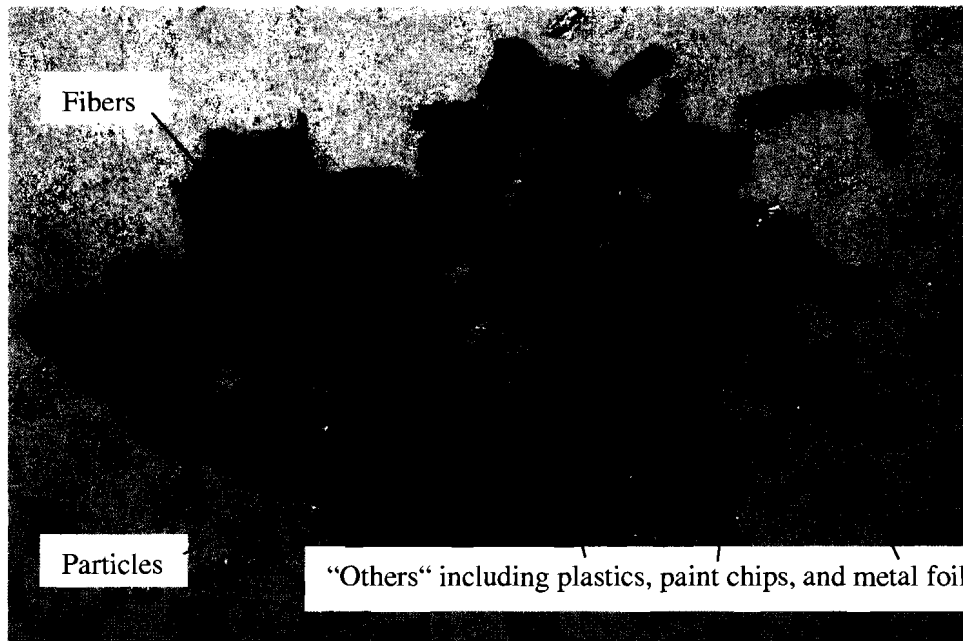


**Figure VII-1. Representative Latent-Debris Components from a Single Volunteer Plant.**

Objects larger than a 0.132-in.-mesh-size sieve were classified as a debris type “other” than particulate or fiber. This category of size, composition, and characteristics should be removed from any plant-specific samples that are collected before applying any mass fractions reported in this appendix. Larger latent debris types are not assumed to be transportable at recirculation pool velocities and so do not contribute to long-term increases in sump-screen head loss. However, any of this debris category that is present on the sump-pool floor may readily transport to the sump during pool fill-up. Table VII-1 presents the range of particulate and fiber mass fractions that were measured for samples that were characterized after the larger pieces were removed. From these data come the generic recommendation that 15% of the transportable latent debris be assumed to be fiber.

Each volunteer plant used a different collection method and sampling scheme. When separating particulates by wet sieving into fractions (>2 mm, 500  $\mu\text{m}$  to 2 mm, 75  $\mu\text{m}$  to 500  $\mu\text{m}$ , and <75  $\mu\text{m}$ ), it became apparent by comparing plants that scraping and bristle-brush collection were not effective at capturing the smaller particulate fractions. This conclusion was further reinforced by SEM photos of filter papers and cloth swipes that showed significant loadings of particles <10  $\mu\text{m}$  in diameter. High-efficiency particulate air (HEPA) filter vacuuming with the brush attachments or manual swiping with lint-free (masslin) cloth are recommended collection methods for characterizing plant-specific latent debris loadings.

**Table VII-1. Particulate and Fiber Mass Fractions for Volunteer Plants A–D**

Plant	Particle Weight	Fiber Weight	% Particle	% Fiber
A	5.42	1.04	84	16
B1	214	20	91	9
B2	369	64	85	15
B3	390	37	91	9
B4	592	47	93	7
B5	792	34	96	4
B6	122	50	71	29
B Total	2479	252	91	9
C	13.77	0.76	95	5
D1	2.51	0.47	84	16
D2	0.29	0	100	0
D3	12.45	0.28	97	3
D4	34.34	2.20	94	6
D6	5.56	0.1	98	2
D8	9.15	0.09	99	1
D10	11.98	0.74	94	6
D15	74.92	7.0	91	9
D Total	151.2	10.88	93	7

Sample Range	Total Particulate	71%–100%
	Total Fiber	0%–29%
Plant Range	Particulate	84%–95%
	Fiber	5%–16%

The material density of characterized fibers was found by water displacement measurements of 10 plant samples to range between 1.0 to 1.9 g/cm<sup>3</sup>. The mean value of 1.5 g/cm<sup>3</sup> is recommended for use if needed in generic latent-debris assessments. However, a more relevant parameter of fiber is the dry-bed bulk density that can be used to estimate the volume of fiber needed to form a 1/8-in.-thick thin bed across the wetted-screen area of a given sump configuration. This property and the suggested application is comparable to the use of the as-manufactured bulk density for fiberglass insulation.

The dry-bed density of latent fiber depends greatly on the amount of compaction applied for the measurement. Several alternatives were tried, but ultimately the staff recommends using the fiberglass density of 2.4 lbm/ft<sup>3</sup> = 38.4 kg/m<sup>3</sup> as a surrogate for dry latent debris. Similarly, fiberglass hydraulic properties should also be used as a surrogate for latent fiber. These recommendations are supported by the following rationale. First, in cases where fiberglass debris is present on the screen, minor inaccuracies in the latent fiber properties will not affect head-loss calculations. Second, where latent fiber is the dominant fibrous debris source and there is sufficient quantity to form a thin-bed filter, maximum head loss will be dominated by the properties of particulates captured on the fiber bed. Again, the difference between the actual hydraulic behavior of latent fiber and the presumed properties of fiberglass will not affect head-loss calculations adversely.

Particulate densities for each size fraction and volunteer plant were measured very accurately using the Brunauer-Emmett-Teller (BET) nitrogen adsorption method. Densities of particulates in the debris range from 2 to 4 g/cm<sup>3</sup> with only a few exceptions, and densities for most of the

samples range between 2.5 and 3.0 g/cm<sup>3</sup>, regardless of their particle size. These data form the basis of the recommendation for a nominal latent particulate density of 2.7 g/cm<sup>3</sup>.

A nominal size distribution of particulates found in the latent debris samples was used as a starting point to develop a formula for surrogate particulate debris that could be tested in a vertical-flow test loop at UNM. This apparatus permits measurement of pressure drop across a debris bed of known composition under a range of water velocities. Hydraulic parameters of the debris bed can then be inferred from differential pressure data by iteratively applying predictive correlations until the model results envelop a range of observed data. Material-specific parameter values, such as the specific surface area that are inferred in this manner, are only appropriate for use with the particular head-loss formula with which they were derived. In this case, the NUREG/CR-6224 head-loss correlation was applied. Microporous flow-resistance tests were performed on both the latent-debris samples and the surrogate formula to confirm that the surrogate could produce reasonably representative yet conservative hydraulic behavior.

Equivalent mass fractions of common sand and clay-based soil were used to recreate the size distribution of the latent particulate. Over a set of well-conditioned head-loss tests where the surrogate particulate was tested in combination with fiberglass insulation, the specific surface area of the surrogate was estimated to be 106,000 ft<sup>2</sup>/ft<sup>3</sup>. Analyses of these tests were complicated by penetration of the debris bed by extremely fine clay silt that continued to circulate in the test loop. Within the range of the tests where flow velocities at the screen are <0.2 ft/s (uncompressed fiber bed) and the estimated particulate-to-fiber mass ratios cannot exceed 3, the estimated particulate loading on a postulated debris bed can be reduced by 7.5% (one-quarter of the <75- $\mu$ m mass fraction) to accommodate realistic debris-bed penetration of latent fine particulates.

The surrogate debris formula was further refined by eliminating the latent-debris fraction with nominal dimensions >2 mm because the particles (sand grains) are not likely to transport at pool velocities <0.5 ft/s that may exist near the screen under recirculation conditions. This size fraction represents ~22% of the particulate mass on average that can be discounted from the particulate inventory that is available for long-term transport under recirculation. This size fraction may be subjected to high-velocity transport during fill-up, and so the fractional decrease was only recommended for latent-particulate inventories residing above the flood level.

GT9990405A

J.T.L



**DISTRIBUTED TO ACRS MEMBERS**

**DISTRIBUTED TO ACNW MEMBERS**

**POLICY ISSUE**  
**(Information)**

August 27, 2004

**RECEIVED** CY-04-0156  
**ACRS/ACNW**  
**US NRC**

SEP 01 2004

**FOR:** The Commissioners  
**FROM:** Luis A. Reyes  
Executive Director for Operations  
**SUBJECT:** SUMMARY OF ACTIVITIES RELATED TO GENERIC SAFETY ISSUES

PURPOSE:

To present the annual summary of activities related to Generic Safety Issues (GSIs).

BACKGROUND:

Since 1983, the staff of the U.S. Nuclear Regulatory Commission (NRC) has adhered to the practice of providing the Commission with an annual update of the progress made in resolving GSIs. The Commission reinforced this practice in a staff requirements memorandum (SRM) dated May 8, 1998, in response to SECY-98-030, "Implementation of [Direction-Setting Issue] DSI-22 Research," in which the Commission directed the staff to provide an annual summary of activities related to open reactor and non-reactor GSIs.

Management Directive (MD) 6.4, "Generic Issues Program," dated December 2001, delineates the NRC's program for addressing reactor and non-reactor generic issues. Specifically, the program described in MD 6.4 comprises seven stages, including (1) identification, (2) initial screening, (3) technical assessment, (4) regulation and guidance development, (5) regulation and guidance issuance, (6) implementation, and (7) verification. Candidate generic issues may be identified by organizations or individuals either within or external to the NRC.

**CONTACT:** Ronald C. Emrit, RES  
(301) 415-6447

**ACRS OFFICE COPY**  
**DO NOT REMOVE FROM ACRS OFFICE**

GT-999

Generally, safety concerns associated with operating events, research results, or risk assessments form the basis for the identification of generic issues (GI) by the staff, the Advisory Committee on Reactor Safeguards (ACRS), the nuclear industry, or the public. After an issue is identified, the staff conducts an initial screening exercise to determine whether it should be processed as a generic safety issue (GSI), excluded from further analysis, or sent to another NRC program for review. In the technical assessment stage, the staff renders a determination as to whether the issue involves adequate protection, safety enhancement, or burden reduction. In addition, the staff's related technical findings become the basis for developing or revising agency rules, guidance, and programs. In the final three stages, the agency issues new or revised regulations or guidance, which are then implemented by licensees and/or certificate holders, and verified by the NRC. GSIs identified after March 1999 have been processed in accordance with MD 6.4.

The NRC's Office of Nuclear Regulatory Research (RES) tracks the status of all generic issues in the agencywide Generic Issue Management Control System (GIMCS) and documents the technical assessments and dispositions of all issues in NUREG-0933, "A Prioritization of Generic Safety Issues."

#### DISCUSSION:

##### Reactor GSIs

For generic issues associated with nuclear reactor power plants, the RES staff is responsible for screening all new generic issues and performing the technical assessments of GSIs. In addition, the Office of Nuclear Reactor Regulation (NRR) is responsible for developing and issuing regulations or guidance that may be recommended in the technical assessments, and subsequently verifies the implementation of the resultant regulation or guidance by licensees and/or certificate holders. The staff also conducts an "adequate protection evaluation" for each newly identified GSI to determine whether plants should continue operating while the issue is being resolved. Since the inception of the generic issues program in 1976, the staff has closed 836 of the 847 identified reactor generic issues. A description of the 11 reactor GSIs that remain open at this time as well as a summary of the status of their various stages of initial screening, technical assessment, or regulation and guidance development are attached. The following is a summary of the activities related to reactor GSIs since the staff issued its last report to the Commission in SECY-03-0124 on July 24, 2003.

##### *Identification*

The staff identified two new GIs for initial screening:

- 196 Boral Degradation
- 197 Iodine Spiking Phenomena

##### *Initial Screening*

The staff completed the initial screening of the following four GIs:

- 186 Potential Risk and Consequences of Heavy Load Drops in Nuclear Power Plants

- 193 Boiling-Water Reactor (BWR) Emergency Core Cooling System (ECCS)  
Suction Concerns
- 194 Implications of Updated Probabilistic Seismic Hazard Estimates
- 195 Hydrogen Combustion in Foreign BWR Piping

#### *Technical Assessment*

The following seven GSIs are undergoing technical assessment:

- 80 Pipe Break Effects on Control Rod Drive (CRD) Hydraulic Lines in the Drywells  
of BWR MARK I and II Containments
- 156.6.1 Pipe Break Effects on Systems and Components
- 163 Multiple Steam Generator Tube Leakage
- 185 Control of Recriticality Following Small-Break LOCAs in Pressurized-Water  
Reactors (PWRs)
- 186 Potential Risk and Consequences of Heavy Load Drops in Nuclear Power Plants
- 188 Steam Generator Tube Leaks/Ruptures Concurrent with Containment Bypass
- 193 Boiling-Water Reactor (BWR) Emergency Core Cooling System (ECCS)  
Suction Concerns

#### *Regulation and Guidance Development*

Regulation and guidance development continued on the following three GSIs:

- 186 Potential Risk and Consequences of Heavy Load Drops
- 189 Susceptibility of Ice Condenser and MARK III Containments to Early Failure from  
Hydrogen Combustion During a Severe Accident
- 191 Assessment of Debris Accumulation on PWR Sump Performance

#### *Closed*

The staff closed the following GSI during this reporting period:

- 168 Environmental Qualification of Electrical Equipment

#### Non-Reactor GSIs

The NRC's Office of Nuclear Material Safety and Safeguards (NMSS) has the primary responsibility for processing non-reactor GSIs through all stages of MD 6.4, and RES tracks the status of the unresolved non-reactor GSIs in the quarterly updates of GIMCS. A description of the 3 non-reactor GSIs that remain open at this time as well as a summary of the status of their various stages of technical assessment or regulation and guidance development are attached. The following is a summary of the activities related to non-reactor GSIs since the staff issued its last report to the Commission in SECY-03-0124 on July 24, 2003.

#### *Identification*

The staff did not identify any new GSI for screening.

*Initial Screening*

No initial screening activities were warranted during this reporting period.

*Technical Assessment*

The following is the status of the ongoing technical assessment of two GSIs:

- NMSS-7      Criticality Benchmarks Greater than 5% Enrichment
- NMSS-14     Surety Estimates for Groundwater Restoration at In Situ Leach Facilities

*Regulation and Guidance Development*

Regulation and guidance development continued on the following GSI:

- NMSS-16     Adequacy of 0.05 Weight Percent Limit in 10 CFR Part 40

CONCLUSION:

Since the staff issued its last report to the Commission on July 24, 2003, two GSIs were dropped from further pursuit, one GSI was closed, and another 14 GSIs remain to be resolved as the staff continued to implement the MD 6.4 process of identifying and resolving reactor and non-reactor GSIs. The staff will continue to provide annual updates to the Commission on GSI-related activities and will inform the Commission of any significant developments.



Luis A. Reyes  
Executive Director  
for Operations

Attachment: Description and Status of Open  
GSIs as of August 16, 2004

DISTRIBUTION:  
Commissioners  
DOC  
OGC  
OCAA  
OIG  
OPA  
OIP  
OCA  
ACRS  
CFO  
EDO  
REGIONS  
SECY

## Description and Status of Open GSIs as of August 16, 2004

GSI Number	Title	Lead Office	Description	Status
80	Pipe Break Effects on Control Rod Drive Hydraulic Lines in the Drywells of BWR MARK I and II Containments	RES	This issue addresses a concern regarding the likelihood and effects of a LOCA, which could cause interactions with the CRD hydraulic lines in a manner that could prevent rod insertion and create the potential for recriticality when the reactor core is reflooded.	The staff's action plan for the combined technical assessment of GSIs 80 and 156.6.1 (see below) was approved in February 2004 and, since that time, the staff has completed studies of the high-energy piping interactions with CRD piping bundles in MARK I and II drywells with no adverse findings. The staff's draft recommendations are scheduled to be finalized in October 2004.
156.6.1	Pipe Break Effects on Systems and Components	RES	This issue addresses a safety concern regarding whether the designs of some plants have adequately addressed the effects of pipe breaks inside containments.	See status of GSI 80 above.
163	Multiple Steam Generator Tube Leakage	NRR	This issue addresses a safety concern regarding multiple steam generator tube leaks during a main steam line break that cannot be isolated.	This issue is an integral part of the NRC's Steam Generator Action Plan (Items 3.1, 3.7, 3.8, and 3.9). The staff is developing a more technically robust position on the treatment of radionuclide releases for use in the safety analyses of design-basis events. Technical assessment of the issue is scheduled for completion by September 2005.
168	Environmental Qualification of Electrical Equipment	NRR	Accelerated aging tests on electrical equipment showed that some environmentally qualified cables either failed or exhibited marginal insulation resistance. Failure of these cables during or following a design-basis event could affect the performance of safety functions.	After review and analysis of six LOCA tests, condition-monitoring tests on instrumentation and control (I&C) cables, and information provided by the nuclear industry, the staff concluded that the existing equipment qualification process is adequate to ensure that I&C cables will perform their intended function. The staff, therefore, issued Regulatory Issue Summary 2003-09 on May 2, 2003, and closed the issue in August 2003 with no new requirements for licensees.

## Description and Status of Open GSIs as of August 16, 2004

GSI Number	Title	Lead Office	Description	Status
185	Control of Recriticality Following Small-Break LOCA in PWRs	RES	This issue addresses small-break LOCA scenarios in PWRs that involve steam generation in the core and condensation in the steam generators, which may cause deborated water to accumulate in part of the reactor coolant system (RCS). In such scenarios, restarting the RCS circulation may cause a recriticality event (reactivity excursion) by moving the deborated water into the core.	In March 2004, the staff completed a draft report describing an assessment of recriticality from the transport of boron-diluted water from loop seals to the core during small-break LOCAs in PWRs. The staff will complete its technical assessment of this issue after all feedback is received. Technical assessment of the issue is scheduled for completion by September 2005.
186	Potential Risk and Consequences of Heavy Load Drops in Nuclear Power Plants	RES	This issue resulted from a staff review of licensees' programs for handling heavy loads, which revealed that dropping a heavy load has a substantially greater potential for severe consequences than the industry previously envisioned.	Initial screening of the issue was completed in August 2003 and resulted in the recommendation to continue work on a technical assessment. The staff prepared NUREG-1774, "A Survey of Crane Operating Experience at U.S. Nuclear Power Plants from 1968 through 2002," dated July 2003. The staff subsequently completed its related technical assessment in November 2003 and provided recommendations for the development of regulatory guidance for licensees. The staff is currently developing a regulatory issue summary, which will be issued to licensees to clarify and reemphasize existing regulatory guidance for the control of heavy loads.

**Description and Status of Open GSIs as of August 16, 2004**

GSI Number	Title	Lead Office	Description	Status
188	Steam Generator Tube Leaks/Ruptures Concurrent with Containment Bypass	RES	This issue addresses the effects on the validity of steam generator tube leak and rupture analyses of resonance vibrations in steam generator tubes during steam line break depressurization.	The issue is an integral part of Item 3.1 of the NRC's Steam Generator Action Plan (SGAP). The staff conducted tests of degraded tubes under pressure and with axial and bending loads to validate analytical results from other SGAP items. Results of the tests showed that dynamic loads associated with a main steam line break will have little impact on the integrity of steam generator tubes unless extensive circumferential cracking is present. The staff is finalizing its draft report and plans to discuss its findings with the ACRS in September 2004.
189	Susceptibility of Ice Condenser and MARK III Containments to Early Failure from Hydrogen Combustion During a Severe Accident	NRR	NUREG/CR-6427, "Assessment of the Direct Containment Heat (DCH) Issue for Plants with Ice Condenser Containments," highlighted this issue with the discovery that the early containment failure probability in ice condensers is dominated by non-DCH hydrogen combustion events. The staff subsequently extended the issue to include BWR MARK III containments because their relatively low free volume and strength are comparable to PWR ice condensers.	The staff concluded that regulatory guidance for providing backup power to one train of hydrogen igniters is warranted for plants with ice condenser or MARK III containments. In November 2003, the ACRS recommended that the staff should proceed with rulemaking to achieve this objective. In pursuing rulemaking, the staff subsequently met with stakeholders in February and March 2004 in its efforts to develop industry guidance that specifies the design criteria for a backup power supply to igniters. A kickoff meeting with the contractor who will perform the regulatory analysis is scheduled for the first week in August 2004. Regulation and guidance development is scheduled to be completed by June 2010.

**Description and Status of Open GSIs as of August 16, 2004**

GSI Number	Title	Lead Office	Description	Status
191	Assessment of Debris Accumulation on PWR Sump Performance	NRR	This issue addresses the possibility of debris accumulating on the ECCS sump screen, which may result in a loss of the net positive suction head (NPSH) margin. This loss of NPSH margin could impede or prevent the flow of water from the sump, which is necessary to meet the criteria of 10 CFR 50.46.	The staff issued a bulletin to request licensees to confirm regulatory compliance, in light of the new concerns, or describe interim compensatory actions that were taken or will be taken to reduce risk until a plant-specific analysis can be completed. The staff also published Revision 3 of Regulatory Guide 1.82, "Water Sources for Long-Term Recirculation Cooling Following a Loss-of-Coolant Accident," dated November 2003. The staff is working with the industry to develop acceptable guidance for plant-specific analyses, and is currently developing a generic letter for issuance to licensees which will reference this industry guidance, and also request licensees to reanalyze their sumps and perform necessary modifications. Regulation and guidance development is scheduled to be completed by March 2007.
193	BWR ECCS Suction Concerns	RES	This issue addresses a concern regarding the possible failure of the ECCS caused by unanticipated, large quantities of entrained gas in the suction piping from BWR suppression pools. The issue applies to MARK I, II, and III containments during large- and medium-break loss-of-coolant accidents (LOCAs), and could potentially result in pump failure or degraded performance as a result of gas binding, vapor locking, or cavitation.	Initial screening of this GSI was completed in October 2003 and resulted in the recommendation to continue work on a technical assessment. The staff's action plan for the technical assessment of this issue was approved in May 2004. The staff has since begun investigating the key issues that were conservatively treated in the initial screening (e.g., air entrainment in the suppression pool and pump failure probabilities).

### Description and Status of Open GSIs as of August 16, 2004

GSI Number	Title	Lead Office	Description	Status
194	Implications of Updated Probabilistic Seismic Hazard Estimates	RES	This issue addressed a concern regarding the seismic design bases of all nuclear power plants in and around the East Tennessee Seismic Zone, based on the new composite seismicity model for the region.	Initial screening of this GSI was completed in September 2003. The staff found that existing NRC programs adequately addressed the safety concern, and the issue was dropped from further pursuit.
195	Hydrogen Combustion in Foreign BWR Piping	RES	This issue addressed the accumulation of combustible gas mixtures in piping. In several foreign events, hydrogen and oxygen gases apparently accumulated to a combustible level, which then damaged the piping systems.	Initial screening of this GSI was completed in February 2004. The staff's analysis indicated that the events posed a low risk to the public, and the issue was dropped from further pursuit.
196	Boral Degradation	RES	This issue addresses a concern regarding degradation mechanisms that could impair the effectiveness of Boral as a neutron absorber in spent fuel casks.	This issue was identified in November 2003. The screening panel met on July 26, 2004, and initial screening issue is scheduled to be completed in August 2004.
197	Iodine Spiking Phenomena	RES	This issue addresses the ACRS concern for the conservative, empirical fashion in which iodine spiking is being treated in accident consequence analyses. The ACRS recommended that the staff develop a mechanistic understanding of iodine spiking phenomena so that analyses would reflect current plant operations and the capabilities of modern fuel rods (to prevent coolant contamination).	This issue was identified in July 2004, and initial screening is scheduled to be completed by January 2005.

### Description and Status of Open GSIs as of August 16, 2004

GSI Number	Title	Lead Office	Description	Status
NMSS-07	Criticality Benchmarks Greater than 5% Enrichment	NMSS	This issue requires the development and confirmation of the adequacy of methods, analytical tools, and guidance for criticality safety software for validating criticality calculations, including requests to process higher enrichments, in the licensing of nuclear facilities.	In June 2004, the staff was provided with, and trained on, sensitivity/uncertainty computer codes available in the SCALE 5.0 modular code system. The acceptability of new methods is scheduled to be communicated to licensees in December 2004. Technical assessment of the issue is scheduled for completion by October 2005.
NMSS-14	Surety Estimates for Groundwater Restoration at In-Situ Leach Facilities	NMSS	This issue addresses the development of methodologies to (1) calculate surety for groundwater restoration activities at in situ leach uranium extraction facilities, and (2) monitor the post-restoration stability of groundwater quality.	Under contract to the NRC, the U.S. Geological Survey (USGS) submitted a draft report, entitled "Consideration of Geochemical Issues in Groundwater Restoration at Uranium In Situ Leach Mining Facilities," dated August 2003. USGS revised its draft report to incorporate additional information provided by the industry and submitted it to the NRC in August 2004. Technical assessment of the issue is scheduled for completion by December 2004.
NMSS-16	Adequacy of 0.05 Weight Percent Limit in Part 40	NMSS	In SECY-00-0201, dated September 2000, the staff forwarded to the Commission a discussion of available options for proceeding with jurisdictional and technical issues concerning the regulation of source material.	On June 24, 2003, the staff notified the Commission in SECY-03-0106 that it planned to postpone work on a Rule until the Commission had an opportunity to review and direct the staff regarding other related issues that could impact the action taken in the final rule. The Commission subsequently issued an SRM in October 2003 in which it responded to SECY-03-0106 by directing the staff to continue reviewing transfers of materials containing less than 0.05 Wt% uranium and thorium using previous Commission guidance.



## **POLICY ISSUE** **(Information)**

August 27, 2004

SECY-04-0156

**FOR:** The Commissioners

**FROM:** Luis A. Reyes  
Executive Director for Operations

**SUBJECT:** SUMMARY OF ACTIVITIES RELATED TO GENERIC SAFETY ISSUES

**PURPOSE:**

To present the annual summary of activities related to Generic Safety Issues (GSIs).

**BACKGROUND:**

Since 1983, the staff of the U.S. Nuclear Regulatory Commission (NRC) has adhered to the practice of providing the Commission with an annual update of the progress made in resolving GSIs. The Commission reinforced this practice in a staff requirements memorandum (SRM) dated May 8, 1998, in response to SECY-98-030, "Implementation of [Direction-Setting Issue] DSI-22 Research," in which the Commission directed the staff to provide an annual summary of activities related to open reactor and non-reactor GSIs.

Management Directive (MD) 6.4, "Generic Issues Program," dated December 2001, delineates the NRC's program for addressing reactor and non-reactor generic issues. Specifically, the program described in MD 6.4 comprises seven stages, including (1) identification, (2) initial screening, (3) technical assessment, (4) regulation and guidance development, (5) regulation and guidance issuance, (6) implementation, and (7) verification. Candidate generic issues may be identified by organizations or individuals either within or external to the NRC.

**CONTACT:** Ronald C. Emrit, RES  
(301) 415-6447

Generally, safety concerns associated with operating events, research results, or risk assessments form the basis for the identification of generic issues (GI) by the staff, the Advisory Committee on Reactor Safeguards (ACRS), the nuclear industry, or the public. After an issue is identified, the staff conducts an initial screening exercise to determine whether it should be processed as a generic safety issue (GSI), excluded from further analysis, or sent to another NRC program for review. In the technical assessment stage, the staff renders a determination as to whether the issue involves adequate protection, safety enhancement, or burden reduction. In addition, the staff's related technical findings become the basis for developing or revising agency rules, guidance, and programs. In the final three stages, the agency issues new or revised regulations or guidance, which are then implemented by licensees and/or certificate holders, and verified by the NRC. GSIs identified after March 1999 have been processed in accordance with MD 6.4.

The NRC's Office of Nuclear Regulatory Research (RES) tracks the status of all generic issues in the agencywide Generic Issue Management Control System (GIMCS) and documents the technical assessments and dispositions of all issues in NUREG-0933, "A Prioritization of Generic Safety Issues."

#### DISCUSSION:

##### Reactor GSIs

For generic issues associated with nuclear reactor power plants, the RES staff is responsible for screening all new generic issues and performing the technical assessments of GSIs. In addition, the Office of Nuclear Reactor Regulation (NRR) is responsible for developing and issuing regulations or guidance that may be recommended in the technical assessments, and subsequently verifies the implementation of the resultant regulation or guidance by licensees and/or certificate holders. The staff also conducts an "adequate protection evaluation" for each newly identified GSI to determine whether plants should continue operating while the issue is being resolved. Since the inception of the generic issues program in 1976, the staff has closed 836 of the 847 identified reactor generic issues. A description of the 11 reactor GSIs that remain open at this time as well as a summary of the status of their various stages of initial screening, technical assessment, or regulation and guidance development are attached. The following is a summary of the activities related to reactor GSIs since the staff issued its last report to the Commission in SECY-03-0124 on July 24, 2003.

##### *Identification*

The staff identified two new GIs for initial screening:

- 196 Boral Degradation
- 197 Iodine Spiking Phenomena

##### *Initial Screening*

The staff completed the initial screening of the following four GIs:

- 186 Potential Risk and Consequences of Heavy Load Drops in Nuclear Power Plants

- 193 Boiling-Water Reactor (BWR) Emergency Core Cooling System (ECCS) Suction Concerns
- 194 Implications of Updated Probabilistic Seismic Hazard Estimates
- 195 Hydrogen Combustion in Foreign BWR Piping

#### *Technical Assessment*

The following seven GSIs are undergoing technical assessment:

- 80 Pipe Break Effects on Control Rod Drive (CRD) Hydraulic Lines in the Drywells of BWR MARK I and II Containments
- 156.6.1 Pipe Break Effects on Systems and Components
- 163 Multiple Steam Generator Tube Leakage
- 185 Control of Recriticality Following Small-Break LOCAs in Pressurized-Water Reactors (PWRs)
- 186 Potential Risk and Consequences of Heavy Load Drops in Nuclear Power Plants
- 188 Steam Generator Tube Leaks/Ruptures Concurrent with Containment Bypass
- 193 Boiling-Water Reactor (BWR) Emergency Core Cooling System (ECCS) Suction Concerns

#### *Regulation and Guidance Development*

Regulation and guidance development continued on the following three GSIs:

- 186 Potential Risk and Consequences of Heavy Load Drops
- 189 Susceptibility of Ice Condenser and MARK III Containments to Early Failure from Hydrogen Combustion During a Severe Accident
- 191 Assessment of Debris Accumulation on PWR Sump Performance

#### *Closed*

The staff closed the following GSI during this reporting period:

- 168 Environmental Qualification of Electrical Equipment

#### Non-Reactor GSIs

The NRC's Office of Nuclear Material Safety and Safeguards (NMSS) has the primary responsibility for processing non-reactor GSIs through all stages of MD 6.4, and RES tracks the status of the unresolved non-reactor GSIs in the quarterly updates of GIMCS. A description of the 3 non-reactor GSIs that remain open at this time as well as a summary of the status of their various stages of technical assessment or regulation and guidance development are attached. The following is a summary of the activities related to non-reactor GSIs since the staff issued its last report to the Commission in SECY-03-0124 on July 24, 2003.

#### *Identification*

The staff did not identify any new GSI for screening.

*Initial Screening*

No initial screening activities were warranted during this reporting period.

*Technical Assessment*

The following is the status of the ongoing technical assessment of two GSIs:

- NMSS-7      Criticality Benchmarks Greater than 5% Enrichment
- NMSS-14     Surety Estimates for Groundwater Restoration at In Situ Leach Facilities

*Regulation and Guidance Development*

Regulation and guidance development continued on the following GSI:

- NMSS-16     Adequacy of 0.05 Weight Percent Limit in 10 CFR Part 40

CONCLUSION:

Since the staff issued its last report to the Commission on July 24, 2003, two GSIs were dropped from further pursuit, one GSI was closed, and another 14 GSIs remain to be resolved as the staff continued to implement the MD 6.4 process of identifying and resolving reactor and non-reactor GSIs. The staff will continue to provide annual updates to the Commission on GSI-related activities and will inform the Commission of any significant developments.



Luis A. Reyes  
Executive Director  
for Operations

Attachment: Description and Status of Open  
GSIs as of August 16, 2004

- DISTRIBUTION:  
Commissioners  
DOC  
OGC  
OCAA  
OIG  
OPA  
OIP  
OCA  
ACRS  
CFO  
EDO  
REGIONS  
SECY

## Description and Status of Open GSIs as of August 16, 2004

GSI Number	Title	Lead Office	Description	Status
80	Pipe Break Effects on Control Rod Drive Hydraulic Lines in the Drywells of BWR MARK I and II Containments	RES	This issue addresses a concern regarding the likelihood and effects of a LOCA, which could cause interactions with the CRD hydraulic lines in a manner that could prevent rod insertion and create the potential for recriticality when the reactor core is reflooded.	The staff's action plan for the combined technical assessment of GSIs 80 and 156.6.1 (see below) was approved in February 2004 and, since that time, the staff has completed studies of the high-energy piping interactions with CRD piping bundles in MARK I and II drywells with no adverse findings. The staff's draft recommendations are scheduled to be finalized in October 2004.
156.6.1	Pipe Break Effects on Systems and Components	RES	This issue addresses a safety concern regarding whether the designs of some plants have adequately addressed the effects of pipe breaks inside containments.	See status of GSI 80 above.
163	Multiple Steam Generator Tube Leakage	NRR	This issue addresses a safety concern regarding multiple steam generator tube leaks during a main steam line break that cannot be isolated.	This issue is an integral part of the NRC's Steam Generator Action Plan (Items 3.1, 3.7, 3.8, and 3.9). The staff is developing a more technically robust position on the treatment of radionuclide releases for use in the safety analyses of design-basis events. Technical assessment of the issue is scheduled for completion by September 2005.
168	Environmental Qualification of Electrical Equipment	NRR	Accelerated aging tests on electrical equipment showed that some environmentally qualified cables either failed or exhibited marginal insulation resistance. Failure of these cables during or following a design-basis event could affect the performance of safety functions.	After review and analysis of six LOCA tests, condition-monitoring tests on instrumentation and control (I&C) cables, and information provided by the nuclear industry, the staff concluded that the existing equipment qualification process is adequate to ensure that I&C cables will perform their intended function. The staff, therefore, issued Regulatory Issue Summary 2003-09 on May 2, 2003, and closed the issue in August 2003 with no new requirements for licensees.

## Description and Status of Open GSIs as of August 16, 2004

GSI Number	Title	Lead Office	Description	Status
185	Control of Recriticality Following Small-Break LOCA in PWRs	RES	This issue addresses small-break LOCA scenarios in PWRs that involve steam generation in the core and condensation in the steam generators, which may cause deborated water to accumulate in part of the reactor coolant system (RCS). In such scenarios, restarting the RCS circulation may cause a recriticality event (reactivity excursion) by moving the deborated water into the core.	In March 2004, the staff completed a draft report describing an assessment of recriticality from the transport of boron-diluted water from loop seals to the core during small-break LOCAs in PWRs. The staff will complete its technical assessment of this issue after all feedback is received. Technical assessment of the issue is scheduled for completion by September 2005.
186	Potential Risk and Consequences of Heavy Load Drops in Nuclear Power Plants	RES	This issue resulted from a staff review of licensees' programs for handling heavy loads, which revealed that dropping a heavy load has a substantially greater potential for severe consequences than the industry previously envisioned.	Initial screening of the issue was completed in August 2003 and resulted in the recommendation to continue work on a technical assessment. The staff prepared NUREG-1774, "A Survey of Crane Operating Experience at U.S. Nuclear Power Plants from 1968 through 2002," dated July 2003. The staff subsequently completed its related technical assessment in November 2003 and provided recommendations for the development of regulatory guidance for licensees. The staff is currently developing a regulatory issue summary, which will be issued to licensees to clarify and reemphasize existing regulatory guidance for the control of heavy loads.

## Description and Status of Open GSIs as of August 16, 2004

GSI Number	Title	Lead Office	Description	Status
188	Steam Generator Tube Leaks/Ruptures Concurrent with Containment Bypass	RES	This issue addresses the effects on the validity of steam generator tube leak and rupture analyses of resonance vibrations in steam generator tubes during steam line break depressurization.	The issue is an integral part of Item 3.1 of the NRC's Steam Generator Action Plan (SGAP). The staff conducted tests of degraded tubes under pressure and with axial and bending loads to validate analytical results from other SGAP items. Results of the tests showed that dynamic loads associated with a main steam line break will have little impact on the integrity of steam generator tubes unless extensive circumferential cracking is present. The staff is finalizing its draft report and plans to discuss its findings with the ACRS in September 2004.
189	Susceptibility of Ice Condenser and MARK III Containments to Early Failure from Hydrogen Combustion During a Severe Accident	NRR	NUREG/CR-6427, "Assessment of the Direct Containment Heat (DCH) Issue for Plants with Ice Condenser Containments," highlighted this issue with the discovery that the early containment failure probability in ice condensers is dominated by non-DCH hydrogen combustion events. The staff subsequently extended the issue to include BWR MARK III containments because their relatively low free volume and strength are comparable to PWR ice condensers.	The staff concluded that regulatory guidance for providing backup power to one train of hydrogen igniters is warranted for plants with ice condenser or MARK III containments. In November 2003, the ACRS recommended that the staff should proceed with rulemaking to achieve this objective. In pursuing rulemaking, the staff subsequently met with stakeholders in February and March 2004 in its efforts to develop industry guidance that specifies the design criteria for a backup power supply to igniters. A kickoff meeting with the contractor who will perform the regulatory analysis is scheduled for the first week in August 2004. Regulation and guidance development is scheduled to be completed by June 2010.

## Description and Status of Open GSIs as of August 16, 2004

GSI Number	Title	Lead Office	Description	Status
191	Assessment of Debris Accumulation on PWR Sump Performance	NRR	This issue addresses the possibility of debris accumulating on the ECCS sump screen, which may result in a loss of the net positive suction head (NPSH) margin. This loss of NPSH margin could impede or prevent the flow of water from the sump, which is necessary to meet the criteria of 10 CFR 50.46.	The staff issued a bulletin to request licensees to confirm regulatory compliance, in light of the new concerns, or describe interim compensatory actions that were taken or will be taken to reduce risk until a plant-specific analysis can be completed. The staff also published Revision 3 of Regulatory Guide 1.82, "Water Sources for Long-Term Recirculation Cooling Following a Loss-of-Coolant Accident," dated November 2003. The staff is working with the industry to develop acceptable guidance for plant-specific analyses, and is currently developing a generic letter for issuance to licensees which will reference this industry guidance, and also request licensees to reanalyze their sumps and perform necessary modifications. Regulation and guidance development is scheduled to be completed by March 2007.
193	BWR ECCS Suction Concerns	RES	This issue addresses a concern regarding the possible failure of the ECCS caused by unanticipated, large quantities of entrained gas in the suction piping from BWR suppression pools. The issue applies to MARK I, II, and III containments during large- and medium-break loss-of-coolant accidents (LOCAs), and could potentially result in pump failure or degraded performance as a result of gas binding, vapor locking, or cavitation.	Initial screening of this GSI was completed in October 2003 and resulted in the recommendation to continue work on a technical assessment. The staff's action plan for the technical assessment of this issue was approved in May 2004. The staff has since begun investigating the key issues that were conservatively treated in the initial screening (e.g., air entrainment in the suppression pool and pump failure probabilities).

## Description and Status of Open GSIs as of August 16, 2004

GSI Number	Title	Lead Office	Description	Status
194	Implications of Updated Probabilistic Seismic Hazard Estimates	RES	This issue addressed a concern regarding the seismic design bases of all nuclear power plants in and around the East Tennessee Seismic Zone, based on the new composite seismicity model for the region.	Initial screening of this GSI was completed in September 2003. The staff found that existing NRC programs adequately addressed the safety concern, and the issue was dropped from further pursuit.
195	Hydrogen Combustion in Foreign BWR Piping	RES	This issue addressed the accumulation of combustible gas mixtures in piping. In several foreign events, hydrogen and oxygen gases apparently accumulated to a combustible level, which then damaged the piping systems.	Initial screening of this GSI was completed in February 2004. The staff's analysis indicated that the events posed a low risk to the public, and the issue was dropped from further pursuit.
196	Boral Degradation	RES	This issue addresses a concern regarding degradation mechanisms that could impair the effectiveness of Boral as a neutron absorber in spent fuel casks.	This issue was identified in November 2003. The screening panel met on July 26, 2004, and initial screening issue is scheduled to be completed in August 2004.
197	Iodine Spiking Phenomena	RES	This issue addresses the ACRS concern for the conservative, empirical fashion in which iodine spiking is being treated in accident consequence analyses. The ACRS recommended that the staff develop a mechanistic understanding of iodine spiking phenomena so that analyses would reflect current plant operations and the capabilities of modern fuel rods (to prevent coolant contamination).	This issue was identified in July 2004, and initial screening is scheduled to be completed by January 2005.

## Description and Status of Open GSIs as of August 16, 2004

GSI Number	Title	Lead Office	Description	Status
NMSS-07	Criticality Benchmarks Greater than 5% Enrichment	NMSS	This issue requires the development and confirmation of the adequacy of methods, analytical tools, and guidance for criticality safety software for validating criticality calculations, including requests to process higher enrichments, in the licensing of nuclear facilities.	In June 2004, the staff was provided with, and trained on, sensitivity/uncertainty computer codes available in the SCALE 5.0 modular code system. The acceptability of new methods is scheduled to be communicated to licensees in December 2004. Technical assessment of the issue is scheduled for completion by October 2005.
NMSS-14	Surety Estimates for Groundwater Restoration at In-Situ Leach Facilities	NMSS	This issue addresses the development of methodologies to (1) calculate surety for groundwater restoration activities at in situ leach uranium extraction facilities, and (2) monitor the post-restoration stability of groundwater quality.	Under contract to the NRC, the U.S. Geological Survey (USGS) submitted a draft report, entitled "Consideration of Geochemical Issues in Groundwater Restoration at Uranium In Situ Leach Mining Facilities," dated August 2003. USGS revised its draft report to incorporate additional information provided by the industry and submitted it to the NRC in August 2004. Technical assessment of the issue is scheduled for completion by December 2004.
NMSS-16	Adequacy of 0.05 Weight Percent Limit in Part 40	NMSS	In SECY-00-0201, dated September 2000, the staff forwarded to the Commission a discussion of available options for proceeding with jurisdictional and technical issues concerning the regulation of source material.	On June 24, 2003, the staff notified the Commission in SECY-03-0106 that it planned to postpone work on a Rule until the Commission had an opportunity to review and direct the staff regarding other related issues that could impact the action taken in the final rule. The Commission subsequently issued an SRM in October 2003 in which it responded to SECY-03-0106 by directing the staff to continue reviewing transfers of materials containing less than 0.05 Wt% uranium and thorium using previous Commission guidance.



## **POLICY ISSUE** **(Information)**

August 27, 2004

SECY-04-0156

**FOR:** The Commissioners

**FROM:** Luis A. Reyes  
Executive Director for Operations

**SUBJECT:** SUMMARY OF ACTIVITIES RELATED TO GENERIC SAFETY ISSUES

**PURPOSE:**

To present the annual summary of activities related to Generic Safety Issues (GSIs).

**BACKGROUND:**

Since 1983, the staff of the U.S. Nuclear Regulatory Commission (NRC) has adhered to the practice of providing the Commission with an annual update of the progress made in resolving GSIs. The Commission reinforced this practice in a staff requirements memorandum (SRM) dated May 8, 1998, in response to SECY-98-030, "Implementation of [Direction-Setting Issue] DSI-22 Research," in which the Commission directed the staff to provide an annual summary of activities related to open reactor and non-reactor GSIs.

Management Directive (MD) 6.4, "Generic Issues Program," dated December 2001, delineates the NRC's program for addressing reactor and non-reactor generic issues. Specifically, the program described in MD 6.4 comprises seven stages, including (1) identification, (2) initial screening, (3) technical assessment, (4) regulation and guidance development, (5) regulation and guidance issuance, (6) implementation, and (7) verification. Candidate generic issues may be identified by organizations or individuals either within or external to the NRC.

**CONTACT:** Ronald C. Emrit, RES  
(301) 415-6447

Generally, safety concerns associated with operating events, research results, or risk assessments form the basis for the identification of generic issues (GI) by the staff, the Advisory Committee on Reactor Safeguards (ACRS), the nuclear industry, or the public. After an issue is identified, the staff conducts an initial screening exercise to determine whether it should be processed as a generic safety issue (GSI), excluded from further analysis, or sent to another NRC program for review. In the technical assessment stage, the staff renders a determination as to whether the issue involves adequate protection, safety enhancement, or burden reduction. In addition, the staff's related technical findings become the basis for developing or revising agency rules, guidance, and programs. In the final three stages, the agency issues new or revised regulations or guidance, which are then implemented by licensees and/or certificate holders, and verified by the NRC. GSIs identified after March 1999 have been processed in accordance with MD 6.4.

The NRC's Office of Nuclear Regulatory Research (RES) tracks the status of all generic issues in the agencywide Generic Issue Management Control System (GIMCS) and documents the technical assessments and dispositions of all issues in NUREG-0933, "A Prioritization of Generic Safety Issues."

#### DISCUSSION:

##### Reactor GSIs

For generic issues associated with nuclear reactor power plants, the RES staff is responsible for screening all new generic issues and performing the technical assessments of GSIs. In addition, the Office of Nuclear Reactor Regulation (NRR) is responsible for developing and issuing regulations or guidance that may be recommended in the technical assessments, and subsequently verifies the implementation of the resultant regulation or guidance by licensees and/or certificate holders. The staff also conducts an "adequate protection evaluation" for each newly identified GSI to determine whether plants should continue operating while the issue is being resolved. Since the inception of the generic issues program in 1976, the staff has closed 836 of the 847 identified reactor generic issues. A description of the 11 reactor GSIs that remain open at this time as well as a summary of the status of their various stages of initial screening, technical assessment, or regulation and guidance development are attached. The following is a summary of the activities related to reactor GSIs since the staff issued its last report to the Commission in SECY-03-0124 on July 24, 2003.

##### *Identification*

The staff identified two new GIs for initial screening:

- 196 Boral Degradation
- 197 Iodine Spiking Phenomena

##### *Initial Screening*

The staff completed the initial screening of the following four GIs:

- 186 Potential Risk and Consequences of Heavy Load Drops in Nuclear Power Plants

- 193 Boiling-Water Reactor (BWR) Emergency Core Cooling System (ECCS) Suction Concerns
- 194 Implications of Updated Probabilistic Seismic Hazard Estimates
- 195 Hydrogen Combustion in Foreign BWR Piping

#### *Technical Assessment*

The following seven GSIs are undergoing technical assessment:

- 80 Pipe Break Effects on Control Rod Drive (CRD) Hydraulic Lines in the Drywells of BWR MARK I and II Containments
- 156.6.1 Pipe Break Effects on Systems and Components
- 163 Multiple Steam Generator Tube Leakage
- 185 Control of Recriticality Following Small-Break LOCAs in Pressurized-Water Reactors (PWRs)
- 186 Potential Risk and Consequences of Heavy Load Drops in Nuclear Power Plants
- 188 Steam Generator Tube Leaks/Ruptures Concurrent with Containment Bypass
- 193 Boiling-Water Reactor (BWR) Emergency Core Cooling System (ECCS) Suction Concerns

#### *Regulation and Guidance Development*

Regulation and guidance development continued on the following three GSIs:

- 186 Potential Risk and Consequences of Heavy Load Drops
- 189 Susceptibility of Ice Condenser and MARK III Containments to Early Failure from Hydrogen Combustion During a Severe Accident
- 191 Assessment of Debris Accumulation on PWR Sump Performance

#### *Closed*

The staff closed the following GSI during this reporting period:

- 168 Environmental Qualification of Electrical Equipment

#### Non-Reactor GSIs

The NRC's Office of Nuclear Material Safety and Safeguards (NMSS) has the primary responsibility for processing non-reactor GSIs through all stages of MD 6.4, and RES tracks the status of the unresolved non-reactor GSIs in the quarterly updates of GIMCS. A description of the 3 non-reactor GSIs that remain open at this time as well as a summary of the status of their various stages of technical assessment or regulation and guidance development are attached. The following is a summary of the activities related to non-reactor GSIs since the staff issued its last report to the Commission in SECY-03-0124 on July 24, 2003.

#### *Identification*

The staff did not identify any new GSI for screening.

*Initial Screening*

No initial screening activities were warranted during this reporting period.

*Technical Assessment*

The following is the status of the ongoing technical assessment of two GSIs:

NMSS-7      Criticality Benchmarks Greater than 5% Enrichment  
NMSS-14     Surety Estimates for Groundwater Restoration at In Situ Leach Facilities

*Regulation and Guidance Development*

Regulation and guidance development continued on the following GSI:

NMSS-16     Adequacy of 0.05 Weight Percent Limit in 10 CFR Part 40

CONCLUSION:

Since the staff issued its last report to the Commission on July 24, 2003, two GSIs were dropped from further pursuit, one GSI was closed, and another 14 GSIs remain to be resolved as the staff continued to implement the MD 6.4 process of identifying and resolving reactor and non-reactor GSIs. The staff will continue to provide annual updates to the Commission on GSI-related activities and will inform the Commission of any significant developments.

  
Luis A. Reyes  
Executive Director  
for Operations

Attachment: Description and Status of Open  
GSIs as of August 16, 2004

DISTRIBUTION:  
Commissioners  
DOC  
OGC  
OCAA  
OIG  
OPA  
OIP  
OCA  
ACRS  
CFO  
EDO  
REGIONS  
SECY

## Description and Status of Open GSIs as of August 16, 2004

GSI Number	Title	Lead Office	Description	Status
80	Pipe Break Effects on Control Rod Drive Hydraulic Lines in the Drywells of BWR MARK I and II Containments	RES	This issue addresses a concern regarding the likelihood and effects of a LOCA, which could cause interactions with the CRD hydraulic lines in a manner that could prevent rod insertion and create the potential for recriticality when the reactor core is reflooded.	The staff's action plan for the combined technical assessment of GSIs 80 and 156.6.1 (see below) was approved in February 2004 and, since that time, the staff has completed studies of the high-energy piping interactions with CRD piping bundles in MARK I and II drywells with no adverse findings. The staff's draft recommendations are scheduled to be finalized in October 2004.
156.6.1	Pipe Break Effects on Systems and Components	RES	This issue addresses a safety concern regarding whether the designs of some plants have adequately addressed the effects of pipe breaks inside containments.	See status of GSI 80 above.
163	Multiple Steam Generator Tube Leakage	NRR	This issue addresses a safety concern regarding multiple steam generator tube leaks during a main steam line break that cannot be isolated.	This issue is an integral part of the NRC's Steam Generator Action Plan (Items 3.1, 3.7, 3.8, and 3.9). The staff is developing a more technically robust position on the treatment of radionuclide releases for use in the safety analyses of design-basis events. Technical assessment of the issue is scheduled for completion by September 2005.
168	Environmental Qualification of Electrical Equipment	NRR	Accelerated aging tests on electrical equipment showed that some environmentally qualified cables either failed or exhibited marginal insulation resistance. Failure of these cables during or following a design-basis event could affect the performance of safety functions.	After review and analysis of six LOCA tests, condition-monitoring tests on instrumentation and control (I&C) cables, and information provided by the nuclear industry, the staff concluded that the existing equipment qualification process is adequate to ensure that I&C cables will perform their intended function. The staff, therefore, issued Regulatory Issue Summary 2003-09 on May 2, 2003, and closed the issue in August 2003 with no new requirements for licensees.

## Description and Status of Open GSIs as of August 16, 2004

GSI Number	Title	Lead Office	Description	Status
185	Control of Recriticality Following Small-Break LOCA in PWRs	RES	This issue addresses small-break LOCA scenarios in PWRs that involve steam generation in the core and condensation in the steam generators, which may cause deborated water to accumulate in part of the reactor coolant system (RCS). In such scenarios, restarting the RCS circulation may cause a recriticality event (reactivity excursion) by moving the deborated water into the core.	In March 2004, the staff completed a draft report describing an assessment of recriticality from the transport of boron-diluted water from loop seals to the core during small-break LOCAs in PWRs. The staff will complete its technical assessment of this issue after all feedback is received. Technical assessment of the issue is scheduled for completion by September 2005.
186	Potential Risk and Consequences of Heavy Load Drops in Nuclear Power Plants	RES	This issue resulted from a staff review of licensees' programs for handling heavy loads, which revealed that dropping a heavy load has a substantially greater potential for severe consequences than the industry previously envisioned.	Initial screening of the issue was completed in August 2003 and resulted in the recommendation to continue work on a technical assessment. The staff prepared NUREG-1774, "A Survey of Crane Operating Experience at U.S. Nuclear Power Plants from 1968 through 2002," dated July 2003. The staff subsequently completed its related technical assessment in November 2003 and provided recommendations for the development of regulatory guidance for licensees. The staff is currently developing a regulatory issue summary, which will be issued to licensees to clarify and reemphasize existing regulatory guidance for the control of heavy loads.

## Description and Status of Open GSIs as of August 16, 2004

GSI Number	Title	Lead Office	Description	Status
188	Steam Generator Tube Leaks/Ruptures Concurrent with Containment Bypass	RES	This issue addresses the effects on the validity of steam generator tube leak and rupture analyses of resonance vibrations in steam generator tubes during steam line break depressurization.	The issue is an integral part of Item 3.1 of the NRC's Steam Generator Action Plan (SGAP). The staff conducted tests of degraded tubes under pressure and with axial and bending loads to validate analytical results from other SGAP items. Results of the tests showed that dynamic loads associated with a main steam line break will have little impact on the integrity of steam generator tubes unless extensive circumferential cracking is present. The staff is finalizing its draft report and plans to discuss its findings with the ACRS in September 2004.
189	Susceptibility of Ice Condenser and MARK III Containments to Early Failure from Hydrogen Combustion During a Severe Accident	NRR	NUREG/CR-6427, "Assessment of the Direct Containment Heat (DCH) Issue for Plants with Ice Condenser Containments," highlighted this issue with the discovery that the early containment failure probability in ice condensers is dominated by non-DCH hydrogen combustion events. The staff subsequently extended the issue to include BWR MARK III containments because their relatively low free volume and strength are comparable to PWR ice condensers.	The staff concluded that regulatory guidance for providing backup power to one train of hydrogen igniters is warranted for plants with ice condenser or MARK III containments. In November 2003, the ACRS recommended that the staff should proceed with rulemaking to achieve this objective. In pursuing rulemaking, the staff subsequently met with stakeholders in February and March 2004 in its efforts to develop industry guidance that specifies the design criteria for a backup power supply to igniters. A kickoff meeting with the contractor who will perform the regulatory analysis is scheduled for the first week in August 2004. Regulation and guidance development is scheduled to be completed by June 2010.

## Description and Status of Open GSIs as of August 16, 2004

GSI Number	Title	Lead Office	Description	Status
191	Assessment of Debris Accumulation on PWR Sump Performance	NRR	This issue addresses the possibility of debris accumulating on the ECCS sump screen, which may result in a loss of the net positive suction head (NPSH) margin. This loss of NPSH margin could impede or prevent the flow of water from the sump, which is necessary to meet the criteria of 10 CFR 50.46.	The staff issued a bulletin to request licensees to confirm regulatory compliance, in light of the new concerns, or describe interim compensatory actions that were taken or will be taken to reduce risk until a plant-specific analysis can be completed. The staff also published Revision 3 of Regulatory Guide 1.82, "Water Sources for Long-Term Recirculation Cooling Following a Loss-of-Coolant Accident," dated November 2003. The staff is working with the industry to develop acceptable guidance for plant-specific analyses, and is currently developing a generic letter for issuance to licensees which will reference this industry guidance, and also request licensees to reanalyze their sumps and perform necessary modifications. Regulation and guidance development is scheduled to be completed by March 2007.
193	BWR ECCS Suction Concerns	RES	This issue addresses a concern regarding the possible failure of the ECCS caused by unanticipated, large quantities of entrained gas in the suction piping from BWR suppression pools. The issue applies to MARK I, II, and III containments during large- and medium-break loss-of-coolant accidents (LOCAs), and could potentially result in pump failure or degraded performance as a result of gas binding, vapor locking, or cavitation.	Initial screening of this GSI was completed in October 2003 and resulted in the recommendation to continue work on a technical assessment. The staff's action plan for the technical assessment of this issue was approved in May 2004. The staff has since begun investigating the key issues that were conservatively treated in the initial screening (e.g., air entrainment in the suppression pool and pump failure probabilities).

### Description and Status of Open GSIs as of August 16, 2004

GSI Number	Title	Lead Office	Description	Status
194	Implications of Updated Probabilistic Seismic Hazard Estimates	RES	This issue addressed a concern regarding the seismic design bases of all nuclear power plants in and around the East Tennessee Seismic Zone, based on the new composite seismicity model for the region.	Initial screening of this GSI was completed in September 2003. The staff found that existing NRC programs adequately addressed the safety concern, and the issue was dropped from further pursuit.
195	Hydrogen Combustion in Foreign BWR Piping	RES	This issue addressed the accumulation of combustible gas mixtures in piping. In several foreign events, hydrogen and oxygen gases apparently accumulated to a combustible level, which then damaged the piping systems.	Initial screening of this GSI was completed in February 2004. The staff's analysis indicated that the events posed a low risk to the public, and the issue was dropped from further pursuit.
196	Boral Degradation	RES	This issue addresses a concern regarding degradation mechanisms that could impair the effectiveness of Boral as a neutron absorber in spent fuel casks.	This issue was identified in November 2003. The screening panel met on July 26, 2004, and initial screening issue is scheduled to be completed in August 2004.
197	Iodine Spiking Phenomena	RES	This issue addresses the ACRS concern for the conservative, empirical fashion in which iodine spiking is being treated in accident consequence analyses. The ACRS recommended that the staff develop a mechanistic understanding of iodine spiking phenomena so that analyses would reflect current plant operations and the capabilities of modern fuel rods (to prevent coolant contamination).	This issue was identified in July 2004, and initial screening is scheduled to be completed by January 2005.

## Description and Status of Open GSIs as of August 16, 2004

GSI Number	Title	Lead Office	Description	Status
NMSS-07	Criticality Benchmarks Greater than 5% Enrichment	NMSS	This issue requires the development and confirmation of the adequacy of methods, analytical tools, and guidance for criticality safety software for validating criticality calculations, including requests to process higher enrichments, in the licensing of nuclear facilities.	In June 2004, the staff was provided with, and trained on, sensitivity/uncertainty computer codes available in the SCALE 5.0 modular code system. The acceptability of new methods is scheduled to be communicated to licensees in December 2004. Technical assessment of the issue is scheduled for completion by October 2005.
NMSS-14	Surety Estimates for Groundwater Restoration at In-Situ Leach Facilities	NMSS	This issue addresses the development of methodologies to (1) calculate surety for groundwater restoration activities at in situ leach uranium extraction facilities, and (2) monitor the post-restoration stability of groundwater quality.	Under contract to the NRC, the U.S. Geological Survey (USGS) submitted a draft report, entitled "Consideration of Geochemical Issues in Groundwater Restoration at Uranium In Situ Leach Mining Facilities," dated August 2003. USGS revised its draft report to incorporate additional information provided by the industry and submitted it to the NRC in August 2004. Technical assessment of the issue is scheduled for completion by December 2004.
NMSS-16	Adequacy of 0.05 Weight Percent Limit in Part 40	NMSS	In SECY-00-0201, dated September 2000, the staff forwarded to the Commission a discussion of available options for proceeding with jurisdictional and technical issues concerning the regulation of source material.	On June 24, 2003, the staff notified the Commission in SECY-03-0106 that it planned to postpone work on a Rule until the Commission had an opportunity to review and direct the staff regarding other related issues that could impact the action taken in the final rule. The Commission subsequently issued an SRM in October 2003 in which it responded to SECY-03-0106 by directing the staff to continue reviewing transfers of materials containing less than 0.05 Wt% uranium and thorium using previous Commission guidance.

GT9990405



MRS

**POLICY ISSUE**

(Information)

**DISTRIBUTED TO ACRS MEMBERS**

RECEIVED  
ACRS/ASNW  
US NRC

SECY-04-0150

AUG 29 2004

August 16, 2004

FOR: The Commissioners

FROM: Luis A. Reyes  
Executive Director for Operations

SUBJECT: ALTERNATE APPROACHES FOR RESOLVING THE PRESSURIZED WATER REACTOR SUMP BLOCKAGE ISSUE (GSI-191), INCLUDING REALISTIC AND RISK-INFORMED CONSIDERATIONS

PURPOSE:

The purpose of this paper is to inform the Commission regarding:

1. staff plans to permit licensees to use alternate approaches for resolution of the pressurized water reactor (PWR) sump blockage issue,
2. the staff's schedule for issuing its safety evaluation report on the industry evaluation guidelines methodology, and
3. the staff's expectations for addressing chemical effects impacts on PWR sump blockage.

SUMMARY:

This paper outlines the regulatory and technical elements necessary to establish a useful and effective alternate approach to resolving Generic Safety Issue (GSI) 191, "Assessment of Debris Accumulation on PWR Sump Performance," and describes the direction the staff is taking to implement such an approach.

CONTACT: Mark Kowal, NRR/DSSA  
301-415-1663

**ACRS OFFICE COPY**  
**DO NOT REMOVE FROM ACRS OFFICE**

GT-999

**BACKGROUND:**

Findings from research performed to resolve the boiling water reactor (BWR) emergency core cooling system (ECCS) strainer plugging issue in the late 1990s raised questions concerning the adequacy of PWR sump designs. These findings prompted the Nuclear Regulatory Commission (NRC) to open GSI-191. The objective of GSI-191 is to ensure that post-accident debris blockage does not impede or prevent the operation of the ECCS and containment spray system (CSS) in the sump recirculation mode in the event of a loss-of-coolant-accident (LOCA) or other high-energy line break (HELB) accident which may require sump recirculation. NRC-sponsored research concluded that recirculation sump clogging is a credible concern for domestic PWRs. The research program mechanistically treated phenomena associated with debris blockage using analytical models of domestic PWRs that were generated with a combination of generic and plant-specific data. As a result of the limitations with respect to plant-specific data and other modeling uncertainties, the research results do not definitively identify whether particular PWR plants are vulnerable to sump clogging.

The staff is implementing a two-step regulatory approach to resolve GSI-191. This approach includes issuing a bulletin and a generic letter. The NRC issued Bulletin 2003-01, "Potential Impact of Debris Blockage on Emergency Sump Recirculation at Pressurized-Water Reactors," in June 2003. The purpose of the bulletin was to inform PWR licensees of the potential for debris blockage of the ECCS and CSS sumps and flowpaths and to request that licensees confirm compliance with Title 10 of the Code of Federal Regulations, Part 50, Section 50.46(b)(5) (10 CFR 50.46(b)(5)) regarding long-term cooling and any other applicable regulatory requirements. Alternatively, licensees were requested to describe any compensatory measures implemented to reduce the potential risk due to post-accident debris blockage until evaluations to determine compliance are completed.

The staff is preparing to issue a generic letter to address final resolution of this issue. The draft generic letter, issued for public comment on March 31, 2004 (ADAMS Accession No. ML040830518), requested licensees to perform analyses to demonstrate compliance with 10 CFR 50.46(b)(5), considering the updated staff position regarding PWR sump performance. Although not yet issued, it is expected that the final generic letter will request the same information. Additionally, it is expected that licensees will be requested to provide information that considers the updated PWR sump design basis requirements no later than September 1, 2005. The generic letter will also request a description of, and implementation schedule for, all corrective actions, including any plant modifications that may be necessary to ensure compliance with the applicable regulations. Licensees will be requested to provide justification for any corrective actions that will not be completed by the end of the first refueling outage that begins after April 1, 2006. The staff expects that all licensees will have completed any necessary modifications, and in turn, resolved this issue by December 31, 2007.

The staff is currently reviewing PWR sump performance evaluation guidance developed by Nuclear Energy Institute (NEI) and the industry. This effort has focused on development of a deterministic and mechanistic methodology for evaluating sump performance under post-accident conditions. In conjunction with developing a deterministic approach, the staff is also developing, through interactions with industry, an alternate approach that licensees could implement to resolve GSI-191.

DISCUSSION:

## Alternate Resolution Approach

For the last several years, the NRC has recognized that probabilistic risk assessment (PRA) has evolved to the point that it can be used increasingly as a tool in regulatory decisionmaking. Through its policy statement on PRA (ADAMS Accession No. ML021980535), the Commission expressed its expectation that enhanced use of PRAs will improve the regulatory process in three ways: through safety decisionmaking enhanced by the use of PRA insights; through more efficient use of agency resources; and through a reduction in unnecessary burden on the licensees.

Specific to GSI-191, the Commission recently requested the staff to "implement an aggressive, realistic plan to achieve resolution and implementation of actions related to PWR ECCS sump concerns." One such resolution path that the staff is considering involves the LOCA break size used in PWR sump analyses. For example, it is well understood that the amount of debris generation to be expected following a LOCA is dependent on the break size, and generally that less debris would be generated with a smaller LOCA break size (although less debris generation may be worse in certain situations when considering debris type and break location). The staff is already working to risk-inform 10 CFR 50.46 to redefine the design basis large-break LOCA break size based on expected LOCA frequencies. A comparable approach for use in GSI-191 resolution would identify a "debris generation" break size which would be used to distinguish between customary and more realistic design basis analyses. To this end, the NRC staff is working to develop alternative approaches which consider realistic and risk-informed elements for use in resolution of GSI-191, and are informed by and consistent with ongoing staff efforts to risk-inform 10 CFR 50.46. The GSI-191 alternate resolution approach is intended to be at least as conservative as any forthcoming revision to 10 CFR 50.46.

On May 25, June 17, and June 29, 2004, the staff met with NEI, industry representatives, and stakeholders in category 2 meetings to discuss alternate realistic and risk-informed approaches for resolution of the PWR sump issue. Throughout these meetings, both NRC and NEI staff presented proposals regarding technical and regulatory elements of alternative approaches, and progress is being made toward reaching an acceptable alternative approach.

The alternative approach includes elements which are both realistic and risk-informed. For such an approach, licensees would continue to perform design basis long-term cooling evaluations and satisfy design basis criteria for all LOCA break sizes up to a new "debris generation" break size. The "debris generation" break size is smaller than a double-ended rupture of the largest pipe in the reactor coolant system (RCS). Long-term cooling must be assured for breaks between the new "debris generation" break size and the double-ended rupture of the largest pipe in the RCS, but the evaluation may be more realistic than a customary design basis evaluation, consistent with the small likelihood of the break occurring. Additionally, any physical modifications to plant equipment or operator actions credited to demonstrate mitigative capability for these larger breaks would not necessarily need to be safety-related or single-failure-proof. Changes to the existing facility designs and credit for operator actions would include risk calculations, consistent with Regulatory Guide 1.174, "An Approach for Using Probabilistic Risk Assessment in Risk-Informed Decisions on Plant-Specific Changes to the Licensing Basis." Licensees would need to ensure that the changes to the

facility design would have sufficient reliability to provide reasonable assurance that SSCs will perform their intended function.

While not a component of the 10 CFR 50.46 ECCS evaluation model, the calculation of sump performance is necessary to determine if the sump and the residual heat removal system are configured properly to provide enough flow to ensure long-term cooling, which is an acceptance criterion of 10 CFR 50.46. Therefore, the staff considers the modeling of sump performance as the validation of assumptions made in the ECCS evaluation model. The modeling of sump performance is a boundary calculation for the ECCS evaluation model, and acceptable sump performance is required for demonstrating long-term core cooling capability (10 CFR 50.46 (b)(5)). On this basis, such an alternative approach might require plant-specific license amendment requests or requests for exemptions from the regulations, depending on each licensee's chosen resolution approach. Licensees could request, on a plant-specific basis, exemptions from requirements associated with demonstrating long-term core cooling capability (10 CFR 50.46 (b)(5)). For example, exemptions from the requirements of 10 CFR 50.46(d) may be required if a licensee chose to classify new equipment as non-safety-related or non-single-failure proof. For purposes of GSI-191 resolution, exemption requests would not be applicable to the other acceptance criteria of 10 CFR 50.46 (peak cladding temperature, maximum cladding oxidation, maximum hydrogen generation, and coolable geometry), and would be submitted in accordance with existing NRC regulations (10 CFR 50.12). License amendment requests may be needed for changes in analytical methodology or assumptions. Licensees would assess the need for license amendment requests in accordance with the requirements of 10 CFR 50.59.

NRC staff review and acceptance of such plant-specific license amendment or exemption requests would consider the following elements:

- ▶ Application of the principles of Regulatory Guide 1.174. (defense-in-depth, safety margins, delta core damage frequency, delta large early release fraction)
- ▶ Consistency with NUREG-0800 (Standard Review Plan), Section 19, "Use of Probabilistic Risk Assessment in Plant-Specific, Risk-Informed Decisionmaking: General Guidance."
- ▶ Design basis, deterministic analyses necessary to verify compliance with 10 CFR 50.46 (b)(5) for break sizes up through the "debris generation" break size.
- ▶ Acceptable mitigative capability up through the double-ended rupture of the largest pipe in the RCS. The equipment needed for mitigative capability would have some functional reliability requirements, but would not necessarily need to be safety-related or single-failure-proof.

One key element of Regulatory Guide 1.174 involves assurance that defense-in-depth is maintained. Although a "debris generation" break size would be selected to distinguish between customary and more realistic design basis analyses, licensees would demonstrate acceptable mitigative capability for LOCA break sizes up through a double-ended rupture of the largest pipe in the RCS. This philosophy is consistent with recent recommendations made by

the Advisory Committee on Reactor Safeguards (ACRS) in its April 27, 2004, letter to the Chairman. However, it is very important to note that an alternative approach for resolving GSI-191 would not redefine the design basis LOCA break size.

The "debris generation" break size to distinguish between customary and more realistic design basis analyses is defined as follows:

- ▶ All American Society of Mechanical Engineers (ASME) Code Class 1 PWR auxiliary piping (attached to RCS main loop piping) up to and including a double-ended rupture of any of these lines.
- ▶ RCS main loop piping (hot, cold and crossover piping) up to a size equivalent to the area of a double-ended rupture of a 14 inch schedule 160 pipe (approximately 196.6 square inches).

The selection of a break size equivalent to the area of a double-ended rupture of a 14 inch schedule 160 pipe for RCS main loop piping generally bounds attached auxiliary piping sizes in PWRs, and is also consistent with 10 CFR 50.46 rulemaking direction (at this time). As mentioned previously, in developing this alternate approach for GSI-191 resolution, the staff intends to remain consistent with the ongoing 10 CFR 50.46 rulemaking effort.

Interactions between the staff and NEI have yielded this alternative GSI-191 resolution approach, which considers realistic and risk-informed elements. NEI documented significant portions of this alternative approach and submitted a revised Section 6 of the evaluation guidelines report on July 13, 2004. The alternative approach discussed in this NEI document incorporates many of the technical and regulatory elements discussed throughout the public meetings on this topic. The staff will review the NEI methodology and document its review as part of the NEI evaluation guidelines safety evaluation report (SER). The staff will note exceptions to and supplement the NEI methodology through the SER, as necessary. The NEI evaluation guidelines SER is scheduled to be issued in October 2004.

#### Schedule Status

On July 16, 2004, Los Alamos National Laboratory (LANL), the contractor working with the staff to review the NEI evaluation guidelines, stopped work due to security and safety concerns. Work was restarted on July 28, 2004; however, certain infrastructure and administrative work remains on hold. Because of this delay, the staff could not provide the Advisory Committee on Reactor Safeguards (ACRS) a draft safety evaluation in time to support a September full committee meeting. The ACRS has asked for a complete safety evaluation a month prior to a full committee meeting. The next opportunity for a full committee meeting is October 7-9. The staff revised a number of intermediary milestones to minimize the impact of this contractor delay. The delay results in rescheduling the issuance of the GSI-191 SER from September 30, 2004, to October 29, 2004, to accommodate the revised ACRS review schedule. This schedule revision will not impact the planned final resolution date for GSI-191, which will remain the end of 2007.

Chemical Effects

The chemical effects impact on PWR sump performance is still being evaluated, and an integrated test program has been developed through a collaborative effort between the NRC and industry. Initial testing is expected to begin in August 2004, and be completed in December 2004. This schedule is also adversely impacted by the recent LANL work stoppage. In order to address chemical effects on a plant specific basis, licensees will initially need to evaluate whether the chemical effects test parameters are sufficiently bounding for their plant specific conditions. If plant specific materials are not bounded by the chemical effects test parameters, licensees should provide technical justification to use any results from the chemical effects tests in their plant specific evaluation. If deleterious chemical effects are observed during these tests, licensees should evaluate the sump screen head loss consequences of this effect in an integrated manner with other postulated post-LOCA effects. In addition, a licensee who chooses to modify their plant sump screens prior to the completion of chemical effects testing and analysis of the test results should consider potential chemical effects in order to ensure a second plant modification is not necessary should deleterious chemical effects be observed during testing. The staff's SER documenting its review of the NEI evaluation guidelines will include this position.

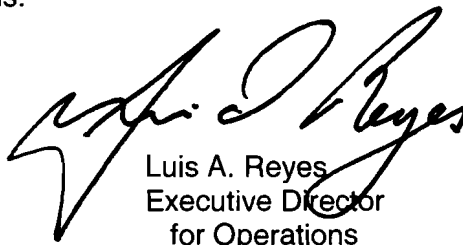
RESOURCES:

There are resources in the budget for GSI-191 resolution through FY2006. The NRR budget for FY2005 and FY2006 includes 2 FTE for each year. The total estimated resources to support the technical work necessary to review and approve license amendment requests and risk-informed exemption requests is considered part of the expected NRR workload involving licensing actions.

COORDINATION:

The Office of the General Counsel has no legal objection to this paper.

The Office of the Chief Financial Officer has reviewed this Commission paper for resource implications and has no objections.



Luis A. Reyes  
Executive Director  
for Operations

**DISTRIBUTION:**

Commissioners  
OGC  
OPA  
OCA  
ACRS  
CFO  
EDO  
COMMUNICATIONS  
REGIONS  
SECY



# **POLICY ISSUE**

## **(Information)**

August 16, 2004

SECY-04-0150

FOR: The Commissioners

FROM: Luis A. Reyes  
Executive Director for Operations

SUBJECT: ALTERNATE APPROACHES FOR RESOLVING THE PRESSURIZED WATER REACTOR SUMP BLOCKAGE ISSUE (GSI-191), INCLUDING REALISTIC AND RISK-INFORMED CONSIDERATIONS

### PURPOSE:

The purpose of this paper is to inform the Commission regarding:

1. staff plans to permit licensees to use alternate approaches for resolution of the pressurized water reactor (PWR) sump blockage issue,
2. the staff's schedule for issuing its safety evaluation report on the industry evaluation guidelines methodology, and
3. the staff's expectations for addressing chemical effects impacts on PWR sump blockage.

### SUMMARY:

This paper outlines the regulatory and technical elements necessary to establish a useful and effective alternate approach to resolving Generic Safety Issue (GSI) 191, "Assessment of Debris Accumulation on PWR Sump Performance," and describes the direction the staff is taking to implement such an approach.

CONTACT: Mark Kowal, NRR/DSSA  
301-415-1663

Chemical Effects

The chemical effects impact on PWR sump performance is still being evaluated, and an integrated test program has been developed through a collaborative effort between the NRC and industry. Initial testing is expected to begin in August 2004, and be completed in December 2004. This schedule is also adversely impacted by the recent LANL work stoppage. In order to address chemical effects on a plant specific basis, licensees will initially need to evaluate whether the chemical effects test parameters are sufficiently bounding for their plant specific conditions. If plant specific materials are not bounded by the chemical effects test parameters, licensees should provide technical justification to use any results from the chemical effects tests in their plant specific evaluation. If deleterious chemical effects are observed during these tests, licensees should evaluate the sump screen head loss consequences of this effect in an integrated manner with other postulated post-LOCA effects. In addition, a licensee who chooses to modify their plant sump screens prior to the completion of chemical effects testing and analysis of the test results should consider potential chemical effects in order to ensure a second plant modification is not necessary should deleterious chemical effects be observed during testing. The staff's SER documenting its review of the NEI evaluation guidelines will include this position.

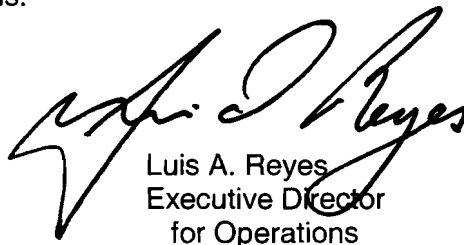
RESOURCES:

There are resources in the budget for GSI-191 resolution through FY2006. The NRR budget for FY2005 and FY2006 includes 2 FTE for each year. The total estimated resources to support the technical work necessary to review and approve license amendment requests and risk-informed exemption requests is considered part of the expected NRR workload involving licensing actions.

COORDINATION:

The Office of the General Counsel has no legal objection to this paper.

The Office of the Chief Financial Officer has reviewed this Commission paper for resource implications and has no objections.



Luis A. Reyes  
Executive Director  
for Operations

**DISTRIBUTION:**

Commissioners  
OGC  
OPA  
OCA  
ACRS  
CFO  
EDO  
COMMUNICATIONS  
REGIONS  
SECY



UNITED STATES  
NUCLEAR REGULATORY COMMISSION  
WASHINGTON, D.C. 20555-0001

JTL  
GT9990404

RECEIVED  
ACRS/AGNW  
US NRC

July 29, 2004

AUG 10 2004

ACRS Engrs.

**DISTRIBUTED TO ACRS MEMBERS**

MEMORANDUM TO: NRR Division Directors  
(See Attached List)

FROM: Catherine Haney, Program Director  
Policy and Rulemaking Program  
Division of Regulatory Improvement Programs  
Office of Nuclear Reactor Regulation

*Catherine Haney*

SUBJECT: DIRECTOR'S QUARTERLY STATUS REPORT

Attached for your information is the July 2004 edition of the Director's Quarterly Status Report. A redline/strikeout version of Attachments 1-6 and the Overview section of this report are available in ADAMS under NRR/DQSR (ADAMS Accession Number ML041940126). To assist in providing updates for the next status report, the appropriate staff level contacts should use the current report located in ADAMS.

The due date for submittal of your next status report updates is October 3, 2004. Please use September 30, 2004, as a cutoff date for your data and provide your updates via E-mail to Beverly Sweeney (E-mail address: BJS3), with a copy to Eileen McKenna (E-mail address: EMM). Attachment 4, the attachment on open petitions for rulemaking will be updated by staff in the RPRP Rulemaking Sections. Attachment 5, entitled, "Generic Communication and Compliance Activities," will be updated by Jack Foster, DIPM/NRR. Attachment 6, an attachment on active user need requests, will be updated by Roy Matthew, ADIP/NRR.

We will target the next Director's Quarterly Status Report for publication on October 31, 2004.

**ACRS OFFICE COPY  
DO NOT REMOVE FROM ACRS OFFICE**

*GT-999*

If you or your staff have any questions regarding the Director's Quarterly Status Report for Action Plans and Rulemaking, please contact Eileen McKenna at 415-2189. Any questions concerning Generic Communication and Compliance Activities (GCCAs) should be directed to Jack Foster at 415-3647.

Attachment: As stated

cc w/att.:	J. E. Dyer, NRR	R.W. Borchardt, NRR
	B. Sheron, NRR	J. Strosnider, NMSS
	C. Paperiello, RES	M. Springer, ADM
	W. Kane, OEDO	E. Merschoff, OEDO
	J. Jolicoeur, OEDO	G. Holahan, OCM/NJD
	R. Croteau, OCM/NJD	J. Sharkey, OCM/EXM
	J. Zimmerman, OCM/JSM	

Distribution w/attachments:

Central Files	RPRP Staff	RPRP R/F	FGillespie, NRR
SBahadur, RES	MMayfield, RES	JRosenthal, RES	REmrit, RES
ACRS (22)	TDietz (3)	DMcCain, NRR	BSt.Mary, IRM
KGray, NRR	JFoster, NRR	DRoberts, NRR	RMathew, NRR
NDudley, NRR	TFrye, NRR	RFranovich, NRR	MKotzalas, NRR
RElliott, NRR	JDonoghue, NRR	MBoyle, NRR	SMoore, NMSS
STreby, OGC	Mltzkowitz, OGC	MLesar, ADM	RZimmerman, NSIR
FEltawila, RES	BGolden, ADM	VVoytko, ADM	TMensah, NRR
RIrish, OIG	JShea, NSIR	GTracy, NSIR	RCaldwell, NSIR
LCupidon, RES	NRR Deputy Div. Dir.	NRR Branch Chiefs	
Regional Office DRP and DRS Dirs.			

ADAMS ACCESSION NUMBER: ML041940126

ADAMS DOCUMENT TITLE: July 2004 Director's Quarterly Status Report

DOCUMENT NAME: MEMOJULY.WPD

To receive a copy of this document, indicate in the box: "C" = Copy without attachment/enclosure "E" Copy with attachment/enclosure "N" = No copy

OFFICE	RPRP:DRIP	<input checked="" type="checkbox"/> IROB:DIPM	<input checked="" type="checkbox"/> SC:RPRP:DRIP	SC:RPRP:DRIP	PD:RPRP:DRIP
NAME	BSweeney:bst	JFoster	DSkiff	EMcKenna	CHaney
DATE	07/29/04	07/15/04	07/29/04	07/29/04	07/29/04

Addressees - Memorandum Dated July 29, 2004

NRR Division Directors

SUBJECT: DIRECTOR'S QUARTERLY STATUS REPORT

Mail Stop

David B. Matthews, Director, DRIP, NRR  
Ledyard B. Marsh, Director, DLPM, NRR  
Bruce A. Boger, Director, DIPM, NRR  
Richard J. Barrett, Director, DE, NRR  
Suzanne C. Black, Director, DSSA, NRR  
Cynthia A. Carpenter, Director, PMAS, NRR

O-12E5  
O-8E1  
O-6E3  
O-9E3  
O-10A1  
O-5E7

ML 041940126

7/29/2004

**INTERNAL**

**DIRECTOR'S QUARTERLY  
STATUS REPORT**

**ACTION PLANS**

**RULEMAKING**

**GENERIC COMMUNICATION AND  
COMPLIANCE ACTIVITIES**

**JULY 2004**

**Office of Nuclear Reactor Regulation**